The Organic Geochemistry of Sedimentary Organic Matter from the Algerian Sahara

by

MEBARKA AZIEZ

A thesis submitted to the University of Newcastle upon Tyne in partial fulfilment of the requirements for the degree of Doctor of Philosophy in the Faculty of Science.

Fossil Fuels and Environmental Geochemistry (Posgraduate Institute): NRG, University of Newcastle upon Tyne, U.K.

March 1992

DECLARATION

I hereby certify that the work described in this thesis is my own, except where otherwise acknowledged, and has not been submitted previously at this or any other university.

MEBARKA AZIEZ

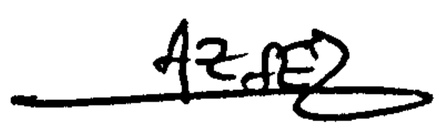

CONTENTS

Structures

Appendix 3: Data for source rocks.

Appendix 4: Data for oils

Appendix 5: Data for source extracts and oils from the Ghadames-El Borma basin.

ACKNOWLEDGEMENTS

I would like to express my gratitude to many people who have contributed to this project. In particular my supervisor in Organic Geochemistry Dr G.D. Abbott and J.M. Jones in Organic petrology are thanked for offering help and supervision when I needed it.

I thank the following who have helped me in a wide of various ways:

Professor S. Larter, Dr. Archie Douglas, Dr. R.V. Tyson, Dr. Paul Farrimond for helpful discussions. Paul Donohoe for GC/MS analysis, Ian Harrison for GC and Rock-Eval analysis, Dr. Mia Moers and Dr. Stuart Petch for proof reading, Dr. Andy Aplin, Dr. J.M. Jones, Yvonne Hall, Rob Hunter, Barbara Brown, Christine Jeans, Lexa Summerbell, Len Rhodes, Ann Thwaites for other assistance. Susan Wood, Effie Lambropoulou, Gavin Law, Andy Bishop, Greg Ewbank, Heather Clegg, Anne Raymond, Wang Yu and Andy Stott for helpful discussion and moral support.

Special thanks go to Nils Telnaes and Arne Steen for GC/MS/MRM analyses.
I would like to express my gratitude to Martin Fowler for high resolution GC/MS analyses of the oils and helpful discussion.

I thank the Algerian government for the research studentship.

Finally I thank my collegues in C.R.D, my relatives and my friends Mia Moers and Leila Mami for their encouragement and my mother for her patience.

Abstract

This study is composed of three parts:

(i) organic geochemical and organic petrological analysis of source rock samples from the Ghadames-El Borma basin are described;

(ii) organic geochemical characterisation of oils from a number of occurrences in Algeria has been carried out to give families or groups of different oil types;

(iii) oil-source rock correlations in the Ghadames-El Borma basin between the oils in the Triassic reservoirs and the putative source rock sections are suggested.

Sixty rock samples ranging from the Triassic to Ordovician in age from the Ghadames-El Borma basin, have been investigated using organic geochemical techniques in order to assess source rock potential. Rock-Eval pyrolysis data indicate that Devonian constitute excellent source rocks, Silurian and Ordovician are considered potentially moderate to good source beds, whereas Triassic sediments have little or no oil potential. Reflected and ultraviolet light microscopy show that amorphous organic matter and Graptolite dominate the Ordovician strata, while Silurian and Devonian contain predominantly liptinitic materials such as acritarchs, algal bodies (*Tasmanites*) and spores; bitumen is moderately abundant. Biological marker investigation using capillary gas chromatography and the combined gas chromatography/mass spectrometry in energy impact (GC/MS/EI) and metastable ion reaction monitoring (GC/MS/MRM) modes together with principal component analysis (PCA) have allowed a discrimination of samples into three groups: (i) Ordovician, (ii) Silurian and Devonian and (iii) Triassic.

Oil-oil correlation procedure has been carried out in areas with a number of different oil occurrences from southern and northern Algeria, namely from the Ghadames-El Borma, Sbaa, Illizi, Triassic province and Southeast Constantine basins. A range of approaches can be used which depend on the nature of the oils. In the present study, correlation parameters include data derived from biological marker distributions as well as gasoline range hydrocarbons.

Distributions of biological marker compounds together with principal component analysis (PCA) of sterane and terpane distributions reveal a discrimination of the well numbers into three groups:

(i) Southeast Constantine (DK1, GKN1), Ghadames-El Borma (ELB9), Sbaa (ODZ1, DECH1), Ain Amenas (TG22).

(ii) Ghadames-El Borma (KA2, ROM1), Ain Amenas (ZR115)

(iii)Gassi Touil (GT6, GT47), Rhourd-Nouss (RN48,RNSE6).

Oils from Illizi basin (MRK16, STAH8, STAH40 and MRK12) are poor in biological marker content and as yet cannot be assigned to any of the above groups. Maturity assessment has been based on paraffin index values (heptane and isoheptane indices) given by Thompson (1983) as well as steroid isomerization and aromatization ratios.

In this situation, oil mixing can be clearly seen using both gasoline derived parameters and biological marker ratios (e.g. sterane isomerization) if there is no loss during migration.

In the final part of this study, oil-source rock correlations have been considered for oils (Keskessa, El Borma and Rom field) and source rocks from the Ghadames-El Borma basin. However, such correlations were, in some cases, difficult to establish because molecular distributions may have changed during migration. Nevertheless, correlations procedures attempted using molecular parameters and PCA results of steranes and terpanes suggest that these particular oils may have been derived from Devonian or Silurian source rocks, as suggested by similarities in sterane and terpane compositions.

Chapter 1 Introduction

1. Introduction

1.1.General Introduction and aims of the project

The large number of hydrocarbon deposits discovered during the last two decades in the Algerian Sahara and northern Algeria have been of great economic significance to the country. The National Oil Company has judged it, therefore, necessary to carry out a detailed study of the organic geochemistry of the crude oils produced in Southeast Constantine (northern Algeria) Sbaa region, Illizi and Ghadames-El Borma basins (Algerian Sahara) as well as source rocks from the Ghadames-El Borma basin. This study will form the basis of an oil-source rock correlation investigation (see Figure 1.1. for geographical locations). The sedimentary sequence involves shales ranging from Triassic to Ordovician in age.

During the last two decades, many attempts have been made at correlating Algerian oils using different approaches such as monoaromatic steroidal hydrocarbon distributions (Tissot et al., 1974b) and gasoline (C_4-C_6) range hydrocarbons (Sonatrach internal report, 1980) from the Illizi basin and the Triassic province. These oils were produced from the Carboniferous, Upper Devonian (F_2) and Middle-Lower Devonian (F_4), Upper Silurian (F_6) and Triassic reservoirs. From the information obtained using the first approach, based on the monoaromatic steroidal hydrocarbon distributions (Tissot et al., 1974b), it is rather difficult to make an objective appraisal because no data was shown (e.g. mass chromatograms or mass spectra). Furthermore, such mature oils do not contain sufficient amounts of monoaromatic steroidal hydrocarbons to allow reliable correlation (Fowler, 1984). As regards the data obtained using the gasoline range C_4-C_6 hydrocarbons, discrimination was based on maturity differences.

The main objective of this thesis has been to conduct an organic geochemical and petrological evaluation of the variation in the organic matter type, maturity

and depositional environment and to investigate the extent to which the geochemical properties have been modified in the oil reservoir by maturation, migration, biodegradation and/or water washing. Several aspects are considered below:

(i) Optical and geochemical characterisation of the organic matter contributing to the sediments ranging from Triassic to Ordovician in age and the detection of any changes in source environment and maturity as a function of age.

(ii) Analysis of oils taken from different geographical areas with a view to establishing (a) the number of different oil families; (b) differences between each oil family by considering the effects of maturation, migration, biodegradation and/or water washing; (c) from the geochemical characteristics of each oil family, the nature and the level of maturity of the source rock (s) at the time of primary migration.

To approach these key questions, sophisticated techniques were applied. The saturated and aromatic hydrocarbon fractions from the source rock extracts and oils were analysed using capillary gas chromatography (GC), combined gas chromatography/mass spectrometry (GC/MS) as well as GC/MS/metastable ion reaction monitoring (GC/MS/MRM). The chemical compositions of the isolated kerogens were determined using flash pyrolysis-gas chromatography (Py-GC). Data from sterane and terpane distributions were then processed using Principal Component Analysis (PCA).

Aliphatic hydrocarbon analysis indicates that the Ordovician can be discriminated from the Triassic, Devonian and Silurian source rock extracts (Chapter3). Biological marker investigation of source rocks suggests that Silurian and Devonian source rocks have roughly similar characteristics.

Distributions of biological marker and gasoline range hydrocarbons together with principal component analysis (PCA) of sterane and terpane distributions (Chapter4) reveal a discrimination of oils into three groups:

(i) Southeast Constantine (DK1, GKN1), Ghadames-El Borma (ELB9), Sbaa (ODZ1, DECH1), Ain Amenas (TG22).

(ii) Ghadames-El Borma Gassi (KA2, ROM1), Ain Amenas (ZR115)

(iii) Gassi Touil (GT6, GT47), Rhourd-Nouss (RN48, RNSE6).

An attempt to correlate the oils from the Ghadames-El Borma basin was made with source rocks (Chapter5) from RE-1 (3346.20m-3438.26m), ZAR-1 (3994.65m) and KA-1 bis (3029.82-3072.85m). These oil-source rock correlations were made difficult by the fact that correlations of source extracts were attempted with migrated and reservoired oils, which may have altered their chemical signatures. One needs to bear in mind the major factors that can affect the composition of oils during and after migration (e.g. water washing, microbial activity and maturation). Correlation procedures made using biomarker parameters together with PCA of sterane and terpane distributions suggest that oils ELB9 (group i) and KA2, ROM1 (group ii) fall in the same group as the Silurian and Devonian source extracts, since these have been previously characterised as having similar chemical composition.

1.2. Geology of the study area

1.2.1.Introduction

This chapter is a brief review of the geology of the Algerian Sahara and northern Algeria (Figure 1.1), particularly in the Southeast Constantine (northern Algeria), Sbaa, Illizi and the Ghadames El-Borma basins (the Algerian Sahara). The geochemical study has been extended to the source rocks in the Ghadames-El Borma basin to enable an oil-source rock correlation to be made. The sedimentary sequences involve marls and shales ranging from Triassic to Ordovician in age. In the following sections, a blef summary of structural and stratigraphic aspects of the Algerian Sahara and each of the basins will be considered.

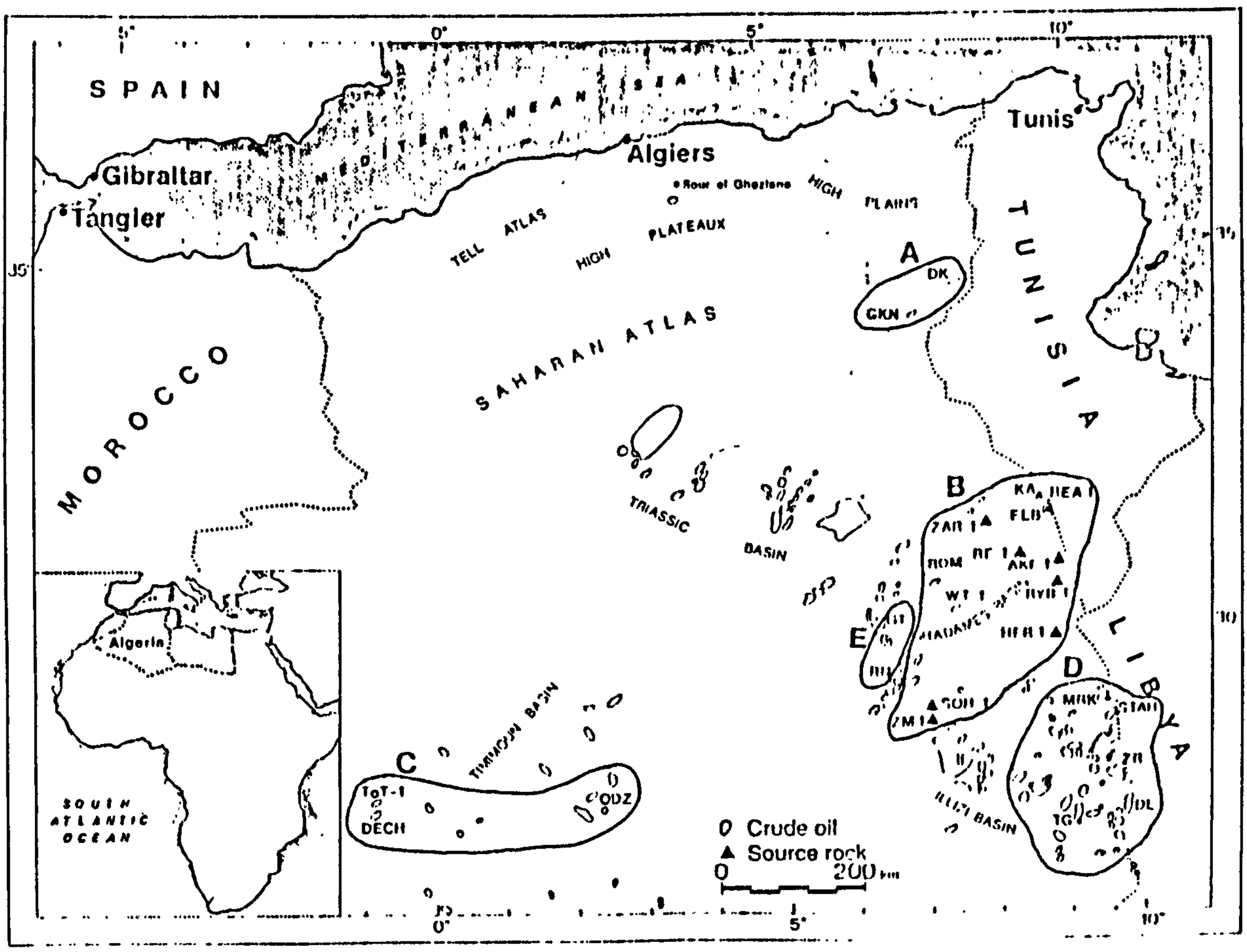

Figure 1.1 Sample location map showing areas of study:

A-the Southeast Constantine basin
B-the Ghadames-El Borma basin
C-the Sbaa basin
D-the Illizi basin (including the geology of Ain Amenas region: TG, DL and ZR)
E-the Triassic basin (Gassi Touil and Rhourd-Nouss regions).

1.2.2. Structure and stratigraphy of the Algerian Sahara

From the tectonic point of view, the Algerian Sahara is related to the western part of the North African plate where the crystalline basement was subjected to substantial subsidence and covered with a thick layer of Paleozoic and Meso-Cenozoic sediments (Chardac et al., 1979).

The Algerian Sahara is bounded to the south by the Reguibat and the Touareg Shields (Hoggar massif) and to the north by the deep Saharan Atlasic fault. The latter separates the Precambrian platform of the Sahara from the epi-Hercynian platform, which existed during the Mesozoic (Saharan Atlas). The thick sedimentary sequence of the Algerian Sahara is made up mainly of transgressive and uncomformable Paleozoic rocks overlying the Precambrian basement. The Paleozoic series consists of rocks ranging from Cambrian to Carboniferous in age; the Permian is absent. The Mesozoic comprises Triassic, Jurassic and Cretaceous continental, lagoonal and marine sediments. From the lithological point of view, the formations are generally sandstones, shales and marls. The main structural elements of the Algerian Sahara are illustrated in Figure 1.2.

1.2.3.The Southeast Constantine basin

The Southeast Constantine basin is situated in northern Algeria, precisely in the eastern part of the Sahara Atlas. The part of northern Algeria has been desribed as being a part of the alpine system (Chardac et al., 1979). The Southeast Constantine basin, being located in the eastern part of the Saharan Atlas, appears to be cut off at the level of Bou-Saada-Biskra high and carries through the Aures and into Tunisia (Figure 1.3). It is bounded to the east by the Tunisian border,to the north by the high plains and to the south by the Sahara Platform (Chardac et al., 1979). During the Cretaceous, in the eastern part of the Sahara Atlas (including the Southeast of Constantine basin), the subsidence has been rapid (Chardac et al.,1979). Thus, thick layers of shales (Neocomian),

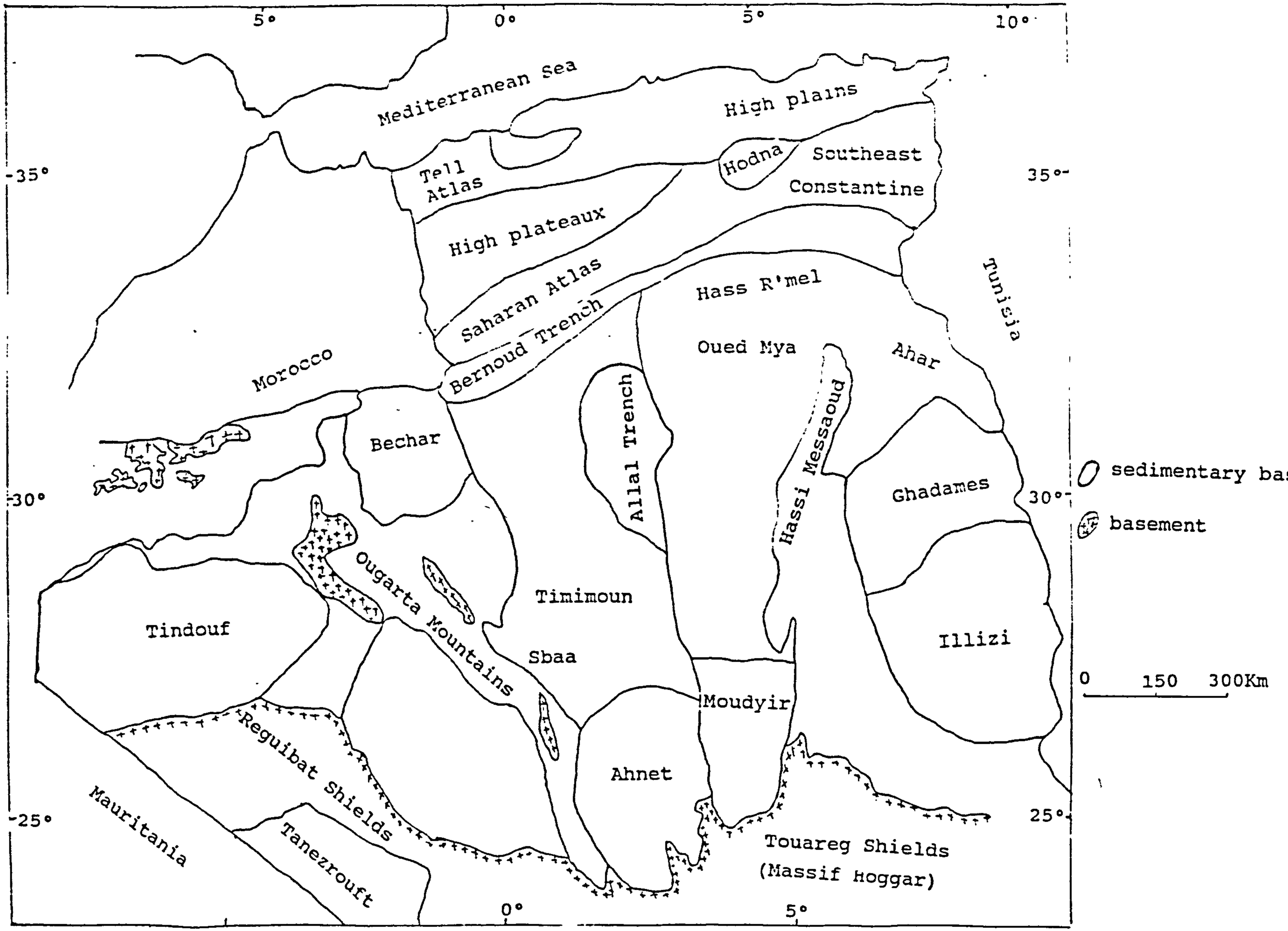

Figure 1.2 Main structural elements of the Algerian Sahara.

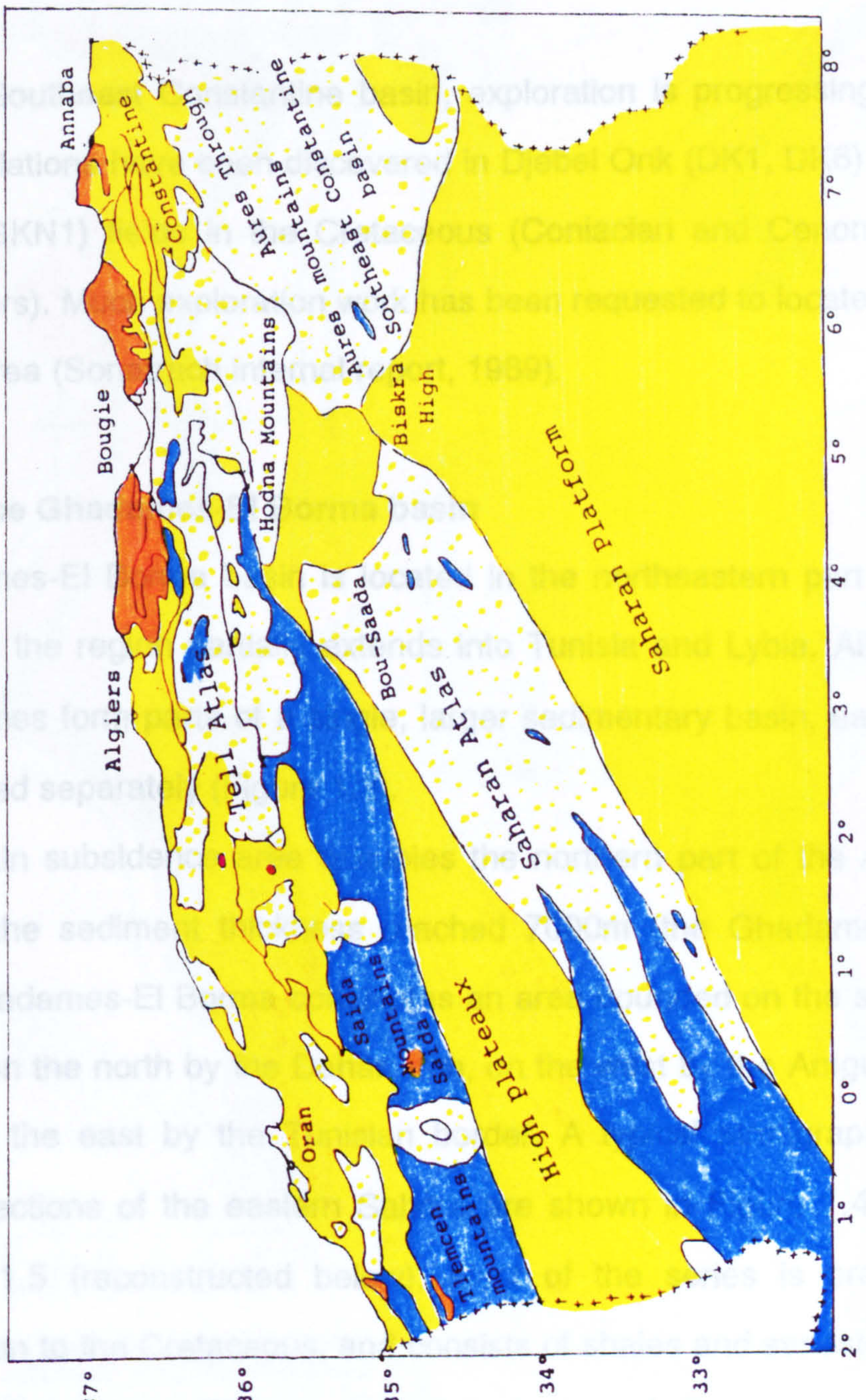

Figure 1.3 Main geological units of northern Algeria.

sandstones (Barremian-Albian), calcareo-dolomites (Aptian), shales (Cenomanian) and clays and carbonates (Turonian-Senonian) were deposited. From the tectonic point of view, this region has been subjected to changes in sea level and to subsidence, commencing during the Aptian (Chardac et al., 1979).

In the Southeast Constantine basin, exploration is progressing, and some oil accumulations have been discovered in Djebel Onk (DK1, DK6) and Guergat-El Kihal (GKN1) fields in the Cretaceous (Coniacian and Cenomacian-Turonian reservoirs). Much exploration work has been requested to locate further oil traps in the area (Sonatrach internal report, 1989).

1.2.4.The Ghadames-El Borma basin

Ghadames-El Borma basin is located in the northeastern part of the Algerian Sahara; the region partially extends into Tunisia and Lybia. Although Illizi and Ghadames form parts of a single, larger sedimentary basin, each basin will be described separately (Figure 1.2).

The main subsidence area occupies the northern part of the Algerian Sahara where the sediment thickness reached 7000m (the Ghadames Depression). The Ghadames-El Borma constitutes an area bounded on the south by the Illizi basin, on the north by the Dahar arch, on the west by the Amguid-El Biod axes and on the east by the Tunisian border. A typical stratigraphic column and cross-sections of the eastern Sahara are shown in Figure 1.4, trace BB' and Figure 1.5 (reconstructed below). Most of the series is present, from the Cambrian to the Cretaceous, and consists of shales and sandstones, except for the marls in the Triassic and limestones of the upper Namurian and Westphalian (Chardac et al., 1979). As can be seen in Figure 1.4, most formations, except the Carbonifereous appears to be limited in extent due to uplift and erosion. The thickness of the beds increases northwards and westwards. The Pre-Mesozoic subcrop map (Figure 1.6) shows that the

Figure 1.4 GEOLOGICAL CROSS SECTION

Western Sahara

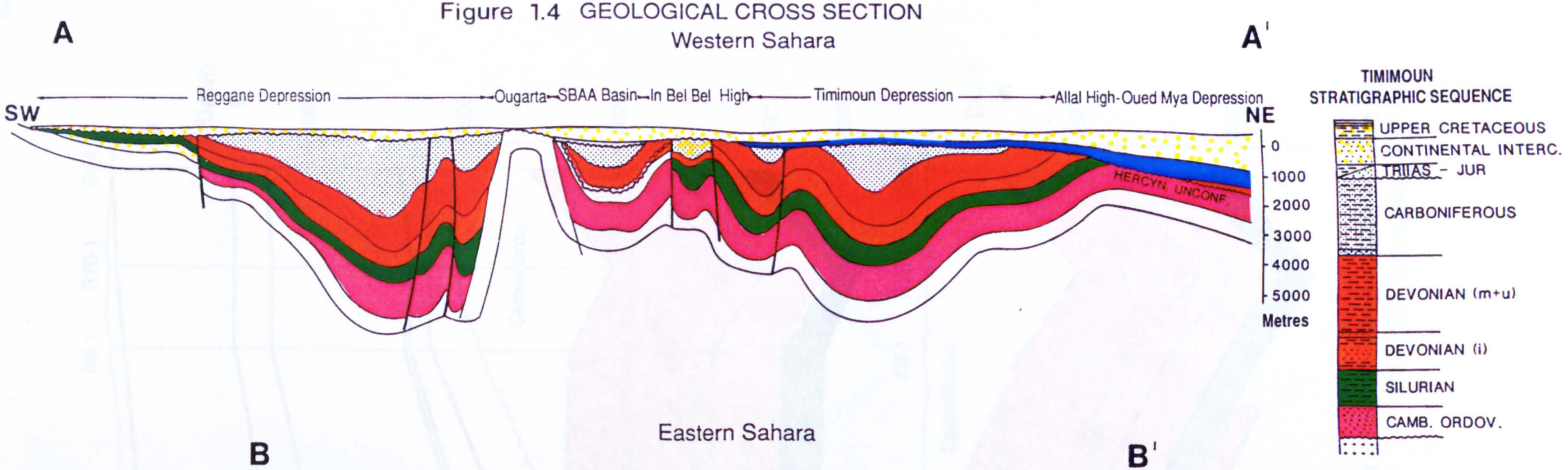

Eastern Sahara

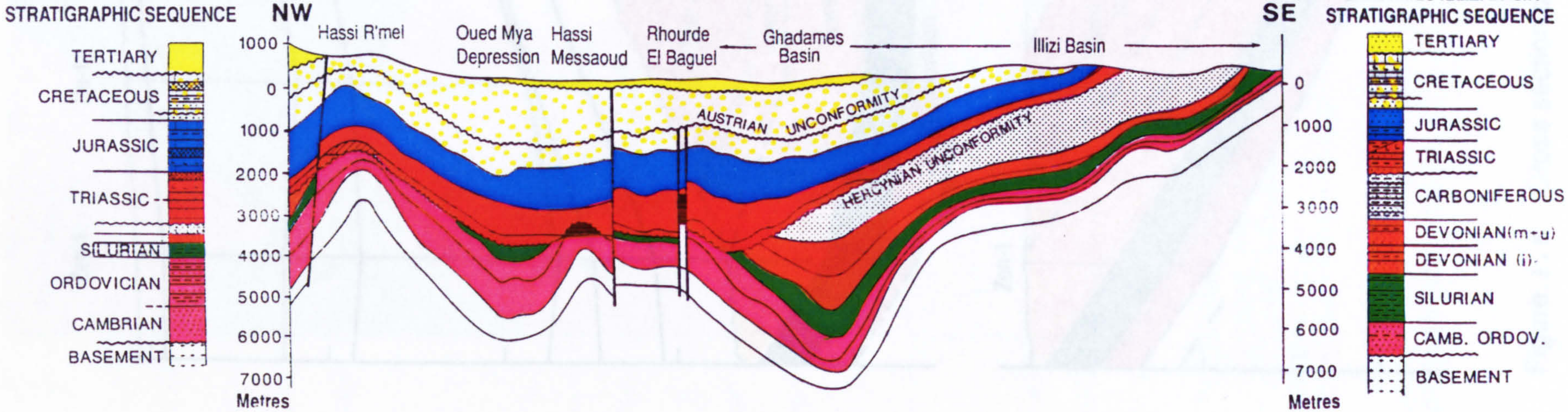

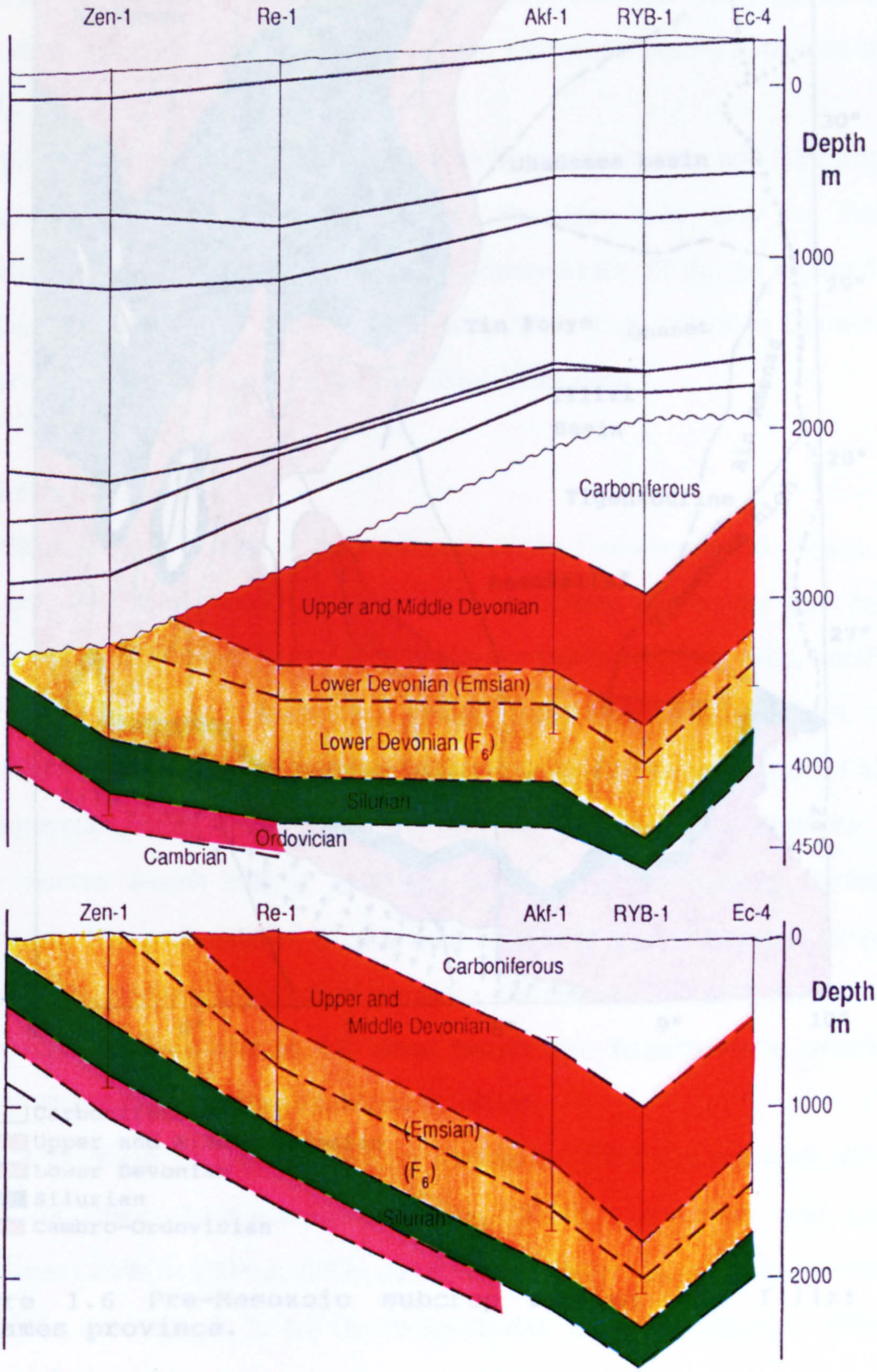

Figure. 1.5 Cross section of part of the Ghadames-El-Borma basin
(Sonatrach Internal Report, 1980)

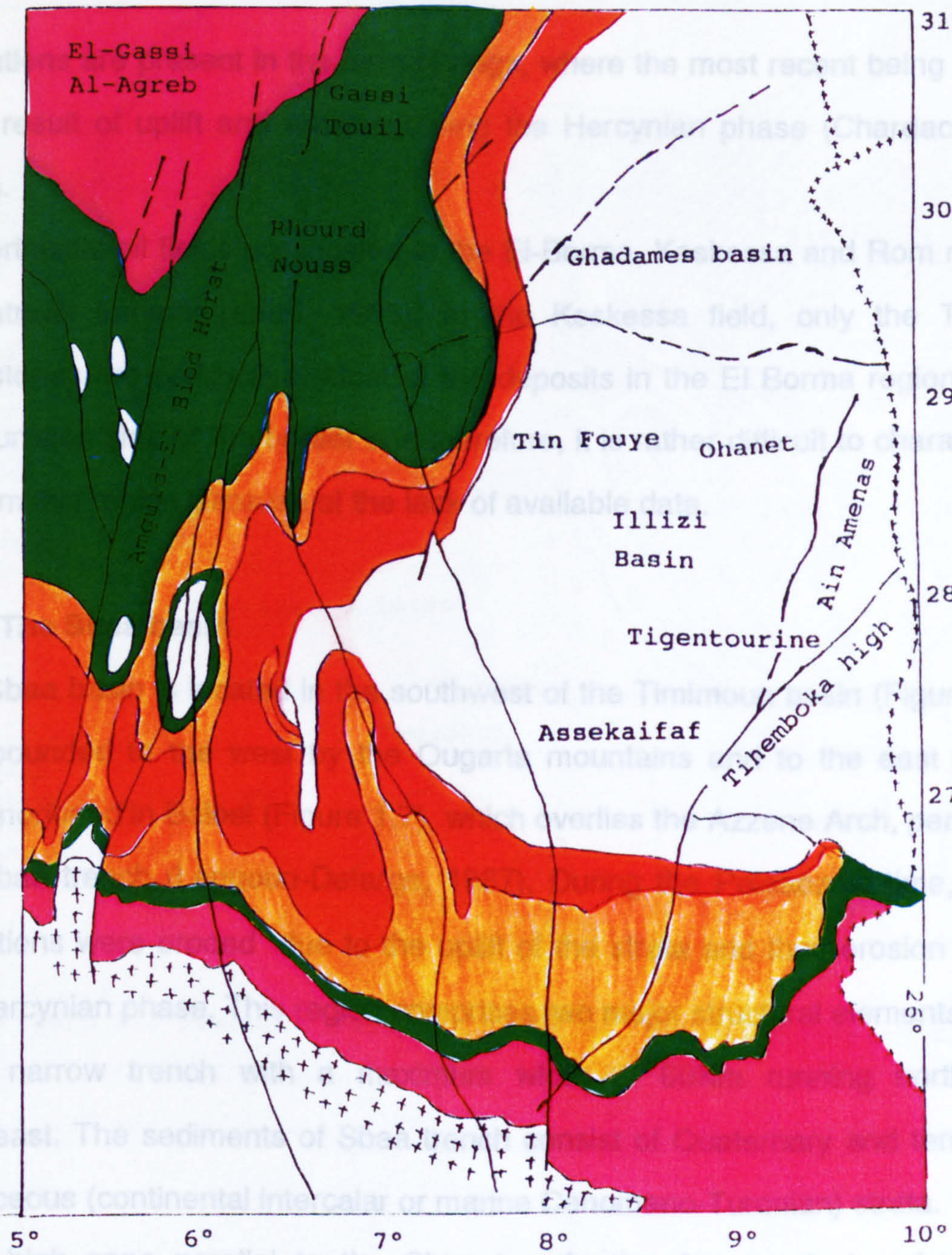

Figure 1.6 Pre-Mesozoic subcrop map of the Illizi and Ghadames province.

formations are present in the form of rings, where the most recent being absent as a result of uplift and erosion during the Hercynian phase (Chardac et al., 1979).

The principal oil fields are located in the El-Borma, Keskessa and Rom regions (Sonatrach internal report, 1985). In the Keskessa field, only the Triassic sandstones are productive. Most of the deposits in the El Borma region lie on the Tunisian side of the border and therefore, it is rather difficult to characterise oil from this region because of the lack of available data.

1.2.5.The Sbaa basin

The Sbaa basin is located in the southwest of the Timimoun basin (Figure 1.2). It is bounded to the west by the Ougarta mountains and to the east by the anticlinorium d'In Belbel (Figure 1.7), which overlies the Azzene Arch, parallel to the Sbaa trench (Laggoun-Defarge, 1987). During the Palaeozoic time, some formations were eroded due to the uplift of the strata and their erosion during the Hercynian phase. This region comprises two major structural elements:

(i) A narrow trench with a maximum width of 60Km running northwest-southeast. The sediments of Sbaa trench consist of Quaternary and terrestrial Cretaceous (continental intercalar or marine Cenomano-Turonian) strata.

(ii) A high zone parallel to the Sbaa trench: the Azzene Arch, where the sediments have a maximum thickness of 3500m.

Most of the oils in the region have been located in TOT-1 (Tournaisian), SBAA-1 (Gres de Sbaa, Tournaisian), LT-1 bis, DECH-1 (Strunian) and ODZ-1 (Namurian) wells at 500m to 600m depth. The tentative source rocks generating these oils are thought to be Devonian-Silurian (Laggoun-Defarge, 1987) or Silurian (Drid, 1989).

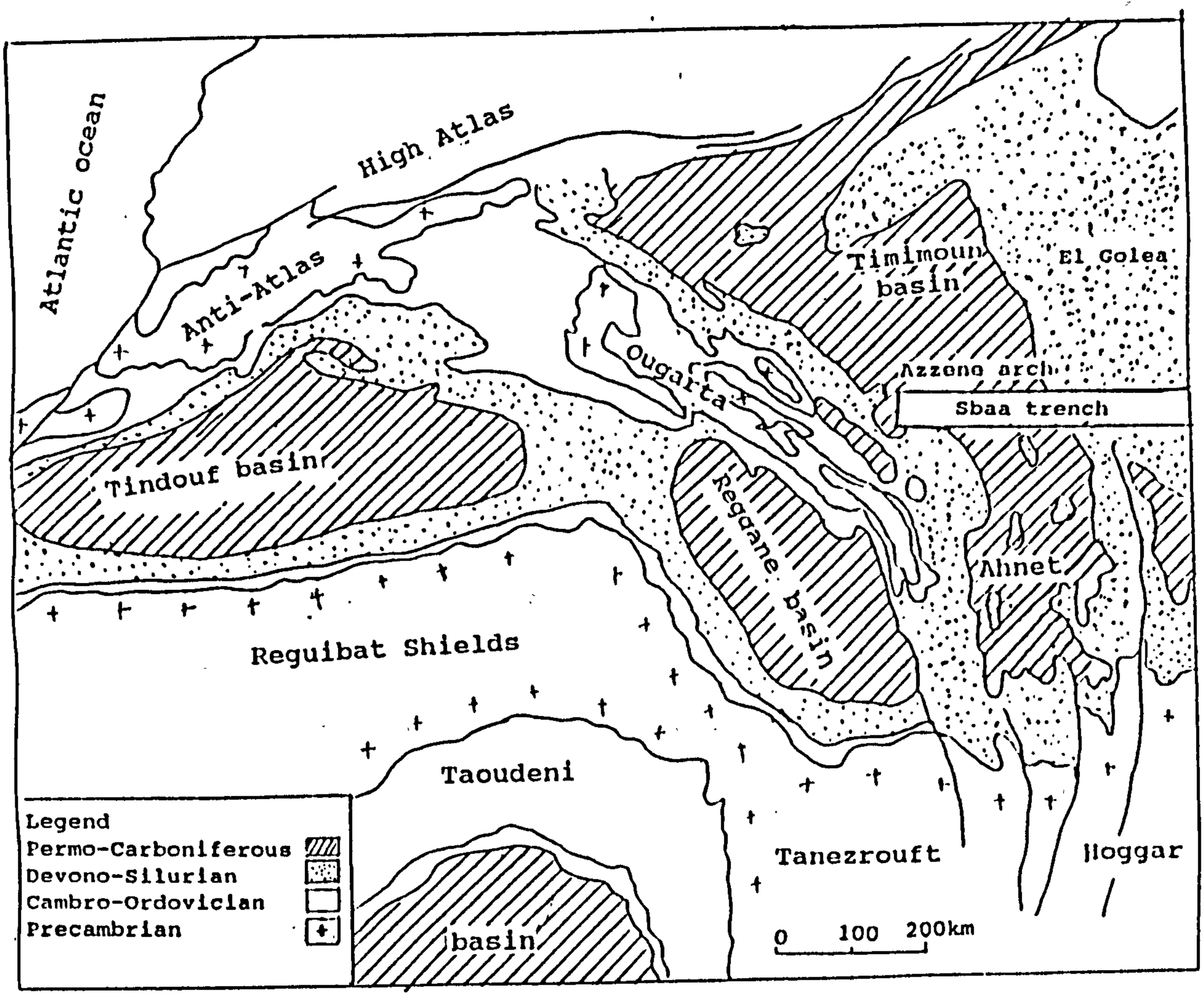

Figure 1.7 Mesozoic subcrop map of the Western Algerian Sahara.

1.2.6.The Illizi basin

The Illizi basin is situated in the southeastern part of Algerian Sahara (Figure 1.2). It is bounded to the south by the Touareg shields (Hoggar massif), to the west by the Amguid-Hassi Messaoud horst-anticlinal, to the north by the Ghadames basin and to the east by the Lybian borders. It is separated from the latter by the Tihemboka trench.

The Illizi basin contains a thick Palaeozoic sequence overlain uncomformably by Mesozoic strata. The basin has been subjected to three major tectonic phases: Hercynian, Autrichian and Alpine; the former played a role in the formation of the basin. In fact, most of the sedimentary events (folding, subsidence etc) are related to the Hercynian phase. Furthermore, during this period the region was oriented northwards adopting the form of a monocline (Latreche, 1982; Sonatrach internal report 1985). The most important structural axes are those of Essaoui-Mellene, Fadnoun, Tihemboka and Ahara; the last two persisted to the end of the Devonian sedimentation (reservoir F_6, Siegenian).

The formations present consist of marls, shales and sandstones with a total thickness of 3500m (Sonatrach internal report, 1980). The Illizi basin is a rich hydrocarbon-bearing basin that has been very well explored. The source rocks are thought to be mainly Devonian and Silurian (Gothlandian shales). The Ordovician and Carbonifereous shales have similar characteristics to the Silurian but are thought to be of less importance. The reservoirs are located in the Cambrian, Ordovician, the Upper Silurian (F_6) and Devonian sandstones (F_2, F_3, F_4, and F_5). The main oilfields in the Illizi basin are located in the Ain Amenas basin, namely Edjleh (DL), Zarzaitine (ZR), and Tiguentourine (TG), and in south Ghadames basin Stah (STAH) and Mereksen (MRK) (Chardac et al., 1979). The main oilfield in Edjleh, are producing from Carbonifereous (Visean), Devonian and the Cambro-Ordovician reservoirs. The structures were divided into northern and southern producing zones by transverse faults. The

Tiguentourine oilfield is situated 40 miles west of Edjleh. It is separated from the latter by a vertical fault. Zarzatine is a faulted monocline accumulation (Tirasoo .,1984).

1.2.7 The Triassic province

The Triassic province is situated in the northern part of the Sahara platform. It comprises the Gassi-Touil and Rhourd-Nouss regions (Figure 1.8). Both areas are situated in the Amghuid-Hassi Messaoud structure, comprising horsts and grabens, which are complicated by the presence of smaller faults. The geological cross-section and stratigraphic column of the Triassic province (Figure 1.4, trace BB') show that the Palaeozoic series is made up of shales and alternations of shales and sandstones. The Devonian and the Carboniferous are limited in extent in the Triassic province by uplift and erosion during the Hercynian phase.

The evolution of the Triassic basin consists a of transgressive Mesozoic series, which unconformably overlies the Upper part of the Palaeozoic (Chardac et al., 1979). Transgression of the sea started in the north during Mesozoic times and in the Upper Cretaceous reached the southern part of the Triassic province. After a period of minimum erosion, the sea withdrew and most of the series consists of continental sediments (Kerdjidj, 1987).

The Silurian (Gothlandian) shales are thought to be the principal source rocks in the area, particularly for Gassi Touil and Rhourd-Nouss fields.

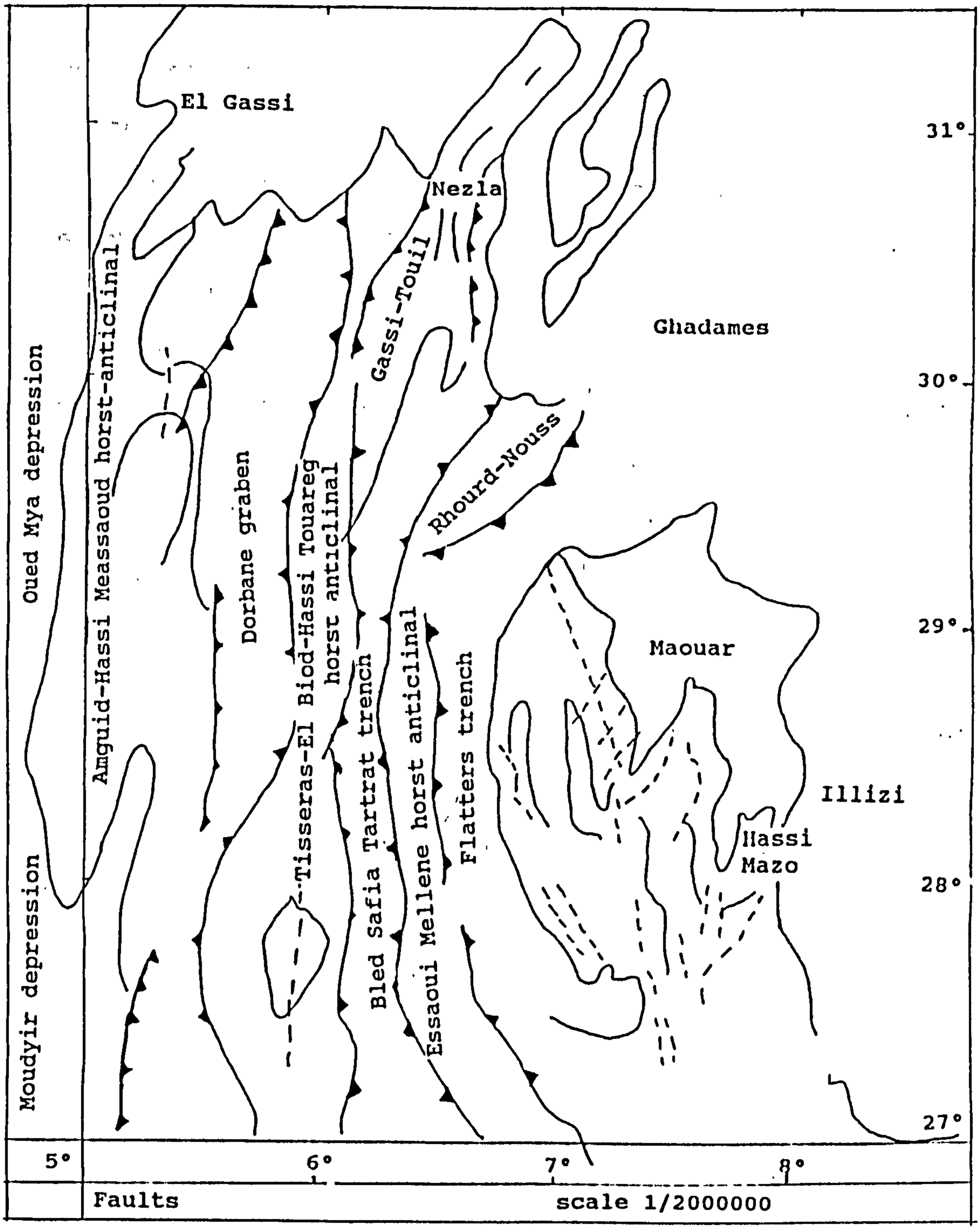

Figure 1.8 Main structural elements of the Triassic province (Kerdjidj, 1987).

1.3. Background review

1.3.1. Introduction

The following provides a review of the literature pertinent to the organic geochemistry of petroleums and their source rocks. The review is divided into two parts. The first describes the application of "bulk" parameters and techniques whereas the second focuses on molecular aspects. The two most important controls on the organic geochemistry of sedimentary organic matter are (i) palaeoenvironment of deposition and (ii) maturation.

1.3.2. Bulk organic geochemistry

Evaluation of potential source rocks in a sedimentary basin is essential to the oil industry. Recognition of source beds is usually based on the richness of organic matter, as measured by the amount of Total Organic Carbon (TOC), and kerogen type. A minimum value of ca 0.5% org.C is a prerequisite for a source rock (e.g. Tissot and Welte, 1984, pp 255) in order to generate commercial oil and gas. The organic carbon content is dependent upon the type and maturity level of organic matter. For example, a value of 2% TOC from a sediment including mainly inertinite, is a poorer source rock than one containing 0.5% TOC of algal origin (Tissot et al., 1974a; Tissot and Welte, 1984, pp 496). Furthermore, the amount of organic matter may vary with lithology in ancient sediments. Carbonates have been reported to contain much less organic matter than shales (Hunt, 1979). Hence, the minimum TOC value is 0.3% for carbonates and evaporites and 0.5% for detrital rocks (Tissot and Welte, 1984, pp 55).

The various types of kerogen are of different chemical compositions, which are influenced by biological source and depositional environment. Input organics can be defined as either autochthonous organic matter, which is mainly planktonic and deposited within a basin, or allochthonous organic matter. The latter consists of higher plant debris or reworked organic matter, which are

brought from areas outside the basin and deposited at a site which is distal from the source.

Rock-Eval, elemental analysis and visual kerogen are generally employed to define the type of sedimentary organic matter. Rock-Eval pyrolysis and elemental analysis can produce similar parameters: hydrogen and oxygen indices (i.e H/C and O/C), which are plotted in the van Krevelen diagram used for classification of various kerogen types (Figure 1.9). This Figure illustrates the evolutionary pathways of three kerogen types (Tissot et al., 1974a). In addition to type I, II and III kerogens, there is a fourth type, residual organic matter, which has low H/C and high O/C ratios. This may contain organic matter recycled and strongly oxidized during transport and deposition. It has no potential for hydrocarbon generation (Tissot et al., 1980).

Type I kerogen is hydrogen-rich, composed mainly of lipidic material derived from algae and bacteria. This organic matter type is associated with lacustrine algae such as *Botryococcus braunii* and similar organisms (e.g. Green River shales in U.S.A.)

Type II kerogen consists of marine organic matter, derived predominantly from phytoplankton, zooplankton and bacteria, which are deposited in a reducing environment. This organic matter type is considered to have a generally good potential for the generation of oil and gas (e.g. as in Devonian and Silurian source rocks from the Algerian Sahara and the Kimmeridge source rocks for the northern North Sea).

Type III kerogen consists of higher plant debris, which may be incorporated into sediments. This organic matter type is poorer than types I and II for oil but it may generate gas, on reaching an appropriate maturity level (e.g. Mahakam

Delta and the Westphalian coal measures for the gas in the southern North Sea). For overmature kerogens, all types plot close to the origin.

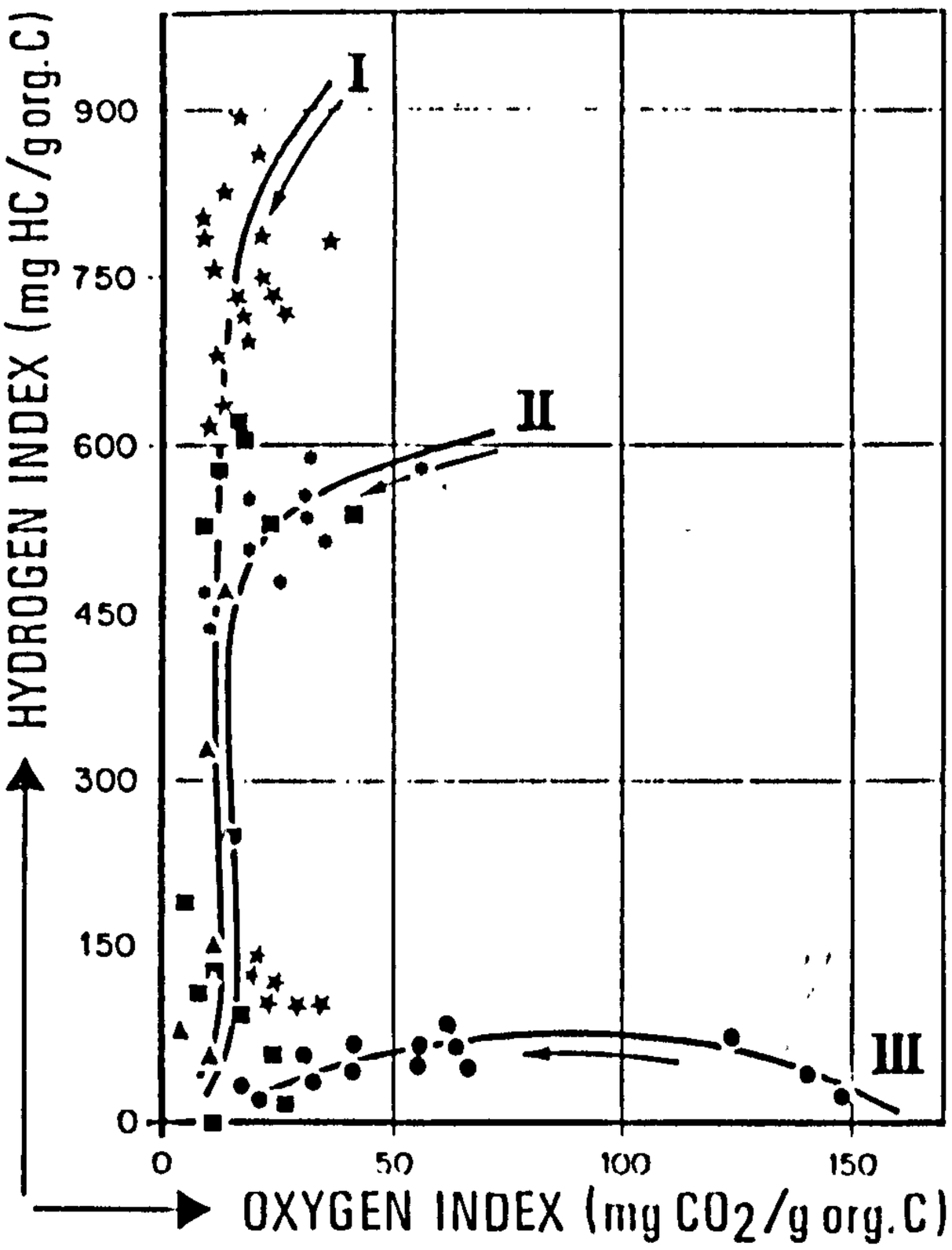

Figure 1.9. A van Krevelen diagram applied to Rock-Eval pyrolysis data. Formation of hydrocarbons as a function of kerogen type. With increasing maturation, hydrogen and oxygen indices tend towards zero. (After Tissot and Welte, 1984 pp 512).

★ Green River shales
✱ Lower Toarcian, Paris Basin
▲ Silurian-Devonian, Algeria-Lybia
● Upper Cretaceous, Douala Basin
■ others

Pyrolysis/gas chromatographic analysis (Py-GC) is used for kerogen typing (e.g. Larter et al., 1978; Solli et al., 1985; Larter, 1985; Larter and Sentfle, 1985; Φygard et al., 1988). A novel diagram (Figure 1.10) has been introduced by Larter (1985) showing the correlation of the sum of normal hydrocarbon yield in the range of C_9-C_{25} and hydrogen index (HI mg S_2/gTOC) for kerogen typing.

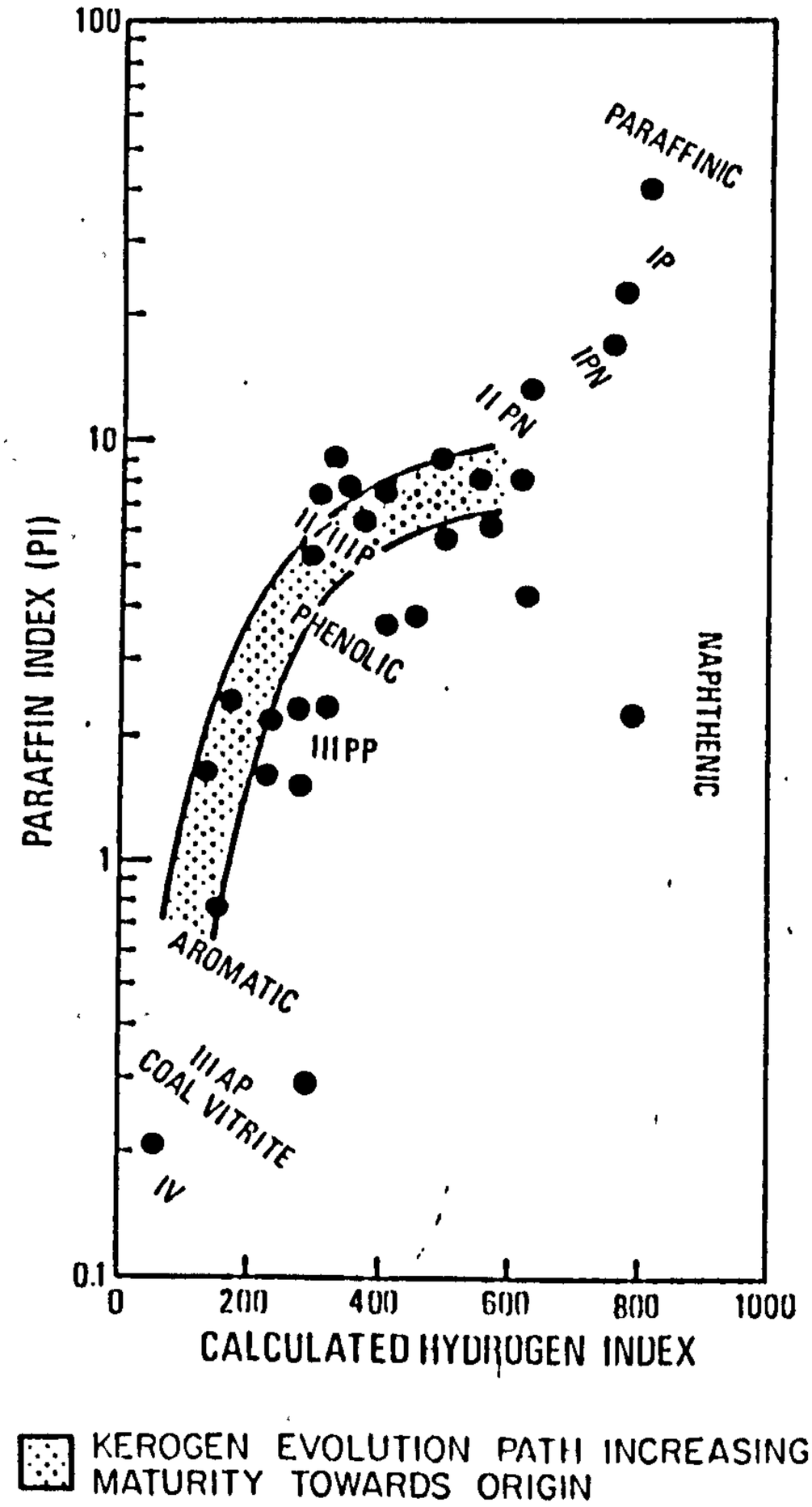

Figure 1.10 Paraffin index as a function of hydrogen index for a number of kerogens. Data from Larter (1985). Paraffin index was calculated from the sum of C_9-C_{30} *n*-alkanes+*n*-alkenes determined from pyrogram peak height data. The three major types are sub-divided into various types depending on their paraffin, naphthenic, phenolic and aromatic contents (after Murchison 1987).

IP paraffinic: kerogens rich in alginite, Torbanite (Botryococcus)

IPN paraffinic-naphthenic: Tasmanite (alginite) rich kerogens .

In naphthenic: Resinite-derived materials

IIPN paraffinic-naphthenic amorphinite-rich kerogens from marine source rocks

II/IIIp exinite rich kerogens

IIIpp paraffinic/phenolic: vitrinite-rich kerogen from marine/ deltaic shales

IIIap aromatic/phenolic: vitrinite-rich kerogens from coal-swamps .

IV aromatic: inertinite-rich kerogens.

He postulated that every kerogen type is characterised by paraffin, naphthene and aromatic yields.

Examination of organic matter using microscopy in reflected and UV fluorescence allows identification of plant debris, algal bodies, spores and amorphous organic matter. This technique was first developed for coal petrography, especially for identification of coal macerals (exinite, vitrinite and inertinite) and has been applied to sedimentary rocks (Hunt, 1979).

1.3.2.1. Palaeoenvironment of deposition

Organic matter composition of source rocks and their related petroleums is a function of a number of factors, which are governed by the palaeoenvironment of deposition (Figure 1.11; Demaison et al., 1983; Powell, 1987). These are (i) biological sources (phytoplankton, zooplankton, bacteria or higher plants), (ii) sedimentation rate, (iii) water column chemistry (oxygen levels, pH (acidic *vs* alkaline), dissolved anions concentrations (CO_3^{2-}, SO_4^{2-} etc), (iv) extent of bacterial reworking during deposition and (v) source rock lithology. The latter is important since it can control the nature of bacterial activity during diagenesis (Powell, 1987). For example, carbonates being characterised by sulphur-rich organic matter, are less sensitive to bacterial degradation than clastic sediments, due to the presence of hydrogen sulphide or elemental sulphur released by sulphate reducing bacteria (Powell, 1987).

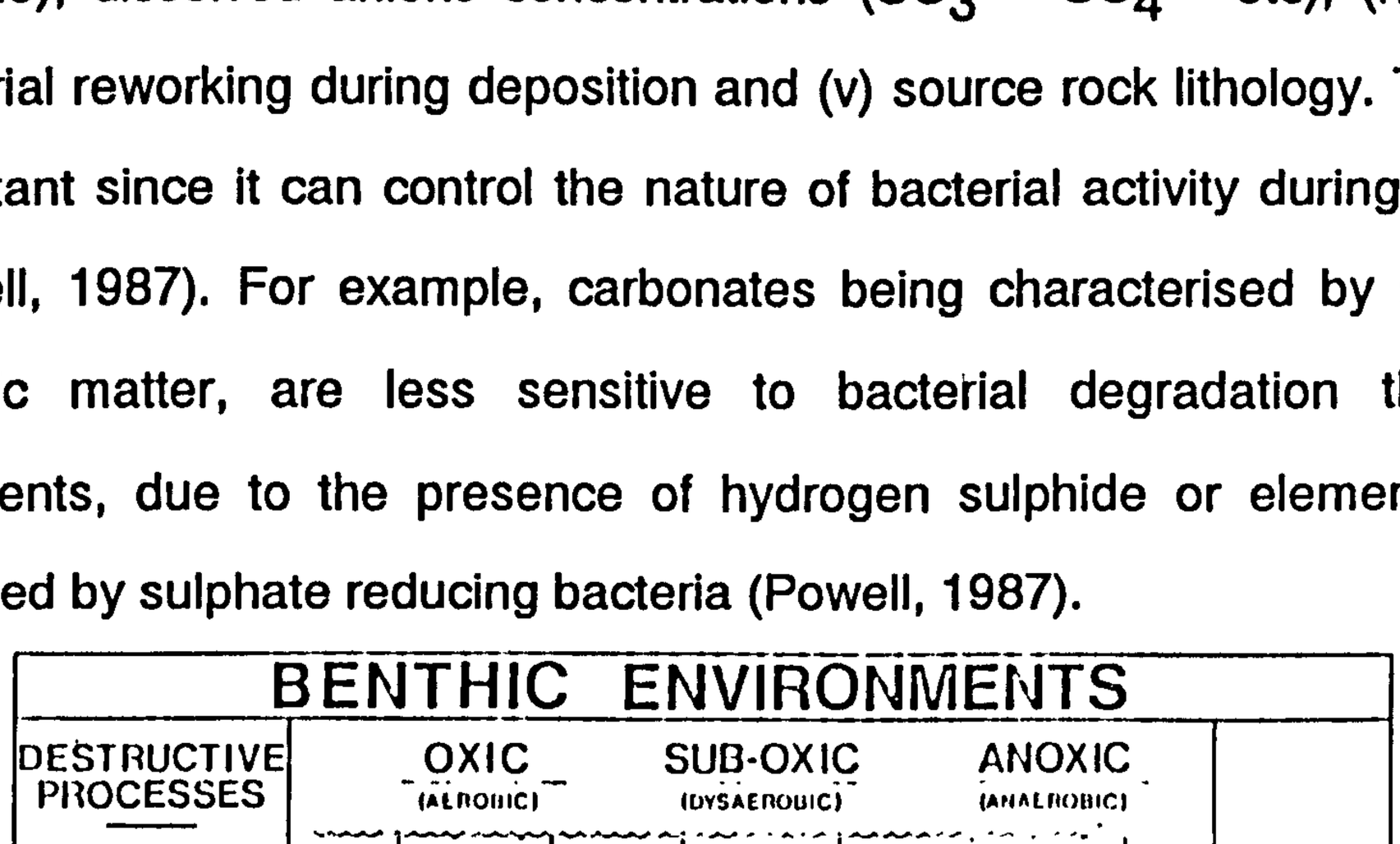

Figure 1.11 Benthic environments and petroleum source bed deposition. Organic facies depends upon the relationship between early depositional factors and kerogen types (after Demaison, 1983).

From the depositional environmental point of view, the Algerian Sahara was a terrain, consisting of detrital rocks of alluvial and fluvial origin. During Palaeozoic times; there was alternating transgression and regression of the sea, leading to marine depositional environments. A high contribution by the fauna, graptolites and brachiopods, is found in Cambrian, Ordovician and Silurian sediments with the predominant lithology ranging from sandy to sandy-argillaceous. The transgression of the sea ended during the Carboniferous, which was marked by continental and lake sediments deposits. The continental facies continued to exist during the Triassic (Aliev et al., 1971).

As already mentioned, organic matter content is controlled by the oxygen level (oxic/anoxic), leading to its preservation or degradation. Therefore, it is worth noting that large numbers of oil accumulations may have been enhanced by minimum oxygen levels during the deposition of the source rocks. Demaison et al. (1983) suggested the presence of four facies in marine and lacustrine environments depending on the oxygen content and the sedimentation rate.

Facies I (producing exclusively oil) arises from highly reducing (anoxic) lacustrine and marine depositional environments, where organic carbon content can reach up to 30%.

Facies II (producing oil) is characterised by anoxic and suboxic conditions of depositional environments, with a high sedimentation rate and organic carbon content varying from 1% to 10%.

Facies III (generating exclusively gas). Conditions of deposition are oxic in marine or lacustrine environments with a lower sedimentation rate than those previously described. Accumulation of organic matter is low with organic carbon content reaching 1% to 5%. The type of organic matter is mainly terrestrial with

some contribution from marine sediments, which have been influenced by bioturbation.

Facies IV (no potential for hydrocarbons) consists of residual organic matter, which remains in areas with high microbial activity (aerobic), low sedimentation rate and high bioturbation. The organic carbon content is low, varying from 0.2% to 0.3%.

Accumulation of organic matter depends on the oxygen level present within a sediment. The lower is the oxygen content, the greater the chances of accumulation of organic matter. It can be favourable in low energy water bodies, corresponding to major transgression periods, which played a major role in the formation of the basin. For instance, these transgressions have played an important role during Silurian and Upper Cretaceous times in the formation of the Saharan Platform (Drid, 1989).

1.3.3.2. Maturation of organic matter

During the three stages of diagenesis, catagenesis and metagenesis (Tissot and Welte, 1984 pp 515), maturation of organic matter can be determined using bulk maturity parameters (e.g vitrinite reflectance, spore colouration, maximum temperature derived from Rock-Eval pyrolysis, (T_{max}). For Rock-Eval derived parameters, see chapter2, Figure 2.1. In addition, hydrogen and oxygen indices (H/C and O/C) decrease with increasing maturity (Tissot and Welte, 1984 pp 524). Using T_{max} as a maturity parameter can, however, be source dependent during diagenesis and early catagenesis (Tissot and Welte, 1984 pp 522). For a good correlation, it is worth using a combination of maturity parameters derived from Rock-Eval as well as reflected and fluorescence microscopy. The production index (S_1/S_1+S_2) is another indicator of maturity. However, this ratio

can be influenced by type and the absorption of organic matter on mineral matrix (e.g Peters, 1986; Langforth and Blanc Valleron, 1990).

Maturity parameters obtained by optical methods such as vitrinite reflectance and spore colouration appear to be more reliable. However, it is rather difficult to evaluate the maturity of cutting samples, consisting of a mixture of fragments with different maturities (Cornford et al., 1979). Examination of block samples using UV fluorescence is very useful particularly for pre-Devonian sediments containing minor amounts or no vitrinite particles, since land plants had not appeared to a significant extent (Traverse, 1988). The UV fluorescence of liptinitic material changes in colour with depth, varying from light orange through middle orange to red and brown at the end of the catagenesis phase (Figure 1.12).

1.3.3. Molecular Organic Geochemistry

This section reviews some biological markers, which can be related to biological source, depositional environment and maturity of source rock extracts and petroleums. A biological marker can be defined as any organic compound, whose structure can be related unequivocally to a known natural product (Mackenzie, 1984). Biological markers (steranes and terpanes) are widespread in sediments and petroleum from the Proterozoic (Aref'ev et al., 1980; Fowler and Douglas, 1984; Fowler et al., 1986; Fowler and Douglas, 1987; Summons et al., 1988) and rocks of younger age. Porphyrins are not reviewed here as they were not used in the present study. Furthermore, development of sophisticated techniques such as combined gas chromatography/mass chromatography using metastable ion monitoring (GC/MS/MS; Gallegos, 1976; Warburton and Zumberge, 1983; Meyers et al., 1984a; Moldowan et al., 1985) have contributed to detection and identification of minor concentrations of biological markers in source rock extracts, oils and from the chemical degradation of kerogens (Michaelis and Albrecht, 1979; Chappe et al., 1980;

Figure 1.12 General scheme of evolution of sedimentary organic matter with burial. Relationship between the palaeo-temperature and optical maturity parameters (modified after Murchison, 1987).

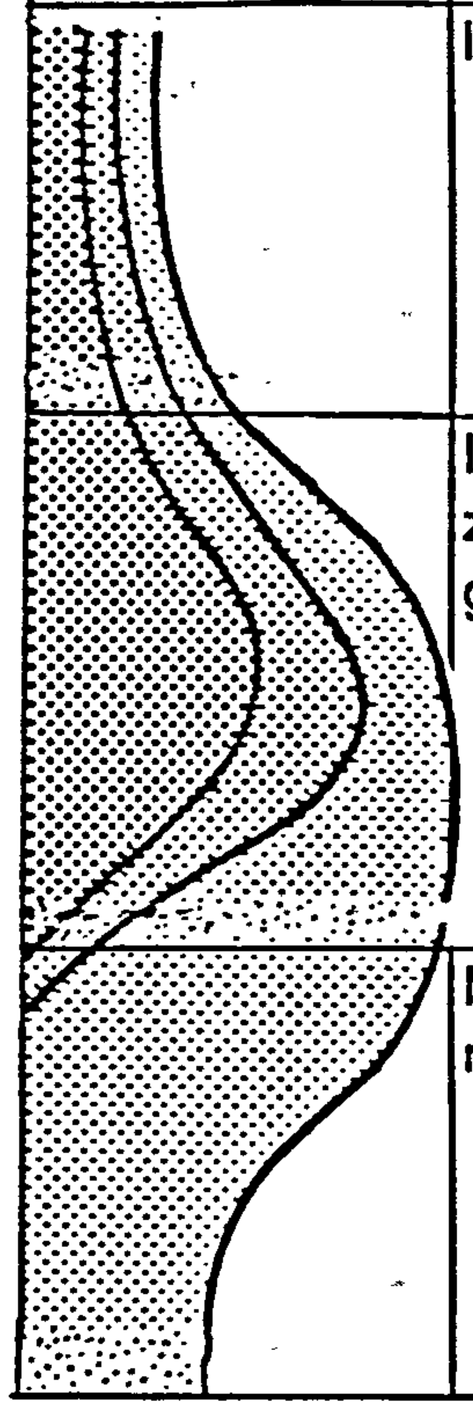

Hydrocarbon maturity	Maximum Palaeo-temperature °C	Vitrinite reflectance (%Ro)	Spore colour index	Spore fluorescence	Hydrocarbon product
Immature	<80	0.3-0.6	2.0-3.0	green-yellow/yelow-orange	Early methane-peak oil
Initial maturity zone of oil generation	80-130	0.6-1.35	3.0-8.0	light orange/deep red	Oil
Mature to post-mature	>130	2.0-3.0	>8.0	Brown	Condensate to dry gas

HEAVY HYDROCARBONS

LIGHT HYDROCARBONS

METHANE

Mycke and Michaelis, 1986; Mycke et al., 1987). During diagenesis, biological marker composition is controlled by chemical reactions, which involve microbial activity eventually, leading to a loss of functional groups, hydrogenation of double bonds and aromatization (Mackenzie, 1984). With increasing maturation, alteration of biological markers continues with generation of new biological markers albeit in low concentrations, which are, therefore, useful for oil-oil and oil-source rock correlations (e.g Seifert and Moldowan, 1978; Mackenzie, 1984). Hence, the following section reviews the major groups of biological markers, which are indicative of source, depositional environment and maturity. These are: *n*-alkanes, branched alkanes including isoprenoid hydrocarbons, tricyclic and tetracyclic terpanes, pentacyclic triterpanes, steranes and aromatic steroidal hydrocarbons (monoaromatic and triararomatic steroidal hydrocarbons). For convenience, the applications of molecular parameters can be divided into three categories: assessments of source input, depostional environment and maturity. The gasoline range hydrocarbons cannot be defined as biological markers and however, these are included in the maturity section, which is their major application.

1.3.3.1.Source indicators

n-alkanes

Individual *n*-alkanes are not biological markers, however, carbon number distributions can be related to biological sources. *N*-alkanes (1) are commonly used for oil-oil and oil-source rock correlations due to their abundance and simple structure (e.g Eglinton et al., 1962; Han and Calvin, 1969; Gelpi et al., 1970). They are derived from algal, bacterial or land plant fatty acids, esters or alcohols, which are defunctionalised during diagenesis of sedimentary organic matter (Martin et al., 1963; Tissot and Welte, 1984 pp 102). *N*-alkanes with an odd carbon numbered predominance in the range of C_{25}-C_{35} were reported in leaf waxes (Eglinton et al., 1962), which are dominated by C_{27}, C_{29} and C_{31} *n*-

Numbers (1) to (41) inclusive refer to molecular structures given at the end of the thesis just after the references section.

alkanes (Eglinton et al., 1962; Caldicott and Eglinton, 1973), although a predominance of C_{23}-C_{32} *n*-alkenes has been observed in oils derived from non-marine sediments, rich in *Botryococcus braunii* (McKirdy et al., 1986). On the contrary, phytoplankton and other algae are characterised by *n*-C_{15}, *n*-C_{17} and *n*-C_{19} predominance (Gelpi et al., 1970). Samples with bacterial contribution are usually dominated by even *n*-alkanes in the range of C_{16}-C_{24} (Han and Calvin, 1969). In addition, hypersaline environments are characterised by even *n*-alkane predominance (Grimalt and Albaiges, 1985; ten Haven et al., 1985; Connan et al., 1986).

Branched alkanes

Acyclic isoprenoid hydrocarbons have been reviewed recently by Volkman and Maxwell, (1986). Short-chain acyclic isoprenoid hydrocarbons (C_n<C_{20}) occur in sediments and oils (e.g pristane 2; 2,6,10,14 pentamethylpentadecane) and phytane 3; 2,6,10,14 pentamethylhexadecane). Pristane and phytane are thought to derive from the phytol side-chain of chlorophyll from photosynthetic organisms (Johns et al., 1966; Brooks et al., 1969; Powell and McKirdy., 1973). Other biological sources for pristane, include zooplankton (Blumer et al., 1963) and archaebacteria (Torbanene et al., 1979; Risatti et al., 1984; Volkman and Maxwell, 1986), whereas phytane has been cited as being sourced from methanogenic bacteria (Risatti et al., 1984; Volkman and Maxwell, 1986). Goossens et al. (1984) have suggested that tocopherols (4) can be a natural precursor for pristane. It is interesting to note that recent isotopic composition analysis reveal that pristane may be derived from algae and phytane from methanogenic bacteria (Freeman et al., 1990) in studies on the Messel shale. Additionally to low molecular weight isoprenoid hydrocarbons (C_{14}-C_{16} and C_{18}-C_{20}), long-chain isoprenoid compounds up to C_{45} have been recorded in sediments and oils, having high archaebacterial contribution from methanogenic bacteria and thermoacidophilic (Han et al., 1982; Torbanene et al., 1979; Risatti

et al., 1984). Acyclic isoprenoids having head-to-tail linkage (e.g. pristane and phytane) are called regular, while those with head-to-head (Moldowan and Seifert, 1979) and tail-to-tail linkages (Brassell et al., 1981) are characteristic of irregular acyclic isoprenoids. Examples of irregular isoprenoid hydrocarbons having tail-to-tail linkages are 2,6,10,15,19-pentamethyleicosane (5), squalane (6) and lycopane are thought to be derived from methanogenic bacteria (Brassell et al., 1981). Occurrence of C_{25} isoprenoid compound has been related to saline environments (Waples et al., 1974; Ten Haven et al., 1985), while the C_{20} acyclic isoprenoid hydrocarbons having 2,6,10-trimethyl-7-(3-methylbutyl)-dodecane (e.g. 7; Yon et al., 1982), has been reported to occur in fresh water and marine sediments derived from Green algae (Rowland et al., 1985). Another irregular isoprenoid C_{34} Botryoccocane has been observed in crude oils derived from non-marine sediments rich in *Botryococcus braunii* algae (McKirdy et al., 1986). However, low concentrations of acyclic isoprenoids ($C_n<C_{20}$) relative to *n*-alkanes, particularly in Ordovician sediments rich in *Gloecapsomorpha prisca* (*G-prisca*), was attributed either to this organism, being a non-photosynthetic lacking the phytyl side-chain (Reed et al., 1986) or to an overwhelming abundance of *n*-alkanes, which could dilute alkylcyclohexanes and isoprenoid hydrocarbons (Hoffmann et al., 1987).

Additional to acyclic isoprenoid hydrocarbons, an homologous series of branched alkanes with one or two methyl groups have been associated with prokaryotic origin (Aref'ev et al., 1979; Klomp, 1986; Fowler and Douglas, 1987; Summons et al., 1988), being prominent contributors to oils and sediments from Precambrian and Palaeozoic age. This series of monomethylalkanes occur as 2-methyl (iso; 8), 3-methyl (anteiso; 9), 4-, 5-, 6-, 7- and 8-methylalkanes and are thought to be indicative of cyanobacterial, bacterial fatty acids contribution (Klomp, 1986; Fowler and Douglas, 1987; Summons et al., 1988), (Johns et al., 1966; Gelpi et al., 1970) and algal mats (Cardoso et al., 1978). The presence of a certain regularity of 2-methyl and 3-methylalkanes may suggest a relationship

between these alkanes and their corresponding iso and anteiso carboxylic acids (Johns et al., 1966; Heoring, 1981; Fowler and Douglas, 1987; Summons, 1987). Recent reports have suggested a series of monomethylalkanes with 2-methyloctadecane, 9-, 8-, 7-methyldecane and a mixture of 9-, 8-, 7- and 6-methyloctadecane in cyanobacterial mats (Robinson and Eglinton, 1990; Shiea et al., 1990), in which dimethylalkanes have been detected and identified as 5,15-dimethylheptadecane (Robinson and Eglinton, 1990).

Monocyclic alkanes

High concentrations of monocyclic alkanes have been reported to occur particularly in Ordovician sediments and oils rich in *Gloecapsomorpha prisca* (Fowler and Douglas, 1984; Reed et al., 1986; Hoffmann et al., 1987; Fowler, 1991). These are assigned as *n*-alkyl (10) and methyl-*n*-alkylcyclohexanes (11) in the range of C_{15}-C_{20} and C_{15}-C_{19} respectively. However, these compounds have been recorded in oils and sediments, irrespective of their age. Similar distributions to the *n*-alkanes may have common input from algal or bacterial fatty acids (e.g Johns et al., 1966; de Rosa et al., 1972); Rubinstein and Strausz, 1979; Hoffmann et al., 1987), although laboratory experiments (Rubinstein and Strausz, 1979; Hoffmann et al., 1987) showed that a combination of decarboxylation during diagenesis, cyclisation, cracking and rearrangment processes could be essential for generation of monocyclic alkanes (Summons et al., 1988). The cis-3-methyl- and trans-4-methyl-1-*n*-alkylcyclohexanes predominate over trans-2- and cis-2-methyl-1-*n*-alkyl isomers in mature samples due to their high stability (Hoffmann et al., 1987). Additional to monocyclic alkanes with normal alkyl side-chain, there have been reports of monocylic alkanes with isoprenoid side-chain c particularly in carbonate-evaporite source rocks (Barbe et al., 1988). These are namely 1-cyclohexyl-3,7,11,15-tetramethyl-hexadecane (e.g 12) and 1-methylcyclohexyl-3,7,11,15-

tetramethyl-hexadecane, indicating sulphur bacteria and/or archaebacteria input although long-chain isoprenoid alkanes were not observed (Barbe et al., 1988).

Tricyclic and tetracyclic terpanes

Tricyclic terpane distributions have been extensively used in oil-oil and oil-source rock correlations (Zumberge, 1983; Curiale, 1985; Palacas et al., 1986). Tricyclic terpanes (13) occur in oils and sediments (Aquino Neto et al., 1982, 1983; Ekweozor and Strausz, 1983; Zumberge, 1983; Chicarelli et al., 1988) in the range of C_{19}-C_{30} and up to C_{45} carbon atom (Moldowan et al., 1983). Extended tricyclic terpanes (C_n>C_{25}) are present in peak doublets, having a chiral centre at C-22. The tricyclohexaprenol has been the only suggested precursor for tricyclic terpanes, being predicted to be a membrane constituent of some prokaryotes (Ourisson et al., 1982). Due to a lack of information on their precursors, tricyclic terpanes have been described as orphan compounds (Summons and Walter, 1990).

Tetracyclic series (14) in the range of C_{24} to C_{27} members occur in sediments and oils derived from source rocks with high terrestrial input. Tetracyclic terpanes including 17,21 secohopanes have been suggested to be the products of thermal maturation or microbial degradation of pentacyclic terpanes (Trendel et al., 1982).

Pentacyclic terpanes

Pentacyclic terpanes (15) are ubiquitous compounds occurring in oils and sediments (Esminger et al., 1974; Van Dorsselaer et al., 1974) in the range of C_{27}-C_{35} carbon number. These are commonly known as degraded hopanes (C_{27}-C_{29}) and extended hopanes (C_{31}-C_{35}) up to C_{40} (Rullkötter and Philp, 1981). Degraded hopanes have been suggested to be the product of degradation of C_{30} hopanoids, probably from Diplopterol or diploptene (16; Ourisson et al., 1982), being constituents of bacterial lipids (Ourisson et al.,

1982; 1987). On the other hand, extended hopanes have been related to C_{35}-bacteriohopanetetrol (17) found in bacteria and cyanobacteria (Ourisson et al., 1979). Further evidence of bacterial origin for hopanoids is consistent with their occurrence in pre-Devonian sediments, since the first megaspores evolved in late lower Devonian (Traverse, 1988).

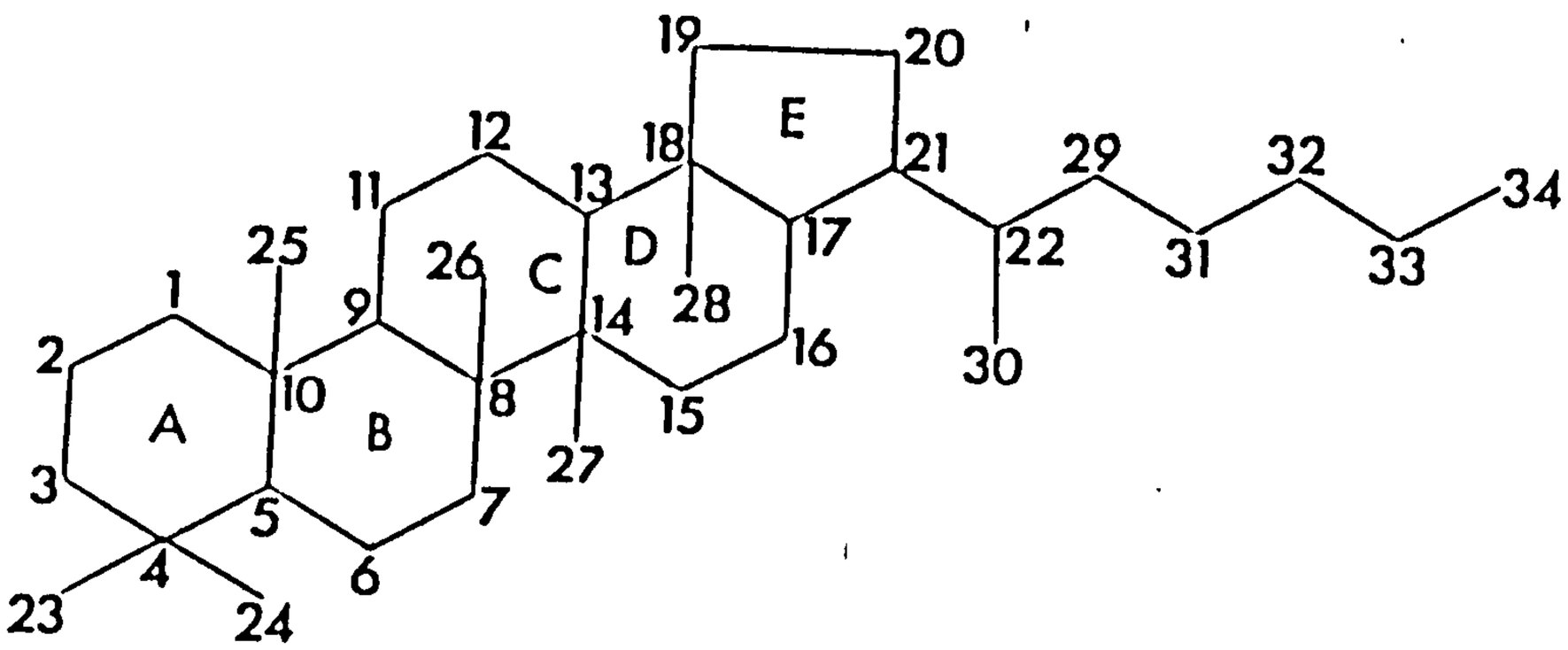

Figure 1.13 Carbon skeleton and numbering system of hopanes

Although, methylhopanes have not been studied during the present work, it is worth noting their occurrences in ancient sediments and oils in the range of C_{28} and C_{30}-C_{36} carbon numbers. Methylhopane isomers have the methyl group at C-2 and C-3 positions of ring A (Seifert and Moldowan, 1978; McEvoy and Giger, 1986; Hoffmann et al., 1987; Summons and Powell, 1987; Summons et al., 1988; Summons and Jahnke, 1990). Their stereochemical structures have been recently elucidated as 2-β-methyl-, 2α-methyl- (18) and 3β-methyl-17α(H),21β(H)-hopanes (19; Summons and Jahnke, 1990). The methylhopane series having 3β-methyl isomers and 2α-methylhopanes appear to occur in mature sediments, while 2β-methyl substituents predominate in immature samples (Summons and Jahnke, 1990). Furthermore, the 2β-methyl hopanoids have been detected in bacteria (Summons and Jahnke, 1990). Additionally to the hopane series, other hopanes with slightly modified hopane structure have been recorded in oils and sediments. The C_{27} 18α(H),17α(H),21β(H)-

trisnorneohopane (20; "T_s", Whitehead, 1973), being termed "terpane stable" (Seifert and Moldowan, 1978), has the methyl group attached to the C-17 instead to the C-18 position (Pym et al., 1975). The C_{28} bisnorhopane has been observed albeit in a limited number of sediments and oils from specific environments, (Seifert and Moldowan, 1978; Cornford et al., 1979; Grantham et al., 1980; Fowler and Douglas, 1984; Curiale et al., 1985; Mello et al., 1989), particularly in highly reducing depositional environments. The possibility of obtaining the C_{28} bisnorhopane from higher homologues is unlikely due to the amount of energy necessary to break the C-C bond at the same carbon atom (Kimble et al., 1974). This compound has been first characterised by Seifert et al. (1978) as 18α(H),17α(H),21β(H)-28,30-bisnorhopane (21). The C_{29} and C_{30} pentacyclic terpanes have been detected in oils and sediments from Proterozoic (e.g. Summons et al., 1988) and younger age (Philp and Gilbert, 1986; Cornford et al., 1988; Philp et al., 1989; Fowler and Brooks, 1990; Riediger et al., 1990); Killops and Howell, 1991; Moldowan et al., 1991). These compounds have been used as source indicators (Philp and Gilbert, 1986) as well as maturity parameters (Cornford et al., 1988; Fowler and Brooks, 1990). Recent work by Moldowan et al (1991) have reported these compounds as "rearranged hopanes" with stereochemical structures as follows:

17α(H)-15α-methyl-27-norhopane (e.g. 17α(H)-diahopane or B_3; 22),

the C_{29} peak is split into 2 compounds being identified as 18α(H)-17α-methyl-28,30-dinorhopane (e.g. 18α(H)-30-norneohoapne or $C_{29}T_s$, 23).

An extended homologous series ranging from C_{29} up to C_{34} diahopanes has also been detected. The 18α(H)-30-norneohopane has been related to the C_{27} trisnorneohopane (T_s). Higher molecular weight nornehopanes have not been reported (Moldowan et al., 1991). Isotopic data for both rearranged and non-rearranged hopanes suggested a common bacterial origin (Moldowan et al., 1991). They have been postulated to be formed as a result of rearrangment of

non-rearranged hopanes by acid clay catalysts in a similar way to rearranged steranes (Rubinstein et al., 1975; Sieskind et al., 1979).

Other pentacyclic triterpanes, that are not based on the hopane skeleton (non-hopanoids) such as the 18α(H)-oleanane (24; Ekweozor et al., 1979) and related compounds, occur in sediments with high terrestrial input (Hoffmann et al., 1984; Mello et al., 1988). Other non-hopanoids such as gammacerane (25) have been recorded in sediments and oils (Schi Ji-Yan et al., 1982; Moldowan et al., 1985) and is thought to be indicative of hypersaline environments (ten Haven et al., 1985; 1988). Gammacerane is believed to be derived from tetrahymanol, a constituent of protozan *Tetrahymena* (Henderson et al., 1969; ten Haven et al., 1989; Venkatasan, 1989).

Steranes

Steranes (26) and other steroidal hydrocarbons (e.g. sterenes, diasterenes and diasteranes; 27) are derived from sterols (28) or steroidal ketones (Mackenzie et al., 1982a; Brassell and Eglinton, 1983; Mackenzie, 1984; McEvoy and Maxwell, 1983), which are ubiquitous in plants and algae (e.g. green algae). A predominance of C_{29} over C_{27} steranes has been mentioned by several workers (e.g. Fowler and Douglas, 1984; Grantham, 1986; Rullkötter et al., 1986; Longman and Palmer, 1987; Grantham and Wakefield, 1988) and has been related to cyanobacteria (e.g. De Sousa and Nes, 1968; Volkman, 1986) but not automatically to higher plants as suggested by Huang and Meinschein, (1979). However, the presence of sterols appear to be minor in bacteria and cyanobacteria and restricted to eukaryotes (Ourisson et al., 1987); C_{27} steranes appears to dominate in marine environments (Brassell and Eglinton, 1983). Furthermore, Grantham and Wakefield (1988) reported that the variation of sterane carbon numbers is a function of diversity of species throughout geological time. The C_{30} desmethylsteranes have been suggested to reflect marine environments (Moldowan, 1984; Moldowan et al., 1985). They are

thought to be derived from C_{30} sterols, which occur in some phytoplankton from *Crytophyacea* and *Chrysophyacea* (Volkman, 1986). The stereochemical structure of C_{30} desmethylsteranes has been recently elucidated as 24-*n*-propylcholestane (Moldowan et al.,1990), being derived from 24-propylencholesterol, detected in marine algae. This type of algae existed during early Ordovician up to Devonian (Moldowan et al., 1990). Rearranged C_{30} steranes have been postulated as 24-*n*-propyl-13β(H),17α(H) (27; 20R and 20S; Moldowan et al., 1990). Steranes with C_{21} and C_{22} carbon number, namely pregnane and homopregnane, have been detected in oils and sediments (Gallegos, 1971; Connan et al., 1980; Wingert and Pomezantz, 1986), but they were only abundant in sediments derived from hypersaline environments (Ten haven et al., 1985).

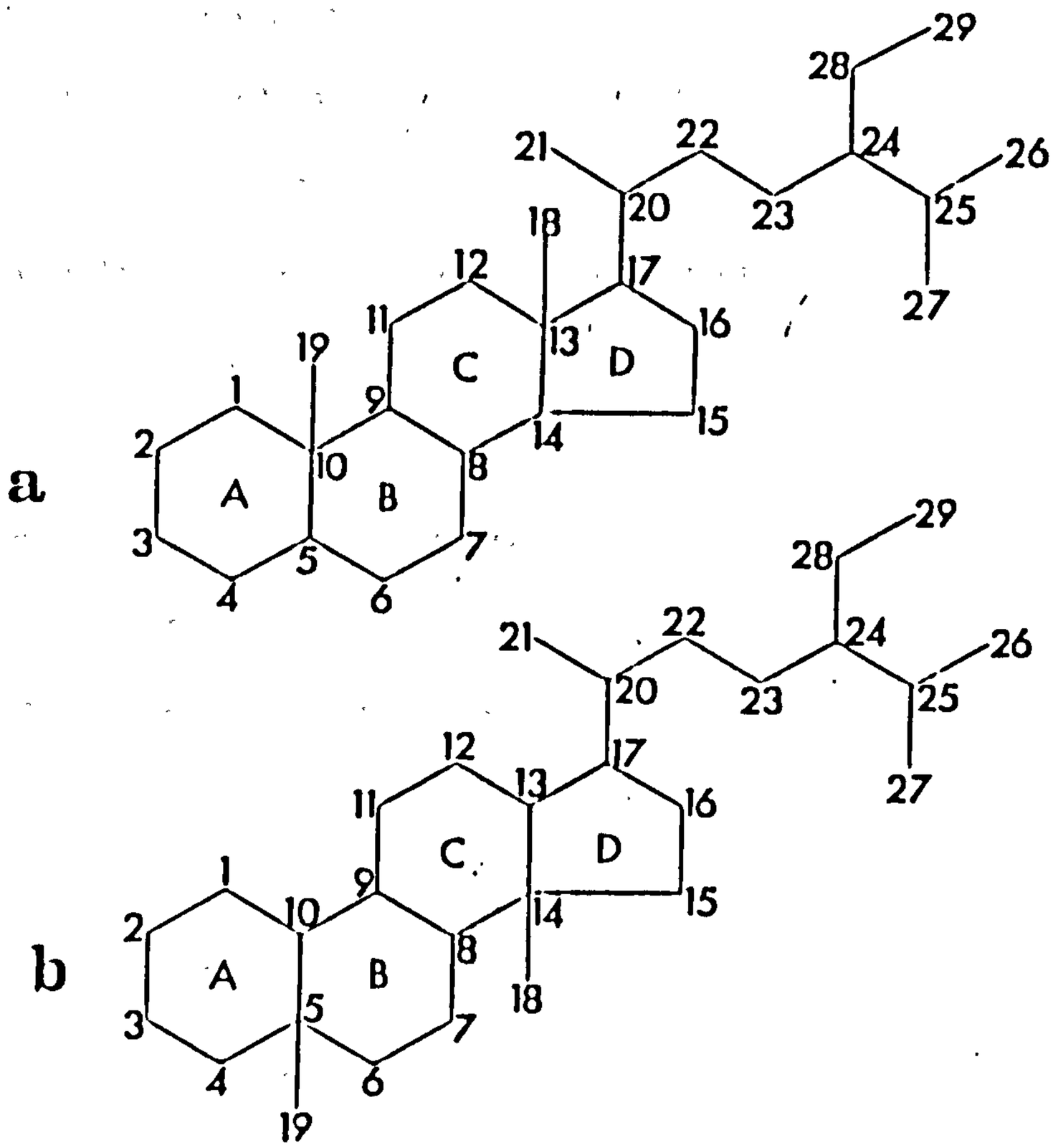

Figure 1.14 Carbon skeleton and numbering system of (a) non-rearranged and (b) rearranged steranes.

Methylsteranes with methyl group at C-4 position have been only observed in sediments with high dinoflagellate contribution (Robinson et al., 1984; Summons et al., 1987; Goodwin et al., 1988). Two types of structures for the C_{30} 4-methylsteranes have been been recognised in marine and non-marine environments. The Dinosterane 4,23,24-trimethylcholestane (29) and the 24-ethyl-4-methylcholestane (30). The former is abundant in marine environments, while the latter compound dominates in non-marine environments (Summons et al., 1987; Goodwin et al., 1988). The 4,23,24-trimethylcholestane is more abundant in marine sediments younger than the Triassic. An additional source for 4-methylsteranes from algae (*Prymnesiophyte*) has been suggested by Volkman et al. (1990a). The second series of methylsteranes occuring with 3β-methyl isomers (31) and 2α-methyl and (32), have been found in sediments from Precambrian and Palaeozoic age (Summons et al., 1987; Summons and Capon, 1988; Summons et al., 1988). In addition, a new series of 3β-alkylsteranes with ethyl and pentyl steranes have been detected in ancient sediments and petroleum (Summons and Capon, 1991; Dahl et al., 1992). The 3β-pentylsteranes may derive from bacteria (Dahl et al., 1992).

1.3.3.2. Palaeoenvironment of deposition

Many geochemical indicators of depositional environments have been suggested. However, they could be affected by source and/or maturity. During diagenesis sterols, rearranged steranes may be formed by catalytic rearrangement of sterenes, which have been first defunctionalised (Rubinstein et al., 1975; Sieskind et al., 1979). Thus, rearrangment seems to occur exclusively in sediments containing aluminosilicates than in carbonates (Rubinstein et al., 1975). Therefore, low proportions of rearranged relative to non-rearranged steranes, pristane to phytane, high abundances of 17α(H)-30-norhopane relative to 17α(H)-hopane as well as short-chain to long-chain steranes have been regarded as characteristic for non-clastic source rocks (e.g.

Rullkötter et al., 1985; Mello et al., 1988; Riediger et al., 1990). High gammacerane and low Pr/Ph ratio may indicate reducing but not necessary hypersaline environments (Peters and Moldowan, 1990). High C_{35} extended hopane with C_{35}/C_{34} greater than one has been observed in carbonate sediments (McKirdy et al., 1983; Zumberge, 1984) and hypersaline environments (ten Haven et al., 1988). However, the homohopane index may be influenced by maturity and lithology (Peters and Moldowan, 1990). High concentrations of 17α(H)-30-norhopane relative to 17α(H)-hopane have been associated with carbonate source rocks (Rullkötter et al., 1985; Zumberge, 1987; Mello et al., 1988) or could result from fractionation and/or biodegradation of oils (Curiale, 1985). The use of Pr/Ph ratio has been suggested as an indicator of conditions of depositional environment. Values<1 indicate reducing environment, while values>1 reflect oxidizing conditions of depositional environment (Didyk et al., 1978). However, the Pr/Ph ratio could be due to hypersaline deposition and to a contribution to the phytane from lipids from the halophilic bacteria (ten Haven et al., 1985; 1987).

1.3.3.3. Maturity

Maturity assessment is essential for reducing risk in the detection and prediction of oil accumulations in the oil industry. Kerogen undergoes maturation during burial as a result of temperature increase (Curiale et al., 1988). Hence, the most commonly used molecular parameters are CPI, Pr/Ph, Pr/*n*-C_{17}, Ph/*n*-C_{18}, sterane, hopane isomerization, steroid aromatization, cracking ratios and methylated triaromatic steroid indices. These parameters will be considered in the following section.

N-alkanes

A predominance of odd to even *n*-alkanes may reflect the maturity level of organic matter. Bray and Evans (1961) suggested a parameter called the

Carbon Preference Index (CPI), which decreases with increasing maturity. However, this parameter may be influenced by source, as indicated by *n*-alkanes inherited from leaf waxes. In addition, there is a tendency towards a dilution of *n*-alkanes by others newly formed by thermal degradation of kerogen (Allan and Douglas, 1977; Curiale et al., 1988).

Acyclic isoprenoids

The Pr/Ph ratio varies with maturity (Tissot et al., 1971). The relatively low abundance of acyclic isoprenoids (C_n<C_{20}) may occur as a result of dilution by *n*-alkane released with increasing maturity (Hoffmann et al., 1987). Alternatively to Pr/Ph ratio, Pr/*n*-C_{17} and Ph/*n*-C_{18} have been used extensively as maturity parameters, which tend to decrease with maturity. *N*-alkanes abundances increase relative to that of isoprenoids, being diluted by *n*-alkanes newly formed as a result of thermal degradation of kerogen. This could be observed at the peak of oil generation and higher maturity (Tissot and Welte, 1984, pp 395).

The Pr/*n*-C_{17} has been found to be affected by the degree of expulsion (Leythaeuser et al., 1984; Leythaeuser and Schwarzkopf, 1986) and dramatically by biodegradation. Thus, these parameters should be used with caution due to effects mentioned above.

Tricyclic terpanes

These occur as a mixture of 13β(H),14α(H) and 13α(H),14β(H) stereoisomers in immature sediments (Aquino Neto et al., 1986). Mature sediments contain relatively high proportions of 13β(H),14α(H), being more stable than 13α(H),14β(H). High molecular weight molecules (C_n>C_{24}) are present as peak doublets, which may have one or more chiral centres. Their relative abundance has been suggested as increasing with increasing maturity (Aquino Neto et al., 1983; Ekweozor and Strausz, 1983; van Graas, 1990; Kruge et al., 1990), although source (Volkman et al., 1990b) and/or fractionation due to migration

(Philp and Engel, 1987; Zhao-An and Philp, 1987; Kruge et al., 1990) cannot be ruled out.

Extended hopanes

The hopane series 17β(H),21β(H) with the biological R configuration at C-22 occurs in immature sediments. With increasing maturity, this compound is converted to the more thermally stable 17α(H),21β(H) (e.g. αβ) and 17β(H),21α(H) (e.g. βα) isomers. αβ and βα isomers have been observed in relative high abundance in mature samples (e.g Meyers et al., 1984b; Raymond and Murchison, 1991), although conversion of βα to αβ has been related to maturity (Seifert and Moldowan, 1980). Peak doublets of extended hopanes series with a chiral centre at C-22 was first reported in oils and sediments by Esminger et al.(1974), where the 22R is the biological synthesised stereoisomer predominating in immature samples. With increasing maturity, extended hopanes (C_n>C_{31}) with a chiral centre at C-22 may show a relative increase of the (22S) stereoisomer to its (22R) counterpart with an end-point ratio of 60:40 (Figure 1.18).

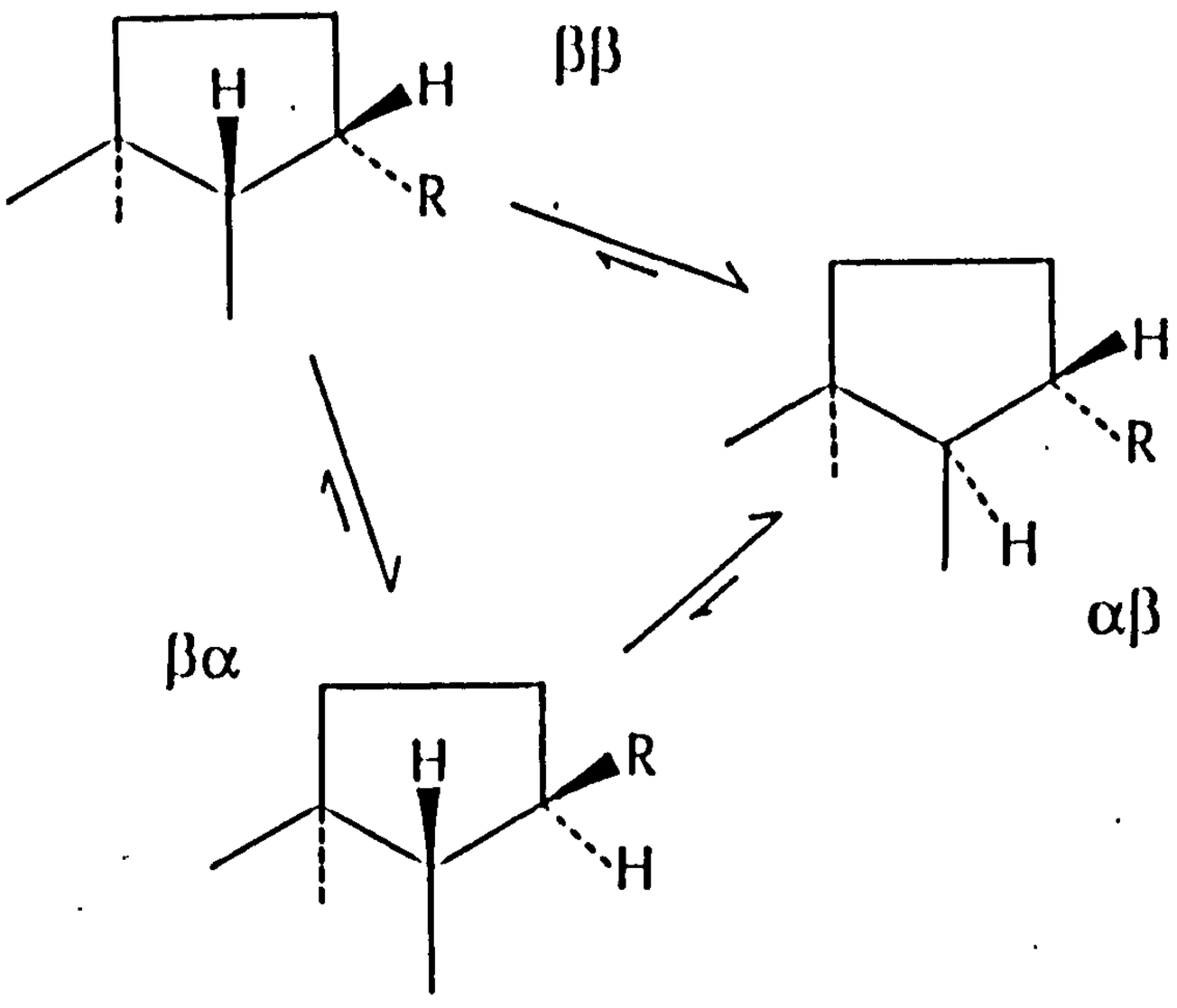

Figure 1.15 The principal isomerisation at C-17 and C-21 positions of hopanes. ββ refers to 17β(H),21β(H) biological configuration. With increasing maturity, stability of hopanes increase in the order ββ<βα<αβ. Therefore, hopanes of αβ-type are abundant in petroleum (Seifert and Moldowan, 1980).

However, a reversal in hopane isomerization has been noted at high temperature during hydrous pyrolysis experiments (Peters et al., 1989; Abbott et al., 1990). Peters et al. (1989) noted that the reversal was especially significant for phosphatic core samples and not for siliceous samples taken from the Monterey source rock section, suggesting a specific mineralogical effect on the hopane isomerization ratio.

The C_{27} T_s ("terpane stable") is more stable than C_{27} T_m ("terpane maturable"). Hence, T_s/T_m ratio tends to increase with maturity. However, this parameter may be affected by source and depositional environment (Seifert and Moldowan, 1978; McKirdy et al., 1983; ten Haven et al., 1985; Moldowan et al., 1986).

Steranes

Steranes occurring with 5α(H),14α(H),17α(H) (20R) configuration are abundant in immature samples. With increasing maturity, isomerization occurs at C-14, C-17 and C-20 chiral centres, giving rise to a mixture of 5α(H),14α(H),17α(H) (20R) and (20S) isomers (ca 50:50) and 5α(H),14β(H),17β(H) (35:75) respectively (Figure 1.16 and 1.18; Mackenzie et al., 1982a).

However, low sterane isomerization ratios (20S/20S+20R) have been observed in oils from the Monterey formation (Curiale et al., 1985) as well as during hydrous pyrolysis experiments (Peters et al., 1989; Strachan, 1989; Peters et al., 1990), suggesting temperature and lithological effects. Abbott et al. (1990) carried out hydrous pyrolysis experiments on kerogen spiked with a deuterated sterane standard with the 5α(H),14α(H),17α(H) (20R) configuration. There was no significant isomerization of this standard at elevated temperatures. On the other hand, there was an increase of the (20S) isomer relative to its (20R) counterpart with increasing temperature and time of the non-deuterated steranes released by the kerogens during hydrous pyrolysis. This apparent isomerization is unlikely to be the result, therefore, of a direct configurational

isomerization in the saturated hydrocarbon fraction at least under the conditions of this particular study.

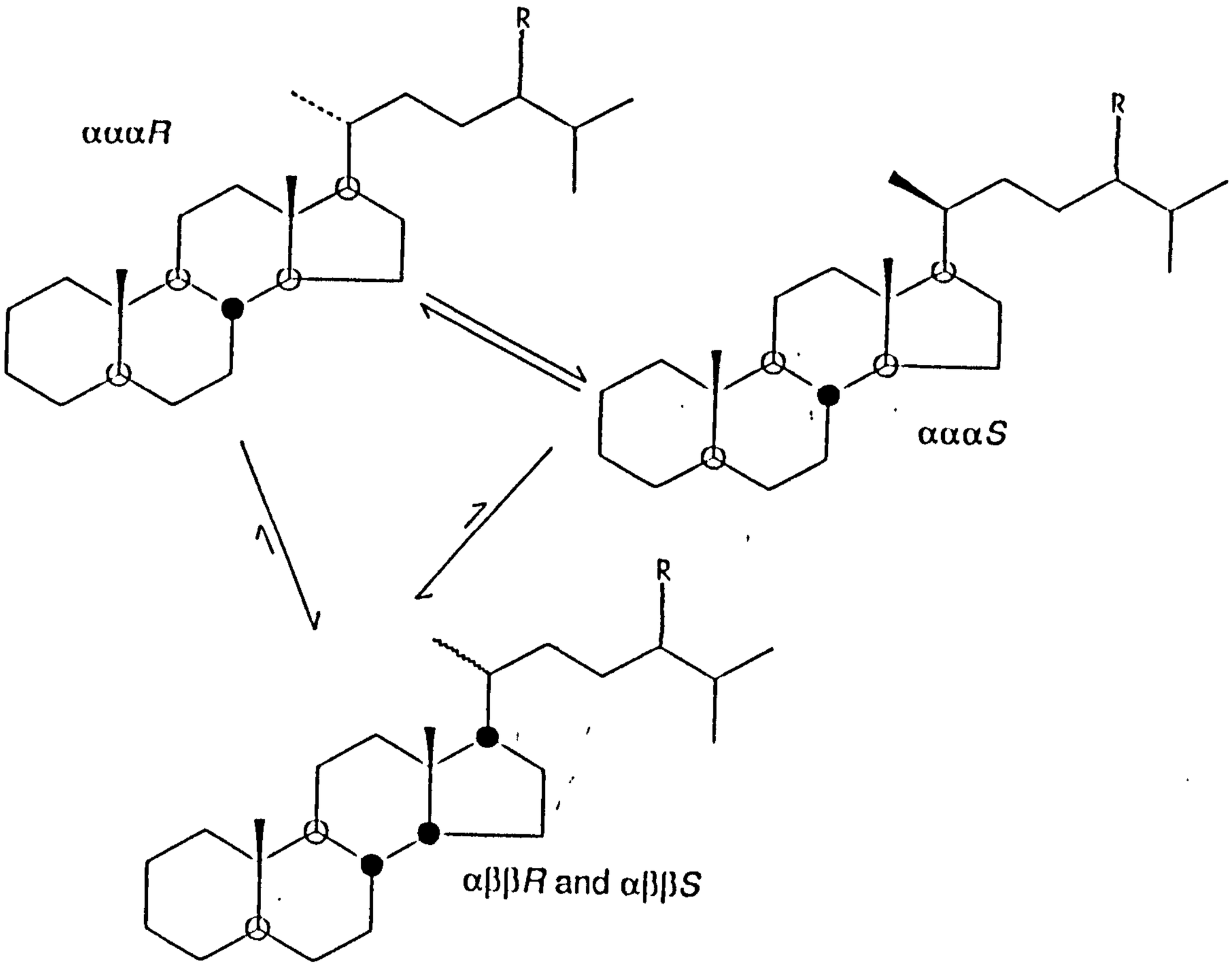

Figure 1.16 The principal isomerisation at C-17 and C-21 positions of hopanes. αααR refers to 5α(H),14α(H),17α(H), (20R). The αααR is inherited from the natural steroid precursors , and consequently dominates the sterane distribution in immature sediments. with increasing maturity, isomerisation of steranes tends towards the end-point values of aaa 20S/20S+20R (50%) and αββ/αββ+ααα (75%), see Figure 1.18, Mackenzie et al., 1982a)

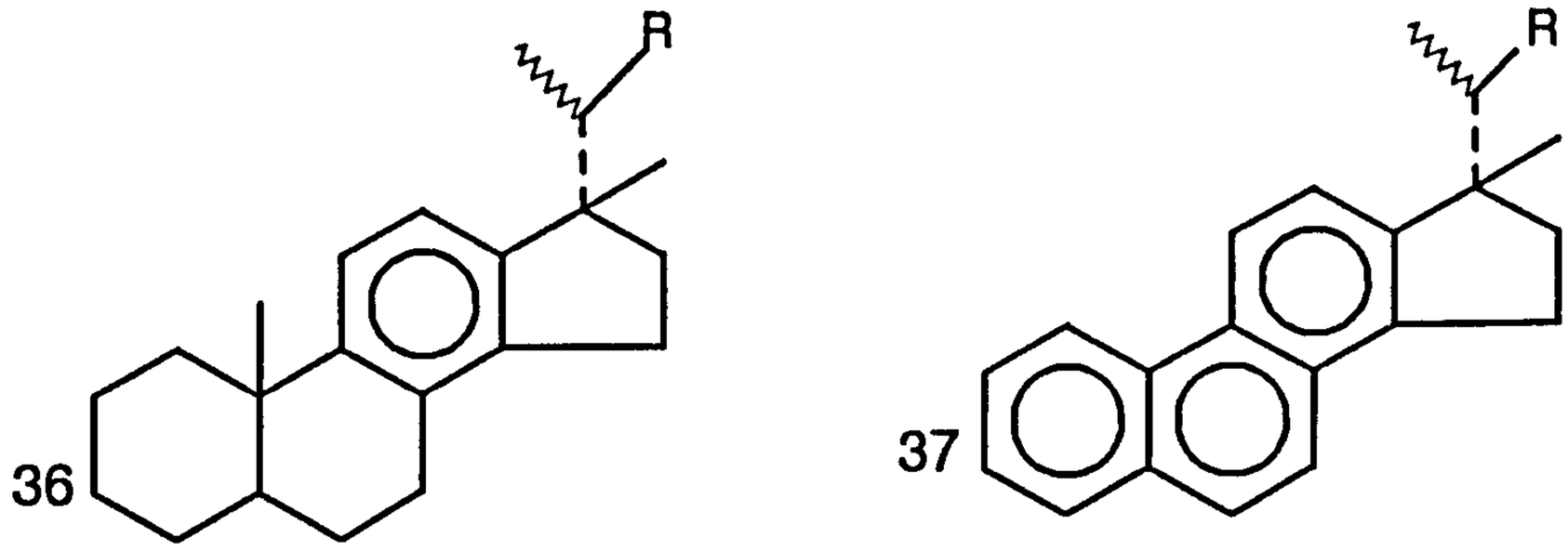

Figure 1.17 Steroid aromatisation of monoaromatic to triaromatic steroidal hydrocarbons (triaromatic steroids/triaromatic +monoaromatic steroids).

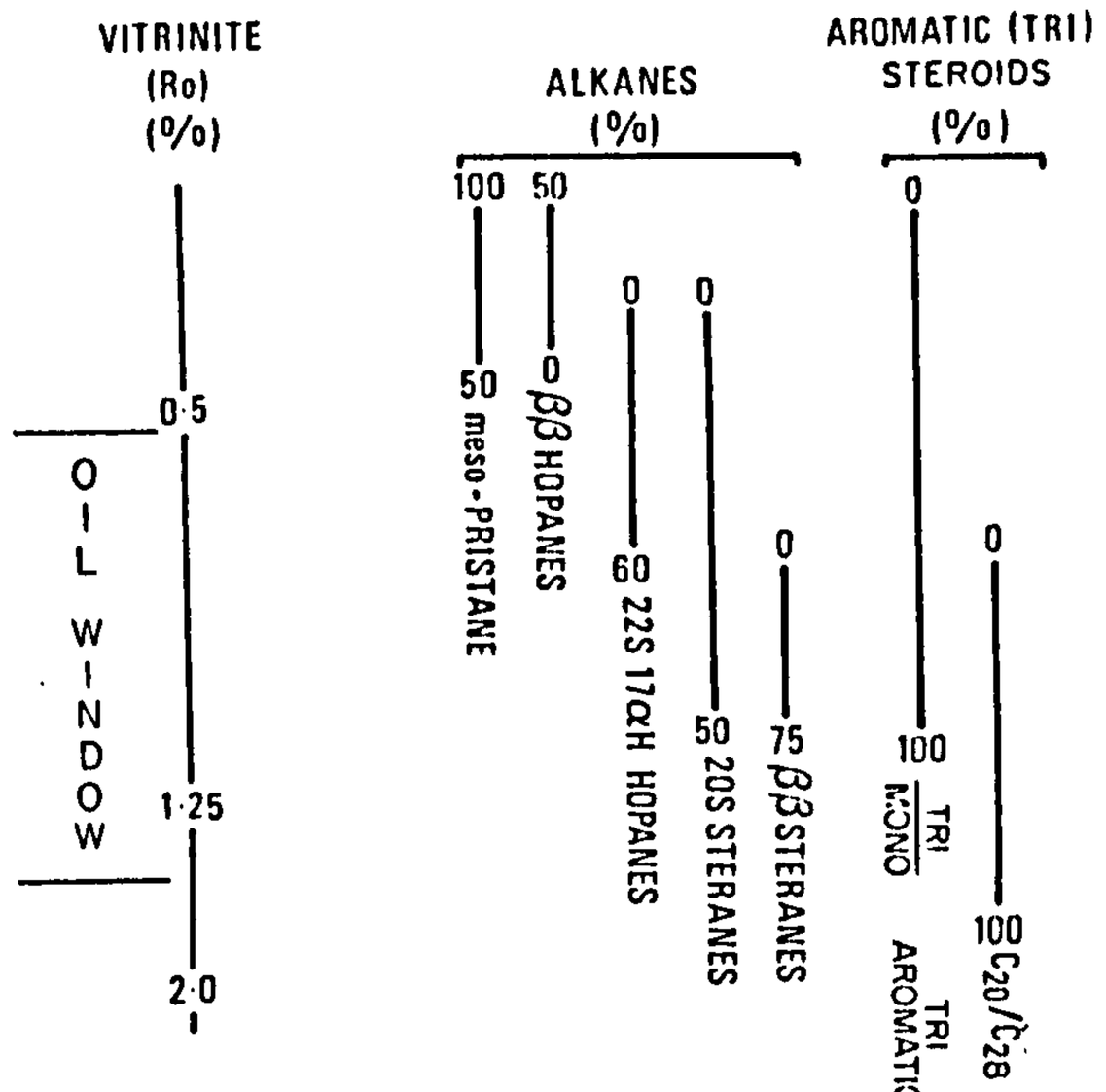

Figure 1.18 Ranges of several maturity parameters plotted against vitrinite reflectance (Ro%) for samples from the Paris Basin (Mackenzie et al., 1982a, modified by Murchisson, 1987).

Aromatic steroid hydrocarbons

Aromatic steroid hydrocarbons are major constituents of sediments and oils. They are derived from diagenetic transformation of biogenic precursors or aromatization of natural products (Douglas et al., 1965). Therefore, they have been applied as indicators of maturity levels of organic-rich sediments and oils (Tissot et al., 1974b; Seifert and Moldowan, 1978; Mackenzie et al., 1981a; 1982b; 1983). C-ring monoaromatic compounds are commonly found in crude oils and rock extracts, while A-ring members have been observed in a limited number of immature sediments (Hussler et al., 1981). C-ring monoaromatic steroidal hydrocarbons have been established first by Tissot et al. (1974b) as potential geochemical parameters for oil-oil correlation studies. Recently, there have been reports of the coexistence of two types of monoaromatic steroid hydrocarbons: rearranged (e.g. RE) and non-rearranged (e.g. NR) compounds (Riolo and Albrecht, 1985; Moldowan and Fago, 1986; Riolo et al., 1986). Rearranged structures may occur in high abundance in certain samples, which are believed to arise from specific types of depositional environment, where the presence of clay and elemental sulphur may have a considerable contribution to the rearrangment process. C-ring monoaromatic steroidal hydrocarbons have been identified in the range of C_{27}-C_{29} carbon numbers. Each compounds has four isomers with A/B cis and trans isomers, where the methyl group is attached to C-5 for rearranged and C-10 for non-rearranged compounds. The major stereochemical configurations are:

5β(CH_3),10β(H) (e.g. cis, RE; 33);

5α(CH_3),10α(H) (e.g. cis RE)

5α(CH_3),10β(H) (e.g trans, RE, 34)

5β(CH_3),10α(H) (e.g. trans, RE)

5β(H),10β(CH_3) (e.g. cis, NR, 35)

5α(H),10α(CH_3) (e.g. cis NR)

5α(H),10β(CH_3) (e.g. trans, NR, 36)

5β(H),10α(CH_3) (e.g. trans, NR).

Cis configuration is considered more stable than trans isomers. Therefore, their relative high abundance may reflect high maturity levels, although, they have been observed in significant amounts in immature samples (Riolo et al., 1986), suggesting other factors may influence the monoaromatic steroidal hydrocarbon distribution such as mineral matrix, type of organic matter, depositional environments and/or maturity (Riolo et al., 1986). Aromatization of monoaromatic to triaromatic steroidal hydrocarbons (Figure 1.18) occurs during burial depth, involving a loss of the 19-methyl group (Mackenzie et al., 1981a; 1982b). The extent of aromatization process has been widely used to measure the maturity levels of the sedimentary organic matter and petroleum (Mackenzie et al., 1981a; 1981b; 1982b). The aromatization parameter is the ratio of triaromatic to itself plus monoaromatic steroidal hydrocarbons (Mackenzie et al., 1982b), which varies from zero to unity. However, due to the coelution of non-rearranged and rearranged components (or their low abundance), the sum of peak heights of total monoaromatic and triaromatic steroidal hydrocarbons has been suggested (Curiale, 1989). In addition, laboratory experiments of steroid aromatization showed that the rates of aromatization of rearranged and non-rearranged compounds may be different (Abbott and Maxwell, 1988). The relative abundance of rearranged structures increases with increasing maturity, leading to a depletion of non-rearranged at high maturity (Riolo et al., 1986; Moldowan and Fago, 1986). Furthermore, the progress of steroid aromatization reaction can be affected by different heating rates (Mackenzie et al., 1982b) as well as by geological conditions (Mackenzie and Mckenzie, 1983). Hence, this reaction proceeds faster than sterane isomerization with increasing temperature (e.g the rapidly subsiding Pannonian basin), while sterane isomerization process is advanced at lower temperature (e.g Dead Sea basin; Rullkötter et al., 1985). Recent reports suggest that sterane isomerization and aromatization are organic facies-dependent (Barwise et al., 1991). However, lithological and type

effects are not totally independent. Conversion of long-chain triaromatic steroidal hydrocarbons (C_{26}-C_{28}) to short-chain (C_{20}, C_{21}) may require high energy for bond breaking and this occurs during the oil generation stage (Figure 1.18). However, based on laboratory experiments, low molecular weight triaromatic steroidal hydrocarbons appear to have precursors other than their high molecular weight homologues (Beach et al., 1989). It needs to be borne in mind that these conclusions are based on simulation experiments and there is always the possibility that sedimentary mechanism may be different from those followed in the laboratory. The fact that long-chain triaromatics do not break down to form short-chain counterparts in the laboratory indicates that it is possible for this same type of behaviour to be followed in the sedimentary column. Triaromatic steroidal hydrocarbons include methylated homologues, which have been detected in sediments and oils (Riolo et al., 1986). These compounds have the methyl group at C-2, C-3, C-4 and C-6 positions of A-ring (Lichtfouse, 1989) with either β or α stereochemistry (Radke, 1987). By analogy to the methylphenanthrene isomers, 2-methyl and 3-methylated triaromatic steroidal hydrocarbons are more stable, being attached to the β position of A-ring (Radke, 1987) and are more abundant in mature sediments. The extent of the rearrangment process has been suggested as an indicator of maturity levels of organic matter. Therefore, the ratios of 2-methyl+3-methyl (e.g. 38) to the sum of itself plus 4-methyl isomers for C_{21} and C_{22} triaromatic steroidal hydrocarbons have been introduced as maturity indices (Lichtfouse, 1989; Lichtfouse et al., 1990; e.g. IMTI1 and IMTI2 respectively).

The gasoline range hydrocarbons

This section involves application of low molecular weight hydrocarbons (C_5-C_9), generally termed "light hydrocarbons" as maturity parameters for correlation procedures. From a geochemical point of view, low molecular weight hydrocarbons vary in yield and composition during burial depth (e.g. Tissot et

al., 1971; Philippi, 1975). Therefore, light hydrocarbons have been extensively applied as maturity parameters for sediments and oils (Tissot et al., 1971; Durand and Espitalié, 1972; Philippi, 1975; Leythaeuser et al., 1979; Thompson, 1979; Connan and Cassou, 1980; Hunt et al., 1980a, 1980b; Thompson, 1983; Hunt, 1984). Different methods have been used for extracting the gasoline range hydrocarbons from sediments, such as the headspace and hydrogen stripping. This later procedure consists of closed gas flow extraction followed by gas chromatographic analysis (Schaefer et al., 1978). A detailed study of the gasoline range hydrocarbon distributions necessitates highly sensitive gas chromatography techniques for a reliable evaluation of the geochemical parameters applied in correlation procedures. Thompson (1979; 1983) suggested two paraffin indices (Heptane value and isoheptane index) for the evaluation of paraffinicity level, in terms of conversion of cyclic and branched alkanes into n-alkanes with increasing maturation. Thompson (1983) considered that normal oils are released at temperature between 139°C-149°C, while mature oils are generated at higher maturity. However, high paraffin contents may have source influence (Snowdon and Powell, 1982; Rullkötter et al., 1986). Furthermore, biodegradation has a different effect on heptane value and isoheptane index. The heptane value having normal heptane in the numerator is more sensitive to biodegradation than the Isoheptane index, having two branched isomers of heptane (see Appendix 4.6) and three cyclic isomers in the denominator. Thus, they may have different response to maturity, biodegradation and migration. In addition, low concentrations of aromatic hydrocarbons (39; benzene, toluene, ethylbenzene, metaxylene, paraxylene and orthoxyxlene) relative to *n*-alkanes may occur as a result of water washing during migration or fractionation, termed "evaporative fractionation" (Thompson, 1987; 1988). This has been defined as an accumulation of gas-saturated oil within the gas-cap. Evaporative fractionation occurs due either to pressure reduction by erosion or fault, or from additional gas in the well (Thompson,

1987; 1988). This system involves a liquid-vapor phase, where low molecular weight hydrocarbons tend to move to the vapor phase, while high molecular weight homologues remain in the liquid phase. Two parameters (toluene/*n*-heptane and *n*-heptane/methylcyclohexane) were introduced based on laboratory and field data (Thompson, 1987; 1988), showing that relatively low toluene and high *n*-heptane abundances do not always reflect high maturity but evaporative fractionation. Recent application of these parameters suggested a source influence (Fowler et al., 1990), since they indicated contradictory results to those shown by Thompson (1987; 1988).

1.3.3.4 Correlations

Biological marker distributions have been extremely useful tools in oil-oil and oil-source rock correlations as a result of the above factors and influences. On the basis of their chemical signatures, oils may be related to each other and to their derived source rocks and hence discriminated into groups or families. Sterane and triterpane distributions are useful for this purpose, although tricyclic terpanes (Curiale, 1985) as well as triaromatic steroid hydrocarbons have also been informative (Brooks et al., 1989). However, distributions of biological markers can be affected by maturity, biodegradation as well as fractionation during migration (e.g Philp and Engel, 1987; Zhao-An and Philp, 1987). To account for biological marker multiple controls, therefore, it is highly desirable that as a broad range of parameters as possible are used in a correlation exercise.

Chapter 2. Experimental

2. Experimental

2.1. General procedures

Solvents used in this work, were distilled in an Oldershaw column (30 theoretical plates), prior to use. Thimbles and cotton wool were previously extracted in dichloromethane and blanks analysed to avoid any trace of contamination. Glassware was soaked overnight in a detergent solution Decon 90 (BDH Ltd), thoroughly cleaned, rinsed with distilled water and dried in an oven. Before use, glassware was rinsed with dichloromethane. During laboratory work up, solvents were partially removed by rotary evaporation. Organic fractions were transferred to pre-weighed vials. The residual solvent was removed under stream of nitrogen (nitrogen blow-down). Weights of all fractions were recorded.

2.2. Extraction of bitumen from rock samples

The surfaces of the rock samples were removed using a brush. They were crushed into small pieces, then washed ultrasonically using dichloromethane (15 minutes), dried and ground to a fine powder in a disc mill (Tema). A known weight of powdered sediment was extracted by a Soxhlet apparatus using a mixture of dichloromethane and methanol in a proportion of (93ml:7ml) for fifty hours. Approximately 1g of copper previously activated with (ca. 4M) hydrochloric acid was used to remove elemental sulphur from the organic extract.

2.3. Asphaltene precipitation

Weighed total extracts were dissolved in a minimum amount of dichloromethane and transferred to a 250ml conical flask. A 40:1 v/v mixture of n-heptane:dichloromethane was added. The solution was left to stir for 15 minutes and to settle overnight. The asphaltene fraction was obtained by filtration in a

sintered funnel. The residue was redissolved in a few millilitres of dichloromethane, precipitated in *n*-heptane. The procedure was repeated at least three times. The asphaltene fraction was dissolved in dichloromethane. Solvents were evaporated and weights recorded.

2.4. Liquid column chromatography.

Silica gel (BDH 60-120 mesh) and alumina adsorbents were pre-extracted in a mixture of dichloromethane and methanol for 8 hours, then activated at a temperature of 110°C for several hours and stored in the same oven. Extracts of source rocks and crude oils were fractionated in a glass column (50cm x 0.75cm i.d.) that was pre-packed with a slurry of activated silica gel and topped with a layer of 2cm to 3cm of a layer of activated alumina. The column was rinsed with light petroleum before use. A known weight of oil or maltene was mixed with activated alumina and allowed to dry. Saturated, "light" aromatic, "heavy" hydrocarbons and NSO compounds were eluted through with 70ml of light petroleum, 50ml:20ml light petroleum: dichloromethane, 70ml dichloromethane and 70ml methanol respectively. All weights were recorded.

2.5. Thin layer chromatography.

This technique requires more sample (20mg) than column chromatography. An aqueous slurry of 45g of Merck Kieselgel G (Nach Stah type 60) and 90ml of distilled water was prepared (for 5 plates). The homogeneous mixture was spread on the plates and left to dry (0.5mm thickness). The coated plates were then activated in an oven at 110°C overnight, developed with ethyl acetate and activated again (1 to 2 hours). Four reference standards (heptadecane, phenyldecane, anthracene and perylene) were spotted on one side of the plate being careful to separate these from the sample. A known weight (10mg to 20mg) of the sample was loaded on the other side of the plate. The plate was developed in hexane. "Light" aromatic and "heavy" aromatic hydrocarbon

fractions were observed under UV light. The saturated hydrocarbon fraction was visualised with Rhodamine 6G. The four fractions were removed separately from the plate and put into short columns, being previously plugged with cotton wool and alumina. Saturated, "light" aromatic (mono and triaromatics), "Heavy" aromatic hydrocarbons (polyaromatic) and NSO fractions were eluted with 50ml of light petroleum, 25ml:25ml of dichloromethane and light petroleum, 50ml of dichloromethane and 50ml of methanol respectively. The different weights were recorded.

2.6. Silicalite adduction

Recently, a new procedure has been developed by Hoering and Freeman, (1984); West et al. (1990) and Armanios et al. (1991) using silicalite sorption as a rapid method for isolating cyclic and branched alkanes for GC/MS analysis. The method employed requires refluxing a solution of paraffins in the presence of molecular sieves for many hours, filtration and evaporation of solvent to obtain the branched/cylic alkane fraction. Silicalite sorption requires less time (1 hour). Silicalite was crushed into small pieces and activated on a flame at high temperature for 15 to 20 minutes and stored in a desiccator for use. 10mg to 20mg of saturated hydrocarbon fraction was dissolved in iso-octane and loaded in a pre-packed pippette with fine grains of activated silicalite. *N*-alkanes were adducted, while the branched/cyclic alkane fraction was eluted using iso-octane. The recovery of normal alkanes was not accomplished since the aim of the procedure was to isolate the cyclic and branched alkanes from the *n*-alkanes, particularly for biological marker investigation (e.g. steranes and triterpanes) and branched alkanes. This operation requires less time than urea and molecular sieve adduction.

2.7. Gas chromatography (GC)

Analyses of saturated and aromatic hydrocarbon fractions were carried out on a Carlo Erba Mega 5160 gas chromatograph fitted with a Grob on column injector and a flame ionization detector. Hydrogen was used as a carrier gas at a flow of 1ml/min supplied at a pressure of 50KPa. Air and hydrogen were supplied to the flame at a pressure of 100kPa and 50kPa respectively. The column oven was programmed from 50°C to 300°C at a rate of 4°C/min and maintained at this temperature for 20 minutes. For the saturated hydrocarbon fraction analysis, the gas chromatograph was equipped with a fused silica capillary column (25m x 0.32mm i.d.) coated with an OV-1 stationary phase (film thickness 0.33 m). For the aromatic hydrocarbon fraction analysis, the gas chromatograph was equipped with a fused silica capillary column (25m x 0.2mm i.d.) coated with a DB5 stationary phase (film thickness 0.33 m).

The gasoline range (C_4-C_9) hydrocarbon fractions of oils makes up approximately 10 to 30 wt% of oil. Crude oils were analysed in a HP588 instrument fitted with a split-splitless injector and a flame ionization detector. The gas chromatograph was equipped with an HP-PONA stationary phase (50m x 0.2mm i.d) fitted with a pre-packed column used for backflushing high molecular weight compounds (C_n>nC_{10}). Helium was used as a carrier gas at a pressure of 32 psi. The column was programmed from 35°C to 80°C at a rate of 1.5°C/min and then to 140°C at a rate of 30°C/min and held isothermal for 10 minutes. The temperature of the detector and injector were 320°C and 280°C respectively. Peak assignments are listed in Table 5.

2.8.Combined gas chromatography-mass spectrometry (GC/MS using electron impact energy mode)

Combined gas chromatographic/mass spectrometric analyses in electron impact energy mode (EI) of the saturated and aromatic hydrocarbon fractions were carried out on a Heweltt Packard 5890 gas chromatograph interfaced with a VG

TS-250 mass spectrometer using an ionization energy of 35eV, an emission current of 2500 A and a source temperature of 175°C. Data was collected using a Digital PDP 11/73 Data system. Helium was used as a carrier gas at a flow of 1ml/min and supplied at a pressure of 60kPa with samples being injected in the split-splitless mode. For GC/MS analysis of the saturated hydrocarbon fractions, the gas chromatograph was equipped with a fused silica capillary column (25m x 0.2mm i.d) coated with an OV-1 stationary phase (0.2 m thickness). For total scanning (SCAN mode) the temperature was initially maintained at 40°C for 3 minutes from then heated up to 300°C at a rate of 4°C/min and held at the final temperature for 20 minutes. A plot of the sum of the intensities of the ions in the mass range from 50 to 500 against scan number provides a total ion current (TIC). A plot of a single selected ion against scan number provides a partial mass chromatogram, which can be used to characterise homologous series with well known mass spectra. Individual compounds were identified by comparison with standard spectra of pure compounds in the literature and by their relative retention times. For the selected ion monitoring (SIM), the column was operated from 50°C for 3 minutes then from 50°C to 300°C at a rate of 4°C/min and finally held at this temperature for 20 minutes. In this mode, each ion was monitored every cycle time. The following ions were monitored during the GC/MS analysis of the saturated hydrocarbon fraction: m/z 83.0860, 97.1020, 217.1950, 218.2040, 259.2430, 177.1640, 191.1794 and 205.1960 for detecting *n*-alkyl and methyl-*n*-alkylcyclohexanes. The others ions are characteristic for steranes and triterpanes. For GC/MS analysis of the aromatic hydrocarbon fractions, the gas chomatograph was equipped with a fused silica capillary column (30m x 0.25mm i.d) coated with a DB5 (5% phenylmethylsilicone, 0.25 m thickness) stationary phase. In SIM mode, the temperature was held at 50°C for 3 minutes then rapidly increased to 175°C at a rate of 10°C/min then to 225°C at a rate of 6°C/min and to 300°C and held at this temperature for 20 minutes. The selected ions were m/z 253.1950, 231.1170,

245.1330 for detecting monoaromatic, triaromatic and methylated triaromatic steroid hydrocarbons respectively.

2.8.1 Compound identification

A homologous series was identified using diagnostic ions, while individual compounds were recognised either by comparison of their mass spectra with those shown in the literature or by coinjection of authentic standards. Diagnostic ion and mass spectral fragmentation patterns of monocyclic, polycyclic alkanes and aromatic steroidal hydrocarbons are illustrated in Figure 2.1, 2.2, 2.3, 2.4, 2.5 and 2.6.

2.9. GC/MS using metastable ion reaction monitoring (MRM)

Application of GC/MS/MRM technique was first introduced by Gallegos (1976) for a mixture of biological marker compounds. It has been defined highly selective, especially for coeluting compounds such as rearranged and non-rearranged steranes as well as steranes and methyl steranes (Warburton and Zumberge, 1983; Meyer et al., 1984a). In the present work, sterane and terpane distributions were obtained using a VG-70E mass spectrometer at Norsk-Hydro research centre, Bergen (Norway). This instrument operated in metastable ion monitoring mode, was interfaced to a HP-5790 gas chromatograph fitted with a 25m, 0.25mm i.d. Ultra HP-1 fused silica column. A programme temperature of 80°C to 150°C at 25°C/min and then to 310°C at 1.5°C/min. Peak data were processed using a Multichrom laboratory data system (VG Laboratory systems).

2.9.1. Calculation of molecular parameters

Values for molecular parameters were calculated from peak heights from narrow peaks of the appropriate mass chromatograms. Abbreviations are explained in each Table of results. These parameters have been selected for their ability to indicate differences in organic matter type (biological marker

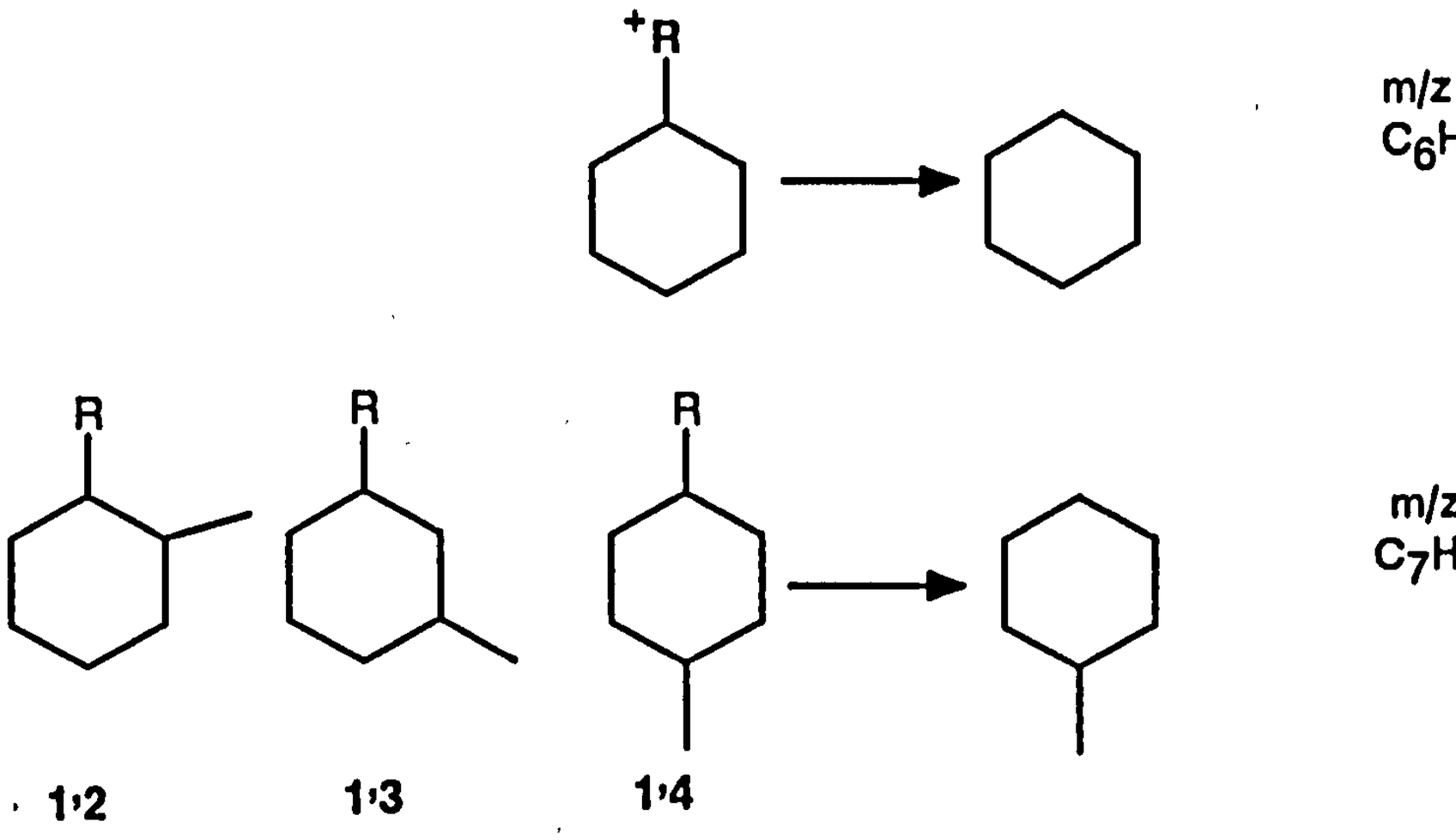

m/z 83+R
C_6H_{11}

m/z 97+R
C_7H_{11}

Figure 2.1 Mass spectral fragmentation pattern of monocyclic alkanes, where R=H, CH_3 or C_nH_{2n+1}
(a) m/z 83+R, C_6H_{11}
(b) m/z 97+R, C_7H_{11}

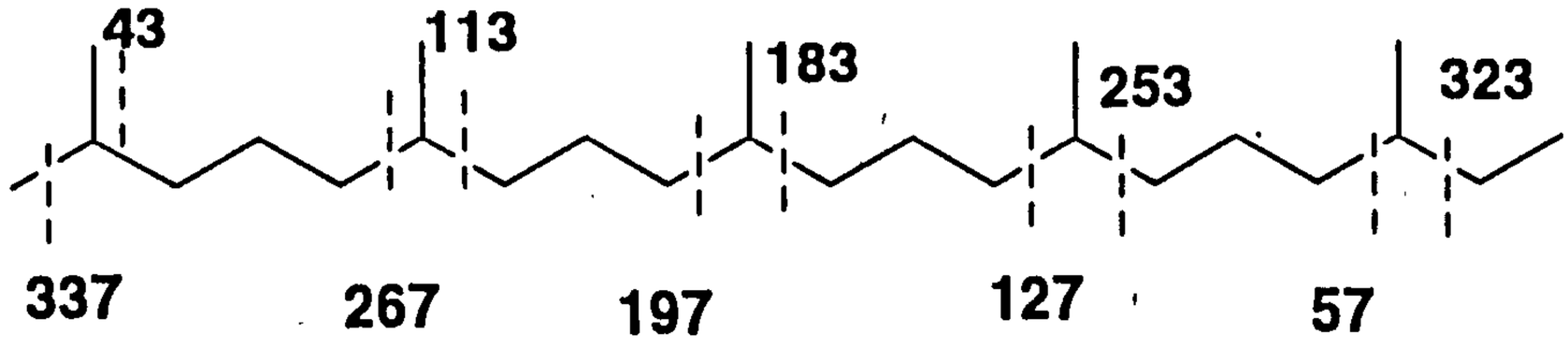

Figure 2.2 Mass spectral of C_{25} head-to-tail isoprenoid hydrocarbon.

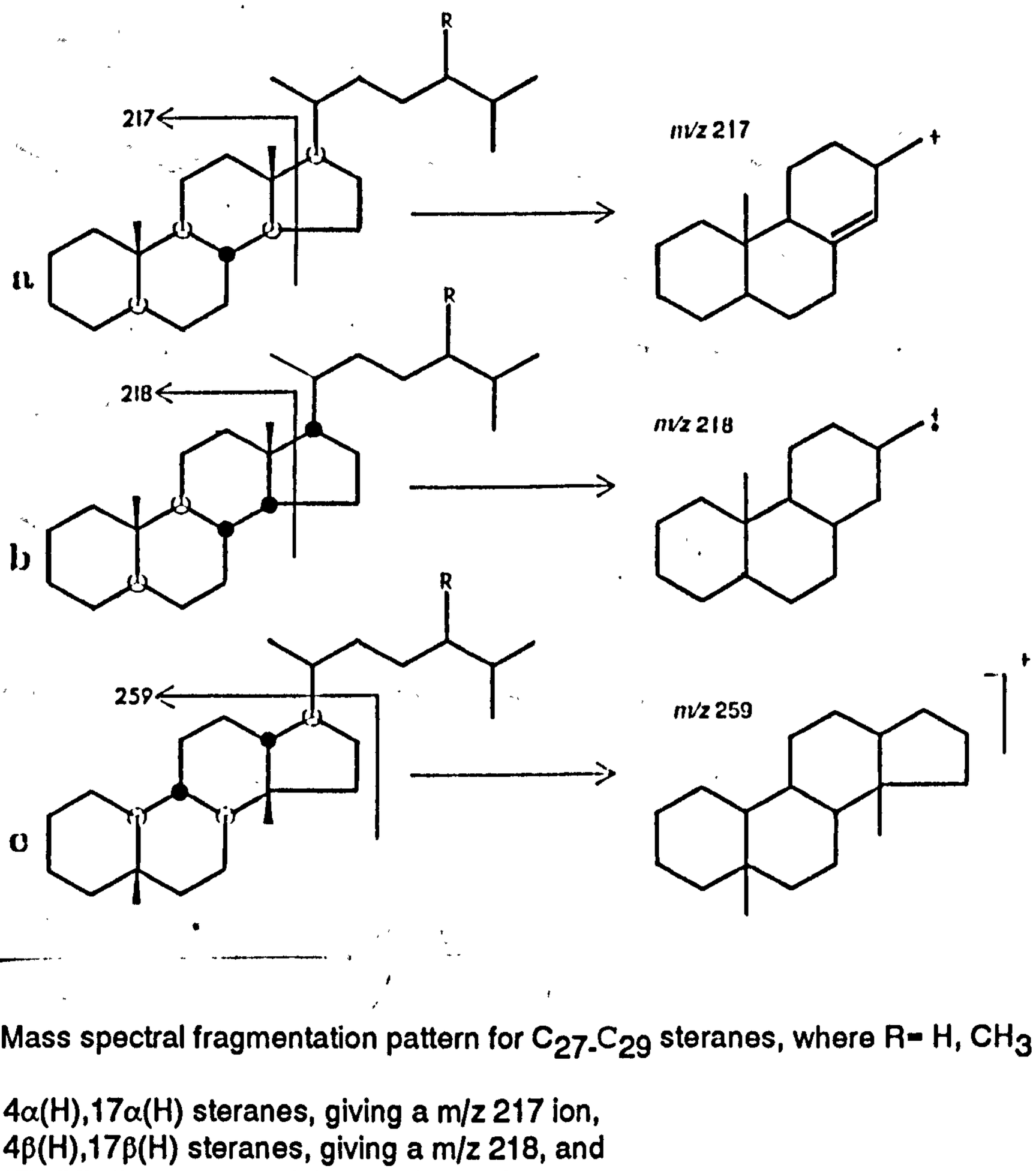

Figure 2.3 Mass spectral fragmentation pattern for C_{27}-C_{29} steranes, where R= H, CH_3 or C_2H_5:
(a) 5α(H),14α(H),17α(H) steranes, giving a m/z 217 ion,
(b) 5α(H),14β(H),17β(H) steranes, giving a m/z 218, and
(c) 13β(H),17α(H) diasteranes, giving a m/z 259 ion.

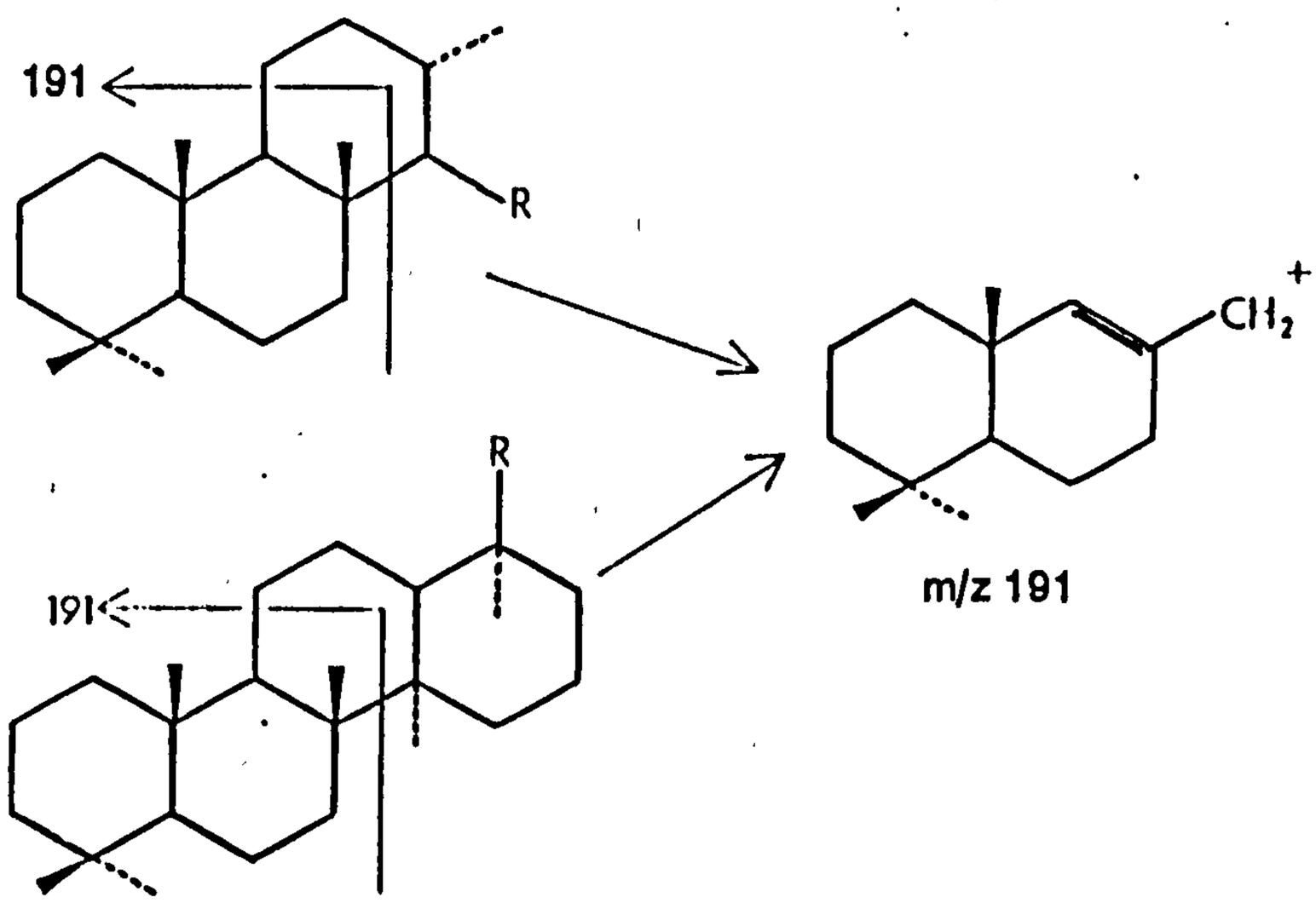

Figure 2.4 Mass spectral fragmentation pattern for tricyclic and tetracyclic terpanes.

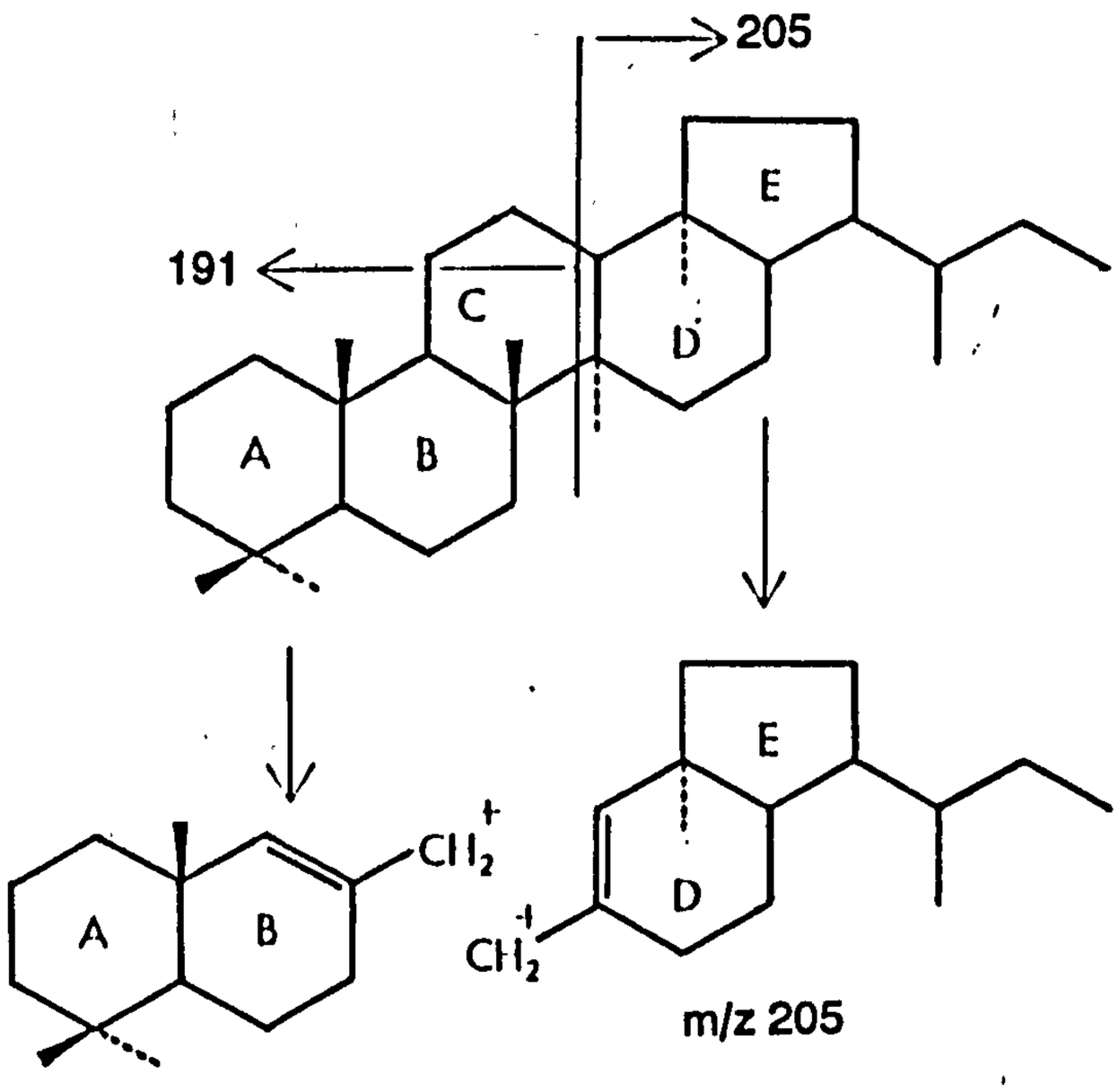

Figure 2.5 Mass spectral fragmentation pattern of a C_{31} hopane.

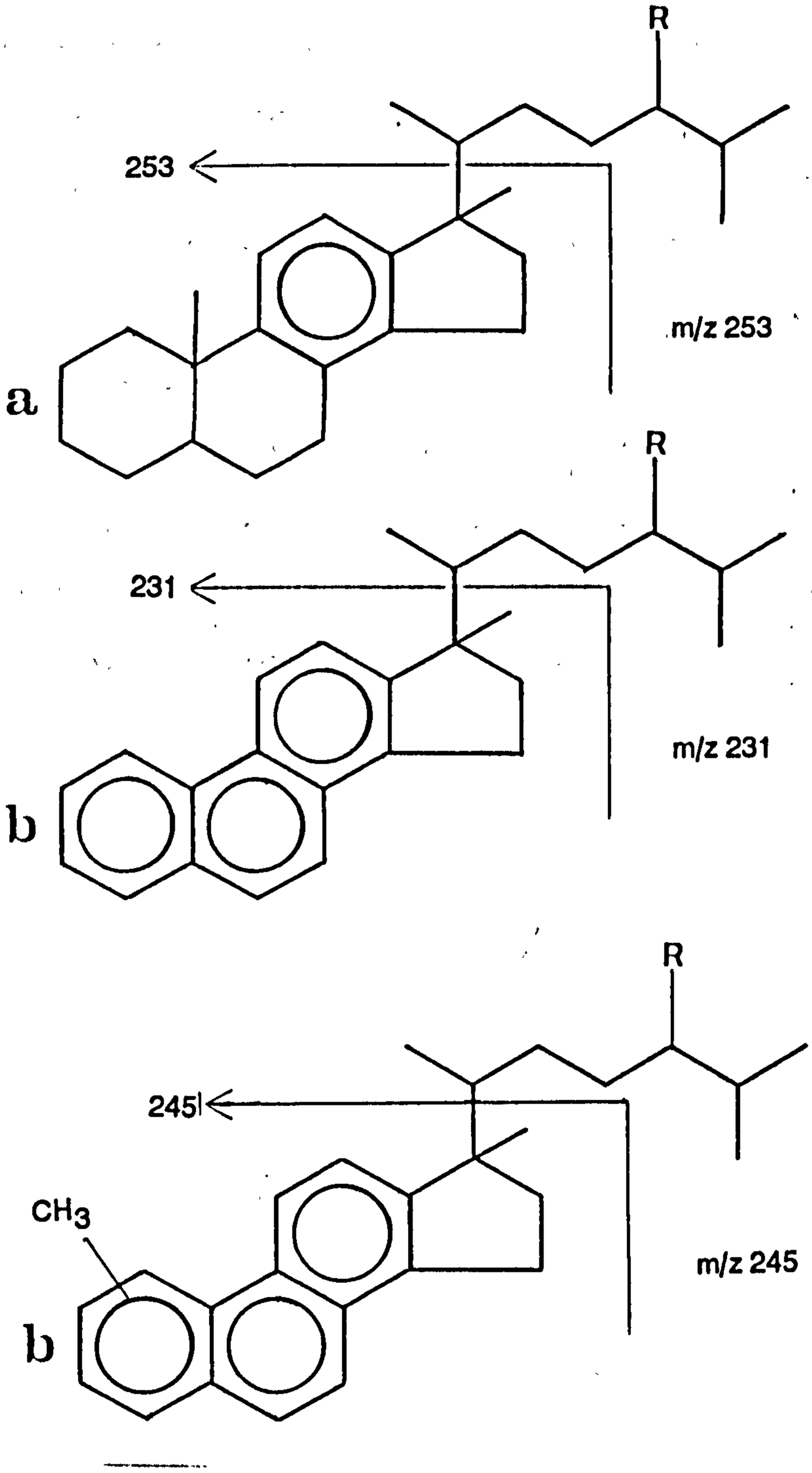

Figure 2.6 Mass spectral fragmentation pattern for aromatic steroids, where R= H, CH_3 or C_2H_5:
(a) C-ring monoaromatic steroidal hydrocarbons, giving a m/z 253 ion,
(b) ABC-ring triaromatic steroidal hydrocarbons, giving a m/z 231 ion and,
(c) Methylated triaromatic steroidal hydrocarbons, giving a m/z 245 ion.

sources), depositional environment and maturity. Obviously, the most useful parameters are those, which are affected by only one of the above factors. Absolute quantification of compound abundances was not attempted. Full details of all molecular parameters are listed in Table 2.1.

2.10 Rock-Eval pyrolysis

The method consists of heating a small amount of rock powder using programmed temperature under helium flow. For details, the reader is referred to Espitalié et al. (1977). The peak chromatographic detected during Rock-Eval pyrolysis with the derived parameters are shown in Figure 2.7.

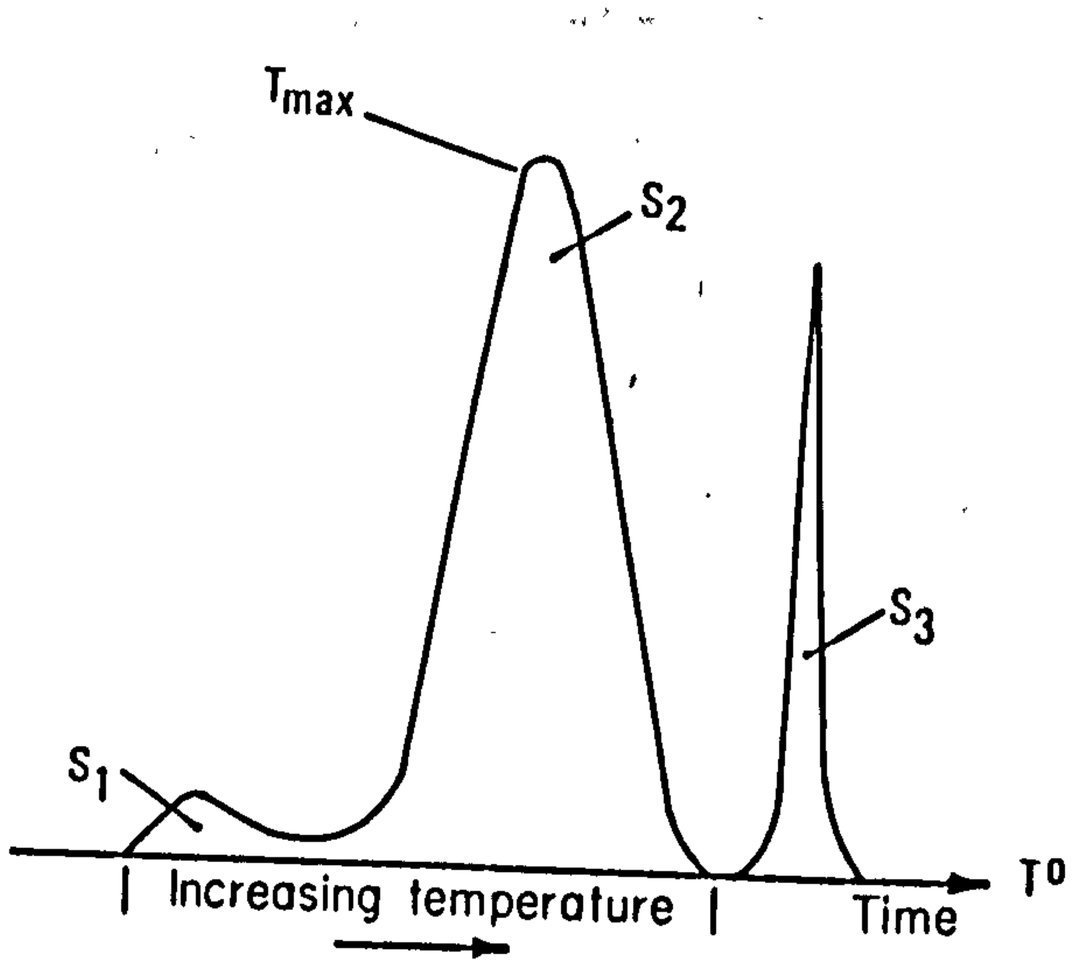

Figure 2.7 Example of three chromatographic peaks generated during Rock-Eval pyrolysis.

Peak S_1 quantity of hydrocarbons desorbed from rock sample during heating at 250°C for 5min.

Peak S_2 quantity of hydrocarbons related material produced during pyrolysis of kerogen over the temperature range 250°C-550°C at 25°C min^{-1}.

Peak S_3 quantity of carbon dioxide produced during pyrolysis over the range of 300°C-390°C.

Tmax Temperature of maximum kerogen decomposition rate (maximum peak S_2 evolution), related to maturity of the sample.

S_1+S_2 Genetic potential
S_1/(S_1+S_2) The production index
S_2/TOC hydrogen index
S_3/TOC oxygen index

2.11. Kerogen isolation

The method involves acid digestion of the inorganic material using hydrochloric and hydrofluoric acids. The aim of this procedure is to obtain good samples for pyrolysis-gas chromatography (Py/GC). An operating system for chemical separation of kerogen was described by Durand and Nicaise (1980). It consists of an isolation of kerogen from the inorganic matrix but not from pyrite, type Framboids. This cannot easily be eliminated since it is the most frequent mineral associated with kerogen. Many attempts have been made by Durand and Nicaise (1980) to isolate kerogen under oxidative and reductive conditions, which may not be ideal because they can alter the chemical composition of kerogen. The first step of this procedure was to remove the carbonate minerals using hydrochloric acid. The pre-extracted rock (by a Soxhlet extraction) was mixed with distilled water in a 500ml teflon beaker. Hydrochloric acid (8M) was then added to the mixture slowly until effervescence ceased and a further volume was added. This was stirred for 24 hours at room temperature and for a further 8 hours at 50°C. The mixture was then centrifuged, the acid decanted and the residue washed twice with distilled water. The supernatant liquid was green due to the dissolved inorganic ions, especially $Fe^{2}+$. A volume of hydrofluoric acid (40%) was then added to the remained mixture until effervescence ceased and a further volume of hydrochloric acid (8M) was added to remove any neo-formed fluorides. The solution was then stirred for 24 hours at room temperature then for few hours at 50°C. Generally a solution of boric acid is used for neutralising the excess of acid and added slowly to maintain the temperature of the mixture. This prevents any formation of thick jelly-like fluorides and silicates, which are then difficult to dissolve. After decanting and washing of the solution several times (10 times) with distilled water, the residue was then allowed to dry at room temperature. Some samples were treated twice to three times to see if minerals could be eliminated and consequently to obtain high concentrations of organic matter.

2.11.1. Optical assessment of samples

Samples were made as polished blocks for reflected light and ultra-violet microscopy.

2.11.2. Sample preparation

For microscopic observations, blocks of samples were prepared. A small piece of rock was crushed and mounted using methyl metacrylate resin and few drops of peroxide accelerator. The samples were first ground on a wet Diamond lap and subsequently on 280 and 600 grade silicon carbide papers. They were then polished with 5/20, 3/50 and Gamma grade alumina powder on 'Selvyt' cloth laps. Propanol-2 is used as a lubricant for sediments whereas water is used for coal.

2.11.3. Measurement of Vitrinite Reflectance

This technique has been used for long time, at the time of Coal Petrology to identify coal macerals and estimate their rank (e.g. Bostick and Foster, 1975). Recently, this technique has been extended to study the finely disseminated organic material in sediments and to evaluate their maturity level (reflectance measurement). The particles of organic matter are present in such a finely dispersed state that they are rather difficult to identify and precisely define their shape. Vitrinite reflectance measurements were obtained using a Zeiss Microscope with a monochromatic green light of 546nm wavelength. The intensity of the reflected light by the sample is converted to an electrical signal by a photomultiplier. The signal is recorded on a pen recorder chart. The deflection is directly proportional to the reflected light by the sample. Then the vitrinite reflectance of the sample (Ro) was determined by comparison with that of the glass standard (R_{st}), using the following formulae:

Vitrinite Reflectance of sample:

$$(Ro)=\frac{\text{Deflection from sample}}{\text{Deflection of St}} \times R_{st}$$

Standards in the range of Ro=0.4536 and 0.9940 were used, depending on the rank of samples. The blocks were observed in an oil immersion with a refractive index of 1.518 (ne) at 23°C. In practice, this was difficult to get because some samples contain little or no vitrinite particles, since land plants evolved in late Silurian. Most of the maturity were based on the intensity of fluorescent liptinic material (spores and algae).

2.11.4. Fluorescence measurement

The polished blocks were also examined using Ultra-Violet light microscopy. The microscope is equipped with a lamp H130 100W Mercury lamp and KP 490 exciter filter, 500nm mirror and an LP 520 barrier filter. This enhances the identification of the liptinic content (spores and algae) in the sample and gives and an estimation of the maturity level based on the intensity of the of the particles fluorescing. One must know that carbonate minerals also fluoresce but they have different spectra.

2.12. Principal Component analysis (PCA)

The most useful Multivariate approaches employed in organic geochemistry in recent years (Kvalheim and Telnaes, 1986; Kvalheim, 1987; Telnaes and Cooper, 1991), is the Principal component analysis (PCA). PCA is a powerful tool for analysing a large volume of data obtained by GC and GC/MS. Consider a large data set consisting of n objects, which are described by several (m) variables (i.e organic and inorganic compositions). This data matrix comprises m columns and n rows. Compounds selected for principal component analysis are illustrated in Table 2.2. To visualize a complete picture of a sample at the molecular level, one needs m-dimensinal space. Thus, PCA can help reducing the m-dimensions to a more practical number two or three dimensions or

Table 2.2 Compound classes selected for the principal component analysis.

N°	compounds
1	C_{20} tricyclic terpane
2	C_{21} tricyclic terpane
3	C_{22} tricyclic terpane
2	C_{23}-tricyclic terpane[13*]
3	C_{24}-tricyclic terpane
4	C_{24}-tetracyclic terpane[14*+]
6	17,21-secohopane[+]
7	C_{25}-tricyclic terpane (a)
8	C_{25}-tricyclic terpane (b)
9	C_{26} tricyclic terpane (a)
10	C_{26} tricyclic terpane (b)
11	T_s[20*]
12	T_m
13	unknown
14	17α(H)-30-norhopane
15	$C_{29}T_s$[23*]
16	17α(H) diahopane or B_3[22*]
17	normoretane
18	17α(H)-hopane[15*]
19	moretane
20	C_{31}-homohopane (22S)
21	C_{31}-homohopane (22R)
22	C_{32}-bishomohopane (22S)
23	C_{32}-bishomohopane (22R)
24	βα-C_{27}-diasterane (20S)
25	βα-C_{27}-diasterane (20R)
26	αβ-C_{27}-diasterane (20S)
27	αβ-C_{27}-diasterane (20R)
28	ααα-C_{27}-sterane (20S)
29	αββ-C_{27}-sterane (20R)
30	αββ-C_{27}-sterane (20S)
31	ααα-C_{27}-sterane (20R
32	βα-C_{28}-diasterane (20S)
33	βα-C_{28}-diasterane (20R)
34	αβ-C_{28}-diasterane (20S)
35	αβ-C_{28}-diasterane (20R)
36	ααα-C_{28}-sterane (20S)
37	αββ-C_{28}-sterane (20R)
38	αββ-C_{28}-sterane (20S)
39	ααα-C_{28}-sterane (20R)
40	βα-C_{29}-diasterane (20S)
41	βα-C_{29}-diasterane (20R)
42	αβ-C_{29}-diasterane (20S)
43	αβ-C_{29}-diasterane (20R)
44	ααα-C_{29}-sterane (20S)
45	αββ-C_{29}-sterane (20R)
46	αββ-C_{29}-sterane (20S)
47	ααα-C_{29}-sterane (20R)
48	βα-C_{30}-sterane (20S)[27*]
49	βα-C_{30}-sterane (20R)
50	ααα-C_{30}-sterane (20S)[26*]
51	αββ-C_{30}-sterane (20R)
52	αββ-C_{30}-sterane (20S)
53	ααα-C_{30}-sterane (20R)

* refers to structures in appendix.

+C_{24} tetracyclic terpane and 17,21 secohopane were barely detectable in oils.

components, describing the maximum variance or contribution. Patterns showing relationships between variables are called loading plot, and those illustrating relationships between samples are called score plots. Variables cluster together carry the same information (Kvalheim and Telnaes, 1986). Thus, due to the orthogonality of the PC's, variables with greater loading may have maximum contribution to this particular PC, indicating that these variables may have the same property as the PC (Telnaes et al., 1987). In an organic geochemical sense, this may describe type, maturity or depositional environment of samples (Kvalheim and Telnaes, 1986; Kvalheim, 1987; Telnaes and Cooper, 1991). In this thesis, PCA was performed using a non-commercial programme written by Dr. Peter Yendle at Bristol University. Results were output to 1,2,3 Lotus illustrating the loadings and scores plots. A detailed background and mathematical study is beyond the scope of this work. For a more detailed study of Multivariate methods, the reader is referred to the book by Davis (1986) and the above references for applications of Multivariate approaches in organic geochemistry. PCA of sterane and terpane as well as gasoline range hydrocarbon distributions are discussed in the relevant Chapters.

Table 2.1 Description and significance of the geochemical parameters used in this thesis (modified after Farrimond, 1987)

Parameters	Quantification	indication	Comment	References
n-C_{17}, n-C_{15}, n-C_{19}	gas chromatogram of saturated hydrocarbon fraction	Biological sources.	Algae are characterised by maximum at n-C_{17}	Gelpi et al. 1970 Brassell et al. (1978).
C_{27}, C_{29} and C_{31}	gas chromatogram of saturated hydrocarbon fraction.	Biological sources.	Higher Plants maximize at C_{27}, C_{29} and C_{31}. Leaf waxes are rich in n-C_{31}.	Eglinton et al. (1962); Caldicott and Eglinton (1973)
CPI, Carbon Preference Index (C_{24}-C_{34})	gas chromatogram of saturated hydrocarbon fraction.	Maturity.	This parameters is also dependent upon source for immature samples.	Brassell et al. (1978).
n-C_{17}/Pr	gas chromatogram of the saturated hydrocarbon fraction.	Maturity	Pristane may derive from photosynthetic organisms. Values<1 indicate algal input. However, this parameter can be influenced by maturity, biodegradation and the degree of expulsion from sediments.	e.g.Brooks et al., 1969; Tissot et al (1971); Leythaeuser and Schwarzkopf (1986).
n-C_{18}/Ph	gas chromatogram of saturated hydrocarbon fraction.	Maturity	High phytane is suggested to be indicative of highly reducing environment and archaebacterial input.	Didyk et al. (1978); Risatti et al. (1984)
Pr/Ph	gas chromatogram of saturated hydrocarbon fraction.	Palaeoenvironment indicator of oxygen content of depositional environment.	This parameter is also influenced by source.	Blumer et al. (1963); Didyk et al. (1978); Goossens et al. (1984); Risatti et al. (1984).
Tricyclic terpanes.	m/z 191 for terpane distribution	biological sources.	Terpane distribution are known to be derived from bacteria and algae. However, their relative concentrations increase with increasing maturity.	Aquino Neto et al. (1982); (1983)

Tricyclic terpanes (tricyclic to hopane ratio, e.g. $C_{23}T/C_{23}T+C_{30}hp$)	m/z 191 (GC/MS SIM) or m/z 318->m/z 191 and m/z 412->m/z 191 (GC/MS/MRM transitions for tricyclic and pentacyclic terpanes respectively.	Biological sources.	This parameter is used for oil-oil and oil-source rock correlations. It is influenced by maturity.	Curiale et al. (1985).
Tetracyclic terpanes	m/z 191 (GC/MS SIM) or m/z 332->m/z 191 metastable ion transitions.	Thermal or microbial degradation.	Tetracyclic terpanes are often related to terrestrial input .	Trendel et al. (1982); Hoffmann et al. (1984).
T_s/T_m: 18α(H)-22,29,30-trisnorneohopane/17α(H)-22,29,30-trisnorhopane	m/z 191 (GC/MS SIM) or m/z 370->m/z 191 metastable ion transitions	Maturity.	This parameter is also dependent upon source and lithology.	e.g. Seifert and Moldowan (1978)
17α(H)-28,30-bisnorhopane	m/z 191 (GC/MS SIM) or m/z 384->m/z 191 metastable ion transitions.	Biological sources and/or depositional environment.	This compound has been found in high abundance in highly reducing sulphur-rich environment.	Grantham et al. (1980).
$C_{29}T_s/C_{29}$ norhopane : 18α(H)-norneohopane/17α(H),21β(H)-norhopane.	m/z 191 (GC/MS SIM) or m/z 398->m/z 191 metastable ion transitions.	Maturity and/or depositional environment.	Relative increase of concentrations of C29Ts with increasing maturity	Cornford et al. (1988); Fowler et al. (1990); Moldowan et al. (1991)
C_{29} hp/C_{30}hp (17α(H),21β(H)-norhopane/17α(H),21β(H) C_{30} hopane.	m/z 191 (GC/MS SIM) or m/z 398->m/z 191 and m/z 412-.m/z 191 metastable ion transitions.	Depositional environment and/or fractionation.	Although low concentrations of norhopane relative to hopane in oils may occur as a result of extensive migration.	Rullkötter et al (1985); Curiale (1985)
17β(H),21α(H)-C_{29} and C_{30} hopanes (normoretane and moretane respectively).	m/z 191 (GC/MS SIM) or m/z 398->m/z 191, m/z 412->m/z 191 metastable ion transitions.	Maturity.	This parameter depends upon source. It is found abundant in coals and sediments rich in algae.	Hoffmann et al. (1984)

17α(H),21β(H)-C_{32} bishomohopane (22S/22S+22R).	m/z 191 (GC/MS SIM) or m/z 426->m/z 191metastable ion transitions.	Maturity.	The biologically compound 22R stereochemistry is partially replaced by the more stable 22S configuration towards an end-point value (%60). A reversal of hopane isomerisation has been observed during hydrous pyrolysis experiments.	Esminger et al. (1977); Peters et al. (1989).
Hopane to sterane ratio (17α(H),21β(H)-C_{30} hopane/C_{29}ααα (20R)).	m/z 191, m/z 217 (GC/MS SIM) or m/z 412->m/z 191, m/z 400->m/z 217 metastable ion transitions.	Biological sources.	This parameter is often used in oil-oil and oil-source rock correlations. High ratio is characteristic of bacterial contribution. Relative increase of hopanes compared to steranes has been observed during hydrous pyrolysis.	Esminger et al. (1974); Eglinton and Douglas (1988).
%(C_{27}-C_{29}) steranes	m/z 217 (GC/MS SIM) or m/z 372->m/z 217, m/z 386->m/z 217 and m/z 400->m/z 217 metastable ion transitions.	Palaoenvironment indicator: C_{27} planktonic, C_{29} terrestrial.	Relatively higher proportions of C_{29} steranes have been observed in marine environments. Therefore, predominance of C_{29} steranes is not automatically indicative of terrestrial input	Huang and Meinschein (1979); Fowler and Douglas (1984); (1987).
C_{30} desmethylsteranes.	m/z 217 (GC/MS SIM) or m/z 414->m/z 217 metastable ion transitions.	Biological sources	This compound is indicative of marine environment.	Moldowan et al. (1985)
Methylsteranes, particularly C_{30} components.	m/z 231 (GC/MS SIM) or m/z 414->231 metastable ion transitions.	Biological sources.	The 4-methylsteranes are thought to be characteristic of Dinoflagellate input in sediments younger than the Triassic age, while 3β-methyl are relatively abundant in Precambrian and Palaeozoic sediments.	Summons et al. (1987); Summons and Capon. (1988); Summons et al. (1988).
C_{27} rearranged/non-rearranged steranes (C_{27}βα (20S)/C_{27}ααα (20S))	m/z 217 and m/z 259 (GC/MS SIM) or m/z 372->m/z 217 metastable ion transitions.	Depositional environment: low value=non-clastic source rock.	Clay minerals presence may control the rearrangment of sterenes, which leads to diasterenes and thus to diasteranes. This ratio is often controled by source and maturity.	Rubinstein et al.(1975); Mackenzie et al. (1982a).

C_{29} ααα (20S/20S+20R)	m/z 217 (GC/MS SIM) or m/z 400->m/z 217 metastable ion transitions.	Maturity, ratio from 0-0.5 by the palaeotemperature of 80°C .	This ratio has been found to vary with increasing maturity. However low sterane isomerisation has been reported in oils.	Curiale et al. (1985)
αββ/αββ+ααα (C_{29} steranes)	m/z 218 and m/z 217 (GC/MS (SIM)	Maturity, ratio rises from 0-0.75 over the oil window	Abundance of αββ isomer increases relative to that of ααα isomer.	Mackenzie and Maxwell (1981).
Sum triaromatic (C_{26}-C_{28})/Sum triaromatic(C_{26}-C_{28})+Sum (C_{27}-C_{29}) monoaromatic steroid ratio (e.g. ARO ratio).	m/z 253 and m/z 231 for monoaromatic and triaromatic steroidal hydrocarbons.	Maturity, ratio rises from 0-0.9 over oil window.	This parameter has been found very useful for oil-source rock correlations. This parameter tends to decrease with increasing extent of secondary migration.	Mackenzie et al. (1981a); Hoffmann et al. (1984).
Cracking ratio of long-chain to short chain triaromatic steroidal hydrocarbons: C_{20}+C_{21}/sum(C_{26}-C_{28})	m/z 231 for triaromatic steroidal hydrocarbons.	Maturity.	This ratio increases with increasing maturity as a result of the cracking of the side-chain.	e.g. Seifert and Moldowan (1978).
MTSI1 and MTSI2: methylated triaromatic steroid indices determined as: 2-methyl+3-methyl/2-methyl+3-methyl+4-methyl-C_{21} and C_{22} methylated triaromatic steroidal hydrocarbons.	m/z 245 for methylated triaromatic steroidal hydrocarbons.	Maturity.	Both MTSI1 and MTSI2 have been very useful maturity parameters, particularly for marine sediments. Immature samples tend to contain high abundance of 4-methyl and 6-methyl, where the 2-methyl and 3-methyl are more abundant in mature samples due to their relatively high stabilities.	Lichtfouse et al. (1990).
Aromaticity ratios: benzene/n-hexane; toluene/n-heptane	gas chromatogram of the gasoline range (C_5-C_9) hydrocarbons.	Maturity and fractionation.	Aromatic hydrocarbons are ususually removed from oil by water washing.	Thompson (1983; 1987).

Paraffinicity ratios: n-heptane/methylcyclohexane; n-hexane/cyclohexane	gas chromatogram of the gasoline range (C_5-C_9) hydrocarbons.	Maturity.	N-alkanes abundance increase with increasing temperature.	Thompson (1983; 1987).
Paraffinicity indices: Isoheptane and Heptane values	gas chromatogram of the gasoline range (C_5-C_9) hydrocarbons.	Maturity.	Abundance of branched alkanes tends to increase with increasing maturity. Using the interval given by Thompson (1983), oils can be distinguished into biodegraded, normal and mature oils.	Thompson (1983).

Chapter 3 Geochemical characterisation and biological marker assessment of source, depositional environment and maturity of Pre-Jurassic sedimentary organic matter from the Ghadames-El Borma basin

3. Geochemical characterisation and biological marker assessment of source, depositional environment and maturity of Pre-Jurassic sedimentary organic matter from Ghadames-El Borma basin.

3.1. Introduction

This chapter is divided into three parts: the first is concerned with petrological descriptions of rock samples while the second contains organic geochemical data on potential source extracts. Sixty rock samples mostly shales ranging from Triassic to Ordovician in age, from the Ghadames-El Borma Basin (Figure 3.1) were examined using reflected and ultraviolet light microscopy (Appendix 3.1). Amorphous organic matter and Graptolites dominate the Ordovician strata, whereas the Silurian and Devonian contain predominantly liptinitic macerals such as acritarchs, *Tasmanites* and spores; bitumen is moderately abundant.

Rock-Eval and pyrolysis/gas chromatography (Py/GC) data in part 2, provides information on kerogen types and their maturity. Devonian, Silurian and Ordovician samples are considered potentially moderate to good source rocks. However, the Triassic rock samples have little oil potential (Appendix 3.2).

The third part of this chapter involves the application of biological marker distributions in the assessment of source, depositional environment and maturity of the sedimentary organic matter. GC, GC-MS/EI (SIM) and GC-MS/MRM analyses of the saturated hydrocarbon fraction together with principal component analysis (PCA) of sterane and terpane distributions allow a discrimination of samples into 3 main groups:

(i) Ordovician

(ii) Devonian and Silurian

(iii) Triassic

This information together with Chapter 4 will then be used in an oil-source rock correlation described in Chapter 5.

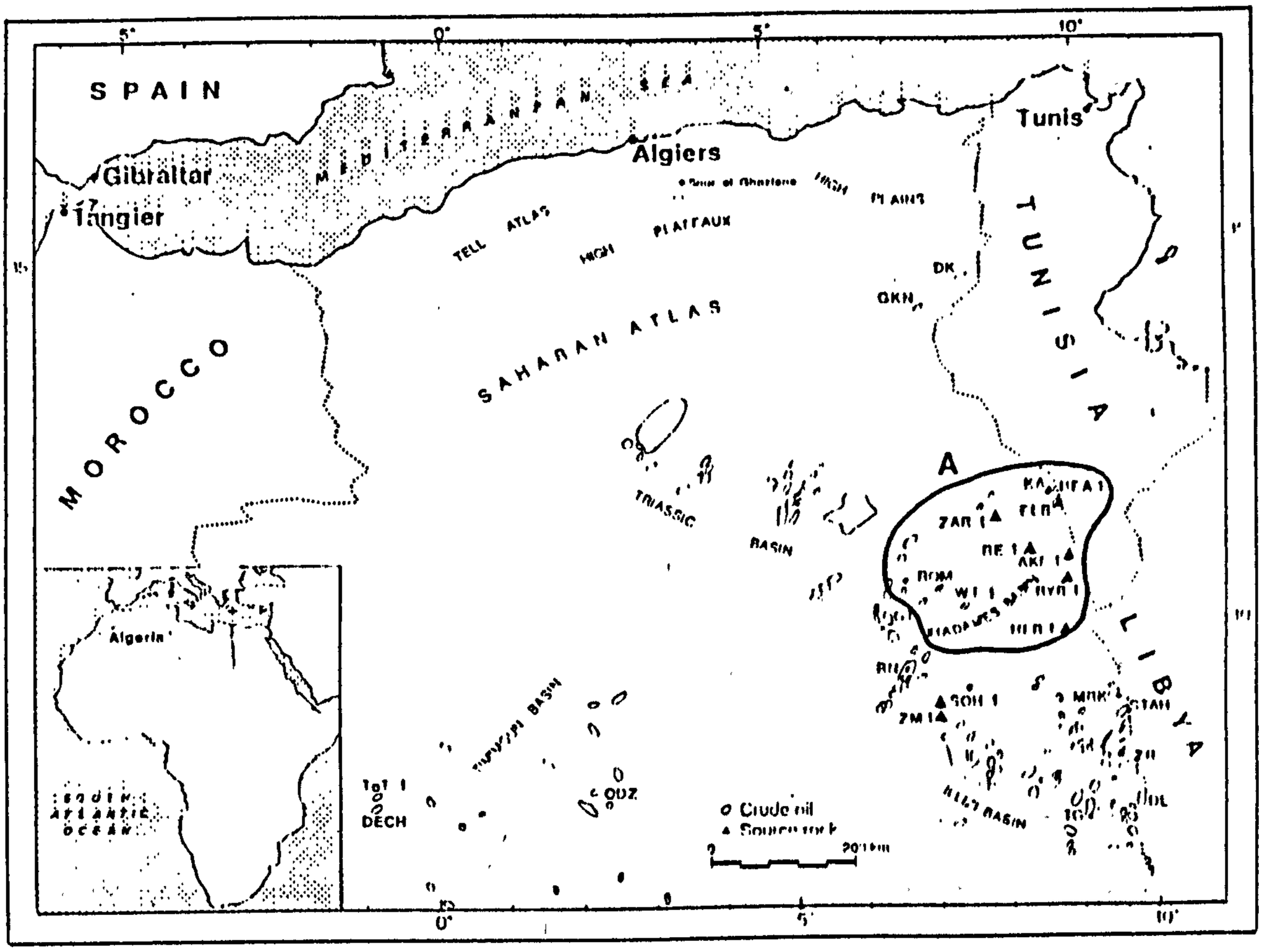

Figure 3.1 Sample location map of the area of study (A= the Ghadames-El Borma basin).

3.2. Petrological description of sediments

3.2.1. Introduction

During the present work, sixty rock samples from 12 boreholes (Appendix 3.1) were examined using reflected and ultraviolet light microscopy. In the absence of vitrinite, thermal maturity assessment was based on spore fluorescence of the liptinitic macerals present. Basically, the dominant organic material present consists of amorphous organic matter in the Triassic and graptolites as well as amorphous organic matter in the Ordovician (photographs N°4 and 5). Examination of argillaceous samples from the Devonian and Silurian shows that liptinitic macerals, especially alginite and sporinite are dominant (photographs N°1, 2 3 and 4). These are associated with abundant framboidal pyrite; which formed as a result of

bacterial reworking. Bacteria utilise the organic matter as an energy source and reduce sulphates to sulphides; in this situation, the organic matter is likely to be preserved (Tissot and Welte, 1984, pp 78).

For an assessment of biological marker distributions, thirty rock samples covering the maturity range VR/E= 0.45%-0.75% were selected.

3.2.2. Triassic

The Triassic sequences are of continental and lake sediments, which overlie in a transgressive and discordant manner the Palaeozoic strata (Figure 1.4 trace BB'). They formed a series called the continental intercalation, which is subdivided into two sections: the lower being argillaceous sandstone and the upper saliferous. The argillaceous sandstone discordantly overlie the eroded Carboniferous and even the Lower Devonian, particularly in the Dahar region of Keskessa and El Borma fields. This sequence includes sandstones, silstones and shales with thin sections of dolomite, marls and salt; anhydrite is present in thin layers. The thickness of the lower clastic series varies from 0 to 175m (Aliev et al., 1971).

The upper, saliferous series, consists of a thick salt with veins of argilites, anhydrite and dolomite. These sediments constitute a good impermeable cover for the retention of oil and gas accumulations (Aliev et al., 1971).

The Lower clastic section contains a moderate abundance of terrestrial organic material, represented by spores and other plant debris with a marine phytoplankton contribution. On the basis of spore fluorescence, KA-1 bis (2605.65m), ELB-3 (2372.20m) and AKF-1 (2250.06m-2252.80m) sequence has not yet reached the oil generation window (Appendix 3.1).

3.2.3. Carboniferous

Most of the Carboniferous sequences are characterised by a marine fauna, of Brachiopods, Crinoids, corals and calcacerous coccoliths (Sonatrach internal report, 1980). However, little work has been done on Carboniferous sediments in this research due to a lack of precise information on the stratigraphy.

3.2.4. Devonian

The Devonian sediments uncomformably overlie the Silurian, being deposited during a marine transgression which reached its maximum at the end of the Silurian and the beginning of the Devonian. During this period, there was a slow rate of sedimentation, where many regions in the Algerian Sahara have been uplifted then eroded, resulting with local unconformities particularly in the Illizi and Ghadames basins (Aliev et al., 1971). Lower Devonian sediments have been located in the north (RE-1), north east (RYB-1; HFR-1), south east (WT-1, STAH-1, MRK-1) of the basin. To the south, the sequence is made up of an alternation of shales and sandstones; the former constituting the main Devonian source rock and the latter the principal reservoir (F_3 and F_6). To the north, in the field RE-1, the thickness of these shales is 400m, containing a large amount of organic material, (varying between 1.00% and 10.8% of org.C, Appendix 3.2). The dominant organic material consists of alginite with subordinate amounts of sporinite (photographs N°1 and 2). Wisps of free hydrocarbons and bitumen staining are also present.

The fluorescence the organic material (RE-1, 3040.00m-3202.20m) indicates a lower maturity level for this succession than those at greater depth

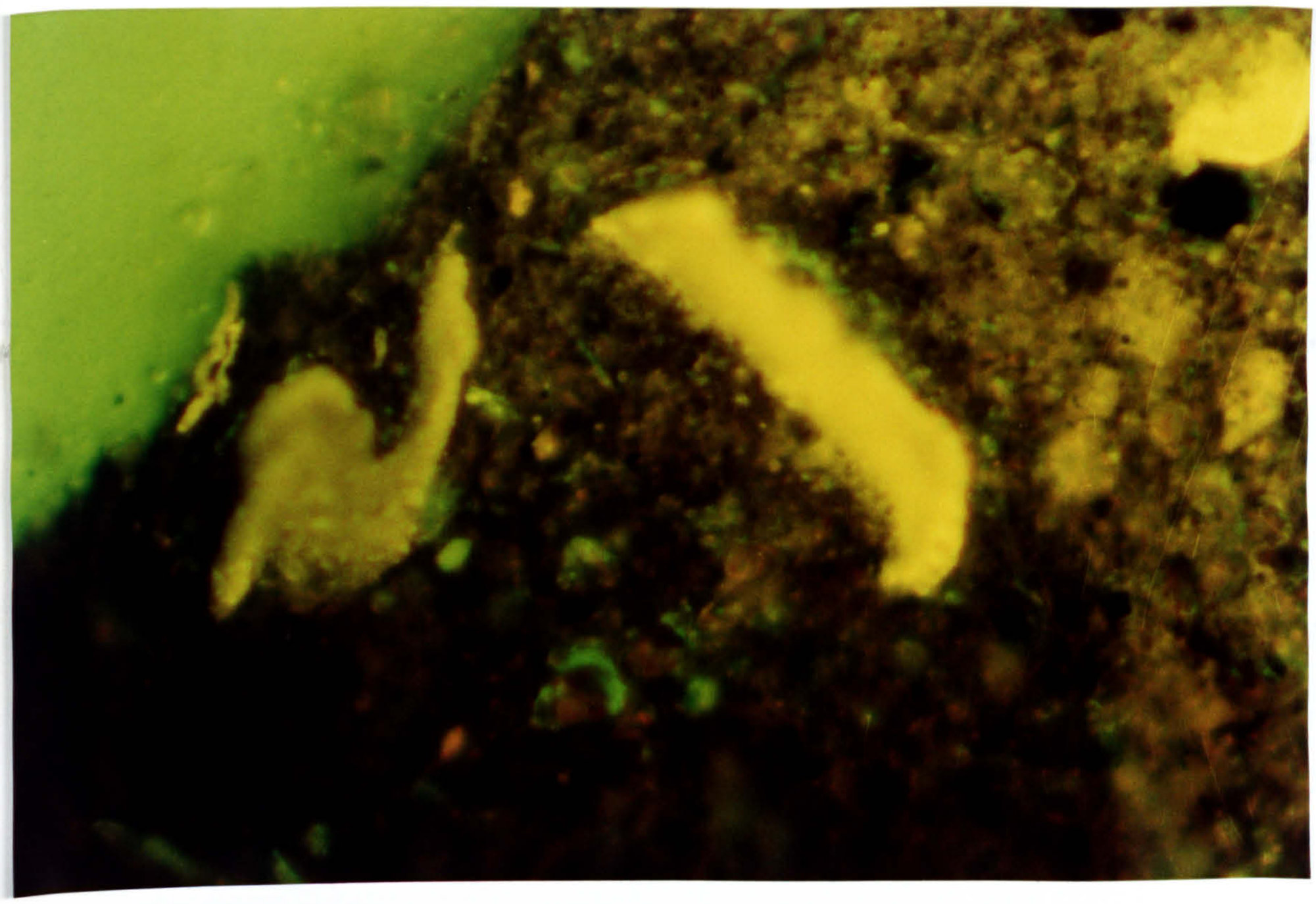

Photograph 1 Devonian sample (RE1, 3040.00m) in ultraviolet light showing algal bodies (block sample x 400).

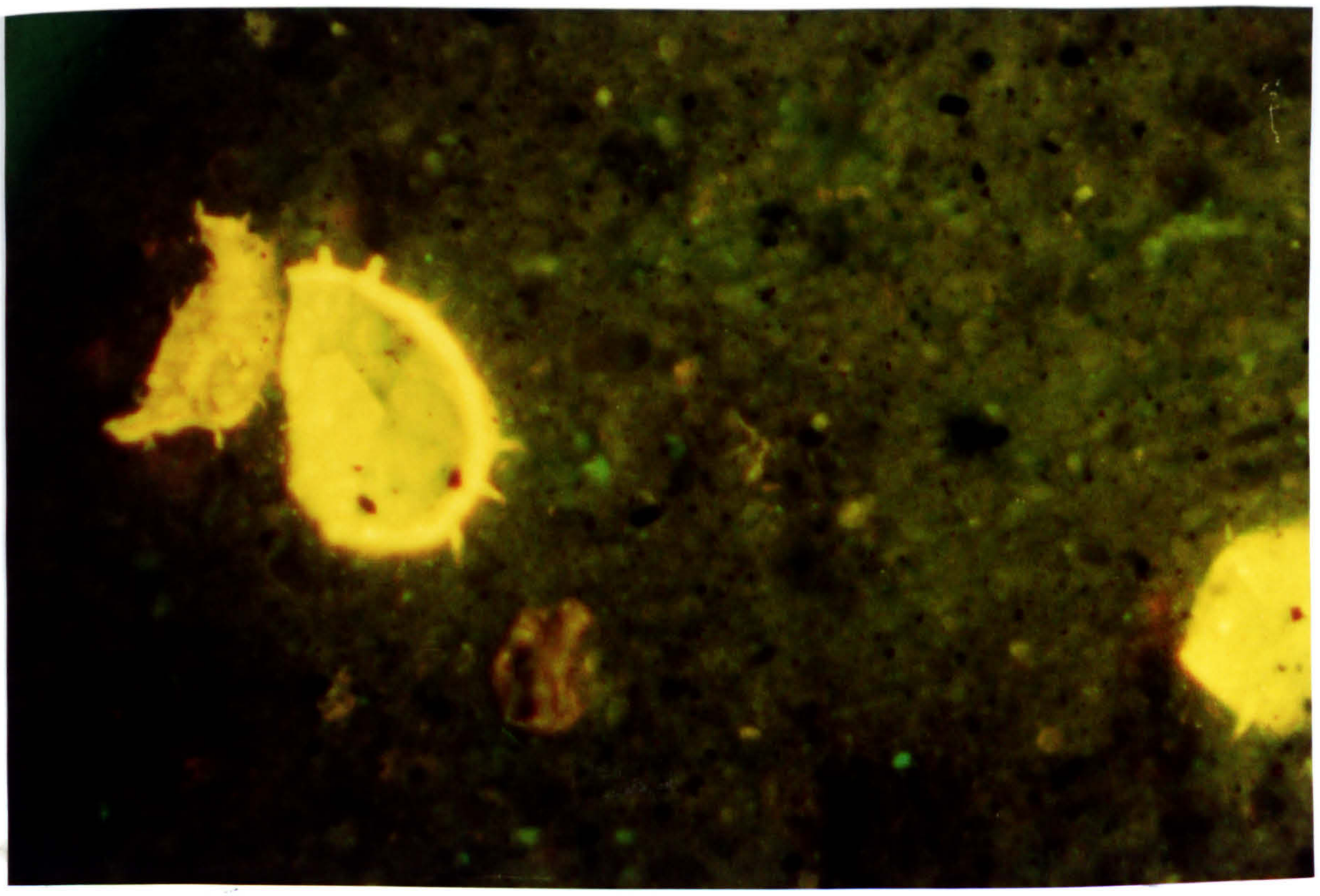

Photograph 2 Devonian sample (RE1, 3114.25m) in ultraviolet light showing acritarchs (block sample x 400).

(3346.20m-3438.26m). However, sediments from boreholes (WT-1, STAH-1, MRK-1) can be considered as overmature.

3.2.5. Silurian

Silurian shales rich in *Tasmanites* and Graptolites have been historically regarded as the best source rocks in the Algerian Sahara (Tissot et al., 1974b). The Silurian strata are represented by a thick layer of black, pyritic shale rich in organic material which overlie conformably the Ordovician. These beds of shales are present in the subsidence area of the Ghadames basin as well as in the Dahar arch and the Khalef structure of Keskessa, as located in KA-1 bis (3029.82m-3072.85m), SOH-1 (3192.50m-3398.40m) and ZM-1 (2388.40m-2483.58m) boreholes. Shales contain moderate to rich amounts of organic material, particularly algae *(Tasmanites*) and spores (photograph N° 3 and 4, ZM1 2388.75m) and can be considered to be a fair potential source facies for petroleum (Appendix 3.2).

3.2.6. Ordovician

Ordovician strata are represented by a sequence of shales and sandstones which lie discordantly on Cambrian sediments. These are regarded as good reservoirs in the Mereksen and Rhourd-Nouss regions, but to the north, the major part of the sequence has been eroded or was not deposited (Sonatrach internal report, 1980). Petrological observations (photographs N°5 and 6, ZM-1 2701.90m) reveal that the organic matter in boreholes ZM-1 (2674.90m-2701.90m) as well as MRK-1 (3196.46m-3309.45m), and KA-1 bis (3168.55m-3182.85m) is mature in ZM-1, becoming overmature in MRK-1 and KA-1 bis (Appendix 3.1).

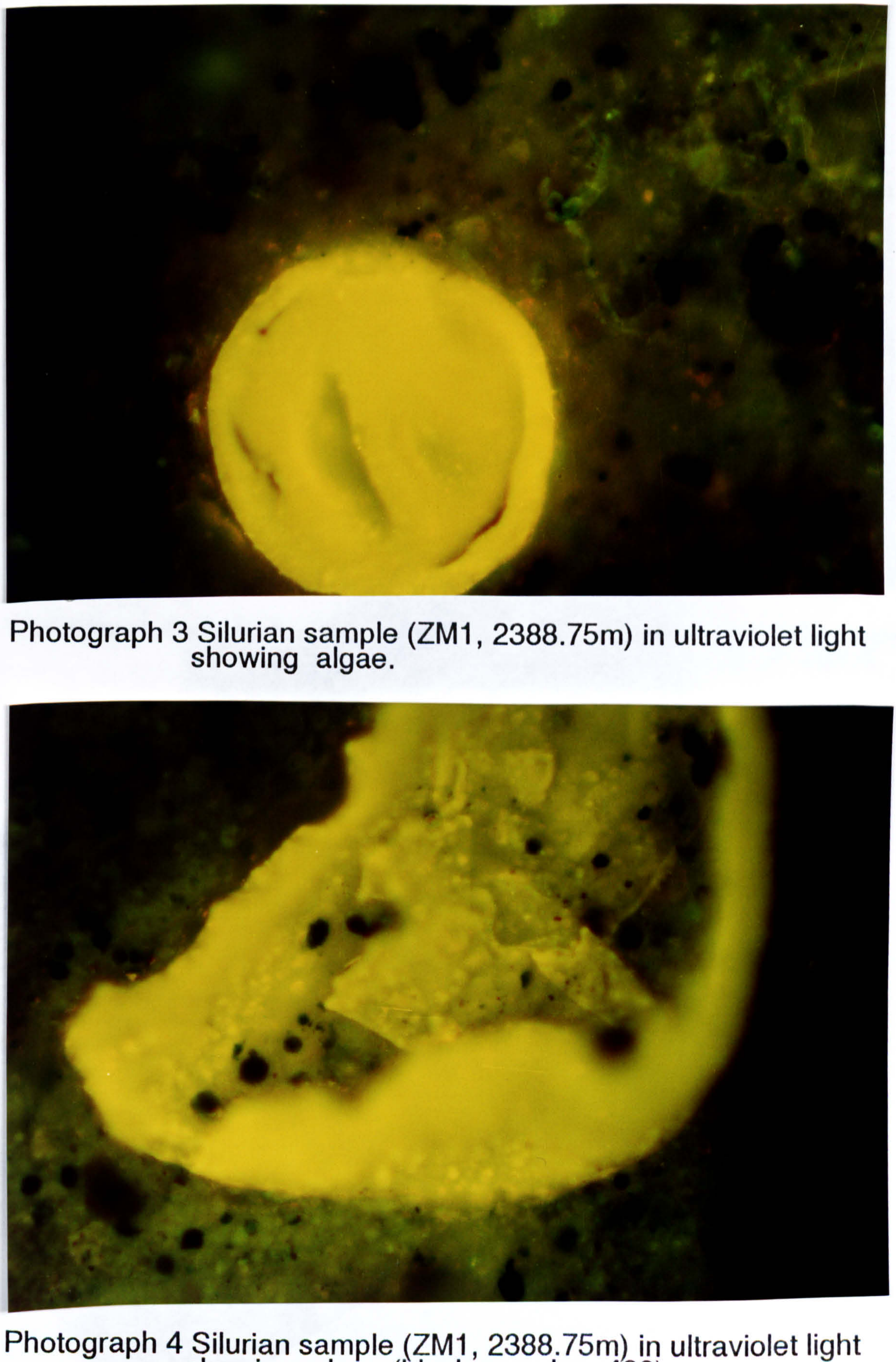

Photograph 3 Silurian sample (ZM1, 2388.75m) in ultraviolet light showing algae.

Photograph 4 Silurian sample (ZM1, 2388.75m) in ultraviolet light showing algae (block sample x 400).

3.3. Bulk geochemistry -results

3.3.1. Rock-Eval pyrolysis

The main parameters applied in this study are T_{max}, genetic potential (S_1+S_2), production index (S_1/S_1+S_2) and hydrogen index (HI, mg S_2/g org.C) (see Figure 2.1. Chapter 2). Rock-Eval and TOC data are listed in Appendix 3.2. During pyrolysis, certain anomalous data from Rock-Eval parameters could be obtained due to contaminants, lithological and heating rate effects. These are discussed in the following section.

3.3.1.1. Genetic potential parameter

Tissot and Welte (1984, pp 513) introduced a parameter S_1+S_2, called genetic potential and gave the following classifications according to its value:

lower than 2kgt^{-1} no oil source rock, some potential for gas

from 2-6kgt^{-1} moderate source rock

above 6kgt^{-1} good source rock

This parameter may be influenced by migrated hydrocarbons.

3.3.1.2. The production index

This is expressed as the ratio of the amounts of generated hydrocarbons by the kerogen to the genetic potential:

S_1/S_1+S_2 production index. Hence, with increasing maturity, this ratio increased due to high amounts of hydrocarbons released by the kerogen. However, this ratio can be influenced by migrated hydrocarbons and adsorption of bitumen on clay minerals (Peters, 1986; Langforth and Blanc Valleron, 1990).

3.3.1.3. T_{max}

T_{max} is defined as the peak temperature of hydrocarbon generation during pyrolysis. T_{max} values vary with heating rate. Therefore, comparison should be based on results obtained in similar pyrolysis conditions. T_{max} is found to be dependent on the kerogen type. Thus, type I and II kerogen exhibit a higher T_{max} than type III kerogen at a given maturity level. At higher maturity, T_{max} can reach similar values for all the various kerogen types (Espitalié et al., 1977).

3.3.1.4. Hydrogen index (HI mg HC/g org.C)

Kerogen type is characterised using hydrogen index (HI), which is defined as as HI= $\frac{S_2 \text{ (mg HC/g org.C)}}{\text{wt \% organic carbon (org.C).}}$

This parameter was reported to be affected by maturity and adsorption of organic material on clay minerals (Peters, 1986; Langforth and Blanc Valleron, 1990).

The two Triassic rock samples analysed show low genetic potential ratios ($S_1+S_2< 2kgt^{-1}$) and low Tmax values (Appendix 3.2), which are consistent with vitrinite reflectance equivalent (VR/E=0.45%). Hence, Triassic rock samples can be considered as immature and poor producing source rocks.

On the contrary, Devonian source rocks are classified as good to excellent type II kerogen, with extremely high genetic potential ratio reaching $71kgt^{-1}$, particularly for borehole RE-1 (3346.20m-3354.40m). RE-1 samples

(3040.00m-3438.26m) have T_{max} values, which cover a wide range of oil generation window.

Silurian samples, particularly those from KA-1 bis (3029.82m-3072.85m), ZM-1 (2388.75m) and ZAR-1 (3994.65m) boreholes can be characterised as moderate source rocks of type II kerogen (Appendix 3.2).

Only one Ordovician sample (ZM-1, 2701.90m) is classified as type II kerogens with good potential for oil, I.e S_1+S_2> 6kgt^{-1} (Appendix 3.2), while mature samples exhibit low transformation ratios and hydrogen index values (S_1/S_1+S_2 and HI mg HC/g org.C).

3.3.2. Pyrolysis/gas chromatography (Py/GC)

Flash pyrolysis/gas chromatography (Py-GC) was applied for kerogen typing (Larter et al., 1978; Solli et al., 1985). This procedure is very useful for kerogen typing in sedimentary rocks for elucidation of the chemical composition of kerogen pyrolysates. A polymeric compound, the poly-tertiary butylstyrene (Poly-t-butylstyrene) was used as an internal standard for absolute quantification of the concentrations of the various pyrolysate components released from kerogen (Larter, 1985; Larter and Senftle, 1985; Φygard et al., 1988).

In Figure 3.2 are displayed the pyrograms of four kerogen pyrolysates from the Triassic, Devonian, Silurian and Ordovician source rocks respectively. Most of the pyrolysates show an abundance of a homologous series of normal hydrocarbons (*n*-alkene and *n*-alkane doublets) from C_7 to C_{30} carbon number and low amounts of aromatic hydrocarbons (I.e alkylaromatic

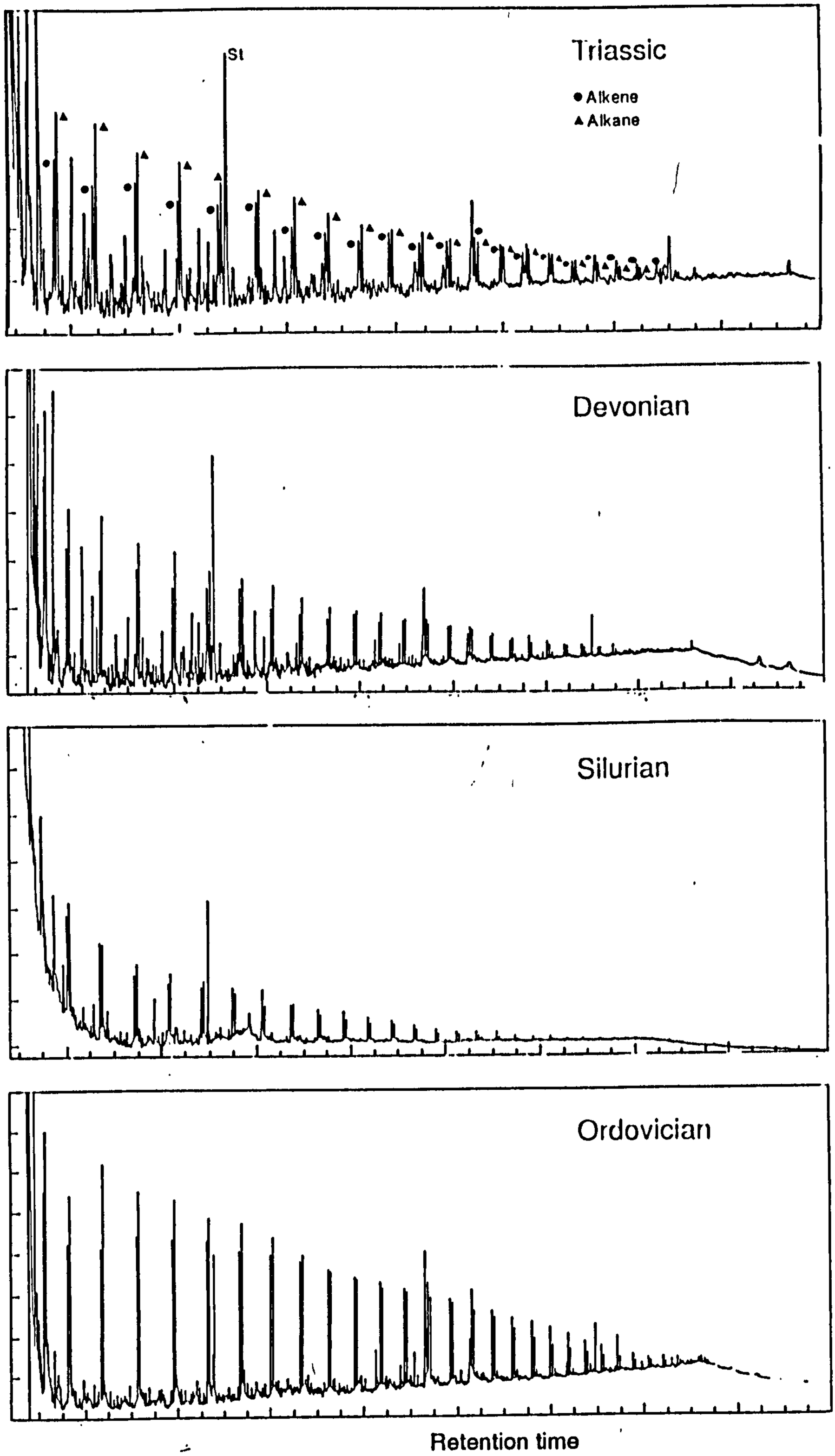

Figure 3.2 displays the pyrograms of four kerogen pyrolysates from the Triassic (KA-1 bis 2605.65m), Devonian (RE-1 3114.70m), Silurian (KA-1 bis 3029.82m) and Ordovician (ZM-1 2701.90m) samples.

compounds). Peak assignments have been made by comparison with published Py-GC traces (Larter, 1985; Larter and Senfle, 1985; Φygard et al., 1988).

Ordovician sample exhibits high abundance of aliphatic (*n*-alkene and *n*-alkane doublets) and relatively lower contents of alkylaromatic hydrocarbons, (i.e toluene, ethylbenzene, meta-, para- and ortho xylenes) compared to Triassic, Devonian and Silurian samples. However, isoprenoids e.g prist-1-ene was relatively minor. Sulphur containing compounds were not detected by flame photometric detector (FPD) except H_2S.

Figure 3.3 illustrates the correlation of the sum of the normal hydrocarbon yields in the range of C_9-C_{25} (i.e Paraffin index, PI) and the hydrogen index (HI) as suggested by Larter (1985; see Figure 1.10) for kerogen typing. This shows that the kerogen samples in this study can be characterised as being either type II paraffinic-naphthenic or type II-III paraffinic, with a discrimination of Ordovician from Triassic, Devonian and Silurian source rocks.

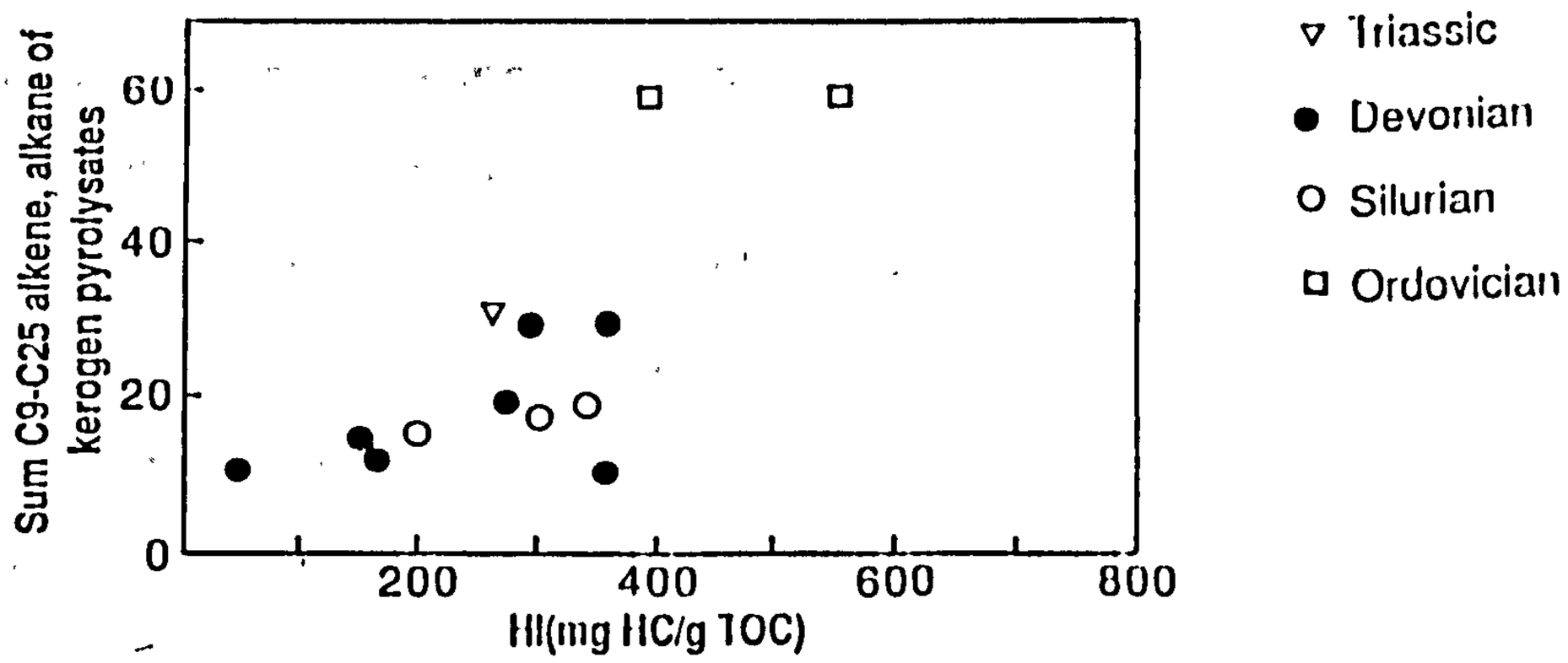

Figure 3.3 Normal aliphatic hydrocarbons from Py/GC data as a function of hydrogen index.

3.4. Bulk geochemistry- discussion

The organic matter for the Devonian, Silurian and Ordovician samples has been shown by optical, and Rock-Eval data to be anywhere between marginally mature and mature (Appendix 3.2 and 3.3). They are considered from the above data as good to excellent type II source rocks. The Triassic, however, can only be considered as being of poor source quality. The low hydrogen index (Appendix 3.2), suggests classification as a mixed type II-III kerogen.

Rock-Eval data and Py-GC of isolated kerogens (Larter, 1985; Larter and Senftle, 1985) reveal that the samples

can be resolved into 2 populations:

(i) Ordovician,

(ii) Triassic, Devonian and Silurian.

This type of feature can be dependent on both source and maturity of organic matter.

3.5. Bulk composition- results

3.5.1. Bitumen extraction and fractionation

The results of the bulk composition of bitumens are listed in Appendix 3.3. Among the methods used for evaluating the organic content was the determination of the amount of extractable organic matter (EOM) as a percentage of the whole rock and the ratio of EOM to the total organic carbon (EOM mg/g org.C). This parameter is termed the transformation ratio (Tissot and Welte, 1984, pp 521).

The two Triassic samples reveal a low transformation ratio (54-89mg/g org.C). This suggests that the Triassic samples are poor source rocks. It is interesting to point out that the Triassic source extracts contain high contents of free, crystallised, elemental sulphur. They also exhibit relatively similar abundances of saturated and aromatic hydrocarbon fractions (Appendix 3.3, Figure 3.4).

Amongst ten Devonian samples, two from RE-1 (3040.00m-3050.25m) are classified as fair, four from RE-1 (3114.70m-3202.26m); ZAR-1 (3450.98m); SED-1 (2642.00m) boreholes as good and four from RE-1 (3346.20m-3438.26m) and RYB-1 (3106.30m-3110.20m) boreholes as excellent source rocks for oil potential. They contain moderate to high saturated relative to aromatic hydrocarbons (Appendix 3.3).

Most of Silurian samples from ZM-1, KA-1 bis and ZAR-1 boreholes contain moderate to high contents of extracts and are classified as fair to good source rocks for oil potential (Appendix 3.3).

Ordovician samples are considered as good source rocks for oil potential (Appendix 3.3). One sample (ZM-1, 2701.90m) exhibits relatively high amounts of extractable organic matter and saturated relative to aromatic hydrocarbons, which are reflected by high amorphous organic matter.

Silurian and Devonian samples are shown to have relatively similar gross chemical composition, being more abundant in saturated hydrocarbon fractions; optical evidence reveals that Devonian, Silurian and Ordovician

sediments are rich in algal bodies and hence highly hydrogen-rich source-rocks.

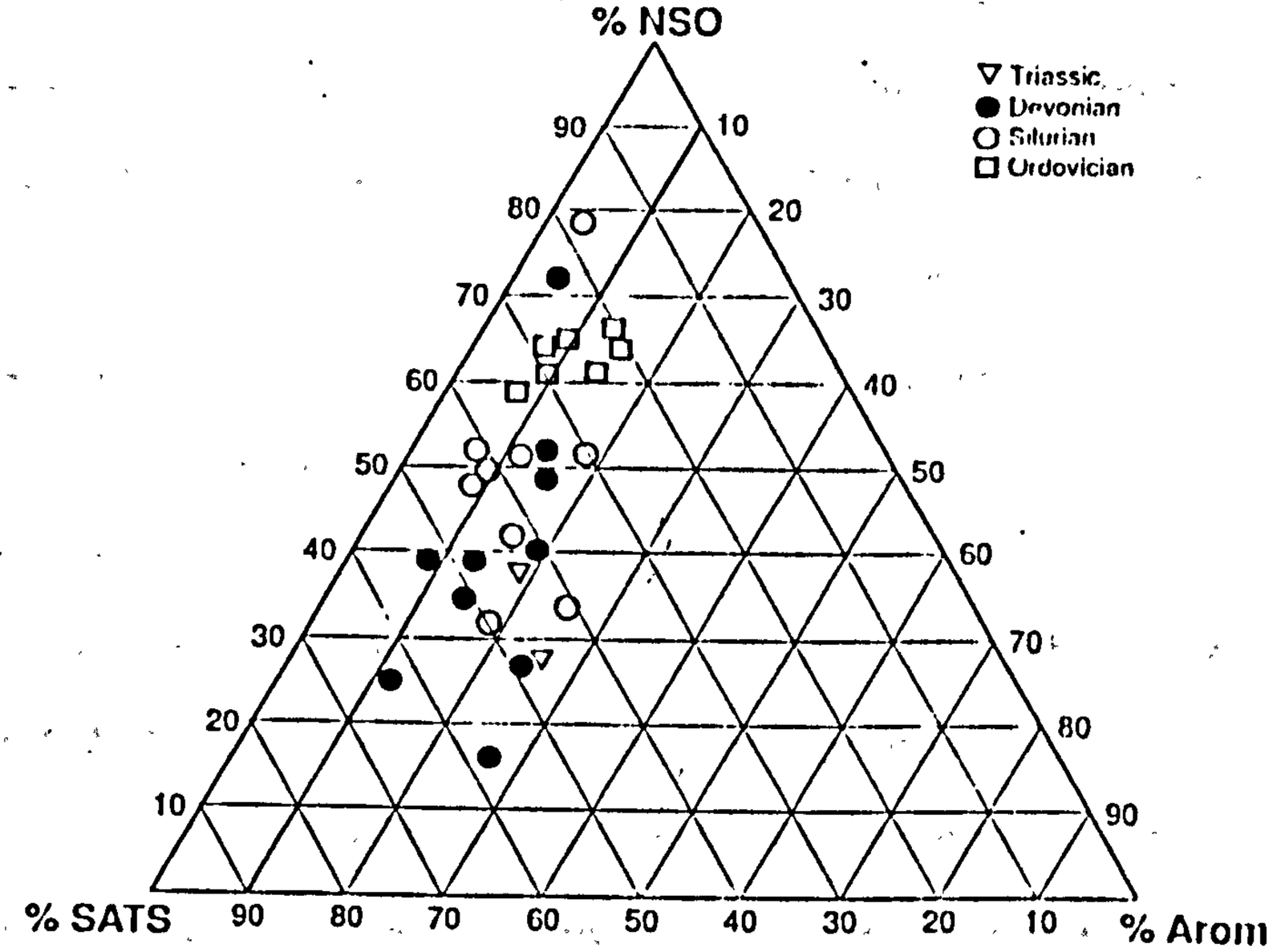

Figure 3.4 Relative proportions of saturated, aromatic hydrocarbons and NSO compounds of source extracts.

3.6. Bulk composition Discussion

There is a trend towards high saturated hydrocarbon contents (up to 68% weight), particularly for Ordovician samples. On the contrary, Triassic samples contain the lowest amounts of saturated hydrocarbons, whereas Devonian and Silurian samples are moderately abundant in aliphatic hydrocarbons.

3.7. Molecular organic geochemistry- Results

3.7.1. Triassic

3.7.1.1. Saturated hydrocarbon fraction

The gas chromatograms for the saturated hydrocarbon fractions of Triassic samples (Figure 3.5a and b) display bimodal distributions, which are dominated by a range of C_{13} to C_{35} *n*-alkanes with slight maxima at *n*-C_{15}, *n*-C_{17}, *n*-C_{19}, *n*-C_{23} and *n*-C_{27}. Waxy high molecular weight *n*-alkanes are prominent although the carbon preference index is close to unity (Appendix 3.3).

Acyclic isoprenoid compounds are present in high abundance (C_n<C_{20}). The GC-MS results of the non-adduct fraction (Figure 3.6), reveal the presence of C_{15}, C_{16}, C_{18}, C_{19} and C_{20} isoprenoids. Peak identification has been made by comparison of the mass spectra (Figure 3.7) with published data (Philp, 1985).

The pristane/phytane ratio (Pr/Ph) varies from 0.8 to 1.08. Pr/*n*-C_{17} and Ph/*n*-C_{18} ratio values are close to one (Appendix 3.3).

N-alkylcyclohexanes and methyl-*n*-alkylcyclohexanes were detected in the range of C_{12}-C_{23} in all samples by monitoring m/z 83 and m/z 97 respectively (Figure 3.8). Identification of compounds has been made by comparison of their mass spectra (Figure 3.9) with published data (Rubinstein and Strausz, 1979; Fowler et al., 1986). Higher homologues C_{21}+ methyl-*n*-alkylcyclohexanes are present in low concentrations. Methyl-*n*-alkylcyclohexane distribution appears to be more complex than that of *n*-alkylcyclohexanes due to the presence of 2-, 3- and 4-methyl-1-*n*-alkylcyclohexane isomers.

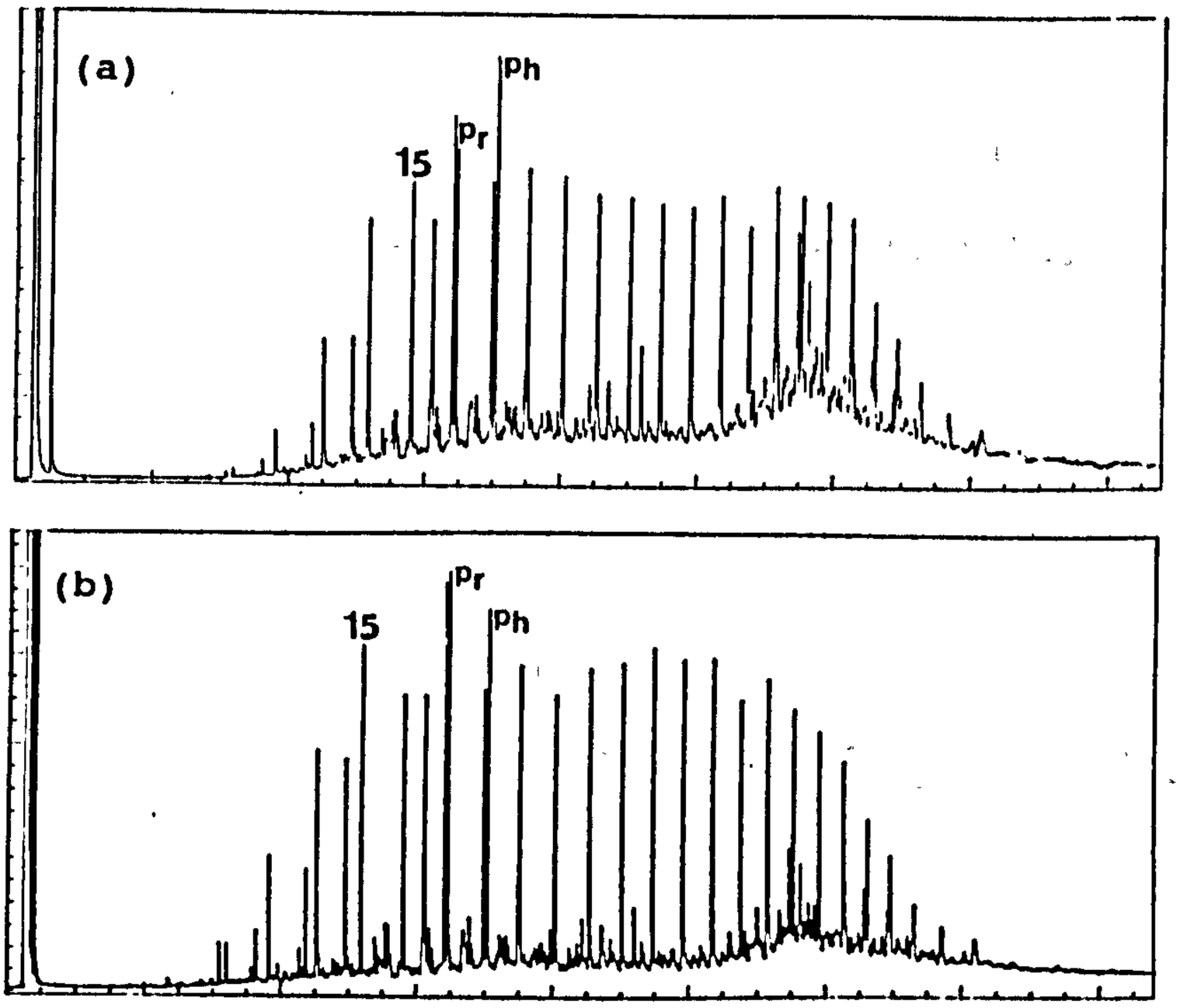

Figure 3.5 Gas chromatograms illustrating the saturated hydrocarbon distributions of two Triassic samples: (a) KA-1 bis (2505.65m), (b) ELB-3 (2372.20m). Cyclic compounds are present in both samples. *N*-alkanes are labelled with their carbon number. Pr= pristane, Ph= phytane.

PAGE
MISSING
IN
ORIGINAL

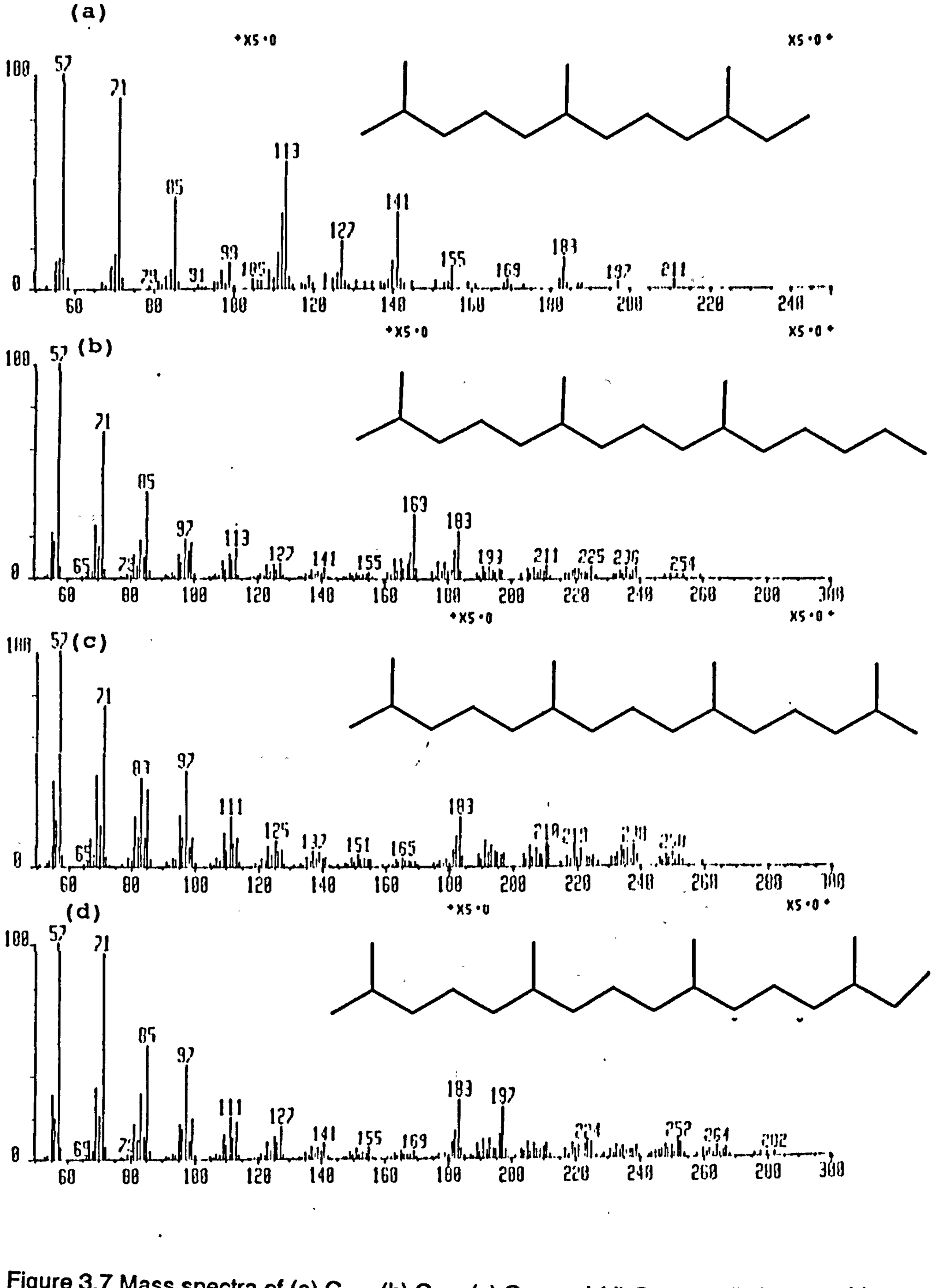

Figure 3.7 Mass spectra of (a) C_{15}, (b) C_{18}, (c) C_{19} and (d) C_{20} acyclic isoprenoid hydrocarbons.

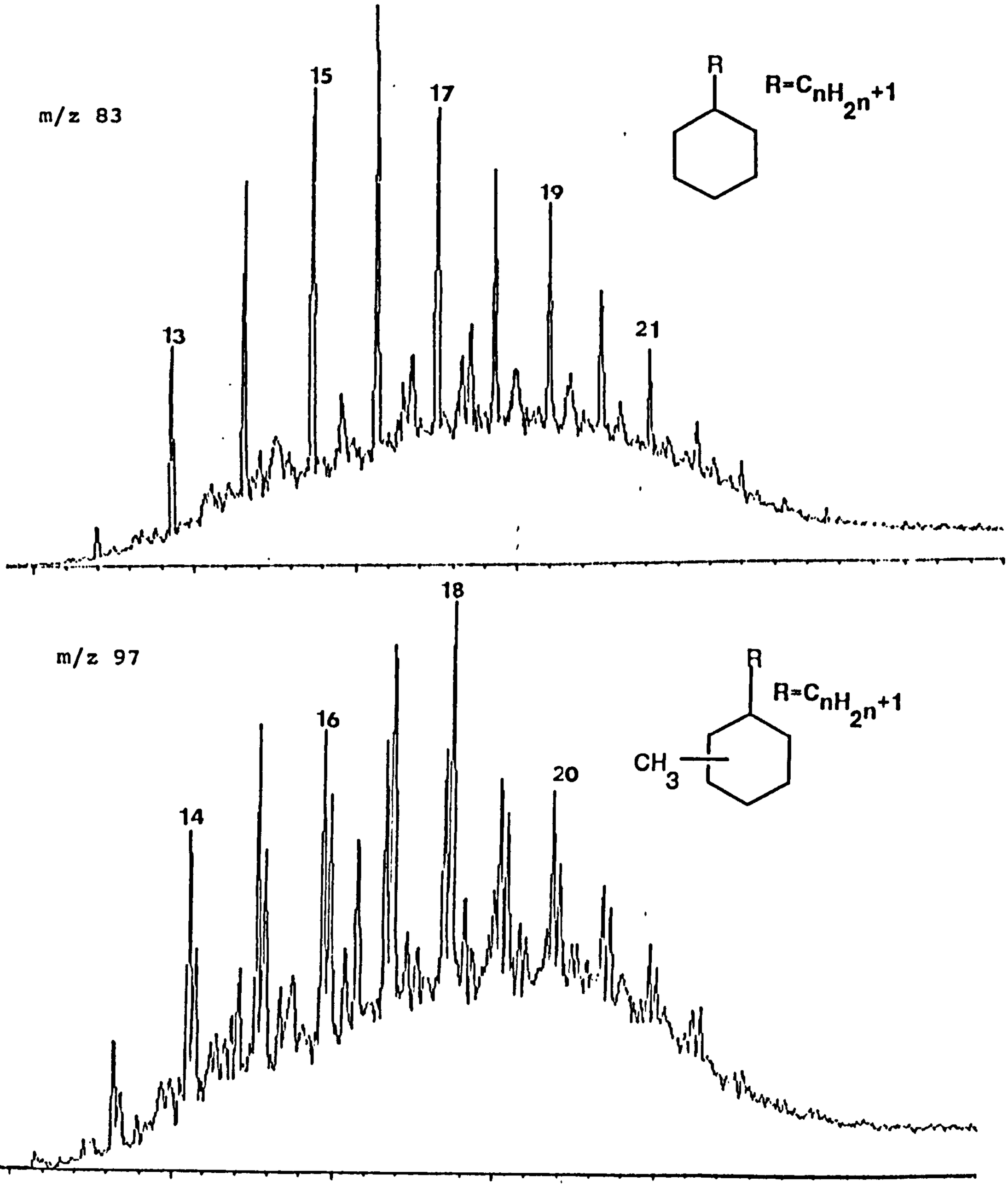

Figure 3.8 An example of *n*-alkylcyclohexanes (m/z 83) and methyl-*n*-alkylcyclohexanes (m/z 97) of a non-adduct saturated hydrocarbon fraction for one selected source extract. Peak are labelled with their carbon number.

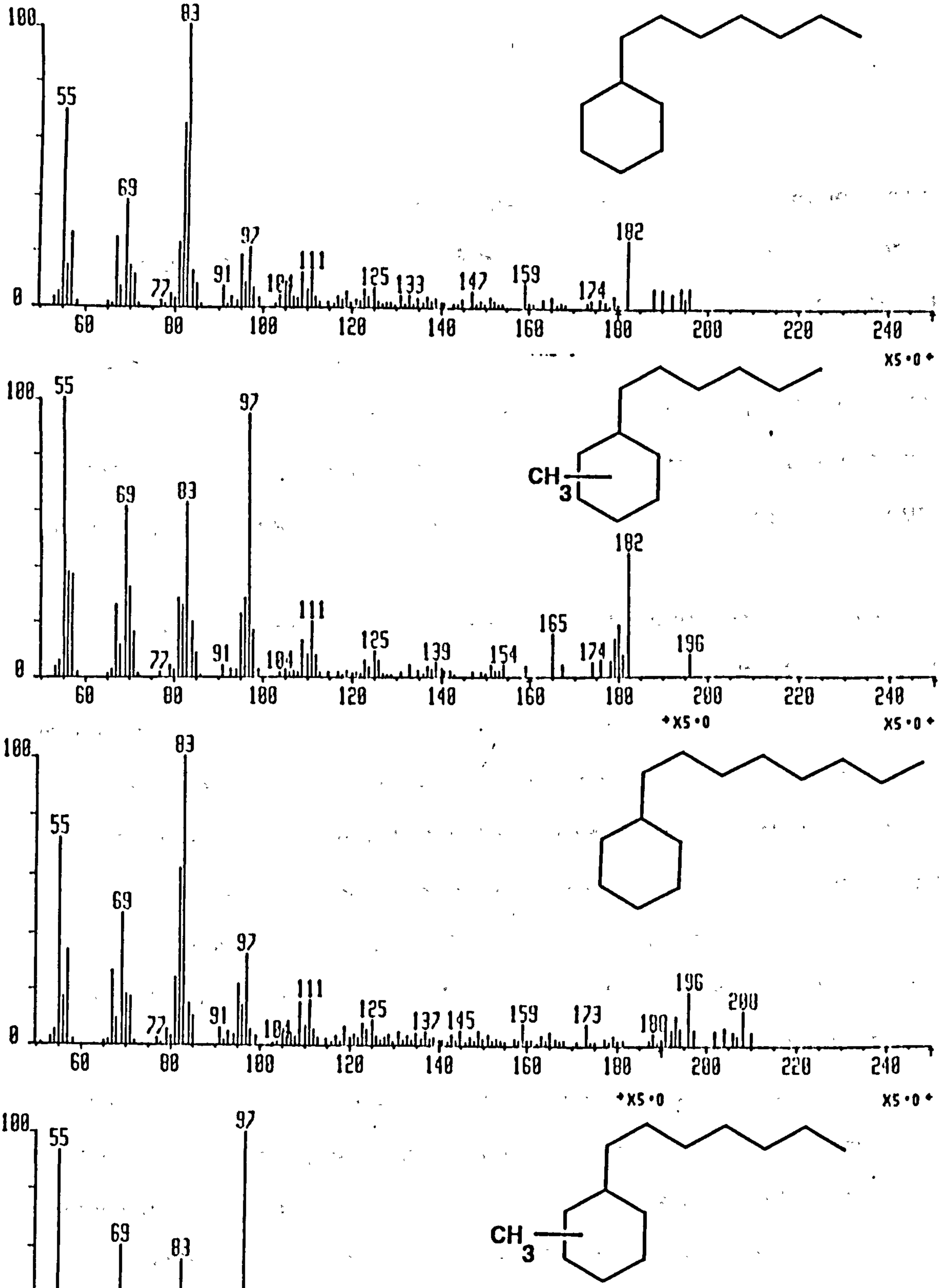

Figure 3.9 Mass spectra of *n*-alkylcyclohexanes (m/z 83) and methyl-*n*-alkylcyclohexanes (m/z 97) in Figure 3.9. (a) $C_{13}H_{26}$, m/z 83 (b) $C_{13}H_{26}$, m/z 97 (c) $C_{14}H_{28}$, m/z 83 (d) $C_{14}H_{28}$, m/z 97.

Sterane and terpane distributions of Triassic samples were determined using both electron impact (EI) and GC/MS metastable reaction ion monitoring (MRM) mass spectrometry. Peak assignments of steranes and terpanes are listed in Table 1 and 2 respectively.

Figure 3.10 and 3.11 display the sterane distributions using GC/MS (SIM) and MRM analyses of Triassic samples, and are dominated by rearranged steranes with a predominance of C_{29} members, as illustrated in Figure 3.12a and 3.12b).

C_{30} steranes were not detected, while C_{30} methylsteranes were observed from the metastable ion reaction monitoring of transition m/z 414-> m/z 231 (Figure 3.13a). C_{30} methylsteranes have been identified by comparison with published data and by coinjection with authentic standards (Summons et al., 1987; Summons and Capon, 1988). Peak assignments are listed in Table 1. It is worth noting the presence of a combination of 24-ethyl-2α-methyl- and 24-ethyl-3β-methyl-5α(H),14α(H),17α(H)-cholestane (e.g 2α-methyl-ααα, 3β-methyl-ααα steranes) in the Triassic samples. However, both isomers were not separated under used GC conditions. Peak 33 has been reported as 4-methyl sterane (Requejo, 1991). However, coelution with C_{30}-ααα (20R) cannot be ruled out (Summons, pers. comm.). Rearranged methylsteranes (peak N° 27 and 28) are relatively less abundant than non-rearranged members. They have been tentatively identified as 24-ethyl-13β(H),17α(H)-3β-methyl and 24-ethyl-13β(H),17α(H)-3β-methyl-cholestane (20S) and (20R) respectively (Summons and Capon, 1988; Requejo, 1991).

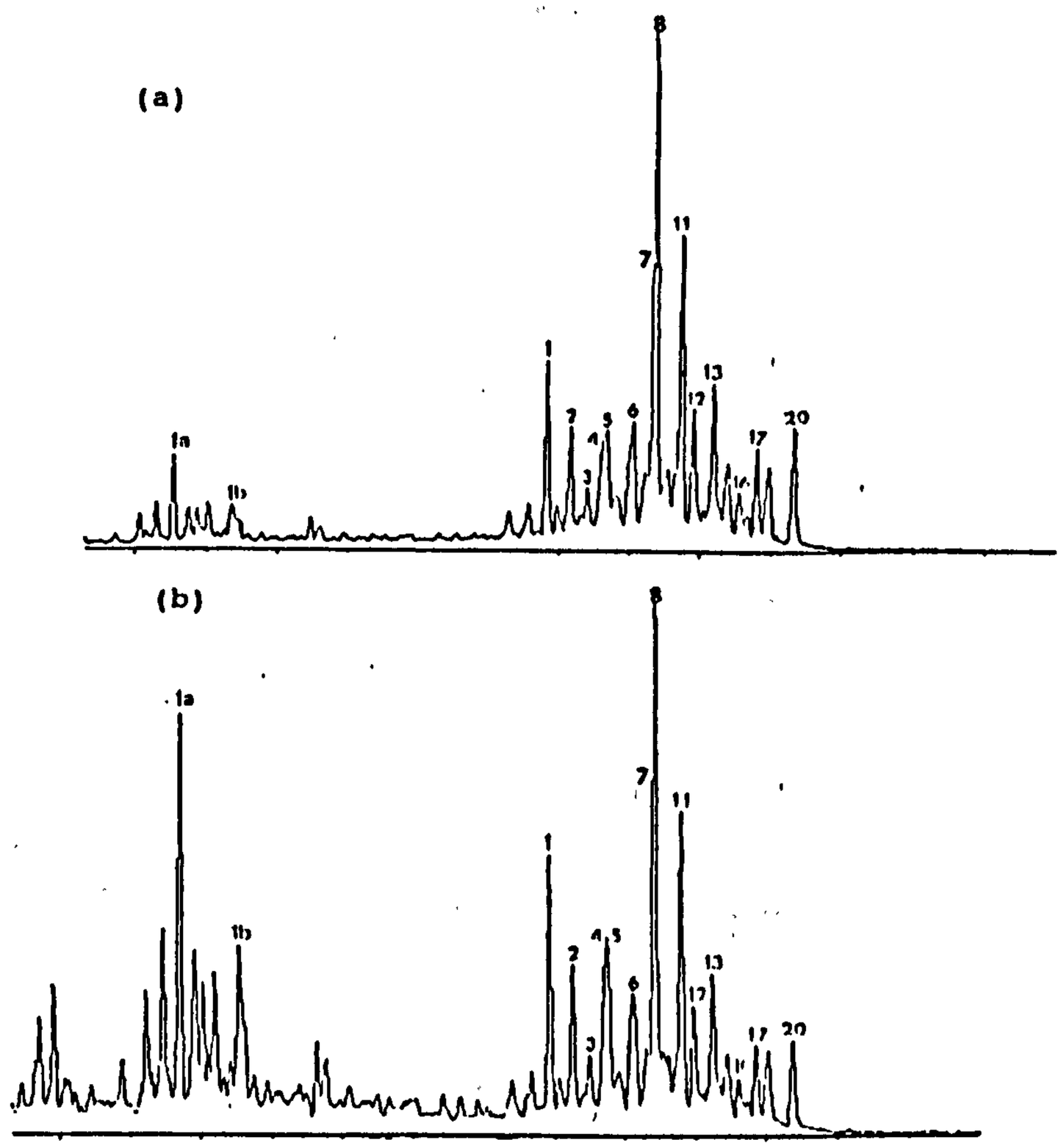

Figure 3.10 m/z 217.1950 mass chromatograms illustrating the sterane distributions of two Triassic source extracts: (a) ELB-3 (2372.20m), (b) KA-1 bis (2605.65m). Peak assignments are listed in Table 1.

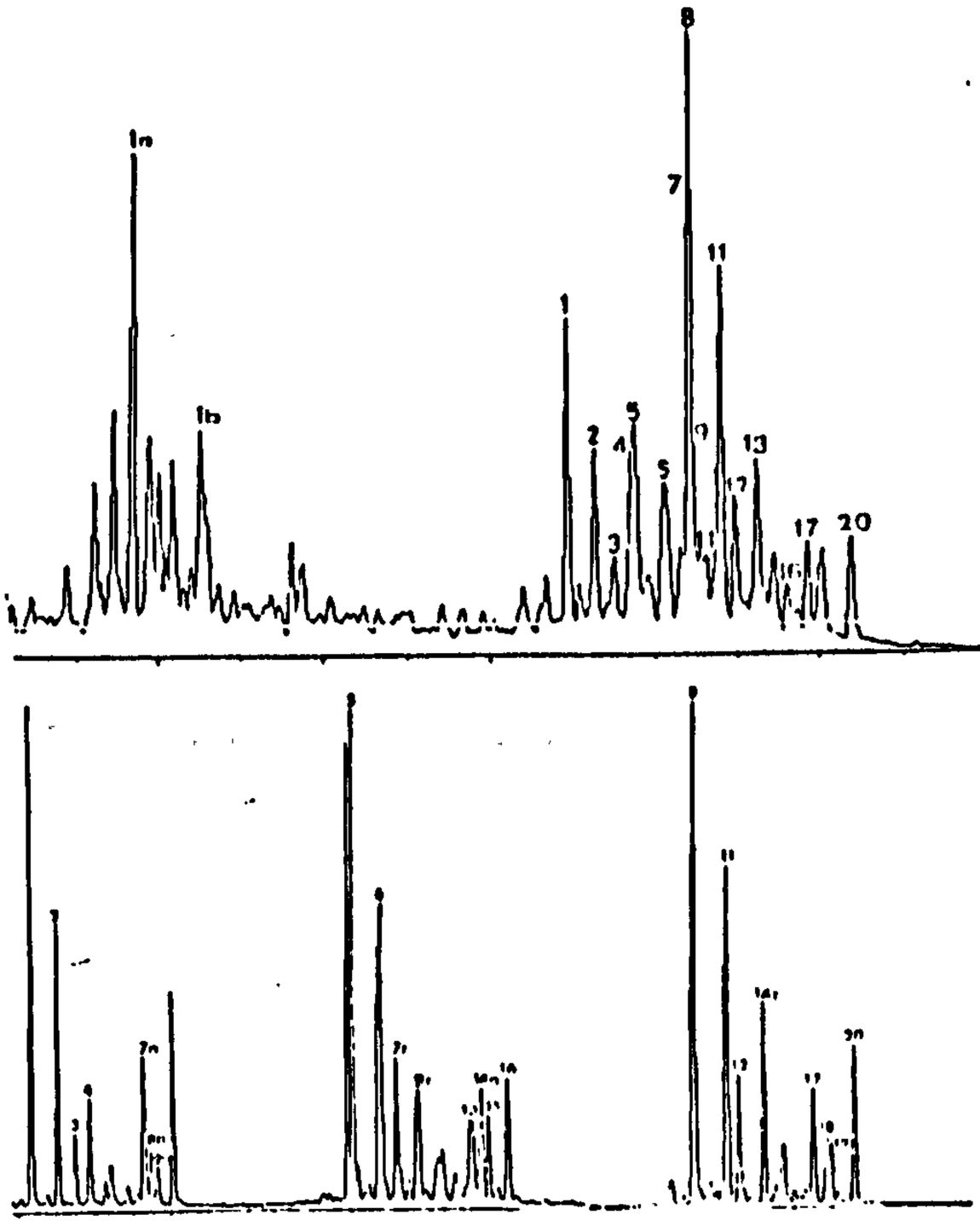

Figure 3.11 Monitoring steranes using GC/MS/EI SIM of (a) 217.1950 mass chromatogram and GC/MS/metastable ion reaction monitoring of transitions (b) m/z 372->217, (c) m/z 386->217 and (d) m/z 400->217 for one selected Triassic sample: KA-1 bis 2605.65m. Peak assignments are listed in Table 1.

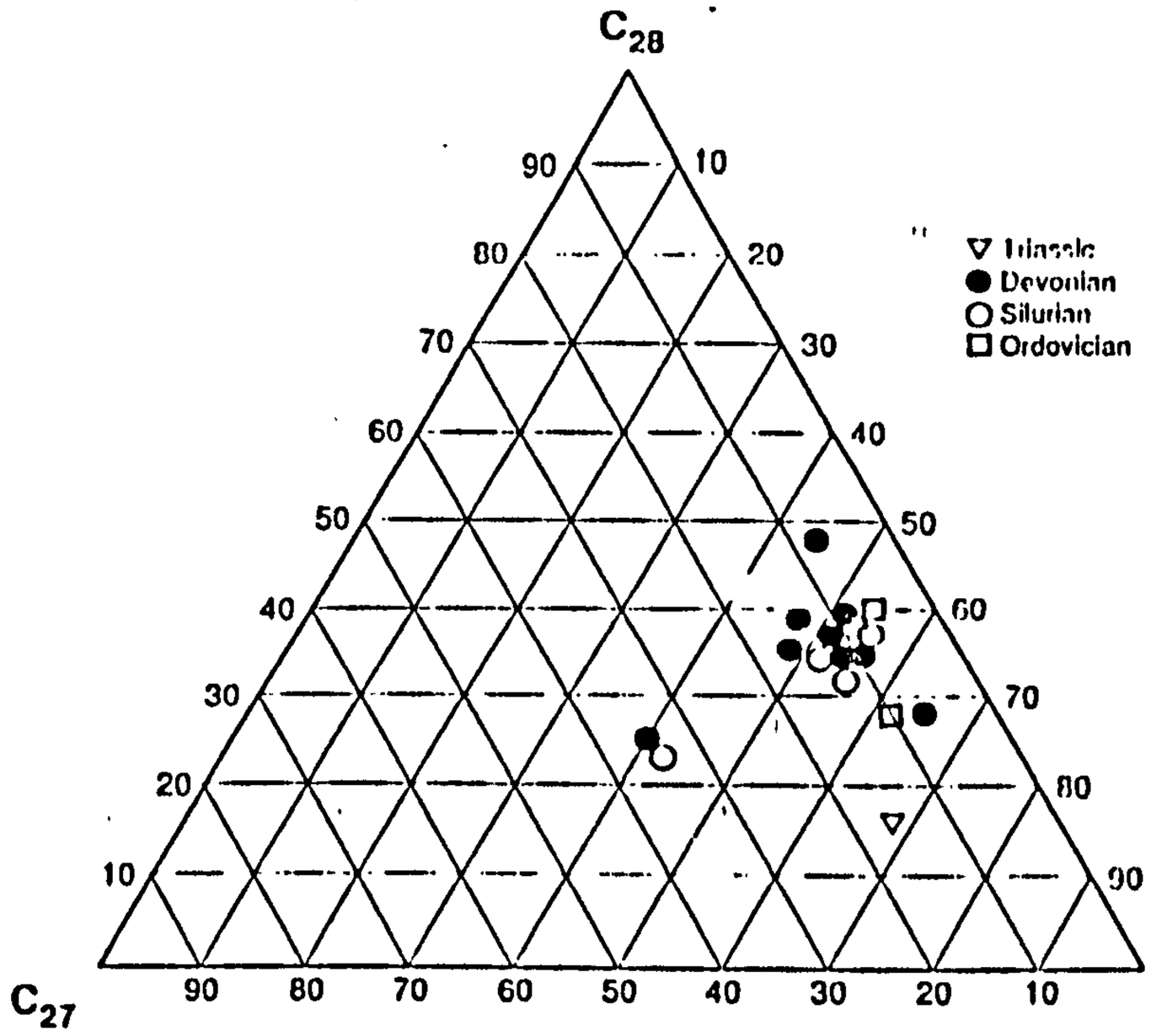

Figure 3.12a Relative proportions of non-rearranged (C_{27}-C_{29}) steranes.

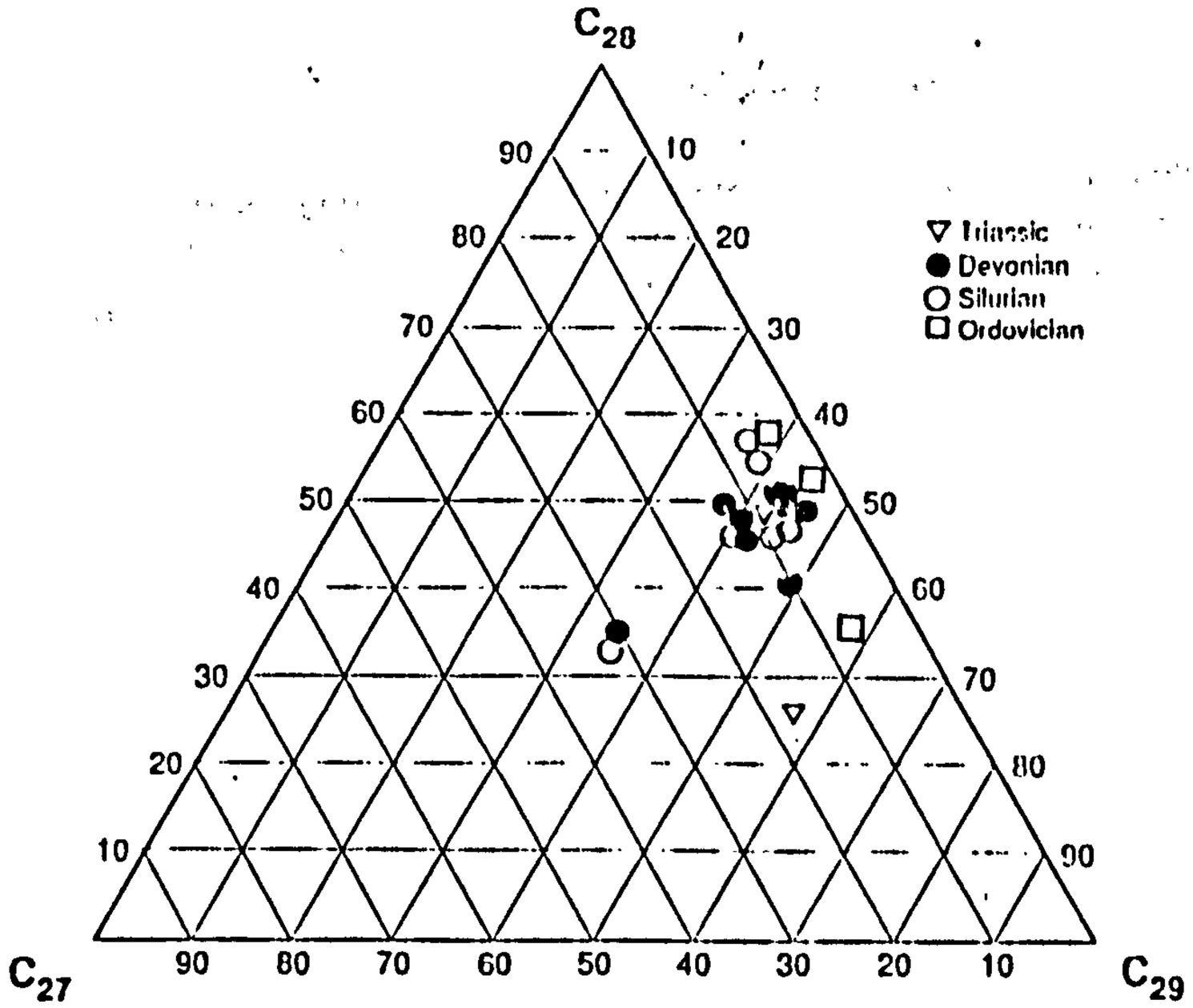

Figure 3.12b Relative proportions of rearranged (C_{27}-C_{29}) steranes.

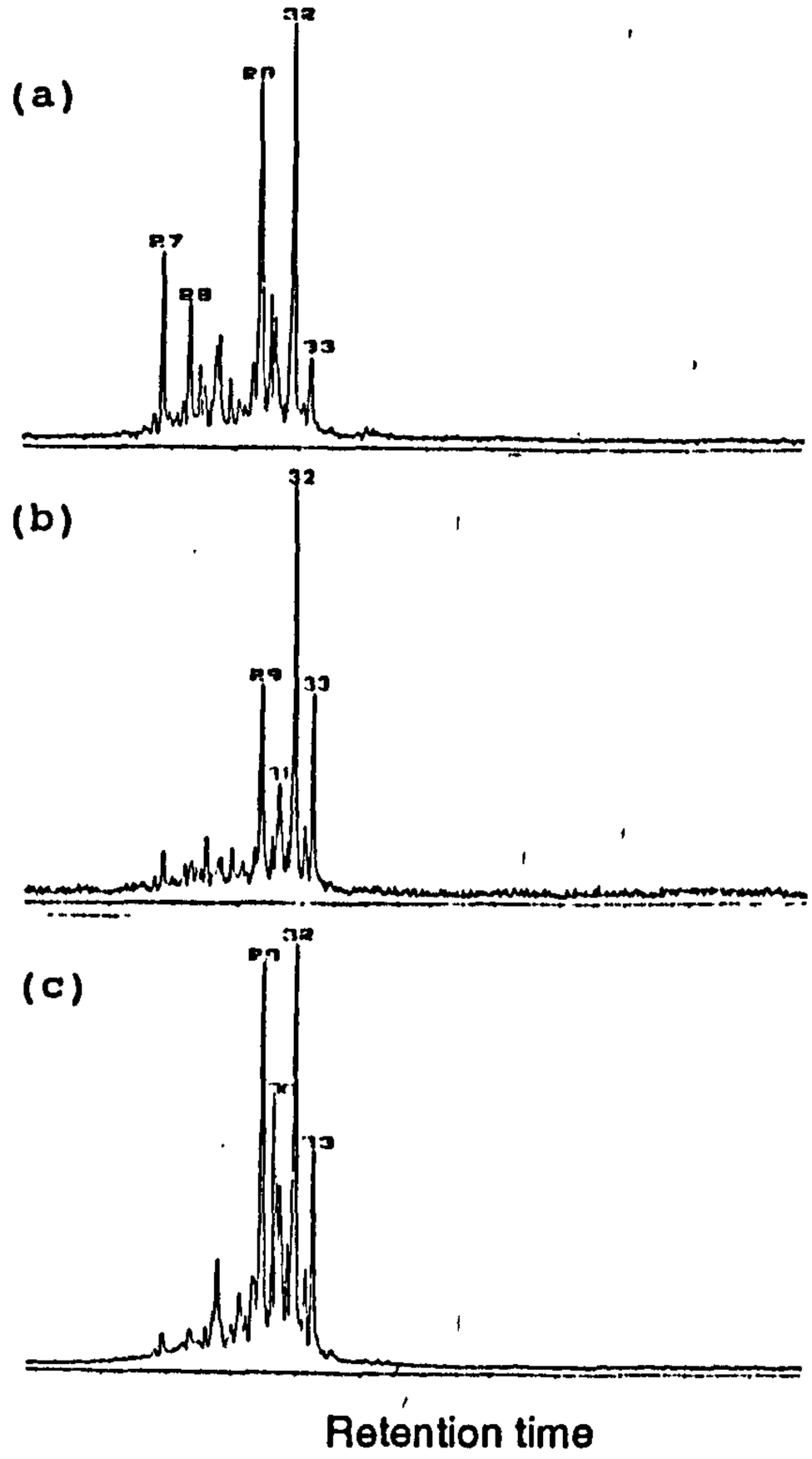

Figure 3.13 Mass chromatogram from metastable ion reaction monitoring transition m/z 414->231 for (a) Triassic sample (KA-1 bis 2605.65m), (b) Devonian sample (RE-1 3050.25m) and (c) Silurian sample (ZM-1 2388.75m). Peak assignments are listed in Table 1.

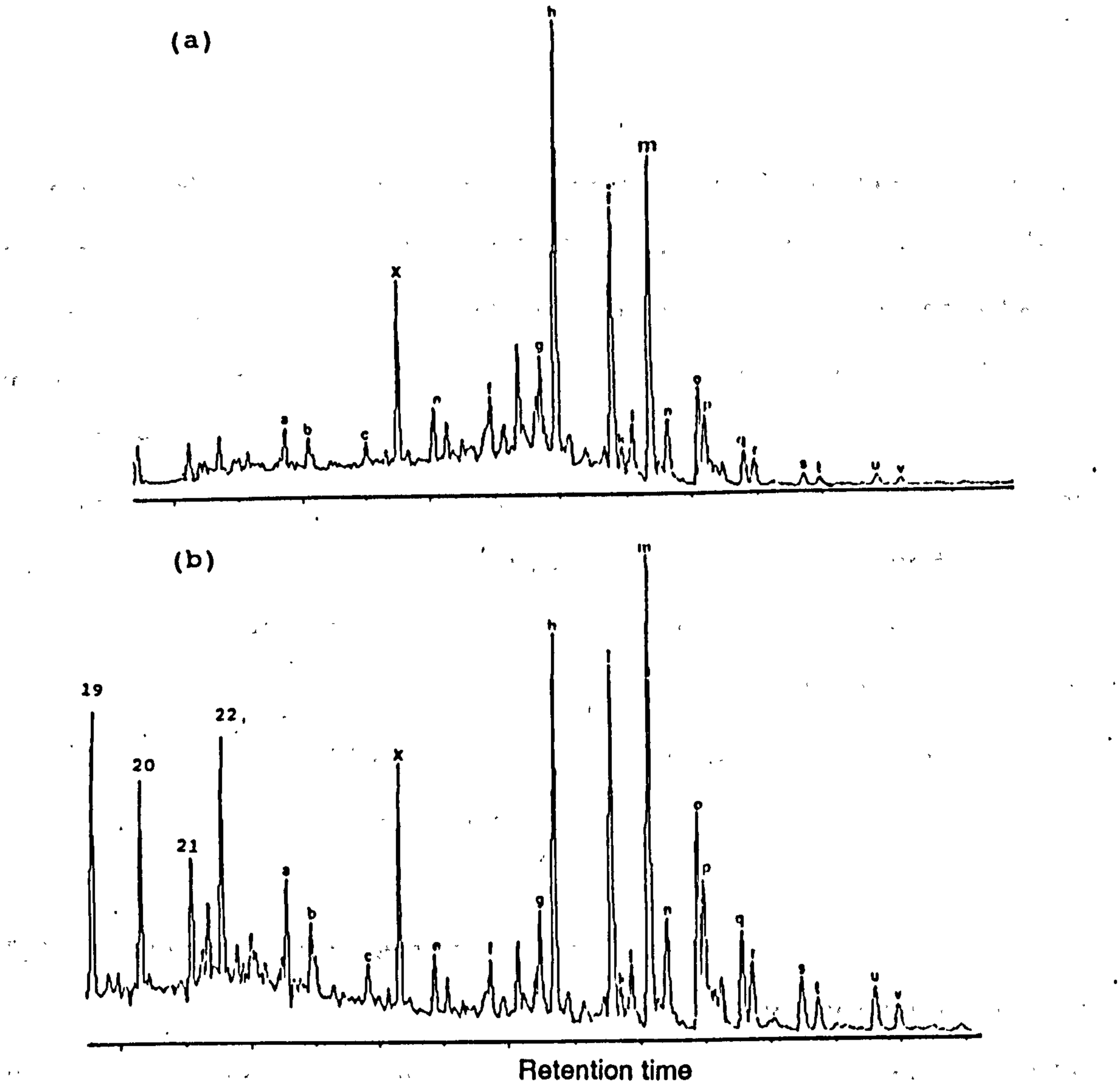

Figure 3.14 m/z 191.1794 mass chromatogram showing terpane distributions of two Triassic samples : (a) ELB-3 (2372.20m), (b) KA-1 bis (2605.65m). Of particular note the relatively high abundance of C_{27} terpane (Tm) in both samples, particularly in ELB-3 (2372.20m). C_{19}, C_{20}, C_{21} and C_{22} tricyclic terpanes are labelled with their carbon number. Peak assignments are listed in Table 2.

There is a tendency towards a relatively high hopanes over steranes as reflected by the 17α(H),21β(H)-C_{30} hopane/5α(H),14α(H),17α(H)-C_{29} (20R) sterane ratio (e.g C_{30}hop/C_{29}st (Appendix 3.5).

Terpane distributions (Figure 3.14 a and b) in the Triassic (ELB-3 (2372.20m) and KA-1 bis (2605.65m)) extracts are dominated by the hopane series ranging from C_{27}-C_{35}, while tricyclic terpanes are relatively low, particularly in ELB-3 (2372.20m). C_{24} tetracyclic (peak X) is relatively abundant in both samples. Note that C_{27} 17α(H)-trisnorhopane (T_m) is

present in relatively higher abundance than 18α(H)-Trisnorneohopane (T_s) and even higher than 17α(H),21β(H)-30 norhopane (e.g $C_{29}\alpha\beta$) in both samples, reflecting a low maturity (Appendix 3.6). T_m was detected in relatively higher concentrations than other homologues in KA-1 bis (2605.65m).

In comparison with the sterane isomerization of 5α(H),14α(H),17α(H)-C_{29} steranes at C-20 (e.g. ααα, 20S/20S+20R) and C-14 and C-17 of 5α(H),14α(H),17α(H)-C_{29} to 5α(H),14β(H),17β(H)-C_{29} (αββ/αββ+ααα), the hopane isomerization at C-22 (22S/22S+22R) and C-17 chiral centres of 17β(H),21α(H)/17β(H),21α(H)+17α(H),21β(H) C_{29} and C_{30} hopanes (eg. βα/βα+αβ) reveal completion (Appendix 3.6).

3.7.1.2. Aromatic hydrocarbon fraction

The distributions of C-ring monoaromatic steroidal hydrocarbon show (Figure 3.16) a prominence of rearranged over non-rearranged compounds in the Triassic source extracts, in which high abundance of rearranged steranes were also observed. Assignment of non-rearranged steroid has been determined by coinjection of non-deuterated C-ring monoaromatic steroidal hydrocarbons standards (Figure 3.15) and by comparison with those shown by Riolo et al. (1986). Peak assignments are listed in Table 3.

A close examination of these mass chromatograms reveals that both samples have complex distributions showing all types of non-rearranged and rearranged monoaromatic steroidal hydrocarbons (C_{27}-C_{29}). However, non-rearranged monoaromatic steroidal hydrocarbons are present in minor amounts (peak N° 4, 13 and 16 in Figure 3.16) relative to rearranged

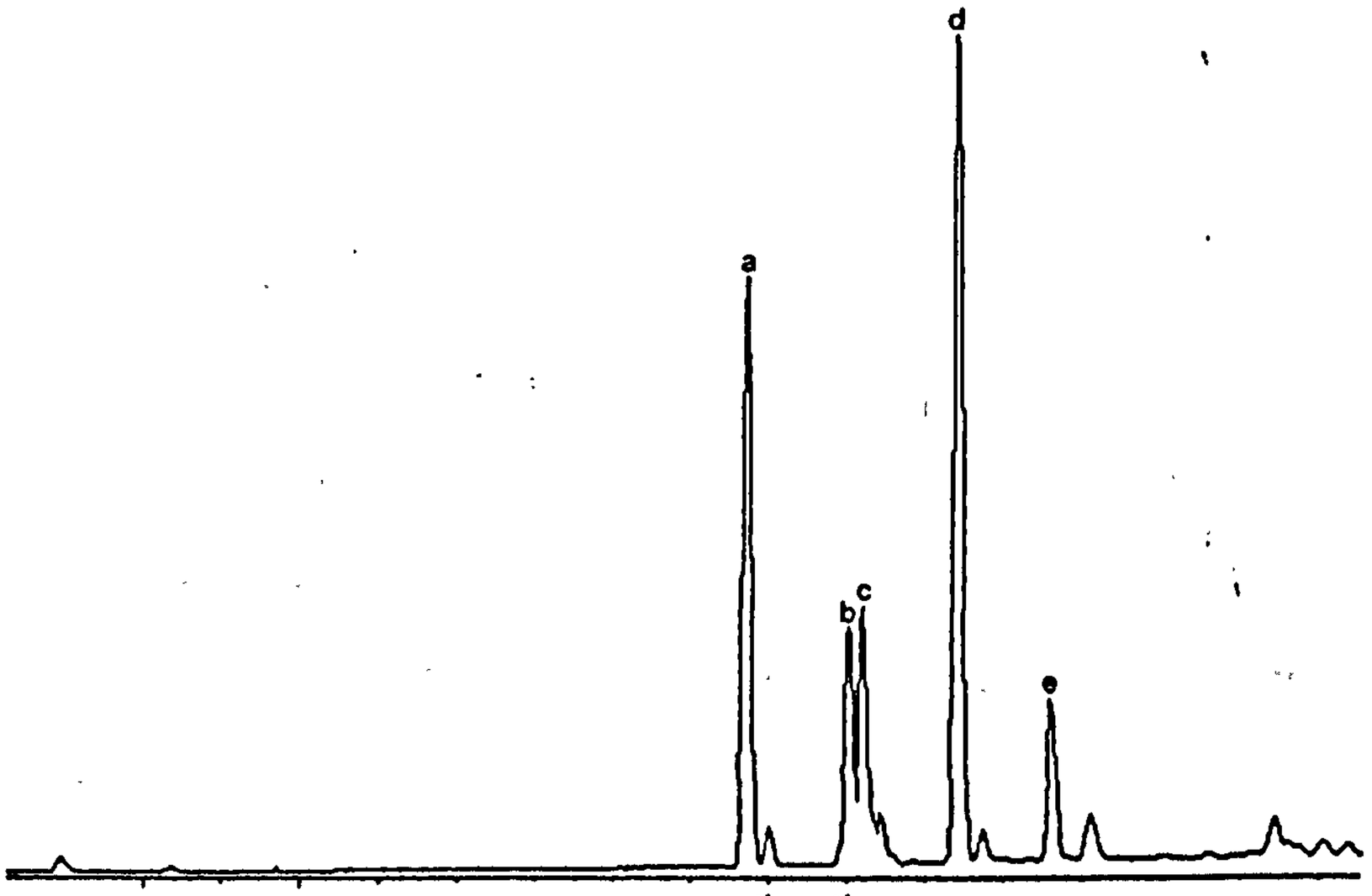

Figure 3.15 m/z 253.1950 mass chromatogram indicative of C-ring monoaromatic steroidal hydrocarbons for a standard mixture of non-deuterated compounds.

Peak assignments:
a 5β(H),10β(CH_3)-C_{27} (20R)
b 5α(H),10β(CH_3)-C_{27} (20R)
c 5β(H),10β(CH_3)-C_{28} (20R)
b 5α(H),10β(CH_3)-C_{28} (20R) & 5β(H),10β(CH_3)-C_{29} (20R)
e 5α(H),10β(CH_3)-C_{29} (20R)

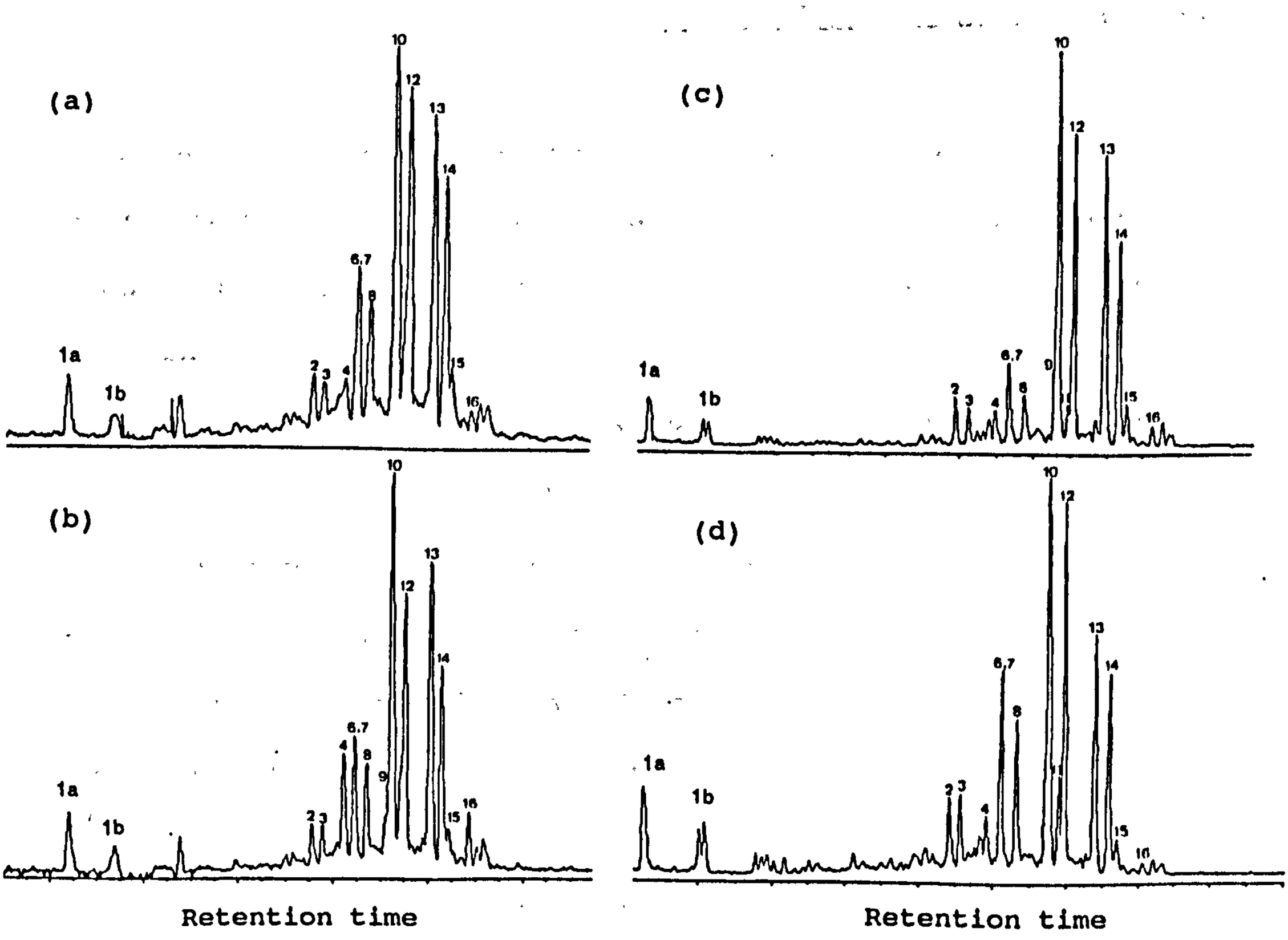

Figure 3.16 m/z 253.1950 mass chromatogram illustrating the C-ring monoaromatic steroidal hydrocarbon distributions in (a) Triassic sample, (b) Triassic & standard mixture of C_{27}, C_{28} and C_{29} non-rearranged components, (d) ELB-3 (2372.20m), (e) KA-1 bis (2605.65m). Of particular note, the relative low presence of non-rearranged compounds (peak 16). Peak assignments are listed in Table 3.

homologues (peak N° 2, 3, 12 and 15). This has been confirmed by coinjection of a standard mixture (Figure 3.16a and 3.16b). However, the quantitative evaluation of the numerous isomers could not be made due to their co-elution using GC-MS analysis only. Low molecular weight homologues (i.e C_{21}, C_{22}) are present in relatively low concentrations in Triassic extracts (Figure 3.16c and 3.16d).

The distributions of triaromatic steroidal hydrocarbons (Figure 3.17, m/z 231.1170) show that both samples contain prominent C_{28} (20R) and (20S), as indicated by high ratio of total $C_{28}/C_{26}+C_{27}+C_{28}$ triaromatic steroidal hydrocarbons (e.g $\%C_{28}t/(C_{26}t+C_{27}t+C_{28}t)$ ratio, Appendix 3.4). This parameter equals about 74% and 63% for ELB-3 (2372.20m) and KA-1 bis (2605.65m) respectively. These compounds have been identified through retention time comparison with published data. Peak assignments are given in Table 4.

The distributions of methylated triaromatic steroidal hydrocarbons (Figure 3.17, m/z 245.1130) show significant amounts of long-chain methylated compounds (C_{27}-C_{29}) and relatively lower amounts of short-chain homologues (C_{21}-C_{22}). The 4-methyl -C_{28} and -C_{29} compounds are present in relatively high abundance. Identification is only tentative (Riolo et al., 1986; Lichtfouse et al., 1990). Peak assignments are listed in Table 4. By analogy with the methylphenanthrene isomers (Radke, 1987), C_{21} and C_{22} methylated triaromatic steroidal hydrocarbons have reported by Lichtfouse et al.(1990) to occur as 2-, 3-, 4- and 6-methyl isomers where 2-methyl and 3-methyl are at β-position and 4-methyl isomers at α-position of the A ring (Radke, 1987). The relative proportions of these isomers were found to increase in this order: 6-methyl>4-methyl>2-methyl+3-methyl with increasing

maturity. Thus, the variation of the relative abundances of 2-methyl + 3-methyl to itself plus 4-methyl isomers of C_{21} and C_{22} triaromatic steroidal hydrocarbons (e.g MTSI1 and MTSI2 for C_{21} and C_{22} components respectively) were suggested by Lichtfouse et al.(1990) as maturity parameters.

The maturity assessment as recorded by the steroid aromatization (e.g ARO ratio equals 0.37 and 0.56), cracking ratios (0.16) as well as MTSI1 and MTSI2 (0.44 and 0.37 for C_{21} and C_{22} for ELB-3 (2372.20m) and KA-1 bis (2605.65m) respectively) suggest a low maturity level of Triassic samples (Appendix 3.7).

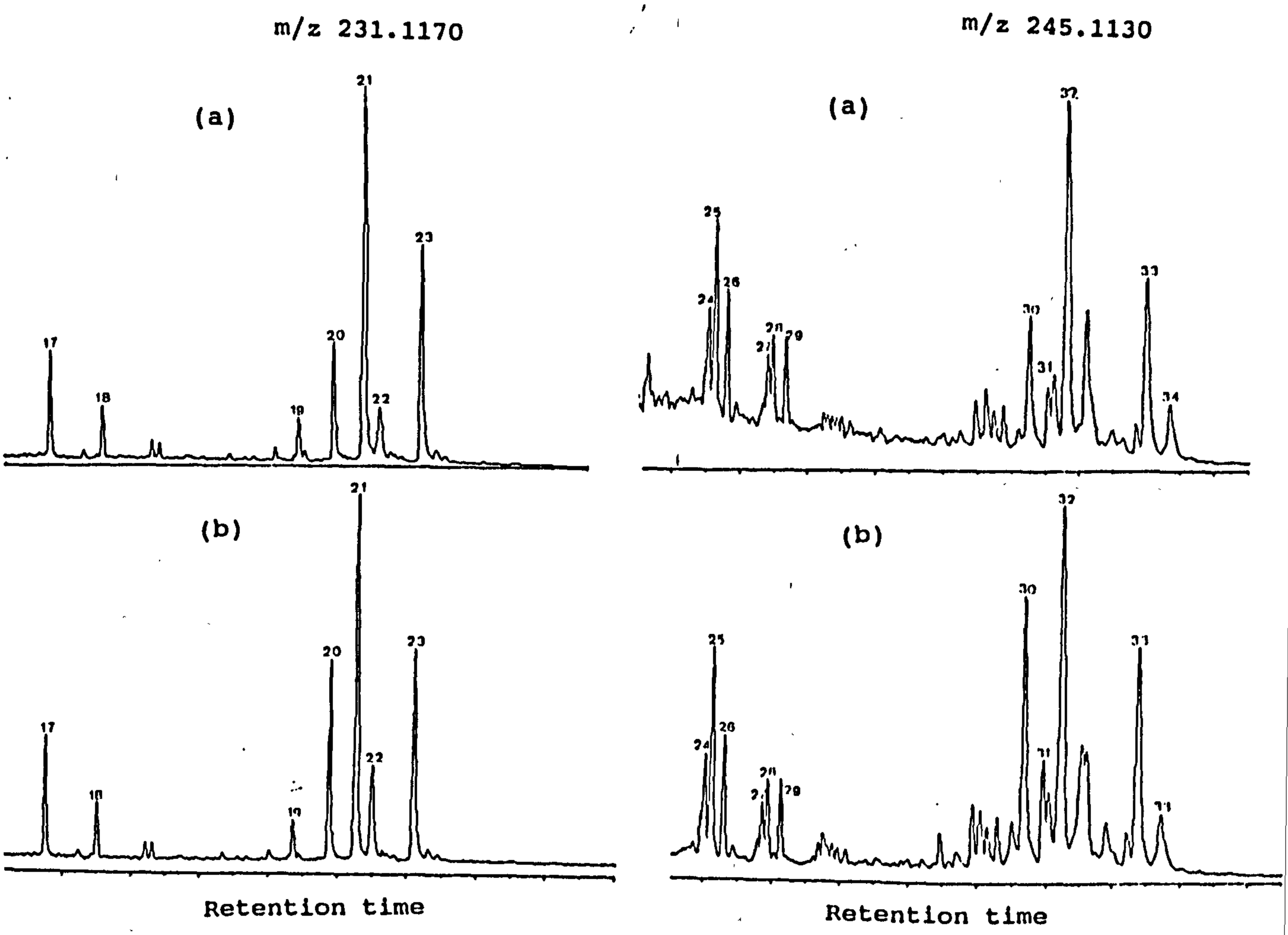

Figure 3.17 m/z 231.1170 and m/z 245.1130 mass chromatograms illustrating the triaromatic steroidal hydrocarbon distributions in (a) ELB-3 (2372.20m), (b) KA-1 bis (2605.65m). Peak assignments are listed in Table 4.

3.7.2. Devonian

3.7.2.1. Saturated hydrocarbon fraction

The distributions of *n*-alkanes in the saturated hydrocarbon fractions of ten Devonian extracts from RE-1 (3040.00m-3438.26m), SED-1 (2642.00m) and ZAR-1(3450.98m) boreholes show a range from C_{12} to C_{36} (Figure 3.18 and 3.19) with a slight odd to even predominance at *n*-C_{15}, *n*-C_{17} and *n*-C_{19}. The most prominent peaks in the gas chromatogram of one selected non-adducted saturated hydrocarbon fraction (Figure 3.6b), are the C_{14}-C_{16} and C_{18}-C_{20} acyclic isoprenoid compounds, whose mass spectra are shown in Figure 3.7. Pristane is higher than phytane, with the Pr/Ph ratio>2 and Pr/*n*-C_{17} ratio>1 (Appendix 3.3). One sample RYB1 (3106.30m) exhibits a distinct and continuous envelope of *n*-alkane distribution ranging from *n*-C_{12} to *n*-C_{36}, probably dominated by waxy *n*-alkanes (Figure 3.19d).

Figure 3.20 shows that the sterane distributions of Devonian source extracts are dominated by C_{27} and C_{29} rearranged steranes, as indicated by the ratio of rearranged to non-rearranged steranes (e.g C27r/C27n and C29r/C29n, Appendix 3.4). Figure 3.21e reveals the presence of relatively lower concentrations of C_{30} rearranged relative to non-rearranged counterparts. The relative proportions of non-rearranged and rearranged (C_{27}-C_{29}) steranes displayed in Figure 3.12a and 3.12b respectively show that most of the Devonian source extracts are similar to each other. As shown in (Figure 3.13b), Devonian samples exhibit a relatively high abundance of the 24-ethyl-ααα-3β-methyl-cholestane (20R), which may coelute with the 24-ethyl-ααα-2α-methyl isomer. These compounds have been assigned by coinjection of a standard mixture (Figure 3.22c), with one selected Devonian saturated hydrocarbon fraction (Figure 3.23b) and by

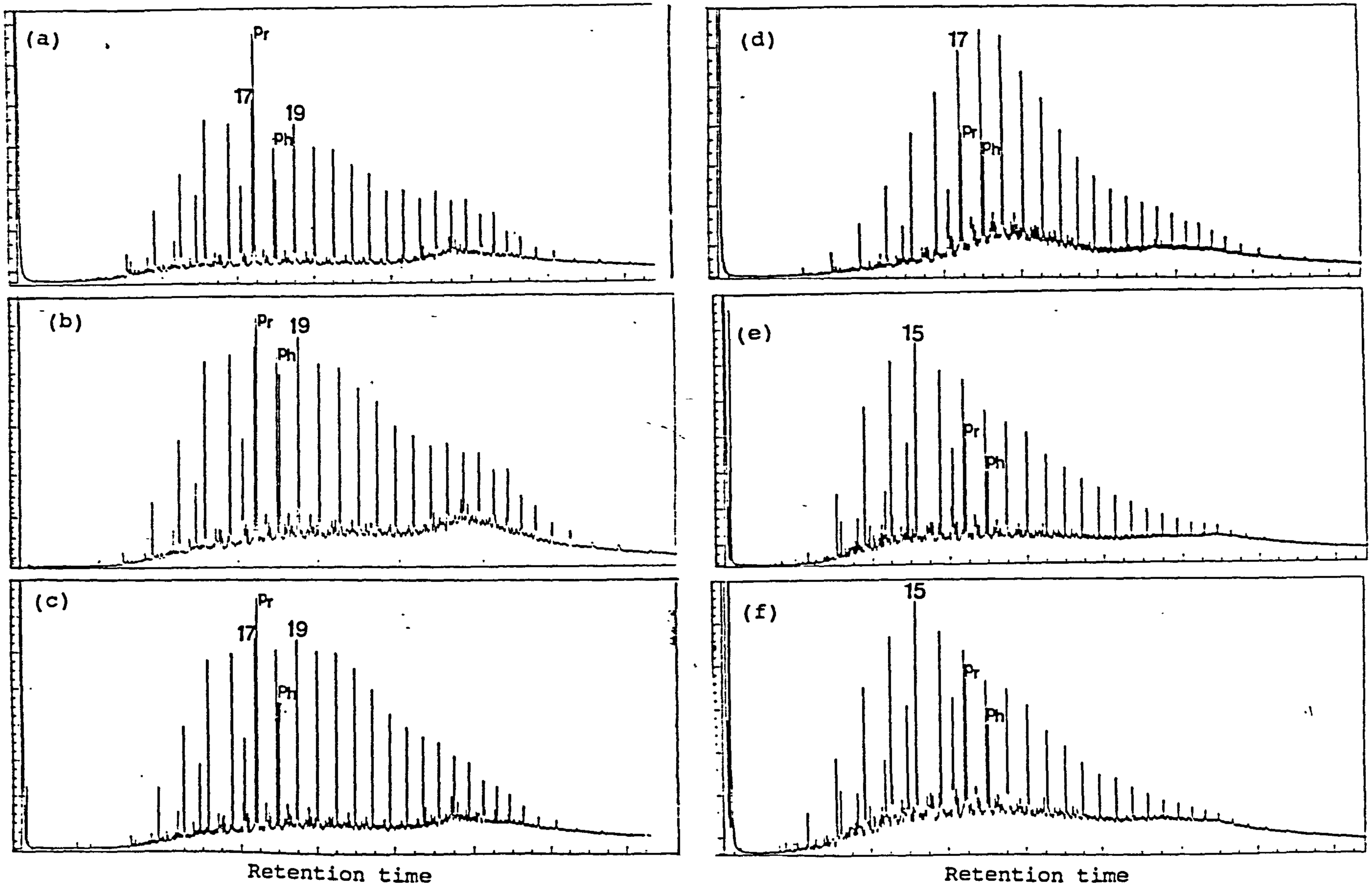

Figure 3.18 Gas chromatograms showing the saturated hydrocarbon distributions of Devonian samples from RE-1 borehole with depth of (a) 3040.00m, (b) 3050.25m, (c) 3314.70m, (d) 3202.30m, (e) 3346.20m, (f) 3354.40m. *N*-alkanes are labelled with their carbon number. Pr= pristane, Ph= phytane. *(e) 3346.30m (f) 3354.40m and (g) 3438.26m.*

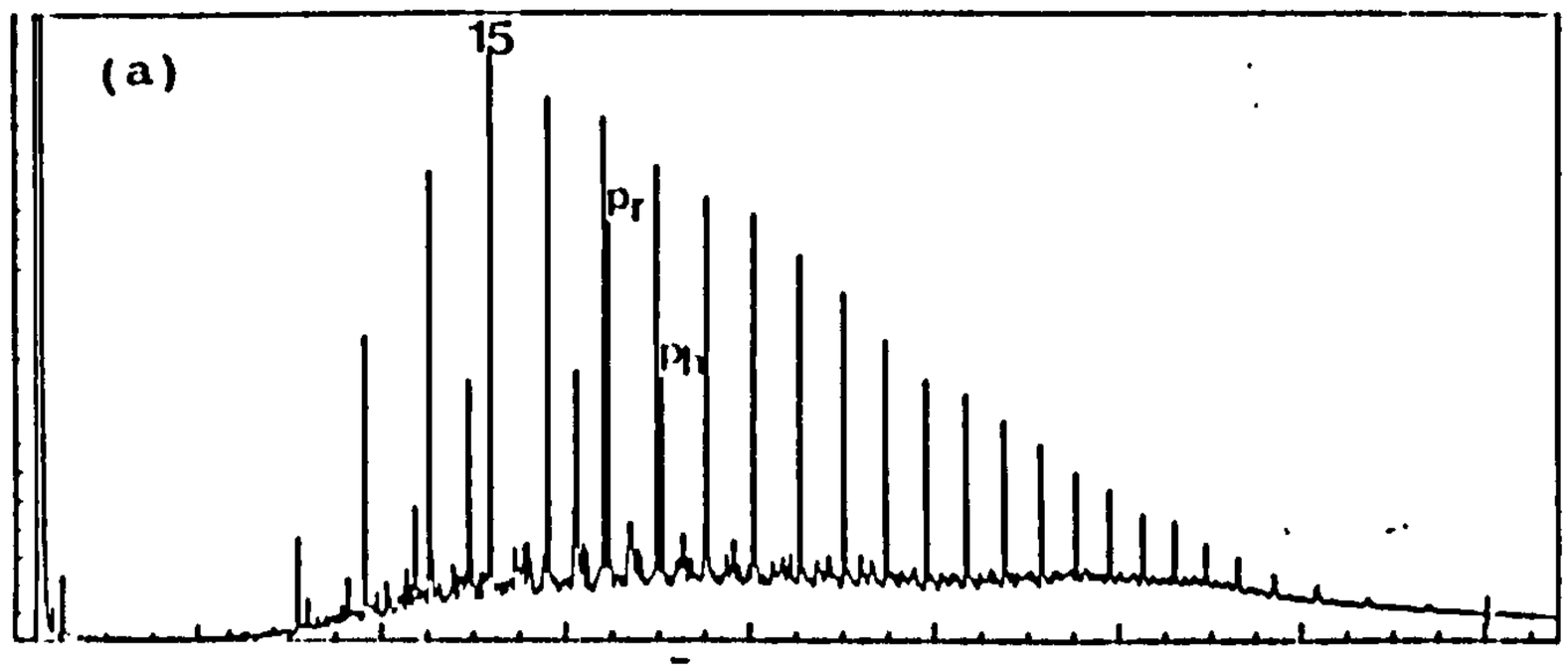

Figure 3.19 Gas chromatograms illustrating the saturated hydrocarbon fractions distributions of four Devonian samples: (a) RE-1 (3438.26m), (b) SED-1 (2642.00m), (c) ZAR-1 (3450.98m), (d) RYB-1 (3106.30m). *N*-alkanes are labelled with their carbon number. Pr= pristane, Ph= phytane.

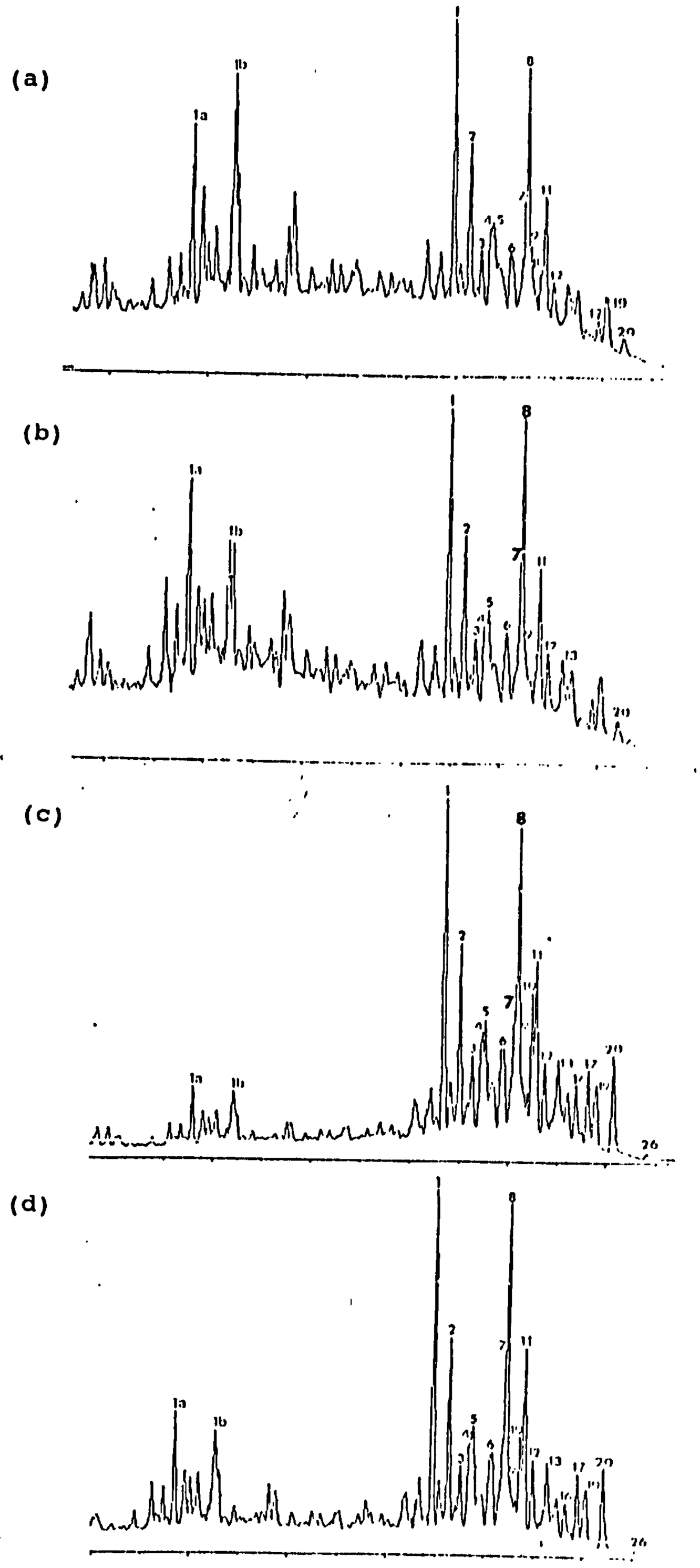

Figure 3.20 m/z 217.1950 mass chromatograms illustrating the sterane distributions of Devonian samples from RE-1 borehole: (a) 3050.25m, (b) 3314.70m, (c) 3354.40m, (d) 3346.20m. Peak assignments are listed in Table 1.

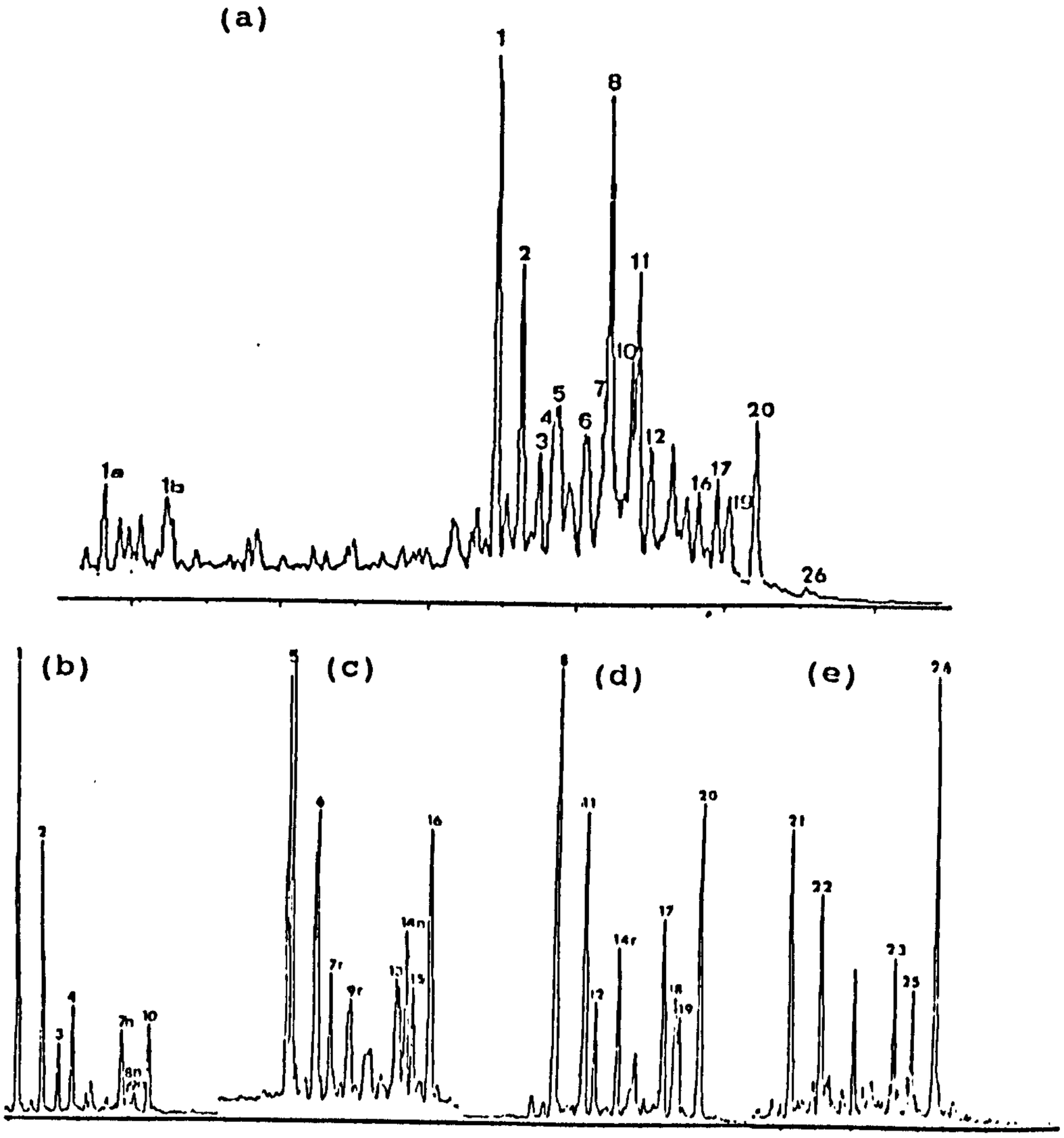

Retention time

Figure 3.21 Monitoring steranes using GC/MS/EI SIM of (a) 217.1950 mass chromatogram and GC/MS/metastable ion reaction monitoring of transitions (b) m/z 372->217, (c) m/z 386->217, (d) m/z 400->217 and (e) m/z 414->217 for one selected Devonian sample (RE-1 3050.25m).

comparison with published data (Summons and Capon, 1988; Requejo, 1991). Peak 33 has been reported as 4-methylsteranes (Requejo et al., 1991), although coelution with C_{30}-$\alpha\alpha\alpha$ (20R) cannot be ruled out (Summons, pers comm.). It is interesting to note the lower abundance of rearranged relative to non-rearranged methylsteranes in Devonian samples.

Tricyclic terpanes (C_{19}-C_{29}) are present in all Devonian samples, irrespective of their maturity levels (Figure 3.24), although they become prominent in mature samples (Figure 3.24c, 3.24d and 3.24e), as indicated by the C_{23} tricyclic to 17α(H),21β(H)-C_{30} ratio (e.g $C_{23}T/C_{23}T+C_{30}hp$, Appendix 3.5. Of particular note, the predominance of T_m over tricyclic and hopanes in sample RE-1 (3040.00m). Furthermore, the $C_{30}hop/C_{29}st$ ratio indicates that steranes and hopanes have roughly similar contribution to the Devonian source extracts, with a relatively higher abundance of hopanes to steranes in mature samples (Appendix 3.5).

There is a trend towards an increase of the relative proportions of compound j, (18α(H)-30-norneohopane, i.e. $C_{29}T_s$ (Moldowan et al., 1991) to 17α(H),21β(H)-30-norhopane with increasing depth for a suite of samples (Figure 3.26) from RE-1 borehole (Cornford et al., 1988; Fowler and Brooks, 1990).

Amongst the commonly used biological marker ratios (Appendices 3.5 and 3.6), there are some parameters such as $C_{30}hop/C_{29}st$, $C_{29}T_s/C_{29}\alpha\beta$ hop, T_s/T_m and C_{29}-($\alpha\beta\beta/\alpha\beta\beta+\alpha\alpha\alpha$) that show convincingly trends with depth (Figure 3.26). However, plots ofC_{29}- and C_{30}-($\beta\alpha/\beta\alpha+\alpha\beta$) as well as 17$\alpha$(H)-$C_{32}$ (22S/22S+22R) ratios versus depth show little response throughout the rank range (VR/E= 0.45%-0.75%) for RE-1 borehole.

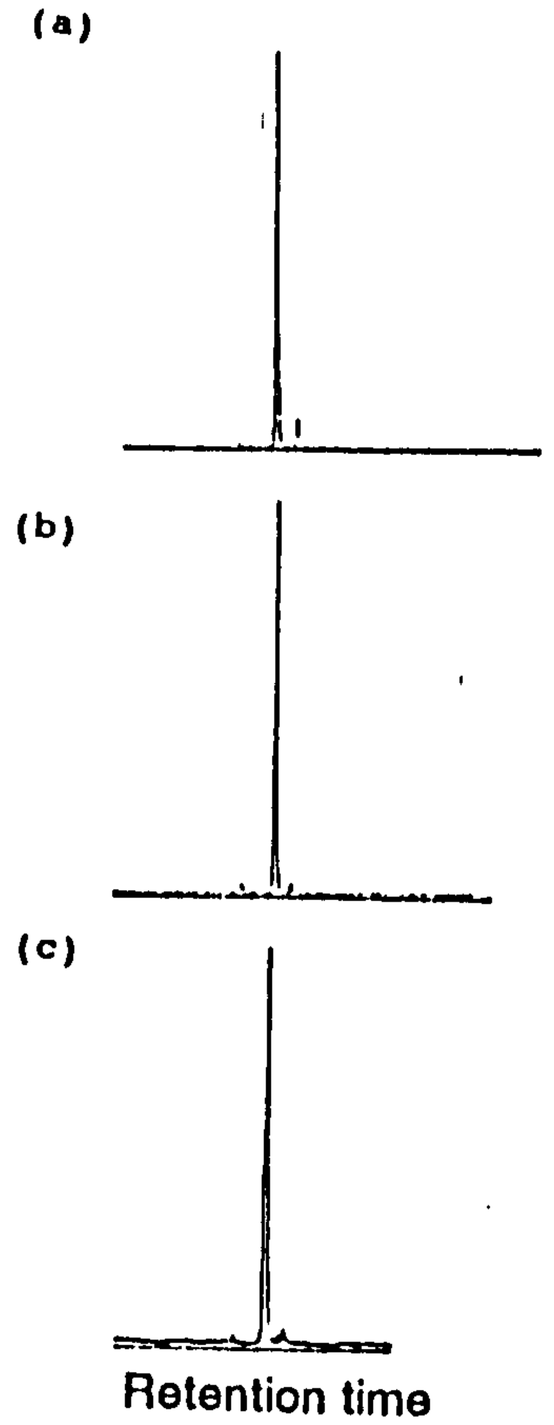

Figure 3.22 GC/MS/MRM traces of transition m/z 414->217 for standard (a):24-ethyl-5α(H),14α(H),17α(H)-2α-methyl-cholestane, standard (b):24-ethyl-5α(H),14α(H),17α(H)-3β-methyl-cholestane and standard (c):mixture of (a) & (b) standards, which coelute within the GC conditions used.

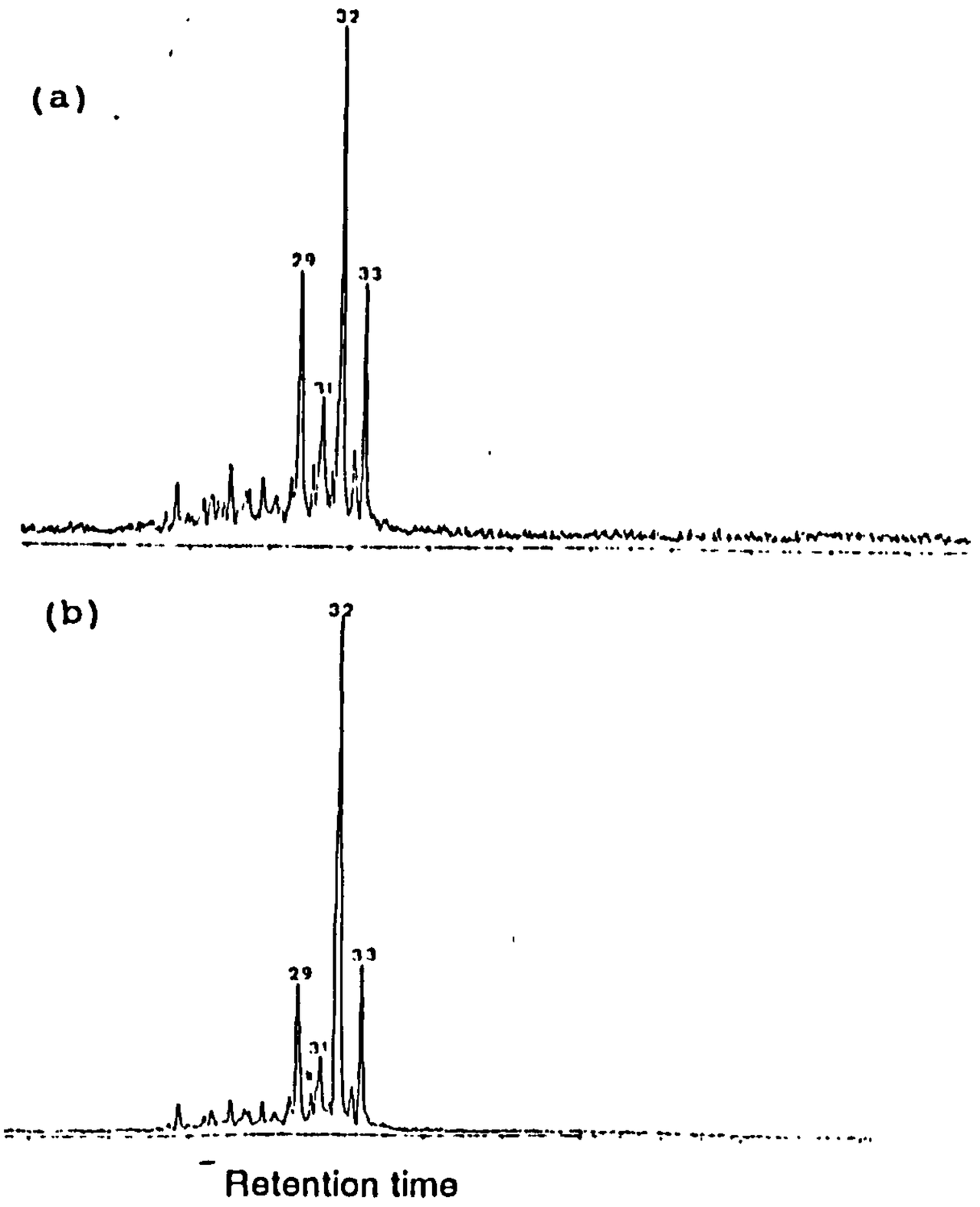

Figure 3.23 GC/MS/MRM traces of transition m/z 414->m/z 231 for (a) one selected Devonian sample (RE-1 3050.25m) and (b) sample (a) + standard mixture (c). Peak assignments are listed in Table 1.

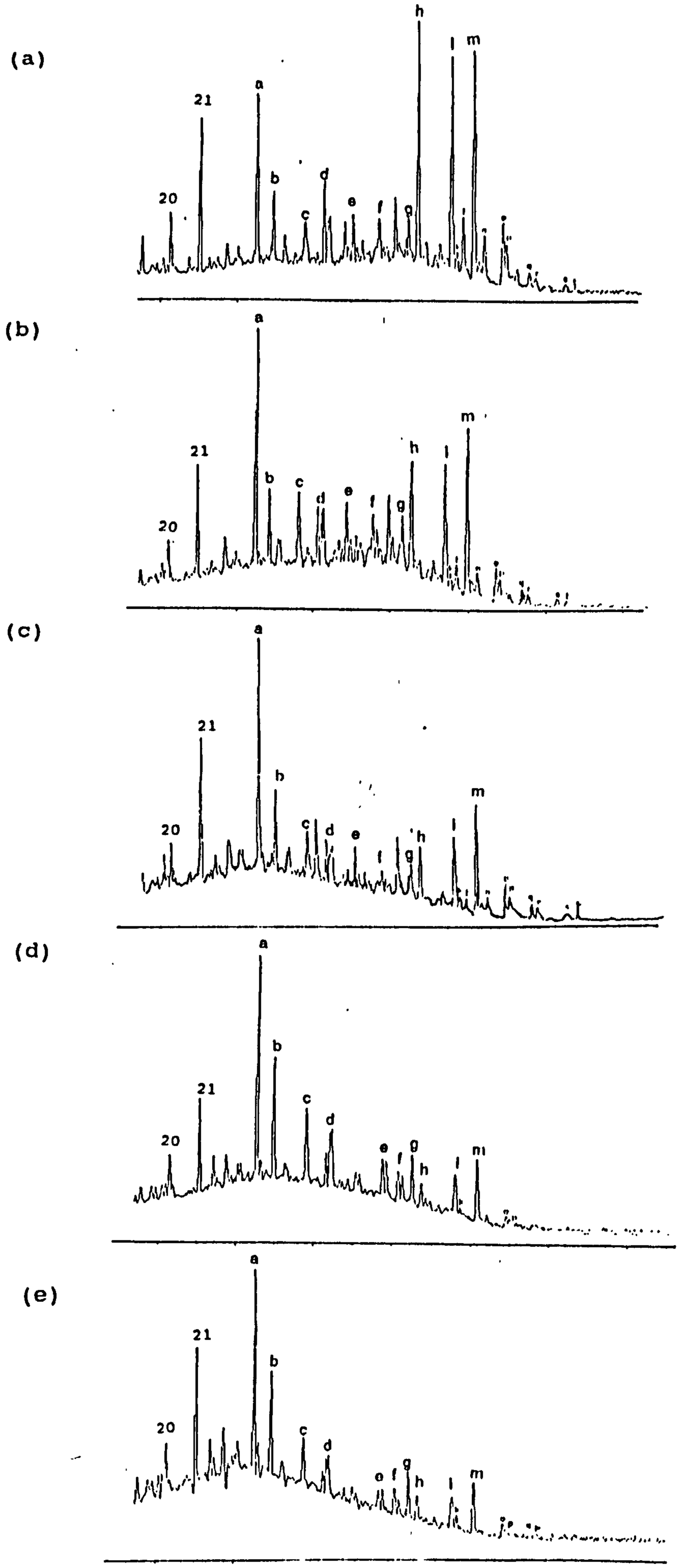

Figure 3.24 m/z 191.1794 mass chromatogram showing terpane distributions of Devonian samples fromRE-1 borehole: (a) 3040.00m, (b) 3050.25m, (c) 3114.70m, (d) 3354.40m and (e) 3438.26m. C_{20} and C_{21} tricyclic terpanes are labelled with their carbon number. Peak assignments are listed in Table 2.

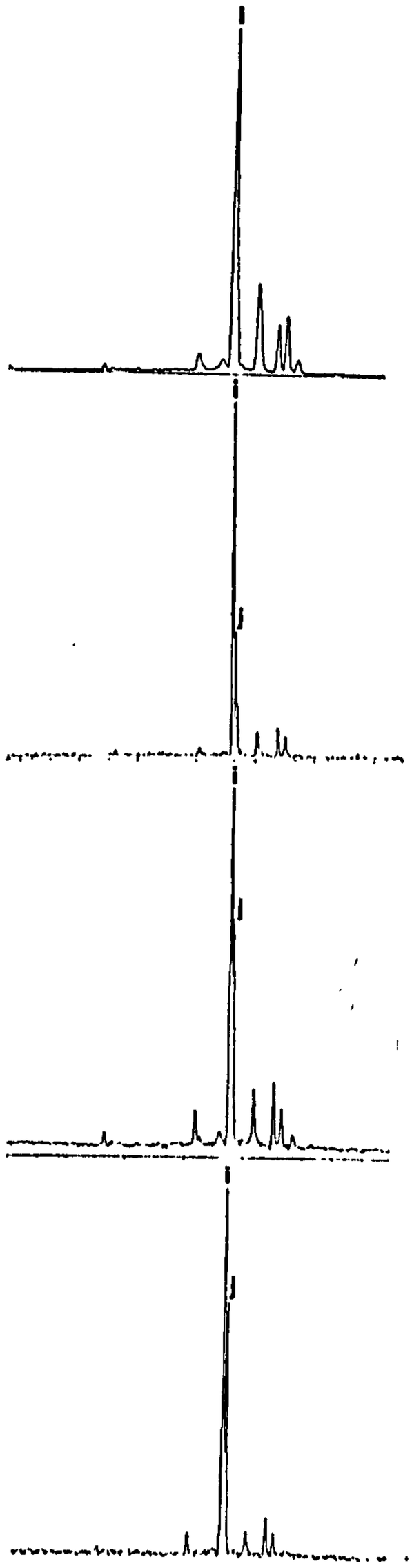

Figure 3.25 Mass chromatograms from metastable ion reaction monitoring of transition m/z 398->m/z 191 for 17a(H),21b(H)-30-norhopane (peak i) and 18a(H)-30-norneohopane (peak j, $C_{29}T_s$). The relative abundance of $C_{29}T_s$ increases with increasing maturity for RE-1 borehole: (a) 3040.00m (b) 3050.25m (c) 3114.70m (d) 3202.26m.

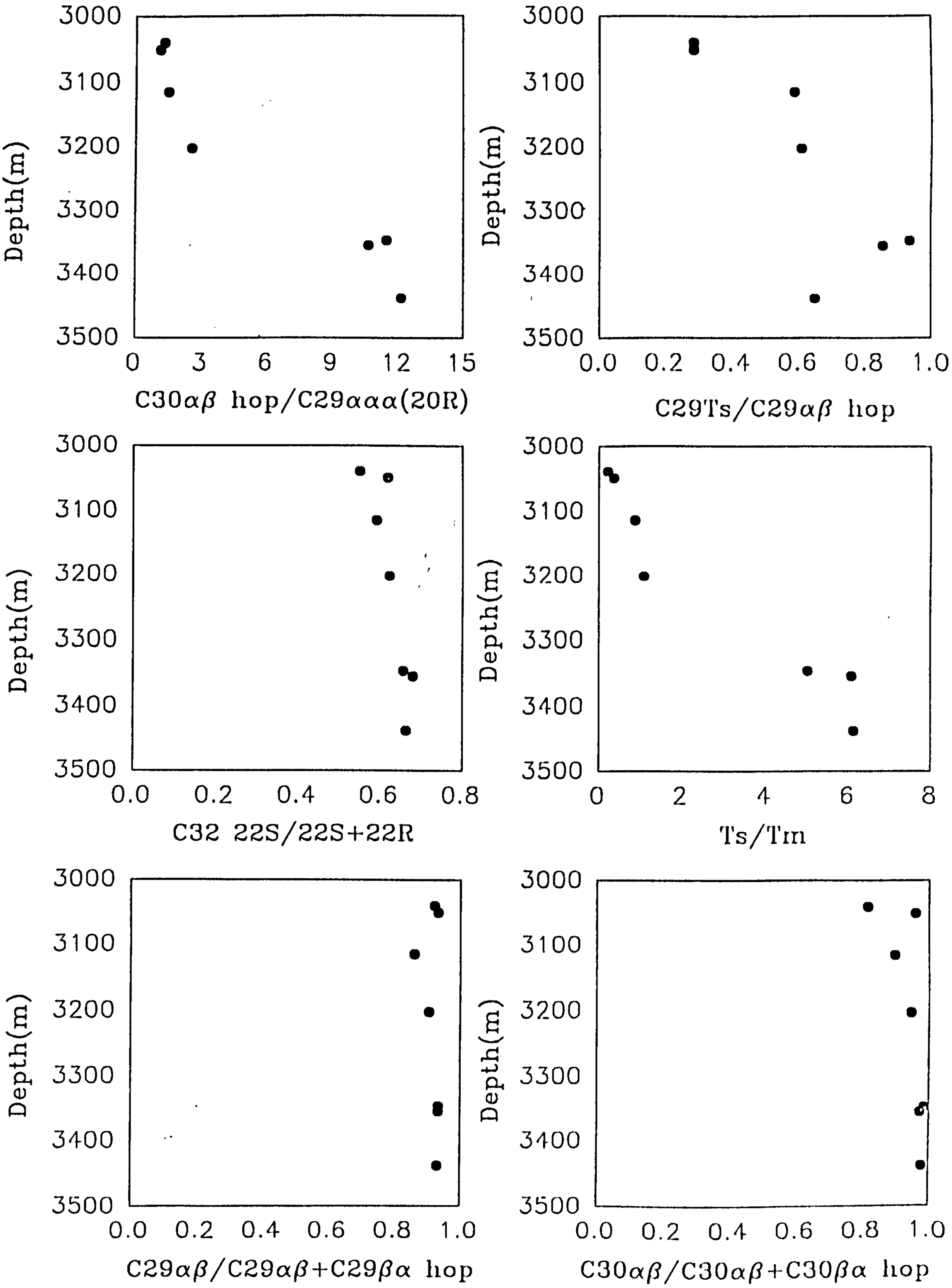

Figure 3.26 Variation of biomarker ratios with increasing depth for RE−1 borehole (see Appendices 3.5 and 3.6, for key to abreviation parameters.

3.7.2.2. Aromatic hydrocarbon fraction

Representative C-ring monoaromatic steroidal hydrocarbon distributions of Devonian extracts (Figure 3.27) show a high abundance of long-chain (C_{27}-C_{29}) relative to short-chain homologues (C_{21} and C_{22}). Rearranged C-ring monoaromatic steroidal hydrocarbons with Cis isomers (peak N° 2, 3, 6+7, 12 and 15) dominate the mass chromatograms, whereas non-rearranged compounds with Trans stereochemical structure are minor (peak N° 5, 13 and 16). There is a tendency towards a decrease of relative concentrations of compound N°2 (i.e cis isomer with 5α(CH_3),10α(H)) with increasing maturity, as illustrated in Figure 3.27.

The distributions of triaromatic steroidal hydrocarbons are displayed in Figure 3.28. Devonian samples exhibit relatively similar abundances of C_{28} triaromatic components as indicated by the $\%C_{28}t/C_{26}t+C_{27}t+C_{28}t$ ratio (Appendix 3.4). There is a less convincingly trend of the cracking with depth for RE1 borehole (Figure 3.29) but generally, steroid aromatization ratio increases as a result of conversion of monoaromatic into triaromatic steroidal hydrocarbons with rank (Seifert and Moldowan, 1978; Mackenzie et al., 1981a; 1981b; 1982b) reaching almost 60% to 80% values, near the peak of oil window. Furthermore, the trend is also observed for C_{29}-ααα (20S/20S+20R) as well as C_{29}-(αββ/αββ+ααα) ratio with increasing maturity (Figure 3.29).

The distributions of methyl triaromatic steroidal hydrocarbons are shown in Figure 3.30. A predominance of the 4-methyl isomers over 2-methyl+3-methyl isomers is observed in less mature samples, while 2-methyl-+3-methyl isomers dominate in mature samples, as indicated by the methyl triaromatic steroid indices (MTSI1 and MTSI2) with depth (Figure 3.29).

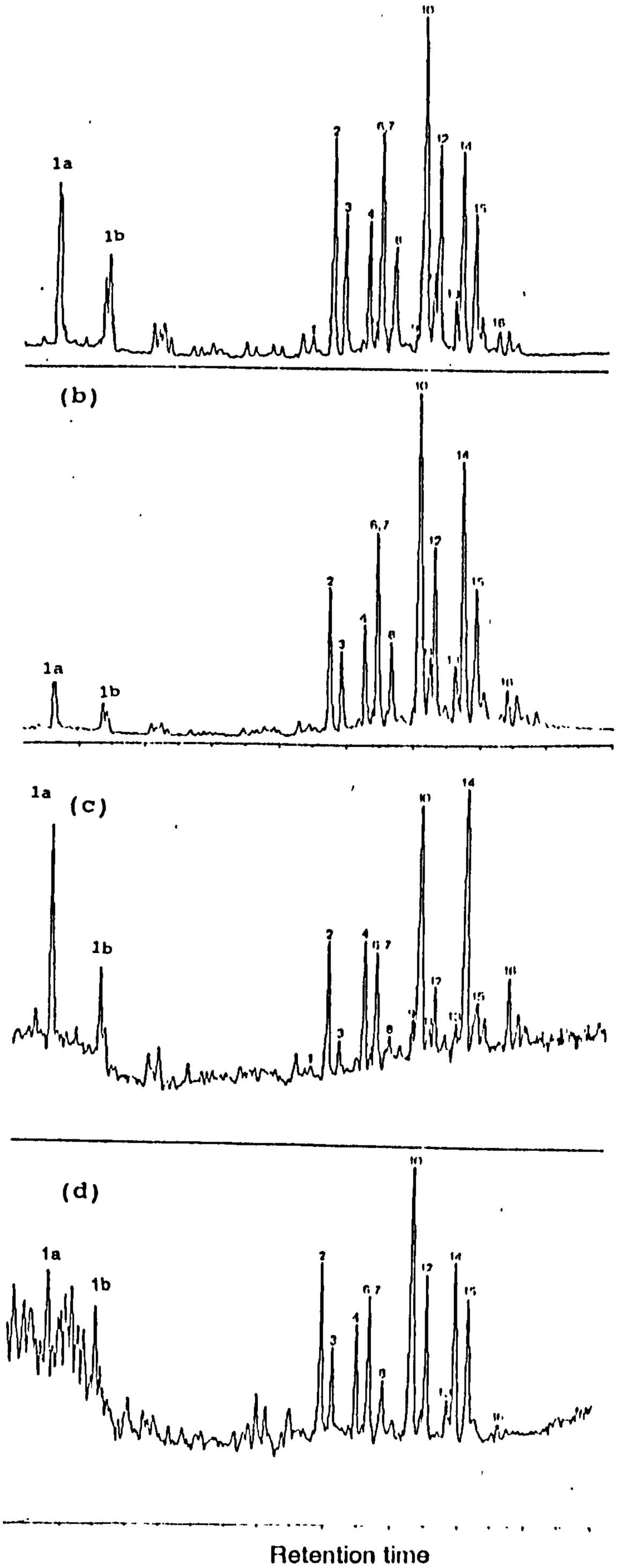

Figure 3.27 m/z 253.1950 mass chromatograms illustrating the C-ring monoaromatic steroidal hydrocarbon distributions of Devonian source-extracts from RE-1 borehole: (a) 3050.25m, (b) 3114.70m, (c) 3354.40m, (d) 3438.26m. Peak assignments are listed in Table 3.

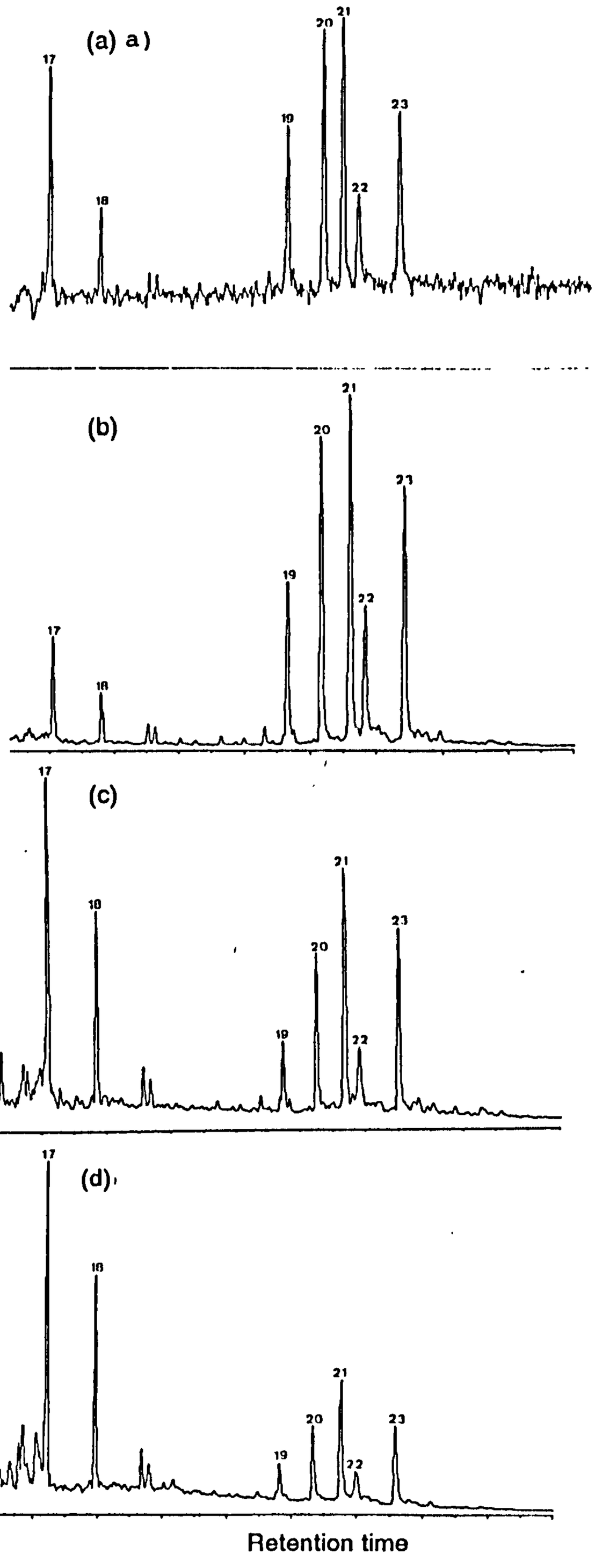

Figure 3.28 m/z 231.1170 mass chromatogram illustrating the triaromatic steroidal hydrocarbon distributions of Devonian samples from RE-1 borehole: (a) 3050.25m, (b) 3114.70m, (c) 3354.40m, (d) 3438.26m. Peak assignments are listed in Table 4.

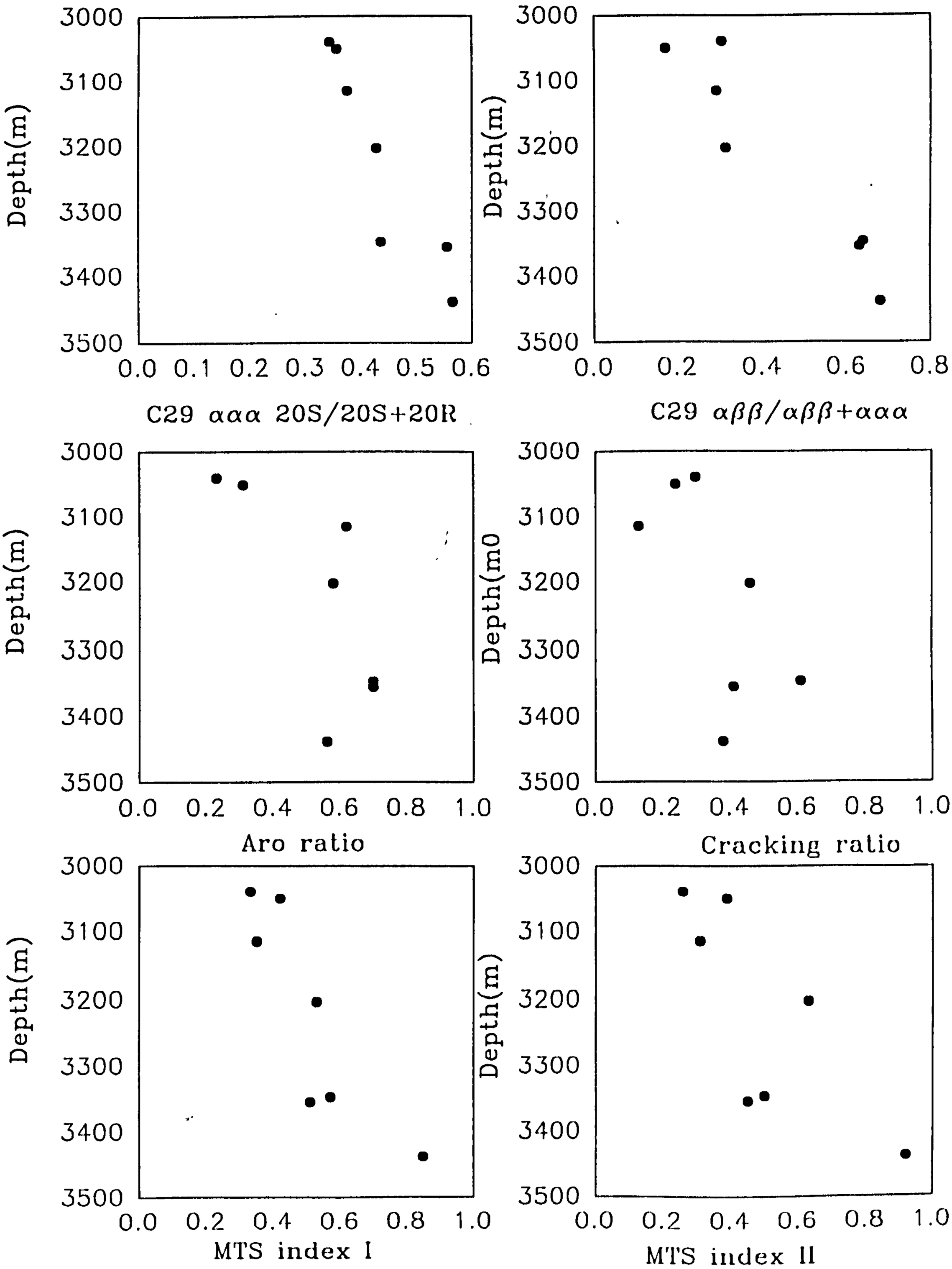

Figure 3.29 . General increase of biomarker ratios, as illustrated in RE-1 borehole (see Appendix 3.7 for key to abreviation parameters).

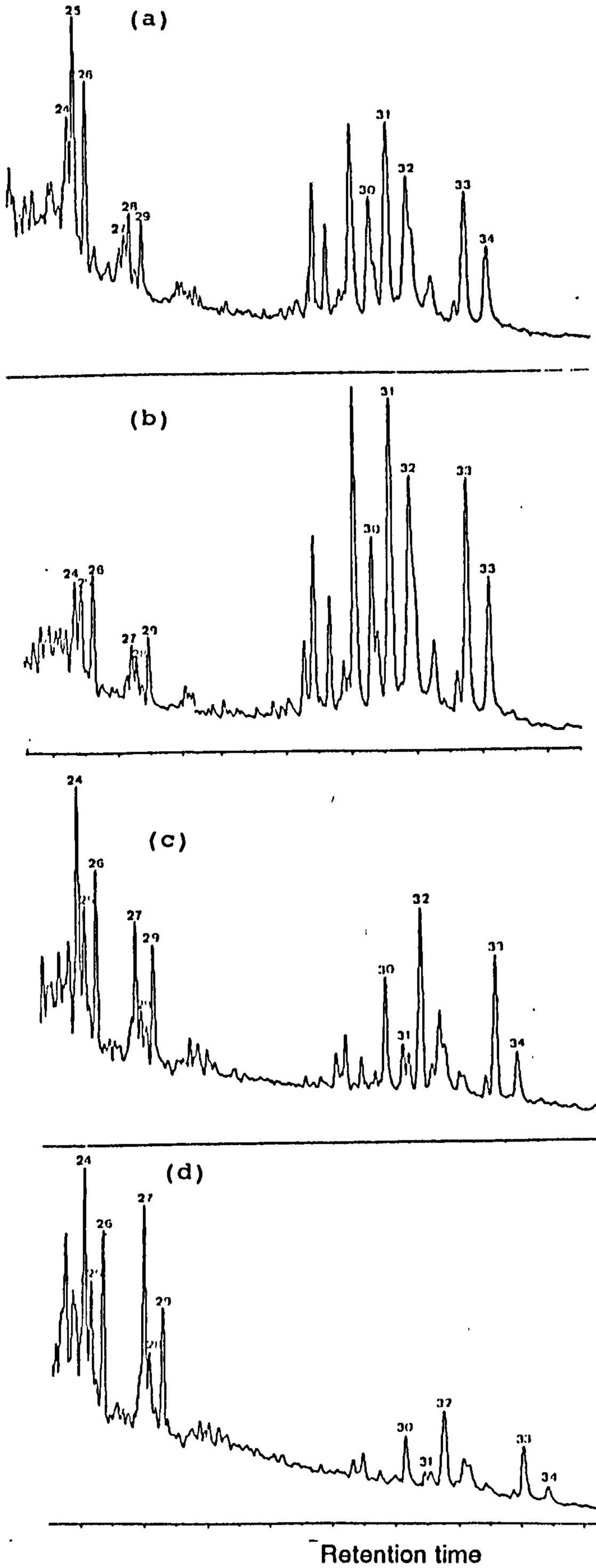

Figure 3.30 m/z 245.1130 mass chromatogram illustrating the distribution of methylated triaromatic steroidal hydrocarbons for Devonian samples from RE-1 borehole: (a) 3050.25m, (b) 3114.70m, (c) 3354.40m, (d) 3438.26m. Peak assignments are listed in Table 4.

3.7.3. Silurian

3.7.3.1. Saturated hydrocarbon fraction

Representative gas chromatograms of the saturated hydrocarbon fractions of Silurian samples are shown in (Figure 3.31). They all display a distribution of *n*-alkanes ranging from C_{12} to C_{36}, with maxima at *n*-C_{15} for KA-1 bis samples, *n*-C_{17} and *n*-C_{19} for REA-1 and ZM-1 samples. Acyclic isoprenoids are less dominant than *n*-alkanes with lower Pr/Ph ratio than Devonian samples (1.30- 1.65) except REA-1, which exhibits higher Pr/Ph and Pr/*n*-C_{17} ratios (Appendix 3.3).

Sterane distributions of three selected Silurian source extracts are shown in Figure 3.32. They exhibit abundant rearranged steranes with a predominance of C_{27} and C_{29} members, particularly for KA-1 bis (3029.82m) and REA-1 (2764.56m) samples as indicated by the rearranged to non-rearranged steranes ratios (e.g. C27r/C27n and C29r/C29n, Appendix 3.4). However, sample ZM-1 (2388.75m) contains relatively much less rearranged than non-rearranged steranes compared to samples previously discussed, although Silurian samples are similar in sterane distribution to Devonian samples (Figure 3.12a and 3.12b). Figure 3.33 displays GC/MS/MRM traces of the C_{27}, C_{28}, C_{29} of C_{30} sterane distributions of one selected Silurian sample (ZM1, 2388.75m) where the $\alpha\alpha\alpha$-C_{27} and -C_{29} (20R) isomers are prominent. It can be seen that non-rearranged steranes are more abundant than rearranged homologues (Figure 3.33a, b, c, d and e).

Methyl steranes were also detected in Silurian source extracts, illustrated in Figure 3.13, being dominated by the 24-ethyl-$\alpha\alpha\alpha$-3β-methyl-cholestane (20R and 20S). Furthermore, peak 33 has been reported as 4-

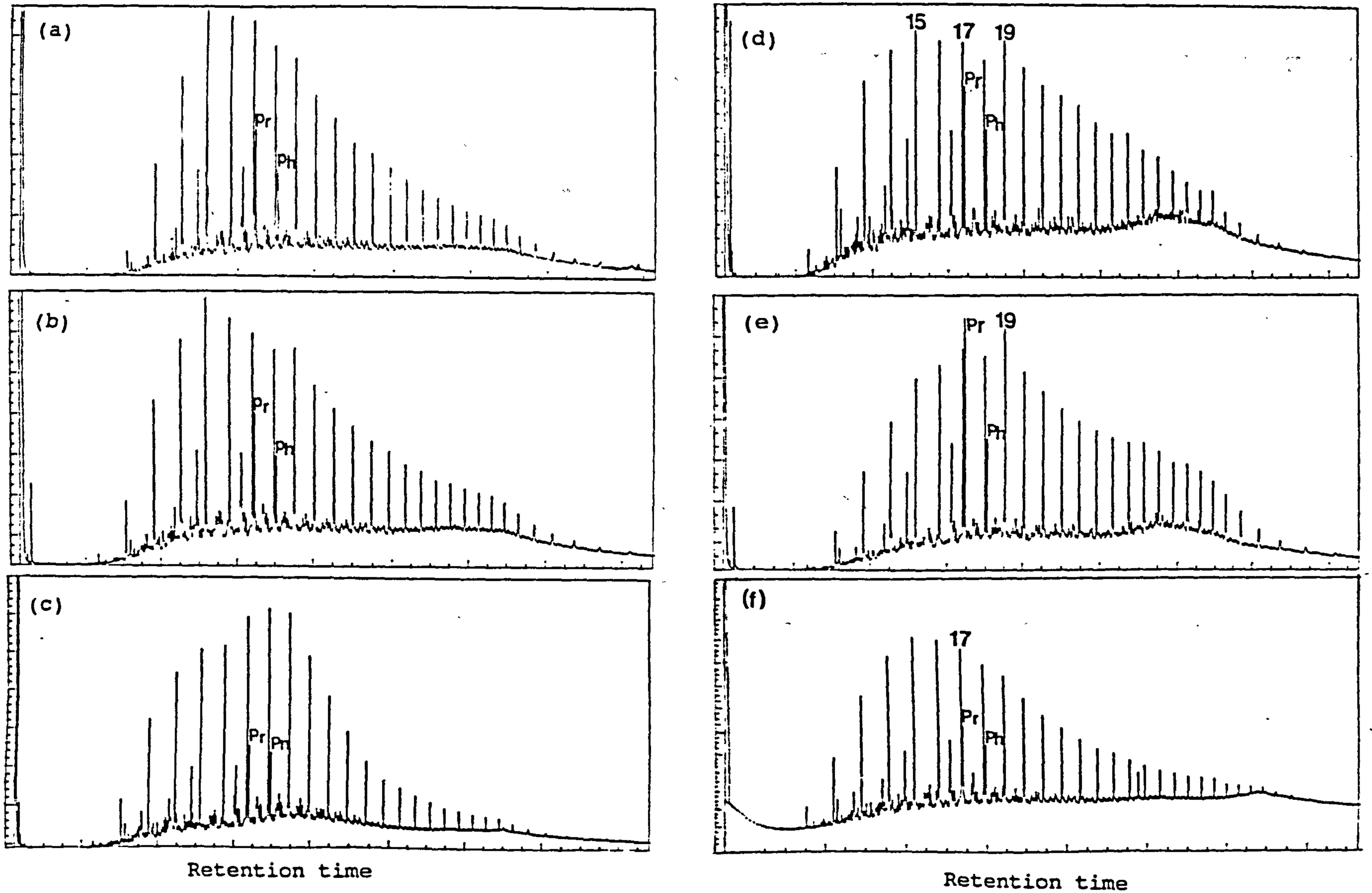

Figure 3.31 Gas chromatograms showing the distributions of saturated hydrocarbon fractions for Silurian samples: (a) ZM-1 (2388.75m), (b) REA-1 (2764.56m), (c) ZAR-1 (3994.65m), (d) KA-1 bis (3029.82m), (e) KA-1 bis (3060.90m) and (f) KA-1 bis (3072.85m). *N*-alkanes are labelled with their carbon number. Pr=phytane, Ph=phytane.

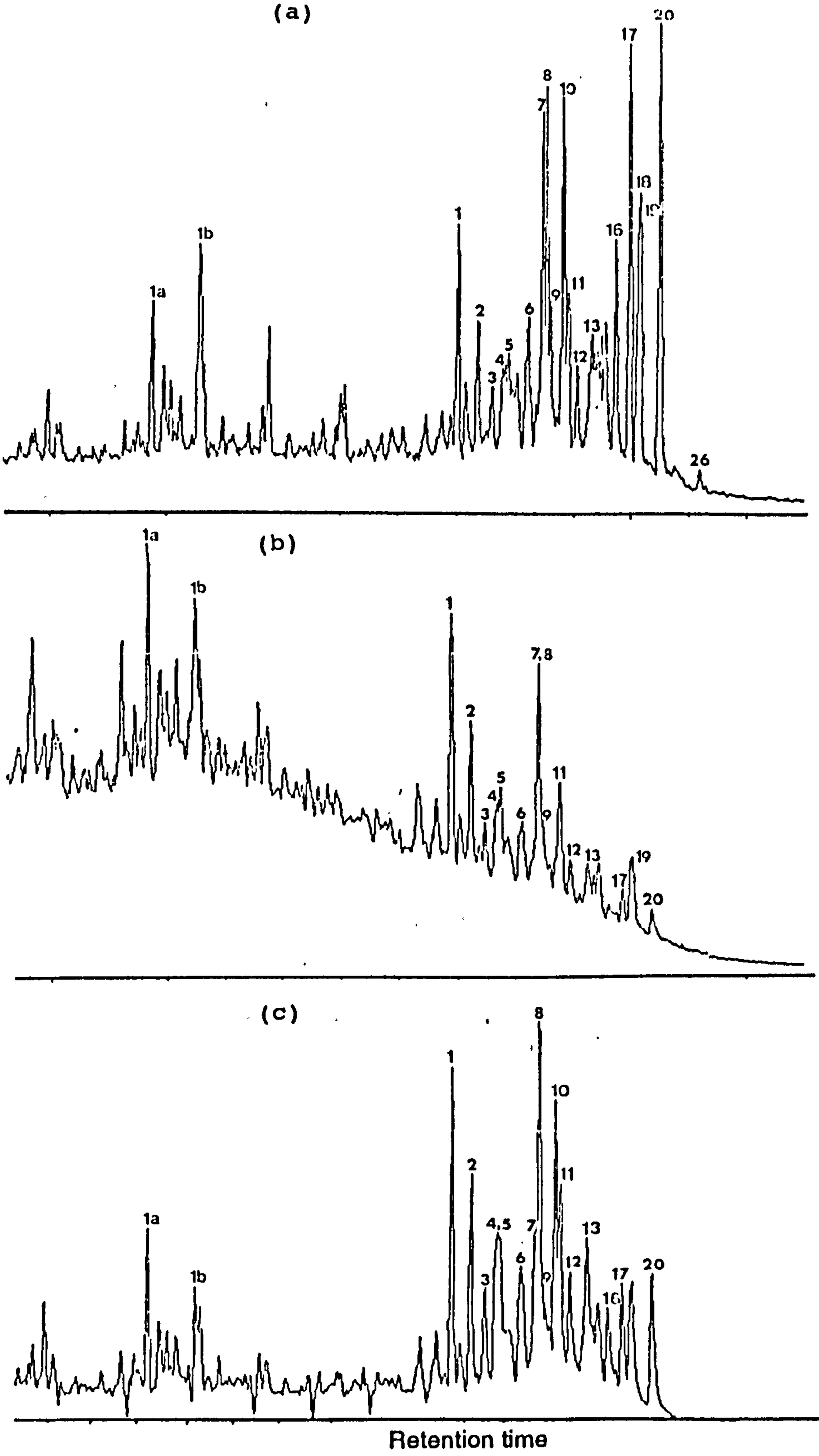

Figure 3.32 m/z 217.1950 mass chromatograms illustrating the sterane distributions of Silurian samples: (a) ZM-1 (2388.75m), (b) KA-1 bis (3029.82m) and (c) REA-1 (2764.56m). Peak assignments are listed in Table 1.

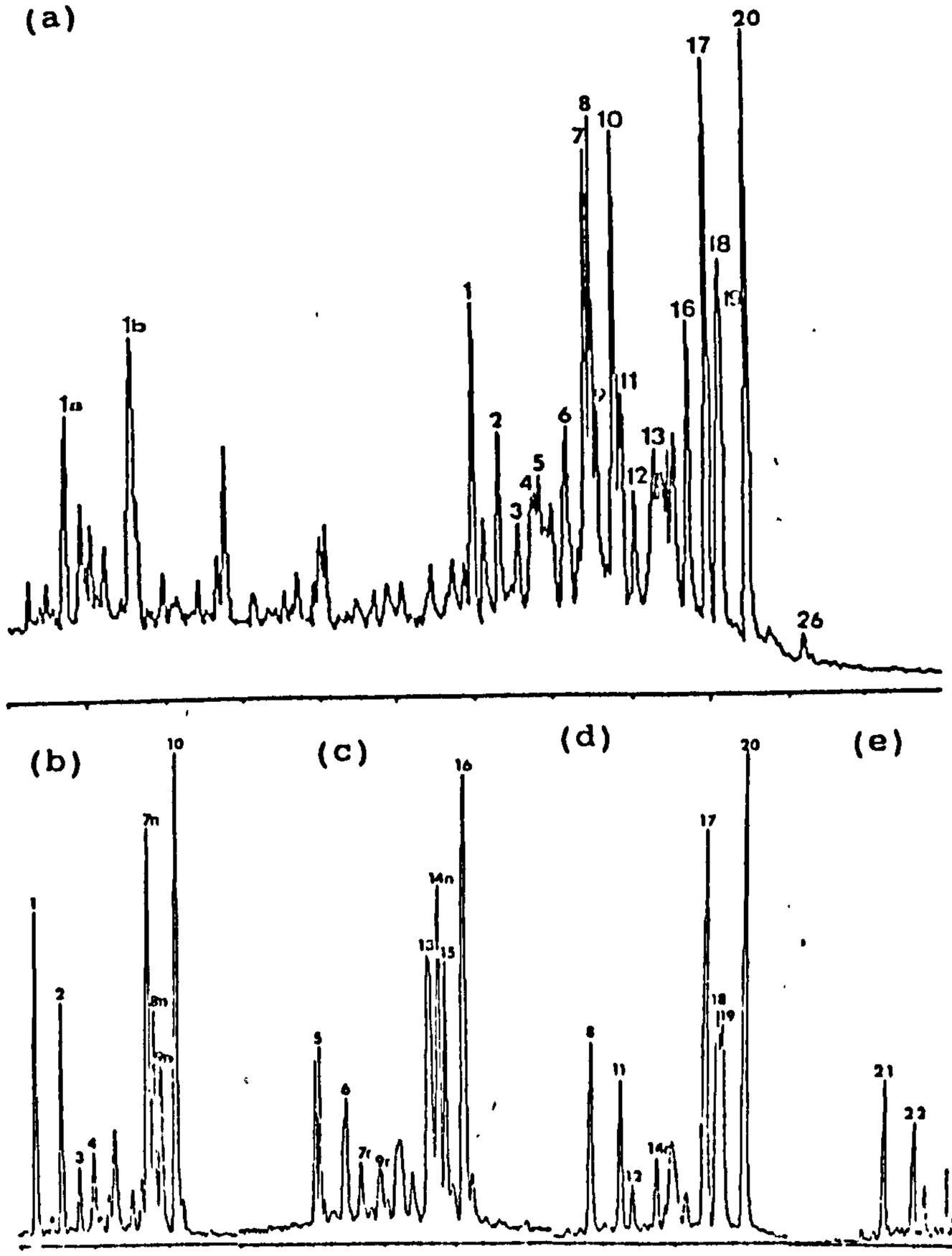

Figure 3.33 Monitoring steranes using GC/MS/EI SIM of (a) 217.1950 mass chromatogram and GC/MS/metastable ion reaction monitoring of transitions (b) m/z 372->217, (c) m/z 386->217 and (d) m/z 400->217 and (e) m/z 414->217 for one selected Silurian (ZM-1 2388.75m). Peak assignments are listed in Table 1.

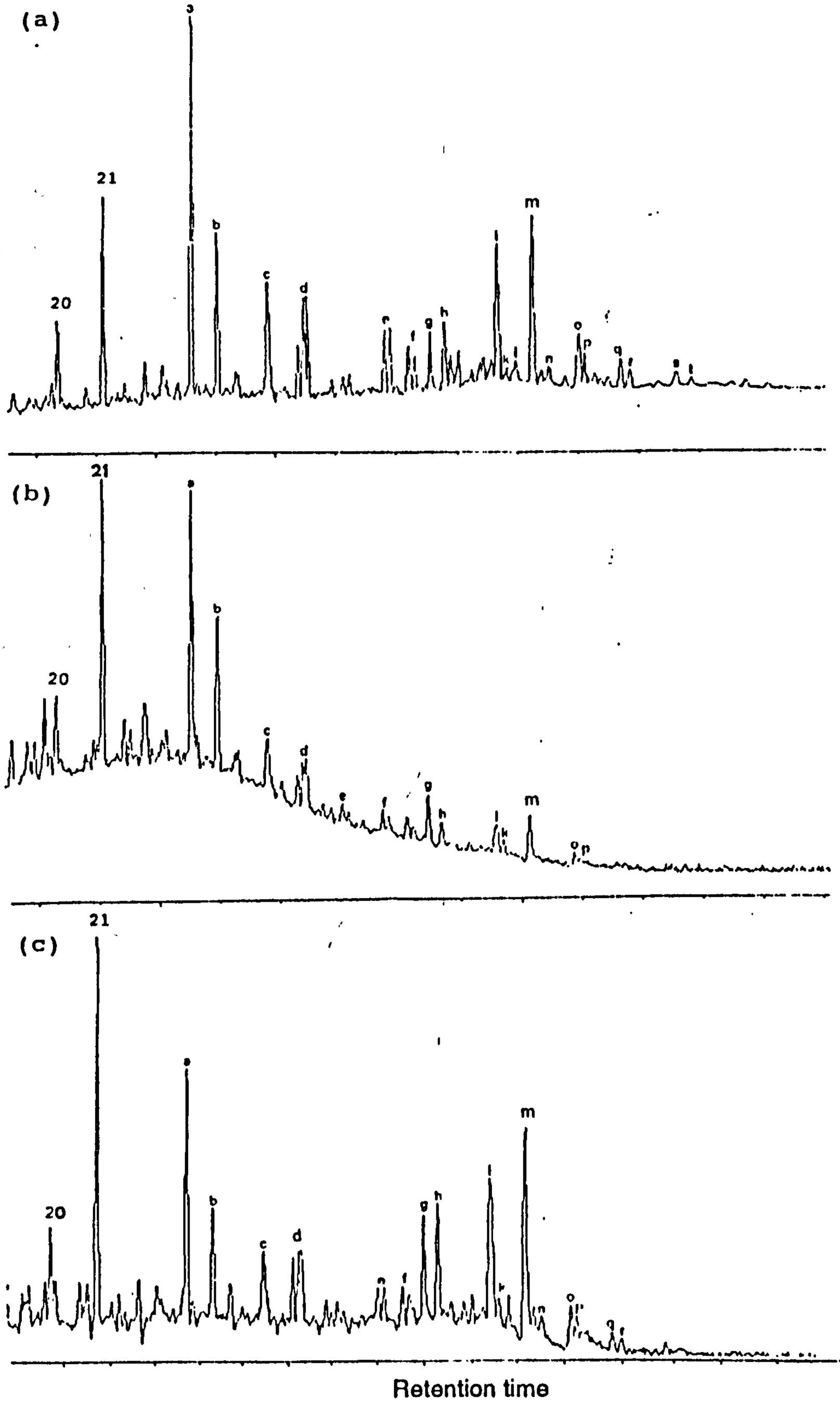

Figure 3.34 m/z 191.1794 mass chromatogram showing the terpane distributions of Silurian samples : (a) ZM-1 (2388.75m), (b) KA-1 bis (3029.82m), (c) REA-1 (2764.56m). C_{20}, C_{21} tricyclic terpanes are labelled with their carbon number. Peak assignments are listed in Table 2.

methylsteranes (Requejo et al., 1991), although coelution with C_{30}-ααα (20R) cannot be ruled out (Summons, pers. comm.). Hopanes are relatively minor in ZM-1 (2388.75m) but major compounds in KA-1 bis (3029.82m-3072.85m) and ZAR-1 (3994.65m), as indicated by the C_{30}hop/C_{29}st ratio (Appendix 3.5).

Terpane distributions of the Silurian source extracts show (Figure 3.34) that tricyclic dominate the chromatogram. The T_s/T_m ratio is close to unity (Appendix 3.6) in ZM-1 (2388.75m) and ZAR-1 (3994.65m), although the former exhibits lower maturity than the latter sample.

3.7.3.2. Aromatic hydrocarbon fraction

The distributions of C-ring monoaromatic steroidal hydrocarbons in the aromatic fractions of Silurian source extracts (Figure 3.35, m/z 253.1950) show a combination of rearranged and non-rearranged of Cis and Trans isomers, where non-rearranged (peak N° 13 and 16) are present in slightly higher amounts than in Devonian and in lesser amounts than in Triassic samples. Relatively low proportions of non-rearranged steroidal hydrocarbons (e.g peak 13, 16) are observed in samples (KA-1 bis, 3029.82m) and REA-1 (2764.56m) compared to ZM-1 (2388.75m). Short-chain (C_{21}, C_{22}) components are present in low abundance relative to long-chain homologues in all Silurian samples.

Triaromatic steroidal hydrocarbon distributions are displayed in Figure 3.35 (m/z 231.1170). The predominance of C_{28} triaromatic steroids in all Silurian samples is indicated by the %C_{28}t/(C_{26}t+C_{27}t+C_{28}t ratio, which reflects similar steroid input (Appendix 3.4).

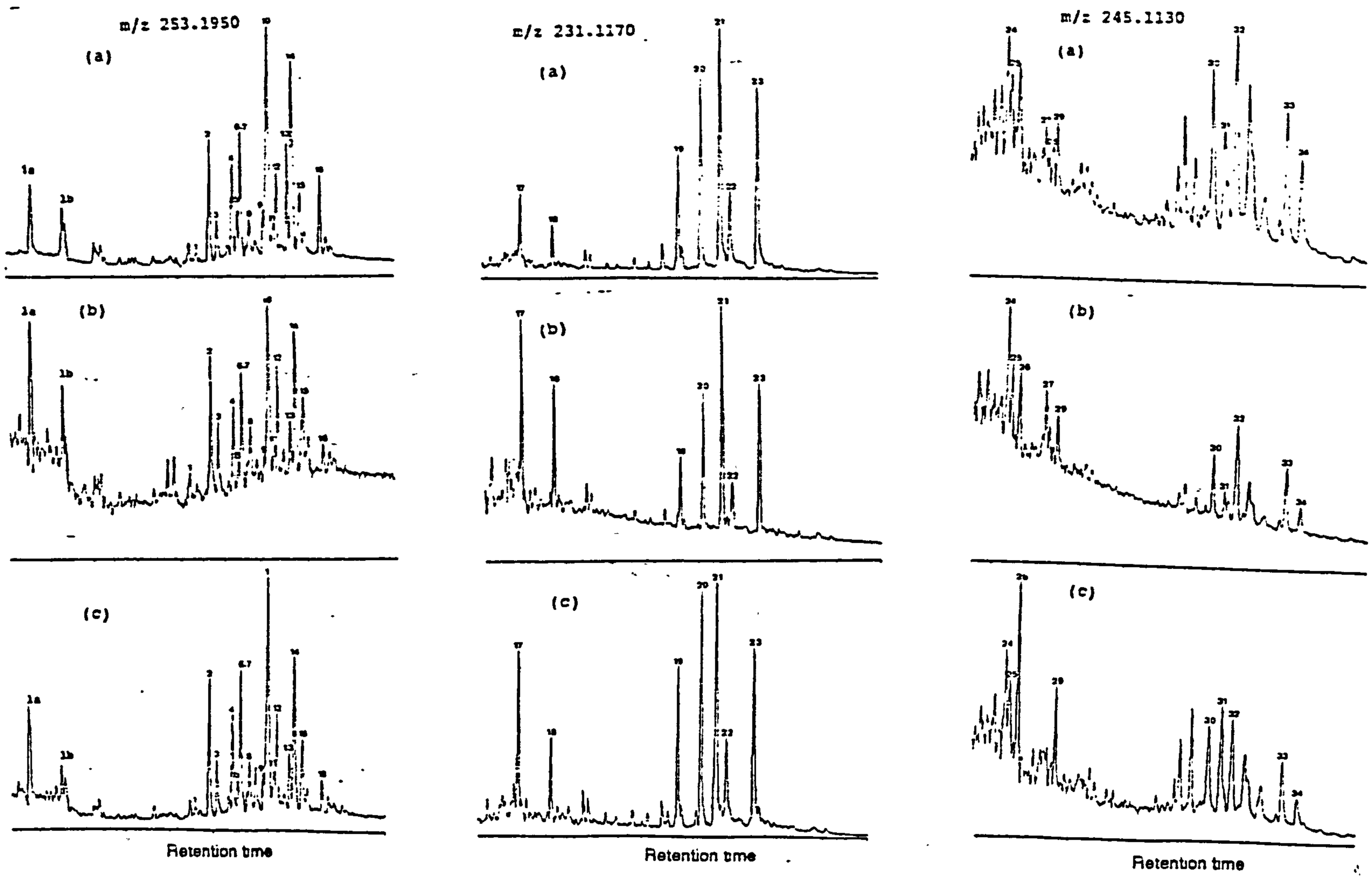

Figure 3.35 Mass chromatograms showing the distributions of C-ring monoaromatic, triaromatic and methylated triaromatic steroidal hydrocarbons for Silurian samples: (a) ZM-1 (2388.75m), (b) KA-1 bis (3029.82m), (c) REA-1 (2764.56m). Peak assignments are listed in Table 3 and 4.

The distributions of methylated triaromatic steroidal hydrocarbons in Silurian extracts (Figure 3.35, m/z 245.1130) indicate relatively high abundances of long-chain compounds (C_{27}-C_{29}) relative to short-chain homologues, particularly in ZM-1 (2388.75m). There is a tendency towards a general increase of steroid aromatization, cracking ratios and methyl triaromatic steroid indices with maturity within the Silurian section (Appendix 3.7).

3.7.4. Ordovician

3.7.4.1. Saturated hydrocarbon fraction

The distribution of the saturated hydrocarbon fractions from Ordovician source extracts (Figure 3.36) show barely detectable levels of acyclic isoprenoids relative to *n*-alkanes, particularly pristane and phytane with low Pr/*n*-C_{17} and Ph/*n*-C_{18} ratios (Appendix 3.3). The gas chromatogram (Figure 3.36a) of the saturated hydrocarbon fraction illustrates a continuous envelope of *n*-alkanes from *n*-C_{11} to *n*-C_{36}, which dominates the gas chromatogram with slight maxima at *n*-C_{15} and *n*-C_{17} and no significant odd carbon number predominance (Appendix 3.3).

Branched alkanes dominate the gas chromatogram of the non-adduct fraction (Figure 3.6d) but acyclic isoprenoids (C_n<C_{20}) are relatively minor. Figure 3.6d displays a homologous series of branched alkanes, which were reported in many oils from Palaeozoic and Precambrian basins (Aref'ev et al., 1979; Hoering, 1981; Klomp, 1986; Fowler and Douglas, 1987; Summons et al., 1988). They have been tentatively identified as monomethyl alkanes, having similar distributions and elution order to those shown by Fowler and Douglas, (1987). The distribution of monomethyl alkanes has been characterised as 3-, 2-, 4-, 5-, 6-, 7-methyl up to 13-methyl isomers; 3-

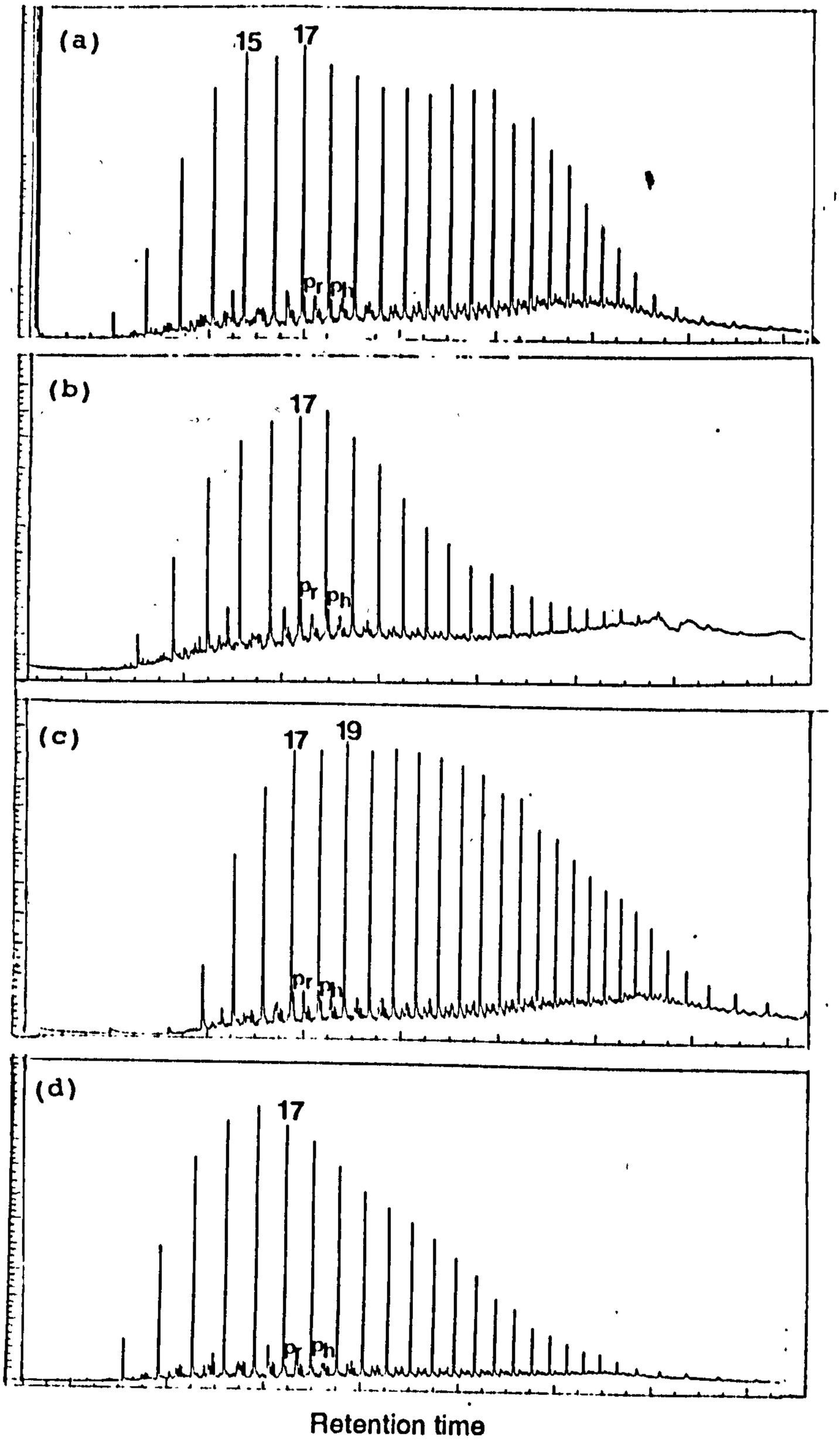

Figure 3.36 Gas chromatograms showing the saturated hydrocarbon distributions of Ordovician samples: (a) ZM-1 (2674.90m), (b) ZM-1 (2694.84m), (c) ZM-1 (2701.90m), (d) KA-1 bis (3179.85m). N-alkanes are labelled with their carbon number. Pr=pristane, Ph=phytane.

methylalkane (i.e anteiso) elutes before 2-methyl isomer (i.e iso). However, the presence of dimethylalkanes cannot be ruled out (Klomp, 1986; Robinson and Eglinton, 1990; Shiea et al., 1990).

Figure 3.37 illustrates the sterane distributions, being dominated by rearranged steranes with a prominence of C_{29} members (Appendices 3.4 and 3.5; Figures 3.12a and 3.12b).

C_{30} sterane was only detected in very low concentrations in ZM-1 (2674.90m) sample. In addition, C_{30} methylsteranes were barely detectable in Ordovician samples.

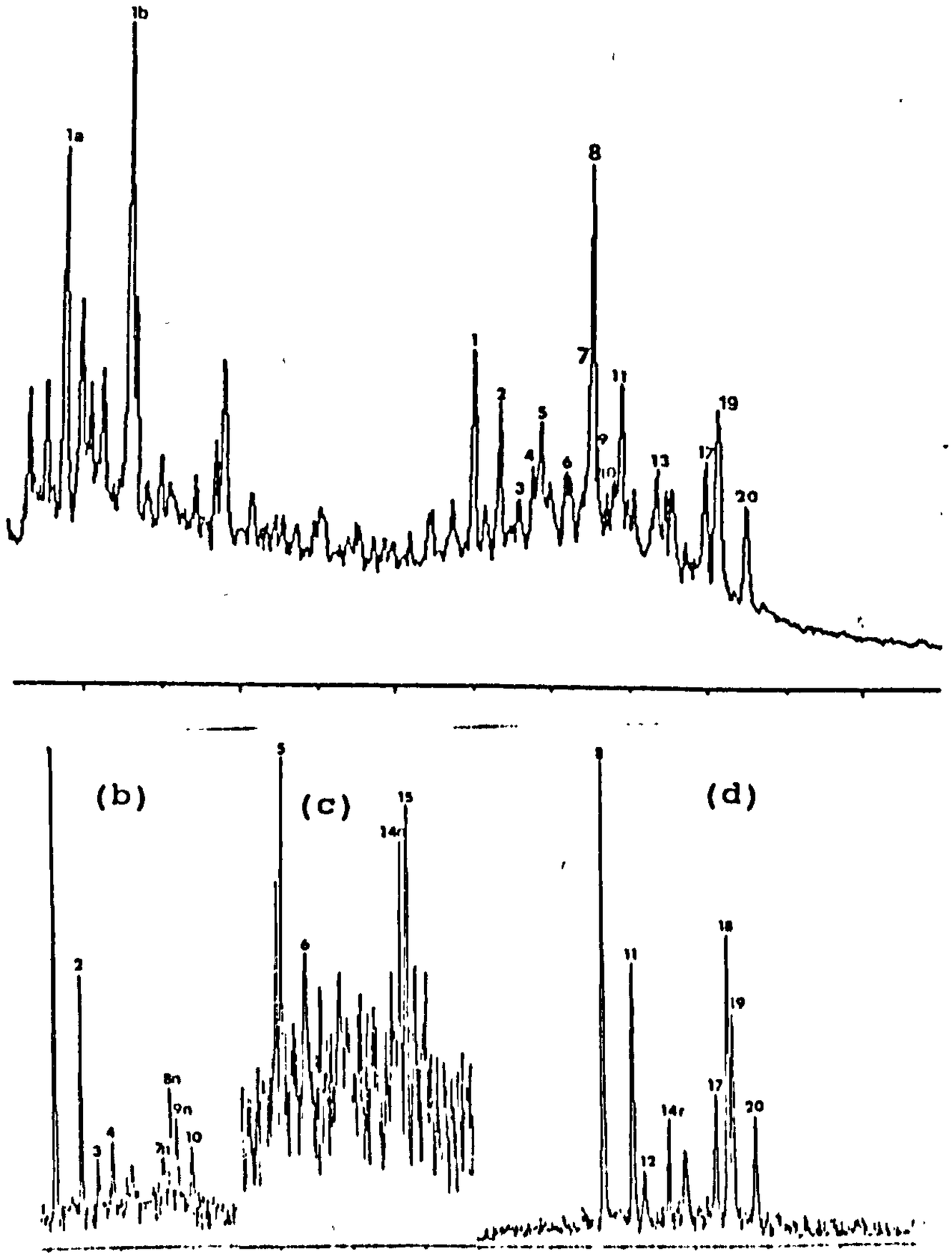

Figure 3.37 Monitoring steranes using GC/MS/EI SIM of (a) 217.1950 mass chromatogram and GC/MS/metastable ion reaction monitoring of transitions (b) m/z 372->217, (c) m/z 386->217 and (d) m/z 400->217 for one selected Ordovician sample (ZM-1 2701.90m). Peak assignments are listed in Table 1.

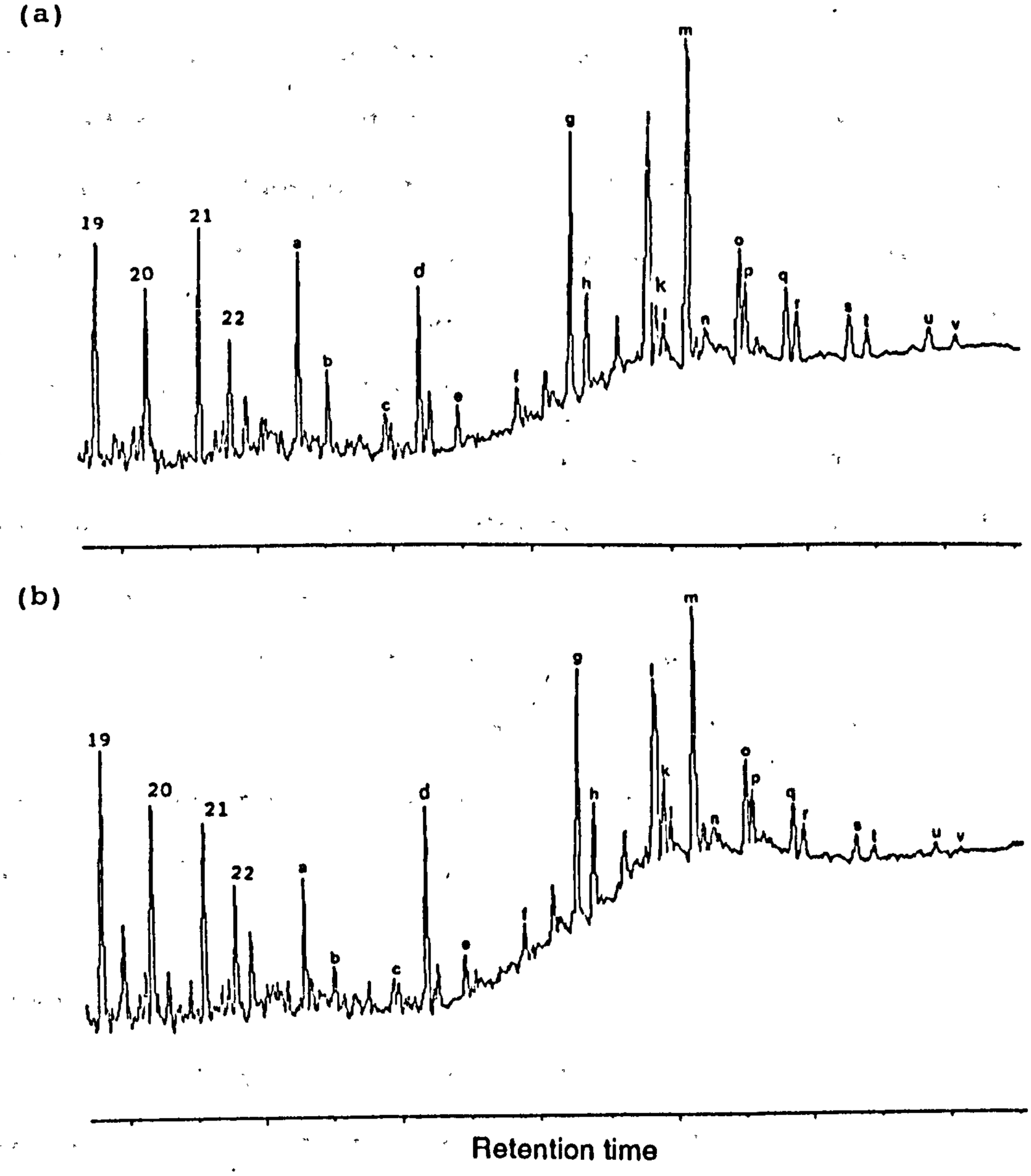

Figure 3.38 m/z 191.1794 mass chromatogram showing terpane distributions of one selected Ordovician sample (ZM-1 2701.90m). C_{20}, C_{21} and C_{22} tricyclic terpanes are labelled with their carbon number. Peak assignments are listed in Table 2.

There is a tendency towards a predominance of hopanes over steranes, as indicated by the $C_{30}\alpha\beta$ hp/C_{29}st ratio (Appendix 3.5).

Tricyclic terpanes are relatively abundant in Ordovician samples, as shown in Figure 3.38. Samples ZM-1 (2674.90m and 2701.90m) have roughly similar T_s/T_m ratio (3.09-3.33), while ZM-1 (2694.84m) exhibits a lower T_s/T_m of this ratio (0.93), suggesting a lithological effect (e.g. Rullkötter et al., 1985; Zumberge, 1987; Mello et al., 1988). Furthermore, component j (i.e 18α(H)-30- norneohopane) was detected in all Ordovician samples in high abundance relative to $C_{29}\alpha\beta$ norhopane, indicating relatively high maturity levels of these samples.

The maturity assessment based on sterane isomerization $C_{29}\alpha\alpha\alpha$ (20S/20S+20R) and hopane isomerization C_{31}-$C_{33}\alpha\beta$ (22S/22S+22R) appear to have reached the end-point values in all Ordovician samples (Appendices 3.6 and 3.7).

3.7.4.2. Aromatic hydrocarbon fraction

The distribution of C-ring monoaromatic steroidal hydrocarbons of one selected Ordovician source extract (ZM-1, 2701.90m) is shown in Figure 3.39, m/z 253.1950. Rearranged compounds with cis isomers (peak N°2 and 3) are present in relatively similar abundances, whereas non-rearranged components are minor. As shown in this Figure, m/z 231.1170, the Ordovician sample exhibits high concentrations of triaromatic steroidal hydrocarbons, particularly C_{28}(20R) relative to C_{26} and C_{27} counterparts. This is reflected by high %$C_{28}t/C_{26}t+C_{27}t+C_{28}t$ ratio (varying from 64% to 70%, Appendix 3.4).

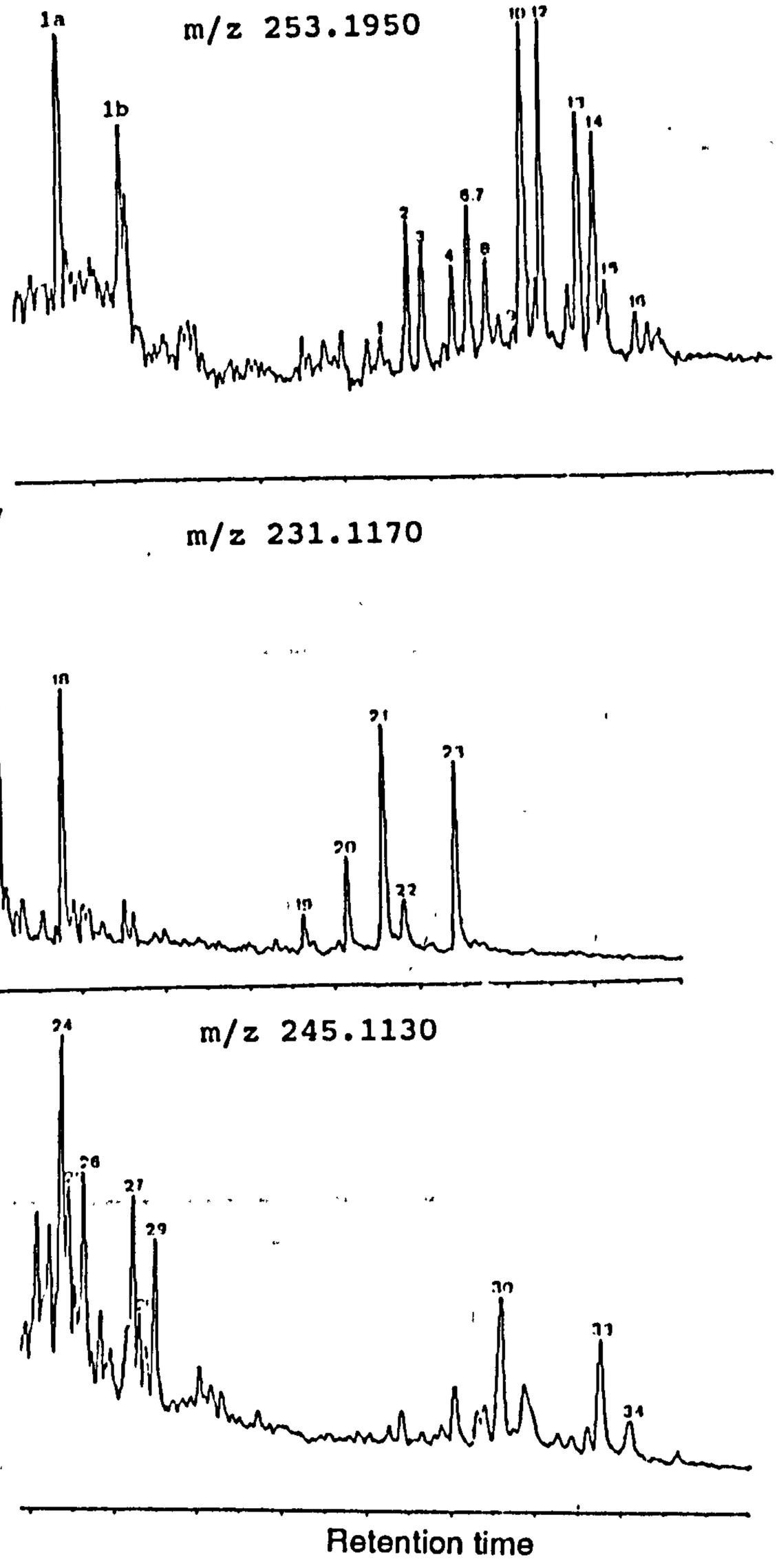

Figure 3.39 m/z 253.1950, m/z 231.1170 and m/z 245.1130 mass chromatograms illustrating the C-ring monoaromatic, triaromatic and methylated triaromatic steroidal hydrocarbon distributions of one selected Ordovician sample (ZM-1 2701.90m). Peak assignments are listed in Table 3 and 4.

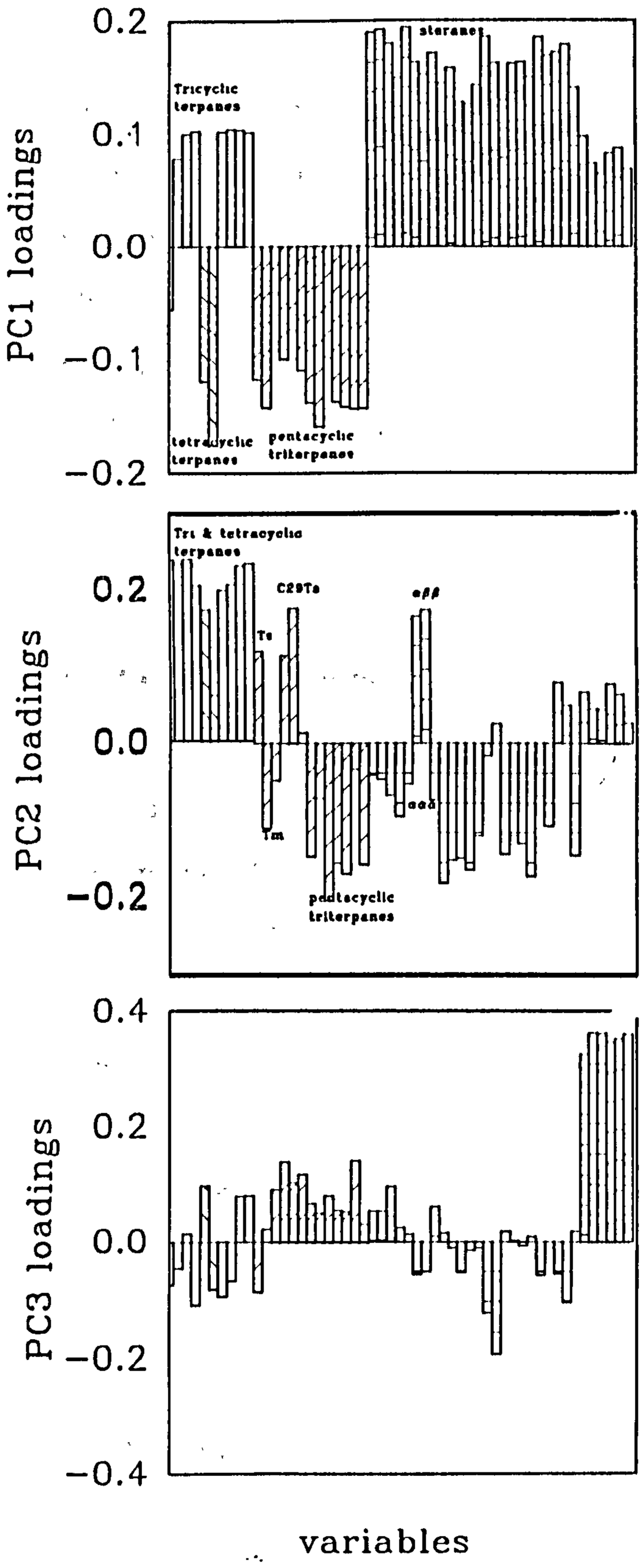

Figure 3.40 Discrimination of source-extracts using PCA. Loadings of the three PCs versus biological markers (steranes and terpanes). Scores of source-extracts on PC1 versus PC2 and PC3.

An example of the distribution of methylated triaromatic steroidal hydrocarbons for one selected Ordovician sample is shown in Figure 3.39, m/z 245.1130. This sample exhibits relatively lower abundances of long-chain (C_{27}-C_{29}) than short-chain (C_{21} and C_{22}), with a predominance of 2-methyl+3-methyl over 4-methyl isomers, as indicated by the MTSI1 and MTSI2 indices (Appendix 3.7). Furthermore, maturity parameters listed in this Appendix for all calculated ratios indicate that this sample has already reached the end-point values.

3.8 Principal component analysis of steranes and terpanes

Correlation of source extracts were carried out using principal component analysis (PCA) to determine the source input, depositional environment and maturation (Kvalheim and Telnaes, 1986; Telnaes and Dahl, 1986; Telnaes and Cook, 1991). The details of principal component analysis procedure are described in Chapter 2.

The sterane and terpane peak heights from GC-MS-MRM analysis, were normalised to percentages and converted to logarithms. This transformation is used to increase the weighting of small peaks and eliminate the dependancy by normalisation, thus minimizing the closure effect (Johanson et al., 1984, Kvalheim and Telnaes, 1986).

3.8.1 Information carried by steranes and terpanes

The principal component analysis of terpanes and steranes data gave three principal components (PC's), which accounted for 32%, 20% and 10% of the total variance for PC_1, PC_2 and PC_3 respectively (Figure 3.40).

The loadings plot on the first principal component (PC_1) exhibits a negative correlation between:

-steranes and pentacyclic terpanes,

-tricyclic and pentacyclic terpanes,

and a positive correlation beteween:

-C_{24} tetracyclic terpane and 17,21 secohopane and pentacyclic terpanes.

This could be interpreted as describing differences in source input (Kvalheim and Telnaes, 1986; Telnaes and Dahl, 1986; Telnaes and Cook, 1991).

The loadings plot of these compounds on PC_2 shows a negative correlation between:

-tricyclic terpanes and pentacyclic terpanes,

-trisnorhopane (T_m) and trisnorneohopane (T_s)

-$\alpha\alpha\alpha$ and $\alpha\beta\beta$ -C_{27} and -C_{29} steranes.

This type of correlation could be attributed to maturity with some influence of source.

3.9. Molecular organic geochemistry-Discussion

3.9.1. Triassic

The presence of an odd carbon numbered predominance, particularly *n*-C_{15}, *n*-C_{17}, *n*-C_{19}, *n*-C_{23} and *n*-C_{27} in the *n*-alkane distributions of Triassic samples indicates a probable common source, as being attributed to algal input (Martin et al., 1963; Johns et al., 1966; Gelpi et al., 1970). The presence of waxy high molecular weight *n*-alkanes indicates a contribution of long-chain lipids from higher plants. Few reports suggested terrestrial organic matter represented by plant debris with a marine phytoplankton contribution to the Triassic sediments (Sonatrach internal report, 1985).

Methyl-*n*-alkylcyclohexanes exhibits a homologous series of peak triplets ranging from C_{13} to C_{23} carbon number. These three isomers have been suggested as cis- and trans- with 2,1- 3,1- and 4-methyl-1-*n*-alkylcyclohexanes with equatorial or axial position of the methyl group (Hoffmann et al. 1987). Mature samples are thought to contain isomers cis-3,1- and methyl-1-n-alkylcyclohexanes, while the least mature samples may exhibit relatively abundant cis-2,1- and trans-2-methyl-1-*n*-alkylcyclohexanes isomers, considering their relative lower stabilities (Hoffmann et al., 1987).

Furthermore, the Pr/Ph<1 may indicate reducing conditions of depositional environment (Didyk et al., 1978), although archaebacterial membrane lipids can be considered as to be the major source for phytane (Chappe et al., 1980; Volkman and Maxwell, 1986). High abundance of rearranged steranes and C-ring monoaromatic steroidal hydrocarbons may suggest suitable clay mineral catalysts present in the Triassic rocks samples (Rubinstein et al., 1975; Sieskind et al., 1979; Riolo et al., 1986). The Pr/*n*-C_{17} and Ph/*n*-C_{18} ratios indicated more likely maturity gradient rather than source.

The high %C_{28}t/C_{26}t+C_{27}t+C_{28}t triaromatic steroid ratio correlates well with a predominance of C_{29} over C_{27} and C_{28} steranes, indicating a high input from from terrestrial debris deposited during the Triassic (Huang and Meinschein, 1979).

The 4-methylsteranes have been reported in many marine and lacustrine depositional environments with dinoflagelate contribution from sediments younger than the Triassic age ((Robinson et al., 1984; Summons et al., 1987; Goodwin et al., 1988; Summons and capon,1988). On the contrary, methylsteranes with the 3β-methyl isomers may either reflect higher input from 3β-methyl precursors or from rearrangment process, which could occur

in the sediments. However, there is no optical evidence showing dinoflagellate contribution to the Triassic organic matter. Therefore, care should be taken in using the presence of methylsteranes as paleoenvironmental indicators, since they have been reported to occur in microlalgae (*Prymnosyophyte*; Volkman et al,. 1990a). The presence of high abundance of bacterially derived hopanes (Ourisson et al., 1979) is reflected by hopane/sterane ratio, suggesting the importance of bacterial lipids in the Triassic, while low contents of tricyclic (KA-1 bis, 2605.65m) terpanes may indicate that the tricyclic terpane precursor was not important contributor. The C_{24} tetracyclic terpane could occur as a result of microbial degradation of pentacyclic terpanes (Trendel et al,, 1982). Low maturity levels of these samples is indicated by low sterane isomerization, steroid aromatization, cracking ratios and steroid methylated triaromatic indices (MTSI1 and MTSI2).

3.9.2. Devonian

The predominance of *n*-C_{17} and *n*-C_{19} and C_{15} and C_{17} in both *n*-alkane distributions can be attributed to algal or bacterial input (Johns et al., 1966; Gelpi et al., 1970).

The pristane over phytane ratio has been used as an indicator of oxic/anoxic conditions of depositional environment (Didyk et al., 1978), although other photosynthetic organisms for isoprenoids (C_n<C_{20}), such as zooplankton (Blumer et al., 1963), archaebacteria (Chappe et al., 1980; Risatti et al., 1984; Volkman and Maxwell, 1986) and algal tocopherols (Goossens et al., 1984) were also reported. The low hopane/sterane ratio, probably reflects high algal sterols input contributing to these samples, while relatively high

concentrations of hopanes may occur as a result of increasing maturity. due to their high stability. Recents reports have shown that hopanes could be released from the kerogen during hydrous pyrolysis experiments (Eglinton and Douglas, 1988), while steranes may degrade thermally faster than hopanes. The predominance of C_{29} and slightly lesser amounts of C_{27} steranes together with the presence of C_{30} desmethyl steranes were thought to be characteristic of a marine input (Moldowan, 1984; Moldowan et al., 1985), since C_{29} steranes were reported to occur in Precambrian as well as Palaeozoic sediments (Fowler and Douglas, 1984; 1987). The triaromatic steroid ratio $\%C_{28}t/C_{26}t+C_{27}t+C_{28}t$ has shown to be very useful as a source indicator for these samples (Curiale, 1989). Hence, all Devonian samples seem to reflect similarities in source. Methyl steranes were reported in many Precambrian studies (Summons et al., 1987). High abundance of 3β-methyl-compounds may suggest a major contribution from the 3β-methyl-precursor if rearrangment process does not take place in the sediments.

High abundance of rearranged steranes is often related to the presence of acid-clay catalysts, which are responsible for the rearrangment of non-rearranged biologically synthetised steroids. (Rubinstein et al., 1975). It is interesting to note high concentrations of rearranged monoaromatic steroidal hydrocarbons in this respect (Connan et al., 1986). The tendency towards high abundance of tricyclic terpanes in Devonian samples is commonly associated with sediments dominated by bacteria (Aquino Neto et al., 1982; 1983) as well as marine algae, (Volkman et al., 1990b) with some influence of maturity.

The trend towards an increase of rearranged hopanes I.e 18α(H)-30-norneohopane with increasing maturity is observed in RE-1 borehole (Cornford et al., 1988; Fowler and Brooks, 1990).

There is a general trend of sterane isomerization, steroid aromatization ratios as well as methyl triaromatic indices. However, the scatter observed for the cracking ratio could indicate maturity and/other unknown effects.

3.9.3. Silurian

Odd predominance in the *n*-alkane distribution (*n*-C_{15}, *n*-C_{17} and *n*-C_{19}) and their individual abundances may be derived from algal source (Johns et al., 1966; Gelpi et al., 1970).

The predominance of C_{27} and C_{29} steranes and the presence of C_{30} desmethyl steranes, abundance of steranes over hopanes suggest a marine organic matter input (Moldowan et al., 1985; Telnaes and Dahl, 1986; Volkman, 1986). The 24-ethyl-3β-methyl-cholestane observed in Silurian oils (Summons et al., 1987; Summons and Capon, 1988) may indicate a contribution from marine algae type *Tasmanites*. It is interesting to note similar distributions of methylsteranes to those of the Devonian samples. High tricyclic terpanes in Silurian is probably further evidence for marine algal input from *Tasmanites* (Volkman et al., 1990b).

The relatively lower abundance of rearranged steranes as well as rearranged C-ring monoaromatic steroidal hydrocarbons, particularly in ZM-1 (2388.75m) compared to other Silurian, Triassic and Devonian source extracts, perhaps reflect differences in mineral matrix content (Rubinstein et al., 1975; Riolo et al., 1986).

3.9.4. Ordovician

The gas chromatograms of the saturated hydrocarbon fractions from the Ordovician are slightly different from the Silurian, Devonian and Triassic source extracts by having a smooth *n*-alkane distribution with no odd to even carbon predominance, abundant branched/cyclic alkanes and minor acyclic isoprenoid compounds (pristane and phytane) relative to *n*-alkanes. This is related to either to an input from a non-photosynthetic organism *Gloecopsamorpha prisca* (*G-prisca*), which lacks the phytyl side-chain (Reed et al., 1986)) or the overwhelming abundance of *n*-alkanes and alkylcyclohexanes, which may dilute the biological markers (Hoffmann et al., 1987). Optical examinations as well as Py-GC of the Ordovician kerogen however, show no evidence of a *G-prisca* contribution to these sediments. In fact, comparative Py-GC traces of both Ordovician kerogen and that presented by Reed et al. (1986) shows different distributions.

The abundance of monomethyl alkanes was observed in many oils and sedimentary organic matter from early Palaeozoic and Proterozoic age (Are'fev et al., 1979; Klomp, 1986; Fowler and Douglas, 1987; Summons et al., 1988). These have been associated with bacterial fatty acids (Johns et al., 1966; Gelpi et al., 1970; Klomp, 1986; Fowler and Douglas, 1987; Summons, 1987; Summons et al., 1988) probably from prokaryotic organisms. Relatively high abundance of 4-, 5-, 6-, 7- and 8-methyl have been suggested to be derived from Blue-green algae (Gelpi et al., 1970; Han and Calvin, 1970).

Other evidence of bacterial-derived organic matter is suggested by high abundance of hopanes (Ourisson et al., 1979; 1982; 1987) a predominance of C_{29} steranes (De Sousa and Nes, 1968; Volkman, 1986). C_{29} sterane

has been associated with Blue-green algae. Therefore, caution should be taken in interpreting high C_{29} steranes as a non-marine indicator, since land plants did not evolve until the Late Silurian (Traverse, 1988).

The abundance of hopanes, C_{29} steranes, monomethyl alkanes and possibly alkylcyclohexanes in Ordovician extracts implies that prokaryotes were very active at the time of depostional environment during Ordovician age.

3.10 General discussion

The organic geochemical data (Rock-Eval and Py-GC) previously discussed for each formation shows that the organic matter is predominantly type II and II-III kerogen. The variation of the saturated, aromatic hydrocarbons and NSO contents reveals that Ordovician source extracts can be classified as highly paraffinic compared to Devonian, Silurian and to a lesser extent Triassic samples.

Molecular information based on *n*-alkane distributions (*i.e.* *n*-C_{15}, *n*-C_{17} and *n*-C_{19}) indicates that Devonian and Silurian sedimentary organic matter is predominantly of algal fatty acid input (Johns et al., 1966; Gelpi et al., 1970). The presence of similar distributions *of* *n*-alkylcyclohexanes and methyl-*n*-alkylcyclohexanes to that of *n*-alkanes may suggest a common source from algal or bacterial fatty acids. However, the abundance of waxy *n*-alkanes indicates terrestrial contribution to the Triassic organic matter. Hence, the PC_1/PC_2 scores (i.e sterane and terpane distributions), the abundance of waxy *n*-alkanes, the lack of C_{30} steranes in the Triassic; the abundance of C_{30} steranes in the Devonian and Silurian; the prominence of hopanes, tricyclic terpanes, the relative low abundance of acyclic isoprenoids, high

concentrations of monomethyl alkanes, predominance of C_{29} steranes in the Ordovician samples allow a discrimination of samples into 3 groups:

1-Ordovician

2-Devonian and Silurian

3-Triassic

The low abundance of acyclic isoprenoids ($C_n<C_{20}$) in Ordovician could be due to an overwhelming abundance of *n*-alkanes and alkylcyclohexanes, which may dilute acyclic isoprenoid hydrocarbons (Hoffmann et al., 1987).

The abundance of *n*-alkanes, monomethyl alkanes and a predominance of C_{29} steranes in the Ordovician suggest a marine contribution perhaps from from Blue-green algae (De Sousa and Nes, 1968; Han and Calvin 1970), as reflected by high abundance of amorphous bitumen. This implies that prokaryotes were very active at the time of depostional environment during Ordovician age.

The presence of methyl steranes 2α-methyl and 3β-methyl steranes may derive from algal source from marine algae but not dinoflagellates, since there were not observed in these particular samples. As suggested by Cornford et al. (1988) and Fowler and Brooks, (1990), the variation of the relative proportions of rearranged hopanes 18α(H)-30-norneohopane (i.e. $C_{29}T_s$) can be used as a maturity parameter. However, like other biological markers (e.g. T_s/T_m,), the rearranged over non-rearranged hopane ratio could be affected by source, maturity and/or lithology.

The sterane isomerization and aromatization ratios have shown trends with increasing maturity. In addition, the rate of aromatization of monoaromatic to triaroamatic steroidal hydrocarbons was found to be not only dependant on the temperature but also on the proportion of the precursors, i.e rearranged

and non-rearranged C-ring monoaromatic steroidal hydrocarbons (Abbott and Maxwell, 1988). In addition, steroid aromatization of rearranged and non-rearranged C-ring monoaromatic to triaromatic steroidal hydrocarbons may be different based on laboratory data. Although, other effects may interfere within geological strata. The methylated triaromatic steroid indices (i.e. MTSI1 and MTSI2) introduced by Lichtfouse et al. (1990), appear to be useful maturity parameters for these samples. Like methyl phenanthrene isomer ratio (MPI), this parameter could be dependent on source and/or lithology (Lichtfouse, pers. comm.).

Chapter 4 Source input and maturity assessment of oils from the northern and southern parts of Algeria. A case of discrimination of oils into oil families.

4. Source input and maturity assessment of oils from the northern and southern parts of Algeria. A case of discrimination of oils into oil families.

4.1. Introduction

This chapter is concerned with oil-oil correlations in the Mesozoic and Palaeozoic reservoirs from a number of different geographical areas in Algeria.

Generally oil-oil correlation studies are carried out in areas with a number of different oil occurrences to determine families or groups of different oil types. A range of approaches can be used which depend on the nature of the oils. For example low density (or high API gravity) oils may require a comparison of the gasoline range hydrocarbon distributions, whilst correlation of oils with low API gravity can be based on biological marker distributions (Hunt, 1979; Welte et al., 1982). In the present study, correlation parameters include data derived from biological marker distributions as well as gasoline range hydrocarbons. Hence, this chapter aims to:

(i)Establish the number of different oil families in the northern and southern parts of the Algerian Sahara.

(ii)Characterise each oil family in terms of its biological marker content (e.g. sterane, terpane, monoaromatic and triaromatic steroids) as well as gasoline range hydrocarbons.

(iii)Discern differences between each group of oils by considering the effects of maturation, migration and biodegradation as well as the influence of depositional environment of the source rocks.

(iv)Determine from the geochemical characteristics of each family, the nature and the level of maturity of each source rock at the time of generation.

The oils analysed in this study can be classified as paraffinic oils (Tissot and Welte, 1984 pp 417). Distributions of biological marker and gasoline range hydrocarbons together with principal component analysis (PCA) of sterane and terpane distributions (i.e PC_1 and PC_2 scores versus triterpane:sterane ratio as well as the correlation of triterpane/sterane ratio with tricyclic/tricyclic+hopane ratio) reveal a discrimination of the well numbers into three groups:

(i) Southeast Constantine (DK1, GKN1), Ghadames-El Borma (ELB9), Sbaa (ODZ1, DECH1), Ain Amenas (TG22).

(ii) Ghadames-El Borma (KA2, ROM1), Ain Amenas (ZR115)

(iii)Gassi Touil (GT6, GT47), Rhourd-Nouss (RN48,RNSE6).

Oils from Illizi basin (MRK16, STAH8, STAH40 and MRK12) are poor in biological marker content and as yet cannot be assigned to any of the above groups.

In order to determine the level of thermal alteration of oils in reservoirs, paraffin indices (Thompson, 1983, 1987) were considered. Oils from the Sbaa basin (TOT1 and DECH1) are shown to be affected by incipient biodegradation (Connan et al., 1985), while the rest of the oils are regarded as mature to overmature.

4.2. Results

The oils are located in seven basins, which are listed below. In the following sections, each one is discussed in turn.

4.2.1. Southeast Constantine basin (DK1, DK6 and GKN1)

4.2.2. Ghadames-El Borma basin (ELB9, KA2, ROM1)

4.2.3. Sbaa basin (DECH1, ODZ1, TOT1)

4.2.4. Illizi basin (MRK12, MRK16, STAH40, STAH8, WT1)

4.2.5. Gassi Touil (GT6, GT47)

4.2.6. Rhourd Nouss (RNSE6, RN48)

4.2.7. Ain Amenas (DL127, TG22, ZR115)

4.2.1.Southeast Constantine basin

This section comprises results of Cretaceous oils, namely DK1 and DK6 from Conacian and GKN1 from Cenomanian reservoirs.

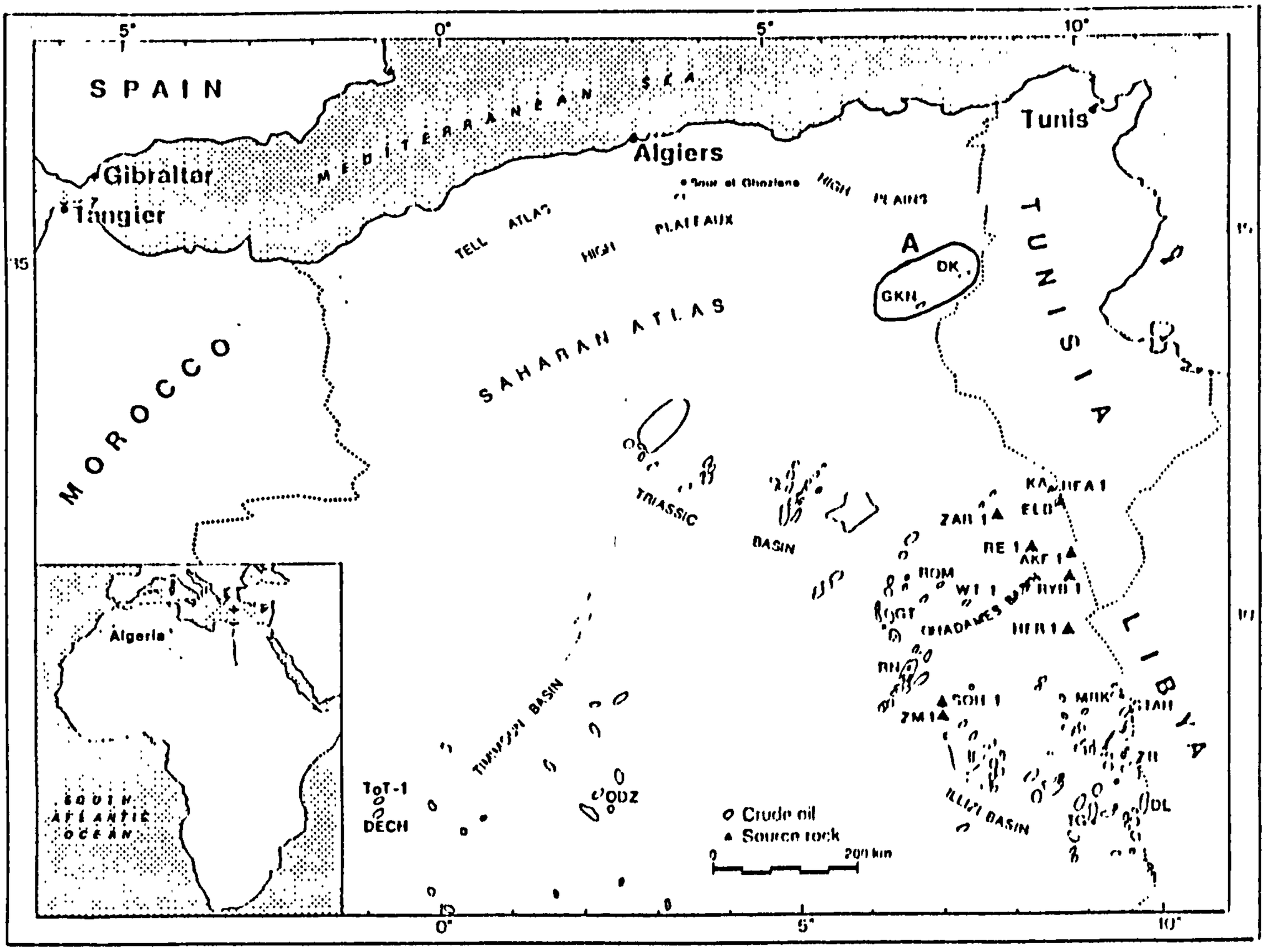

Figure 4.1a: Sample location map showing the area of study (A= Southeast Constantine basin), which group of oils were investigated.

4.2.1.1.Bulk composition

The bulk composition data (% saturates, %aromatics and %NSO (including asphaltenes), Table 4.1a) are displayed in Figure 4.2a. This shows that DK1 and DK6 form a separate group from GKN1 oil, being characterised by relatively high saturated hydrocarbons and low NSO contents and low density values. Therefore, only DK1 and GKN1, have be considered for a biological marker and gasoline range investigation.

Table 4.1a: Bulk composition data

well	%Sats	%Aro	%NSO	Pr/Ph	D*
DK1	66.75	17.63	15.62	2.37	0.847
DK6	66.80	18.16	15.04	2.54	0.847
GKN1	85.09	12.63	2.28	2.66	0.807

* D is the density of oils measured at 20°C (g/cm^3).

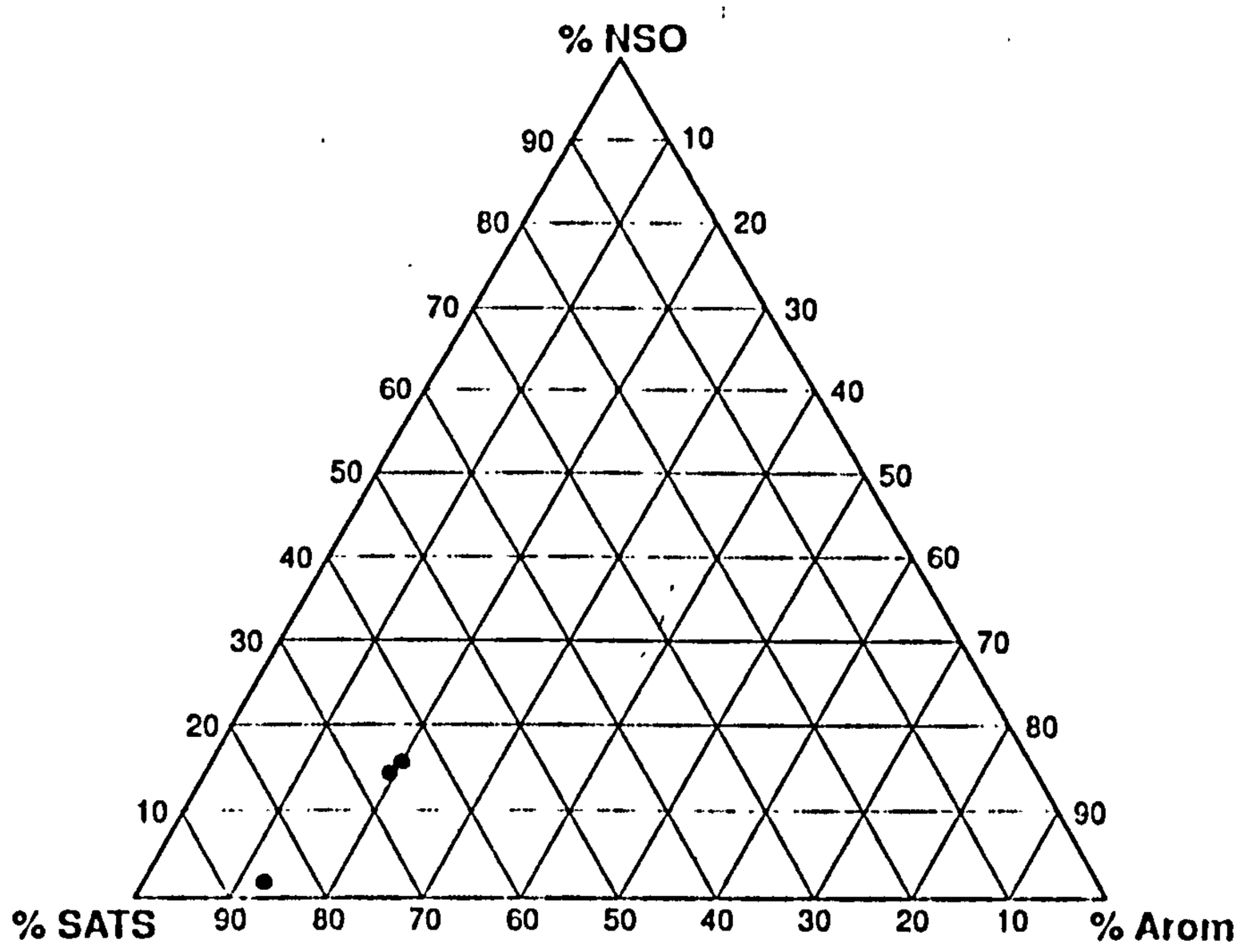

Figure 4.2a Relative proportions of saturated, aromatic hydrocarbons and NSO compounds of oils from the Southeast Constantine basin.

4.2.1.2. Saturated hydrocarbon fraction

As described above, DK1, DK6 and GKN1 are dominated by saturated hydrocarbons, as clearly seen in the whole oil gas chromatograms (Figure 4.3). The *n*-alkanes form a smooth distribution with prominent low molecular weight components, and no odd or even carbon number predominance. The Pr/Ph is greater than two in every case (Table 4.1a).

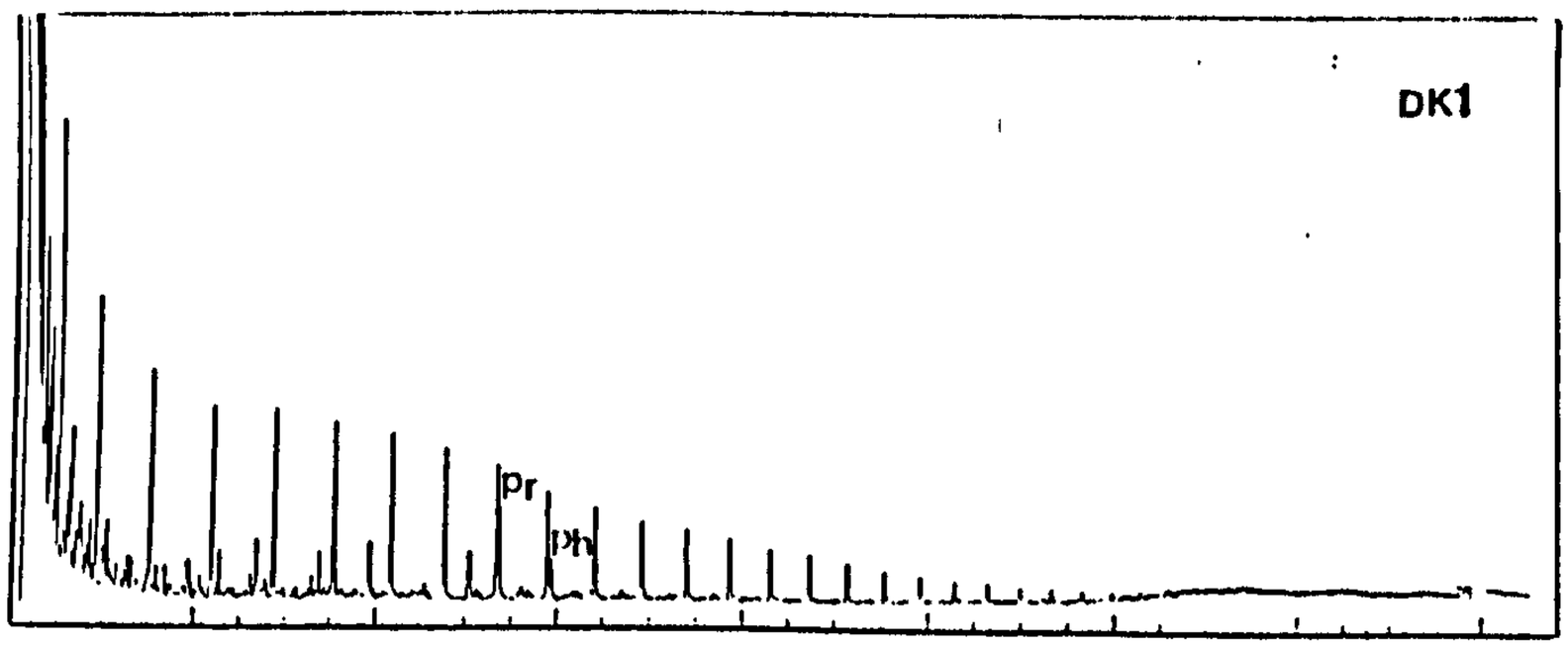

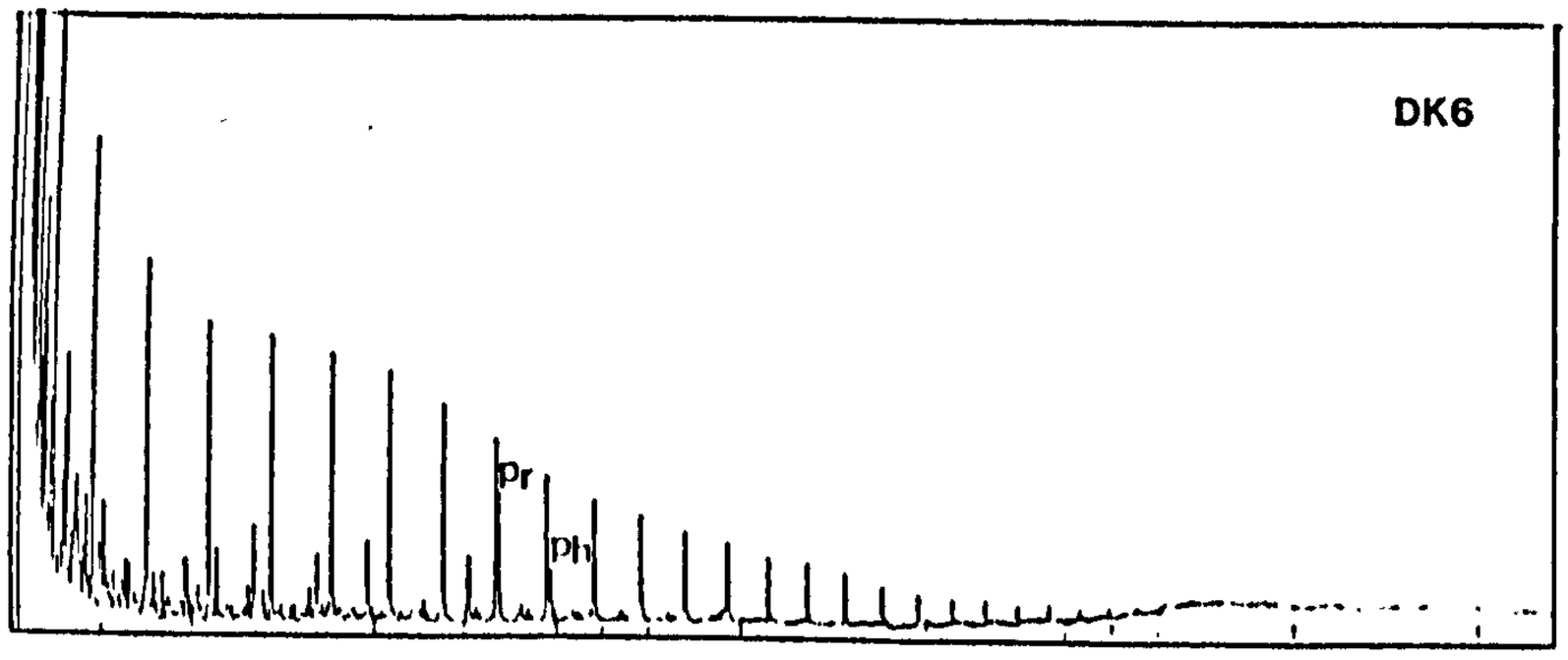

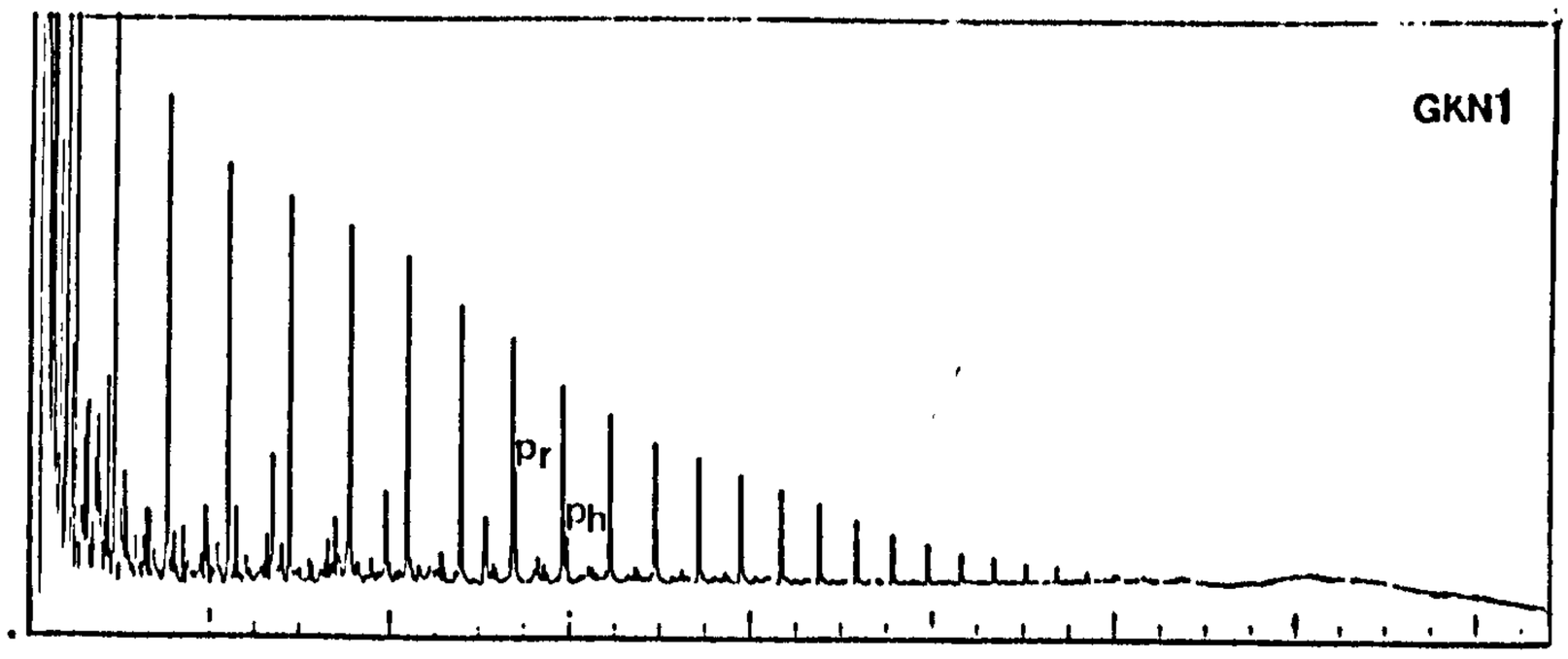

Retention time

Figure 4.3 Gas chromatograms of oils from the Southeast Constantine basin.

Monocyclic alkanes were detected by gas chromatography/mass spectrometric analysis (GC/MS) of the non-adducted saturated hydrocarbon fraction, using the m/z 83 and m/z 97 mass chromatograms for *n*-alkylcyclcohexanes and methyl-*n*-alkylcyclohexanes respectively (Figure 4.4a and 4.4b). Peak assignments have been made based on comparison of their mass spectra with those shown in the literature (Rubinstein and Strausz, 1979; Philp, 1985; Fowler et al., 1986). Mass spectra of *n*-alkylcyclohexanes and methyl-*n*-alkylcyclohexanes are displayed in Figure 3.10, Chapter 3). Biological marker distributions were determined using gas chromatography mass spectrometry operated at high resolution (GC/MS) in a selected-ion monitoring mode (SIM) and metastable ion reaction monitoring (MRM). Monoaromatic (m/z 253.1950), triaromatic (m/z

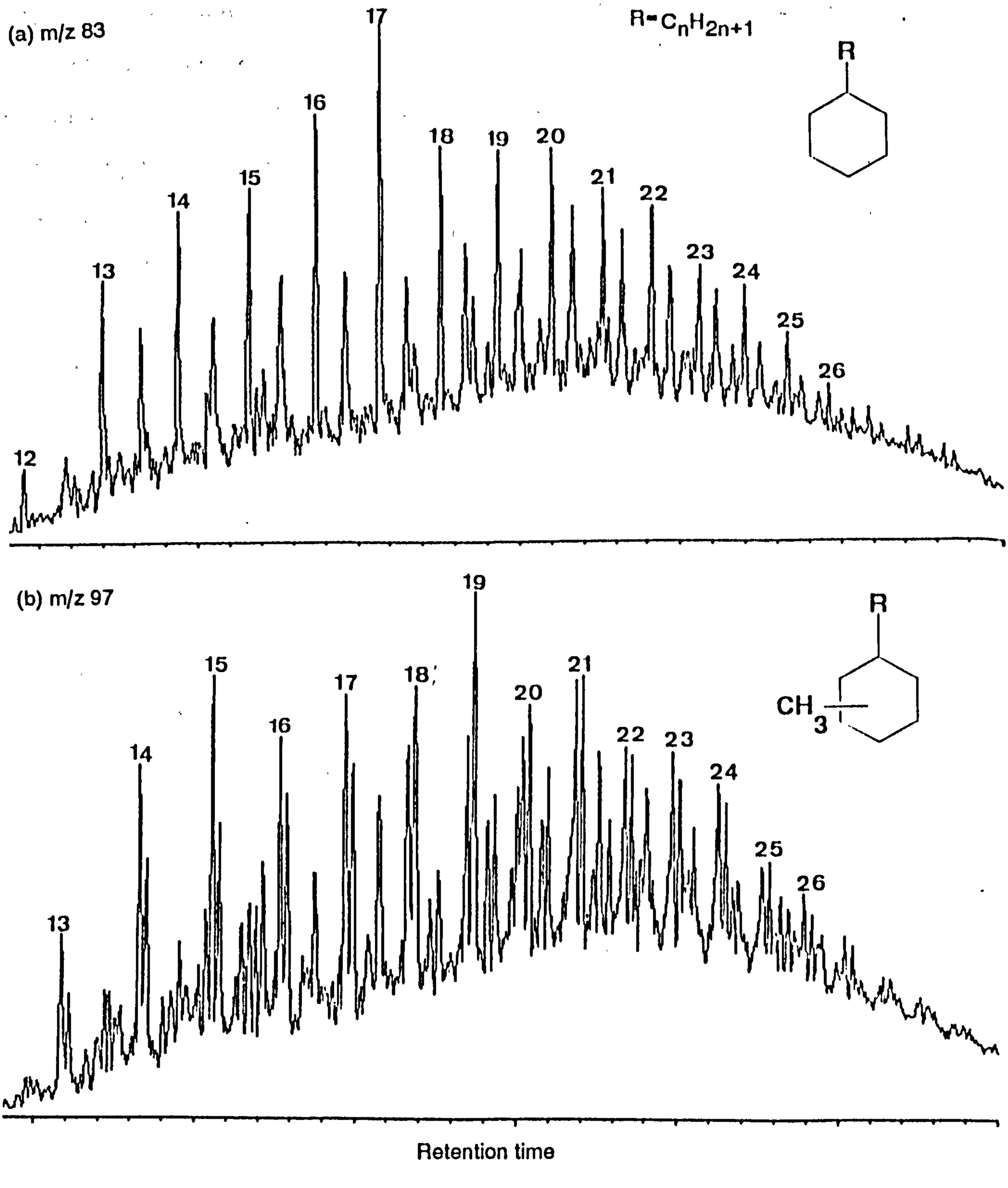

Figure 4.4 (a) m/z 83 and (b) m/z 97 mass chromatograms showing the distributions of *n*-alkyl and methyl-*n*-alkylcyclohexanes in one selected oil from the Southeast Constantine basin (DK1). Peaks are labelled with their carbon number.

231.1170) and methylated triaromatic steroidal hydrocarbon distributions (245.1330) were only detected using high resolution (GC/MS) in selected ion monitoring mode (SIM). The corresponding peak assignments are shown in Tables 1, 2, 3 and 4 respectively.

Representative sterane distributions are shown in Figure 4.5a, b, c, d and e (SIM and MRM traces).

Figure 4.6 shows that the C_{27} and C_{29} components dominate the sterane distributions of both oils, with a predominance of rearranged steranes in GKN1, as expressed by the 13β(H),17α(H)-C_{27} and -C_{29}(20S)/ 5α(H),14α(H),17α(H)-C_{27} and -C_{29} (20S) sterane ratios (e.g. C_{27}r/C_{27}n and C_{29}r/C_{29}n respectively, Appendix 4.2), while 5α(H),14α(H),17α(H) (ααα) and 5α(H),14β(H),17β(H) (αββ)(20R) steranes are major components in DK1. Furthermore, the relative proportions of (C_{27}-C_{29}) non-rearranged and rearranged steranes displayed similar pattern in Figure 4.7a and 4.7b, showing a close relationship between DK1 and GKN1.

C_{30} steranes are minor components in GKN1 but present in fairly high amounts in DK1 (Figure 4.6d) with a prominence of (ααα) (20R) and (20S). It is important to point out that rearranged C_{30} steranes occur in much less abundance their rearranged counterparts (Figure 4.5d). Short-chain steranes, pregnane (C_{21}) and homopregnane (C_{22}) are low in relative abundance compared to long-chain (C_{27}-C_{29}) homologues in DK1.

Methylsteranes occur in the range of C_{27}-C_{30} carbon numbers. As mentioned in Chapter 3, C_{30} methylsterane distributions (Figure 4.8) have been identified by coinjection of authentic standards and comparison with of mass chromatograms with those shown in the literature (Summons et al., 1987; Summons and Capon, 1988). Peak assignments are listed in Table 1. Methylsteranes were barely detectable in GKN1, while they were recorded in relatively higher abundance in DK1. It is worth noting the predominance of 24-ethyl-5α(H),14β(H),17β(H)-3β-methyl-cholestane (20R) (e.g 24-ethyl-αββ-3β-methyl-cholestane) in DK1. Peak 33 has been reported as 4-

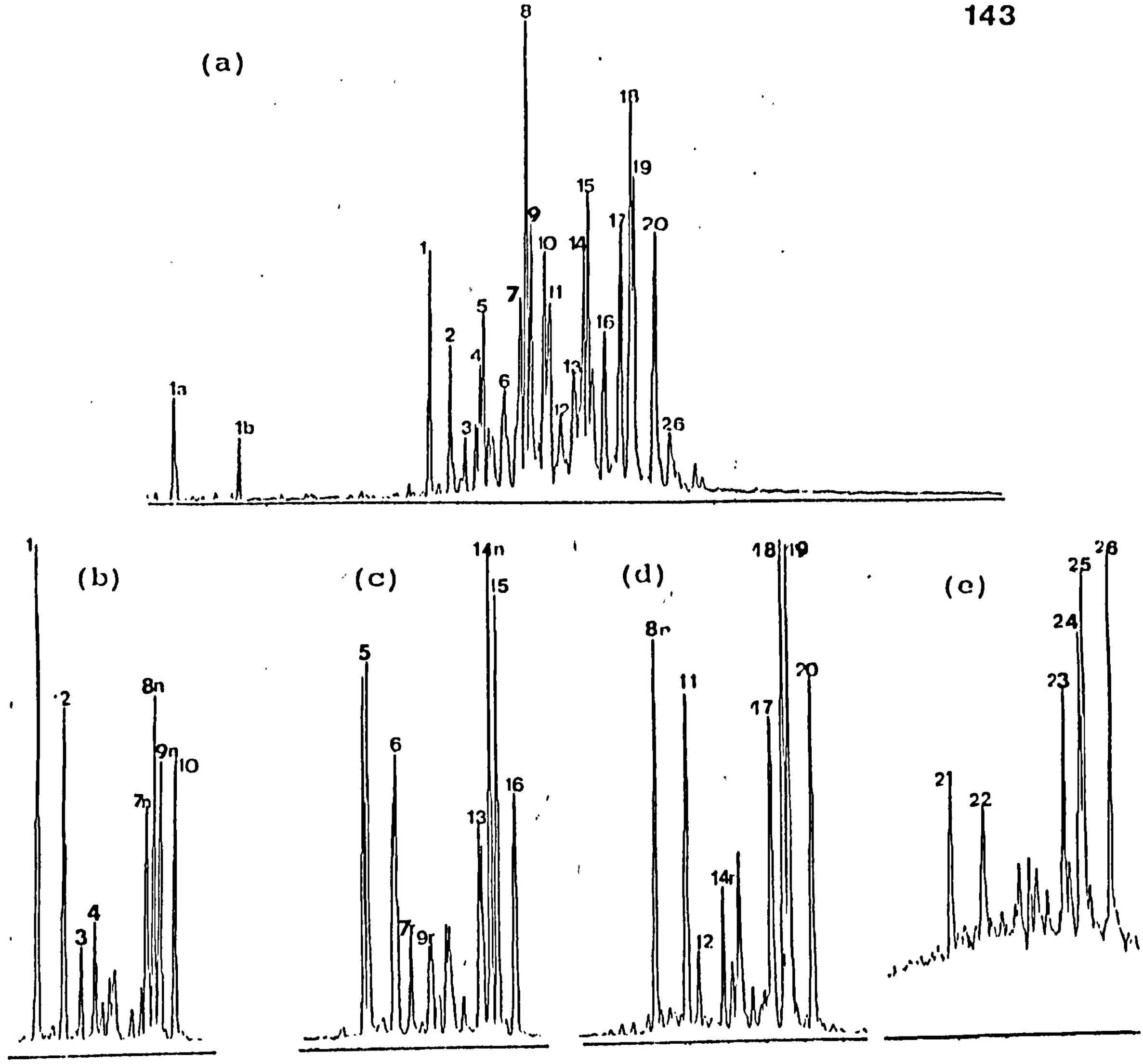

Figure 4.5 Monitoring steranes using GC/MS: high resolution SIM monitoring of (a) 217.1950 mass chromatogram ; (b) m/z 372->217, (c) m/z 386-> 217, (d) m/z 400->217 and (e) m/z 414->217 metastable ion transitions. The sample is an oil (DK1) from the Southeast Constantine basin. The C_{30} steranes are low in relative abundance. Their low concentrations and interference with methylsteranes can be determined using GC/MS metastable ion reaction monitoring (GC/MS/MRM). Furthermore, rearranged and non-rearranged steranes are resolved. Peak assignments are listed in Table 1.

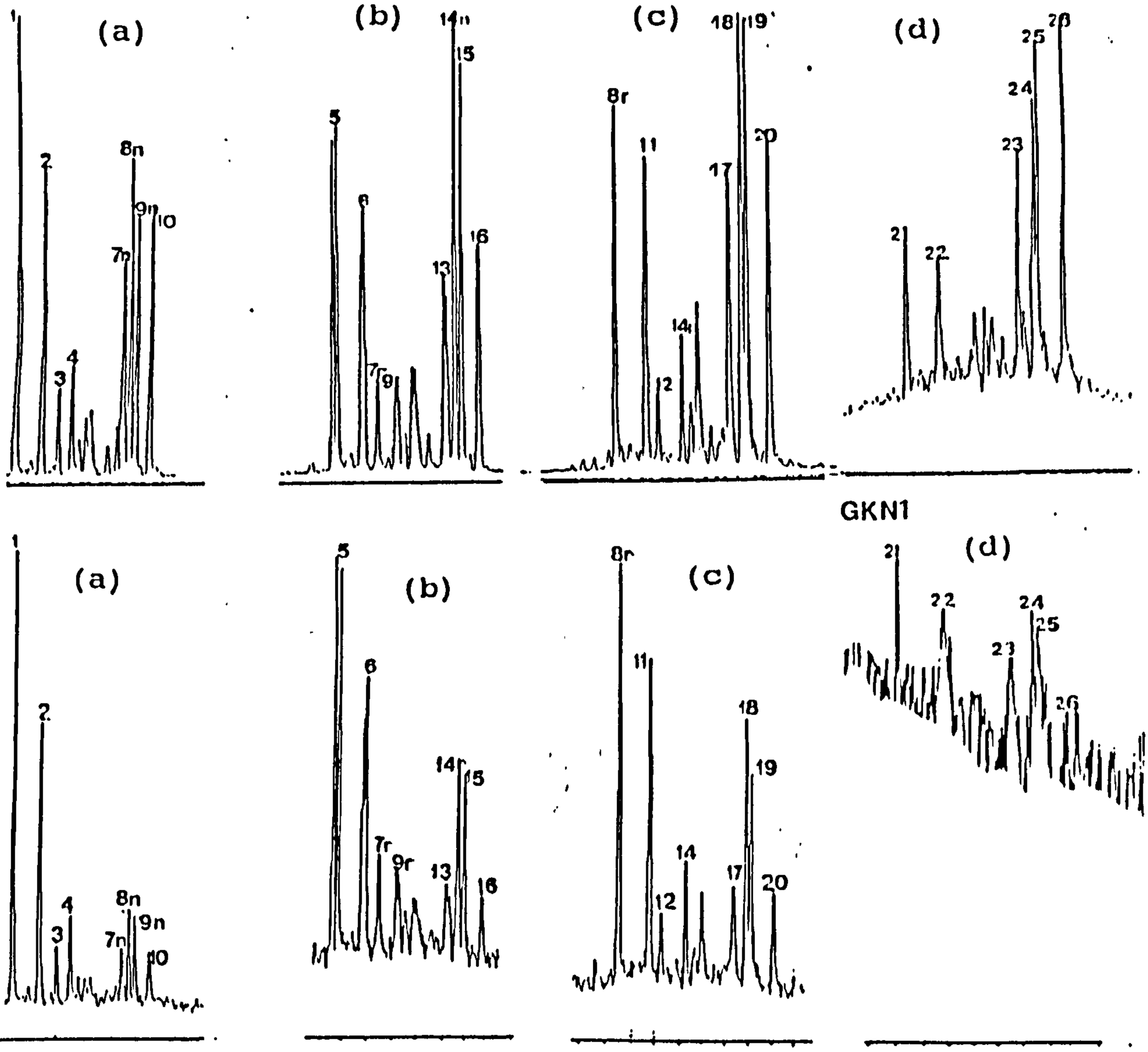

Figure 4.6 Metastable ion transitions of (a) m/z 372->217, b) m/z 386-> 217, (c) m/z 400->217 and (d) m/z 414->217 for oils from the Southeast Constantine basin (DK1 and GKN1). Peak assignments are listed in Table 1.

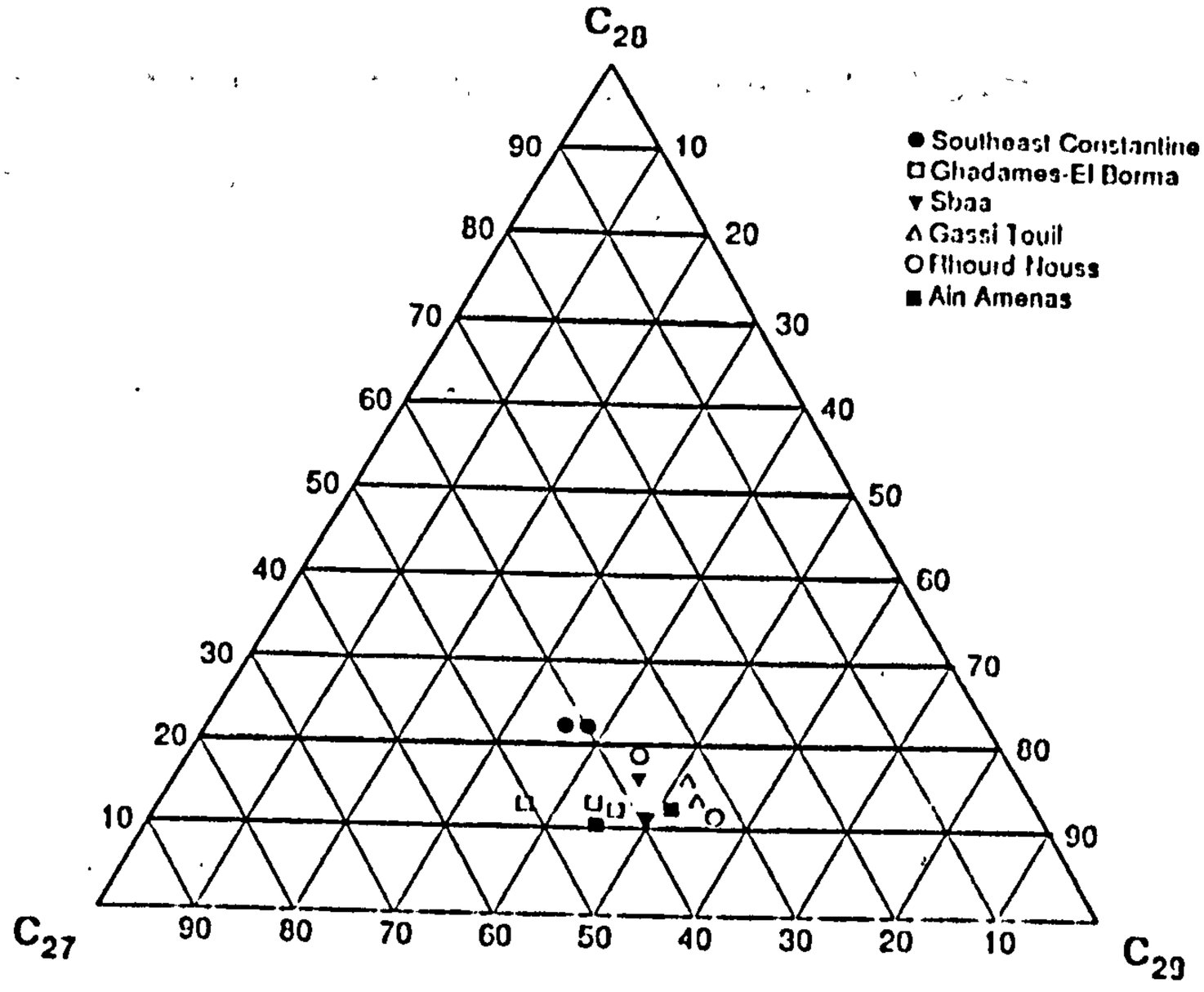

Figure 4.7a Relative proportions of non-rearranged (C_{27}-C_{29}) steranes of oils.

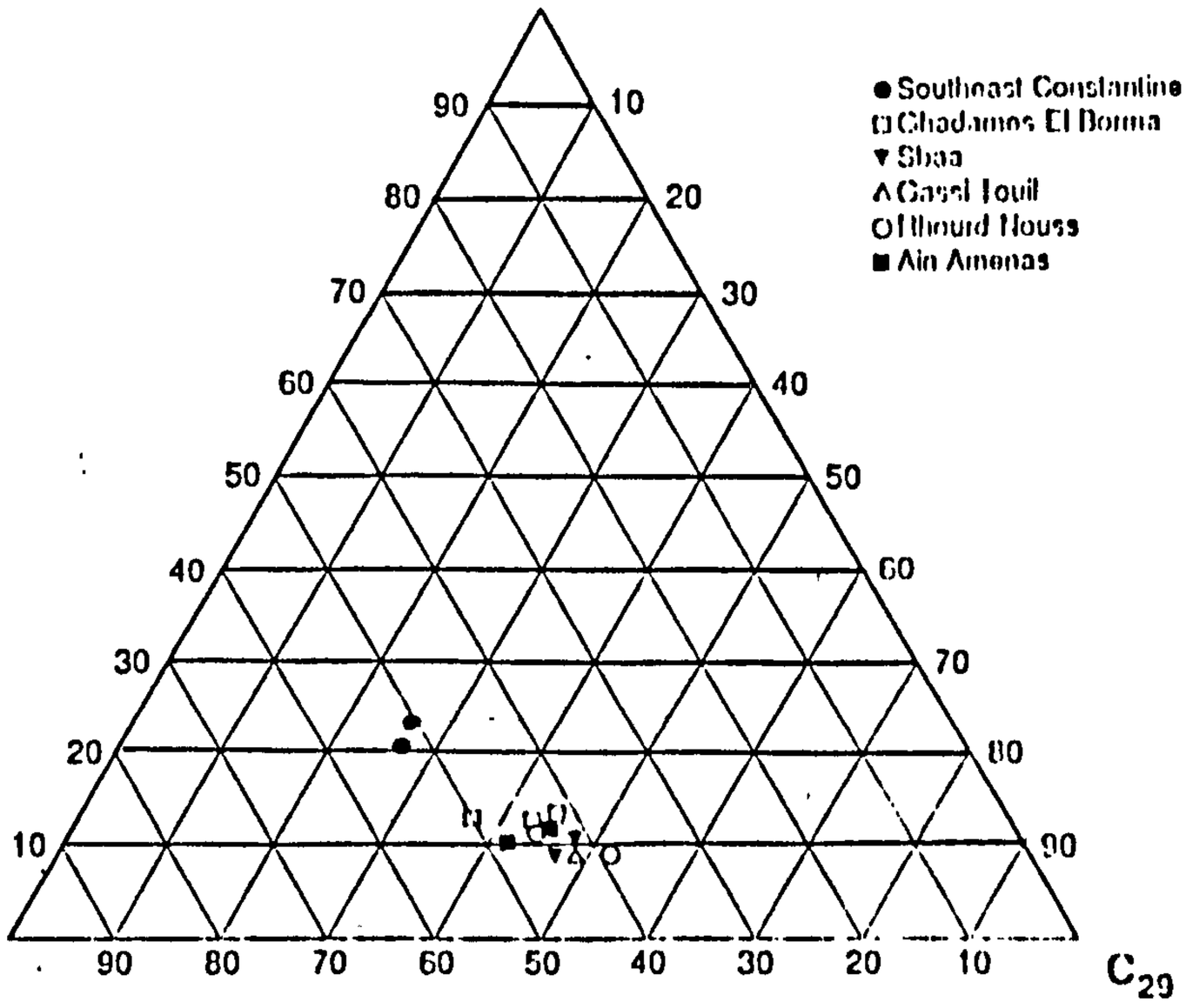

Figure 4.7b Relative proportions of rearranged (C_{27}-C_{29}) steranes of oils.

methylsteranes, although coelution with C_{30}-ααα (20R) cannot be ruled out (Summons, pers. comm.).

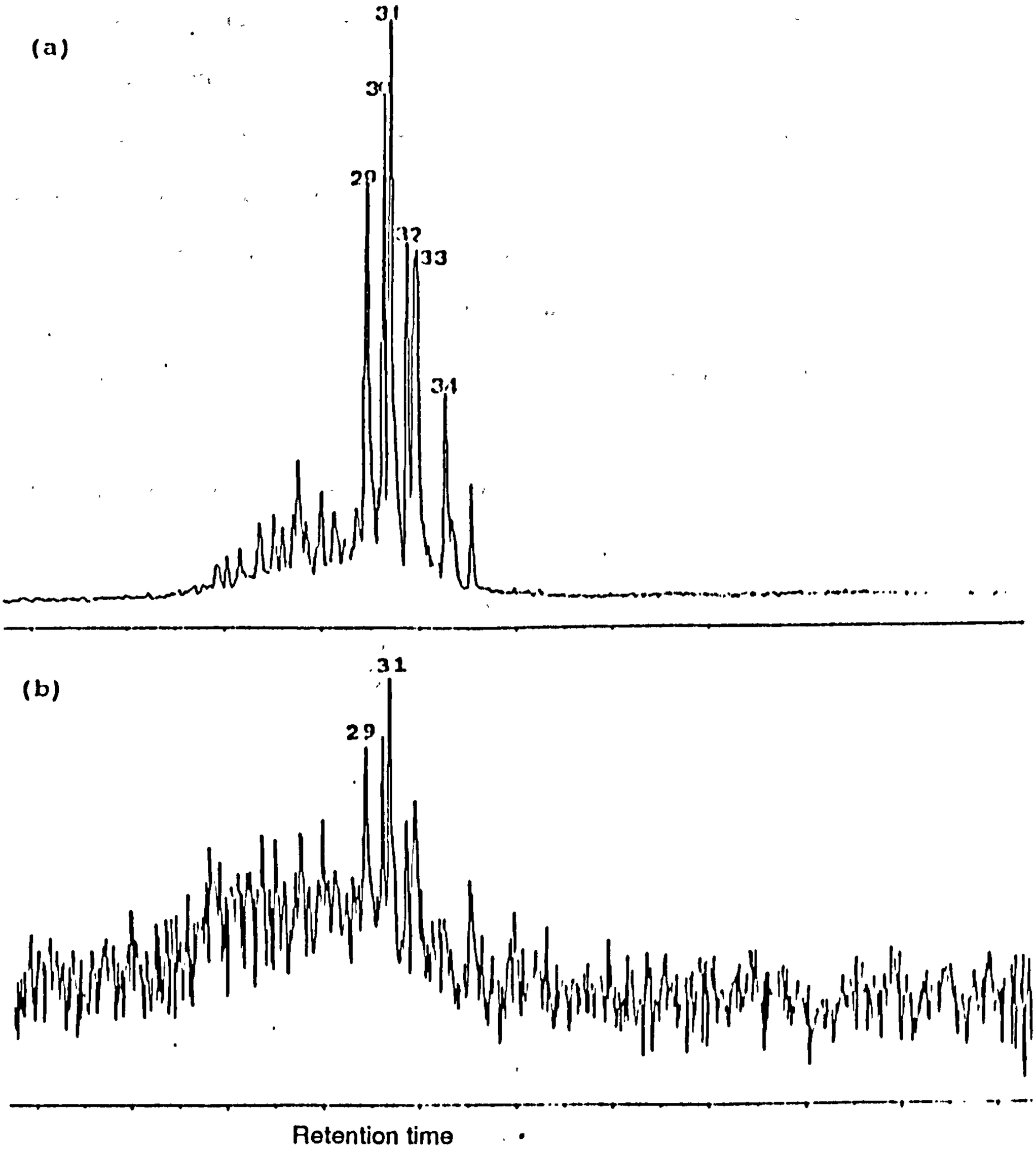

Figure 4.8 Mass chromatogram from metastable ion reaction monitoring of transition m/z 414->231 for C_{30} methyl steranes in oils from the Southeast Constantine basin: (a) DK1 and (b) GKN1. Peak assignments are listed in Table 1.

Hopane abundances are relatively higher than steranes, as the hopane to sterane ratio (e.g. C_{30}hp/C_{29}st in Appendix 4.4). There is a low abundance of tricyclic terpanes (T) relative to hopanes (hop) in both oils as shown in Figure 4.9, 4.56a and 4.56b.

Compounds (j and k) eluting just after $C_{29}\alpha\beta$ norhopane, have been detected in these oils, albeit in low concentrations in DK1. As previously mentioned in Chapter3, these compounds have been tentatively identified by comparison with published MRM traces (Moldowan et al., 1991) as :

j=18α(H)-17α-methyl-28,30-dinorhopane (e.g. 18α(H)-30-norneohopane or $C_{29}T_s$),

k=17α(H)-15α-methyl-27-norhopane (e.g. 17α(H) diahopane or B_3).

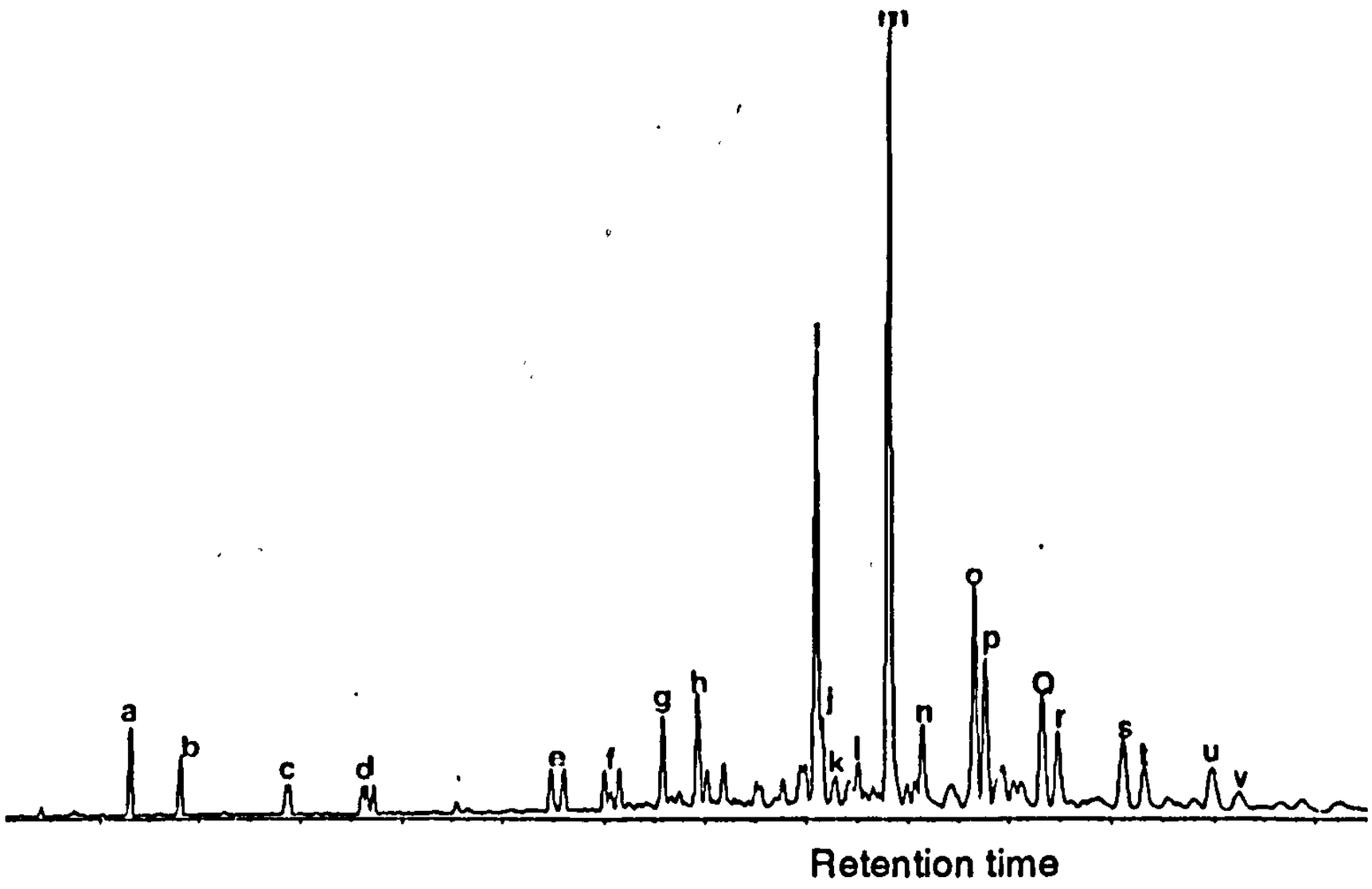

Figure 4.9 m/z 191.1794 mass chromatogram showing terpane distributions of one selected oil from the Southeast Constantine basin. Peak asssignments are listed in Table 2.

These rearranged hopanes occurring in organic extracts, are also present in oils in various proportions.

There is a general increase of the $C_{29}T_s$ relative to 17a(H),21b(H)-30 norhopane (e.g.$C_{29}\alpha\beta$ norhop). The plot of $C_{29}\alpha\beta$ norhop/$C_{30}\alpha\beta$ hop versus C_{29}Ts/$C_{29}\alpha\beta$ norhop (Figure 4.10) indicates relatively higher

abundance of $C_{29}T_s$ than GKN1, suggesting probably higher maturity levels of GKN1 than DK1 (Cornford et al., 1988; Fowler et al., 1990). The lower maturity level of DK1 is also indicated by the presence of 17β(H),21α(H)-C_{29} normoretane (C_{29}βα) and 17β(H),21α(H)-C_{30} moretane (C_{30} βα) and the similar concentrations of the C_{27} 18α(H),21β(H)-22,29,30-trisnorneohopane (T_s) relative to 17α(H),21β(H)-22,29,30- trisnorhopane (T_m), with T_s/T_m close to unity.

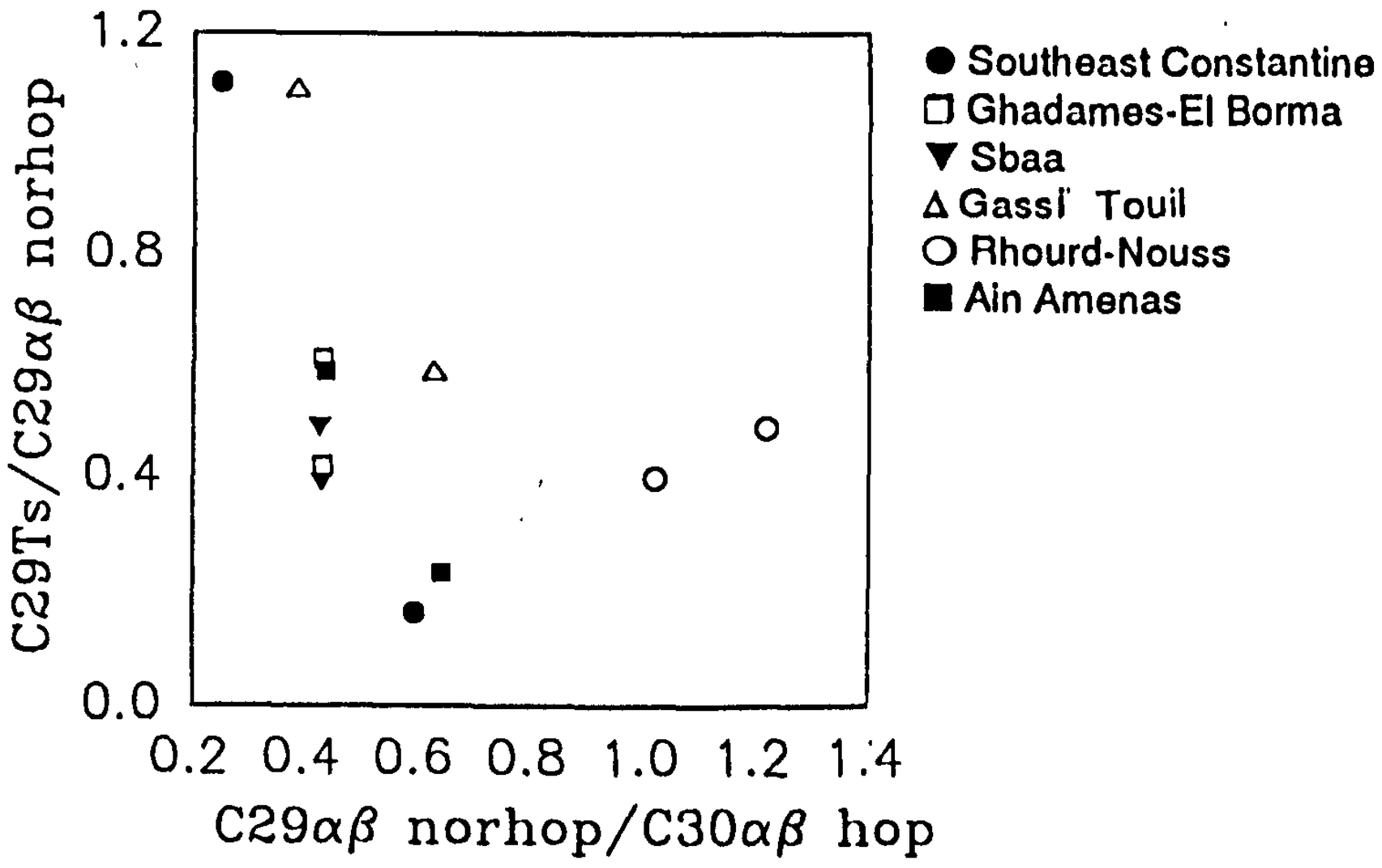

Figure 4.10 Correlation of $C_{29}T_s/C_{29}$αβ norhop versus C_{29}αβ norhop/C_{30}αβ hop.

4.2.1.3. Aromatic hydrocarbon fraction

A feature of particular interest in the C-ring monoaromatic hydrocarbon distribution of DK1 oil (Figure 4.11, m/z 253.1950 mass chromatogram) is the presence of prominent C_{28} ring-C monoaromatic steroidal hydrocarbon (peak N° 6). Non-rearranged isomers are minor components relative to rearranged compounds, with a predominance of cis-isomers (e.g. 5β-methyl). Short-chain monoaromatic steroidal hydrocarbons (C_{21} and C_{22}) are present albeit in very low abundance in DK1.

The distribution of triaromatic steroidal hydrocarbons is displayed in Figure 4.11 (m/z 231.1170 mass chromatogram), showing prominent C_{28} components (i.e peak N°23), as reflected by the ratio of total C_{28} triaromatic/total $C_{26}+C_{27}+C_{28}$ triaromatic steroid (e.g. $\%C_{28}t/C_{26}t+C_{27}t+C_{28}t$, Appendix 4.2). Short-chain homologues are observed in relatively low abundance, as indicated by low cracking ratio (Appendix 4.5). Furthermore, measurement of the extent of sterane isomerization reveals low level of maturity of DK1. In contrast, steroid aromatization has proceeded extensively to more than 80% conversion of monoaromatic to triaromatic components (Appendix 4.5).

The methylated triaromatic steroidal hydrocarbon distribution is displayed in Figure 4.11, m/z 245.1130 mass chromatogram. Long-chain components are dominant. Peak N° 24, 25 and 26 as well as 27, 28 and 29 have been reported to be 2-methy+3-methyl-, 4-methyl- and 6-methyl-C_{21} and -C_{22} isomers by comparison with published mass chromatograms (Lichtfouse, 1989; Lichtfouse et al., 1990). The 4-methyl components are dominant. Hence, both the methylated triaromatic steroid indices (2-methyl+3-methyl/2-methyl+3-methyl+4-methyl-C_{21} and -C_{22} (e.g. MTSI1 and MTSI2 for C_{21} and C_{22} components respectively) reveal low extent of methyl triaromatic isomerization for DK1 oil (0.31 and 0.32 respectively).

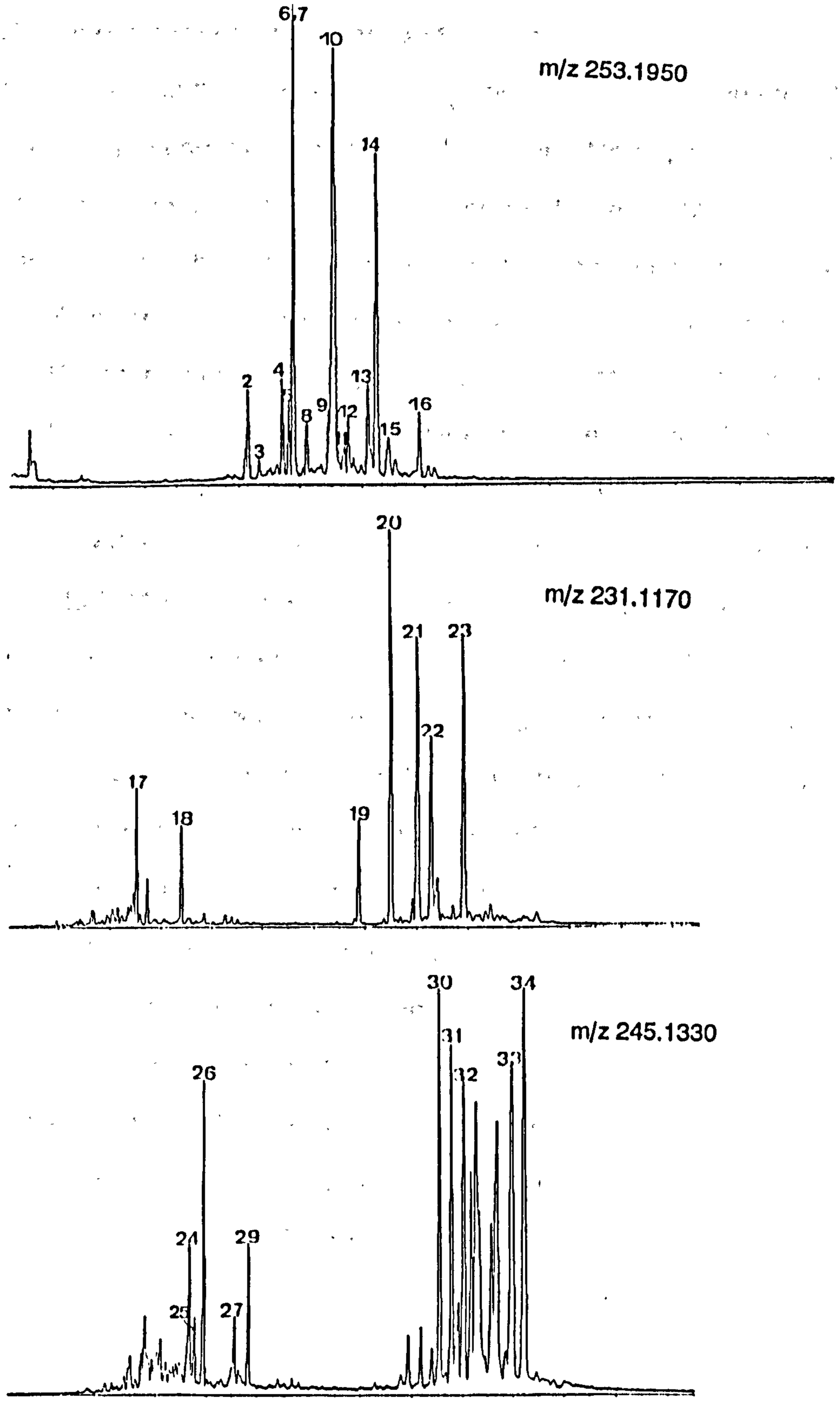

Figure 4.11 mass chromatograms illustrating C-ring monoaromatic, triaromatic and methylated triaromatic steroidal hydrocarbon distributions of DK1 oil. Peak assignments are listed in Tables 3 and 4.

4.2.1.4. Gasoline range hydrocarbon fraction

The gasoline range hydrocarbons (C_5-C_8) provide useful parameters for oil-oil and oil-source correlation studies (Erdman and Morris, 1974; Thompson, 1979; 1983; Schaefer et al., 1984; Schaefer and Littke, 1987).

Oils were analysed by capillary gas chromatography for characterisation of their gasoline range hydrocarbon distributions. Gas chromatograms of DK1 and GKN1 are presented in Figure 4.12a and 4.12b. Peak assignments have been made by comparison with published gas chromatograms (Schaefer and Littke, 1987). Peak assignments are listed in Table 5. It worth noting the predominance of (C_4-C_7) gasoline range hydrocarbons in GKN1 compared to DK1 oil. Normal alkanes are significant compared to branched, cyclic alkanes and aromatic hydrocarbons. Thompson (1979, 1983; 1987) has shown that the composition of the gasoline range hydrocarbons changes as oil generation proceeds. He introduced paraffinicity and aromaticity indices to determine the extent of maturation, biodegradation and water washing. The paraffin indices were calculated using the concentrations of the gasoline range hydrocarbons (C_4-C_8). Paraffin indices I and II (e.g. Heptane and Isoheptane values and other parameters are reviewed in Chapter 1, section 1.3.1.3). Thompson (1983) gave the following classification of oils on the basis of gasoline range hydrocarbons:

Petroleum class	class limits	
	Isoheptane index	Heptane index
biodegraded	0-0.8	0-18
normal paraffinic	0.8-1.2	18-22
mature	1.2-2.0	22-30
overmature	2.0-4.0	30-60

According to this classification, DK1 and GKN1 can be regarded as normal paraffinic oils. Furthermore, both oils exhibit similar aromaticity ratios (Appendix 4.6). In addition to these paraffin indices, Thompson, (1987,

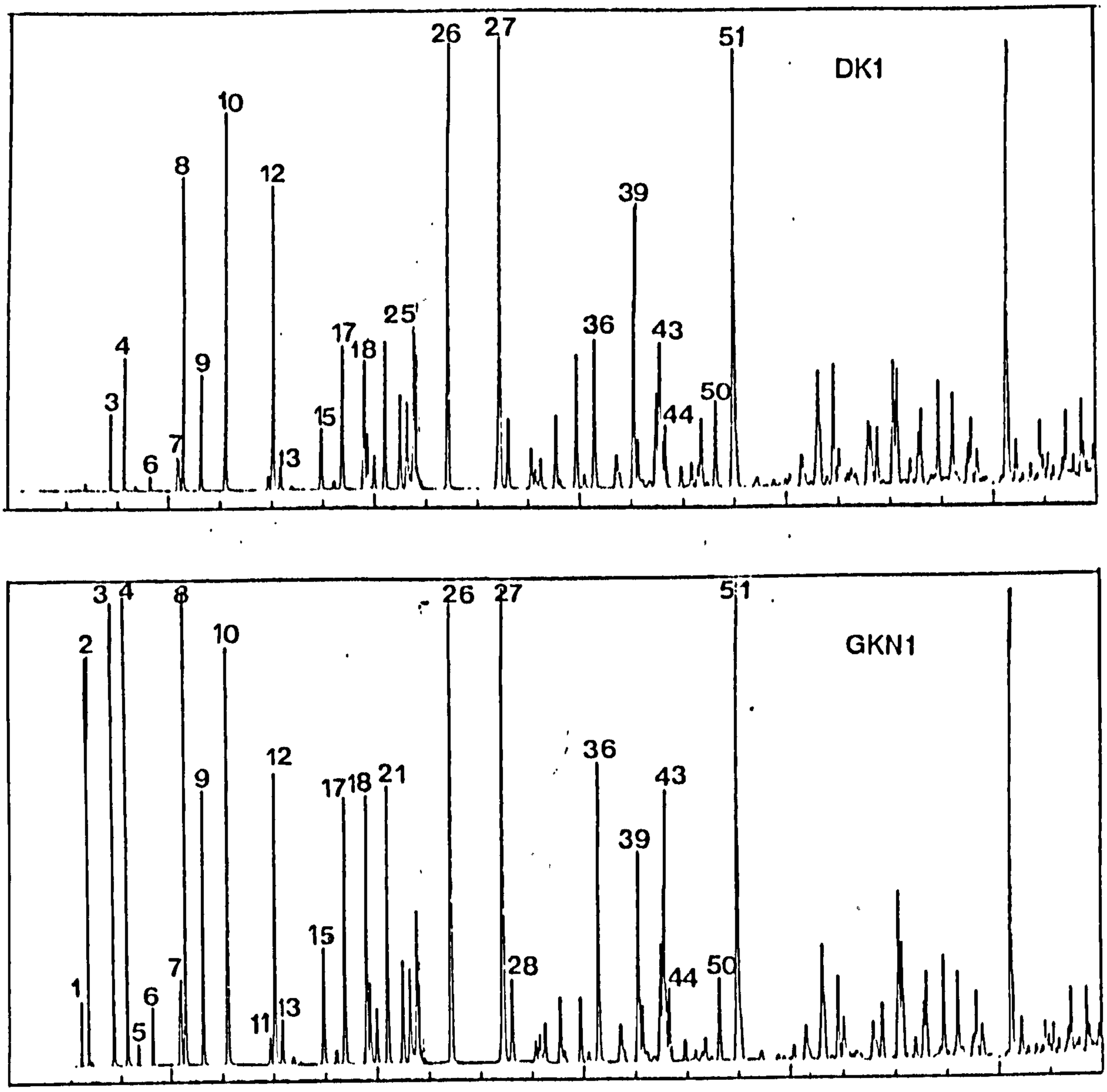

Figure 4.12 Gas chromatograms of the gasoline range hydrocarbon fractions of two oils from the Southeast Constantine basin: (a) DK1, (b) GKN1. Peak assignments are given in Table 5.

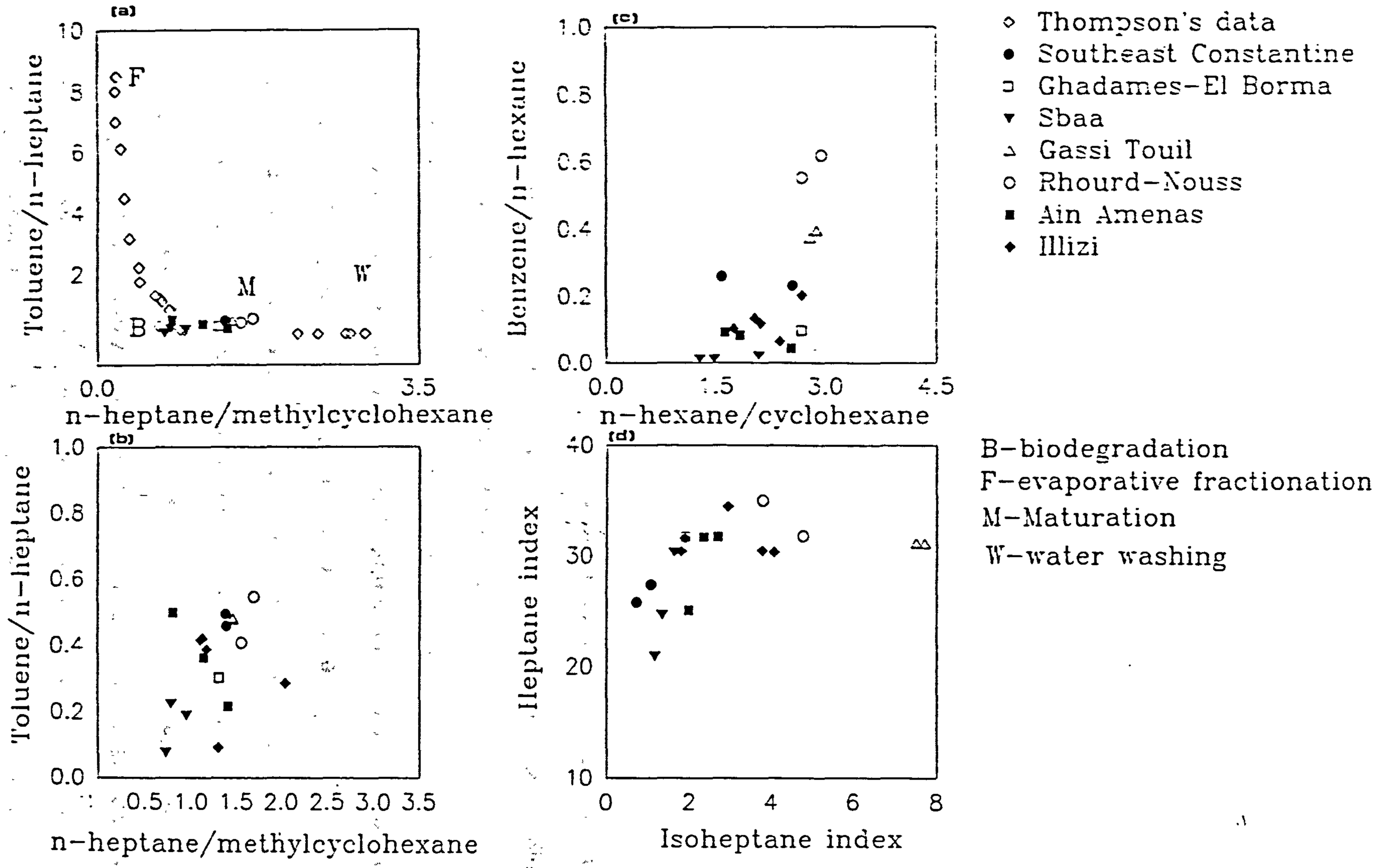

Figure 4.13 Relationship between paraffinicity and aromaticity indices in 18 selected oils.

1988) defined two other parameters namely *n*-heptane/methylcyclohexane and toluene/*n*-heptane (e.g *n*-C_7/MCH and tol/*n*-C_7) to determine effects of maturation, biodegradation and water washing of oils in reservoirs. Based on field and laboratory work, Thompson (1987; 1988) reported some anomalous values of the paraffinicity and aromaticity ratios (*n*-C_7/MCH and tol/*n*-C_7) and related this phenomenon to a fractionation of light hydrocarbons by gas extractions, known as evaporative fractionation. As a result of this, the residual fraction is enriched in the less volatile compounds, whereas the evaporative fraction contain the more volatile compounds. According to his findings, a value of 0.69 for the tol/*n*-C_7 ratio represented a single phase and a higher value was obtained during evaporative fractionation of oils. Hence, when using this diagram (Thompson, 1987; 1988), both DK1 and GKN1 are plotted in the direction indicative of increasing maturation as shown in Figure 4.13a.

4.2.2. Ghadames-El Borma basin

This section comprises results of ELB9, KA2 and ROM1 (test 3 and test 1E), which are located in Triassic reservoirs. ELB9, KA2 and ROM1 test 3 (e.g. ROM1) have been selected for biological marker assessment.

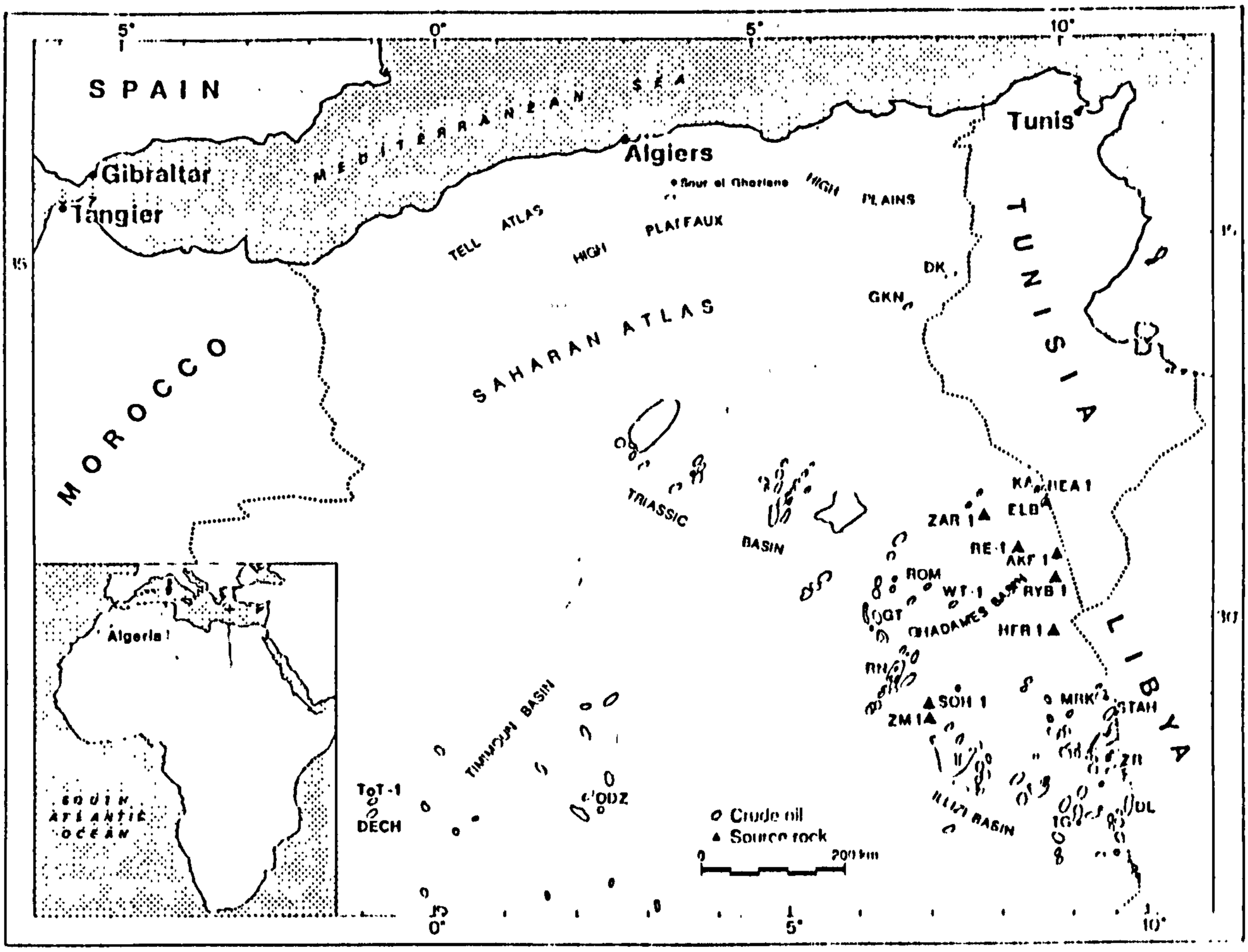

Figure 4.1b Sample location map showing the area (A) of study (A=The Ghadames-El Borma basin) which group of oils were investigated.

4.2.2.1. Bulk composition

Oils from Ghadames-El Borma basin exhibit higher density values particularly ELB9 and KA2. This, however, is reflected by a total absence of the gasoline range hydrocarbons (C_n<C_{10}). In general, they possess similar chemical composition (Figure 4.2b) including high content of saturates and low NSO compounds. Therefore, only ELB9, KA2 and ROM1 test 3 have been considered for a biological marker and gasoline range hydrocarbon characterisation.

Table 4.1b: Bulk composition data

Well	%Sats	%Aro	%NSO	Pr/Ph	D*
ELB9	76.95	19.94	3.11	1.63	0.876
KA2	80.35	17.07	2.57	1.53	0.877
ROM1 test3	91.29	7.47	1.24	1.61	0.818
ROM1 test1E	88.29	10.37	1.34	1.66	0.820

* D is the density of oils measured at 20°C (g/cm^3).

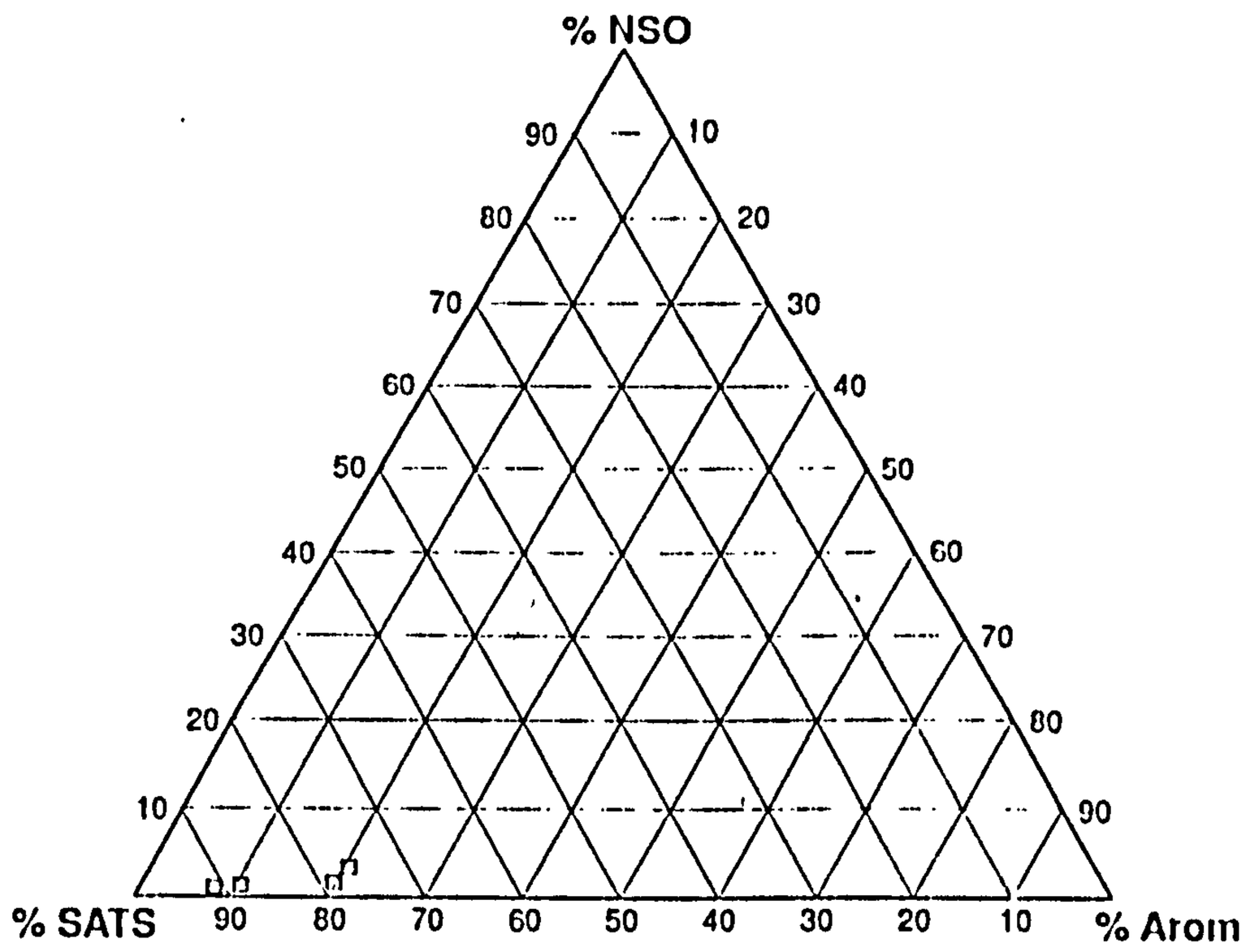

Figure 4.2b Relative proportions of saturated, aromatic hydrocarbons and NSO compounds from the Ghadames-El Borma basin.

4.2.2.2.Saturated hydrocarbon fraction

High abundance of saturated hydrocarbons is clearly seen in the whole oil gas chromatograms of ELB9, KA2, ROM1 (Figure 4.14), particularly *n*-alkanes, with a total absence of the gasoline range hydrocarbons in ELB9 and KA2. They exhibit roughly similar Pr/Ph ratio (Table 4.1b).

N-alkylcyclohexanes and methyl-*n*-alkylcylohexanes have similar patterns as the *n*-alkanes, ranging from C_{12} to C_{26} carbon number, as previously described for DK1 oil.

Sterane distributions of these oils are displayed in Figure 4.15. Rearranged steranes are prominent with a predominance of C_{29} members. The relative

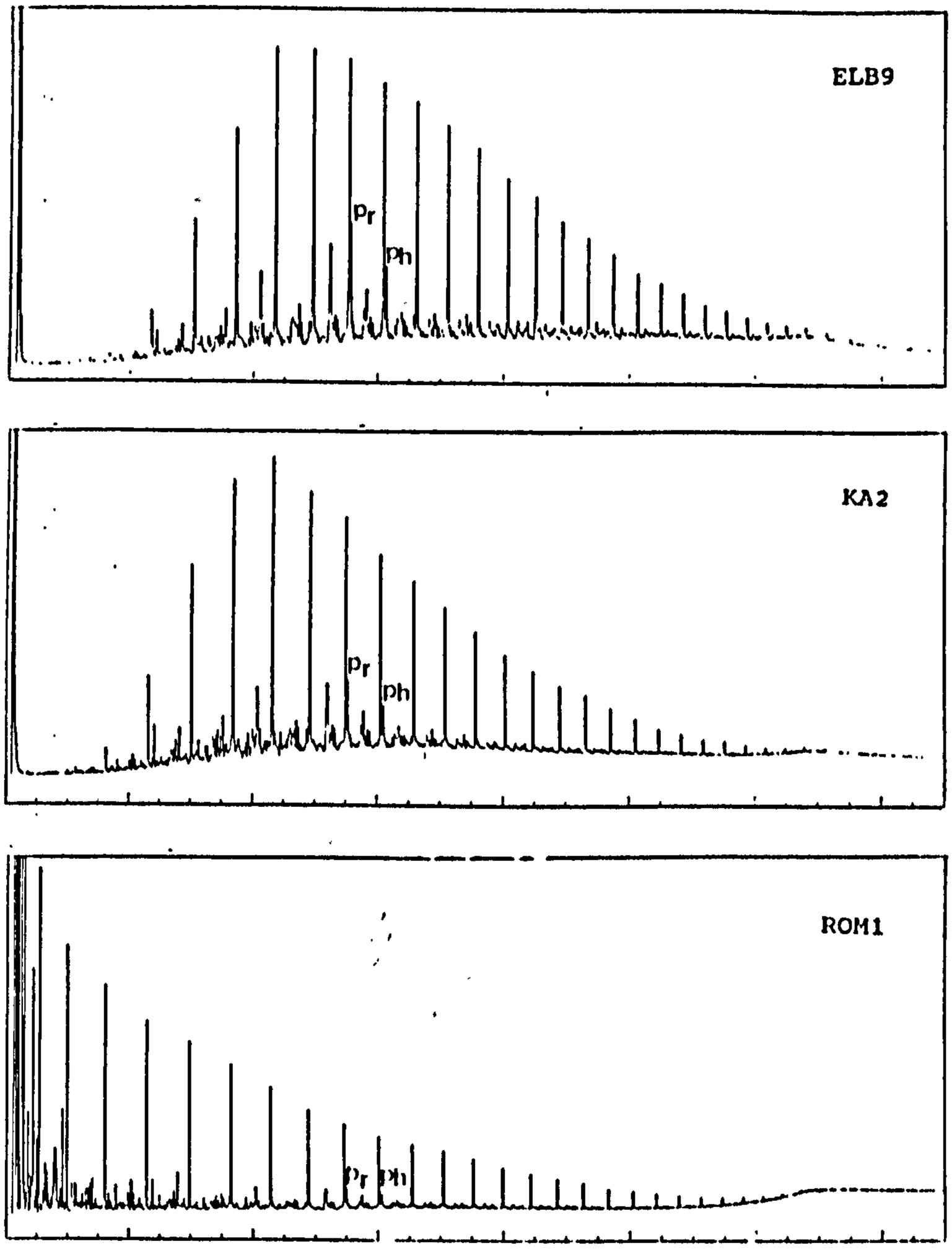

Figure 4.14 Gas chromatograms of oils from the Ghadames-El Borma basin.

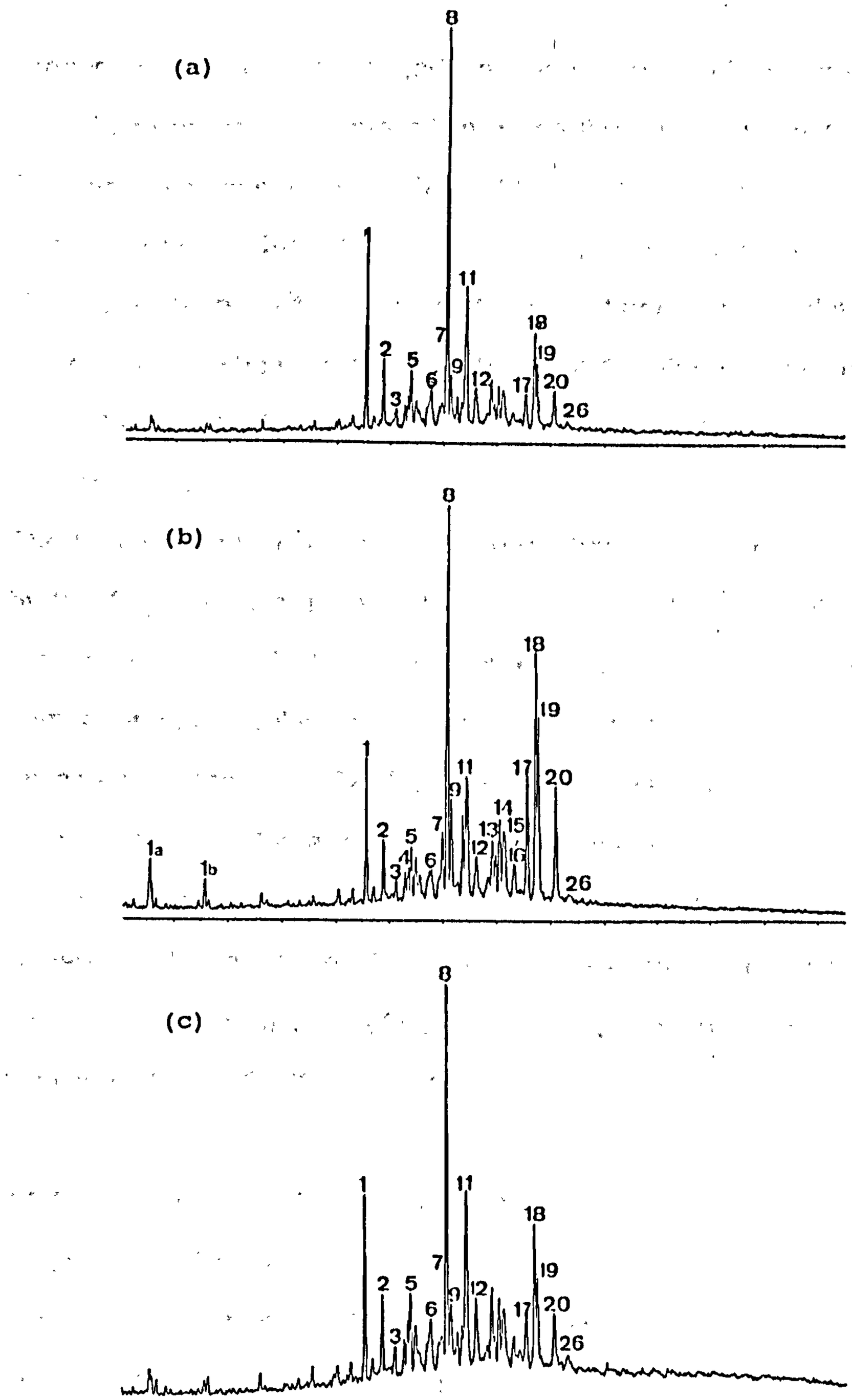

Figure 4.15 m/z 217.1950 mass chromatograms illustrating sterane distributions of oils from the Ghadames-El Borma basin: (a) ELB9, (b) KA2 and (c) ROM1. Peak assignments are listed in Table 1.

proportions of both rearranged and non-rearranged steranes (C_{27}-C_{29}) reveal similar sterane composition of the three oils (Figure 4.7a and 4.7b). Enhanced concentrations of 5α(H),14β(H),17β(H) (20R) (e.g. αββ) sterane relative to 5α(H)14α(H),17α(H) (20S) (e.g. ααα) isomer are also observed. Both C_{30} desmethylsteranes and methylsteranes were detected in one selected oil as shown in Figure 4.16 and 4.17, albeit in low concentrations. The 24-ethyl-αββ-3β-methyl-cholestane dominate the mass chromatogram (Figure 4.17).

The hopane contribution is much higher than that of steranes, as indicated by the C_{30} hp/C_{29}st ratio (6.80, 3.50 and 3.47 for ELB9, KA2 and ROM1 respectively). As illustrated in Figure 4.18, tricyclic terpanes are minor components, particularly in ELB9 and KA2, but relatively higher in ROM1 as indicated by the ratio $C_{23}T/C_{23}T+C_{30}\alpha\beta$ hop (0.36 and 0.35 and 0.59 respectively). All three oils contain rearranged hopanes i.e $C_{29}T_s$ and 17α(H)- diahopane, however, in various proportions (Figure 4.18 and Appendix 4.3). In addition Figure 4.10 shows that the correlation of $C_{29}\alpha\beta$ nohop/$C_{30}\alpha\beta$ hop and C_{29}Ts/$C_{29}\alpha\beta$ norhop may indicate a lower maturity level of KA2 than ELB9 and ROM1.

4.2.2.3. Aromatic hydrocarbon fraction

As shown in Figure 4.19 the C-ring monoaromatic steroidal hydrocarbons were barely detectable in ROM1 compared to KA2 and ELB9. Non-rearranged compounds are minor in these oils (peak N° 13 and 16).

The triaromatic steroidal hydrocarbon distributions (Figure 4.20) show that ELB9 and ROM1 are dominated by short-chain homologues, while KA2 contains relatively high concentrations of long-chain (C_{26}-C_{28}) members. The C_{28} triaromatic is present in similar proportions in all three oils, as reflected by the ratio of $\%C_{28}t / C_{26}t+C_{27}t+C_{28}t$ (68.02, 64.05 and 68.10 for KA2, ELB9 and ROM1 respectively). ROM1 displays increased relative proportions of short-chain homologues compared to ELB9 and KA2, as

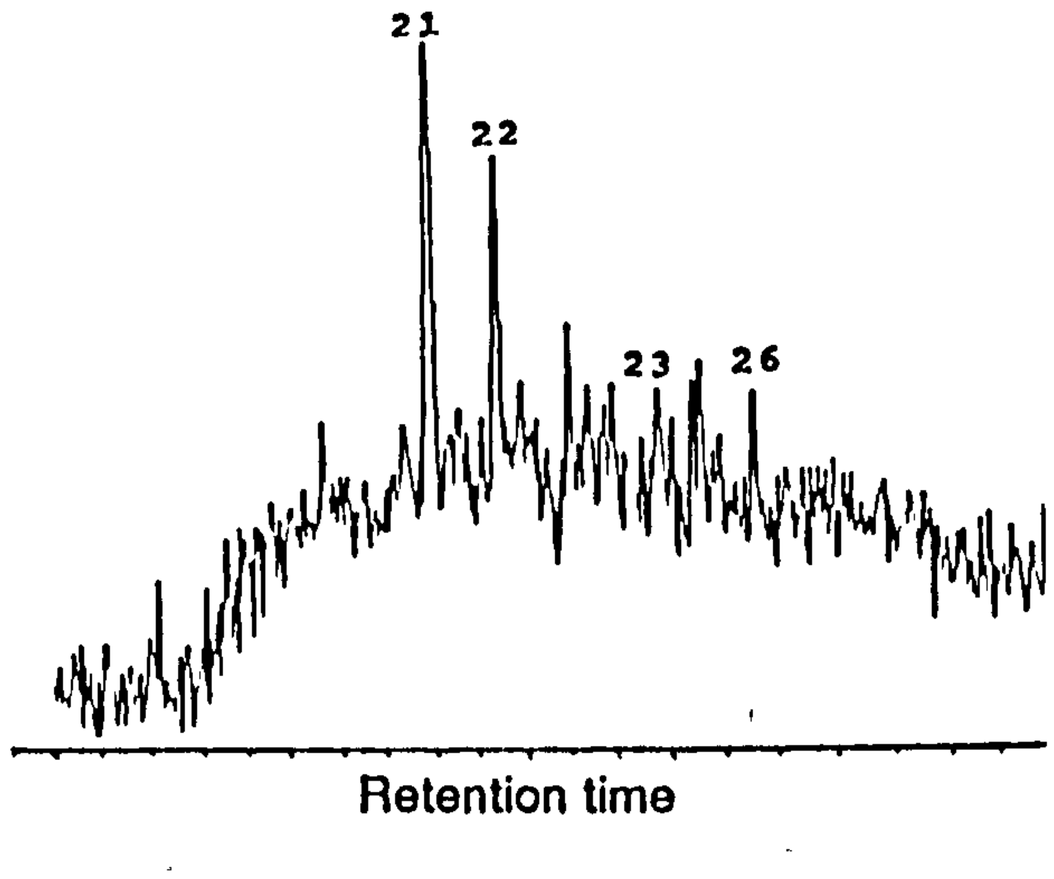

Figure 4.16 Mass chromatogram from metastable ion reaction monitoring of transition m/z 414->m/z 217 for C_{30} steranes in one selected oil from the Gahdames-El Borma basin: (ELB9). Peak assignments are given in Table 1.

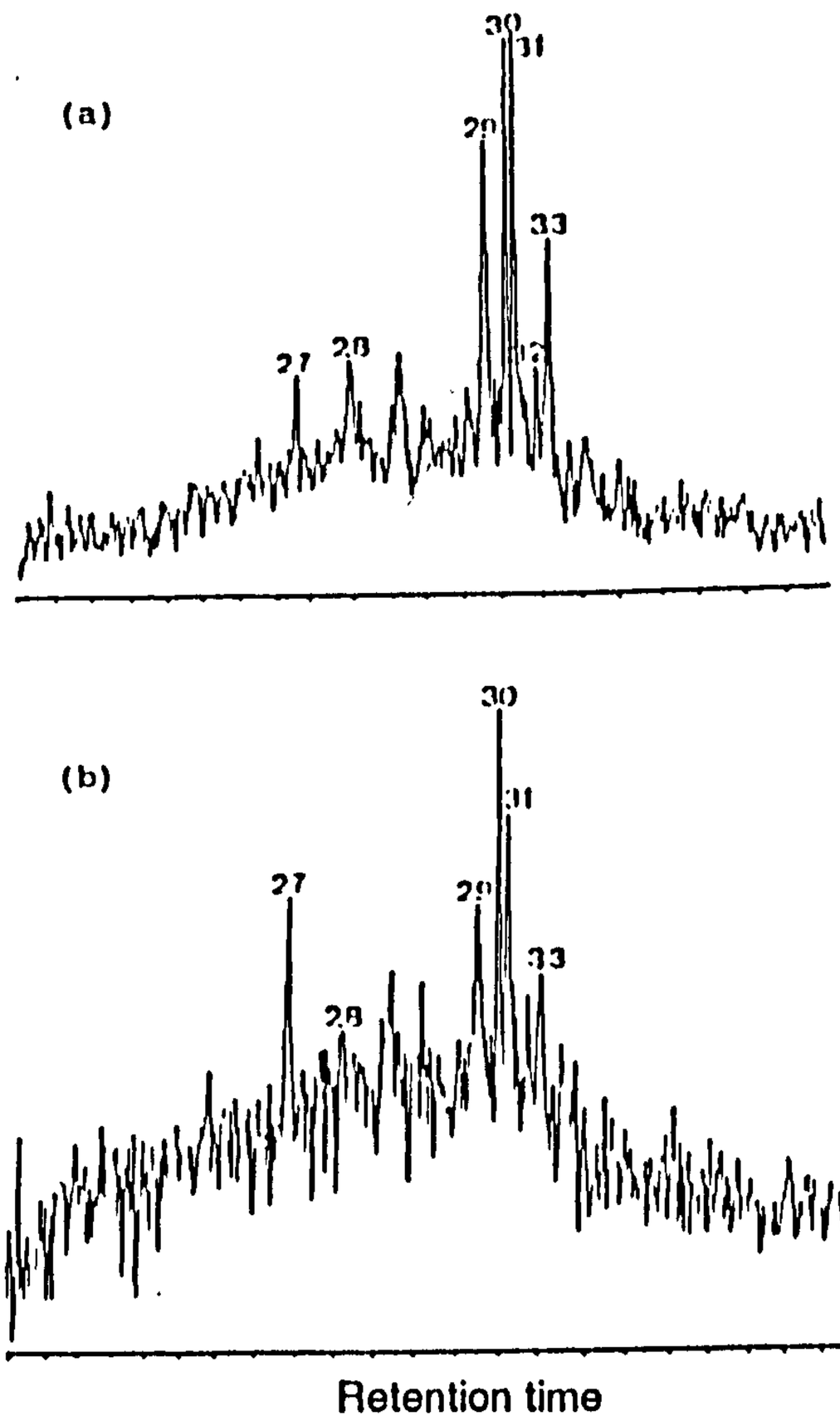

Figure 4.17 Mass chromatograms from metastable ion reation monitoring of transition m/z 414->m/z 231 in two selected oils from the Ghadames-El Borma basin: (a) KA2, (b) ROM1. Peak assignments are listed in Table 1.

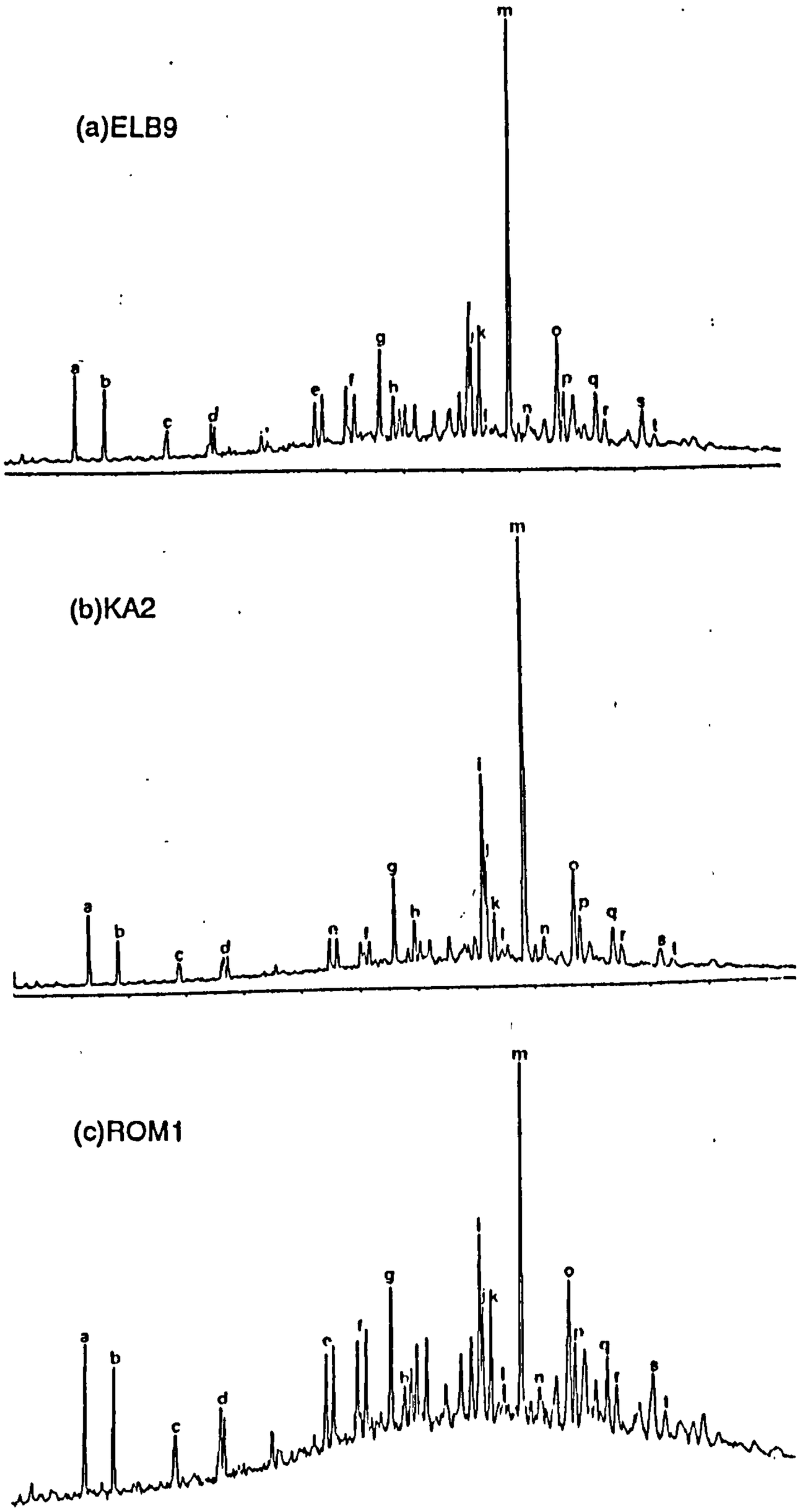

Figure 4.18 m/z 191.1794 mass chromatogram showing the terpane distribution of one selected oil from the Ghadames-El Borma basin. Peak assignments are listed in Table 2.

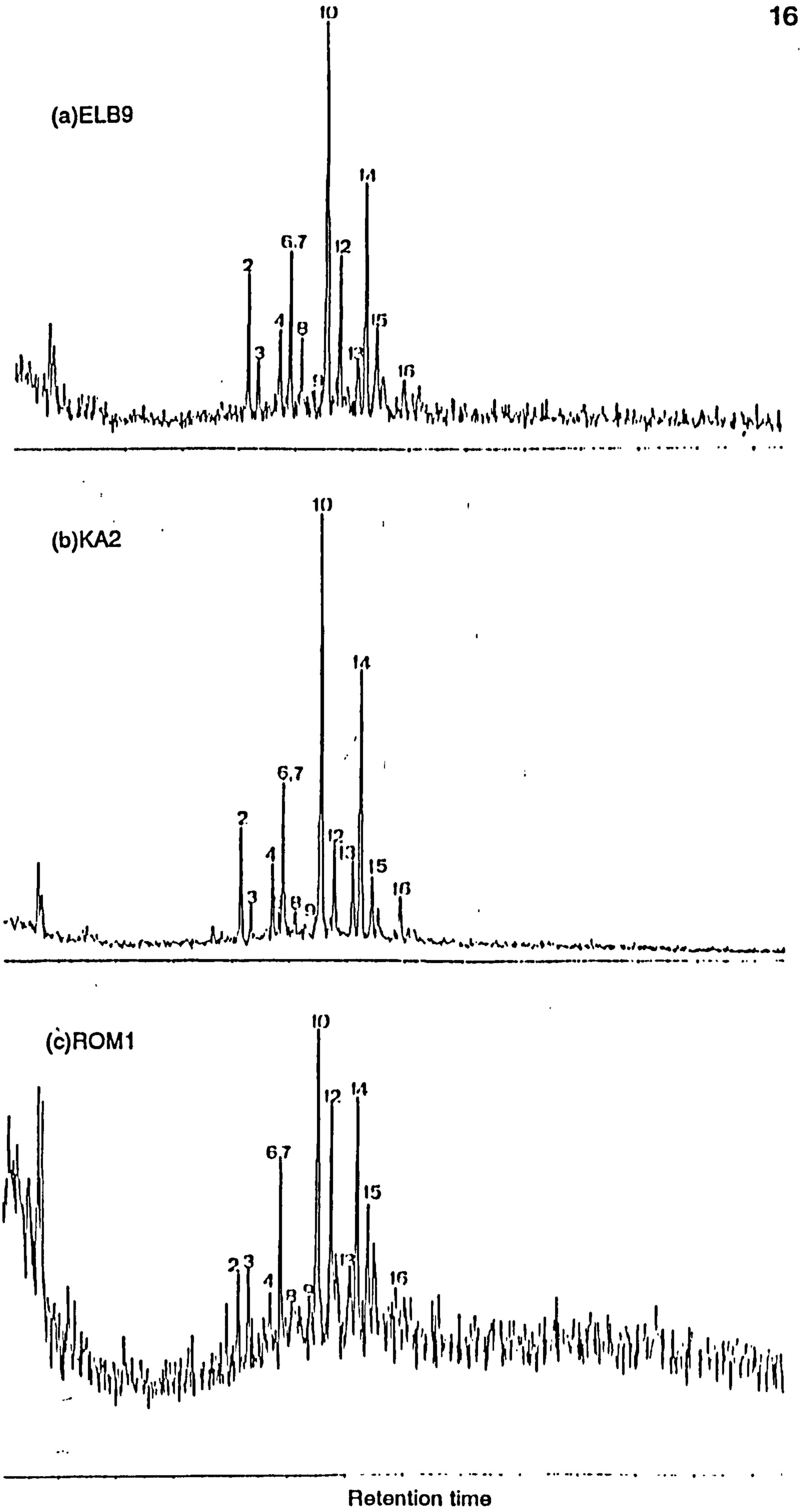

Figure 4.19 m/z 253.1950 mass chromatograms showing the C-ring monoaromatic steroidal hydrocarbon distributions of oils from the Ghadames-El Borma basin: (a) ELB9, (b) KA2 and (c) ROM1. Peak assignments are listed in Table 3.

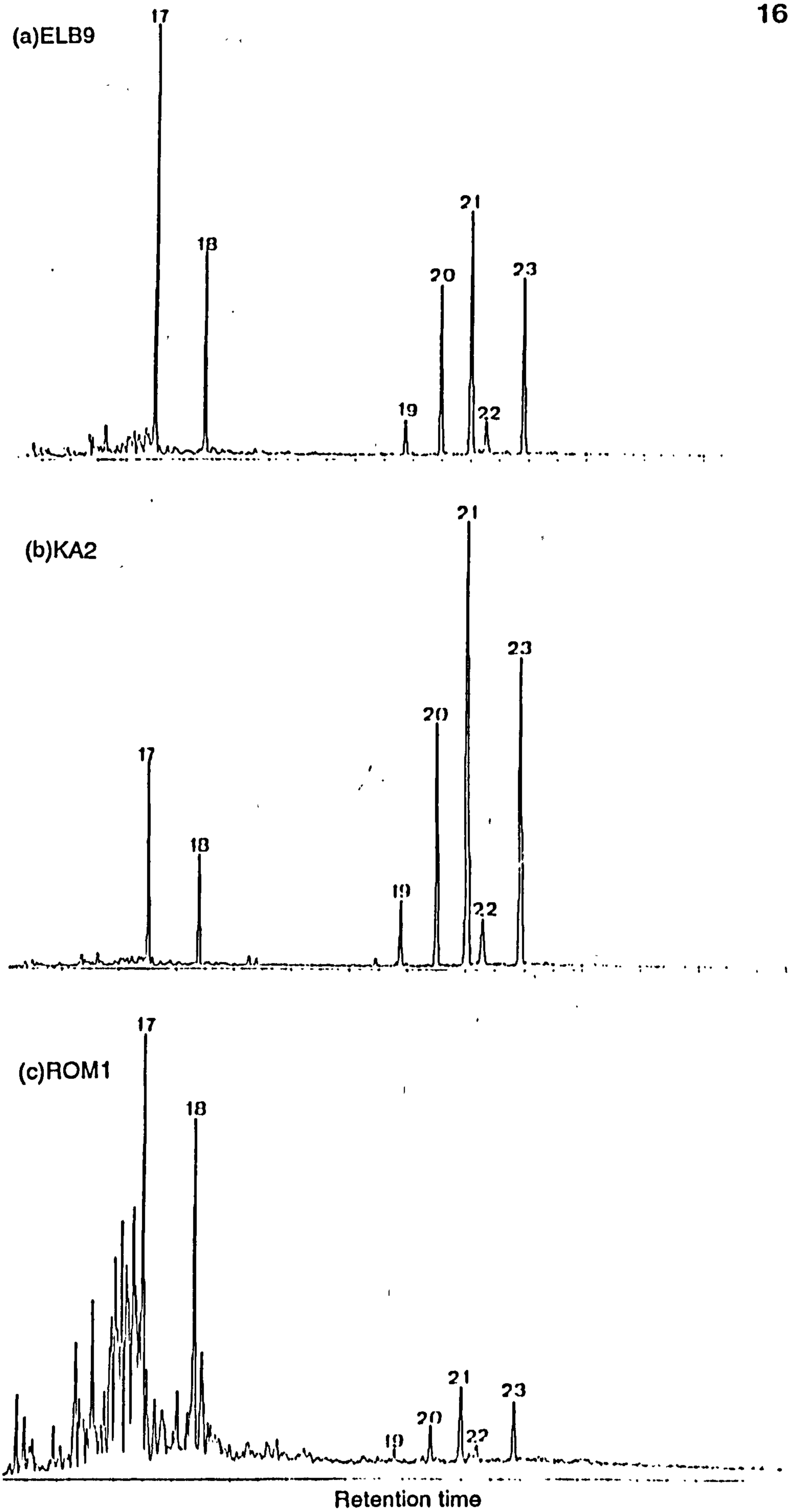

Figure 4.20 m/z 231.1170 mass chromatograms showing triaromatic steroidal hydrocarbon distributions of oils from the Ghadames-El Borma basin: (a) ELB9, (b) KA2 and (c) ROM1. Peak assignments are listed in Table 4.

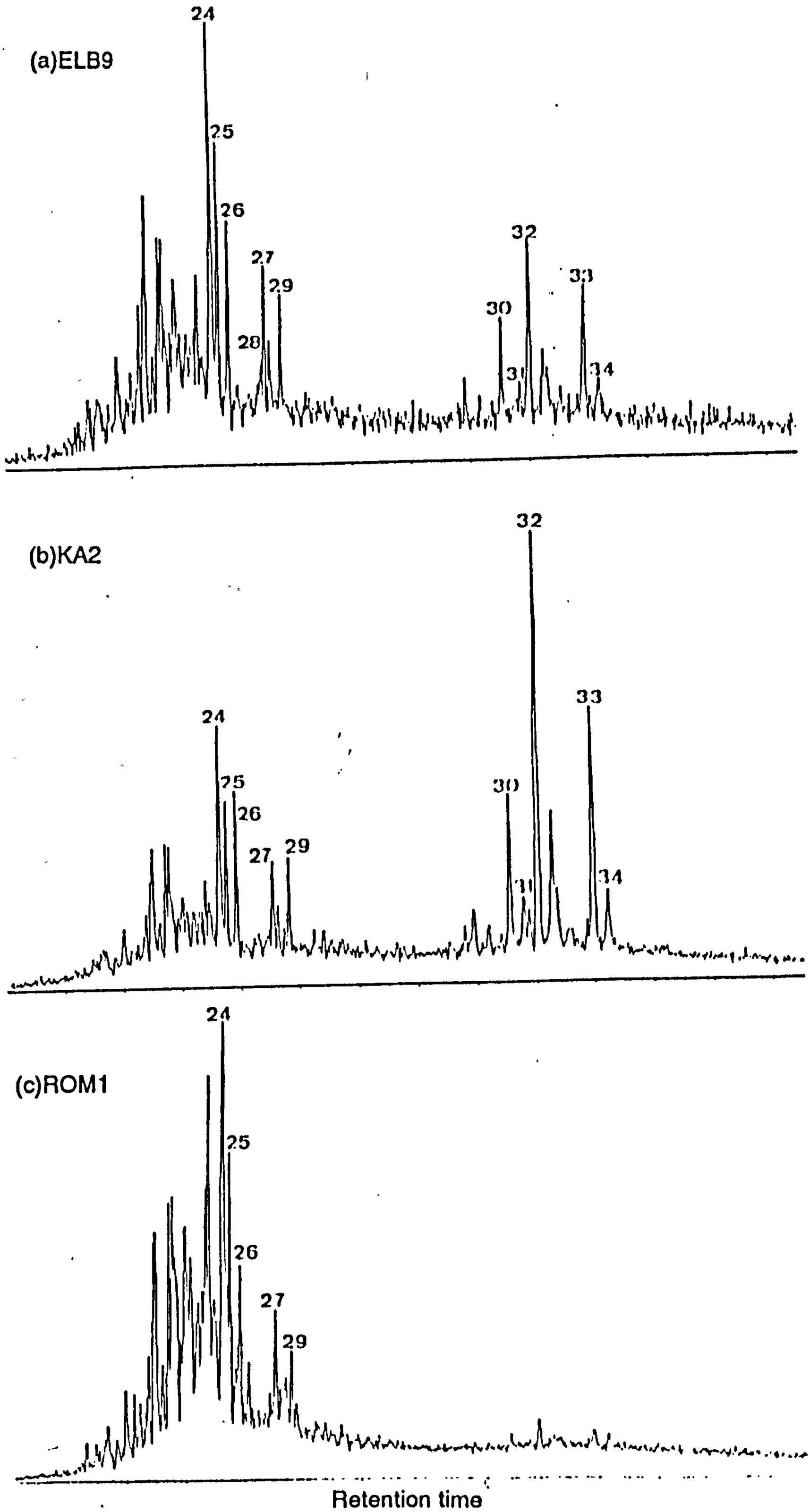

Figure 4.21 m/z 245.1330 mass chromatograms showing methylated triaromatic steroidal hydrocarbon distributions of oils from the Ghadames-El Borma basin: (a) ELB9, (b) KA2 and (c) ROM1. Peak assignments are listed in Table 4.

indicated by the cracking ratio (0.77, 0.48 and 0.22 for ROM1, ELB9 and KA2 respectively. The steroid aromatization ratio has reached the end-point values for ELB9 and KA2) (0.86 and 0.88 respectively).

The methyl triaromatic steroid hydrocarbons were barely detectable in ROM1 (Figure 4.21c), but relatively higher in ELB9 and KA2 (Figure 4.21a and 4.21b). The 2-methyl+3-methyl isomers are represented in relatively high concentrations as revealed by the MTSI1 and MTSI2 indices (0.48-0.61). Hence, the extent of methyl triaromatic steroid isomerization continues to rise in a similar way to the cracking ratio (Appendix 4.5).

4.2.2.4. Gasoline range hydrocarbon fraction

No gas chromatograms of the gasoline range hydrocarbons were recorded for both KA2 and ELB9, while ROM1 exhibits the whole range (C_4-C_9) hydrocarbons (Figure 4.22). As described previously, both heptane and isoheptane values (Thompson, 1983; 1987) and other paraffinicity indices (e.g n-C_7/MCH, n-C_6/CHX, Appendix 4.6), reveal that ROM1 can be regarded as overmature. ROM1 exhibits low values of aromaticity ratios (Bz/*n*-C_6 and tol/*n*-C_7), suggesting water washing (Figure 4.13b and 4.13c).

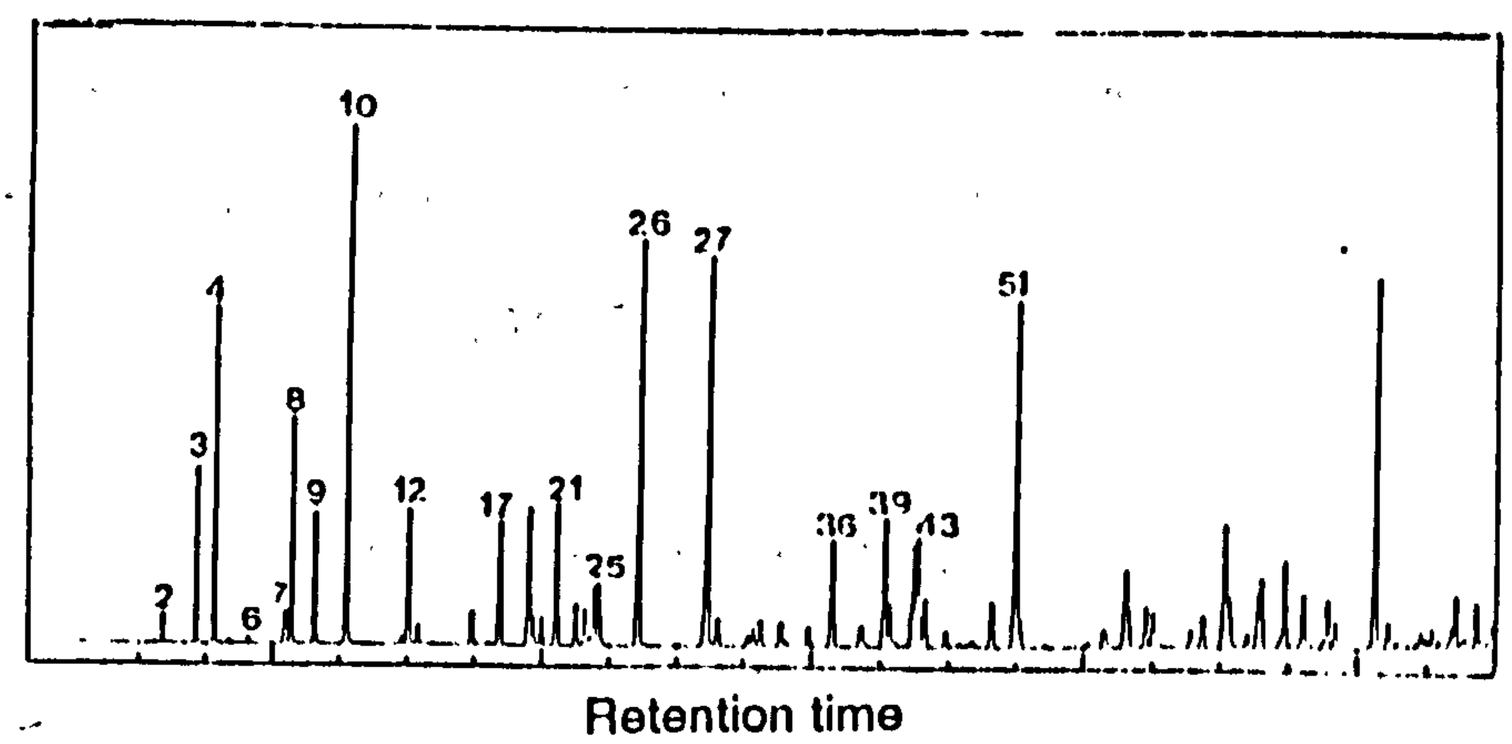

Figure 4.22 Gas chromatograms of the gasoline range hydrocarbon fractions of one selected oil from the Ghadames-El Borma basin (ROM1). Peak assignments are given in Table 5.

4.2.3. Sbaa basin

This section comprises results of oils from the Famenian (ODZ1 test1 and test2), Strunian (DECH1 test3, test4 and test5) and Tounaisian (TOT1) reservoirs.

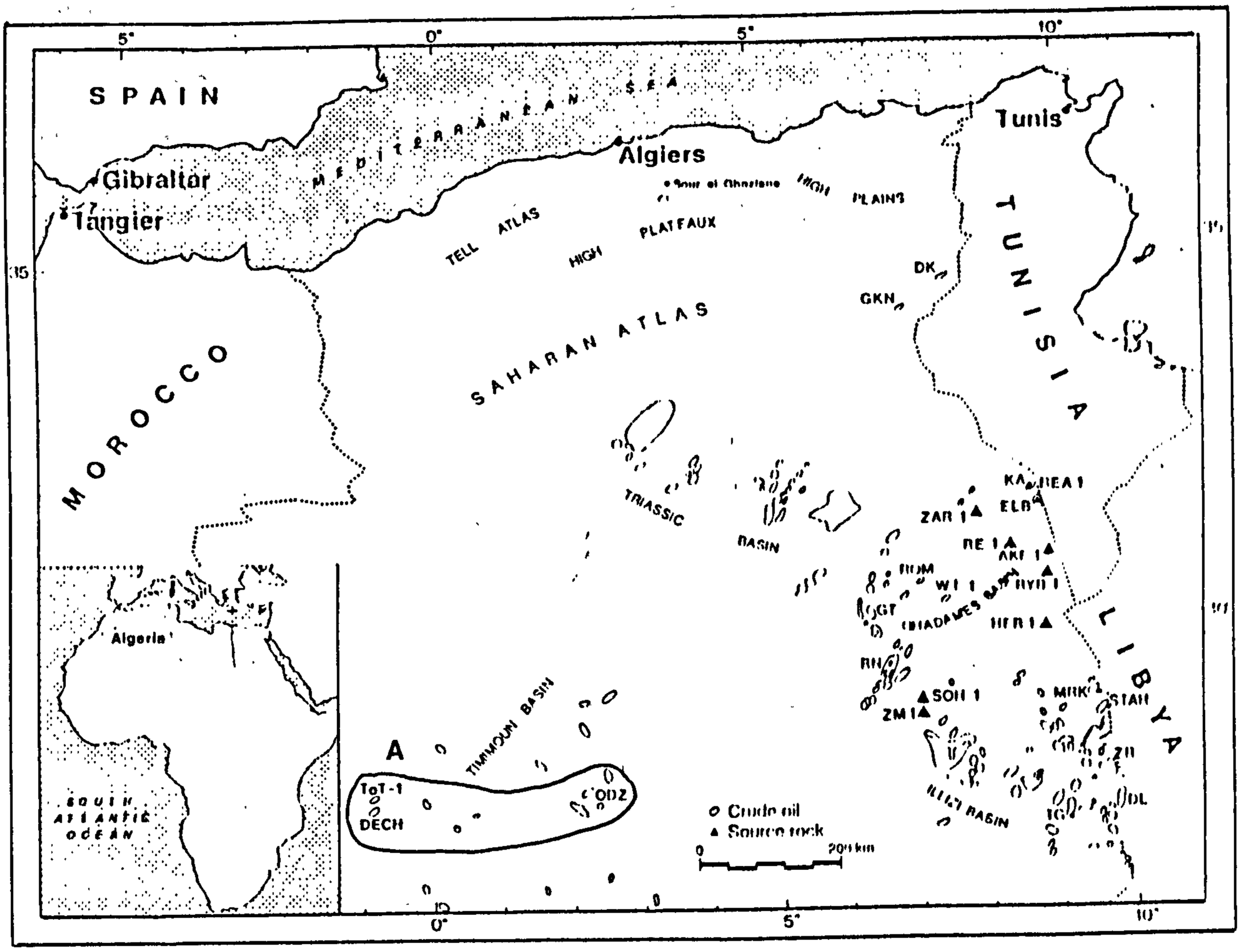

Figure 4.1c Sample location map showing the area of study (A=Sbaa basin), which group of oils were investigated.

4.2.3.1. Bulk composition

The ternary diagram (Figure 4.2c) showing the relative proportions of the saturated, aromatic hydrocarbons and NSO (including asphaltenes), reveals similar chemical composition of oils from Sbaa basin. For a biological marker and gasoline range hydrocarbons investigation, only DECH1 test 5, ODZ1 test 2 and TOT1 have been considered. Higher density for TOT1 is reflected by relatively higher NSO contents than DECH1 and ODZ1.

Table 4.1c: Bulk composition data

Well	%Sats	%Aro	%NSO	Pr/Ph	D*
TOT1	76.11	16.64	7.25	2.19	0.868
ODZ1 test1	78.79	17.24	3.97	2.01	0.826
ODZ1 test2	80.42	16.64	2.94	2.01	0.825
DECH1 test3	74.72	21.78	3.50	2.11	0.810
DECH1 test4	74.49	23.69	0.82	2.11	0.810
DECH1 test5	75.60	21.37	3.03	2.01	0.810

* D is the density of oils measured at 20°C (g/cm^3).

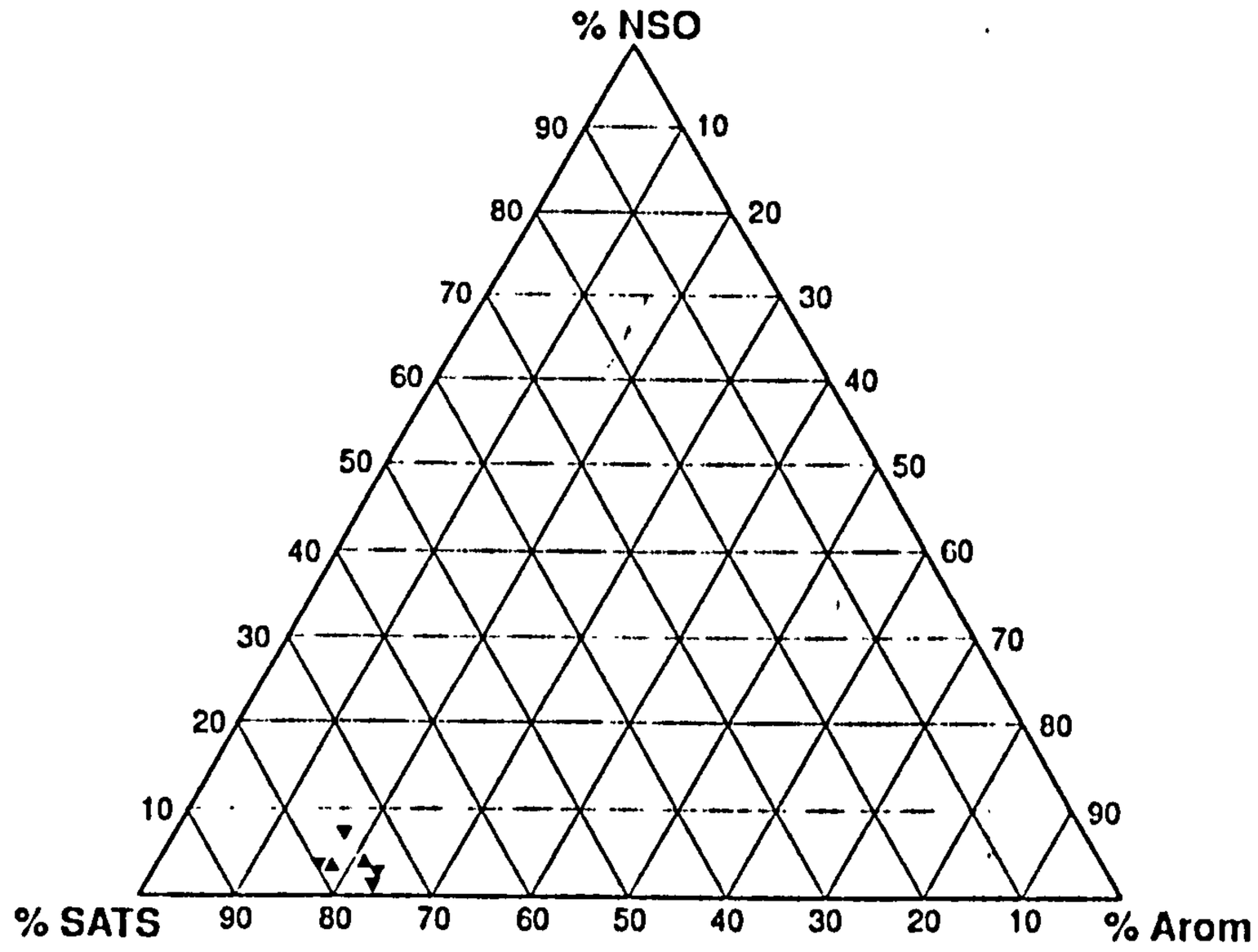

Figure 4.2c Relative proportions of saturated, aromatic hydrocarbons and NSO compounds of oils from the Sbaa basin.

4.2.3.2. Saturated hydrocarbon fraction

These oils are dominated by saturated hydrocarbons, as shown in the whole oil gas chromatograms (Figure 4.23). The C_{12}+ saturated hydrocarbon distributions are similar to each other with prominent n-alkanes and minor acyclic isoprenoids (C_n<C_{20}). The Pr/Ph ratio is about 2.0. Low molecular weight hydrocarbons are generally present in ODZ1, while the range of *n*-C_9

to *n*-C_{12} are slightly depleted in TOT1 and totally absent in DECH1, as indicated by the lack of peaks in Figure 4.23.

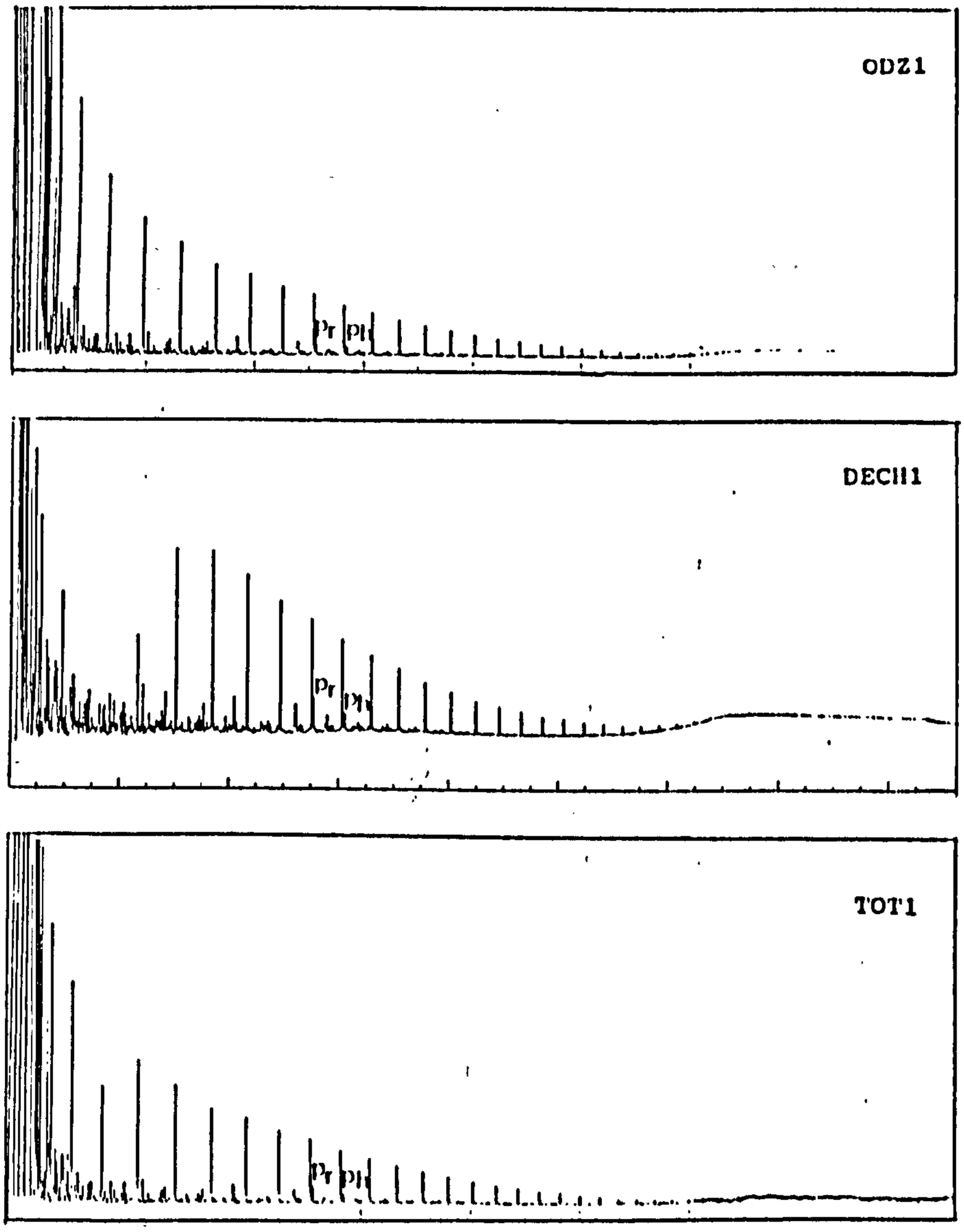

Figure 4.23 Gas chromatograms of oils from the Sbaa basin.

Biological markers are recorded in much less abundance in TOT1 and than in ODZ1 and DECH1. Representative sterane distributions of these oils are displayed in Figure 4.24, in which rearranged steranes are appreciably greater than non-rearranged steranes with a predominance of C_{29} components. The ternary diagram (Figure 4.7a and 4.7b) showing the relative proportions of C_{27}-C_{29} steranes, reveals that they oils share similarities with each other.

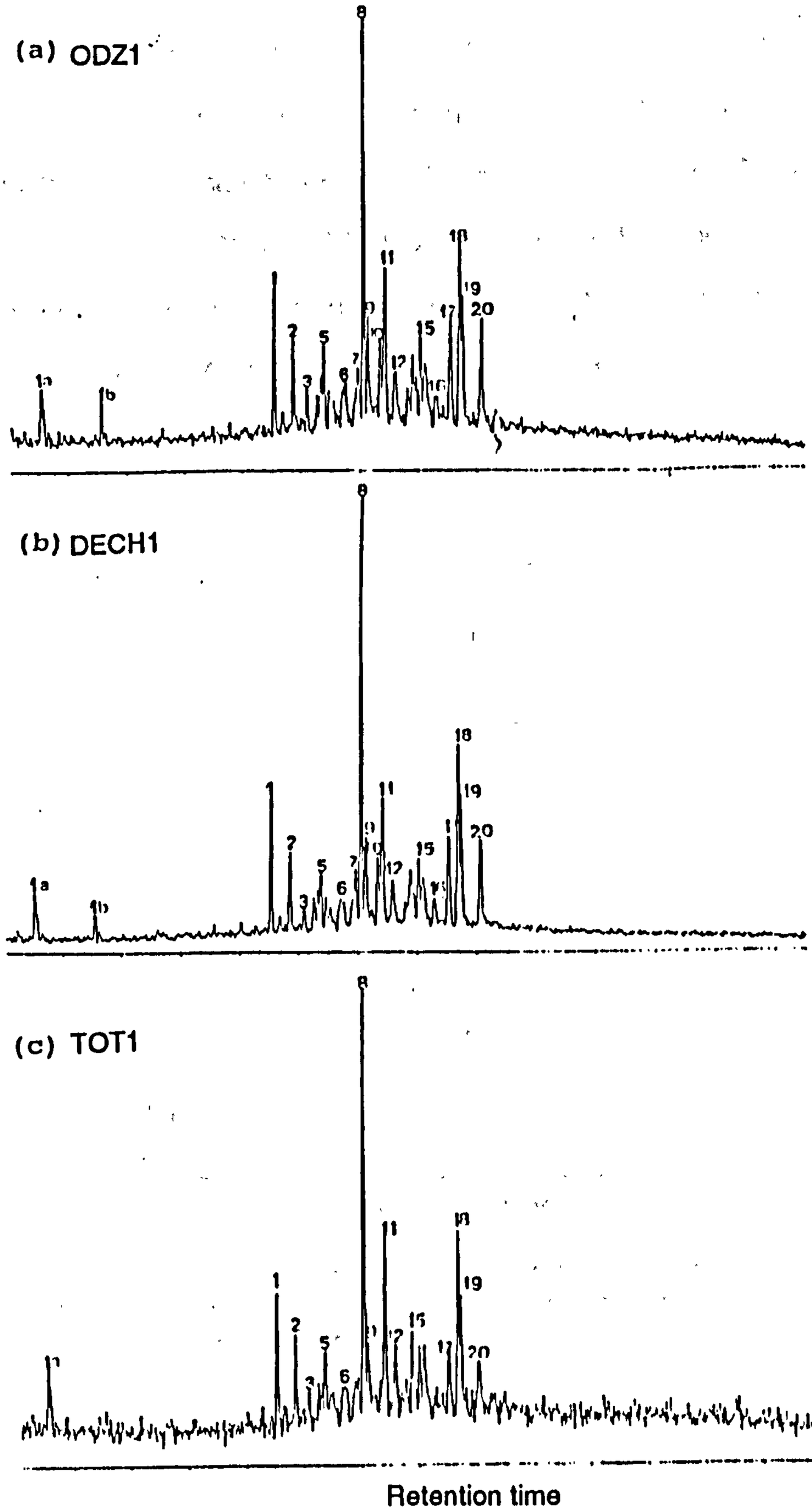

Figure 4.24 m/z 217.1950 mass chromatograms illustrating sterane distributions of oils from the Sbaa basin: (a) ODZ1, (b) DECH1 and (c) TOT1. Peak assignments are listed in Table 1.

C_{30} steranes were recorded in very low concentrations, while C_{30} methylsteranes (Figure 4.25) occur in DECH1 and ODZ1 with prominent 24-ethyl-αββ-3β-methyl-cholestane ((20S) and 20R). The 24-ethyl-ααα-3β-methyl-cholestane (20R) and 24-ethyl-ααα-2α-methyl-cholestane (20R) are present in similar proportions in both oils (peak N° 32 and 33 respectively). However, C_{30}-ααα (20R) sterane appears to give a similar response in the m/z 231->414.

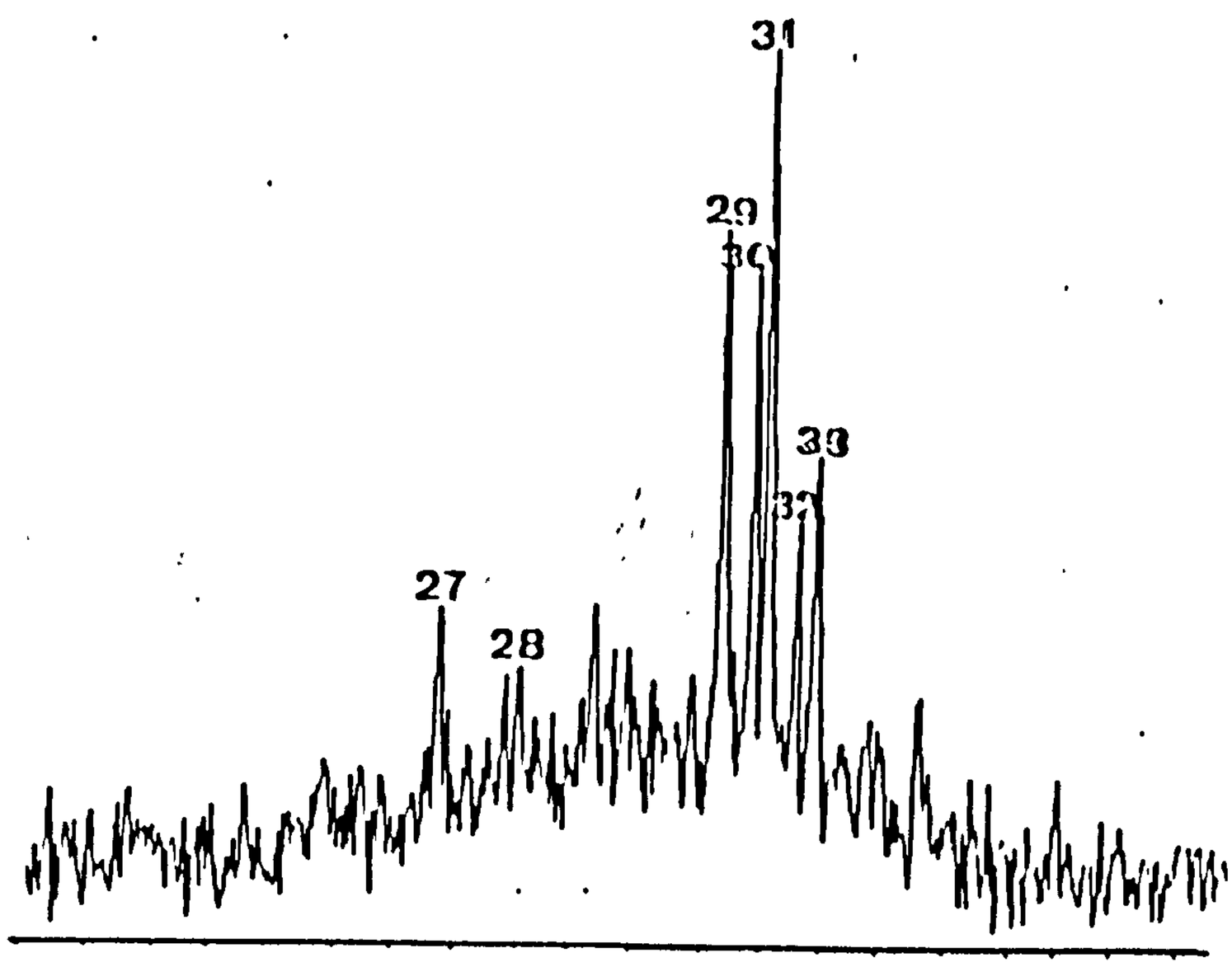

Figure 4.25 Mass chromatogram from metastable ion reaction monitoring of transition m/z 414->m/z 231 for C_{30} methylsteranes of one selected oil from the Sbaa basin (ODZ1). peak assignments are listed in Table 1.

Enhanced concentrations of hopanes is reflected by high abundance of hopanes relative to steranes as well as tricyclic terpanes, as shown in Appendix 4.4 and Figure 4.10. The C_{29}αβ norhopane is relatively less significant than C_{30}αβ hopane, particularly in TOT (Figure 4.26c). As illustrated in Figure 4.26, the C_{29}Ts seems to have relatively similar abundances in all three oils. Furthermore, Figure 4.10 displays the C_{29}αβ norhop/$C_{29}T_s$ ratio versus C_{29}αβ norhop/C_{30}αβ hop ratio, which shows that DECH1 and ODZ1 may have similar maturity levels.

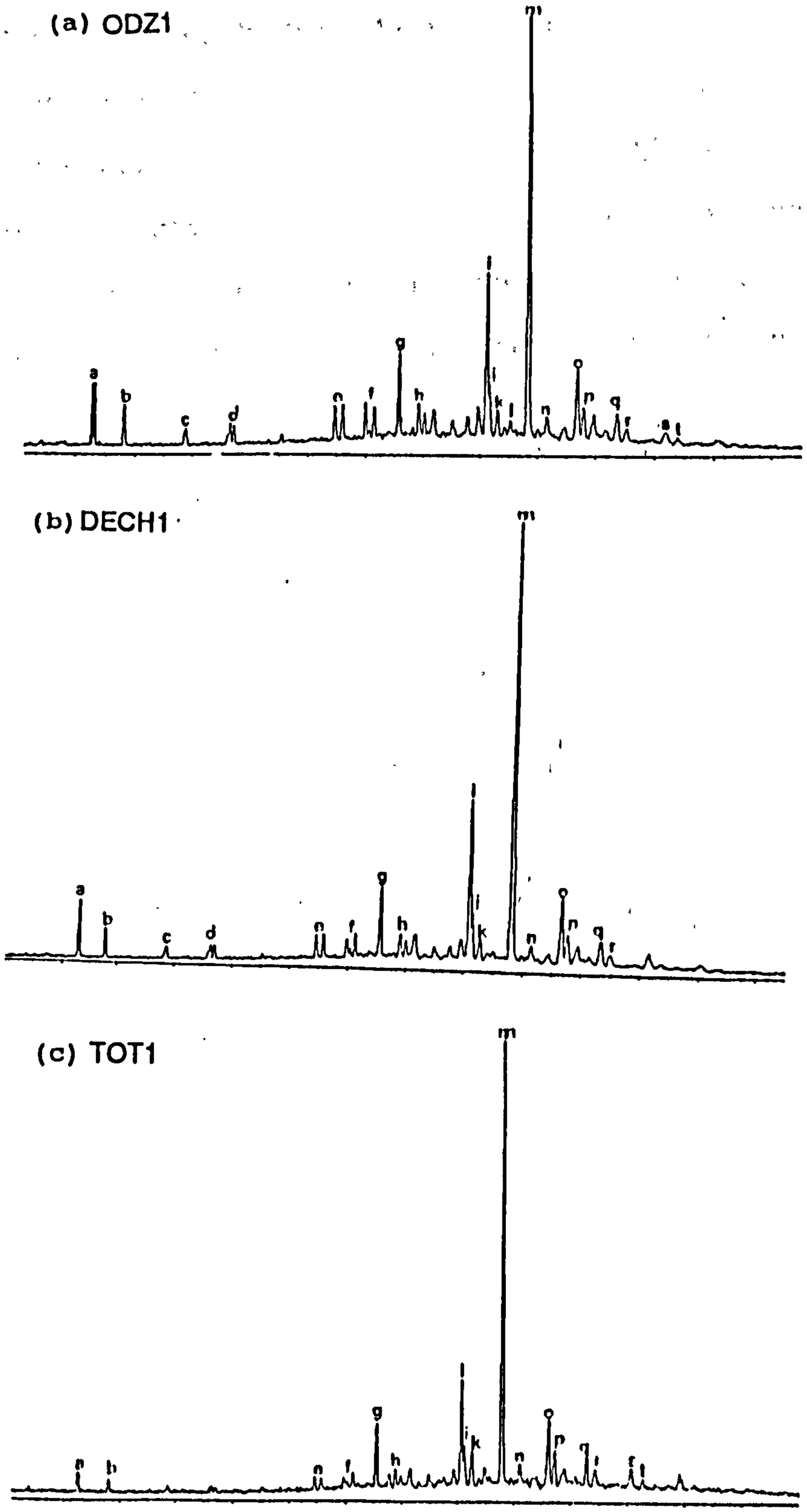

Figure 4.26 m/z 191.1794 mass chromatogram showing distributions of terpanes in oils from the Sbaa basin: (a) ODZ1, (b) DECH1 and (c) TOT1. Peak assignments are listed in Table 2.

4.2.3.3. Aromatic hydrocarbon fraction

The missing values in Appendix 4.5 reflect very low concentrations of C-ring monoaromatic steroidal hydrocarbons in ODZ1 and TOT1, while DECH1 contains relatively higher amounts of these compounds (Figure 4.27). Rearranged compounds monoaromatic steroid (peak N°2, 4, 10 and 14) are more abundant than non-rearranged counterparts (e.g peak N° 13, 16).

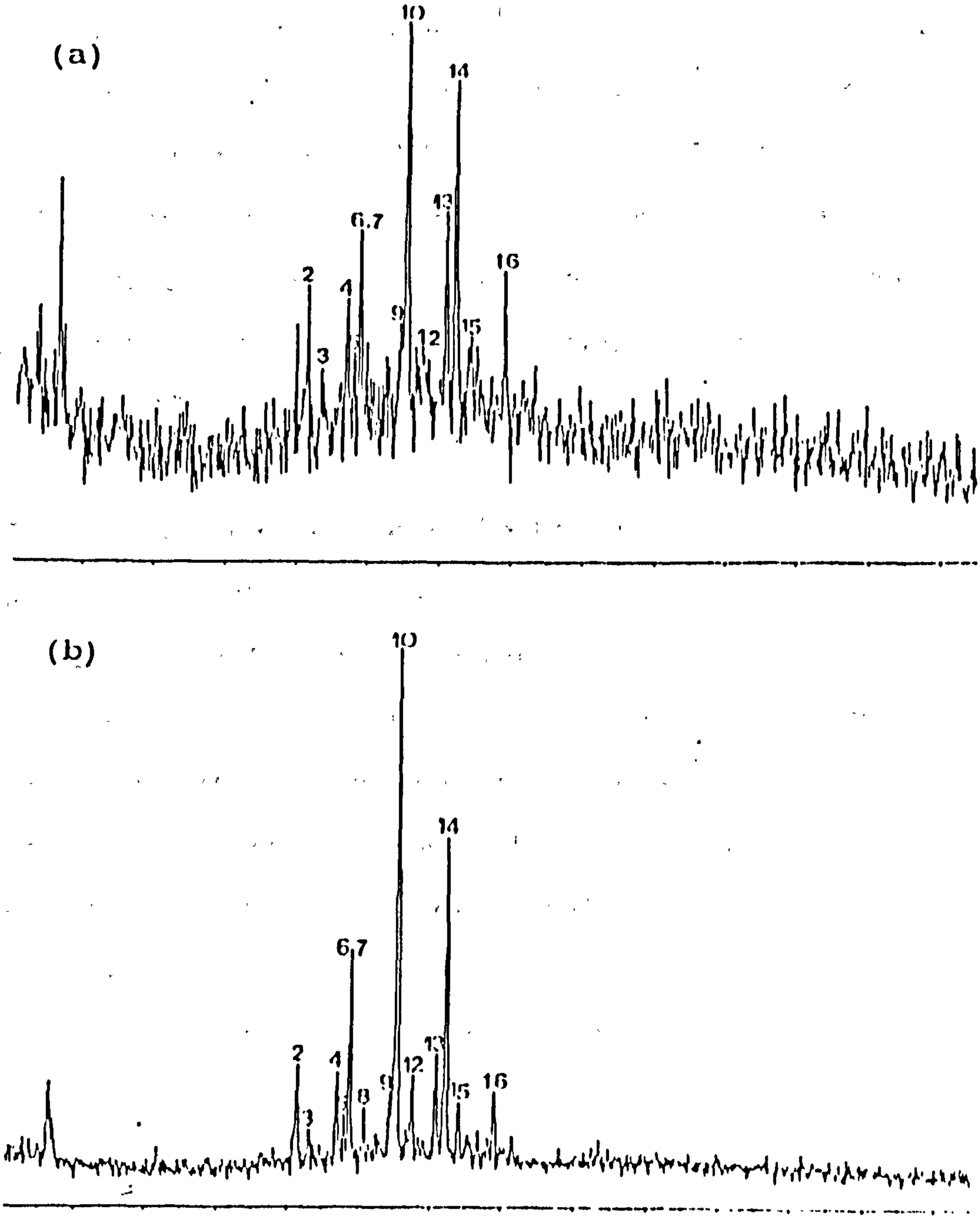

Figure 4.27 m/z 253.1950 mass chromatograms showing C-ring monoaromatic steroidal hydrocarbon distributions of oils from the Sbaa basin: (a) ODZ1, (b) DECH1. Peak assignments are listed in Table 3.

The triaromatic steroidal hydrocarbon distributions are shown in Figure 4.28. The predominance of C_{29} steranes is reflected by high C_{28} triaromatic steroid, as indicated the $\%C_{28}t/C_{26}t+C_{27}t+C_{28}t$ (Appendix 4.2). DECH1 exhibits low abundance of short-chain triaromatic (C_{20}-C_{21}), as indicated by low cracking ratio (0.15) compared to ODZ1 and TOT1 (0.31 and 0.37 respectively). Steroid aromatization ratio was only calculated for DECH1, due to the low abundance of monoaromatic components in ODZ1 and their total absence in TOT1. Therefore, conversion of monoaromatic to triaromatic steroidal hydrocarbons has reached more than 70%, as revealed by the aromatization ratio for DECH1 (i.e. ARO ratio in Appendix 4.5).

The methyl triaromatic steroidal hydrocarbon distribution are relatively minor in DECH1 and ODZ1 and barley detectable in TOT1. The 2-methyl+3-methyl isomers predominate over 4- and 6-methyl isomers, as indicated by the MTSI1 and MTSI2 ratios (Appendix 4.5).

4.2.3.4. Gasoline range hydrocarbon fraction

A close examination of the gasoline range (C_4-C_9) hydrocarbons (Figure 4.29) reveals that ODZ1 and TOT1 contain much less significant amounts of C_4-C_7 range hydrocarbons than DECH1, which may have been lost by evaporation during storage. Furthermore, these oils exhibits low aromaticity ratios, as shown in Figure 4.13 and Appendix 4.6. This Figure displays Heptane index versus Isoheptane index as well as the summary diagram of paraffinicity versus aromaticity (Thompson, 1987, 1988). These indicate that only TOT1 can be regarded as normal paraffinic, DECH1 and ODZ1 as mature oils.

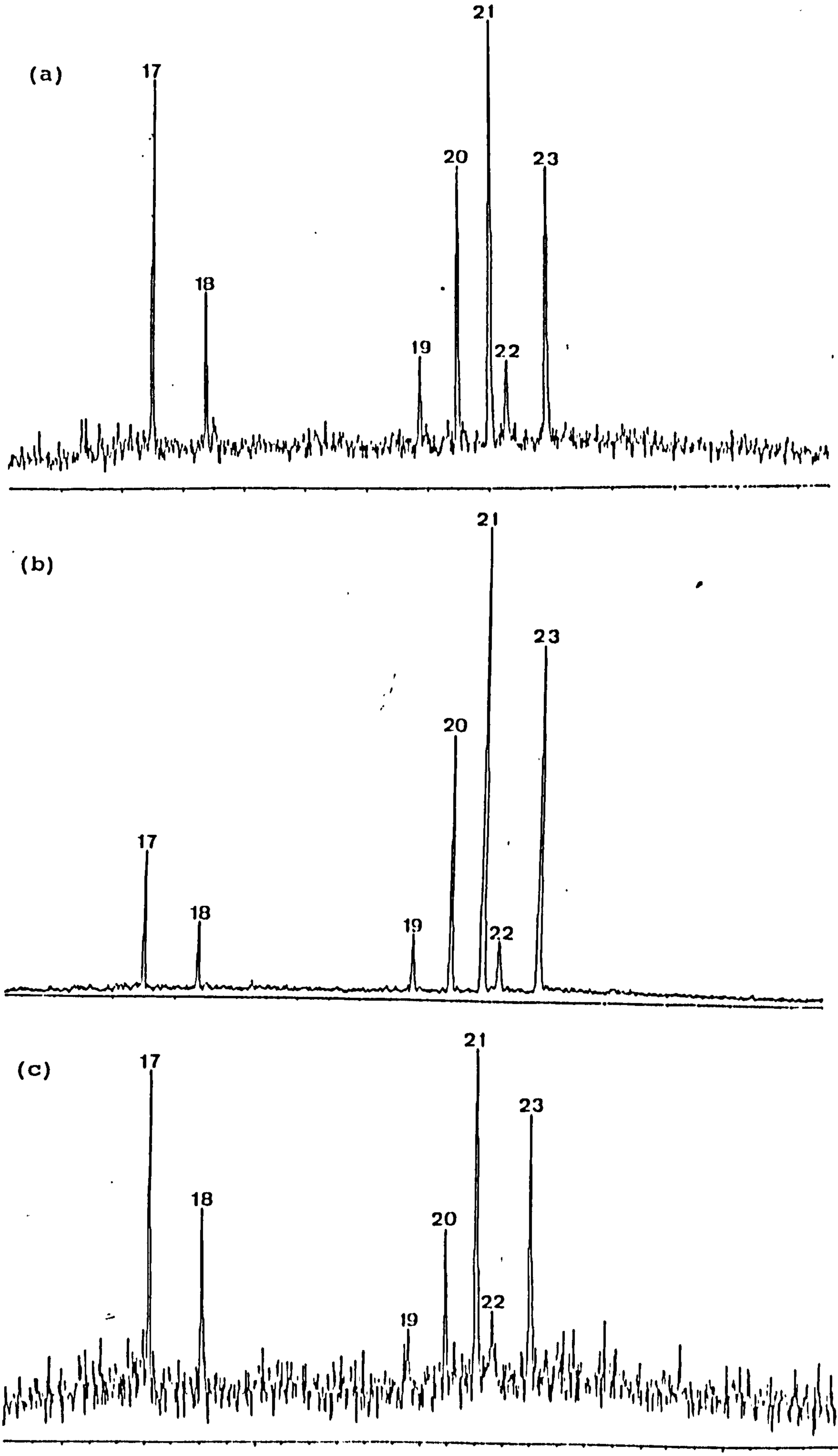

Figure 4.28 m/z 231.1170 mass chromatograms showing triaromatic steroidal hydrocarbon distributions of oils from the Sbaa basin: (a) ODZ1 (b) DECH1 and (c) TOT1. Peak assignments are listed in Table 4.

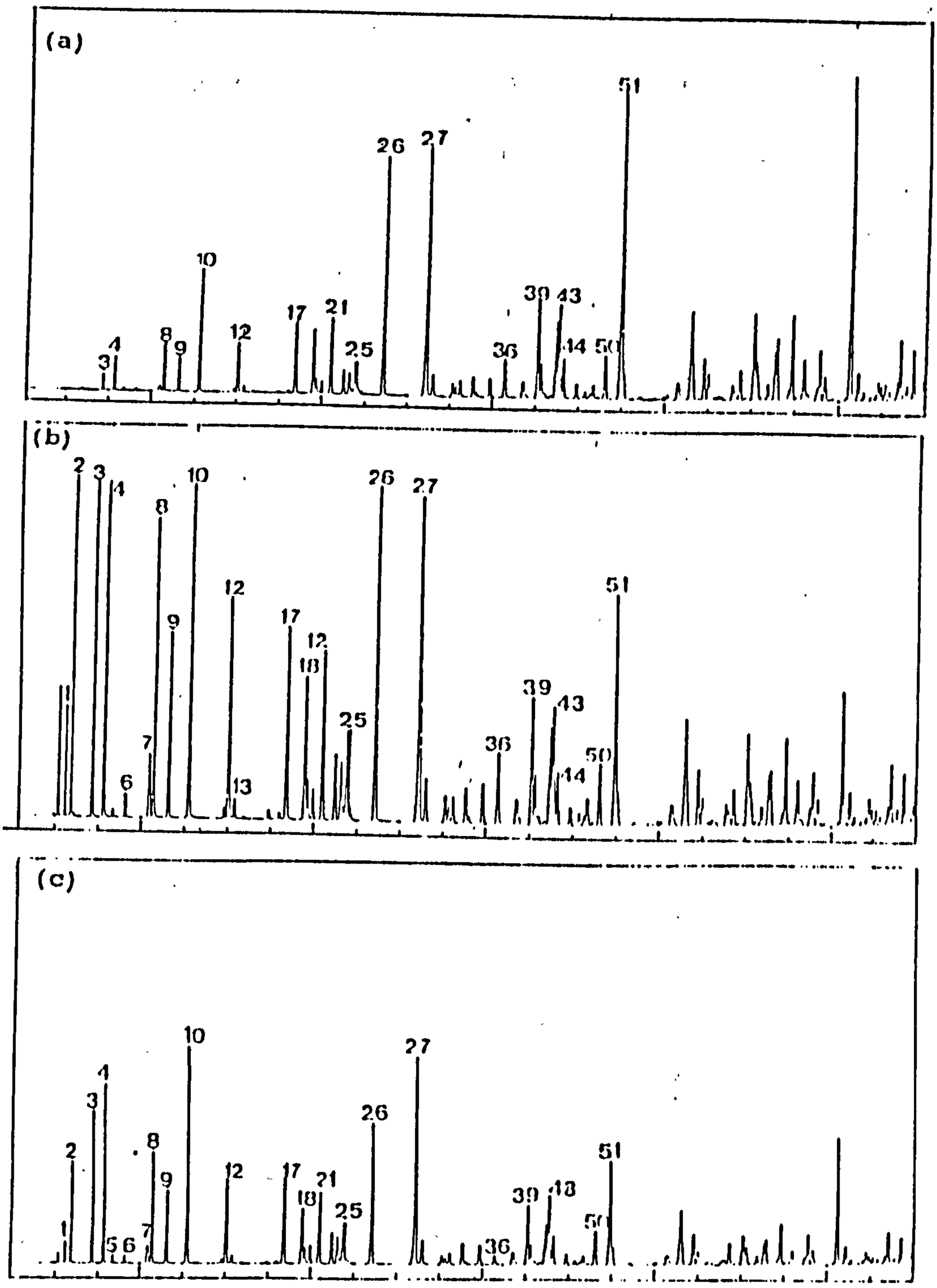

Retention time

Figure 4.29 Gas chromatograms of the gasoline range hydrocarbon fractions of three selected oils from the Sbaa basin: (a) ODZ1, (b) DECH1 and (c) TOT1. Peak assignments are given in Table 5.

4.2.4. Illizi basin

This section comprises results of oils from the Upper Devonian (e.g. F2 and F3), Lower Devonian reservoirs (F6 and TAGI) reservoirs.

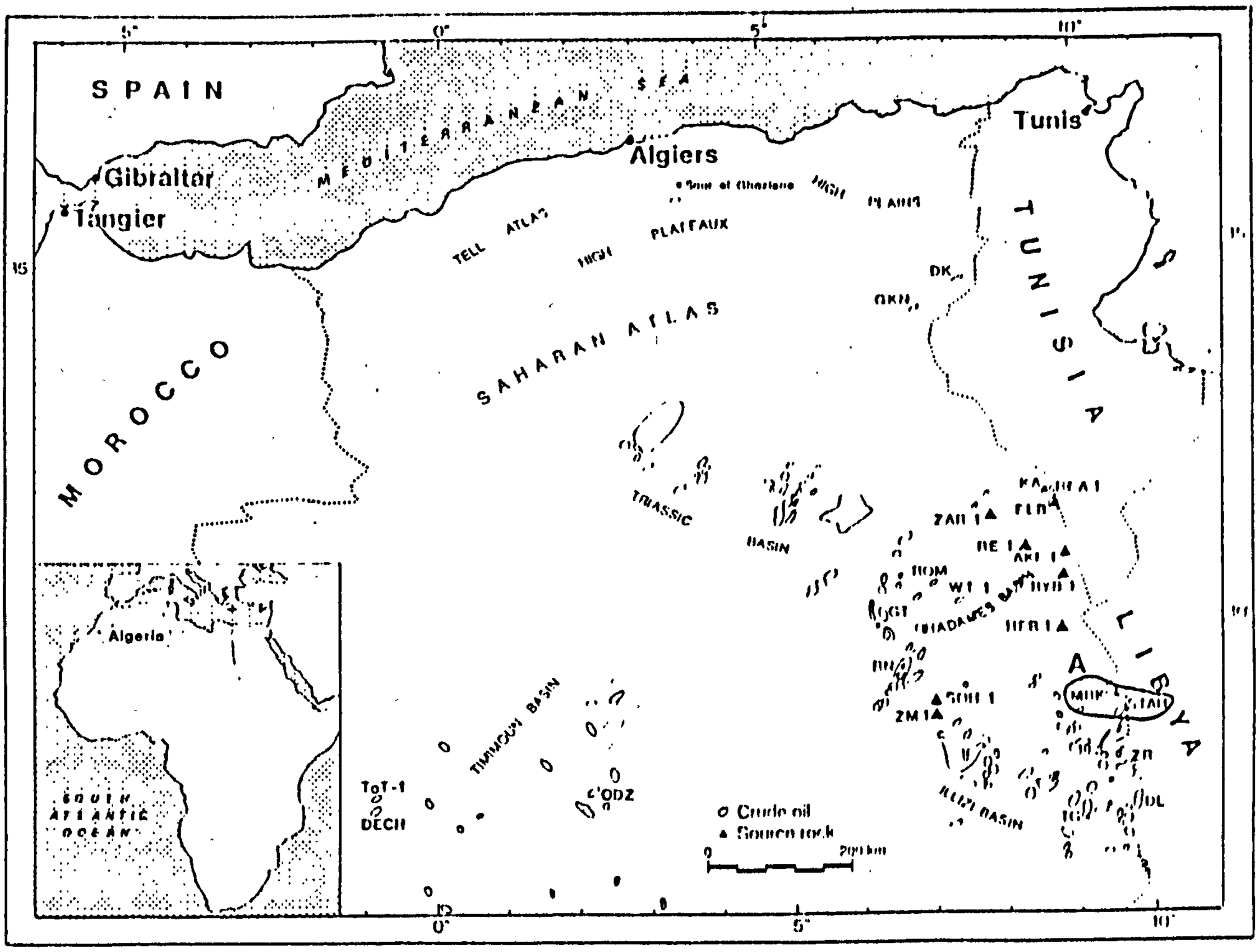

Figure 4.1d Sample location map showing the area of study (A=the Illizi basin), which group of oils were investigated.

4.2.4.1. Bulk composition

In general, NSO fraction consists of 2% to 8% of the total weight of oil (Table 4.1d). Oils reservoired from F_6 and F_3 (Lower and Upper Devonian reservoirs respectively) are highly mature compared to the other oils, as indicated by high saturates and low NSO contents. A slight distinction between oils from F_3, F_6 and TAGI (Lower Devonian reservoir) is recorded by higher amounts of saturated hydrocarbons with increasing reservoir depth (Welte et al., 1982). Figure 4.2d shows that Illizi oils fall in the same group. Hence, only STAH3F_3, STAH40 F_6 and WT1 TAGI have been

considered for a biological marker and gasoline range hydrocarbon investigation.

Table 4.1d: Bulk composition data

Well	%Sats	%Aro	%NSO	Pr/Ph	*D
$MRK6F_3$	85.05	12.63	2.32	1.44	0.819
$MRK9F_3$	81.28	17.28	1.44	1.41	0.819
$MRK16F_3$	79.43	14.25	6.32	1.33	0.819
$MRK17F_3$	85.01	13.56	1.44	1.31	0.819
$STAH3F_3$	87.74	10.68	1.58	1.42	0.787
$STAH8F_3$	78.45	12.87	8.68	1.45	0.787
$STAH37F_3$	91.45	7.16	1.40	1.42	0.787
$STAH43F_3$	88.22	10.53	1.26	1.45	0.787
$STAH29F_6$	90.22	8.92	0.86	1.61	0.810
$STAH40F_6$	93.09	4.32	2.59	1.73	0.810
$STAH44F_6$	88.19	9.55	2.26	1.66	0.810
WT1(TAGI)	90.09	8.29	1.61	1.61	0.812

* D is the density of oils measured at 20°C (g/cm^3).

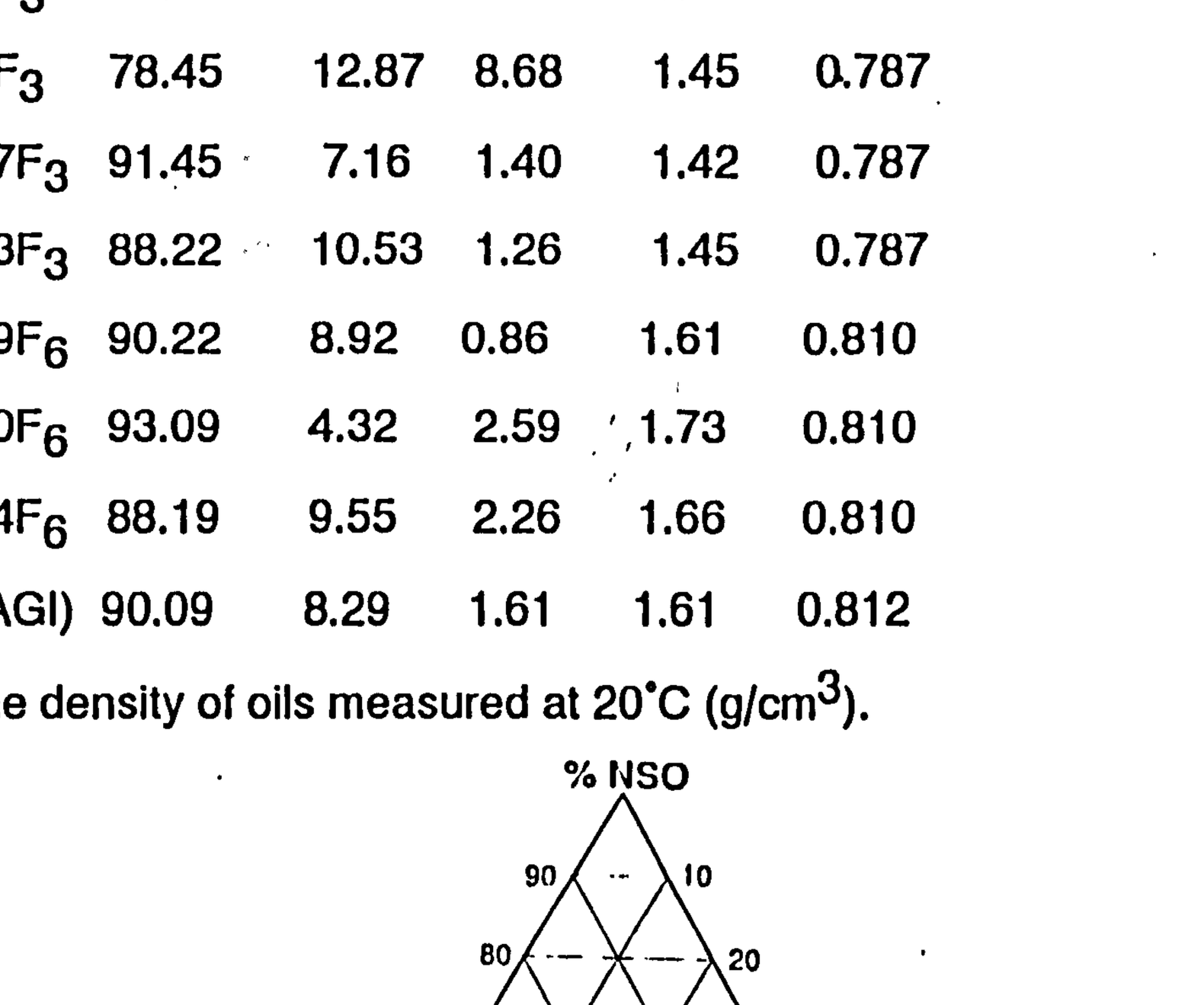

Figure 4.2d Relative proportions of saturated, aromatic hydrocarbons and NSO compounds of oils from the Illizi basin

4.2.4.2. Saturated hydrocarbon fraction

The most dominant hydrocarbons are the saturates as revealed by the gas chromatograms of the whole oils (Figure 4.30).

The gas chromatogram of non-adduct saturated hydrocarbon fraction ($MRK12F_6$, Figure 4.31) shows an abundance of a homologous series of monomethylalkanes, which have been tentatively identified by comparison with published chromatograms (Fowler et al., 1987), as 3-methyl, 2-methyl, 4-methyl, 5-methyl, 6-methyl and 7-methyl isomers. Acyclic hydrocarbons ($C_n<C_{20}$) are prominent, as indicated in this Figure.

Low concentrations of biological markers were recorded in these oils, suggesting high maturity, although rearranged steranes dominate the sterane distributions with prominence of C_{29} components (Figure 4.32).

Tricyclic terpanes are minor relative to hopane series, particularly C_{29} and C_{30} hopanes (Figure 4.32).

4.2.4.3. Aromatic hydrocarbon fraction

Missing data in Appendix 4.5 indicate that C-ring monoaromatic and triaromatic steroidal hydrocarbons were not detected in these oils due either to high maturity and/or water washing.

4.2.4.4. Gasoline range hydrocarbon fraction

Gas chromatograms of the gasoline hydrocarbon fractions of oils from Illizi basin (F_6, F_3 and TAGI reservoirs) are displayed in Figure 4.33. $STAH8F_3$ appears to contain relatively higher amounts of gasoline-range (C_4-C_7) hydrocarbons than $MRK12F_6$ (Figure 4.33a and 4.33b respectively). All these oils appear to have been water washed, as suggested by low aromaticity ratios (Appendix 4.6 and Figure 4.13).

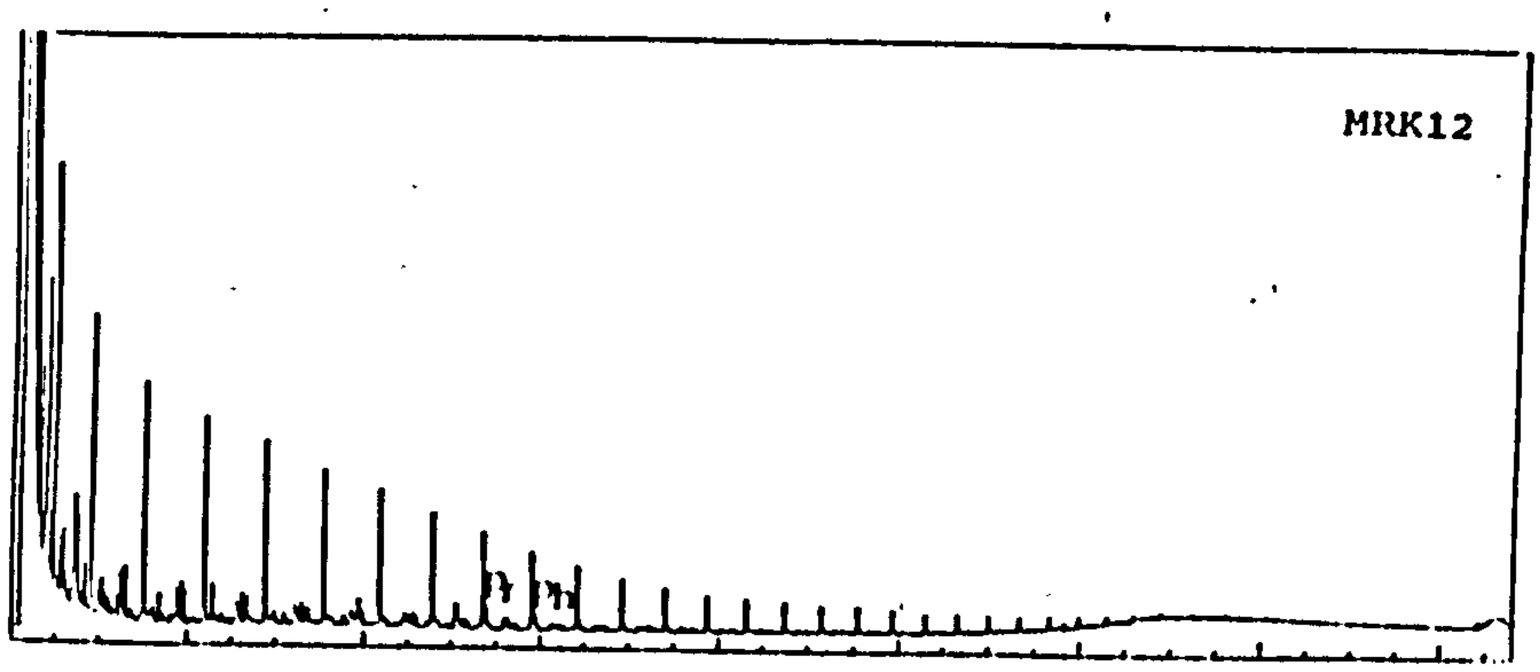

Figure 4.30 Gas chromatograms of oils from the Illizi basin.

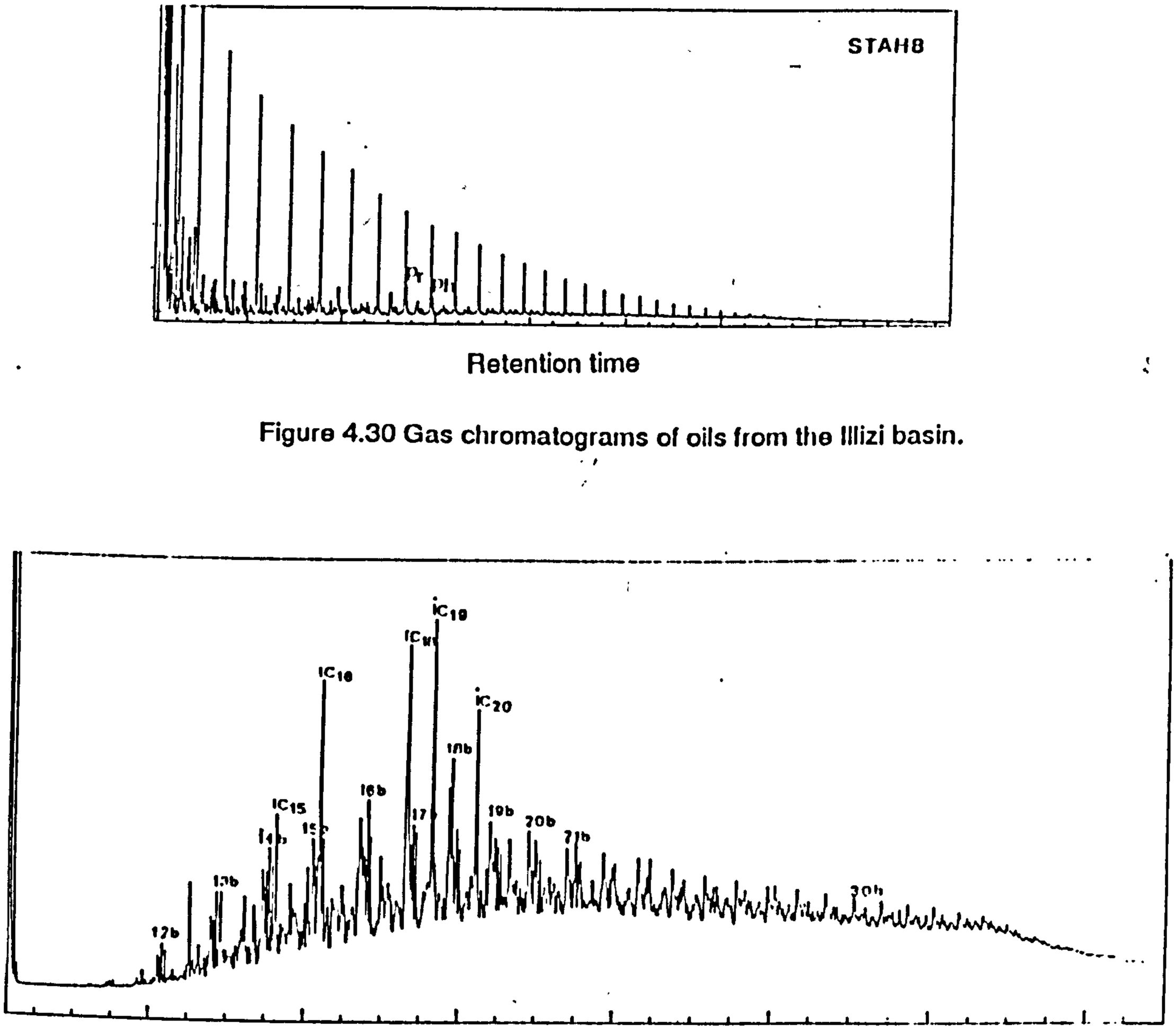

Figure 4.31 Gas chromatogram of non-adduct hydrocarbon fraction of one selected oil from the Illizi basin (MRK12F_6), showing a homologous series of branched alkanes (b), which have been tentatively identified as monomethylalkanes. These are labelled with their carbon number. 'i' refers to isoprenoid hydrocarbons.

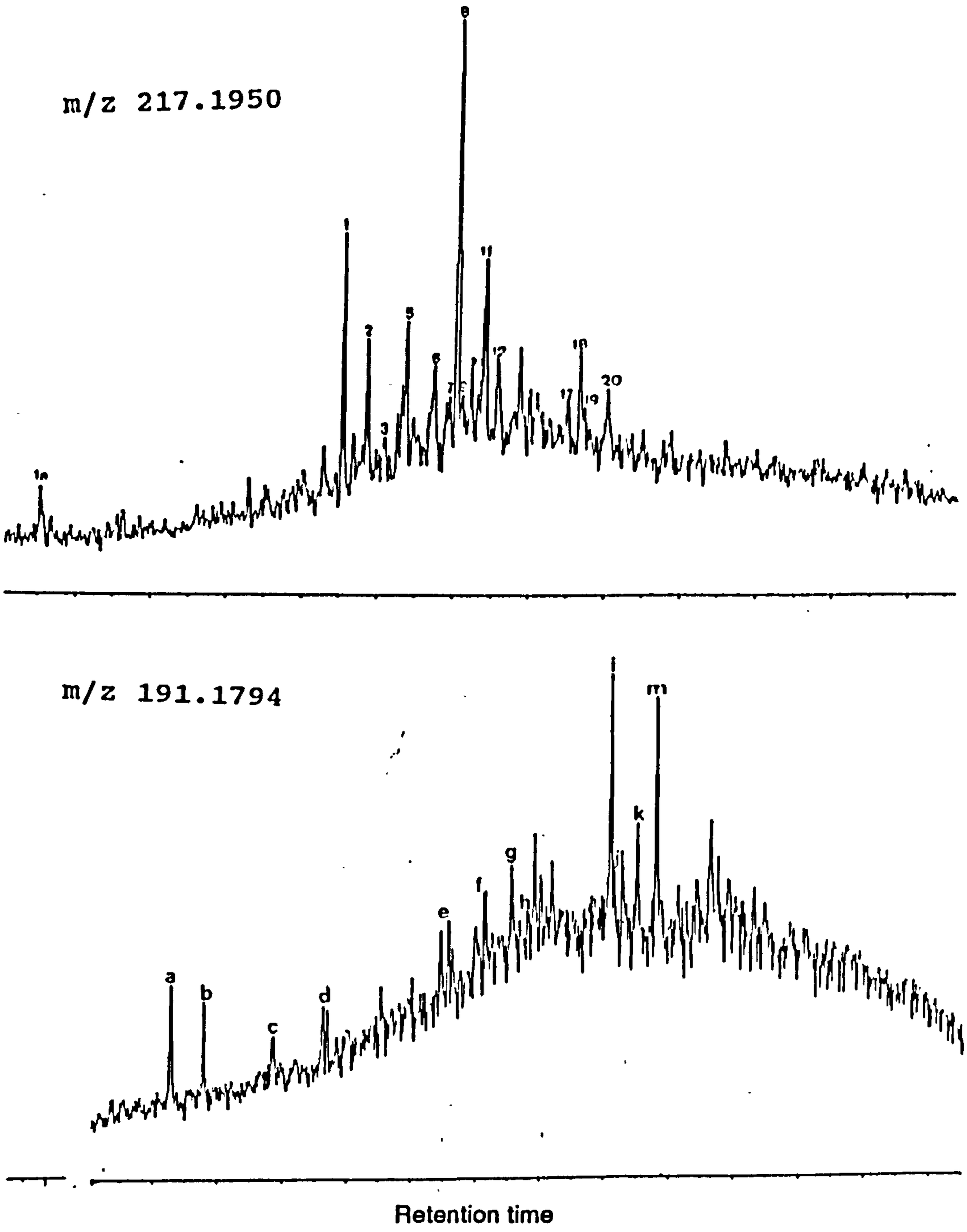

Figure 4.32 m/z 217.1950 and m/z 191.1794 mass chromatograms showing sterane and terpane distributions of one selected oil from the Illizi basin (STAH40F$_6$). Peak assignments are listed in Tables 1 and 2 respectively.

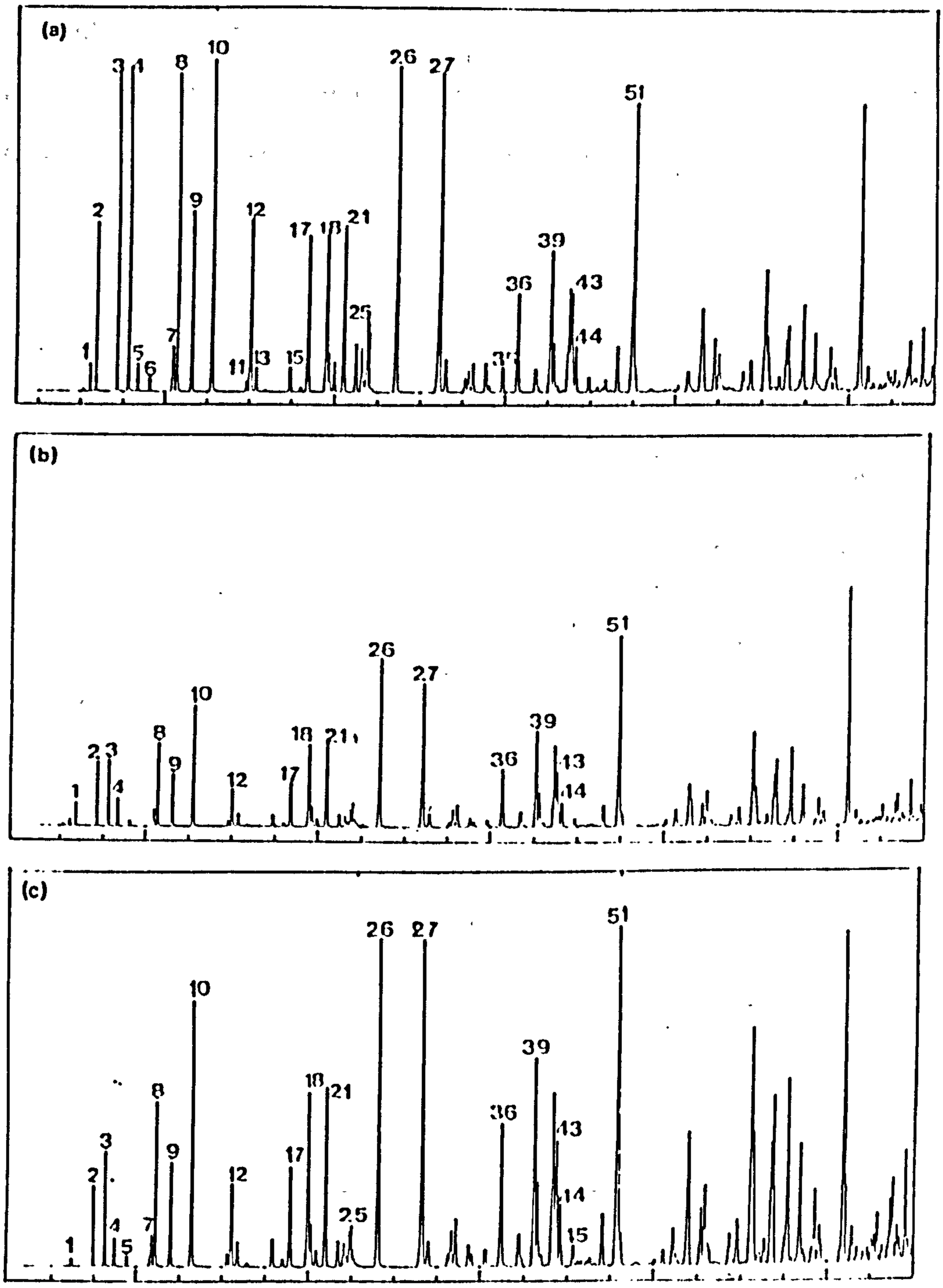

Figure 4.33 Gas chromatograms of the gasoline range hydrocarbon fractions of three selected oils from the Illizi basin: (a) STAH8F_3, (b) MRK12F_6 and (c) STAH40F_6. Peak assignments are given in Table 5.

4.2.5. Gassi Touil basin

This section comprises results of oils from the Upper Devonian (e.g. TAGS) and Lower Devonian reservoirs (TAGI) reservoirs.

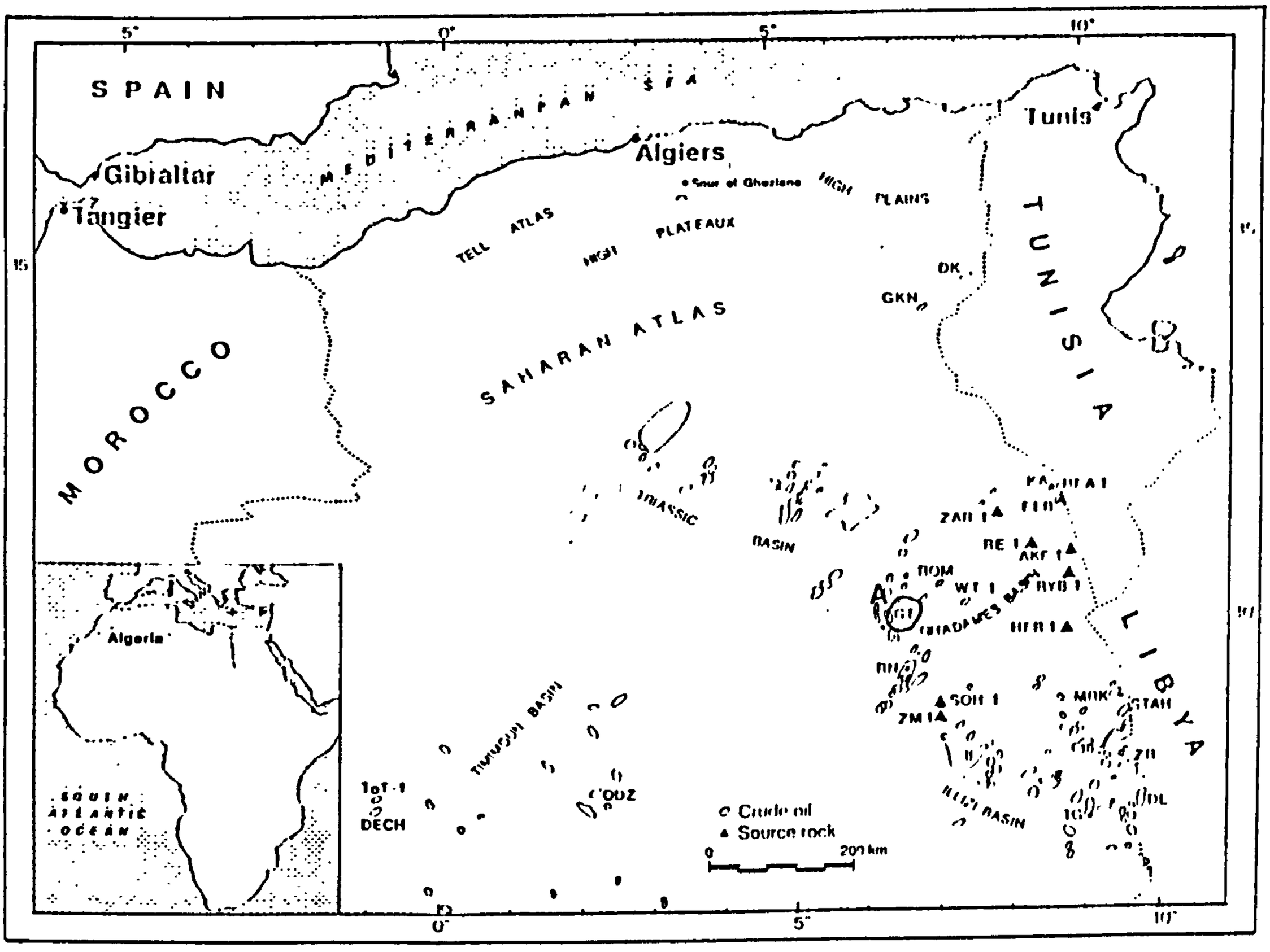

Figure 4.1e Sample location map showing the area of study (A= the Gassi Touil basin), which group of oils were investigated.

4.2.5.1. Bulk composition

The bulk composition presented in Table 4.1e and displayed in Figure 4.2e reveals slight differences between these two oils, although a slight higher increase in saturates is observed for GT47 than GT6

Table 4.1e: Bulk composition data

Well	%Sats	%Aro	%NSO	Pr/Ph	*D
GT47 TAGI	89.47	6.68	3.85	1.53	0.802
GT6 TAGS	78.82	20.31	0.87	1.39	0.812

* D is the density of oils measured at 20°C (g/cm^3).

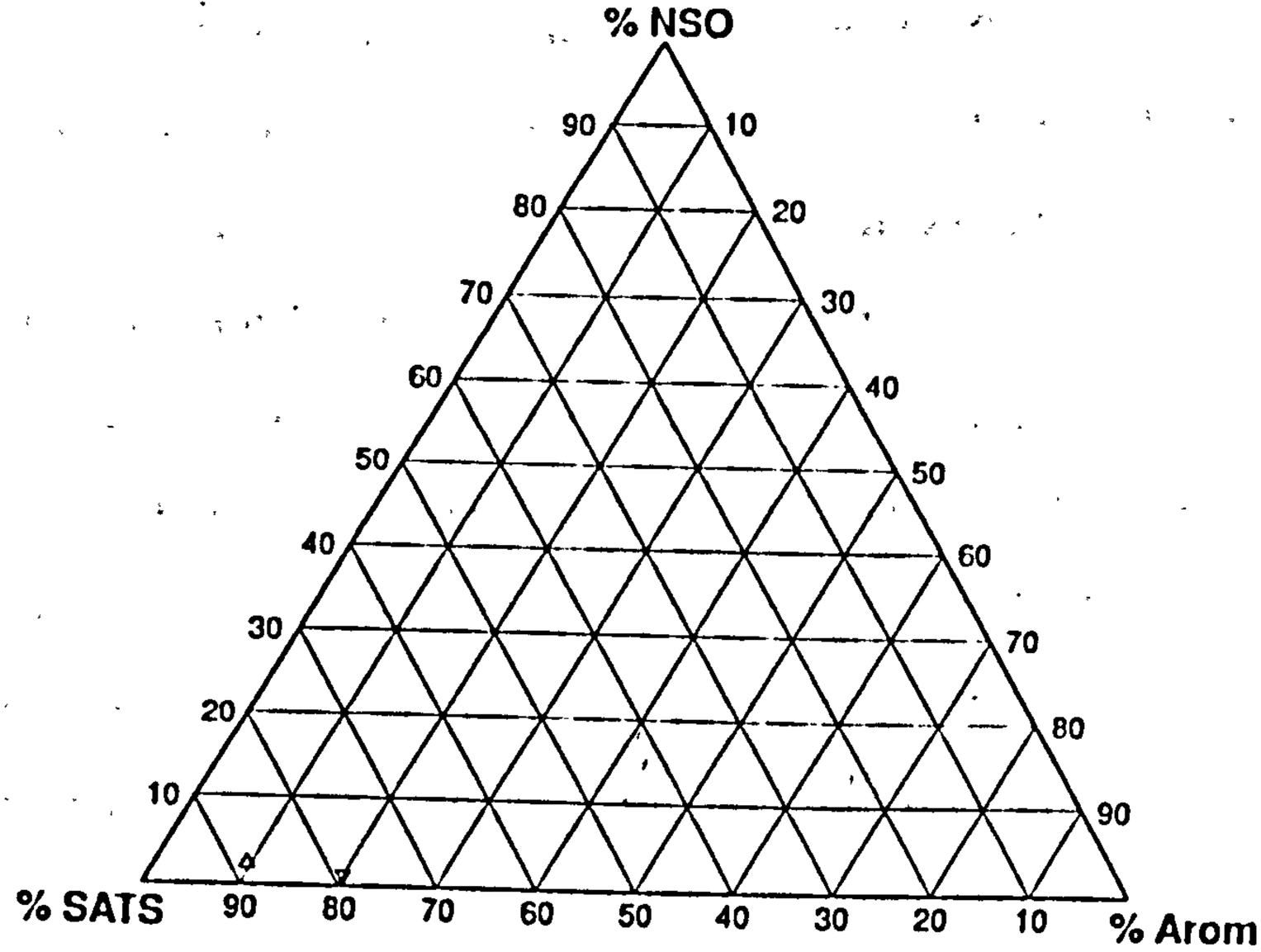

Figure 4.2e Relative proportions of saturated, aromatic hydrocarbons and NSO compounds of oils from the Gassi Touil basin.

4.2.5.2. Saturated hydrocarbon fraction

The molecular distributions are dominated by low molecular weight *n*-alkanes, with only minor acyclic isoprenoid alkanes (Table 4.1e), as clearly seen in the whole oil gas chromatograms (Figure 4.34).

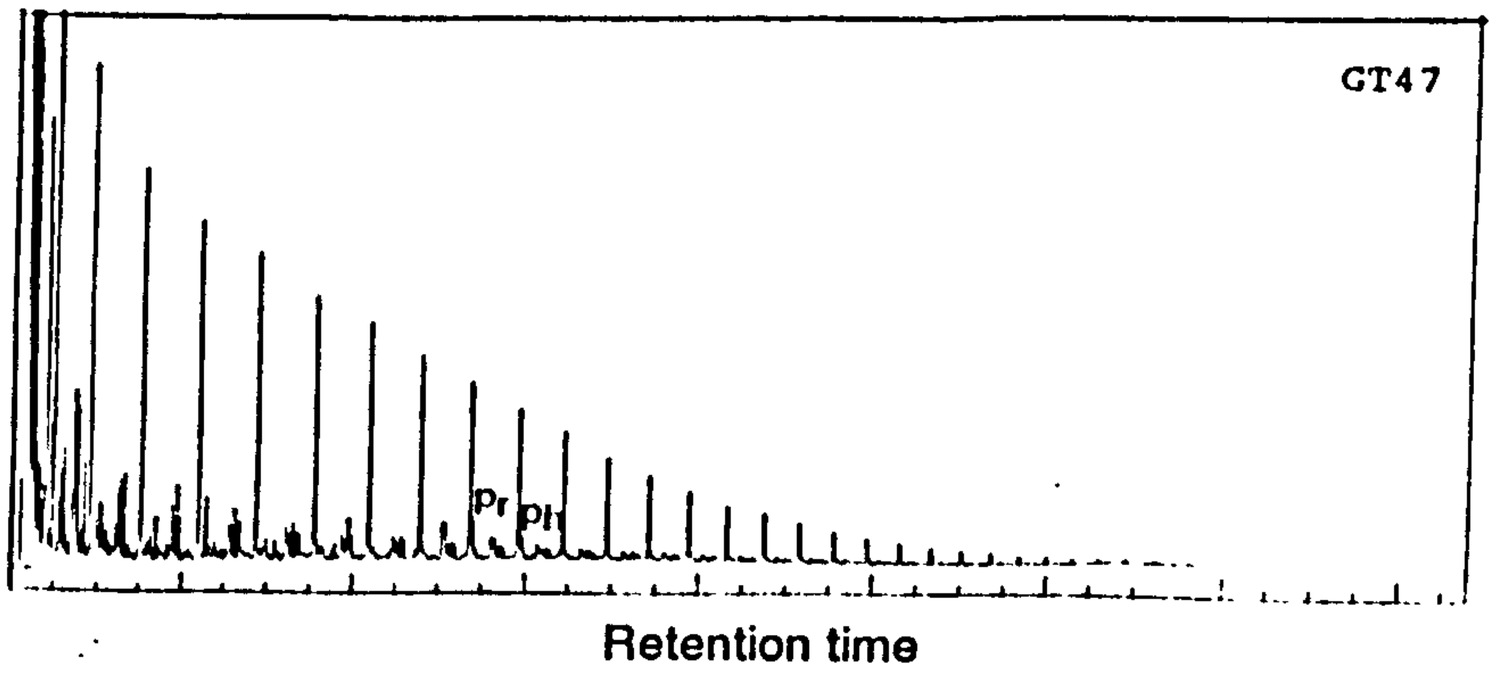

Figure 4.34 Gas chromatograms of oils from the Gassi Touil basin.

These oils contain low concentrations of biological marker compounds. Sterane distributions were barely detectable, being dominated by relatively low amounts of rearranged steranes, with a predominance of C_{29} components (Figure 4.35). The similarity in steranes distributions is clearly seen on the ternary diagram (Figure 4.7a and 4.7b). C_{30} steranes occur in minor abundance in both oils, while C_{30} methylsteranes (Figure 4.36) are dominated by the 24-ethyl-αββ-3β-methyl-((20R) and (20S)).

Hopanes and steranes have roughly similar contribution in both oils, as indicated in Appendix 4.4. It worth noting the relatively higher abundances of tricyclic relative to pentacyclic terpanes in GT6 and GT47 (Figure 4.37) than in the other oils, as indicated by high $C_{23}T/C_{23}T+C_{30}\alpha\beta$ hop ratio (0.83 and 0.69 for GT47 and GT6 respectively). The $C_{23}T/C_{23}T+C_{30}\alpha\beta$ hop ratio versus $C_{30}\alpha\beta/C_{29}\alpha\alpha\alpha$ (20R) ratio (Figure 4.56) shows that these oils can be discriminated from the other oils. The variation of the relative proportions of $C_{29}T_s$ to $C_{29}\alpha\beta$ norhop and $C_{29}\alpha\beta$ norhop/$C_{30}\alpha\beta$ hop illustrated in Figure 4.10, reveal similar maturity levels of GT6 and GT47.

4.2.5.3. Aromatic hydrocarbon fraction

C-ring monoaromatic steroidal hydrocarbons were barely detectable in both oils. Only triaromatic distributions are present in fairly small amounts (Figure 4.37), showing relatively similar and high proportions of C_{28} triaromatic in GT6 and GT47, as indicated by the $\%C_{28}t/C_{26}t+C_{27}t+C_{28}t$ ratio (Appendix 4.2). Short-chain triaromatic steroidal hydrocarbons are major components in GT47 but moderately abundant in GT6 as indicated by the cracking ratio (0.33-0.57).

4.2.5.4. Gasoline range hydrocarbon fraction

A close examination of the gas chromatograms of the gasoline (C_4-C_9) range hydrocarbons of GT6 and GT47 (Figure 4.39) and the data derived from this fraction (Appendix 4.6) show that these two oils are similar. Figure

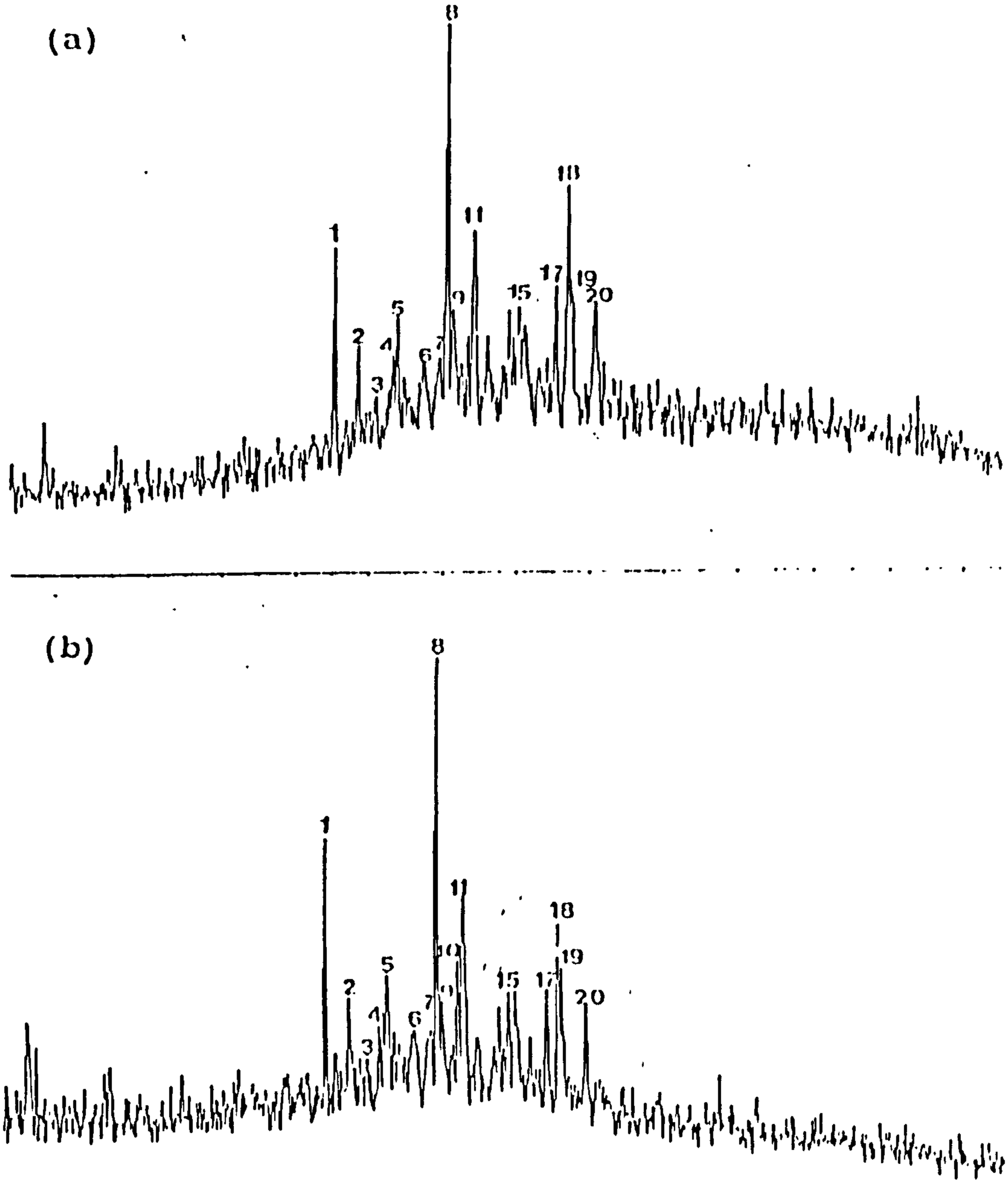

Figure 4.35 m/z 217.1950 mass chromatograms illustrating sterane distributions of oils from the Gassi Touil basin: (a) GT6, (b) GT47. Peak assignments are listed in Table 1.

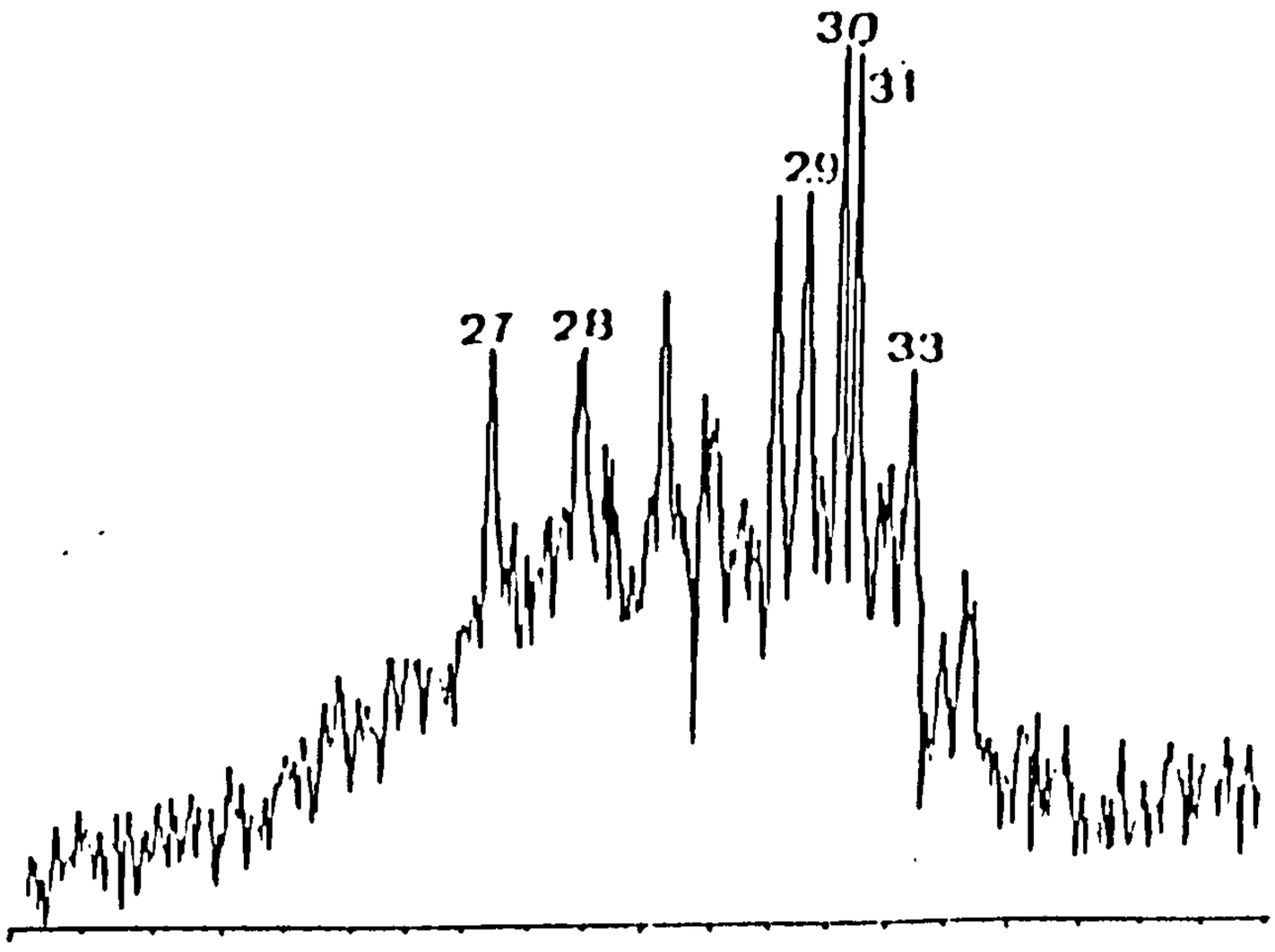

Figure 4.36 Mass chromatogram from metastable ion reaction monitoring of transition m/z 414->m/z 231 for methylsteranes (C_{30} components) in one selected oil (GT6) from the Gassi Touil basin. Peak assignments are listed in Table 1.

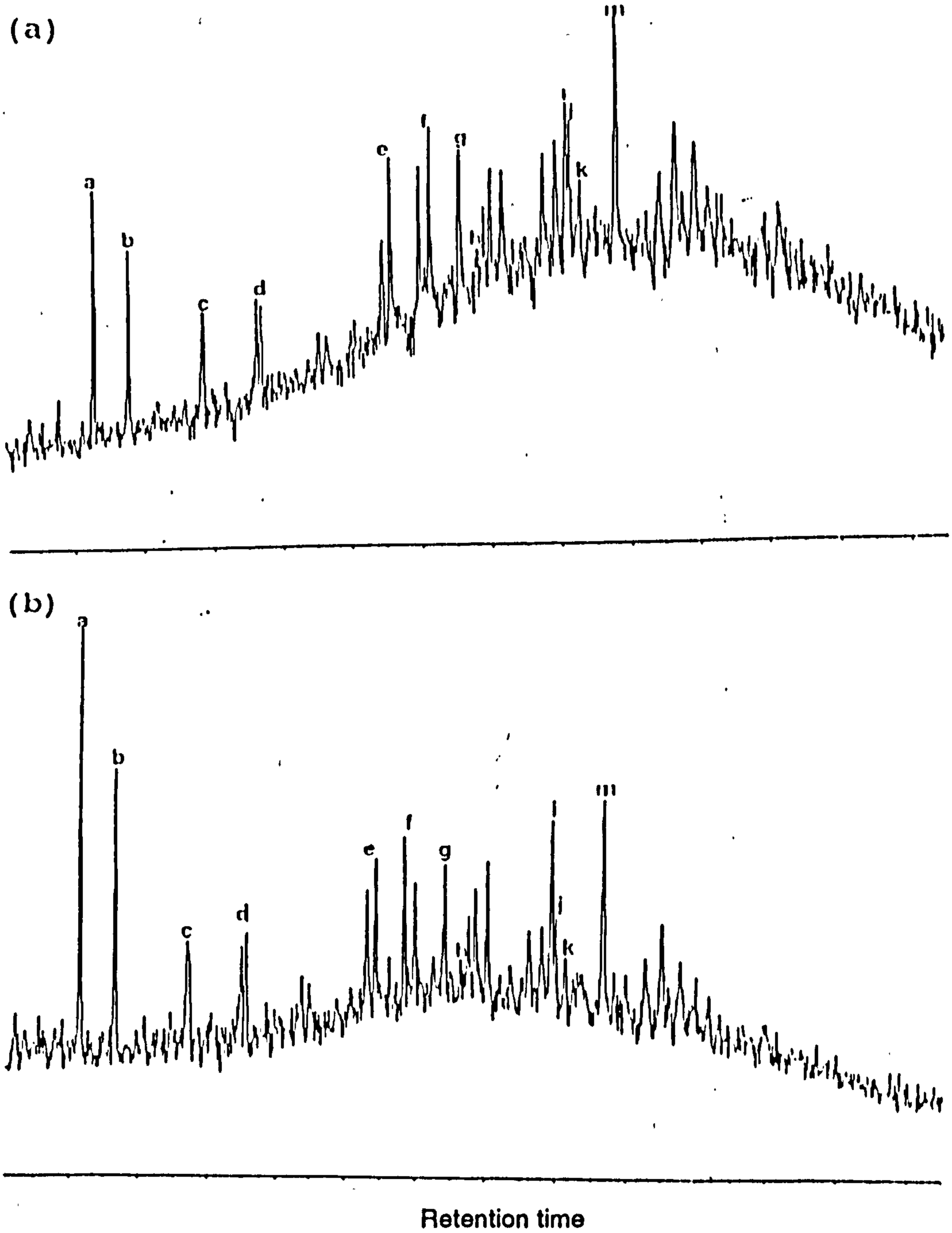

Figure 4.37 m/z 191.1794 mass chromatogram showing terpane distributions of oils from the Gassi Touil basin: (a) GT6, (b) GT47. Peak assignments are listed in Table 2.

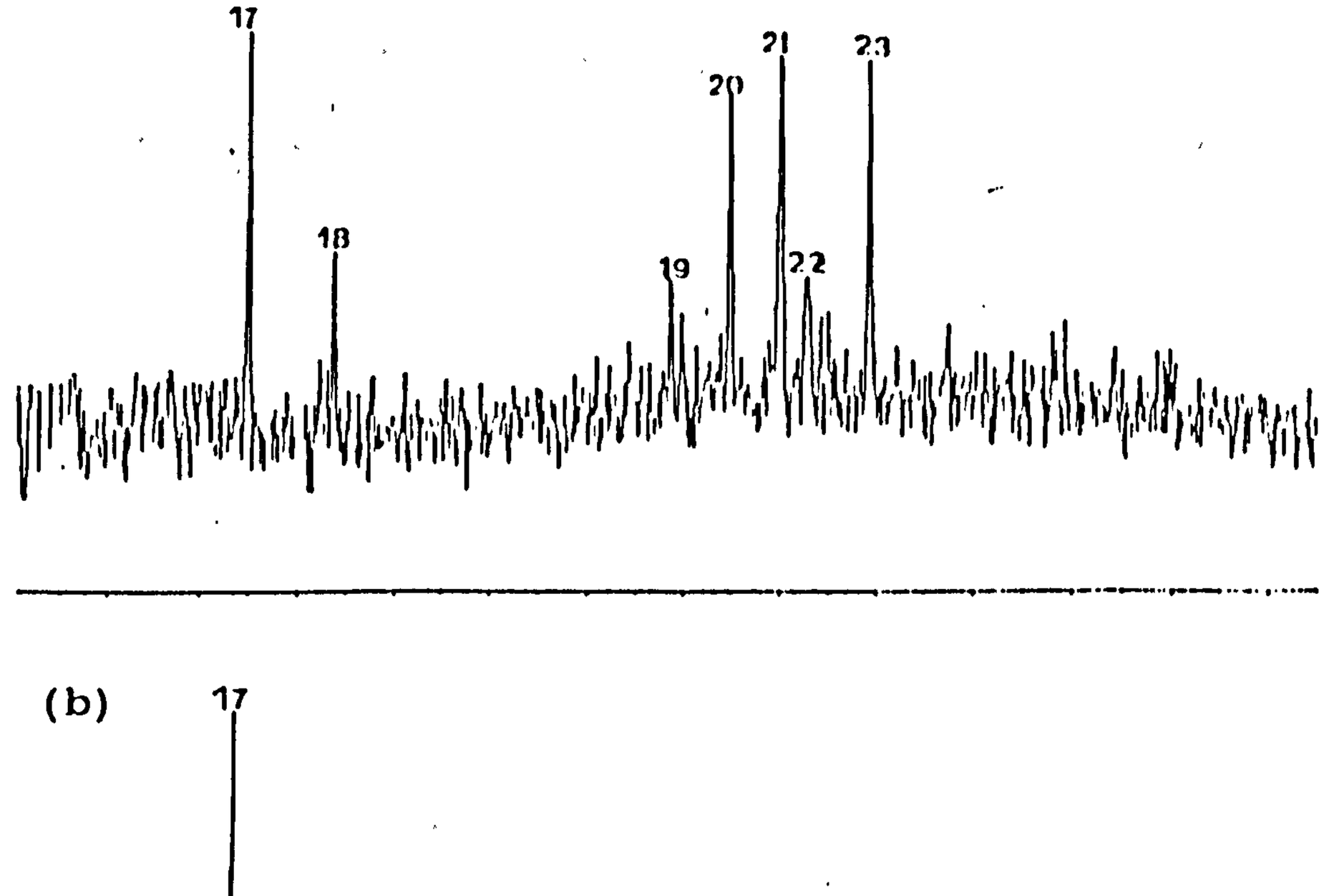

Figure 4.38 m/z 231.1170 mass chromatograms showing triaromatic steroidal hydrocarbon distributions in oils from the Gassi Touil basin: (a) GT6, (b) GT47. Peak assignments are listed in Table 4.

4.13 shows that oils from Gassi Touil exhibit high paraffinicity indices (e.g Heptane and Isoheptane indices and others). Furthermore, on the summary diagram (i.e *n*-C_7/MCH versus Tol/*n*-C_7 diagram) of Thompson (1987;1988), these oils plot on the direction indicative of high maturity.

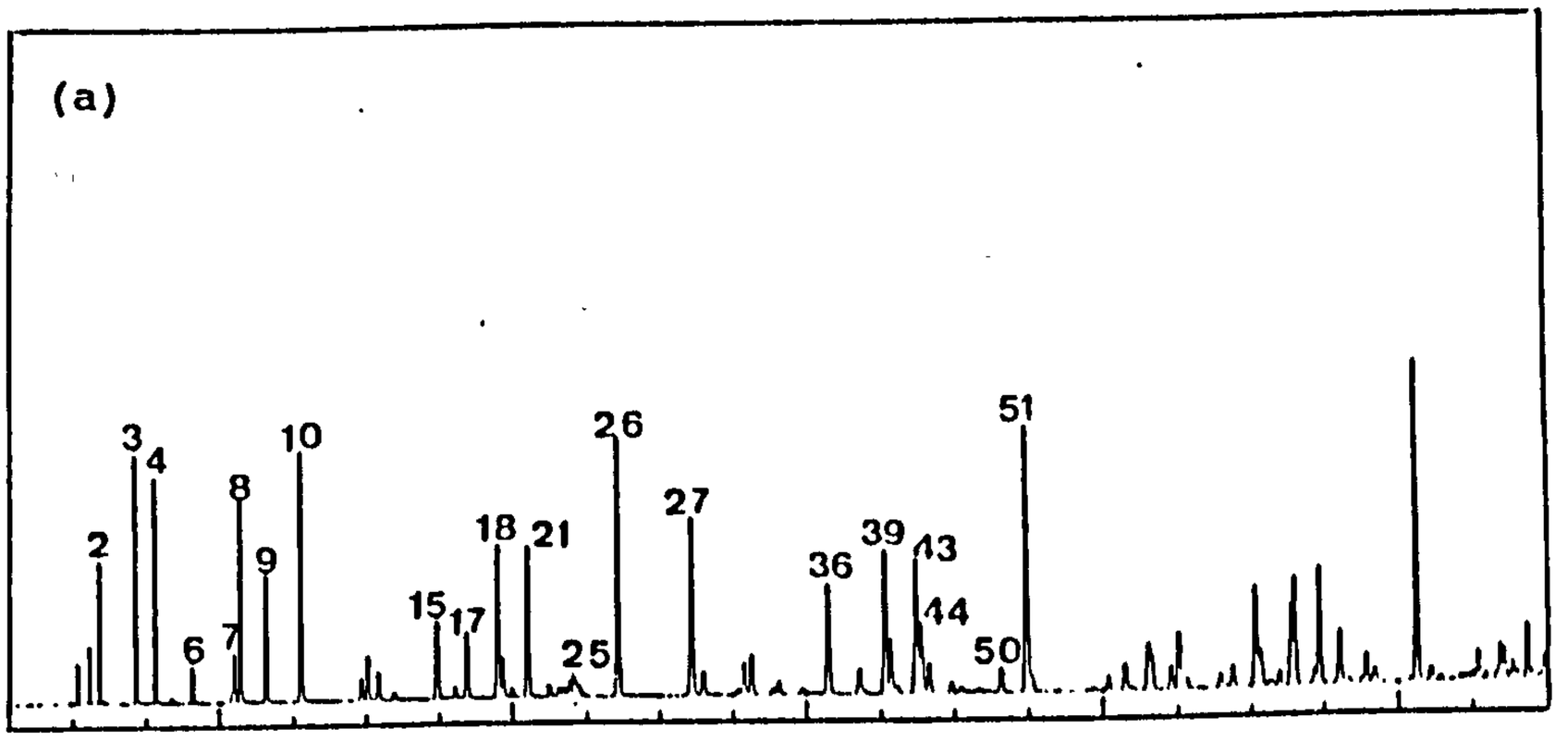

Figure 4.39 Gas chromatograms of the gasoline range hydrocarbon fractions of oils from the Gassi Touil basin: (a) GT6, (b) GT47. Peak assignments are given in Table 5.

4.2.6. Rhourd-Nouss basin

This section comprises results of oils from the Upper Devonian (e.g. TAGS) and Lower Devonian reservoirs (TAGI) reservoirs.

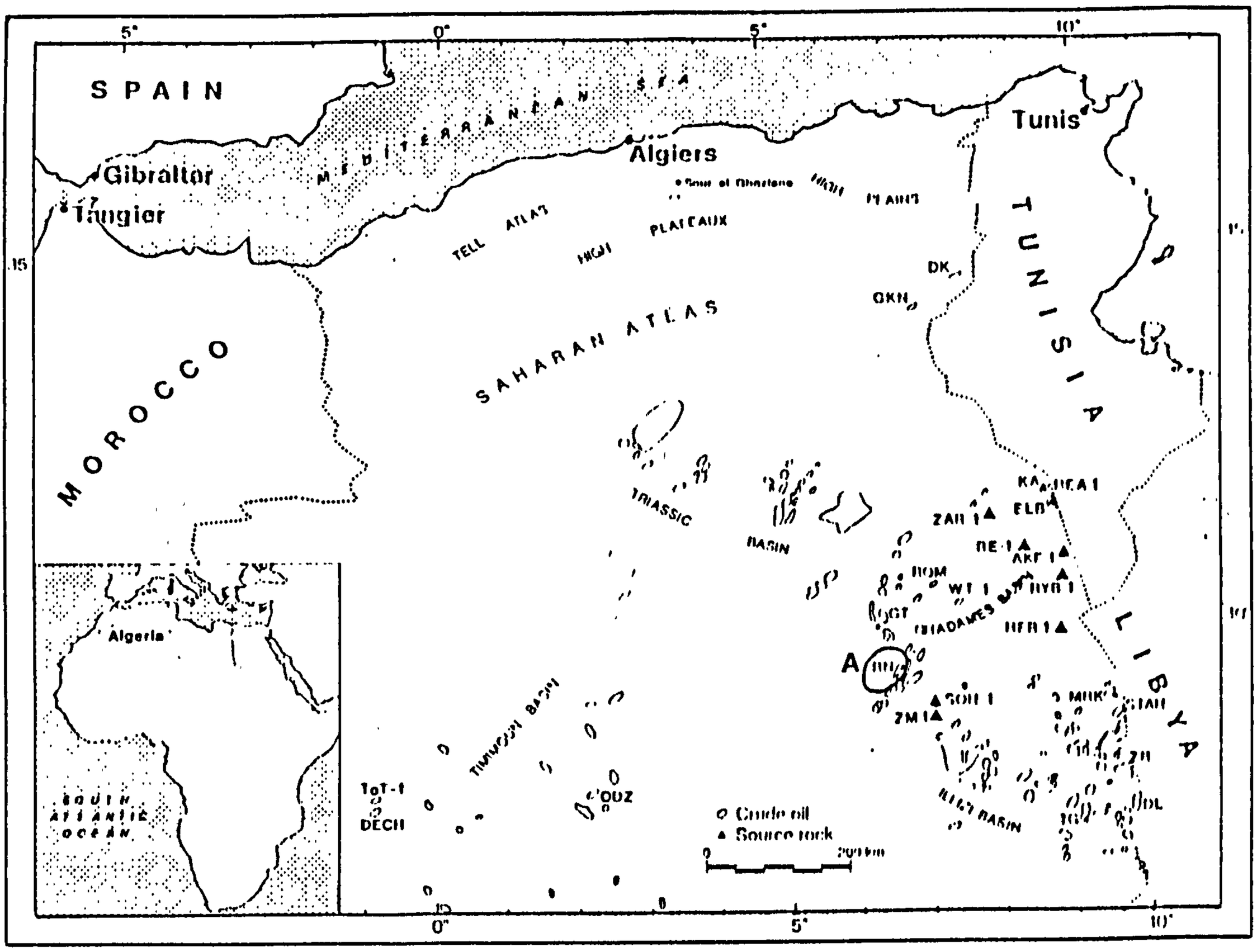

Figure 4.1f Sample location map showing the area of study (A= the Rhourd-Nouss basin), which group of oils were investigated.

4.2.6.1. Bulk composition

The bulk composition (Table 4.1f) displayed in Figure 4.2f, show a little or no difference between RN48 and RNSE6.

Table 4.1f: Bulk composition data

Well	%Sats	%Aro	%NSO	Pr/Ph	D*
RN48 TAGI	89.18	9.13	1.68	1.36	0.808
RNSE6 TAGS	79.52	18.33	2.14	1.61	0.853

* D is the density of oils measured at 20°C (g/cm^3).

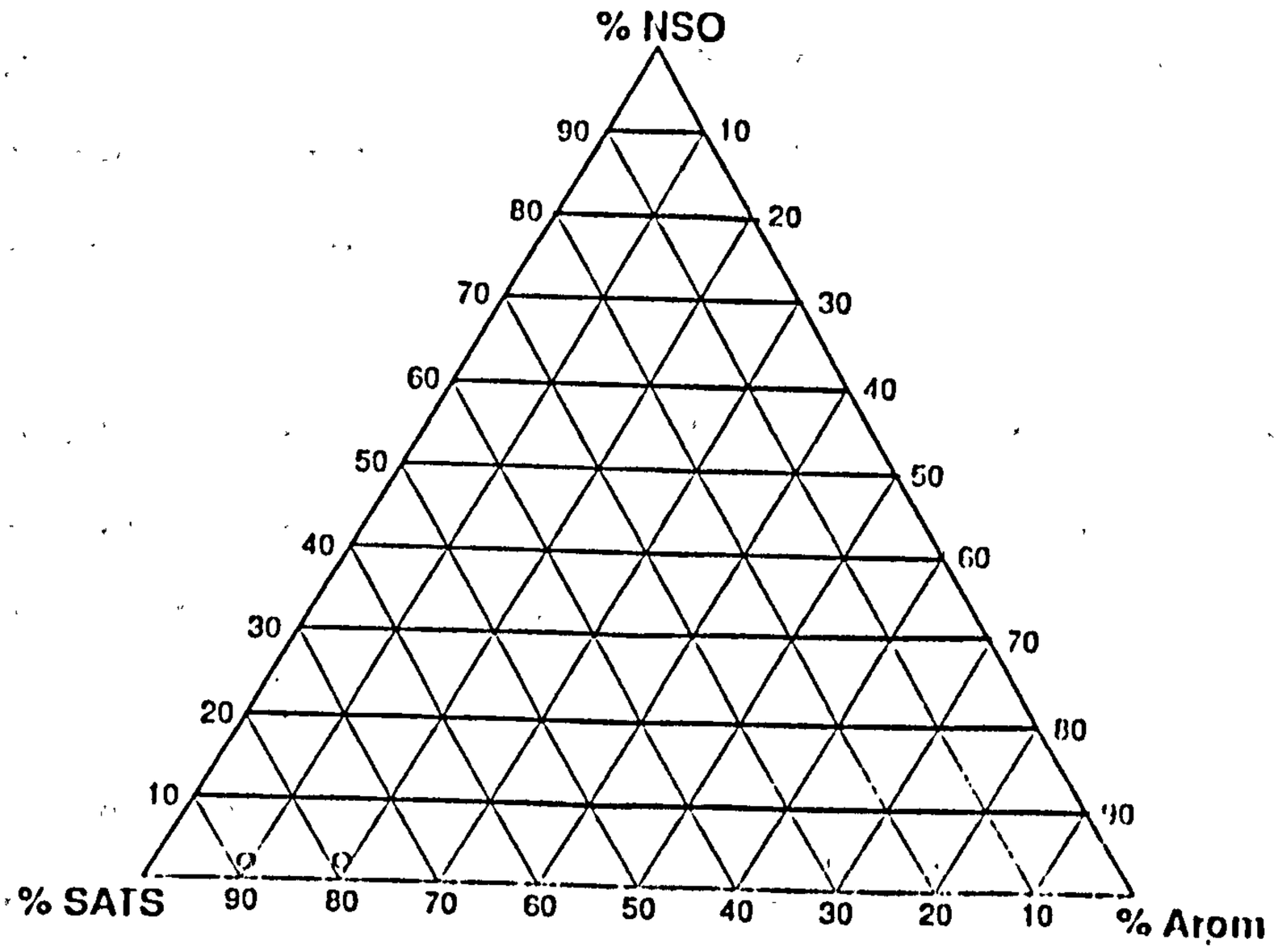

Figure 4.2f Relative proportions of saturated, aromatic hydrocarbons and NSO compounds of oils from the Rhourd-Nouss basin.

4.2.6.2. Saturated hydrocarbon fraction

The tendency towards high abundance of *n*-alkanes is reflected in the whole oil gas chromatograms (Figure 4.40), with minor acyclic isoprenoids giving Pr/Ph ratio in the range of 1.36 and 1,61.

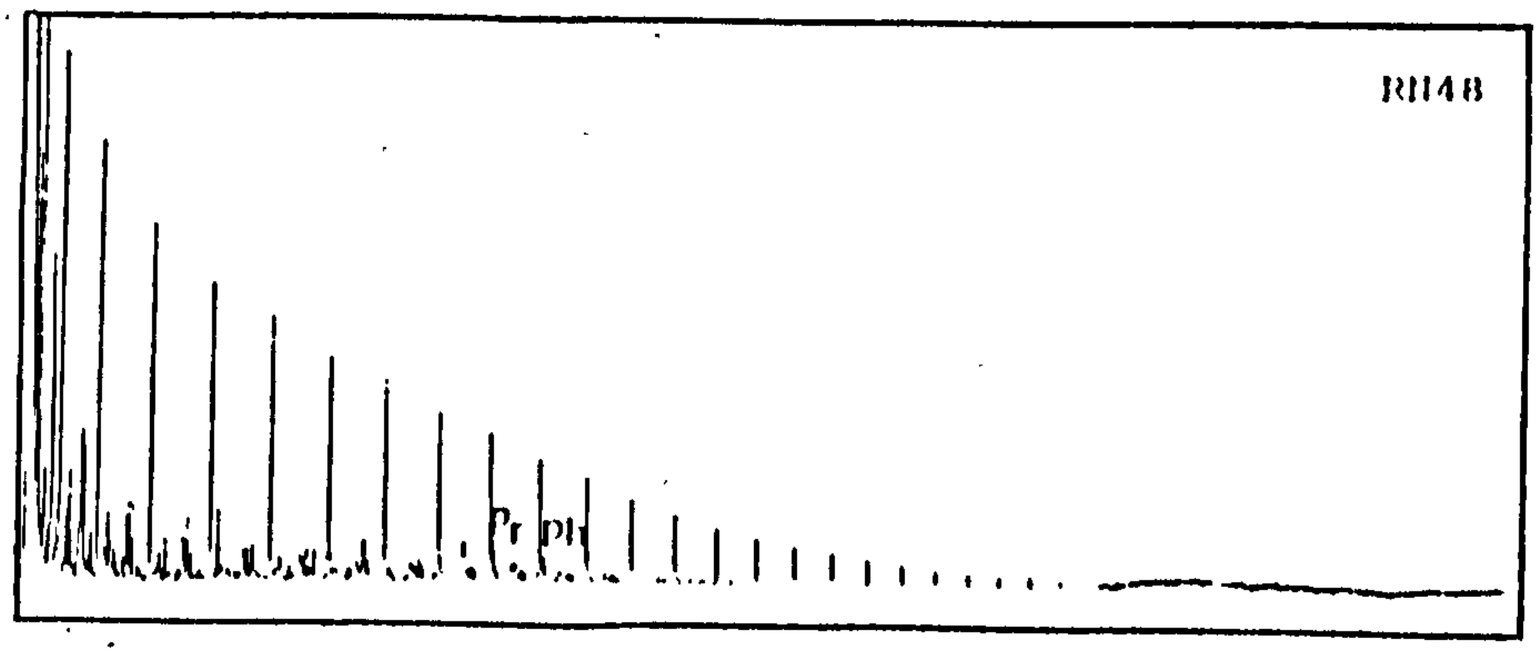

Figure 4.40 Gas chromatogram of one selected oil from the Rhourd-Nouss basin.

Sterane distributions are dominated by rearranged steranes with C_{29} members in both oils (Figure 4.41). They were detected in relatively lower concentrations in RN48 than RNSE6. Pregnane and homopregnane are minor relatively to long chain homologues. Methylsteranes were recorded in low abundance, as shown in Figure 4.42 with prominent 3β-methyl (αββ ((20R) and (20S)).

As displayed in Figure 4.43, oils from the Rhourd-Nouss basin exhibit the lowest content of hopanes, as reflected by the highest $C_{30}\alpha\beta$ norhop/C_{29}st ratio (0.87 and 0.64 for RN48 and RNSE6 respectively), suggesting higher contribution of steranes than hopane. Furthermore, tricyclic predominate over pentacyclic terpanes in a similar to those from Gassi Touil basin with prominent C_{23} tricyclic terpane, as indicated by the $C_{23}T/C_{23}+C_{30}\alpha\beta$ hop (0.63, 0.79 for RN48 and RNSE6 respectively. Figure 4.56 shows that RN48 and RNSE6 falls in the same group as GT6 and GT47 oils, sharing similarities in source and maturity level.

4.2.6.3. Aromatic hydrocarbon fraction

The C-ring monoaromatic steroidal hydrocarbons were barely detectable in the aromatic hydrocarbon fractions of both oils, in which only moderate amounts of triaromatic components are observed (Figure 4.44). The tendency towards high C_{29} steranes in RNSE6 is reflected by high C_{28} triaromatic steroidal hydrocarbons, as indicated by the $\%C_{28}t/C_{26}t+C_{27}t+C_{28}t$ (i.e 80%). Both triaromatic and methyl triaromatic steroidal hydrocarbon distributions are dominated by short-chain homologues (Figure 4.44 and 4.45), as reflected by high cracking ratios (0.64 and 0.73) and MTSI1 and MTSI2 (0.68 and 0.55). Long-chain methyl triaromatics were barely detectable, as shown in Figure 4.45.

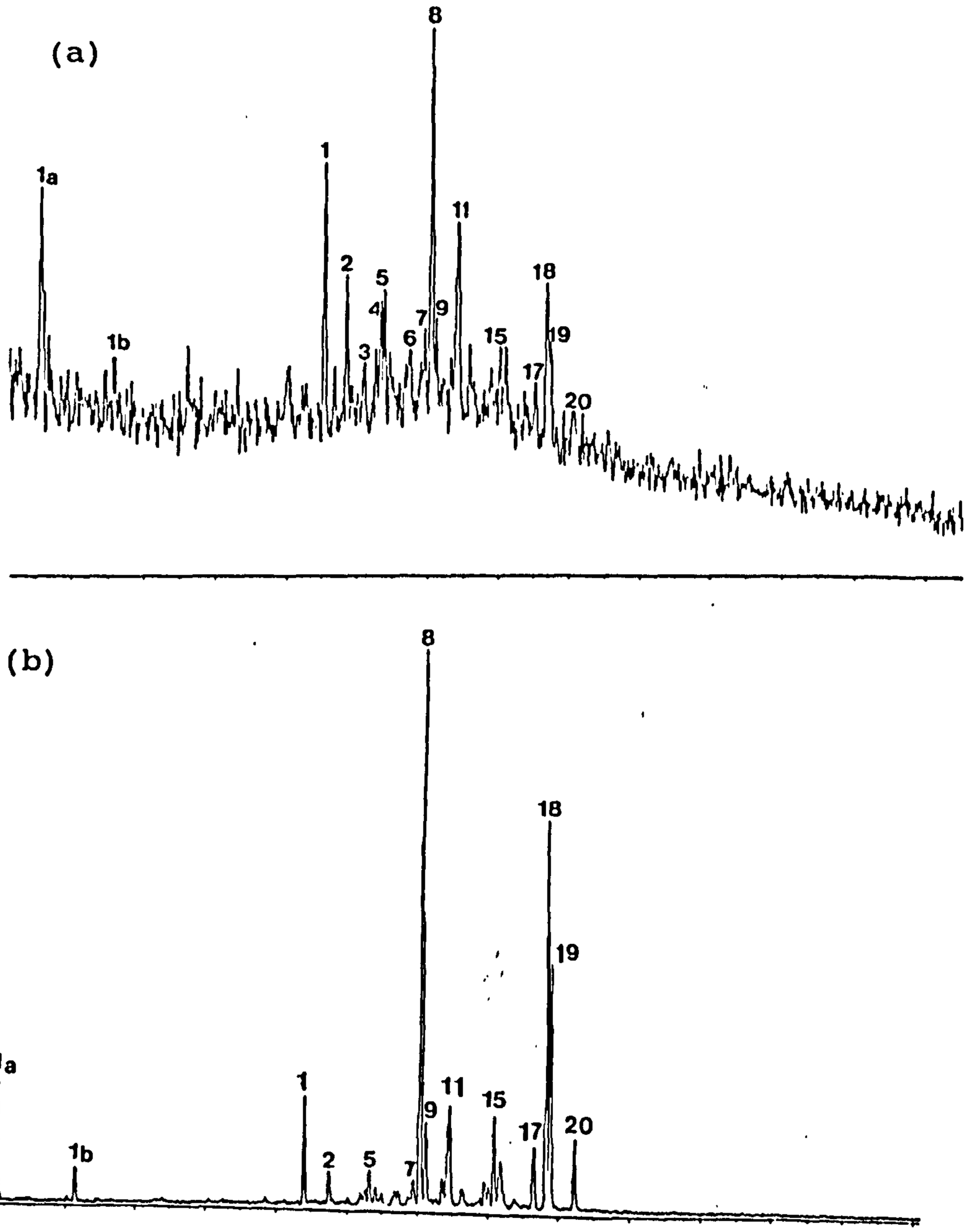

Figure 4.41 m/z 217.1950 mass chromatograms illustrating sterane distributions of oils from the Rhourd-Nouss basin: (a) RN48, (b) RNSE6. Peak assignments are listed in Table 1.

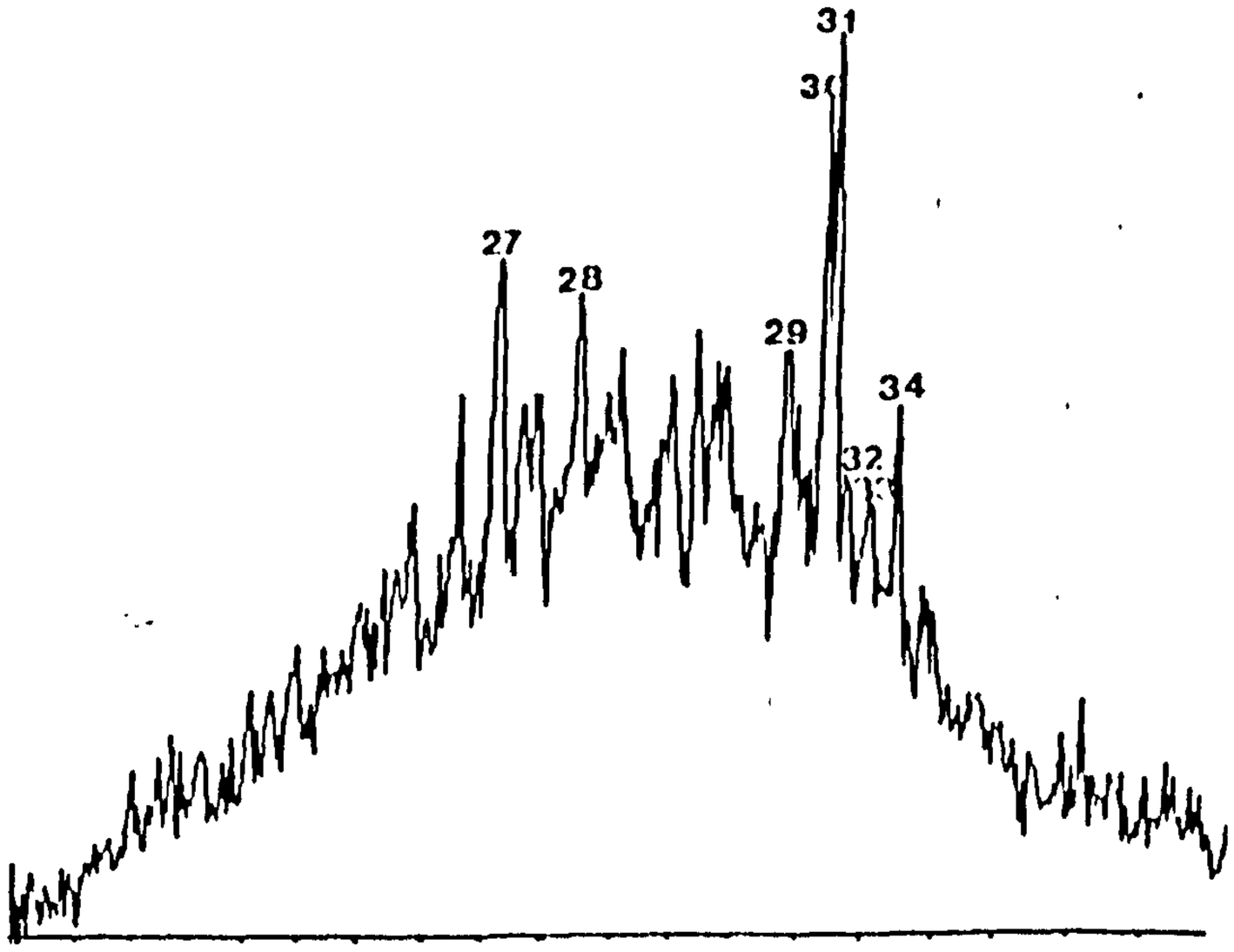

Figure 4.42 Mass chromatogram from metastable ion reaction monitoring of transition m/z 414->m/z 231 for methylsteranes (C_{30} components) in one selected oil from the Rhourd-Nouss basin (RNSE6). Peak assignments are listed in Table 1.

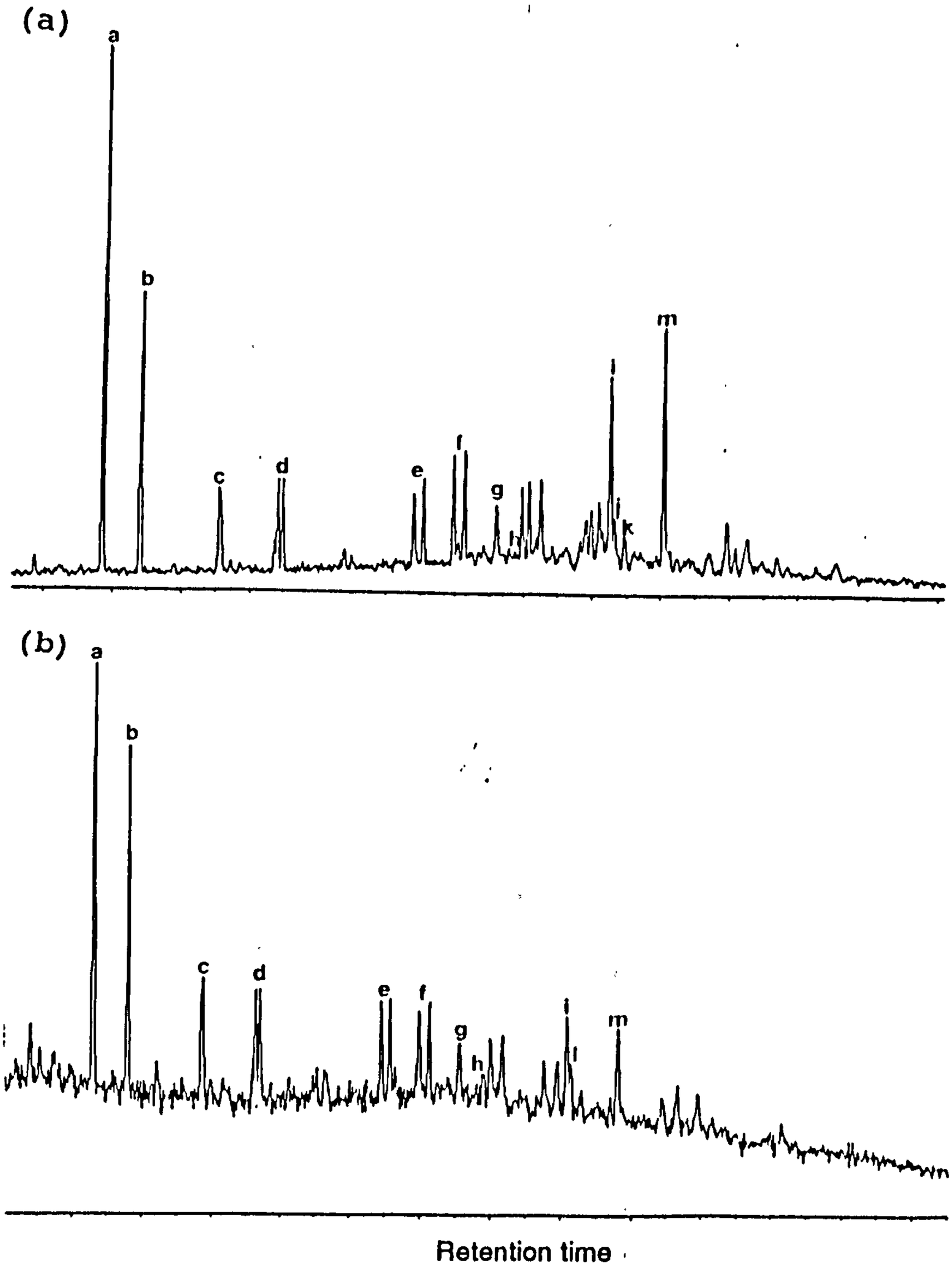

Figure 4.43 m/z 191.1794 mass chromatogram showing terpane distributions of oils from the Rhourd-Nouss basin: (a) RN48, (b) RNSE6. Peak assignments are listed in Table 2.

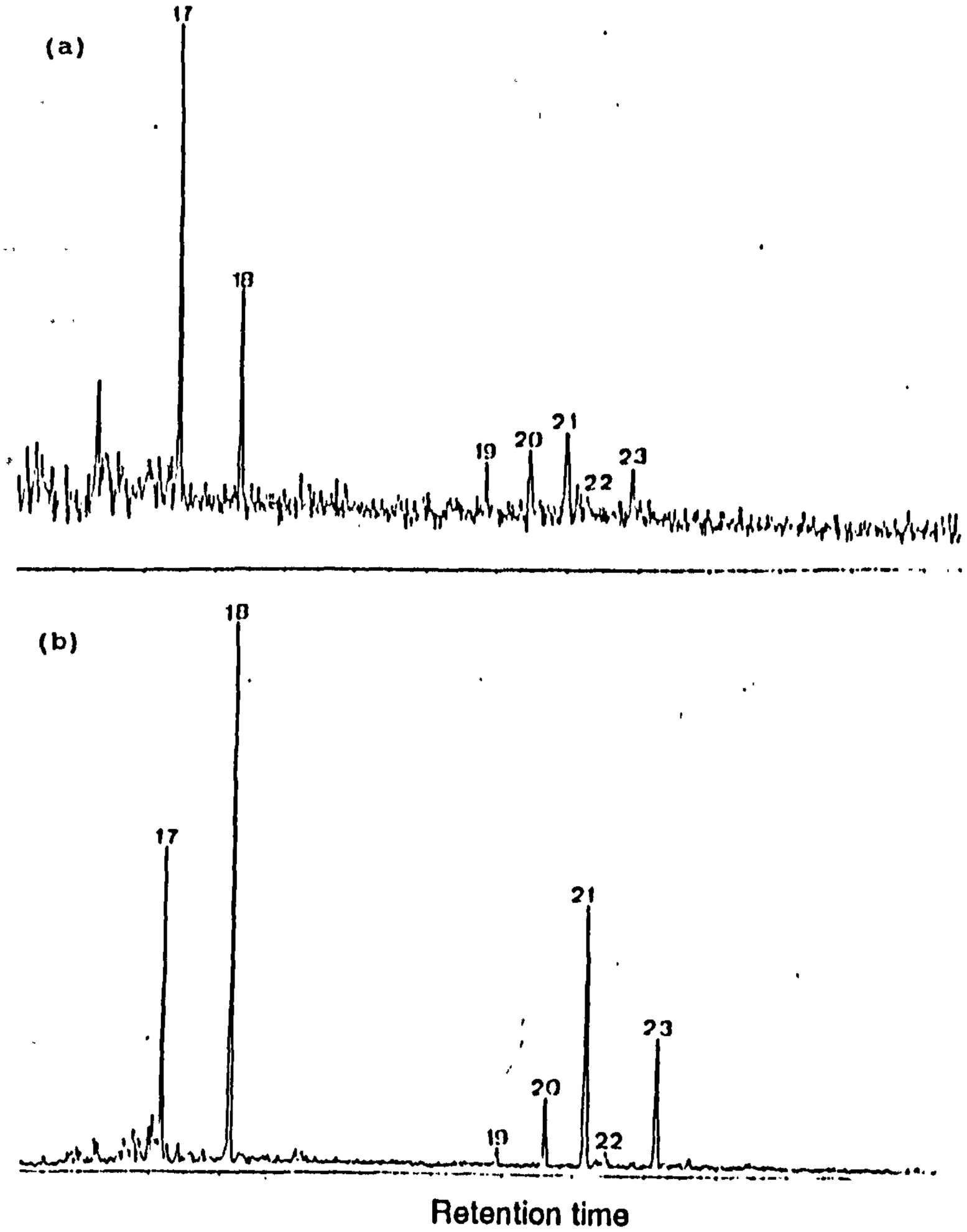

Figure 4.44 m/z 231.1170 mass chromatograms showing triaromatic steroidal hydrocarbon distributions of oils from the Rhourd-Nouss basin: (a) RN48, (b) RNSE6. Peak assignments are listed in Table 4.

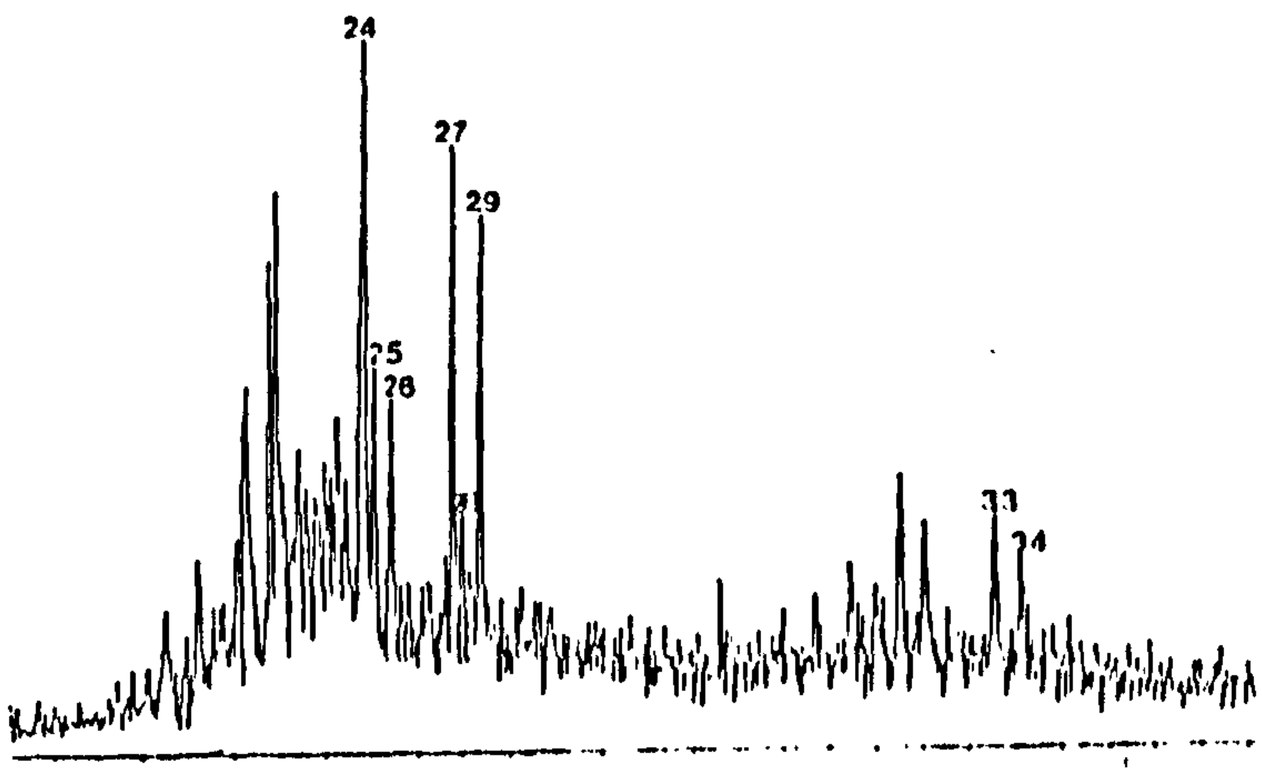

Figure 4.45 m/z 245.1330 mass chromatograms showing methylated triaromatic steroidal hydrocarbon distributions of one selected oil from the Rhourd-Nouss basin (RNSE6). Peak assignments are listed in Table 4.

4.2.6.4 Gasoline range hydrocarbon fraction

Gas chromatograms of the gasoline range (C_4-C_9) reveal higher abundance of light ends in RNSE6 than in RN48 oil, as shown in Figure 4.46. The data derived from the gasoline range (C_5-C_8) hydrocarbons (Appendix 4.6 and Figure 4.13) indicate high maturity levels of both oils, I.e RNSE6 as mature and RN48 as overmature (Thompson, 1983; 1987).

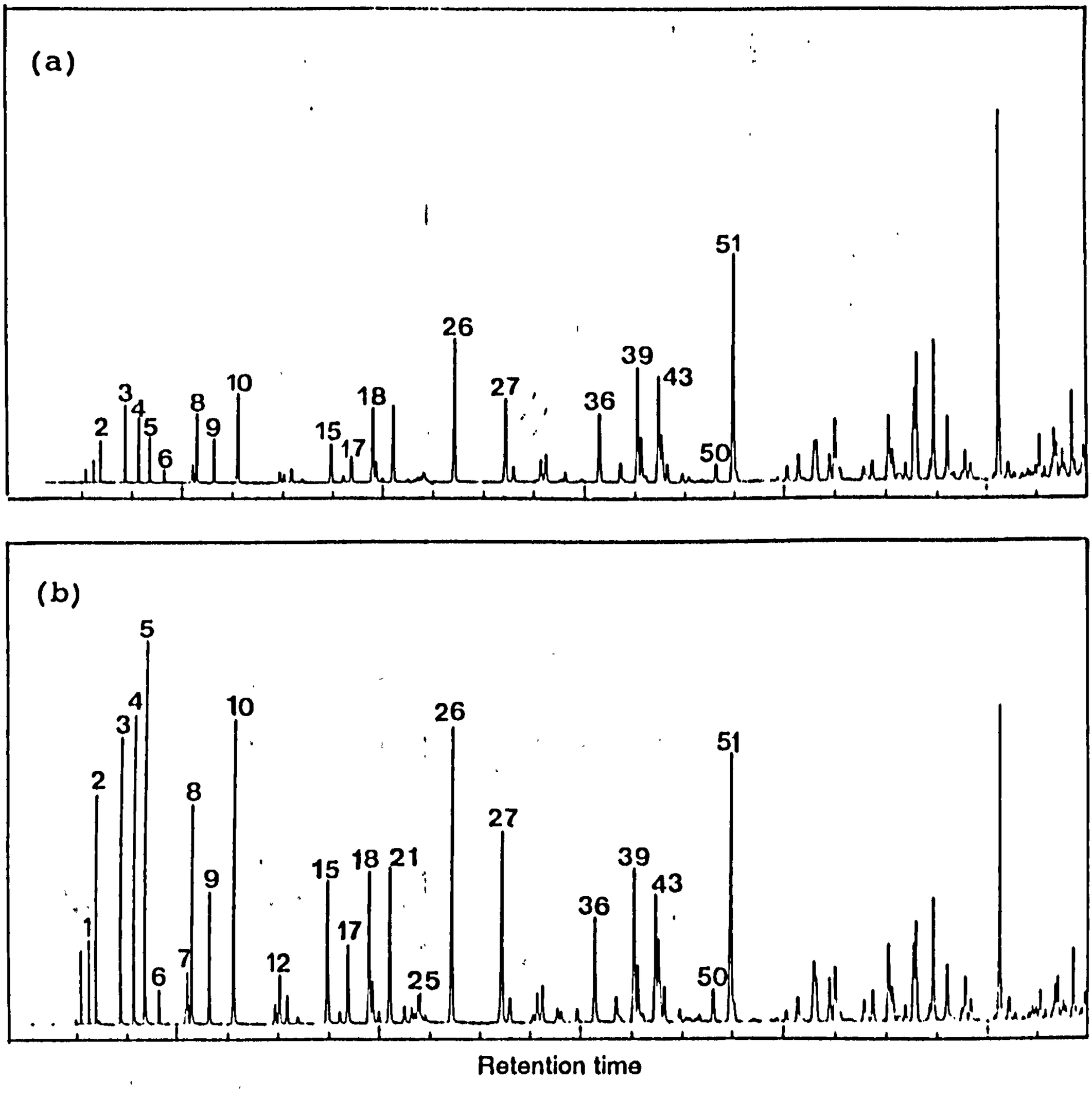

Figure 4.46 Gas chromatograms of the gasoline range hydrocarbon fractions of oils from the Rhourd-Nouss basin: (a) RN48, (b) RNSE6. Peak assignments are given in Table 5.

4.2.7. Ain Amenas basin

This section comprises results of oils from Upper Devonian (e.g. F_2) and Carboniferous (e.g Carb) reservoirs.

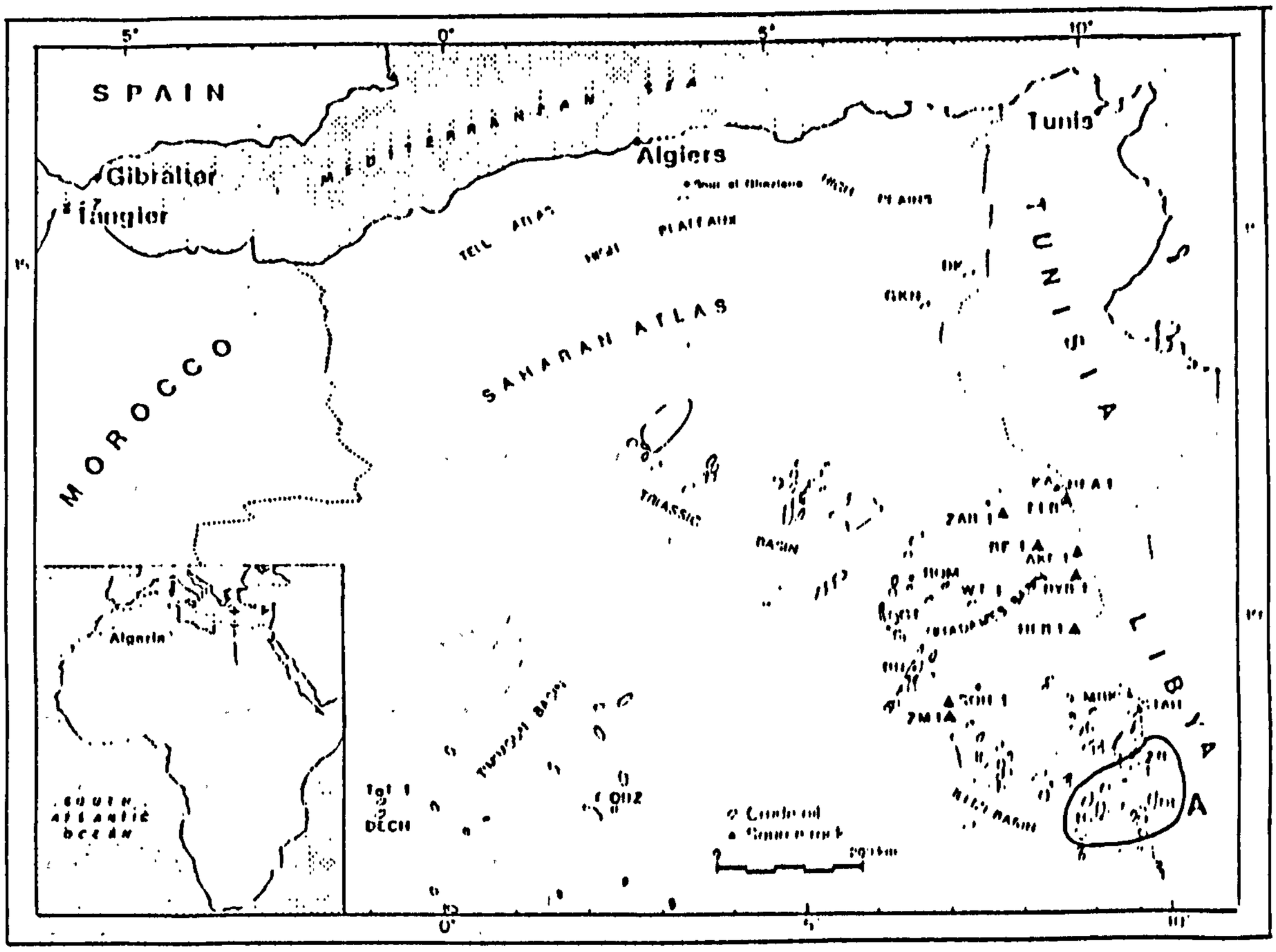

Figure 4.1g Sample location map of the area of study (A= the Ain Amenas basin), which group of oils were investigated.

4.2.7.1. Bulk composition

The bulk composition data displayed in Table 4.1g and Figure 4.2g reveals no distinction between these two oils.

Table 4.1g: Bulk composition data

Well	%Sats	%Aro	%NSO	Pr/Ph	*D
ZR115 Carb	89.46	9.86	0.68	1.74	0.789
DL127F_2	76.25	15.21	8.54	1.46	0.829
TG22F_2	88.57	10.34	1.09	1.26	0.829

* D is the density of oils measured at 20°C (g/cm^3).

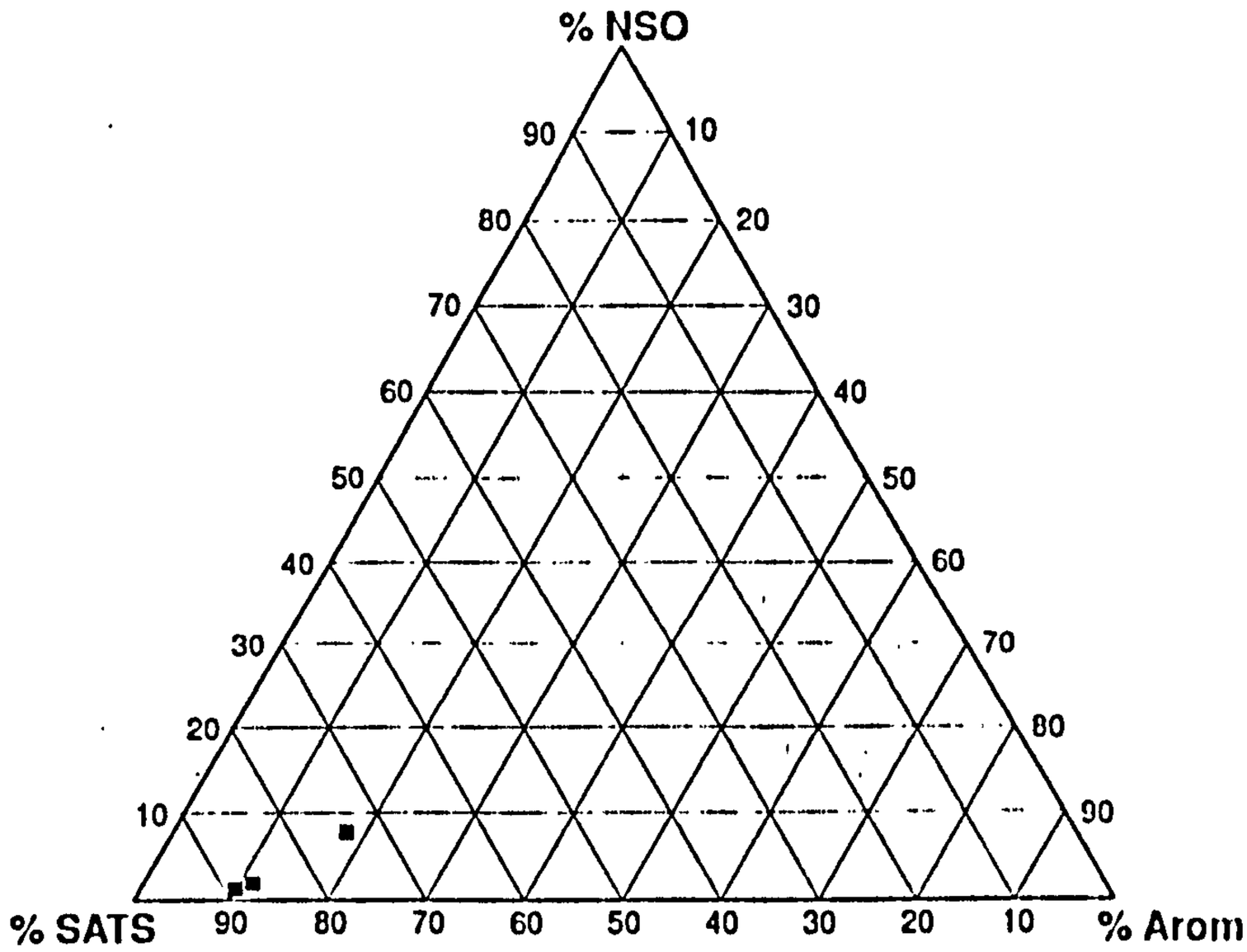

Figure 4.2g Relative proportions of saturated, aromatic hydrocarbons and NSO compounds of oils from the Ain Amenas basin.

4.2.7.2. Saturated hydrocarbon fraction

Despite differences in age of oil reservoirs, *n*-alkanes are prominent as it is clearly seen in the whole oil gas chromatograms (Figure 4.47) relative to isoprenoid hydrocarbons. The Pr/Ph ratio varies in the range of 1.39-1.74, revealing higher contents of pristane in ZR115 (Carb) than in TG22 (F_2) and DL127 (F_2).

Representative mass chromatograms of sterane distributions for TG22 (F_2) and ZR115 (Carb) are shown in Figure 4.48.

Rearranged C_{29} steranes dominate the sterane distributions of both oils (Figure 4.48), while pregnane and homopregnane were low in ZR115 (carb) bu not detected in TG22 (F_2). ZR115 (Carb) exhibits relatively higher contents of $\alpha\alpha\alpha$ and $\alpha\beta\beta$ ((20R) and (20S)) than TG22 (F2) with lower extent of sterane isomerization (20S/20S+20R) and ($\alpha\beta\beta/\alpha\beta\beta+\alpha\alpha\alpha$) for ZR115 (0.48 and 0.38 respectively) and TG22 (0.57 and 0.82 respectively).

Methylsteranes were detected in both oils (Figure 4.49). It is thought that peak N° 33 (i.e 24-ethyl-$\alpha\alpha\alpha$-4α-methyl-cholestane (20R) may arise from

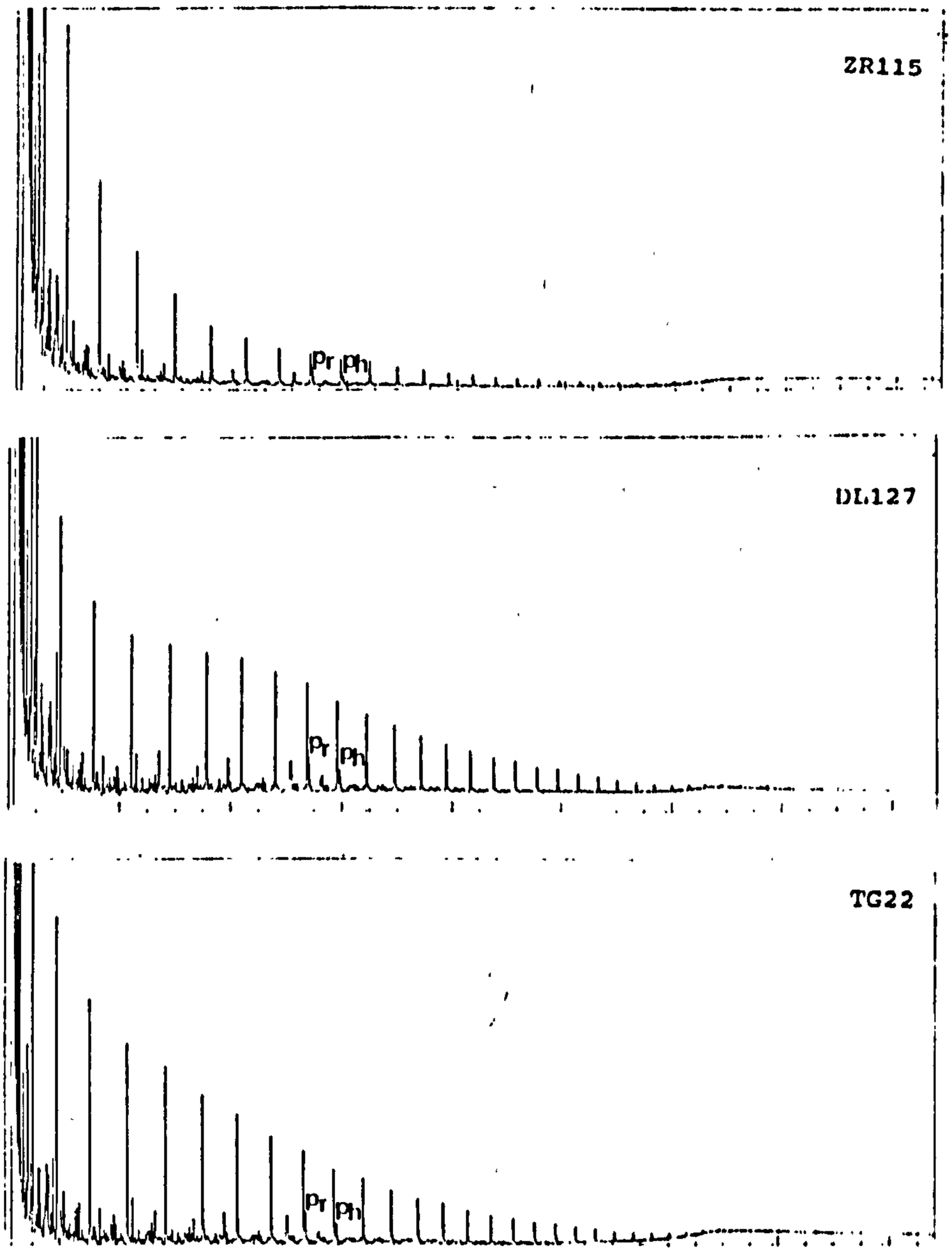

Figure 4.47 Gas chromatograms of oils from the Ain Amenas basin.

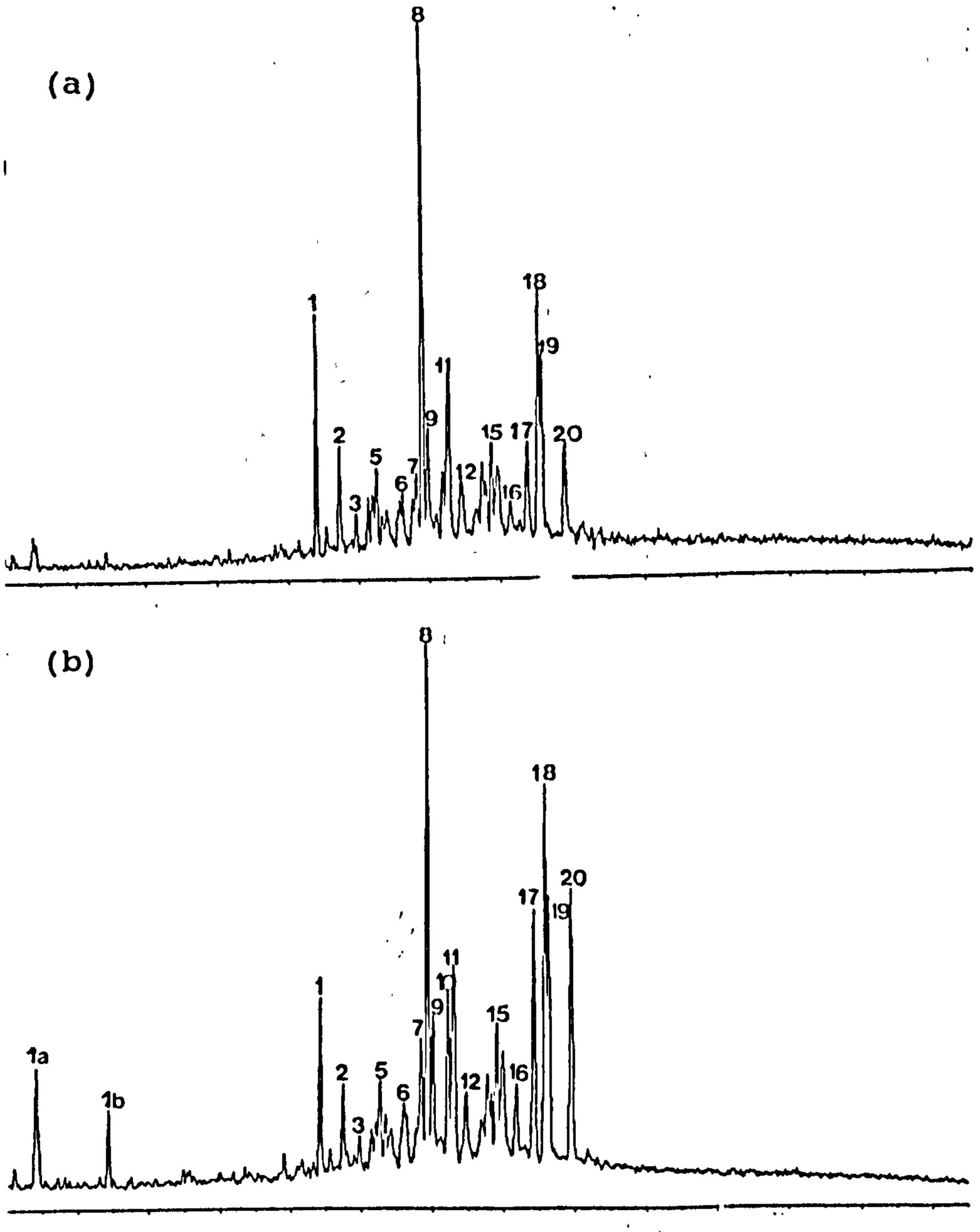

Figure 4.48 m/z 217.1950 mass chromatograms illustrating sterane distributions of two selected oils from the Ain Amenas basin: (a) TG22 F_2, (b) ZR115 (Carb). Peak assignments are listed in Table 1.

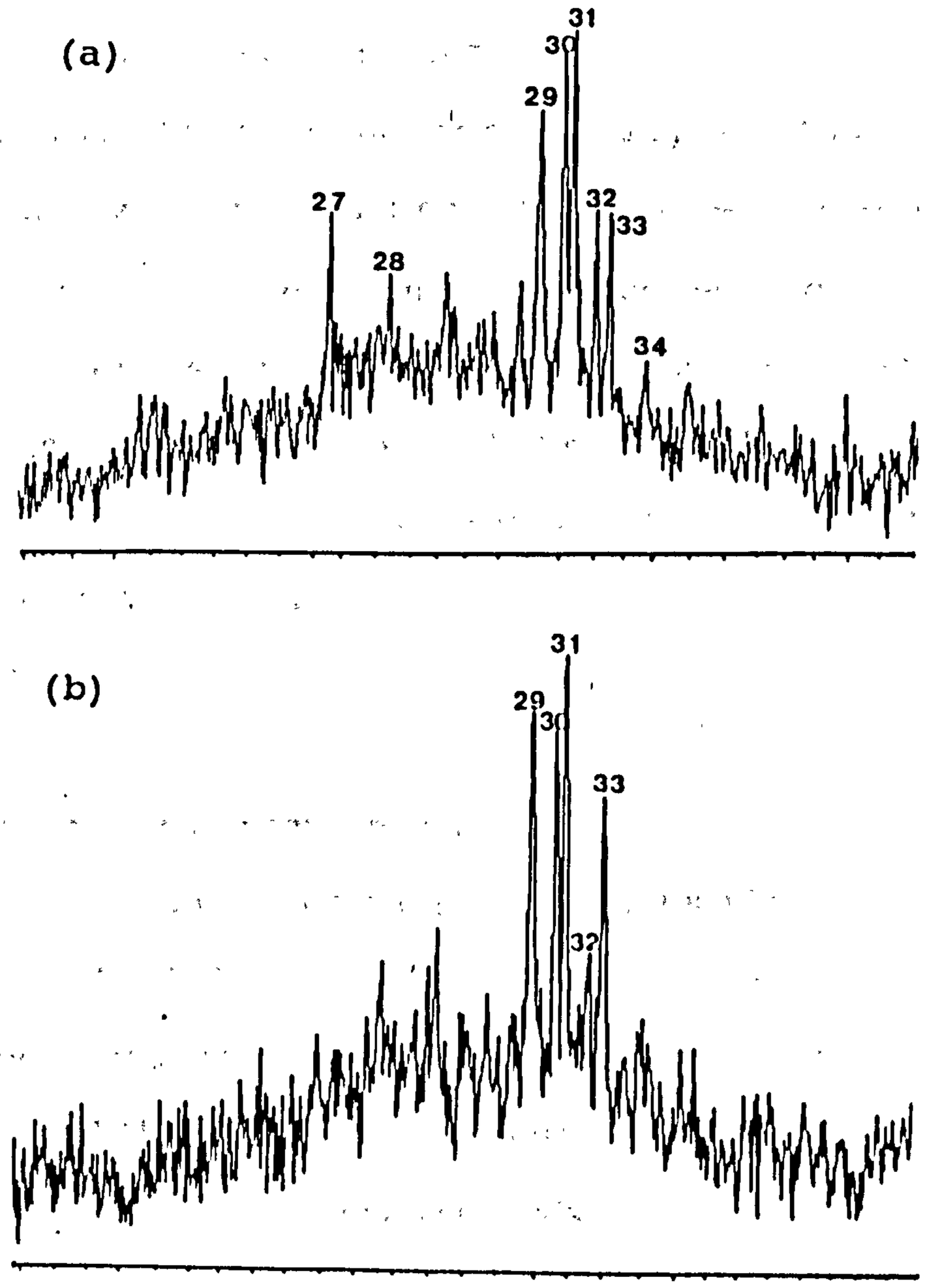

Figure 4.49 Mass chromatogram from metastable ion reaction monitoring of transition m/z 414->m/z 231 for methylsteranes (C_{30} components) in two selected oils from the Ain Amenas: (a) TG22 F_2, (b) ZR115 (Carb). Peak assignments are listed in Table 1.

coelution with C_{30}-ααα (20R) steranes; Summons, pers. comm.), although none of this component was detected in ZR115 oil (Carb).

Terpane distributions of ZR115 and TG22 are shown in Figure 4.50. As illustrated in Figure 4.56, ZR115 and TG22 fall in distinct group using source (Figure 4.56a, 4.56c and 4.45d) and maturity parameters (Figure 4.56b).The difference in the relative proportions of $C_{29}T_s$ and $C_{29}\alpha\beta$ norhop is a further evidence for lower maturity levels for ZR115 than TG22 (Figure 4.10). This is reflected by low T_s/T_m ratio (i.e. 1.02) and the presence of moretane and normoretane in ZR115 oil.

Tricyclic terpanes are minor components in ZR115 oil.

4.2.7.3. Aromatic hydrocarbon fraction

An example of C-ring monoaromatic steroidal hydrocarbon distributions in ZR115 (Carb) and TG22 (F_2) are displayed in Figure 4.51. The barely detectable concentrations of these compounds may indicates a lower maturity levels of ZR115 than TG22. Furthermore, ZR115 exhibits relatively higher amounts of non-rearranged compounds with trans isomers (peak N° 16) than TG22.

The triaromatic steroidal hydrocarbon distributions (Figure 4.52) show slightly different patterns with a prominent C_{28} triaromatic component in ZR115 but relatively lower in TG22, as indicated by the $\%C_{28}t/(C_{26}t+C_{27}t+C_{28}t$ ratio (72% and 65%). Steroid aromatization ratio have values ranging between 0.61 and 0.81 for ZR115 and TG22 respectively, reflecting almost completion of conversion of monoaromatic to triaromatic steroidal hydrocarbons. On the contrary, both oils display minor amounts of short-chain compounds, as indicated by low cracking ratio (0.15 and 0.17).

The methylated triaromatic steroidal hydrocarbon distributions appear to be minor, being dominated by short-chain homologues with 2-methyl+3-methyl isomers for C_{21} and C_{22} components in TG22. On the contrary, ZR115

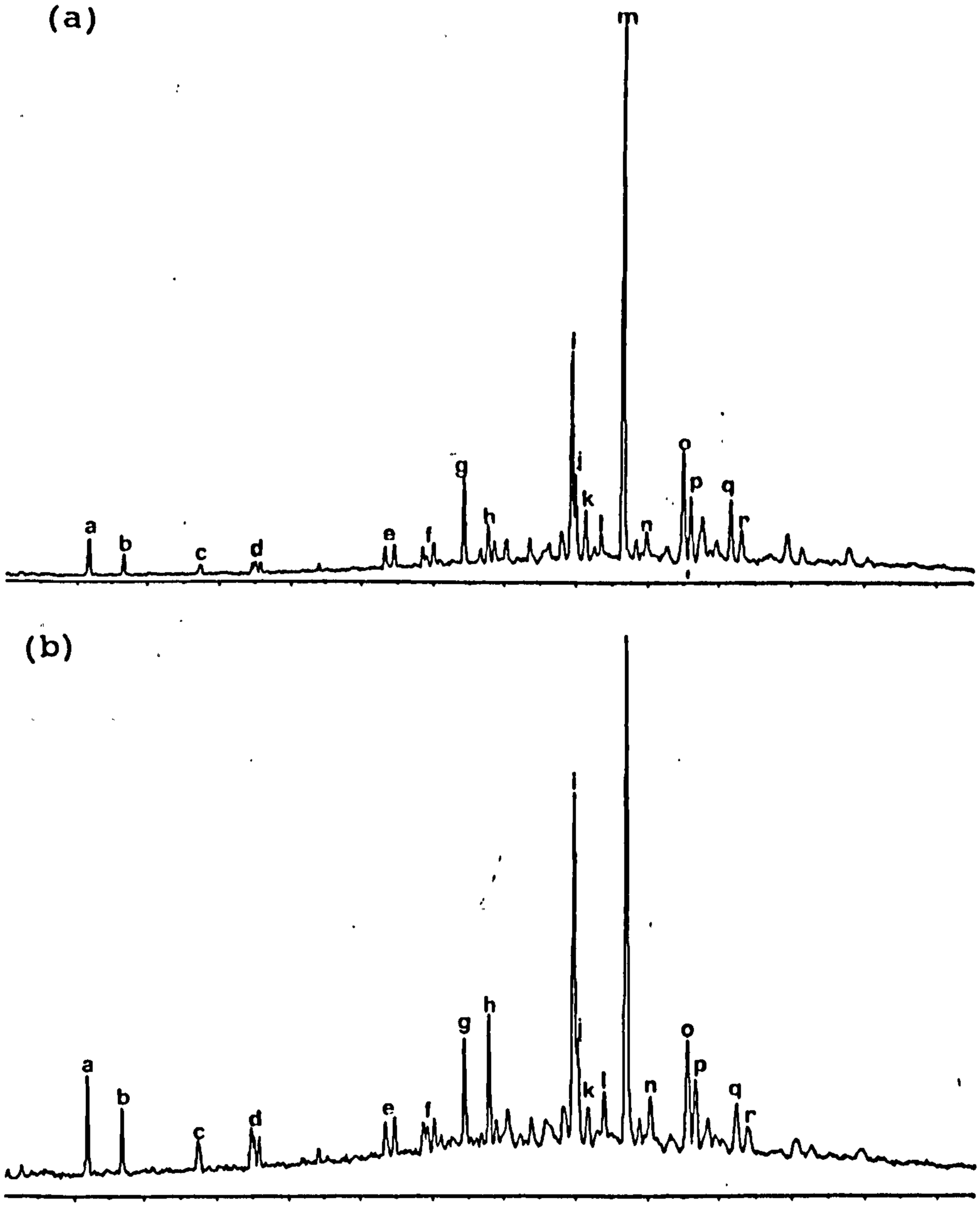

Figure 4.50 m/z 191.1794 mass chromatogram showing terpane distributions of two selected oils from the Ain Amenas basin: (a) TG22 F_2, (b) ZR115. Peak assignments are listed in Table 2.

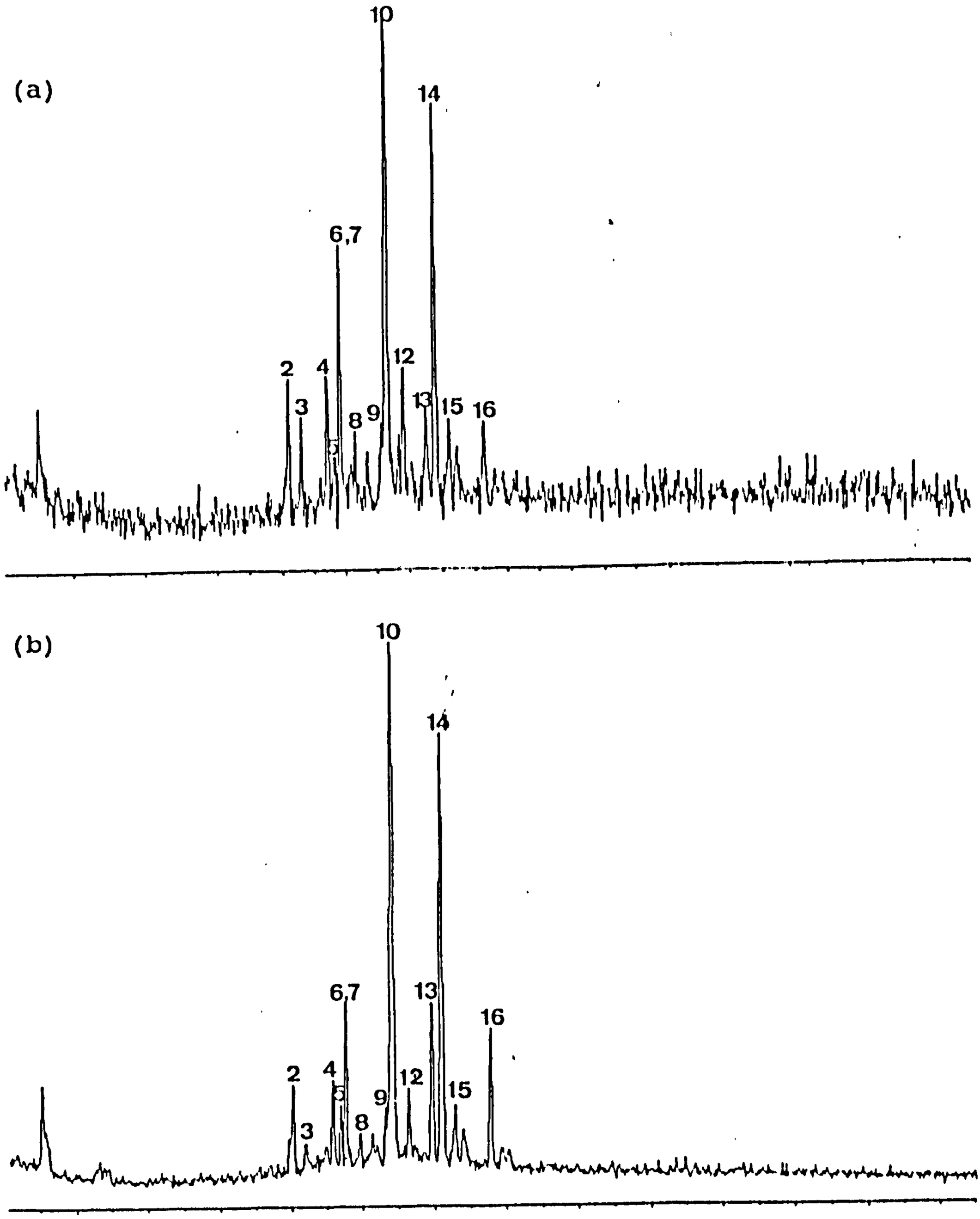

Figure 4.51 m/z 253.1950 mass chromatograms showing C-ring monoaromatic steroidal hydrocarbon distributions of two selected oils from the Ain Amenas basin: (a) TG22 F_2, (b) ZR115 (Carb). Peak assignments are listed in Table 3.

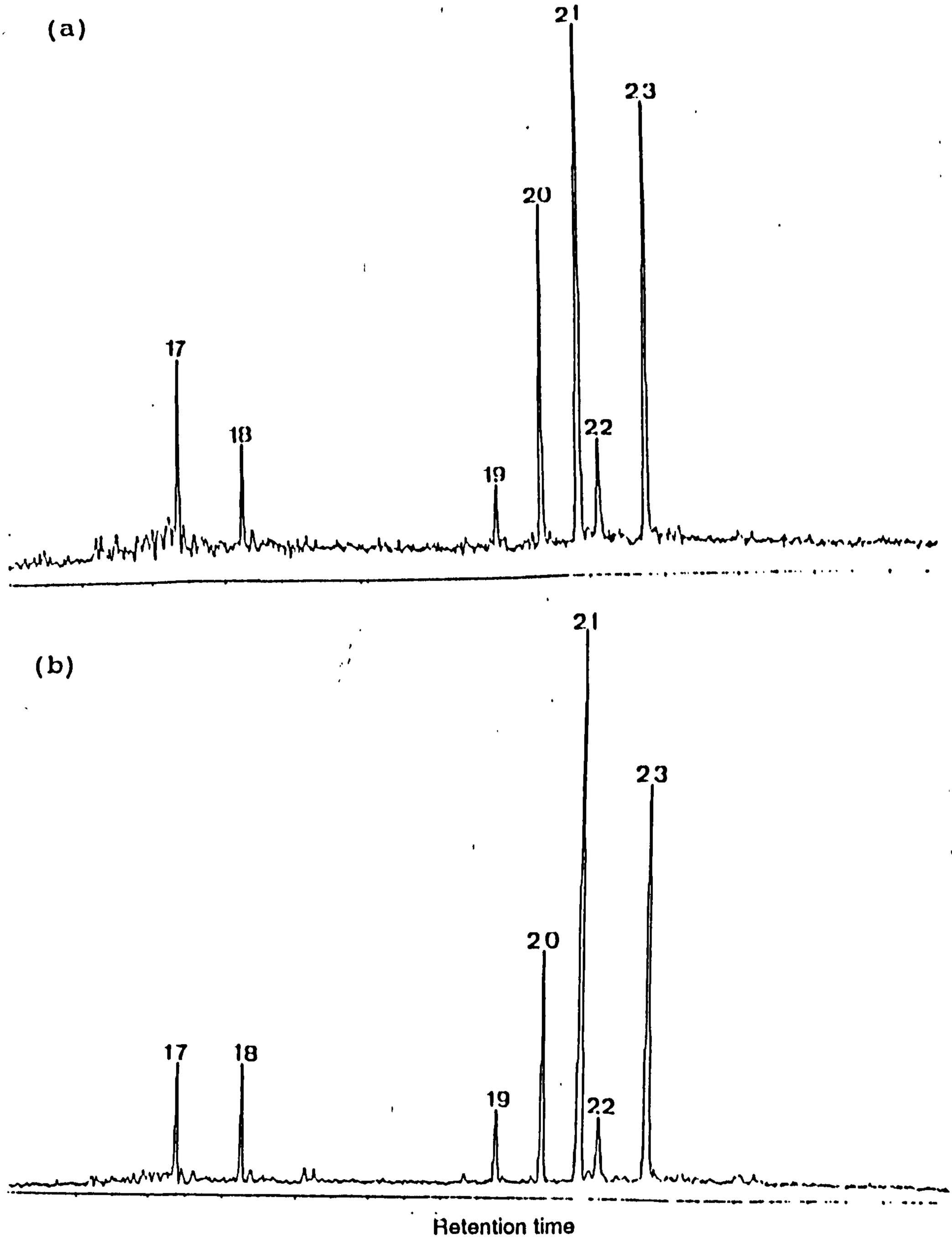

Figure 4.52 m/z 231.1170 mass chromatograms showing triaromatic steroidal hydrocarbon distributions of two selected oils from the Ain Amenas basin: (a) TG22 F_2, (b) ZR115 (Carb). Peak assignments are listed in Table 4.

exhibits slightly higher amounts of 4-methyl-C_{21} and -C_{22} isomers (peak N°26 and 29, Figure 4.53), as indicated by the MTSI1 and MTSI2 indices in Appendix 4.5.

4.2.7.4. Gasoline hydrocarbon fraction

The gasoline range hydrocarbon distributions of TG22, DL127 and ZR115 are shown in Figure 4.54. *N*-alkanes are less prominent in TG22 (F_2) than DL127 (F_2) and ZR115 (Carb). There is a low abundance of aromatic hydrocarbons relative to *n*-alkanes, as indicated by low aromaticity ratios (Appendix 4.6 and Figure 4.13). Furthermore, Isoheptane and Heptane indices (Figure 4.13d, 4.13a respectively) as well as the summary diagram (Thompson (1987; 1988) indicate high maturity levels of these oils (Thompson, 1983; 1987; 1988).

4.3. Principal component analysis

Principal component analysis (PCA) has proved to be a very useful procedure for oil-oil and oil-source rock correlations using both biological marker (Telnaes and Dahl, 1986; Kvalheim and Telnaes, 1986; Telnaes and Cook, 1991) and gasoline range hydrocarbon distributions (Kvalheim, 1987). The data were calculated from peak heights, which were normalised to percentages and converted to logarithms. As mentioned in Chapter 3, this transformation has been used to minimize the dependency effect created by normalisation (Johanson et al., 1984; Kvalheim, 1987).

4.3.1. Information carried by steranes and terpanes

For sterane, tricyclic, tetracyclic and pentacyclic terpane distributions, the first three principal components were calculated with PC_1, PC_2 and PC_3 accounting for 35.5%, 20.5% and 19.5% respectively of the total variance.

To interpret the score plots, it is necessary to understand in a geochemical sense the distribution of each variable or class of variables on PC_1, PC_2

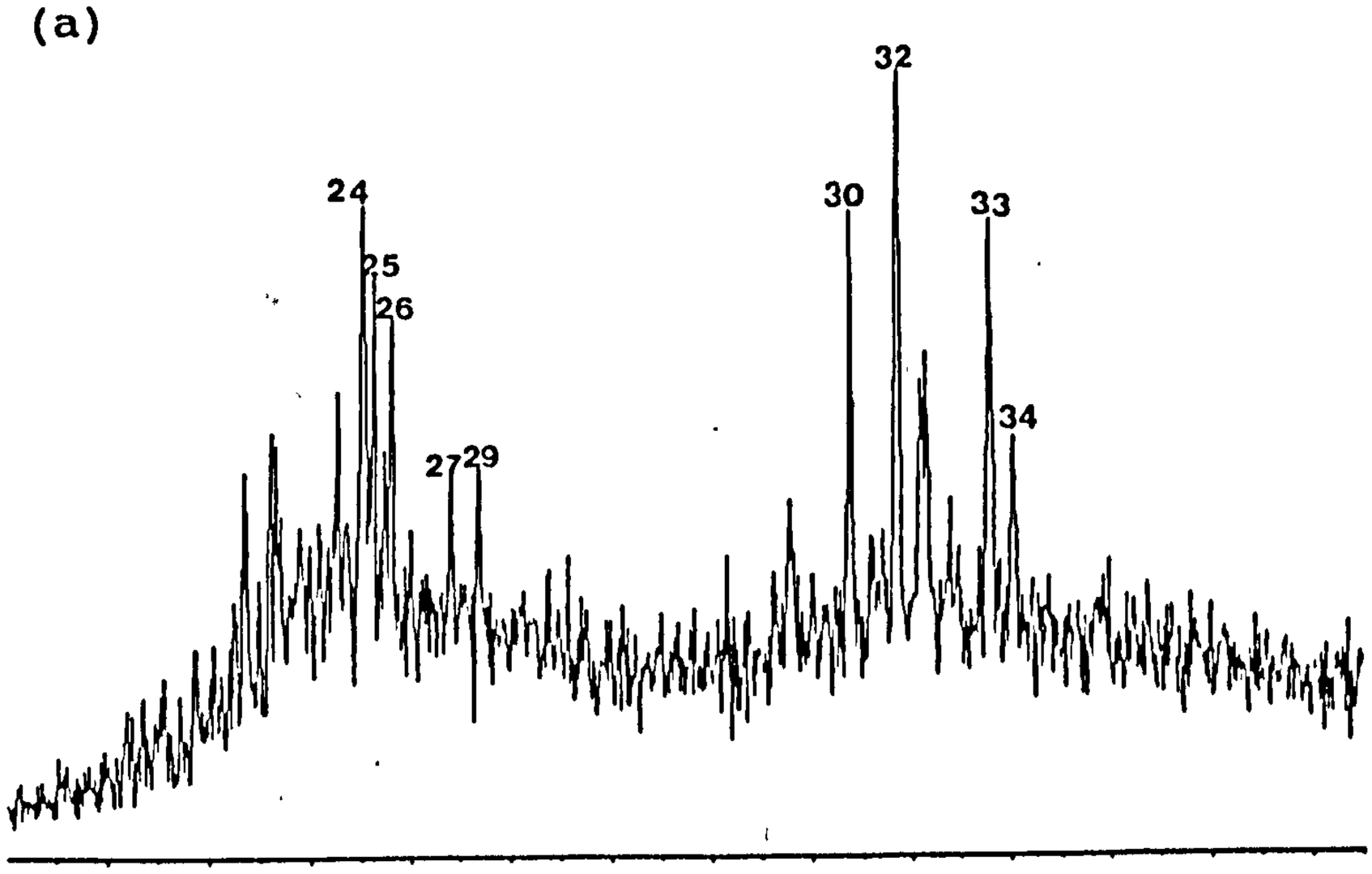

Figure 4.53 m/z 245.1330 mass chromatograms showing methylated triaromatic steroidal hydrocarbon distributionsof two selected oils from the Ain Amenas basin: (a) TG22 F_2, (b) ZR115 (Carb). Peak assignments are listed in Table 4.

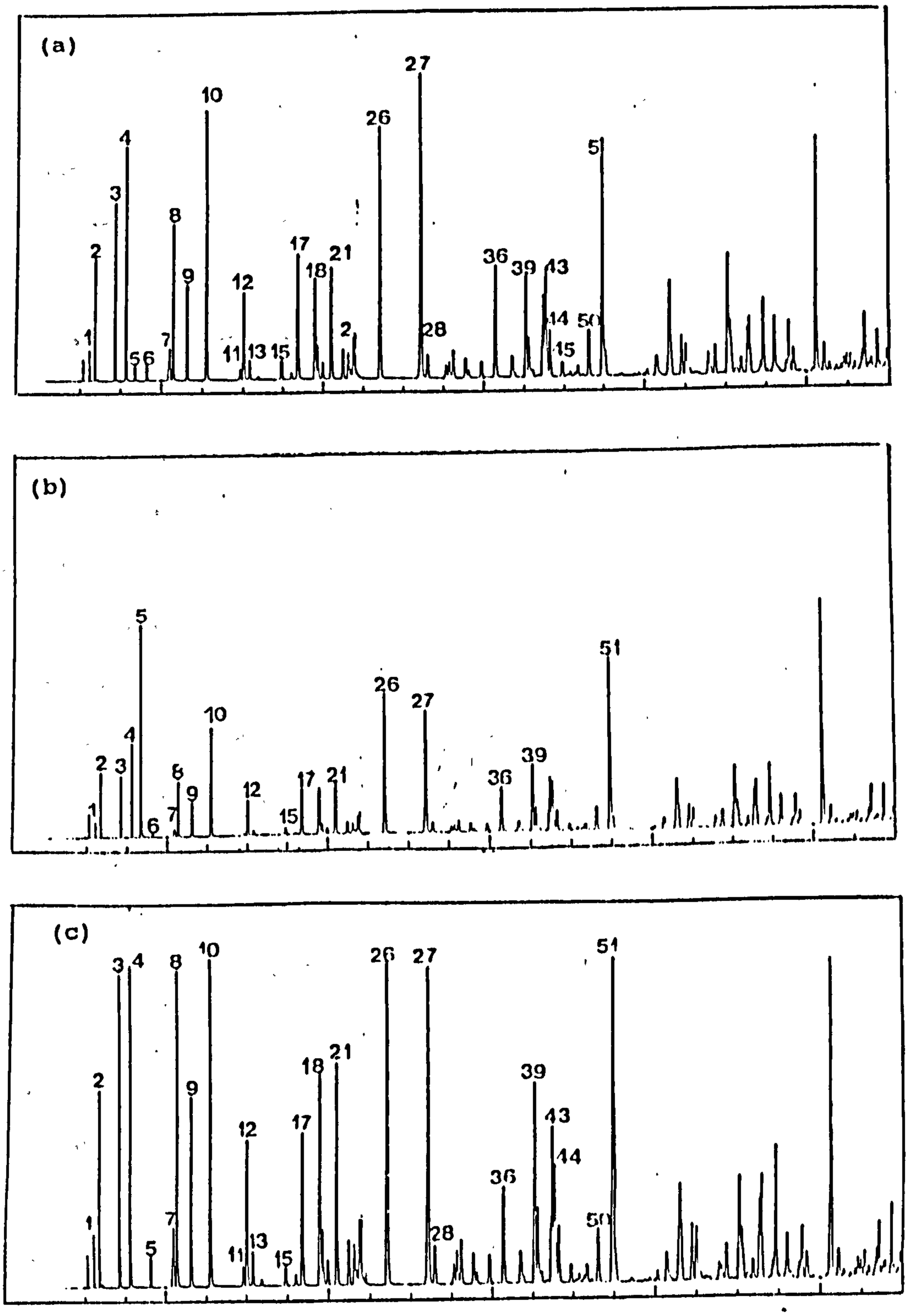

Figure 4.54 Gas chromatograms of the gasoline range hydrocarbon fractions of oils from the Ain Amenas basin: (a) DL127 F_2, (b) TG22 F_2, (c) ZR115 (Carb). Peak assignments are given in Table 5.

and PC_3, namely loading plots. These are plotted versus biomarker variables (Figure 4.55). The loadings of the pentacyclic terpanes and non-rearranged steranes are negatively correlated with the loadings of tricyclic terpanes and rearranged steranes on PC_1. The loadings on PC_2 shows a negative correlation between:

-tricyclic terpanes, steranes and pentacyclic terpanes,

-C_{30} components and the rest of the steranes.

The loadings of terpanes on PC_3 are negatively correlated with steranes.

The PC_1 loading plot may be interpreted in terms of differences in organic input and depositional environment, while PC_2 loadings may be explained in terms of differences in input.

The score of plots of oils on PC_1 is plotted versus the score on PC_2 (Figure 4.56). To enhance maturity or source dependence, PC_1 and PC_2 scores were plotted versus $C_{23}T/C_{23}T+C_{30}\alpha\beta$ hop and $C_{30}\alpha\beta$ hop/$C_{29}\alpha\alpha\alpha$ (20R) (Figure 4.57). As clearly seen in this Figure, plots of $C_{30}\alpha\beta/C_{29}\alpha\alpha\alpha$ (20R) versus $C_{23}T/C_{23}T+C_{30}\alpha\beta$ hop, PC_1 versus $C_{30}\alpha\beta$ hop/$C_{29}\alpha\alpha\alpha$ (20R) as well as PC_2 versus $C_{30}\alpha\beta$ hop/$C_{29}\alpha\alpha\alpha$ (20R) gives rise to three genetic groups:

(i) Southeast Constantine (DK1, GKN1), Ghadames-El Borma (ELB9), Sbaa (ODZ1, DECH1), Ain Amenas (TG22).

(ii) Ghadames-El Borma (KA2, ROM1), Ain Amenas (ZR115)

(iii) Gassi Touil (GT6, GT47), Rhourd-Nouss (RN48, RNSE6).

However, maturity differences is reflected in the PC_1 versus $C_{23}T/C_{23}T+C_{30}\alpha\beta$ hop (Figure 4.57B) diagram, which suggests a discrimination of oils into three groups from the least mature, mature to overmature:

(i) Southeast Constantine (DK1), Ain Amenas (ZR115)

(ii) Southeast Constantine (GKN1), Ghadames-El Borma (ELB9, KA2), Sbaa (ODZ1, DECH1), Ain Amenas (TG22).

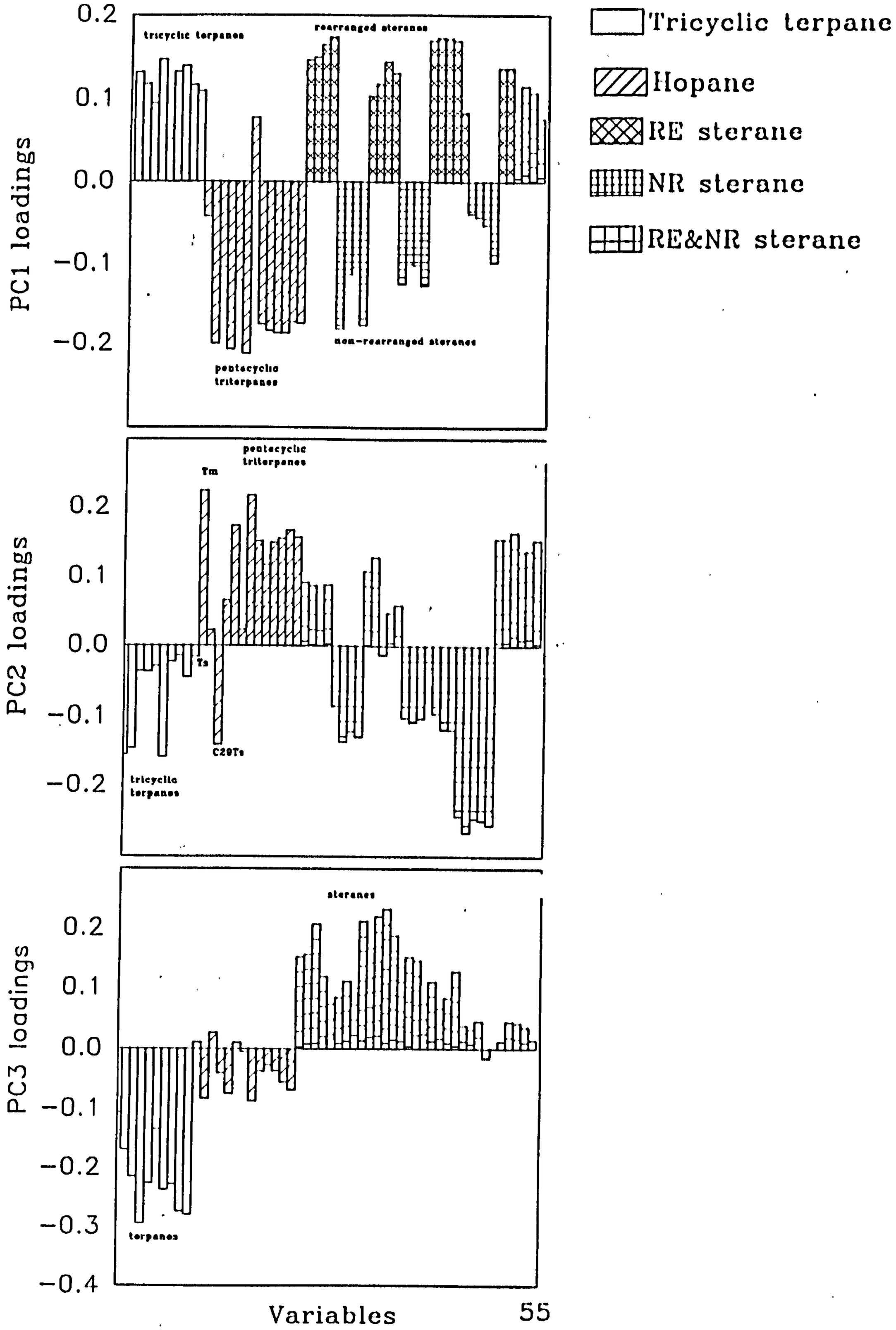

Figure 4.55 Oil–oil correlation (biomarkers). Loadings for the three PCs plotted versus biomarker variables.

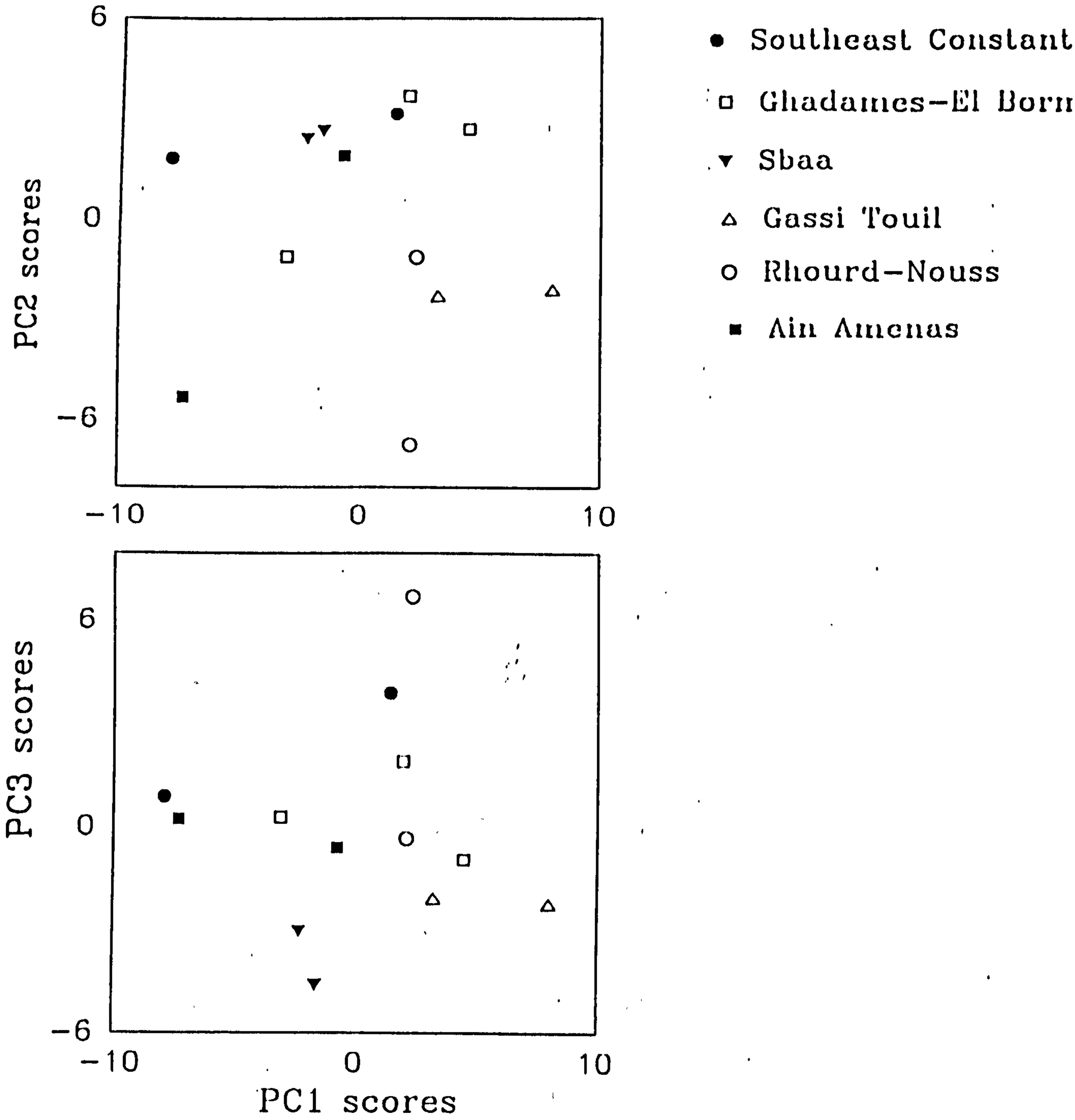

Figure 4.55 Oil-oil correlation (biomarkers). Loadings for the three PCs plotted against biomarker variables (i.e steranes and terpanes).

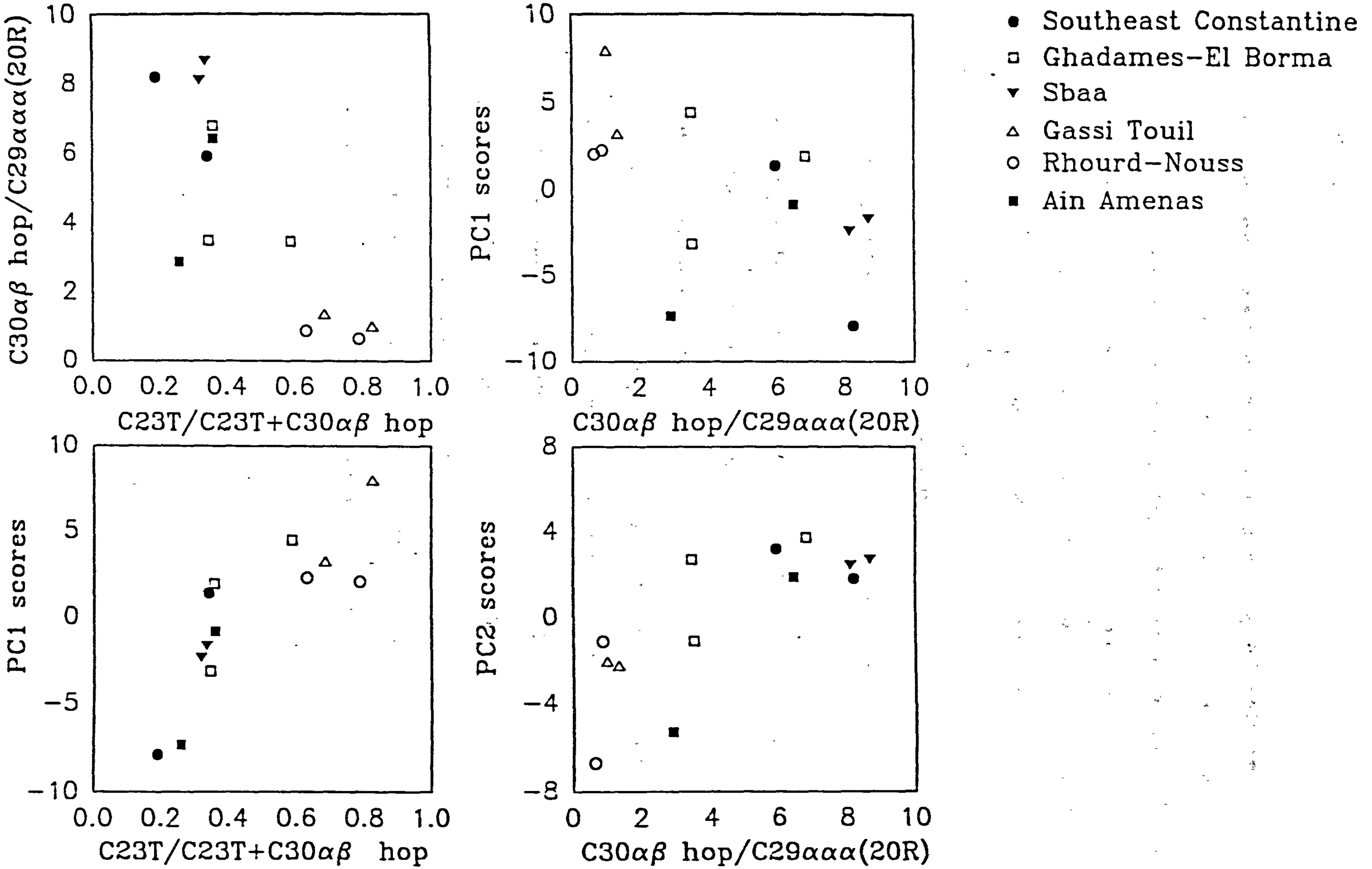

Figure 4.57 PCA scores for steranes and terpanes, C23T/C23T+C30αβ hop and C30αβ hop/C29ααα(20R) showing possible discrimination of oils.

(iii) Rhourd-Nouss (RN48, RNSE6), Gassi Touil (GT6, GT47), Ghadames-El Borma (ROM1).

4.3.2.Information carried by the gasoline-range (C_5-C_8) hydrocarbons.

Similar procedure of calculation has been applied to the gasoline range hydrocarbons. Principal component analysis of these data gave 46.7%, 20.8% and 11.5% of the total variance for PC_1, PC_2 and PC_3 respectively. Figure 4.58 displays the loadings plots of the components on the three principal components (PC_1), (PC_2) and (PC_3). The loadings plots on exhibits a negative correlation between:

-normal, cyclic and branched alkanes on PC_1,

-volatile components (C_5-C_7) and less-volatile hydrocarbons (C_7-C_8) on PC_2.

The score plot of PC_1 versus PC_2 plot (Figure 4.58) does not give a clear discrimination of oils, while PC_1 versus PC_3 gives rise to three oil groups:

(i) Southeast Constantine (DK1)

(ii) Southeast Constantine (GKN1), Ghadames-El Borma (ROM1), Sbaa (ODZ1, DECH1, TOT1), Illizi (MRK12F_6, MRK16F_3, STAH40F_6, STAH8F_3, WT1 TAGI) and Ain Amenas (DL127F_2, TG22F_2, ZR115 Carb).

(iii) Gassi Touil (GT6, GT47) and Rhourd-Nouss (RN48, RNSE6).

However, ZR115 oil seems to fall in the same group of mature to overmature oils. On the contrary, based on biological marker distributions, it has been classified as immature to marginally mature.

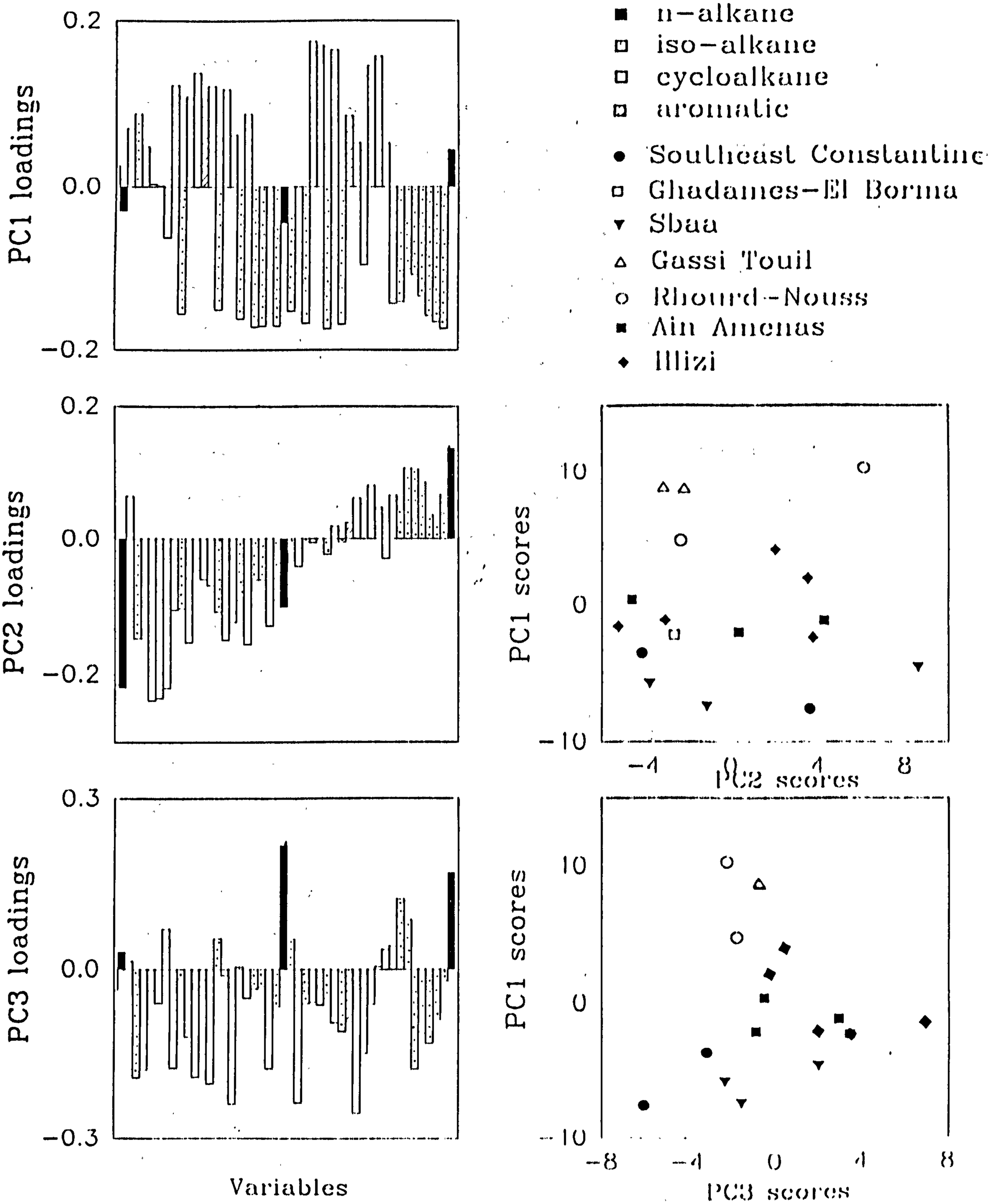

Figure 4.58 Oil−oil correlation (gasoline range hydrocarbons). Loadings for the three PCs plotted vesus (C5−C8) hydrocarbons Scores of the oils on PC1 plotted versus PC2 and PC3.

4.4. Discussion

4.4.1. Southeast Constantine basin

From the bulk composition data given in Table 4.1a and presented pictorially in Figure 4.2a, GKN1 is obviously of higher maturity than DK1 and DK6, being characterised by enhanced concentrations of saturates and gasoline range hydrocarbons as well as low NSO (including asphaltenes) and biological markers contents. In addition, the aromatic hydrocarbon content is low (12%- 18%), which suggest a paraffinic classification (Tissot and Welte, 1984 pp 417). Furthermore, a number of parameters allows DK1 oils to be classified as immature, i.e the presence of $C_{29}\beta\alpha$ normoretane, $C_{30}\beta\alpha$ moretane, low T_s/T_m ratio (0.99), low extent of sterane isomerization (20S/20S+20R=0.48), cracking ratios (0.15) as well as methyl triaromatic steroid isomerization parameters (e.g MTSI1 and MTSI2 equal 0.31 and 0.32 respectively). These reflect presumably less deeper burial of the tentative source rock (s) of DK1 compared to that of GKN1 oils. The tendency towards high and similar maturity level of DK1 and GKN1 is only indicated by Heptane index, while Isoheptane index reveals a normal paraffinic classification (Thompson, 1983; 1987). This feature could possibly indicate a type of organic matter control on both paraffinicity indices (Snowdon and Powell, 1982; Rullkötter et al., 1986; Fowler et al., 1990). Furthermore, Snowdon and Powell (1982) suggested high Heptane indices in sediments highly rich in algae.

According to biological marker parameters related to source and/or depositional environment, DK1 and GKN1 oils share similarities in sources of organic matter such as:

-the generally high Pr/Ph ratios reflects either a prominent input of pristane from zooplankton (Blumer et al., 1963) or algal tocopherol (Goossens et al., 1984). Furthermore, the presence of C_{30} steranes may be a reflection of marine input for the source rock (s) of DK1 and GKN1 oils (Moldowan et al.,

1985; Telnaes and Dahl, 1986). However, DK1 shows a low rearranged/non-rearranged sterane ratios (i.e $C_{27}r/C_{27}n$=2.35 and $C_{29}r/C_{29}n$=1.29, Appendix 4.2) compared to the GKN1 oil (9.29 and 4.62 respectively). This parameter has been related to depositional environment of the organic matter that generated oils (Moldowan et al., 1986), also increases with thermal maturity (Seifert and Moldowan, 1978; Peters et al., 1989). Furthermore, the presence of methylsteranes (i.e 24-ethyl-3β-methyl- and 24-ethyl-2α-methyl-ααα (20R)) in both oils may indicate common input for the source rocks that generates these oils, although no precursors have been yet suggested. Further evidence of a close relationship between oils from the Southeast of Constantine basin, is reflected in the triangular diagrams of non-rearranged and rearranged steranes (C_{27}-C_{29}, Figure 13a and 13b and Appendix 4.4). High hopanes relative to steranes (triterpane:sterane ratio>5) may indicate that bacteria are common contributors in the Mesozoic organic matter during its source rock deposition.

The relatively minor abundance of tricyclic relative to pentacyclic terpanes suggests that there was a little contribution from tricyclic precursor, although no evidence of migration affecting tricyclic terpanes has been reported in the literature.

As regards the lithology and depositional environment of the tentative Coniacian and/or Cenomanian source-rock (s) for petroleum accumulations in the Djebel Onk area (northern Algeria), there have been reports that the source rock could be laminated bituminous marls and limestones (Internal report Sonatrach, 1985), although no detailed geochemical study has been made in the present work, due to a lack of samples in the area.

4.4.2. Ghadames-El Borma basin

A close examination of the whole oil gas chromatograms of (ELB9 and KA2) allows us to make some preliminary remarks regarding the distribution of light hydrocarbons. KA2 and ELB9 oils seem to have been depleted totally in their gasoline fraction either by degradation effect during storage. Hence, discrimination these three oils can only be based on biological marker distributions. All three oils (ELB9, KA2 and ROM1) are obviously of relatively high maturity, being characterised by complete sterane isomerization (20S+20S+20R=0.54), steroid aromatization and cracking ratios, except for KA2. Sterane isomerization and aromatization reactions proceeded at similar rates, while relatively lower cracking ratio may suggest that KA2 could have been generated at a lower maturity than ELB9 and ROM1. High sterane isomerization ratio ($\alpha\beta\beta/\alpha\beta\beta+\alpha\alpha\alpha$ (20R)) may indicate that migration and/or maturation effects are greater for ELB9 and ROM1 than for KA2 (Seifert and Moldowan, 1981). These data imply that ELB9 and ROM1 have been associated with source-rocks having vitrinite reflectance equivalent (VR/E>0.8%) at the time of generation, while KA2 has been probably expelled before reaching this value (Figure 1.13, Mackenzie and Maxwell, 1981). The tendency towards high maturity levels of ROM1 is also indicated by paraffinicity indices.

According to molecular parameters related to source input, the three oils share similarities as indicated in the ternary diagrams of non-rearranged and rearranged (C_{27}-C_{29}) steranes as well as by a consistent ratio of $\%C_{28}t/(C_{26}t+C_{27}t+C_{28}t)$ (Curiale, 1989). Furthermore, the presence albeit low concentrations of C_{30} steranes may reflect a marine input from the source rock generating these oils. In addition, the 24-ethyl-3β-methy-$\alpha\alpha\alpha$ and -$\alpha\beta\beta$ ((20S) and 20R) and probably 2α-methyl isomers may indicate a common input.

As regards the terpane distributions, variation in the tricyclic to pentacyclic terpane ratio may be explained in terms of source input and/or maturity

differences. Volkman et al. (1990) have reported that sediments rich in algae type *Tasmanites* have high tricyclic terpanes contents.

4.4.3. Sbaa basin

Oils from the Sbaa basin are generally similar to each other. Relatively low NSO contents and biological marker distributions may reflect higher maturity levels of ODZ1 and TOT1 than DECH1. Low aromaticity ratios of these oils may be due to water washing, resulting in partially depleted oil. The diminished peak heights of *n*-C_9 to *n*-C_{12} alkanes relative to the other *n*-alkanes indicates a mild incipient biodegradation of TOT1 and DECH1 (Connan et al., 1985), which is possible at shallow depth reservoirs (500m-600m). Low concentrations of aromatic relative to *n*-alkanes may due to water washing during migration or evaporative fractionation (Thompson, 1987, 1988). Lower Heptane values for a mature oil than those indicated by Thompson (1983) could result from biodegradation. This parameter has been reported to be more sensitive to biodegradation than the Isoheptane index (Snowdon and Powell, 1982; Rullkötter et al., 1986).

The generally high Pr/Ph ratios may indicate oxic conditions of depositional environment of the source rocks generating these oils (Didyk et al., 1978), although high input for pristane from algal tocopherols (Goossens et al., 1984).

The tendency towards a predominance of C_{29} steranes is consistent with that of C_{28} triaromatic steroidal hydrocarbons, as measured by the $\%C_{28}t/C_{26}t+C_{27}t+C_{28}t$, appendix 4.2). The presence of the 24-ethyl-3β-methyl-ααα and αββ ((20R) and (20S)) and probably 24-ethyl-2α-methylsteranes may suggest a marine algal input, although no evidence of source has been yet reported in the literature.

The low abundance of tricyclic terpanes relative to hopanes reveals that their source-rock (s) may not contain high contribution from tricyclic terpane precursor.

4.4.4. Illizi Basin

There is a tendency towards high maturity levels of the Illizi oils, as suggested by relatively high saturate and low aromatic hydrocarbons and NSO contents and subsequently barely detectable concentrations of biological markers. These results are found in good agreement with those shown by Fowler, (1984). All paraffinicity parameters derived from the gasoline hydrocarbons are indicative of thermal alteration of these oils. Greater depth of reservoirs supports this argument (>3000m).

The predominance of C_{29} steranes and low abundance of tricyclic terpanes indicated a possible common source input for F_3 and F_6 oil reservoired.

Tissot et al. (1974b), stated the existence of monoaromatic steroidal hydrocarbon distributions, especially tetracyclic compounds in oils from Illizi basin (F_3 and F_6 reservoirs). However, no data were presented (e.g. mass chromatograms or mass spectra) for comparative study. Furthermore, such mature oils do not contain sufficient amounts of biological markers to allow reliable correlations with the other oils. Hence, they are unlikely to give information on the source type and the depositional environment of organic matter generating these oils.

4.4.5. Gassi Touil basin

The bulk composition data and the barely detectable biological marker distributions as well as high paraffinicity parameters derived from gasoline-range (C_4-C_9) hydrocarbons suggest high maturity levels of these oils. Furthermore, relatively high abundances of $C_{29}T_s$ rearranged hopanes are indicative of high maturity levels of the organic matter that generated these oils (Cornford et al., 1988; Fowler and Brooks, 1990; Moldowan et al., 1991), while the diminishing abundance of $C_{29}\alpha\beta$ norhopane relative to $C_{30}\alpha\beta$ hopane could result from fractionation (Curiale, 1985). The consistency in C_{29} sterane and C_{28} triaromatic steroid carbon number predominance together the abundance tricyclic terpane relative to pentacyclic terpanes

indicate that these oils may have a common input probably from marine algae, since high tricyclic terpanes have been reported in immature sediments rich in *Tasmanites* (Volkman et al., 1990b). The presence of C_{30} steranes and prominence of C_{29} steranes indicate a marine origin of these oils, since abundant C_{29} steranes have been observed in marine sediments (Grantham, 1986; Fowler et al., 1987; Summons et al., 1988).

4.4.6. Rhourd-Nouss basin

High abundance of saturated relative to aromatic hydrocarbons and low NSO contents as well as very low concentrations of biological markers suggest high maturity levels of these oils. Further evidence of high maturity levels of these oils is reflected by high cracking ratios as well as paraffinicity ratios (i.e Heptane, Isoheptane indices and others, Appendix 4.6). Higher aromaticity indices than the other oils may indicate that oils from the Rhourd-Nouss basin have been less affected by water washing.

Figure 4.56 showing the correlation of $C_{30}\alpha\beta$ hop versus $C_{23}T/C_{23}T+C_{30}\alpha\beta$ hop, PC_1 versus $C_{30}\alpha\beta$ hop/$C_{29}\alpha\alpha\alpha$ (20R), PC_2 versus $C_{30}\alpha\beta$ hop/$C_{29}\alpha\alpha\alpha$ (20R), reveals that oils from Rhourd-Nouss fall in the same field as those from Gassi Touil basin (GT6 and GT47). The prominence of tricyclic relative to pentacyclic terpanes could be related to either thermal maturity (e.g., Zumberge, 1983) or source, since high abundance of tricyclic terpanes have been reported to occur in immature sediments rich in *Tasmanites* (Volkman et al., 1990b).

4.4.7. Ain Amenas basin

The similarity in the bulk composition of ZR115 (Carb), DL127(F_2) and TG22 (F_2) is not reflected at the molecular level of steroidal and terpenoidal distributions.

The occurrence of normoretane and moretane in ZR115 (Carb), low T_s/T_m, low extent of sterane isomerization, aromatization and cracking ratios are

indicative of lower maturity of ZR115 (Carb) than·TG22 F_2. On the contrary, the paraffinicity indices indicate high maturity levels of both oils. This may reveal a certain ambiguity of the gasoline hydrocarbon derived parameters, suggesting that these ratios like some other parameters could be affected by source (Snowdon and Powell, 1982; Rullkötter et al., 1986; Fowler and Brooks, 1990). Oil mixing of a gas-condensate with relatively less mature oil is another possibily.

The similar sterane composition (C_{27}-C_{29}) may indicate a common source of input for ZR115 (carb) and TG22(F_2). However, Figure 4.56 shows that ZR115 (Carb) and TG22(F_2) are belong to different groups. Hence, ZR115 contains higher sterane content than TG22 and barely detectable tricyclic terpanes. The lack of C_{30} steranes probably reveal a non-marine input for ZR115 oil.

The low abundance of tricyclic terpanes may be the result of no contribution from tricyclic terpane precursor or due to water washing, as suggested by laboratory experiments, although no field data have been reported in this matter.

4.5. General discussion

In an effort to establish oil-oil correlations, several geochemical analyses were applied for the bulk composition and molecular information, leading towards an understanding of source input, depositional environment, maturation and possibly biodegradation, and water washing. The general bulk composition·indicate a normal paraffinic oil classification (Tissot and Welte, 1984, pp 417). Among all oils analysed during this study, those from the Southeast Constantine basin (ie. DK1, DK6) and one from Ain Amenas (ZR115) are the least mature; depletion of light hydrocarbons may be due to incipient biodegradation in those from the Sbaa basin (TOT1 and DECH1), or during storage for oils from the Ghadames-El Borma basin (ELB9 and KA2). With the exception of the effects described above, all oils contain

relatively high proportions of saturated hydrocarbons. Oils from the Illizi basin contain the highest values. Molecular parameters derived from the gasoline range hydrocarbons appear to reflect both source and maturity controls (Snowdon and Powell, 1982; Rullkötter et al., 1986; Fowler and Brooks, 1990).

The occurrence of *n*-alkylcyclohexanes and methyl-*n*-alkyl cyclohexanes in these oils can be attributed to algal and/or bacterial derived fatty acids (Johns et al., 1966; Rubinstein and Strausz, 1979; Fowler and Douglas, 1986; Hoffmann et al., 1987). Laboratory simulation by Hoffmann et al. (1987) led to the suggestion that *n*-alkylcyclohexanes can be formed as a result of a combination of diagenetic factors, e.g. decarboxylation, cyclisation and cracking of fatty acids (Summons et al., 1988).

The high Pr/Ph ratio (greater than two) suggests that oils from the southeast Constantine and Sbaa basins, may be related to high input of pristane from algal tocopherols (Goossens et al., 1984).

Distinction between oils has been based on the presence or absence of tricyclic terpanes, $C_{30}\alpha\beta$ hop/$C_{29}\alpha\alpha\alpha$ (20R) versus $C_{23}T/C_{23}T+C_{30}\alpha\beta$ hop ratios, PC_1 scores versus $C_{30}\alpha\beta$ hop/$C_{29}\alpha\alpha\alpha$ (20R) and PC_2 scores versus $C_{30}\alpha\beta/C_{29}\alpha\alpha\alpha$ (20R). Hence, oils can be discriminated into three groups:

(i) Southeast Constantine (DK1, GKN1), Ghadames-El Borma (ELB9), Sbaa (ODZ1, DECH1), Ain Amenas (TG22).

(ii) Ghadames-El Borma (KA2, ROM1), Ain Amenas (ZR115)

(iii) Gassi Touil (GT6, GT47), Rhourd-Nouss (RN48, RNSE6).

As discussed previously, the major abundance of tricyclic terpanes in group (iii) oils indicates that one of the tentative source-rock (s) oils may contain these compounds, while none of the source-rock (s) for group (i) and (ii) oils may possess them, if no loss during migration has taken place (Curiale, 1985). Based on laboratory experiments, low molecular weight in the range of C_{17}-C_{20} tricyclic components could be removed by water washing while

abundance of C_{22} and C_{23} can be reduced to 10% (Hoffmann and Strausz, 1986).

The presence of C_{30} steranes in most of the oils suggest marine source-rocks (Moldowan, 1984; Moldowan et al., 1985; Telnaes and Dahl, 1986). Hence, the distribution of methylsteranes with C_{30} carbon number and 24-ethyl-3β-methyl-ααα and -αββ) and 24-ethyl-2α-methyl-ααα isomers is indicative of a probable marine algal input, as algae were the most dominant organisms in Palaeozoic era.

Chapter 5 Oil-source correlation in the Ghadames-El Borma basin

5. Oil-Source correlation in the Ghadames-El Borma basin.

5.1. Introduction

This chapter is concerned with an oil-source rock correlation involving seven source rock samples and three oils from the Ghadames-El Borma basin. The second part of the chapter includes the summary and conclusions for the study. The Ghadames-El Borma basin is less well explored than the Illizi basin, although they form part of one single, larger sedimentary basin, in that they have the same geological history. From the data presented in Chapter 3 and Chapter 4, it should be noted that there are some excellent Devonian and moderate to good Silurian source rocks in the area. Therefore, the aim of the first part of this Chapter will be an attempt to identify the specific source beds generating oils from KA2, ELB9 and ROM1 fields. For this purpose, potential source rocks have been selected on the basis of their organic-richness (i.e %TOC, EOM mg/g TOC), type (HI mg HC/g TOC), maturity of kerogen (%VR/E, T_{max}) and source extracts (biomarker parameters).

In the present study, only samples from RE-1 (3346.20m-3438.26m), ZAR-1 (3994.65m) and KA-1 bis (3029.82m-3072.85m) have been selected for oil-source rock correlation based upon preliminary geochemical evidence. In our biological marker investigation of source rocks (Chapter 3), Silurian and Devonian source rocks appear to have roughly similar characteristics, although the tricyclic terpane to hopane ratio indicates that these intervals can be distinguished. However, oil-source rock correlations can be made difficult by the fact that source extracts are correlated to migrated and reservoir oils. Many factors such as water washing, microbial activity and maturation can affect the composition of oils during and after migration. Nevertheless, correlation procedures were attempted using biomarker parameters together with PCA of sterane and terpane distributions. The PCA data suggests that group (i) oils (ELB9) and group (ii) KA2 and ROM1 fall in the same group as Silurian and Devonian source extracts. In other words, there are three possibilities for the

source of either group (i) or (ii). Firstly a Silurian source, secondly a Devonian source or thirdly an admixture of Devonian and Silurian sources.

It is worth noting that the oils were produced from the Triassic reservoirs, which lie unconformably on the Silurian and Devonian strata, where oil mixing could occur.

5.2 Results and Discussion

Data from the gross composition of source extracts (Chapter 3, Appendix 3.3) and oils (Chapter 4, Table 4.1b) indicate that most oils contain relatively higher proportions of saturated hydrocarbons and lower concentrations of NSO compounds than the source extracts. This type of feature was reported by Hunt and Jamieson (1956); Hunt (1979) and Tissot and Welte, (1984 pp 333). However, it is known that correlation can be made difficult due to some physical processes such as adsorption of polar compounds on the mineral matrix occurring during migration rather than variation in the type and maturity of the organic matter in the source rocks (Tissot and Welte, 1984, pp 333).

In Figure 5.1, the saturated hydrocarbon fraction gas chromatograms of oil-like extracts from rock samples of KA-1 bis (3039.82m), RE-1 (3354.40m) and ZAR-1 (3994.65m) and each reservoir oil are compared. As it can be clearly seen, the $C_{15}+$ saturated hydrocarbon gas chromatograms and the various Pr/Ph ratios seem to indicate a possible relationship between reservoir oils and source extracts from only RE-1 (3346.20m-3438.26m), KA-1 bis (3029.82m-3072.85m) and ZAR-1 (3994.65m) with all possessing a smooth *n*-alkane distribution, which reflects a marine input. However, the Pr/Ph ratio needs to be used with caution due to source, maturity and migration effects (Leythaeuser et al., 1983; Leythaeuser and Schwarzkopf, 1986). Combined geochemical data of oils and oil-like source extracts are listed in Appendix 5.1 and 5.2. The Devonian, Silurian source extracts and the oils seem to be related (Figures 5.2a and 5.2b respectively). Furthermore, principal component analysis (PCA) of sterane and terpane distributions provide another evidence for a close relationship between

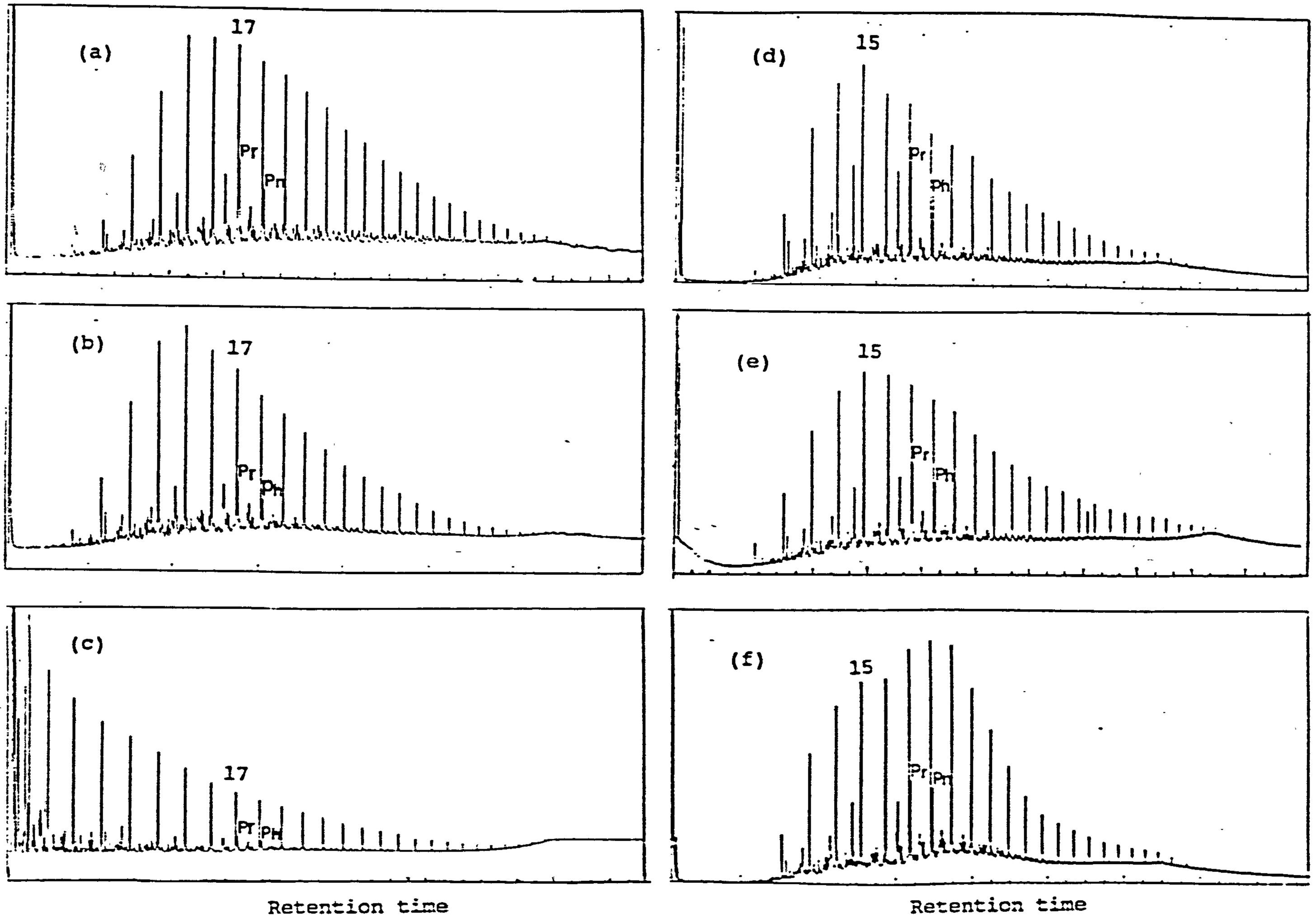

Figure 5.1 Gas chromatograms showing the saturated hydrocarbon distributions of oils: (a) ELS9, (b) (KA2, (c) ROM1 and selected mature source extracts: (d) RE1 (3346.20m), (e) KA1 (3072.85m), (f) ZAR1 (3994.65m). n-alkanes are labelled with their carbon number. Pr=pristane, Ph=phytane.

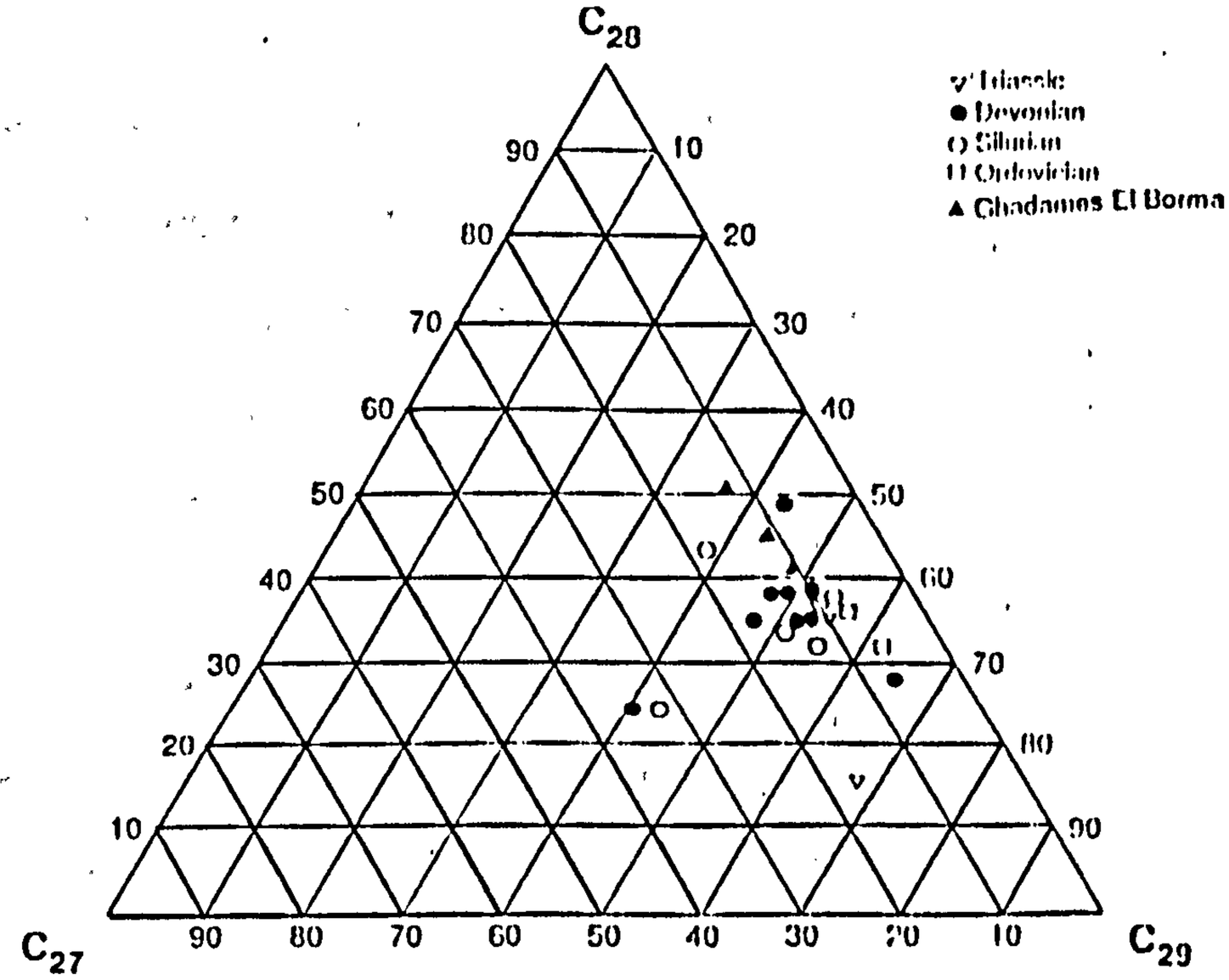

Figure 5.2a: Relative proportions of non-rearranged steranes (C_{27}-C_{29}) of oils and source extracts from the Ghadames-El Borma basin.

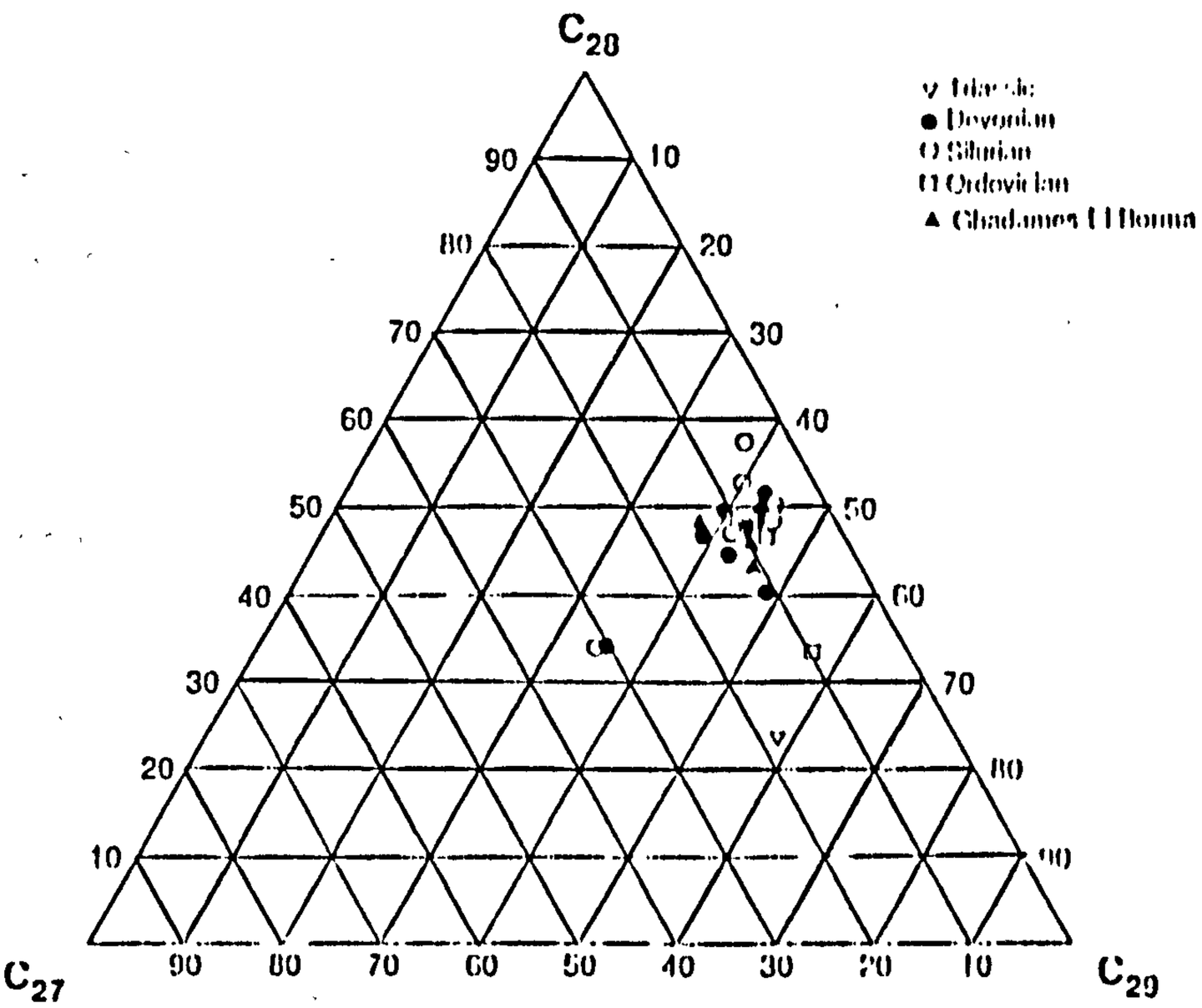

Figure 5.2b: Relative proportions of rearranged steranes (C_{27}-C_{29}) of oils and source extracts from the Ghadames-El Borma basin.

Devonian, Silurian source rocks and KA2, ELB9 and ROM1 oils. The three principal components analysis accounted for 44.7%, 22.5% and 8.0% for PC_1, PC_2 and PC_3 respectively. It is worth examining the loading plots of sterane and terpane distributions. On the loading of PC_1, there is tendency towards a negative correlation between:

-steranes and pentacyclic terpanes.

-tricyclic and pentacyclic terpanes

and a positive correlation between:

-tetracyclic terpanes (including C_{24} and 17,21 secohopane and pentacyclic terpanes

The loading on PC_2 shows a negative correlation between:

-tricyclic and pentacyclic terpanes,

-T_s and T_m,

-$\alpha\alpha\alpha$ and $\alpha\beta\beta$ steranes.

The loading on PC_3 indicates a negative correlation between:

-T_s and T_m,

-non-rearranged and rearranged steranes

The PC_1 loading may be interpreted in terms of differences in organic input. The PC_2 loadings may be explained in terms of maturity, while PC_3 may represent lithology and/or maturity. As it can be seen in the score plot PC_1/PC_2 and PC_1/PC_3, the oils are likely to be derived from Devonian or Silurian but not from Ordovician source rocks.

Furthermore, the C_{29} steranes predominance together with C_{28} triaromatic member (i.e. $\%C_{28}t/C_{26}t+C_{27}t+C_{28}t$) and the presence of C_{30} steranes, albeit in low concentrations in the oils and source extracts suggest a common marine input. As regards the discrimination of oils from the Ghadames-El Borma basin, the correlation of the ($C_{23}T/C_{23}T+C_{30}\alpha\beta$ hop) versus $C_{30}\alpha\beta$ hop/$C_{29}\alpha\alpha\alpha$ (20R) ratios (Figure 4.57) has been found useful in distinguishing group (I) oil (ELB9) from group (ii) oil (KA2, ROM1) as previously discussed in Chapter 4. Furthermore, based on this criterion, KA2 and ELB9 oils seem to correlate with

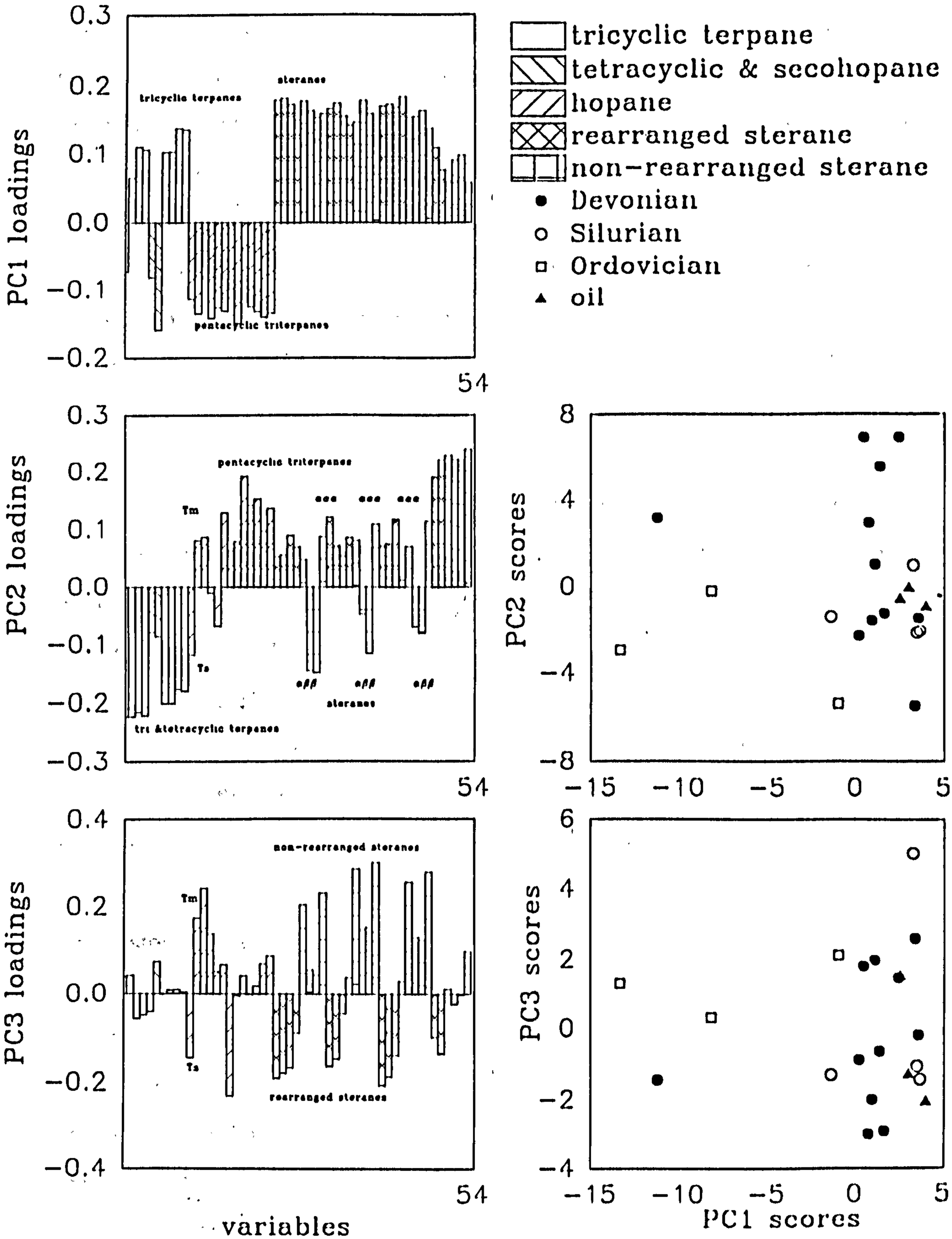

Figure 5.3 Oil−source rock correlation (biomarkers). Loadings for the three PCs plotted versus biomarker variables. Scores of oils and source extracts from Ghadames−El Borma basin.

the Devonian samples from RE-1 (3346.20m-3438.26m), while ROM1 have similar characteristics to the Silurian source extracts from ZAR-1 (3994.65m). However, based on the hopane to sterane ratio (C_{30} hop/C_{29}st), group (ii) oil (KA2 and ROM1) seem to show a good correlation with only source extracts from KA-1 bis (3029.82m-3072.85m), while none of the source extracts show a close relationship with group (ii) oil (ELB9). Figure 5.5 shows that the major source rocks lie in the Devonian from RE-1 field. In addition, oils and source extracts correlate well on the basis of GC/MS metastable ion transitions for C_{29} steranes (i.e m/z 414-217). However, the T_s/T_m ratio seems to show no correlation between oils and all source extracts. As clearly seen in Appendix 5.2, group (ii) oil (ROM1) has comparable values of T_s/T_m ratio only with source extracts from RE-1 (3346.20m-3438.26m). A lower value of this parameter particularly for groups (i) ELB9 and (ii) oils (KA2), indicates that these oils could have been expelled from their source rock(s) at an earlier stage than those currently studied. There is no evidence in the literature of migration effect on this parameter, which is rather influenced by source, maturity and/or lithology (Moldowan et al., 1986). Migration influence is not significant in the present study, since the Palaeozoic series consist of alternation of shales and sandstones. Such a pattern facilitates the drainage of oil from the source rocks. The maturity of oils and source extracts has been assessed (Appendix 5.2) using sterane isomerisation (C_{29} (20S/20S+20R), steroid aromatisation (Aro ratio) and methylalted triaromatic steroid indices (MTSI1 and MTSI2), which reveal similar maturity levels of KA2, ELB9 oils to source extracts from RE1 field (3346.20m-3354.40m), while ROM1 seems to have been generated at a later stage of oil, probably from deeper sediments, as suggested by the presence of low concentrations of triaromatic steroid hydrocarbons. It needs to be borne in mind maturity and water washing effects on aromatic compounds.

Tentative description of oil generation and accumulation in the Ghadames-El Borma basin.

From the combined information obtained from biomarker parameters and principal component analysis of sterane and terpane distributions of oils and source extracts and the thermal history of the basin, only a tentative reconstruction of some of the features of oil generation and accumulation in the Ghadames-El Borma basin is postulated. It is apparent that all the oils were produced within rich Devonian and Silurian source rocks. All the oils are mature with probably ROM1 being generated at a higher maturity level than ELB9 and KA2 oils.

The present-day geothermal gradient has been reported to be about 30°C/km (Sonatrach internal report, 1980), as shown in Figure 5.4a, 5.4b and 5.4c illustrating the thermal history of the basin during the Middle Devonian, Upper Devonian and Silurian periods (Sonatrach internal report, 1980). These Figures show that the Ghadames-El Borma basin has been subjected to two cycles of subsidence in a similar way to the Illizi basin (Tissot et al., 1974b). The first of these two events was described as the Hercynian orogeny and erosion during Palaeozoic times, since major unconformities exist at the top of the Carboniferous, Devonian and Silurian strata, indicating possible uplift and erosion during this period. This created migration pathways for hydrocarbons from the source rocks to the traps. However, due to tectonic movements, many oil accumulations were lost and others newly formed.

The second major cycle of subsidence occurred during Mesozoic times. In the northeastern part of the basin, the burial depth was extensive with the organic matter reaching the metagenesis phase (cracking). During this period, massive amounts of salt and evaporites emerged to form caps for good preservation of hydrocarbons in the Triassic reservoirs. Sediments were subjected to high pressure and temperature. All the succession including the Carboniferous reached the peak of oil generation, while during Palaeozoic times, only Ordovician and Silurian strata were heated enough to reach the peak of oil

MIDDLE DEVONIAN

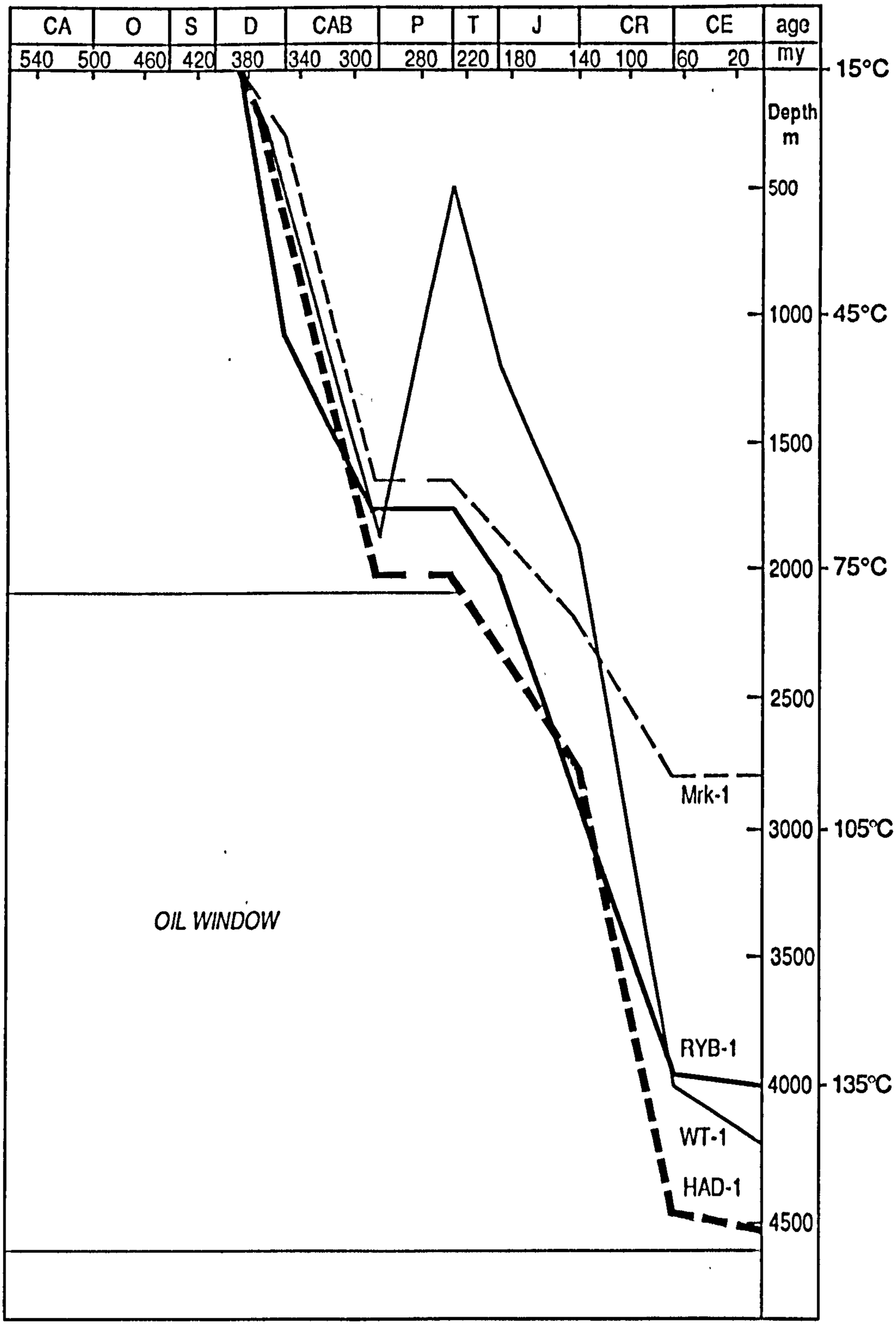

Figure 5.4a Burial history of the base of the Middle Devonian as a function of geological time. *(Modified after Sonatrach Internal Report, 1980)*

UPPER DEVONIAN

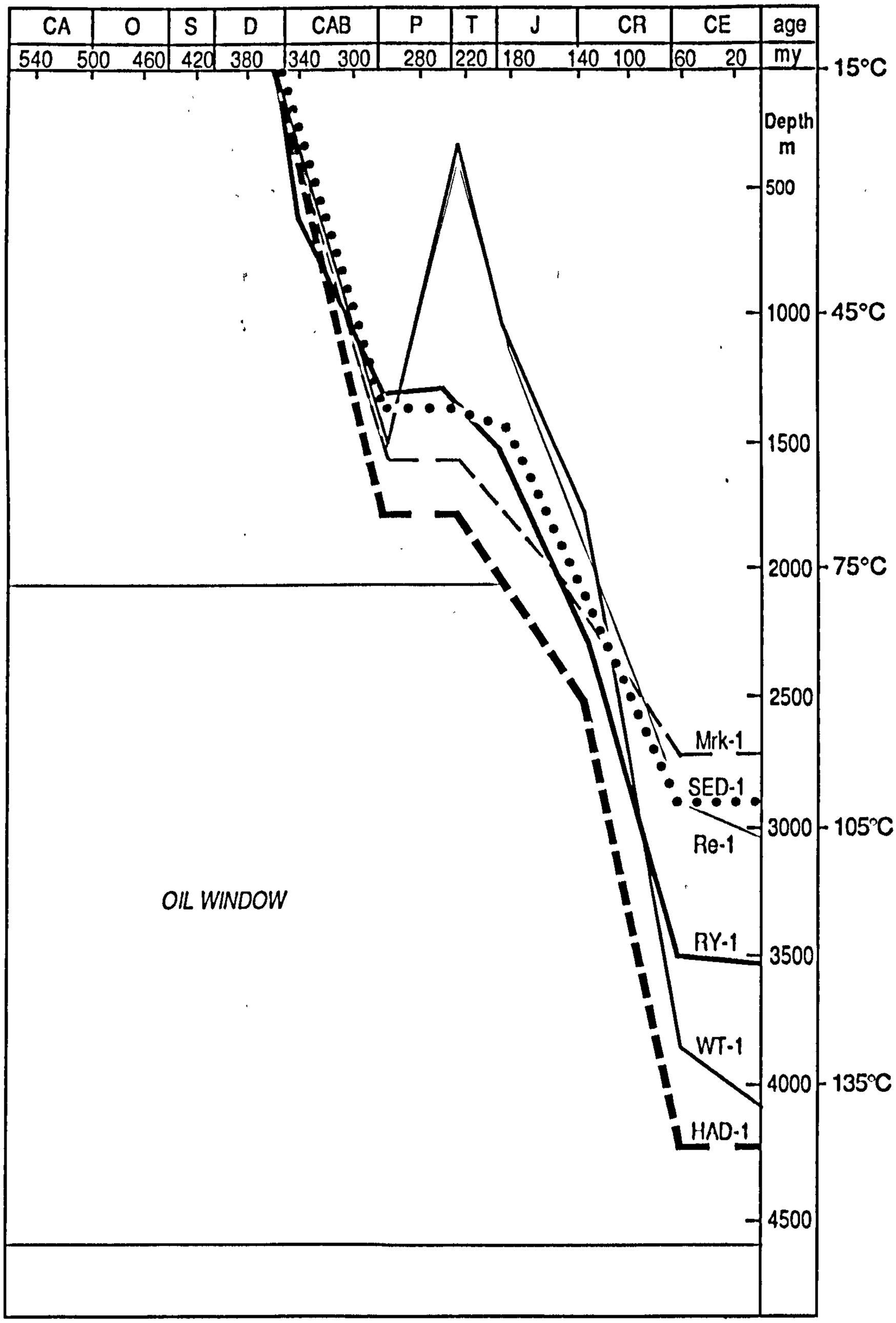

Figure 5.4b Burial history of the base of the Upper Devonian as a function of geological time. *(Modified after Sonatrach Internal Report, 1980)*

SILURIAN

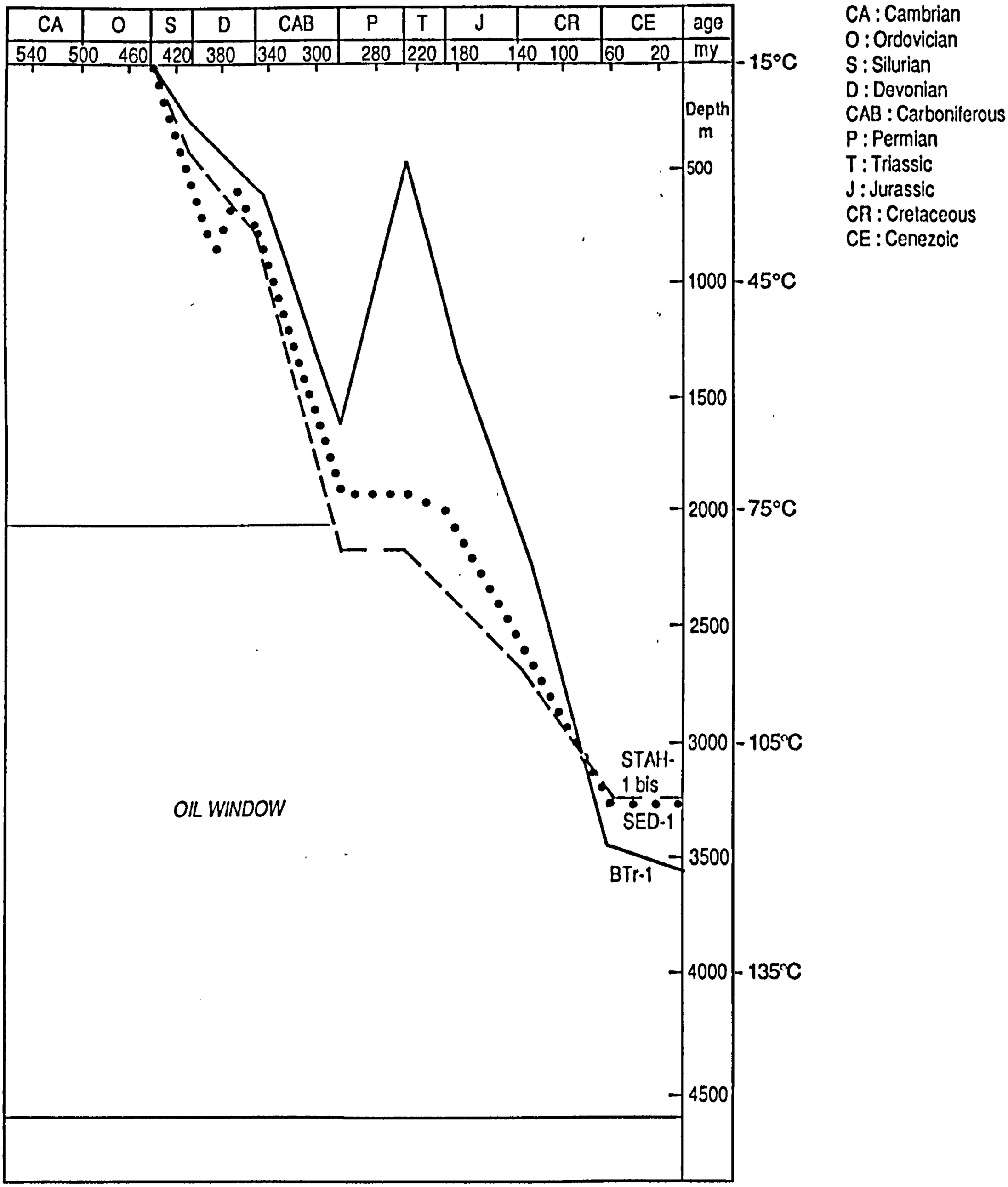

Figure 5.4c Burial history of the base of the Silurian as a function of geological time. *(Modified after Sonatrach Internal Report, 1980)*

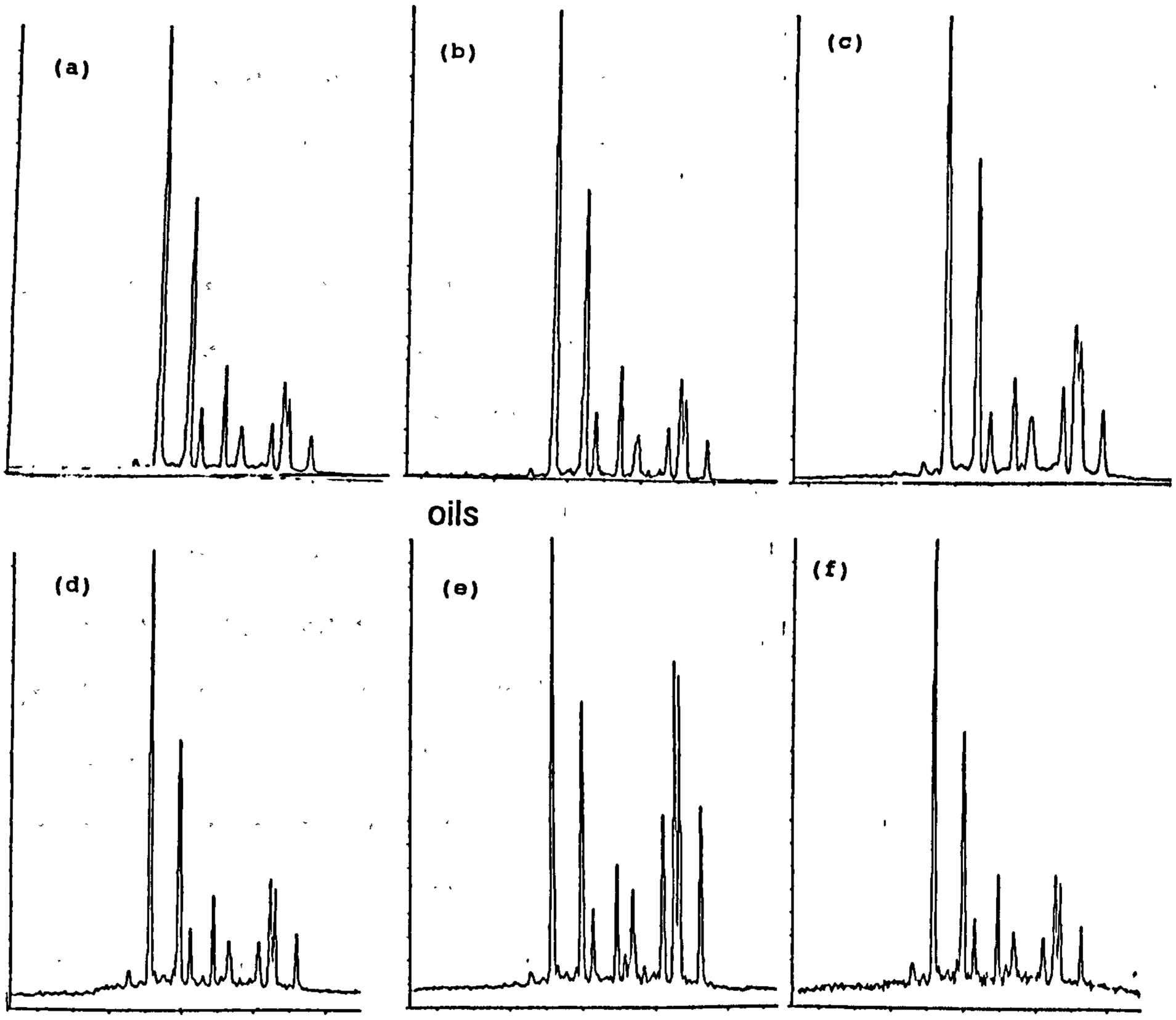

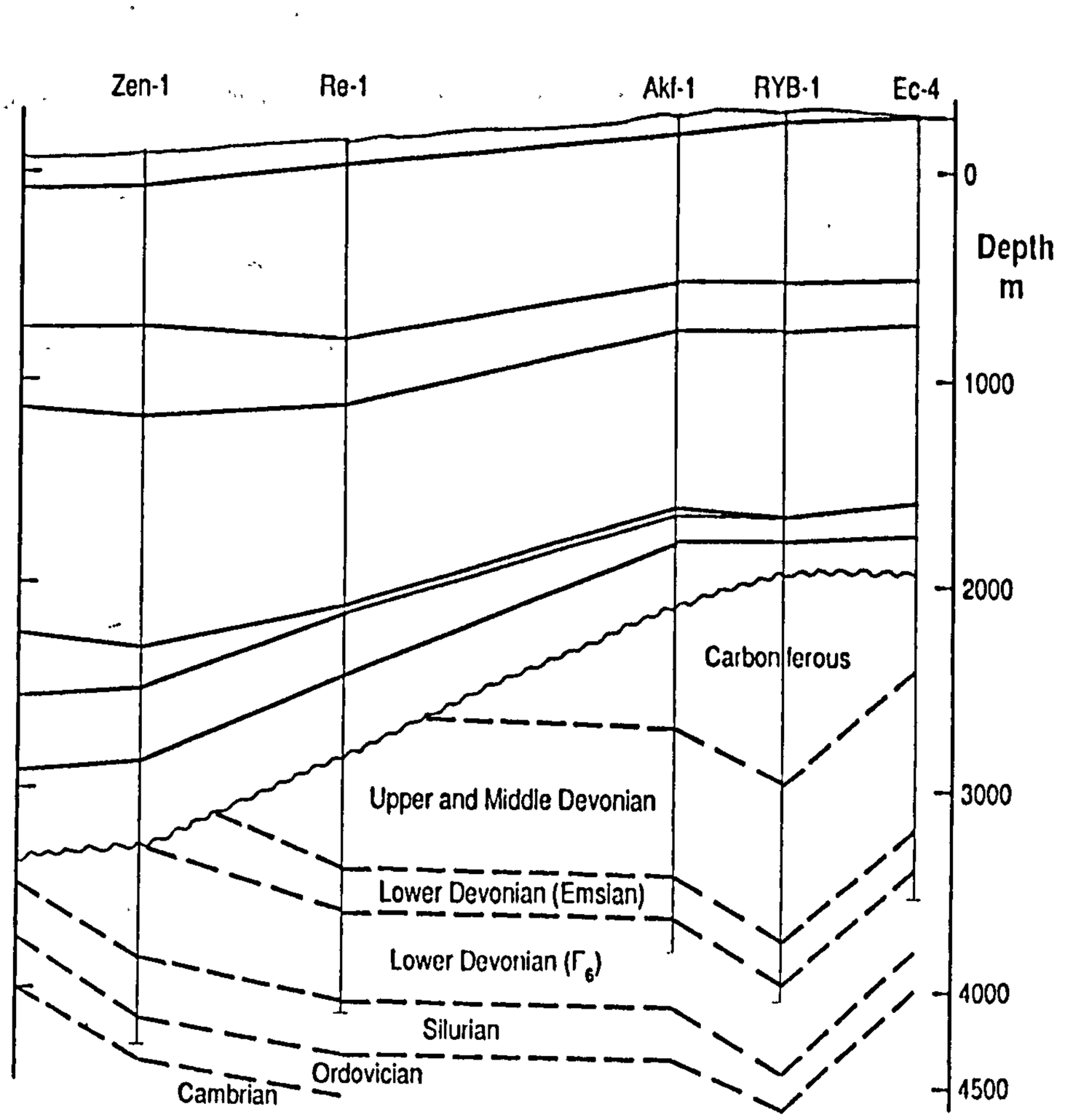

Figure 5.5 Oil-source correlation procedure using GC/MS/metastable ion transition for C_{29} steranes (i.e m/z 400-217) for source extracts: (a) RE-1 (3346.20m), (b) (3354.40m) and (c) KA-1 bis (3072.85m) and oils: (d) ELB9, (e) KA2 and (f) ROM1. These oils and source extracts are similar in sterane composition, suggesting possible Devonian or Silurian source rocks in the area.

generation. It is worth noting that the generation of hydrocarbons finished at the end of the Cretaceous (Sonatrach internal report, 1985).

5.3. Summary and Conclusions

In summary, data from biological marker investigation as well as the Pre-Mesozoic subcrop map (Figure 1.6) imply that all three oils KA2, ELB9 and ROM1 could have been derived from source rocks of marine input and depositional environments, probably from Devonian, Silurian or even an admixture of these sources. Despite the fact that the set of rock samples analysed was not sufficiently complete for an oil-source rock correlation procedure in the Ghadames-El Borma basin, a certain number of conclusions can be drawn from the present study:

-Group (i) includes DK1 and GKN1 oils, which obviously originate from the pre-Cretaceous sediments. The sterane distribution reveals relatively higher proportions of C_{28} steranes as well as C_{28} monoaromatic steroid hydrocarbons, suggesting marine algae or from other marine organism contribution to their source rock(s). Basically, all maturity parameters indicate a lower maturity level of DK1 than GKN1. As far as the tentative source rock(s) is concerned, there have been few reports suggesting laminated bituminous marls and limestones for generating these oils.

This group comprises oils from the Ghadames-El Borma (ELB9), Sbaa (ODZ1, DECH1) and Ain amenas oils (TG22) as well. According to molecular information, ELB9, ODZ1, DECH1 and TG22 appear to have similar features in their biological markers distributions. These include

a) predominance of C_{29} steranes in all these oils

b) similar tricyclic terpane to hopane ratio (0.32-0.36)

c) roughly similar hopane to sterane ratio, particularly for ELB9, ODZ1, DECH1 and TG22. This may suggest another possibility that Devonian and Silurian source rocks are involved in the Sbaa basin (Laggoun-Defarge, 1987; Drid, 1989). Possible explanations for the depositional environment and source input

may be ascertained from a detailed biological marker investigation for sediments in the Sbaa and Ain Amenas fields. Biological marker and gasoline (C_4-C_9) range hydrocarbon investigation postulate an oil mixture of a mature oil or gas condensate with a less mature to DECH1 reservoir oil (Connan et al., 1985; Drid, 1989). A similar feature has been reported by Drid (1989) for Visean sediments from DECH1 borehole. As regards the gasoline range hydrocarbons, ELB9 as well as KA2 oils seem to have been depleted either by water washing or more likely during the storage.

Group (ii) includes oils Ghadames-El Borma (KA2 and ROM1) and Ain Amenas (ZR115), as suggested by PCA of steranes and terpanes and $C_{23}T/C_{23}T+C_{30}$ $\alpha\beta$ hop versus C_{30} $\alpha\beta/C_{29}\alpha\alpha\alpha$ (20R) plots (Figure 4.57). The maturity parameters based on biological markers as well as paraffin indices indicate that ZR115 oil accumulation could occur from an oil mixing of a mature and a less mature oils, although no evidence of biodegradation or water washing was shown.

Group (iii) includes oils from the Gassi Touil (GT6, GT47), Rhourd-Nouss (RNSE6, RN48) basins. As shown in Figure 4.57, these oils can be distinguished from the remained groups by higher tricyclic to hopane and lower hopane to sterane ratios, which may suggest high input from algae. Oils from the Gassi Touil and Rhourd-Nouss regions in the Triassic province are thought to be derived from Silurian source rocks (Gothlandian shales), as the only potential source rocks in the area and shown in the Pre-Mesozoic subcrop map (Figure 1.6). However, oil from Ain Amenas (ZR115) produced in the Carboniferous reservoir could be differentiated from the other group of oils due to the lack of C_{30} steranes as well as tricyclic terpanes.

5.4. Ideas for future research

This study is the first detailed organic geochemical investigation of oils from the northern part of Algeria (Southeast Constantine basin), northeastern (Ghadames-El Borma, Illizi, Ain Amenas basins) and southwestern (Sbaa) parts of the Algerian Sahara and sediments from the Ghadames-El Borma basin, in which biological marker distributions in the saturated and aromatic fractions have been examined. Oil-oil and oil-source rock correlations have been attempted in order to discriminate oils into oil families and identify specific strata for the oil accumulations in the Ghadames-El Borma basin. It is hoped to analyse the gasoline range (C_4-C_9) hydrocarbons of both oils and source rocks for an oil-source rock correlation in many Algerian basins. Furthermore, work will be needed to determine the chemical structures of C_8 and C_9 branched alkanes, methylsteranes as well as the separation and identification of rearranged and non-rearranged monoaromatic steroidal hydrocarbons. It would also be necessary to use chemical and physical degradation of kerogen in order to determine the biological markers attached to the kerogens. Further work will be considered for investigating the influence of kerogen type and lithology on the steroid aromatisation, cracking ratio and methylated triaromatic steroid indices. Another important key question to be answered is whether Cenomanian/Turonian Oceanic Anoxic Event detected in the Bahloul formation, Tunisia (Farrimond et al., 1990) can be extended to the Cenomanian/Turonian formation in the southeast of Constantine (Algeria).

Tables: Peak assignments

Table 1: Peak assignments illustrating the m/z 217.1950 mass chromatogram and m/z 372->m/z 217, m/z 386->m/z 217, m/z 400->m/z 217 and m/z 414->m/z 217 as well as m/z 414-> m/z 231 metastable ion transitions for steranes and methylsteranes respectively.

N°	sterane compounds
1a	C_{21} pregnane
1b	C_{22} homopregnane
1	13β(H),17α(H)-diacholestane (20S)
2	13β(H),17α(H)-diacholestane (20R)
3	13α(H),17β(H)-diacholestane (20S)
4	13α(H),17β(H)-diacholestane (20R)
5	24-methyl-13β(H),17α(H)-diacholestane (20S)
6	24-methyl-13β(H),17α(H)-diacholestane (20R)
7	24-methyl-13α(H),17β(H)-diacholestane (20S) (r) 5α(H),14α(H),17α(H)-cholestane (20S) (n)
8	24-ethyl-13β(H),17α(H)-diacholestane (20S) (r) 5α(H),14β(H),17β(H)-cholestane (20R) (n)
9	24-methyl-13α(H),17β(H)-diacholestane (20R) (r) 5a(H),14b(H),17b(H)-cholestane (20S) (n)
10	5α(H),14α(H),17α(H)-cholestane (20R)
11	24-ethyl-13β(H),17α(H)-diacholestane (20R)
12	24-ethyl-13α(H),17β(H)-diacholestane (20S)
13	24-methyl-5α(H),14α(H),17α(H)-cholestane (20S
14	24-ethyl-13α(H),17β(H)-diacholestane (20R) (r) 24-methy-5α(H),14b(H),17β(H)-cholestane (20R) (n)
15	24-methyl-5a(H),14β(H),17β(H)-cholestane (20S)
16	24-methyl-5α(H),14α(H),17α(H)-cholestane (20R)
17	24-ethyl-5α(H),14α(H),17α(H)-cholestane (20S)
18	24-ethyl-5α(H),14β(H),17β(H)-cholestane (20R)
19	24-ethyl-5α(H),14β(H),17β(H)-cholestane (20S)
20	24-ethyl-5α(H),14α(H),17α(H)-cholestane (20R)
21	24-*n*-propyl-13β(H),17α(H)-diacholestane(20S)[27*]
22	24-*n*-propyl-13β(H),17α(H)-diacholestane(20R)
23	24-*n*-propyl-5α(H),14α(H),17α(H)-cholestane (20S)
24	24-*n*-propyl-5α(H),14β(H),17β(H)-cholestane (20R)
25	24-*n*-propyl-5α(H),14β(H),17β(H)-cholestane (20S)
26	24-*n*-propyl-5α(H),14α(H),17α(H)-cholestane (20R)[26*]
27	24-ethyl-13β(H),17α(H)-3β-methyl-diacholestane (20S)
28	24-ethyl-13β(H),17α(H)-3β-methyldiacholestane(20R)
29	24-ethyl-5α(H),14α(H),17α(H)-3β-methyl-cholestane (20S)[31*] 24-ethyl-5α(H),14α(H),17α(H)-2α-methylcholestane (20S)[32*]
30	24-ethyl-5α(H),14β(H),17β(H)-3β-methyl-cholestane (20R)
31	24-ethyl-5α(H),14β(H),17α(H)-3β-methyl-cholestane (20S)
32	24-ethyl-5α(H),14α(H),17α(H)-2α-methyl-cholestane (20R) 24-ethyl-5α(H),14α(H),17α(H)-3β-methyl-cholestane (20R)
33	24-ethyl-5α(H),14α(H),17α(H)-4α-methyl-cholestane (20R)

* refers to structures in appendix, (r) and (n) to rearranged and non-rearranged steranes respectively.

Table 2: Peak assignments of terpane compounds illustrated in the m/z 191.1794 mass chromatogram.

Peak	elemental composition	Assignment
a	$C_{23}H_{42}$	C_{23}-tricyclic terpane[13*]
b	$C_{24}H_{44}$	C_{24}-tricyclic terpane
c	$C_{25}H_{46}$	C_{25}-tricyclic terpane
x	$C_{24}H_{42}$	C_{24}-tetracyclic terpane[14*]
d	$C_{26}H_{48}$	C_{26}-tricyclic terpane
e	$C_{28}H_{50}$	C_{28}-tricyclic terpane
f	$C_{29}H_{52}$	C_{29}-tricyclic terpane
g	$C_{27}H_{46}$	18α(H)-22,29,30-trisnorneohopane (T_s)[20*]
h	$C_{27}H_{46}$	17α(H)-22,29,30-trisnorhopane (T_m)
i	$C_{29}H_{50}$	17α(H),21β(H)-30-norhopane
j	$C_{29}H_{50}$	18α(H)-30-norneohopane ($C_{29}T_s$)[23*]
k	$C_{29}H_{50}$	17α(H)-15α-methyl-27- norhopane (e.g. 17α(H) diahopane)[22*]
l	$C_{29}H_{50}$	17β(H),21α(H)-30-norhopane (normoretane)
m	$C_{30}H_{52}$	17α(H),21β(H)-hopane[15*]
n	$C_{30}H_{52}$	17β(H),21α(H)-hopane (moretane)
o	$C_{31}H_{54}$	17α(H),21β(H)-30-homohopane (22S)
p	$C_{31}H_{54}$	17α(H),21β(H)-30-homohopane (22R)
q	$C_{32}H_{56}$	17α(H),21β(H)-bishomohopane (22S)
r	$C_{32}H_{56}$	17α(H),21β(H)-bishomohopane (22R)
s	$C_{33}H_{58}$	17α(H),21β(H)-trishomohopane (22S)
t	$C_{33}H_{58}$	17α(H),21β(H)-trishomohopane (22R)
u	$C_{34}H_{60}$	17α(H),21β(H)-tetrakishomohopane(22S)
v	$C_{34}H_{60}$	17α(H),21β(H)-tetrakishomohopane(22R)

* refers to structures in appendix.

Table 3: Peak assignments of C-ring monoaromatic steroidal hydrocarbons, based on m/z 253.1950 mass chromatogram.

peak N°	elemental composition	stereochemistry
1a	$C_{21}H_{30}$	unknown
1b	$C_{22}H_{32}$	unknown
1	$C_{27}H_{42}$	5β(H), 10β(CH_3) (20S)[33*]
2	$C_{27}H_{42}$	5β(CH_3),10β(H)(20S)
3	$C_{27}H_{42}$	5α(CH_3),10α(H)(20S)
4	$C_{27}H_{42}$	5β(H),10β(CH_3)(20R) [39*]
		5β(CH_3),10β(H)(20R)
5	$C_{27}H_{42}$	5α(H),10β(CH_3)(20S)
6	$C_{28}H_{44}$	5β(H),10β(CH_3)(20S)
7	$C_{27}H_{42}$	5α(CH_3),10α(H)(20R)
	$C_{28}H_{44}$	5β(CH_3),10β(H)(20S)
8	$C_{28}H_{44}$	5α(CH_3),10α(H)(20S)
9	$C_{27}H_{42}$	5α(H),10α(CH_3)(20R)[34*]
	$C_{28}H_{44}$	5α(H),10β(CH_3) (20S)
10	$C_{28}H_{44}$	5β(H),10β(CH_3) (20R)
	$C_{28}H_{44}$	5β(CH_3),10β(H) (20R)[35*]
	$C_{29}H_{46}$	5β(H),10β(CH_3) (20S)
	$C_{29}H_{46}$	5β(CH_3),10β(H) (20S)
11	$C_{28}H_{44}$	5α(CH_3),10α(H) (20R)
12	$C_{29}H_{46}$	5α(CH_3),10α(H) (20S)
13	$C_{29}H_{46}$	5α(H),10β(CH_3) (20S)
14	$C_{28}H_{44}$	5α(H),10β(CH_3) (20R)[36*]
	$C_{29}H_{46}$	5β(H),10β(CH_3) (20R)
	$C_{29}H_{46}$	5β(CH_3),10β(H) (20R)
15	$C_{29}H_{46}$	5α(CH_3),10α(H) (20R)
16	$C_{29}H_{46}$	5αH),10β(CH_3)(20R)

* refers to structures in Appendix

Table 4: Peak assignments for triaromatic steroidal hydrocarbons, based on the m/z 231.1170 and m/z 245.1330 mass chromatograms.

Peak N°	m/z	elemental composition	structure
17	231	$C_{20}H_{20}$	
18	231	$C_{21}H_{22}$	
19	231	$C_{26}H_{32}$ (20S)	
20	231	$C_{26}H_{32}$ (20R)	
	231	$C_{27}H_{34}$ (20S)	
21	231	$C_{28}H_{36}$ (20S)	
22	231	$C_{27}H_{34}$ (20R)	
23	231	$C_{28}H_{36}$ (20R)[37*]	
24	245	$C_{21}H_{22}$	2-methyl+ 3-methyl-C_{21}[38*]
25	245	$C_{21}H_{22}$	6-methyl-C_{20}
26	245	$C_{21}H_{22}$	4-methyl-C_{20}
27	245	$C_{22}H_2$	2-methyl+3-methyl-C_{21}
28	245	$C_{22}H_{24}$	6-methyl-C_{21}
29	245	$C_{22}H_{24}$	4-methyl-C_{21}
30	245	$C_{27}H_{34}$	4-methyl-C_{26}
31	245	$C_{27}H_{34}$	3-methyl-C_{26}
32	245	$C_{27}H_{34}$	4-methyl-C_{26}
33	245	$C_{29}H_{38}$	3-methyl-C_{28}
34	245	$C_{29}H_{38}$	4-methyl-C_{28}

* refers to structures in appendix.

Table 5: Peak assignments for the gasoline range (C_4-C_8) hydrocarbons of crude oils.

Peak N°	elemental composition	structure
1	C_4H_{10}	isobutane
2	C_4H_{10}	*n*-butane
3	C_5H_{12}	isopentane
4	C_5H_{12}	*n*-pentane
5	C_6H_{14}	2,2-dimethylbutane
6	C_5H_{10}	cyclopentane
7	C_6H_{14}	2,3-dimethylbutane
8	C_6H_{14}	2-methylpentane
9	C_6H_{14}	3-methylpentane
10	C_6H_{14}	*n*-hexane
11	C_7H_{16}	2,2-dimethylpentane
12	C_7H_{12}	methylcyclopentane
13	C_7H_{16}	2,4-dimethylpentane
14	C_7H_{16}	2,2,3-trimethylbutane
15	C_6H_6	benzene[39*]
16	C_7H_{16}	3,3-dimethylpentane
17	C_7H_{12}	cyclohexane[40*]
18	C_7H_{14}	2-methylhexane
19	C_7H_{14}	2,3-dimethylpentane[41*]
20	C_7H_{12}	1,1-dimethylcyclopentane
21	C_7H_{14}	3-methylhexane
22	C_7H_{12}	cis-1,3-dimethylcyclopentane
23	C_7H_{12}	trans-1,3-dimethylcyclopentane
24	C_7H_{14}	3-ethylpentane
25	C_7H_{12}	trans-1,2-dimethylcyclopentane
26	C_7H_{14}	*n*-heptane
27	C_7H_{12}	methylcyclohexane& cis-1,2DMCP
28	C_8H_{18}	2,2-dimethylhexane
29	C_8H_{18}	ethylcyclohexane
30	C_8H_{18}	2,5-dimethylhexane
31	C_8H_{18}	2,4-dimethylhexane
32	C_8H_{16}	1,2,4-trimethylcyclopentane
33	unknown	
34	unknown	
35	unknown	
36	C_7H_9	toluene
37	unknown	
38	unknown	
39	C_8H_{18}	2-methylheptane
40	C_8H_{18}	4-methylheptane
41	unknown	
42	unknown	
43	C_8H_{18}	3-methylheptane
44	C_8H_{16}	cis-1,2-dimethylcyclohexane
45	C_8H_{16}	trans-1,4-dimethylcyclohexane
46	C_8H_{16}	1,1-dimethylhexane
47	C_8H_{16}	cis-1,4-dimethylcyclohexane
48	unknown	
50	C_8H_{16}	trans-1,2-dimethylcyclohexane
51	C_8H_{18}	*n*-octane

*refers to structures in appendix.

References

Abbott G.D. and Maxwell J.R. (1988) Kinetics of the aromatisation of rearranged ring-C monoaromatic steroid hydrocarbons. *Org.Geochem.* **13**, 881-885.

Abbott G.D., Wang G.Y., Eglinton T.I., Home A.K. and Petch G.S. (1990) The kinetics of sterane biological marker release and degradation processes during hydrous pyrolysis of vitrinite kerogen. *Geochim.Cosmochim.Acta.* **54**, 2451-2461.

Aliev M., Ait Laoussine N., Avrov V., Aleksine G., Barouline G., Lakovlev B., Korj M., Kouvykine J., Makarove V., Mazanov V., Medvedev E., Mkrtchiane O., Moustafinov R., Oriev L., Oroudjeva D., Oulmi M. and Saïd A. (1971) Geological structures and estimation of oil and gas in the Sahara in Algeria. Sonatrach. Rotopress, S.A. 265pp.

Allan J. and Douglas A.G. (1977) Variations in the content and distribution of *n*-alkanes in a series of Carboniferous vitrinites and sporinites of bituminous rank. *Geochim.Cosmochim.Acta.* **41**, 1223-1230.

Aquino Neto F.R., Restle A., Connan J., Albrecht P. and Ourisson G. (1982) Novel tricyclic terpanes (C_{19}-C_{20}) in sediments and petroleum. *Tetrahedron.Lett.* **23**, 2027-2030.

Aquino Neto F.R., Trendel A., Restle A., Connan J. and Albrecht P. (1983) Occurence and formation of tricyclic and tetracyclic terpanes in sediments and petroleums. *In Advances in Organic Geochemistry* 1981 (Edited by Bjorıy M. et al.). Wiley, Chichester, 659-667.

Aquino Neto F.R. Cardoso J.N. Rodrigues R. and Trindale L.A.F. (1986) Evolution of tricyclic alkanes in the Espirito Santo Basin, Brazil. *Geochim.Cosmochim.Acta.* **50**, 2069-2072.

Aref'ev O.A., Kulibakina I.B., Rabrotrov V.T, Makushina V.m and Zabrodina M.N. (1979) Genetic features and catagenenic transformation of petroleum from the Upper Precambrian and Lower Cambrian of the Siberian platform. *Izv.Akd.Nauk.SSR.Ser.Geol.* 2, 135-140 (in russian).

Armanios C., Alexander R. and Kagi R.I. (1991) Separation of diahopanes and 22S and 22R diastereomers of the extended hopanes using large-pore, high-silica molecular sieves. *Organic Geochemistry, Advances and Applications in Energy and the Natural environment.* 15th Meeting of the European Association of Organic Geochemists. Poster Abstracts (Edited by Manning D.). Manchester University Press, 613-614.

Barbe A., Grimalt J.O., and Albaigés J. (1988) A novel cyclohexyl isoprenoid hydrocarbons in carbonate-evaporite crude oils. *Naturwissenschaften* **75**, 624-625.

Barwise A.J.G., Ducan A.D. and Pepper A.S. (1991) The kinetics of molecular maturity reactions- calibration of organofacies effects using basin data. *Organic Geochemistry, Advances and Applications in Energy and the Natural environment.* 15th Meeting of the European Association of Organic Geochemists. Poster Abstracts (Edited by Manning D.). Manchester University Press. 275-277.

Beach F., Peakman T.M., Abbott G.D., Sleeman R. and Maxwell J.R. (1989) Laboratory thermal alteration of triaromatic steroid hydrocarbons. *Org.Geochem.* **14**, 109-111.

Blumer M., Mullin M.M. and Thomas D.W. (1963) Pristane in zooplankton. *Science* **140**, 974.

Bostick N. and Foster W. (1975) Comparison of vitrinite in coal seams and kerogen of sandstones, shales and limestones in the same part of sedimentary section. *Colloque International Petrographie de la matière organique des sediments*, (Edited by Alpern B.)., 13-25.

Brassell S.G., Eglinton G., Maxwell J.R. and Philp R.P. (1978) Natural background of alkanes in the aquatic environment. *In Aquatic polluants: transformation and biological effects* (Edited by Huzinger O. Van Lelyveld I.H. and Zoeteman B.C.J). Pergamon press, Oxford, 1978. 69-86.

Brassell S.C., Wardroper A.M.K., Thompson I.D., Maxwell J.R. and Eglinton G. (1981) Specific acyclic isoprenoids as biological markers of methanogenic bacteria in marine sediments. *Nature* **290**, 293-296.

Brassell S.C. and Eglinton G. (1983) steroids and terpenoids in deep sea sediments as environmental and diagenetic indicators. *In Advances in Organic Geochemistry* 1981 (Edited by Bjorıy M. et al.). Wiley, Chichester. 684-697.

Bray E.E. and Evans E.D. (1961) Distribution of *n*-paraffins as a clue to recognition of source beds. *Geochim. Cosmochim. Acta.* **22**, 2-15.

Brooks J.D., Gould K. and Smith J.W. (1969) Isoprenoid hydrocarbons in coal and petroleum. *Nature* **222**, 257-259.

Brooks P.W., Fowler M.G. and Macqueen R.W. (1989) Use of biomarkers including aromatic steroids to indicate relationships between oil sands/heavy oils/bitumens and convential oils, Western Canada basin. *In Proceedings of the 1989 Eastern Oil shale Symp. Lexington, Kentucky.*

Caldicott A.B. and Eglinton G. (1973) Surface waxes. *In Phytochemistry 3, Inorganic elements and special Groups of Chemicals* (Edited by Miller L.P.). Van Nostrand Reinhold, New York. 162-

Cardozo J., Watts C.D., Maxwell J.R. Goodfellow R., Eglinton G. and Golubic S. (1978) A biochemical study of the abu-Dhabi algal mats: a simplified ecosystem. *Chem. Geol.* **23**, 273-291.

Chappe B., Michaelis W. and Albrecht P. (1980) Molecular fossils of archaebacteria as selective degradation products of kerogen. *In Advances in Organic Geochemistry* 1979 (Edited by Douglas A.G. and Maxwell J.R.). Pergamon Press, Oxford, 265-274.

Chappe B., Albrecht P. and Michaelis W. (1982) Polar lipids of archaebacteria in sediments and petroleum. *Science* **217**, 65-67.

Chardac J.L., Dupont A., Edmundson H., Gartner J., Guindy A., Mons F., Noïk S., Orlandi, Y., Pirard Y.M., Serra O., Sodeke T., Souhaité Ph., Trassard J. and Wittmann M. (1979) Applications des diagraphies et méthodes associées. (Edition Schlumberger, France).

Chicarelli M.I., Aquino Neto F.R. and Albrecht P. (1988) Occurrence of four stereoisomeric tricyclic terpane series in immature Brazilian shales. *Geochim. Cosmochim. Acta.* **52**, 1955-1959.

Connan J. and Cassou A.M. (1980) Properties of gases and petroleum liquids from terrestrial kerogen at various maturation levels. *Geochim. Cosmochim. Acta.* **44**, 1-23.

Connan J., Restle A. and Albrecht P. (1980) Biodegradation of crude oil in the Aquitaine basin. *In Advances in Organic Geochemistry* 1979 (Edited by Douglas A.G. and Maxwell J.R.). Pergamon Press, Oxford, 1-17.

Connan J., DesAutels D.A. and Aldridge A.K. (1985) Petroleum Geochemistry of north slope of Alaska: source rocks, crude oils properties and migration of hydrocarbons. Alaska north slope oil/rock correlation study. *In: A.A.P.G. studies in Geology* #20. (Edited by Magoon L.B. and Claypool G.E.). 243-279.

Connan J., Bouroullec J., Dessort D. and Albrecht P. (1986) The microbial input in carbonate-anhydrite facies of a shabka palaeoenvironment from Guatemala: A molecular approch. *Org. Geochem.* **10**, 29-50.

Cornford C., Rullkötter J. and Welte D. (1979) organic geochemistry of DSDP project Leg 47A, site 397 eastern North Atlantic: organic petrography and extractable hydrocarbons. In initial reports of the Deep Sea Drilling Project (Edited by von Rad V., Ryan B.F et al.), 47Pt1., Chap2, 511-522. U.S. Govt Printing office.

Cornford C., Christie O., Endresen U., Jensen P. and Myhr M.B. (1988) Source rock and seep oil maturity in Dorset, southern England. *Org. Geochem.* **13**, 399-409.

Curiale J.A. (1985) Oil types and source rock-oil correlation on the North slope, Alaska -A cooperative USGS-Industry Study. Alaska north slope oil/rock correlation study. *In: A. A. P. G. studies in Geology* #20. (Edited by Magoon L.B. and Claypool G.E.), 203-231.

Curiale J.A., Cameron D. and Davis D.V. (1985) Biological marker distribution and significance in oils and rocks of the Monterey Formation, California. *Geochim. Cosmochim. Acta.* **49**, 271-288.

Curiale J.A., Larter S.R., Sweeney R.E. and Bromley B.W. (1988) Molecular thermal maturity indicators in oil and gas source rocks. *In Thermal History of Sedimentary basins* (Edited by Naeser N.D and McCulloh T.H.). Springer-Verlag, New York. 53-72.

Curiale J.A. (1989) Integrated biological marker correlations among mature oils of the Sverdrup Basin. *In:symp.Seifert W.K. Biomarker. Petrol. Amer. Chem. Soc. Div. Petrol. Chem. Dallas*, 9-14 April. Preprints **34**, 122-125.

Curiale J.A. and Odermatt J.R. (1989) Short-term biomarker variability in the monterey Formation, Santa Maria basin. *Org. Geochem.* **14**, 1-13.

Dahl J., Moldowan J.M., McCaffrey M.A. and Lipton P.A. (1992) A new class of natural products revealed by 3ß-alkylsteranes in petroleum. *Nature* **335**, 154-157.

Davis J.C. (1986) Statistics and data analysis in geology. (third edition). 646pp, John and wiley Sons, New York.

Demaison G., Holck A.J.J., Jones R.W. and Moore G.T. (1983) Predictive source bed stratigraphy; a guide to regional petroleum occurrence, North Sea basin and eastern North American margin. *In: Origin, migration and accumulations of hydrocarbons.* Proc. eleventh. World. Pet. Cong., London. 17-29.

De Rosa M., Gambacorta A., Minale L. and Bu'lock J.D. (1972) The formation of ω-cyclohexyl-fatty acids from Shikimate in an Acidophilic Thermophilic Bacillus. A new biosynthetic pathway. *Biochem. J.* **128**, 751-754.

De Sousa N.J. and Nes W.R. (1968) sterols: isolation from a blue-green algae. *Science* **162**, 363.

Didyk B.M., Simoneit B.R.T., Brassel S.C. and Eglinton G. (1978) Organic geochemical indicators of palaeoenvironmental conditions of sedimentation. *Nature* **272**, 216-222.

Douglas A.G. and Mair B.J. (1965) Sulphur: Role in genesis of petroleum. *Science* **147**, 499-501.

Drid M. (1989) Sur quelques aspects de la diagénese organique et minerale dans le bassin de Timimoun et le sillon de Sbaa (Sahara central algerien). Thèse de Doctorat de l'Université de Bordeaux III en Sciences de la terre.

Durand B. and Espitalié J. (1972) Formation et evolution des hydrocarbure de C_1 à C_{15} et des gas permanents dans les argiles du Toarcian du bassin de Paris. *In Advances in Organic Geochemistry 1971* (Edited by Gaertner H.R.V. and Wehner H.). Pergamon Press. 455-468.

Durand B. and Monin J.C. (1980) Elemental analysis of kerogen (C,H,O,N,S,Fe). In: Kerogen: Insoluble Organic Matter from Sedimentary Rocks (edited by Durand B.) edition technip, Paris. 113-142.

Durand B., and Nicaise G. (1980) Procedures for kerogen isolation. In:Kerogen: Insoluble Organic Matter from Sedimentary Rocks (Edited by Durand B.). Edition technip, Paris. 35-53.

Eglinton G., Hamilton R.J., Raphael R.A. and Gonzalez A.G. (1962). Hydrocarbon constituents of the wax coatings of plant leaves: a taxanomy survey. *Nature* **193**, 739-742.

Eglinton T.I. and Douglas A.G. (1988) Quantitative study of biomarker hydrocarbons released from kerogens during hydrous pyrolysis. *Energy and Fuels*. **2**, 81-88.

Ekweozor C.M., Okogun J.I., Ekong D.E.U. and Maxwell J.R. (1979) Preliminary organic geochemical studies of samples from the Niger Delta (Nigeria), II. Analysis of shales for triterpenoid derivatives. *Chem. Geol.* **27**, 29-37.

Ekweozor C.M. and Strausz O.P. (1983) Tricyclic terpanes in Athabasca Oil sands: their geochemistry. *In Advances in Organic Geochemistry* 1981. (Edited by Bjoroy M. et al.). Wiley Chichester. 746-766.

Erdman J.G. and Morris D.A. (1974) Geochemical correlation of petroleum. *A. A. P. G. Bull.* **58**, 2326-2337.

Esminger A., van Dorssalaer A., Spyckerelle C., Albrecht P. and Ourisson G. (1974) Pentacyclic triterpenes of the hopane type as ubiquitous geochemical markers: origin and significance. *In Advances in Organic Geochemistry* 1973 (Edited by Tissot B. and Bennier F.). Editions Technip, Paris. 245-260.

Espitalié J., Laporte J.L., Madec M., Marquis E., Leplat P., Paulet J. and Boutefeu A. (1977) Méthode rapide de caractérisation des roches mères, de leur potentiel pétrolier et de leur degré d'évolution. *Revue. Inst. Francais. du Pétrole.* **32**, 23-43.

Farrimond P. (1987) The Toarcian and Cenomanian/Turonian oceanic anoxic event. PhD thesis, Bristol University.

Farrimond P., Eglinton G. Brassell S.C. and Jenkyns H.C. (1990) The Cenomanian/Turonian anoxic event in Europe: Organic geochemical study. *Mar. Pet. Geol.* **7**, 75-89.

Fowler M.G. (1984) Organic geochemistry of Pre-Carboniferous sedimentary organic matter. Ph.D. thesis, University of Newcastle-upon-Tyne

Fowler M.G. and Douglas A.G. (1984) Distribution and structure of hydrocarbons in four organic-rich Ordovician rocks. *Org. Geochem.* **6**, 105-114.

Fowler M.G., Abolins P. and Douglas A.G. (1986) Monocyclic alkanes in Ordovician organic matter. *Org. Geochem.* **10**, 815-823.

Fowler M.G. and Douglas A.G. (1987) Saturated hydrocarbon biomarkers in oils of Late Precambrian age from Eastern Siberia. *Org. Geochem.* **11**, 201-213.

Fowler M.G. and Brooks P.W. (1990) Organic geochemistry as an aid in the interpretation of the history of oil migration into different reservoirs at the Hibernia K-18 and Ben Nevis I-45 wells, Jeanne d'Arc basin, Offshore eastern Canada. *In Advances in Organic Geochemistry* 1989 (Edited by Durand B and Behar F). Pergamon Press, 461-475.

Fowler M.G. (1991) The influence of Gleocapsomorpha prisca on the organic geochemistry of oils and organic-rich rocks of late Ordovician age from Canada. *Proc.9th Alfred Wegner conference, Early organic evolution*: implications for Mineral and Energy Ressources, Maria Loach, West Germany, Springer (in press).

Freeman K.H., Hayes J.M., Trendel J.M. and Albrecht P. (1990) Evidence from carbon isotope measurements for diverse origins of sedimentary hydrocarbons. *Nature* **343**, 254-256.

Gallegos E.J. (1971) Identification of new steranes, terpanes ans branched paraffins in Green River Shale by combined capillary gas chromatography and mass spectrometry. *Anal. Chem.* **43**, 1151-1160.

Gallegos E.J. (1976) Analysis of organic mixtures using metastable transition spectra. *Anal. Chem.* **48**, 1348-1351.

Gelpi E., Schneider H., Mann J. and Oró J. (1970) Hydrocarbons of geochemical significance in microscopic algae. *Phytochem* **9**, 603-612.

Goodwin N.S., Mann A.L. and Patience R.L. (1988) structure and significance of C_{30} 4-methyl steranes in lacustrine shales and oils. *Org. Geochem.* **12**, 495-506.

Goossens H., de Leeuw J.W., Schrenck P.A. and Brassell S.C. (1984) Tocopherols as likely precursors of pristane in ancient sediments and crude oils. *Nature* **312**, 440-442.

Grantham P.J., Posthuma J. and De Groot K. (1980) Variation of C_{27} and C_{28} triterpane content of a North Sea core and various North Sea oils. *In Advances in Organic Geochemistry* 1979 (Edited by Douglas A.G. and Maxwell J.R.). Pergamon Press, Oxford, 29-88

Grantham P.J. (1986) The occurence of unsual C_{27} and C_{29} sterane predominances in two types of of Oman crude oil. *Org. Geochem.* **9**, 1-10.

Grantham P.J. and Wakefield L.L (1988) Variations in the sterane carbon number distribution of marine source rock derived crude oils through geological time. *Org. Geochem.* **12**, 61-73.

Grimalt J. and Albaigés J. (1985) *N*-alkanes distributions in surface sediments from the Arabian Gulf. *Naturwissenschaften* **72**, 35-37.

Han J. and Calvin M. (1969) Hydrocarbon distribution of algae and bacteria and microbiological activity in sediments. *Proc. Nat. acad. Sci. USA.* **64**, 436.

Han J. and Calvin M. (1970) Branched alkanes from blue-green algae. *Chem. Comm.* 1490-1491.

Han J (1982) Geochemical fossils of a possibility archaebacterial origin in ancient sediments. *Zbl. Bakt. Hyg., I. Abt. orig.* **3**, 40-52.

ten Haven H.L, De Leeuw J.W. and Schenck P.A. (1985) Organic geochemical studies of a Messinian evaporitc basin, northern Apennines (Italy)I: hydrocarbon biological markers for a hypersaline environment. *Geochim. Cosmochim. Acta.* **49**, 2181-2191.

ten Haven H.L., de Leew J.W., Rullkotter J. and Sinningue Damsté J.S. (1987) Restricted utility of the pristane/phytane ratio as a palaeoenvironmental indicator. *Nature* **330**, 641-643.

ten Haven H.L., De Leeuw J.W., Sinnigue Damste J.S., Schenck P.A., Palmer S.E. and Zumberge J.E. (1988) *In: Lacustrine Petroleum Source rocks* (Edited by Fleet A.J. et al.). Blakwell, Oxford, 123-130.

ten Haven H.L., Rohmer M., Rullkötter J. and Bisseret P. (1989) Tetrahymanol, the most likely precursor of gammacerane occurs ubiquitously in marine sediments. *Geochem. Cosmochim. Acta.* **53**, 3073-3079.

Henderson W., Wollrab V. and Eglinton G. (1969) Identification of steranes and triterpanes from a geological source by capillary gas liquid chromatography and mass spectrometry. *In Advances in Organic Geochemistry* 1968 (Edited by Schenck P.A. and Havenaar I.). Pergamon press, London. 181-207.

Hoering T.C. (1981) Monomethyl acyclic hydrocarbons in petroleum and rock extracts. *Carnegie. Inst. Wash. Yearbook.* **80**, 389-393.

Hoering T.C. and Freeman D.H. (1984) Shape-selective sorption of monomethylalkanes by silicalite, a zeolite form of silica. *J. Chrom.* **316**, 333-341.

Hoffmann C.F., Mackenzie A.S., Lewis C.A., Maxwell J.R., Oudin J.L., Durand B. and Vadenbroucke M. (1984) A biological marker study in coals, shales and oils from the Mahakam Delta, Katlimantan, Indonesia. *Chem. Geol.* **42.** 1-23.

Hoffmann C.F. and Strausz O.P. (1986) Bitumen accumulation in Grosmont Platform complex, Upper Devonian, Alberta, Canada. *A. A. P. G. Bull.* **70**, 1113-1128.

Hoffmann C.F., Foster C.B., Powell T.G. and Summons R.E. (1987) Hydrocarbon biomarkers from Ordovician sediments and the fossil algae *Gloecopsomorpha Prisca zalessky 1917. Geochim. Cosmochim. Acta.* **51**, 2681-2697.

Huang W.Y. and Meinschein W.G. (1979) Sterols as ecological indicators. *Geochim. Cosmochim. Acta.***43**, 739-745.

Huges W.B., Holba A.G., Miller D.E. and Richardson J.S. (1985) Geochemistry of greater Ekofisk crude oils. *In Petroleum Geochemistry in exploration of the Norwigian Shelf* (Edited by Thomas B.M et al.). Graham and Trotman, London, 75-92.

Hunt J.M. and Jamieson G.W. (1956) Oil and organic matter in some source rocks of petroleum. *A. A. P. G. Bull.* **40**, 477-488.

Hunt J.M. (1979) Petroleum Geochemistry and Geology. N.H.Freeman and Co., San Fransisco. 617pp.

Hunt J.M (1984) Generation and migration of light hydrocarbons. *Science* **226**, 1265-1270.

Hunt J.M. Huc A.Y. and Whelan J.K. (1980a) Correlation of light hydrocarbons in sedimentary rocks. *Nature* **288**, 688-690.

Hunt J.M. Miller R.J. and Whelan J.K. (1980b) Formation of C_4-C_7 hydrocarbons from bacterial degradation of naturally occurring terpenoids. *Nature* **288**, 577-578.

Hussler G., Chappe P., Wehrung P., and Albrecht P. (1981) C_{27}-C_{29} ring A monoaromatic steroids in Cretaceous black shales. *Nature* **294**, 556-558.

Johanson E., Wold S. and SjÖdin K. (1984) Miniminzing effects of closure on analytical data. *Anal. Chem.* **56**, 1685-1688.

Johns R.B., Belsky T., McCarthy E.D., Burlingame A.L., Haug P., Schnoes H.K., Richter W.J. and Calvin M. (1966) The organic geochemistry of ancient sediments II. *Geochim. Cosmochim. Acta.* **30**, 1191-1222.

Kerdjidj M.K. (1987) Application de la petrographie et de la geochimie organique à l'histoire thermique de la partie sud-est du bassin Triasique du Sahara Nord-oriental (Algerie). These, Doctorat de l'Université d'Orléans, France.

Killops S.D. and Howell V.J. (1991) Complex series of pentacyclic triterpanes in lacustrine sourced oil from Korea Bray Basin. *Chem. Geol.* **91**, 65-79.

Kimble B.J., Maxwell J.R., Philp R.P. and Eglinton G. (1974) Identification of steranes and triterpanes in geolipids extracts by high resolution gas chromatography and mass spectrometry. *Chem. Geol.* **14**, 173-198.

Klomp U.C. (1986) The chemical structure of a pronounced series of iso-alkanes in South Oman crudes. *Org. Geochem.* **10**, 807-814. Pergamon Press, Oxford.

Kruge M.A., Hubert J.F. Jay Akes R. and Meriney P.E. (1990) Biological marker in Lower Jurassic Synrift lacustrine black shales, Harrfort Basin, Connicut, U.S.A. *Org. Geochem.* 15, 281-289.

Kvalheim O.M and Telnaes (1986) Visualizing information in multivariate data: applications to petroleum geochemistry part 2. Interpretation and correlation of North sea oils using three different biomarker fractions. *Analytica. Chimica. Acta*, **191**, Elsvier Science Publishers B.V., Amsterdam. 97-110.

Kvalheim O.M. (1987) Multivariate correlation of oils and source rocks by the combined use of principal components modelling, analysis of variance and a coefficient of congruence. *Chemometrics and Intelligent Laboratory Systems*, **2**. 127-136.

Laggoun-Defarge F. (1987) Etude de la diagenèse organique des series Paleozoiques du bassin de Sbaa (Algerie). Approche geochimique et petrographique. Thèse de Doctorat de l'Université d'Orléans, France.

Langford F.F. and Blanc-Valleron M.M. (1990) Interpreting Rock-Eval pyrolysis data using graphs of pyrolizable hydrocarbons vs. total organic carbon. *A. A. P. G. Bull.* **74**, 799-804.

Larter S.R., Solli H. and Douglas A.G. (1978) Analysis of kerogens by pyrolysis-gas chromatography-mass spectrometry using selective ion detection. *J. Chrom.* **167**, 421-431.

Larter S.R (1985) Integrated kerogen typing in the recognition and quantitative assessment of petroleum source rocks. *In petroleum Geochemistry in exploration of the Norwegian Shelf*, Norwegian Petroleum Society. Graham and Trottman, London. 269-286.

Larter S.R. and Sentfle J.T. (1985) Improved Kerogen typing for petroleum source rock analysis. *Nature* **318**, 277-280.

Latreche S. (1982) Evolution structurale du bassin d'Illizi (Sahara Oriental Algerien) au Paleozoique superieur. Diplome d'Etudes superieures. Sciences. Université de Droit, d'Economie et des Sciences, d'Aix Marseille. Faculté des Sciences et Techniques de St Jerome.

Leythaeuser D., Schaefer R.G., Cornford C. and Weiner B. (1979) Generation and migration of light hydrocarbons (C_2-C_7) in sedimentary basins. *Org. Geochem.* **1**, 191-204.

Leythaeuser D., BjorΦy M., Mackenzie A.S., Schaefer R.G. and Altebaumer F.J. (1983) Recognition of migration and its effects within two corholes in shale/sandstone sequences from Svalbard, Norway. *In Advances in Organic Geochemistry* 1981 (Edited by BjorΦy M. et al.). Wiley, Chichester. 136-146.

Leythaeuser D., Mackenzie A.S. Schaefer R.G and BjorΦy M. (1984). A novel approach for recognition and quantification of hydrocarbons migration effects in shale-sandstaone sequences. *A. A. P. G. Bull.* **68**, 196-219.

Leythaeuser D. and Schwarzkopf T.H. (1986) The pristane/*n*-heptadecane ratio as an indicator for recognition of migration effects *In Advances In Organic Geochemistry* 1985 (Edited by Leythaeuser D. and Rullkötter J.). Pergamon Press, Oxford. 191-197.

Longman M.W. and Palmer S.E. (1987) Organic Geochemistry of Mid-Continent Middle and Late Ordovician oils. *A. A. P. G. Bull.* **71**, 938-950.

Lichtfouse E. (1989) Nouveaux stéroides aromatiques fossiles. Thesis de Doctorat de l'université Louis Pasteur de Strasbourg.

Lichtfouse E., Riolo J. and Albrecht P. (1990) Occurrence of 2-methyl-, 3-methyl- and 6-methyltriaromatic steroid hydrocarbons in geological samples. *Tetrahedron. Lett.* **31**, 3997-3940.

Mackenzie A.S., Patience R.L., Maxwell J.R. Vadenbroucke M. and Durand B. (1980) Molecular parameters of maturation in the Toarcian shales, Paris Basin, Francel. Changes in the configurations of acyclic isoprenoid alkanes, sterane and triterpanes. *Geochim. Cosmochim. Acta.* **44**, 1709-1722.

Mackenzie A.S. and Maxwell J.R. (1981) Assessment of thermal maturation in sedimentary rocks by molecular measurements. *In Organic Maturation Studies and Fossil Fuel Exploration.* (Edited by Brooks J.). Academic press, London. 239-254.

Mackenzie A.S., Hoffmann C.F. and Maxwell J.R. (1981a) Molecular parameters of maturation in the Toarcian shales, Paris Basin, FranceIII. Changes in aromatic steroid hydrocarbons. *Geochim. Cosmochim. Acta.* **45**, 1345-1355.

Mackenzie A.S., Lewis C.A. & Maxwell J.R (1981b) Molecular parameters of maturation in the Thoarcian shales, Paris basin, FranceIV. Laboratory thermal alteration studies. *Geochim. Cosmochim. Acta.* **45**, 2369-2376.

Mackenzie A.S., Brassell S.C., Englinton G. and Maxwell J.R. (1982a) Chemical fossils: The geological fate of steroids. *Science* **217**, 491-504.

Mackenzie A.S., Lamb N.A. and Maxwell J.R. (1982b) Steroid hydrocarbons and the thermal history of sediments. *Nature* **295**. 223-226.

Mackenzie A.S. and Mckenzie D. (1983) Isomerization and aromatization of hydrocarbons in sedimentary basins formed by extention. *Geol. Mag.* **120**, 417-528.

Mackenzie A.S. (1984) Applications of biological markers in petroleum geochemistry. *In Advances in Petroleum Geochemistry* 1983 (Edited by Brooks J. and Welte D.H.). Vol 1 Academic Press, New York. 115-214.

Martin R.L., John C.W. and Williams J.A. (1963) Distributions of *n*-paraffins in crude oils and their implications to origin of petroleum. *Nature* **199**, 110-113.

McEvoy J. and Maxwell J.R. (1983) diagenesis of steroidal compounds in sediments from the south california Bight (DSDP Leg 63, site 467) *In Advances in Organic Geochemistry* 1981 (Edited by BjorΦy M. et al.). Wiley, Chichester, 449-464.

McEvoy J. and Giger W. (1986) Origin of hydrocarbons in Triassic Serpiano oil shales: hopanoids. *In Advances in Organic Geochemistry* 1985 (Edited by Leythaeuser D. and Rullkötter J.). Pergamon Press, Oxford. 943-949.

McKirdy D.M., Aldridge C.F. and Maxwell J.R. (1983) A geochemical comparison of some crude oils from Pre-Ordovician carbonates rocks. *In Advances in Organic Geochemistry* 1981 (Edited by BjorΦy M. et al.). Wiley, Chichester. 99-107.

McKirdy D.M. Cox R.E. Volkman J.K. and Howell V.G. (1986) Botryococcane in a new class of Australian non-marine crude oils. *Nature* **320**, 57-59.

Mello M.R. Telnaes N. Gaglionone P.C. Chicarelli M.I. Brassell S.C. and Maxwell J.R. (1988) Organic geochemical characterisation of depositional paleoenvironment of source rocks and oils in Brazilian margin basins. *In Advances in Organic Geochemistry* 1987 (Edited by Mattavalli L. and Novelli L.). Pergamon Press, Oxford. 31-45.

Mello M.R., Koutsoukos E.A.M., Hart M.B., Brassell S.C. and Maxwell J.R. (1989) Late Cretaceous anoxic events in the Brazilian continental margin. *Org. Geochem.* **14**, 529-542.

Meyer T., Christie O.H.J. and Brooks P.W. (1984a) Aspects of biomarker analysis by gas chromatography/mass spectrometry with selective metastable ion monitoring. *Anal. Chim. Acta.* **161**, 65-74.

Meyers P.A., Leenher M.J., Kawka O.E. and Trull T.W. (1984b) Enhanced preservation of marine-derived organic matter in Cenomanian black shales from the southern Angola Basin. *Nature* **312**. 356-359.

Michaelis W. and Albrecht P. (1979) Molecular fossils of archaebacteria in kerogen. *Naturwissenschaften* **66**, 420-422.

Moldowan J.M. and Seifert W.K. (1979) Head to head linked isoprenoid hydrocarbons in petroleum. *Science* **204**, 169-171.

Moldowan J.M., Seifert W.K. and Gallegos E.J. (1983) Identification of an extented series of tricyclic terpanes in petroleum. *Geochim. Cosmochim. Acta.* **47**, 1531-1534.

Moldowan J.M. (1984) C_{30}-Steranes, novel markers for marine petroleum and sedimentary rocks. *Geochim. Cosmochim. Acta.* **48**, 2767-2768.

Moldowan J.M., Seifert W.K. and Gallegos E.J. (1985) Relationship between petroleum composition and deposional environment of petroleum source rocks. *A. A. P. G. Bull.* **69**, 1225-1268.

Moldowan J.M. and Fago J.F. (1986) Structure and significance of novel rearranged monoaromatic steroid hydrocarbons in petroleum. *Geochim. Cosmochim. Acta.* **50**, 343-351.

Moldowan J.M., Sundararaman P. and Schoell M. (1986) Sensitivity of biomarker properties to depositional environment and/or source input in the lower Toarcian of SW-Germany. *In Advances in Organic Geochemistry* 1985 (Edited by Leythaeuser D. and Rullkötter J.). Pergamon Press, Oxford. 915-926.

Moldowan J.M. Fago F.G. cathy Y.L. Jacobson S.R. Watt D.S. Slougui N.S. Jeganathan W. and Young D.C. (1990) Sedimentary 24-*n*-propylcholestane, molecular fossils diagnostic of marine algae. *Science* **247**, 309-312.

Moldowan J.M., Fago F.J., Young D.C., Carlson R.M.K, Dwyne G.V., Clardy J., Schoell M., Pillinger C.T. and Watt D.S. (1991) rearranged hopanes in sediments and petroleum. *Geochem. Cosmochim. Acta.* **55**, 3333-3353.

Murchison D.G. (1987) Recent advances in organic petrology and organic geochemistry: an overview with some reference to 'oil from coal'. *In: Coal and Coal-bearing Strata*: Recent advances, Geological Society special publication. **32**, 257-302.

Mycke B. and Michaelis W. (1986) Molecular fossils from chemical degradation of macromolecular organic matter. *In Advances in Organic Geochemistry* 1985 (Edited by Leythaeuser D. and Rullkötter J.). Pergamon Press, Oxford. 847-858.

Mycke B., Narjes F. and Michaelis W. (1987) Bacteriohopanetetrol from chemical degradation of an oil shale kerogen. *Nature* **326**, 179-181.

Ourisson G., Albrecht P. and Rohmer M. (1979) the hopanoids. Palaeochemistry and biochemistry of a group of natural products. *Pure. Appl. Chem.* **51**, 709-729.

Ourisson G., Albrecht P. and Rohmer M. (1982) Predictive microbilal biochemistry: from molecular fossils to procaryotic membranes. *Trends. Biochem. Sci.* **7**, 233-239.

Ourisson G., Rohmer M. and Parolla K. (1987) Procaryotic hopanoids and other polyterpenoid sterol surrogates. *Ann. Rev. Microbiol.* **41**, 301-333.

Φygard K., Larter S. and Sentfle J. (1988) The control of maturity and kerogen type on quantitative analytical pyrolysis data. *Org. Geochem.* **13**, 1153-1162.

Palacas J.G., Monopolis D., Nicolaou C.A. and Anders D.E. (1986) Geochemical correlation of surface and subsurface oils, Western Greece. *In Advances in Organic Geochemistry* 1985 (Edited by Leythaeuser D. and Rullkötter J.). Pergamon Press, Oxford., 417-423.

Peters K.E. (1986) Guidelines for evaluating petroleum source rocks using programmed pyrolysis. *A. A. P. G. Bull.* **70**, 318-329.

Peters K.E., Moldowan J.M. and Sundararaman P. (1989) Effects of hydrous pyrolysis on biomarker thermal maturity parameters: Monterey Phosphatic and Siliceous members. *Org. Geochem.* **15**, 249-269.

Peters K.E. and Moldowan J.M. (1990) effects of source, thermal maturity and biodegradation on the distribution and isomerisation of homohopanes in petroleum. *Org. Geochem.* **15**, 249-265.

Philp R.P (1985) Fossil fuel biomarkers, applications and spectra. Elsvier Science Publishers.

Philp R.P. and Gilbert T.D. (1986) Biomarker distributions in Australian oils predominantly derived from terrigenous source material. *Org. Geochem.* **10**, 73-84.

Philp R.P. and Engel M.H (1987) The effects of migration on the distribution of biomarkers and stable carbon isotopic composition of crude oils. Migration of hydrocarbons in sedimentary basins. (Edition Technip). 615-632.

Philp R.P. Jinggui L. and Lewis C.A. (1989) An organic geochemical investigation of crude oils from Shanganing, Jianghan, Chaidamu and Zhunger Basins, People's Republic of China. *Org. Geochem.* **14**, 447-460.

Philippi G.T. (1975) The deep subsurface temperature controlled origin of the gaseous and gasoline range hydrocarbons of petroleum. *Geochim. Cosmochim. Acta.* **39**, 1353-1373.

Powell T.G. and McKirdy D.M. (1973) Relationship between ratio of pristane and phytane, crude oil composition and geological environment in Australia. *Nat. Phys. Sci.* **243**, 37-39.

Powell T.G. (1987) Depositional controls on source rock character and crude oil composition. *In.Proc.Twelveth.World.Pet.Cong.* **2.** Exploration. Wiley., 31-42.

Pym J.M., Ray J.E., Smith G.W. and Whitehead E.V. (1975) Petroleum triterpane fingerprinting of crude oils. *Anal. Chem.* **47**, 1617-1622.

Radke M. (1987) Organic Geochemistry of aromatic hydrocarbons.*In Advances in Petroleum Geochemistry* (Edited by Brooks J. and Welte D.H.). Vol **2**. Academic Press, London. 141-207.

Raymond A.C. and Murchison. D.C. (1991) Effect of igneous activity on molecular indices in different types of organic matter. *Org. Geochem.* (in press).

Reed J.D., Illich H.A. and Horsfield B. (1986) Biochemical evolutionary significance of Ordovician oils and their source rocks. *In Advances in Organic Geochemistry* 1985 (Edited by Leythaeuser D. and Rullkötter J.). Pergamon Press, Oxford. 347-358.

Requejo A.G. Hsu C.S. and Dechert G. (1991) Methyl steranes in marine source rocks. *Organic Geochemistry, Advances and Applications in Energy and the Natural environment.* 15th Meeting of the European Association of Organic Geochemists. Poster Abstracts (Edited by Manning D.). Manchester University Press, 201-205.

Riediger C.L., Fowler M.G., Brooks P.W. and Snowdon L.R. (1990) Triassic oils and potential Mesozoic source rocks, Piece River Arch, Western Canada Basin. *In Advances in Organic Geochemistry* 1989 (Edited by Durand B. and Behar F.). Pergamon press, 295-305.

Riolo J. and Albrecht P. (1985) Novel rearranged ring C-monoaromatic steroid hydrocarbons in sediments and petroleums. *Tetrahedron. Lett.* **26**, 2701-2704.

Riolo J., Ludwig B. and Albrecht P. (1985) Synthesis of ring C-monoaromatic steroid hydrocarbons occuring in geological samples. *Tetrahedron. Lett.* **26**, 2697-2700.

Riolo J., Hussler G., Albrecht P., and Connan J.L. (1986) Distribution of aromatic steroids in geological samples. Their evaluation as geochemical parameters. *In Advances in Organic Geochemistry* 1985 (Edited by Leythaeuser D. and Rullkotter J.). Pergamon Press, Oxford, 981-990.

Risatti J.B., Rowland S.J., Yon D.A. and Maxwell J.R. (1984) Stereochemical studies of acyclic isoprenoids -XII. Lipids of methanogenic bacteria and possible contributions to sediments. *In Advances in Organic Geochemistry* 1983 (Edited by Schenck P.A., De Leeuw J.W. and Limbach G.W.M.). Pergamon Press, 93-104

Robinson N. and Eglinton G. (1990) Lipid chemistry of Icelandic hot spring microbial mats. *Org. Geochem.* **15**, 291-298.

Robinson N., Eglinton G., Brassell S.C. and Cranwell P.A. (1984) Dinoflagellate origin for sedimentary 4α-methyl steroids and 5α-stanols. *Nature* **308**, 439-441.

Rowland S.J., Yon D.A., Lewis C.A. and Maxwell J.R. (1985) Occurrence of 2,6,10-trimethyl-7-(3-methylbutyl)-dodecane and related hydrocarbons in the green alga Enteromorpha prolifera and sediments. *Org. Geochem.* 8, 207-213.

Rubinstein I., Sieskind O. and Albrecht P. (1975) Rearranged sterenes in a shale: Occurrence and simulated formation. *J. chem. Soc. Perkin. 1*, 1833-1836.

Rubinstein I. and Strausz O.P (1979) Geochemistry of the thiourea adduct fraction from an Alberta petroleum. *Geochim. Cosmochim. Acta.* **43**, 1387-1392.

Rullkötter J. and Philp R.P. (1981) Extended hopanes up to C_{40} in Thorton bitumen. *Nature* **292**, 616-618.

Rullkötter J., Spiro B. and Nissenbaum A. (1985) Biological marker of oils and asphalts from carbonate source rocks in a rapidly subsiding graben, Dead Sea, Israel. *Geochim. Cosmochim. Acta.* **49**, 1357-1370.

Rullkötter J. Meyers P.A. Schaefer R.G. Dunham K.W. (1986) oil generation in the Michigan Basin: a biological marker and stable isotope approach. *Org. Geochem.* **10**, 359-375.

Schaefer R.G., Weiner B. and Leythaeuser D. (1978) Determination of sub-nanogram per gram quantities of light hydrocarbons (C_2-C_9) in rock samples by hydrogen stripping in the flow system of a capillary gas chromatograph. *Anal. Chem.* **50**, 1848-1854.

Schaefer R.G., Welte D.H. and Pooch H. (1984) Geochemistry of low molecular weight hydrocarbons in two exploration wells of the Elmworth gas field (Western Canada Basin). *Org. Geochem.* **6**, 695-701.

Schaefer R.G. and Littke R. (1987) Maturity-related compositional changes in the low-molecular-weight hydrocarbon fraction of Toarcian shales. *Org. Geochem.* **13**, 887-892.

Schi Ji Yang, Mackenzie A.S., Alexander R., Gomar A.P., Wolff G.A. and Maxwell J.R. (1982) A biological marker investigation of petroleum and shales from the Shengli oilfield, the People's Republic of China. *Chem. Geol.* **35**, 1-31.

Seifert W.K. and Moldowan J.M. (1978) Application of steranes, terpanes and monoaromatic steroids to the maturity, migration for source-rocks and crude oils. *Geochim. Cosmochim. Acta.* **42**, 77-95.

Seifert W.K., Moldowan J.M., Smith G.W. and Whitehead E.V. (1978) First proof of structure of a C_{28}-pentacyclic triterpane in petroleum. *Nature* **271**, 436-437.

Seifert W.K. and Moldowan J.M. (1980) The effect of thermal stress on source rock quality as measured by hopane stereochemistry. *In Advances in Organic Geochemistry* 1979 (Edited by Douglas A.G. and Maxwell J.R.). Pergamon Press, Oxford. 229-237.

Seifert W.K. and Moldowan J.M. (1981) Paleoreconstruction by biological mnarkers. *Geochim. Cosmochim. Acta.* **45**, 783-794.

Shiea J. Brassell S.C. and Ward D.M. (1990) Mid-chain branmched mono- and dimethylalkanes in hot spring cyanobacterial mats: a direct biogenic source for branched alkanes in ancient sediments?. *Org. Geochem.* **15**, 223-232.

Sieskind O., Joly G. and Albrecht P. (1979) Simulation of the geothermal transformations of sterols. Superacid effect of clay minerals. *Geochim. Cosmochim. Acta.* **43**, 1675-1679.

Snowdon L.R. and Powell T.G. (1982) Immature oil and condensate. Modification of hydrocarbon generation model for terrestrial organic matter. *A. A.P. G. Bull.* **66**, 775-788.

Solli H., Schou L. Krane J., Skjetne T. and Leplat P. (1985) Characterisation of sedimentary organic matter using nuclear magnetic resonance and pyrolysis techniques. *In Petroleum Geochemistry in exploration of the Norwegian Shelf*, Norwegian Petroleum Society. Graham and Trottman, London. 309-317.

Sonatrach internal report (1971) Geological and estimation of oil and gas in the Sahara in Algeria.

Sonatrach internal report (1980) Evaluation des potentialités en hydrocarbure. Depression de Ghadames.

Sonatrach internal report (1985) Etude geochimique de la region d'El Borma-Ghadames.

Sonatrach internal report (1989) Etude geochimique de la region de Gherguit-El-Kihal (GKN1).

Strachan M.G., Alexander R., Subroto E.A. and Kagi R.I. (1989) Constraints upon the use of 24-ethylcholestane diastereomer ratios as indicators of thermal maturity of petroleum. *Org. Geochem.* **14**, 423-432.

Summons R.E. (1987) Branched alkanes from ancients and modern sediments: Isomer discrimination by GC/MS with multiple reaction monitoring. *Org. Geochem.* 11. 281-289.

Summons R.E. and Powell T.G. (1987) Identification of aryl isoprenoids in some source rocks and crude oils: Biological marker from the Green Sulphur bacteria. *Geochim. Cosmochim. Acta.* **51**, 557-566.

Summons R.E., Volkman J.K. and Boreham C.J. (1987) Dinosterane and other hydrocarbons of dinoflagellate origin in sediments and petroleum. *Geochim. Cosmochim. Acta.* **51**, 3075-3082.

Summons R.E. and Capon R.J. (1988) Fossil steranes with unprecedented methylation in ring-A. *Geochim. Cosmochim. Acta.* **52**, 2733-2736.

Summons R.E., Powell T.G. and Boreham C.J. (1988) Petroleum geology and geochemistry of the Middle Proterozoic McArthur Basin, Northern Australia: III. Composition of extractable hydrocarbons. *Geochim. Cosmochim. Acta.* **52**, 1747-1763.

Summons R.E. and Jahnke L.L. (1990) Identification of the methylhopanes in sediments and petroleum. *Geochim. Cosmochim. Acta.* **54**, 247-251.

Summons R.E. and Walter M.R. (1990) Molecular and microfossils of prokaryotes and protistes from Proterozoic sediments. *Am. J. Sci.* **290**, 212-244.

Summons R.E and Capon R.J. (1991) Identification of 3ß-ethyl- steranes in sediments and petroleum. *Geochim. Cosmochim. Acta.* **55**, 2391-2395.

Telnaes N. and Dahl B. (1986) Oil-oil correlation using multivariate techniques. *Org. Geochem.* **10**, 425-432.

Telnaes N., Bjorseth A., Christy A.A. and Kvalheim O.M. (1987) Interpretation of multivariate data: Relationship between phenanthrene in crude oils. *Chemometrics and intelligent Laboratory Systems*, Vol **2**, 149-153.

Telnaes N. and Cooper B.S. (1991) Oil-source rock correlation using biological markers, Nowegian continental shelf. *Mar. Pet. Geol.* **8**, 302-310.

Thompson K.F.M. (1979) Light hydrocarbons in subsurface sediments. *Geochim. Cosmochim. Acta.* **43**, 657-672.

Thompson K.F.M (1983) Classification and thermal history of petroleum based on light hydrocarbons. *Geochim. Cosmochim. Acta.* **47**, 303-316.

Thompson K.F.M (1987) Fractionated aromatic petroleum and the generation of gas-condensates. *Org. Geochem.* **11**, 573-590.

Thompson K.F.M (1988) Gas-condensate migration and oil fractionation in Deltaic sediments. *Mar. Pet. Geol.* **5**, 237-246.

Tirasoo E.N. (1984) Oilfields of the world (third edition). Scientific Press Ltd. Beaconsfield, England.

Tissot B.P., Califet-Debyser Y., Deroo G. and Oudin J.L. (1971) Origin and evolution of hydrocarbons in early Toarcian shales, Paris basin, France. *A. A. P. G. Bull.* **55**, 2177-2193.

Tissot B., Durand B., Espitalié J. and Combaz A. (1974a) Influence of nature and diagenesis of organic matter in formation of Petroleum. *A. A. P. G. Bull.* **58**, 499-506.

Tissot B., Espitalié J., Deroo G., Temper C. and Jonathan D. (1974b) Origin and migration of hydrocarbon in the Oriental Sahara (Algeria). *In Advances in Organic Geochemistry* 1973 (Edited by Tissot B. and Bennier F.). Editions Technip, 315-334.

Tissot B.P. Demaison G., Masson P., Delteil J.R. and Combaz A. (1980) Paleoenvironment and petroleum potential of Middle Cretaceous Black shales in Atlantic Basins. *A. A. P. G. Bull.* **64**, 2051-2063.

Tissot B.P. and Welte D.H. (1984) Petroleum Formation and occurrence, 2nd edn, 699 pp. Springer, Berlin.

Tornabene T.B., Langworthy T.A., Holzer G. and Oro J. (1979) Squalene, phytanes and other isoprenoids as major neutral lipids of methanogenic and thermoacidophilic "archaebacteria". *J.Mol.evol.* **13**, 73-83.

Traverse A. (1988) Paleopalynology. Unwin Hyman Ltd, London.

Trendel J.M., Restle A., Connan J. and Albrecht P. (1982) Identification of a novel series of tetracyclic terpane hydrocarbons (C_{24}-C_{27}) in sediments and petroleums. *J. Chem. Soc. Chem. Comm*um. 304-306.

Van Dorsselear A., Esminger A., Spyckerelle C., Dastillung M., Sieskind D., Arpino P., Albrecht P. and Ourisson G. (1974) Degraded and extended hopane derivatives (C_{27}-C_{35}) as ubiquitous geochemical markers. *Tetrahedron. Lett.* **14**, 1349-1352.

Van Graas W.G. (1990) Biomarker maturity parameters for high maturities. Calibration of the working range up to the oil/condensate threshold. *In Advances in Organic Geochemistry* 1989 (Edited by Durand B. and Behar F.). 1025-1032.

Vankatesan M.I. (1989) Tetrahymanol: its widespread occurrence and geochemical significance. *Geochim. Cosmochim. Acta.* **53**, 3095-3101.

Volkman J.K., Alexander R. and Kagi R.I. (1983) GC-MS characterisation of C_{27} and C_{28} triterpanes in sediments and Petroleum. *Geochim. Cosmochim. Acta.* **47**, 1033-1040.

Volkman J.K. (1986) A review of sterols markers for marine and terrigenous organic matter. *Org. Geochem.* **9**, 83-99.

Volkman J.K. and Maxwell J.R. (1986) Acyclic isoprenoids as biological markers. *In Biological markers in sedimentary record.* Amsterdam., Eslvier, 1-42.

Volkman J.K., Kearney P. and Jeffrey S.W. (1990a) A new source of 4-methyl sterols and 5α(H)-slanols in sediments: *Prymnesiophyte* microalgae of the genus Pavlova. *Org. Geochem.* **15**, 489-497.

Volkman, J.K., Banks, M.R., Denwer, K. and Aquino Neto, F.R. (1990b) Biomarker composition and depositional setting of Tasmanite oil shale from Northern Tasmania, Australia. *Org. Geochem.* (In press).

Waples D.W., Haug P. and Welte D.H. (1974) Occurrence of a regular C_{25} isoprenoid hydrocarbon in tertiary sediments representing a lagoonal saline environment. *Geochim. Cosmochim. Acta.* **38**, 381-387.

Warburton G.A. and Zumberge J.E. (1983) Determination of petroleum sterane and triterpane distributions by mass spectrometry with selective metastable ion monitoring. *Anal. Chem.* **55**, 123-125.

Welte D.H. Kratochvil H., Rullkötter J., Ladwein H. and Schaefer R.G. (1982) Organic geochemistry of crude oils from the Vienna Basin and an assessment of their origin. *Chem. Geol.* **35**, 33-68.

West N., Alexander R. and Kagi R.I. (1990) The use of silicalite for rapid isolation of branched and cyclic alkane fractions of petroleum. *Org. Geochem.* **15**, 499-501.

Whitehead E.V. (1973) The structure of petroleum pentacyclanes. *In Advances in Organic Geochemistry* 1973 (Edited by Tissot B. and Bennier F.). Editions Technip, 225-243.

Winger M.G. and Pomerantz M. (1986) Structure and significance of some twenty-one and twenty-two carbon petroleum steranes. *Geochim. Cosmochim. Acta.* **50**, 2763-2769.

Yon D.A Maxwell J.R and Ryback G. (1982) 2,6,10-trimethyl-7-(3-methylbutyl)-dodecane, a novel sedimentary biological marker compound. *Tetrahedron. Lett.* **23**, 2143-2146.

Zhao-An F. and Philp R.P. (1987) Laboratory biomarker fractionation and implications on migration studies. *Org. Geochem.* **11**, 169-175.

Zumberge J.E. (1983) tricyclic diterpane distributions in the correlation of Paleozoic crude oils from the Williston Basin. *In Advances in Organic Geochemistry* 1981 (Edited by BjorFy M. et al.). Wiley Chichester, 738-745.

Zumberge J.E. (1984) Source rocks of the Luna Formation (Upper Cretaceous) in the Middle Magdalena Valley. *In Petroleum Geochemistry and Source Rocks Potential of Carbonate Rocks. A.A.P.G., studies In Geology* #18 (Edited by Palacas J.G. et al.)., 127-133.

Zumberge J.E. (1987) Prediction of source rock characterised based on terpane biomarkers in oils: A multivariate statistical approach. *Geochim. Cosmochim. Acta.* **51**, 1625-1637.

Structures

1

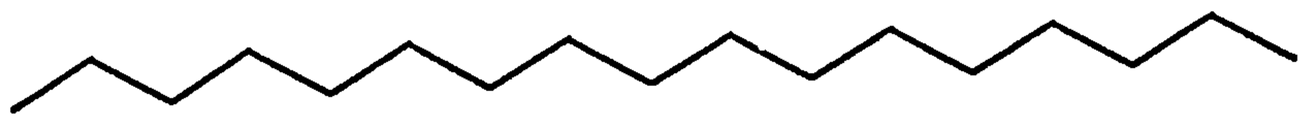

2

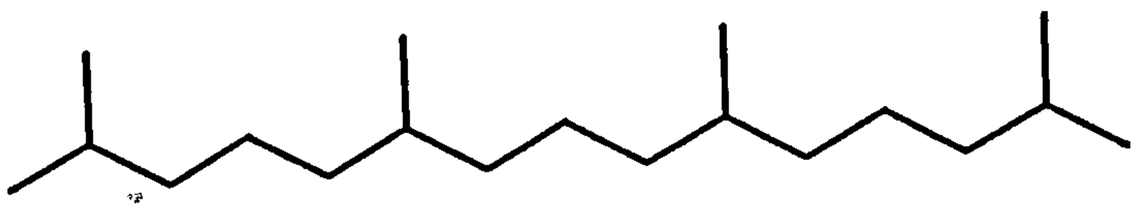

3

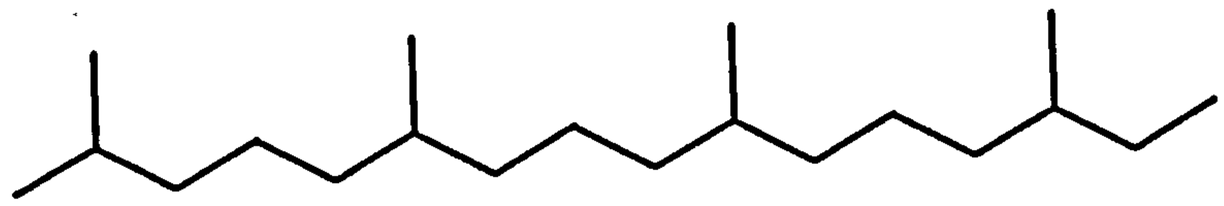

4

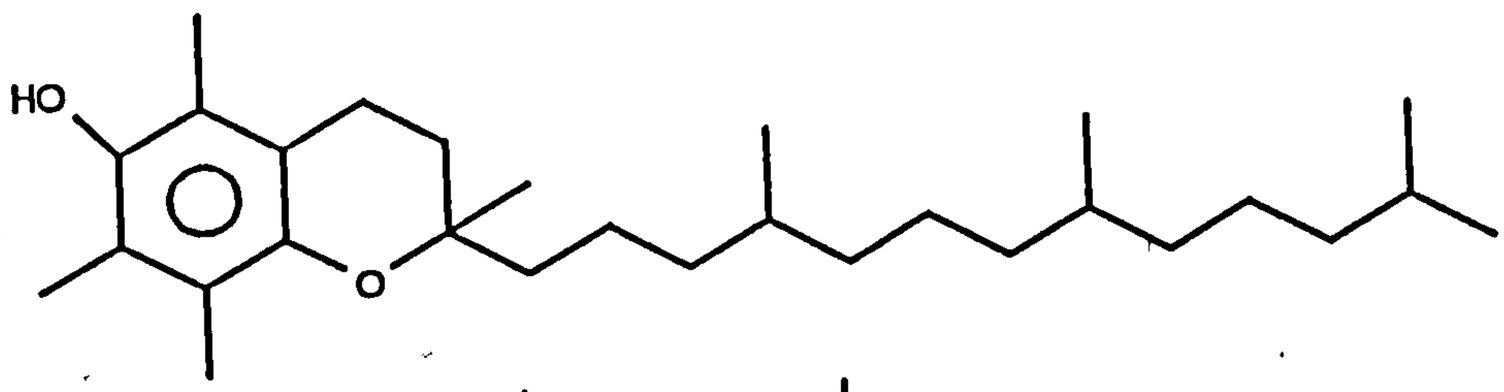

5

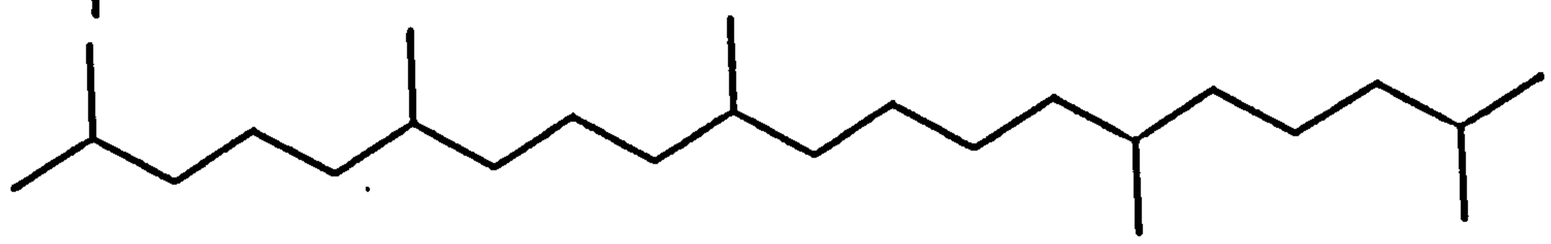

6

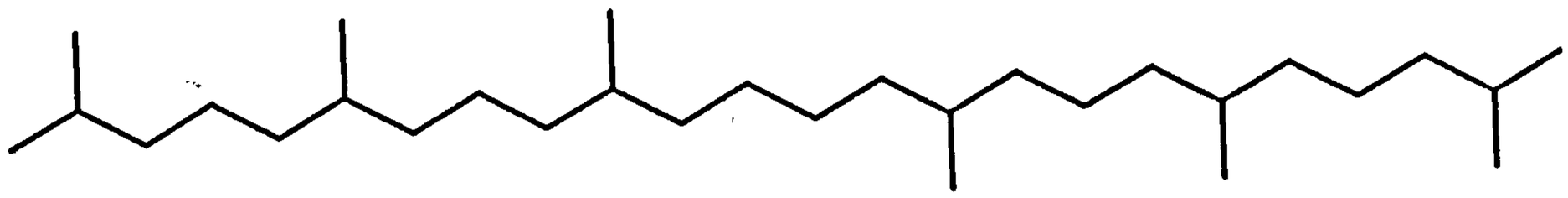

7

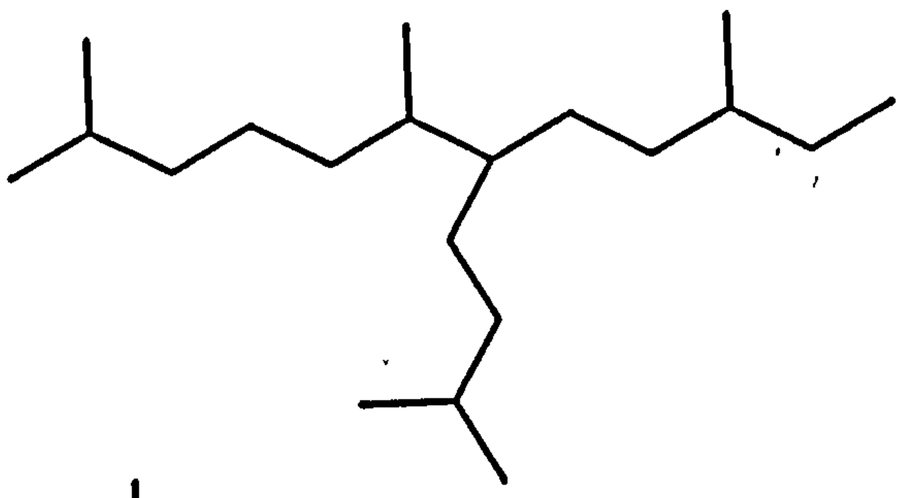

8

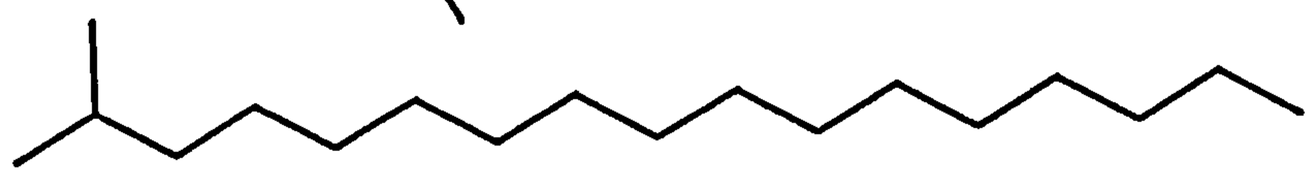

9

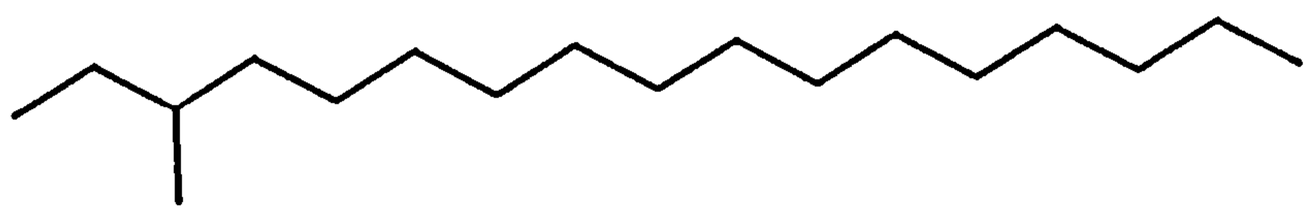

10

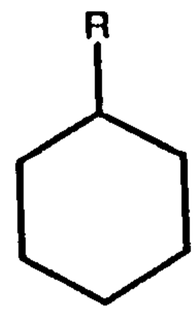

11

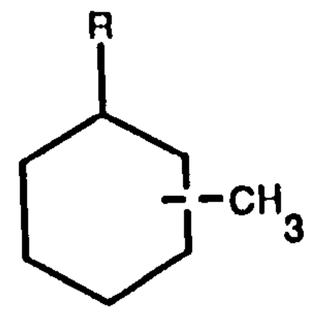

12

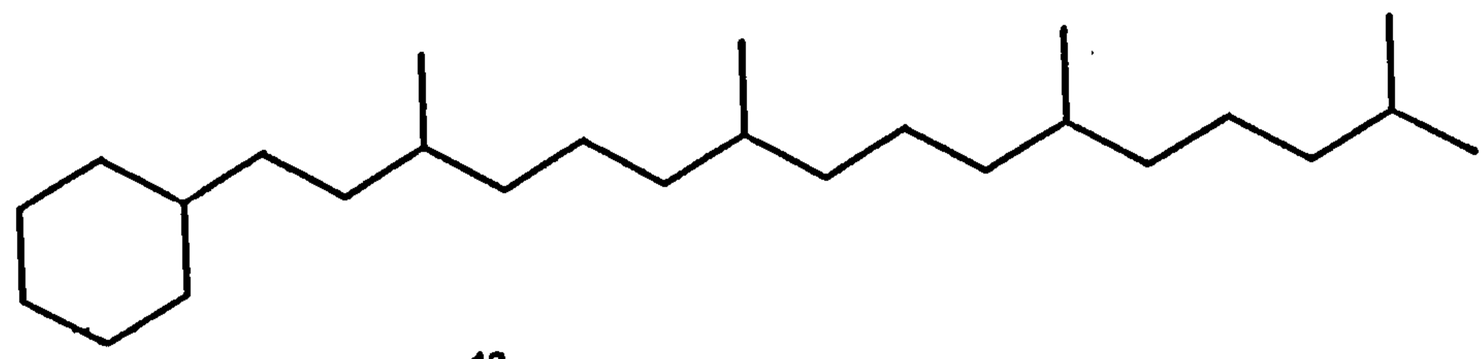

13

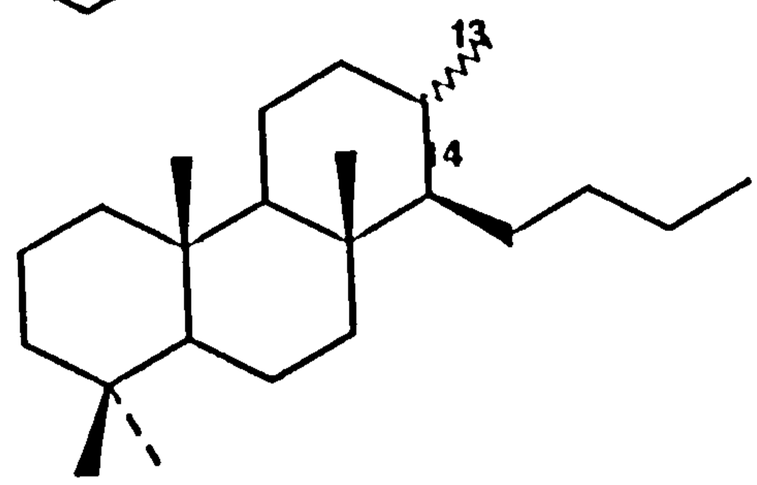

14

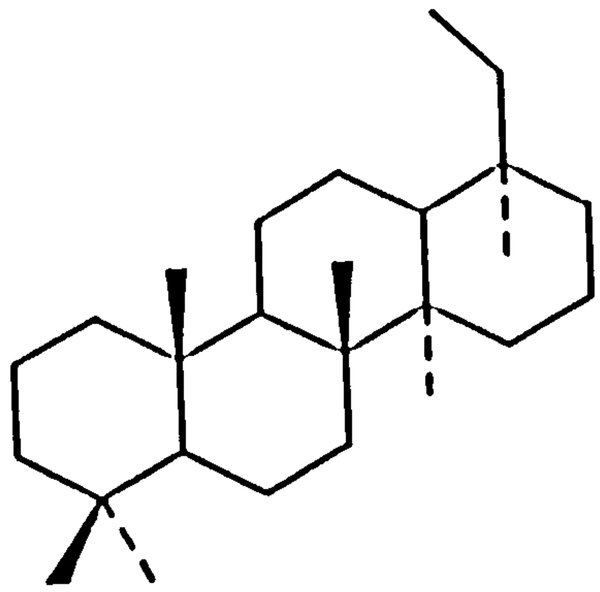

15

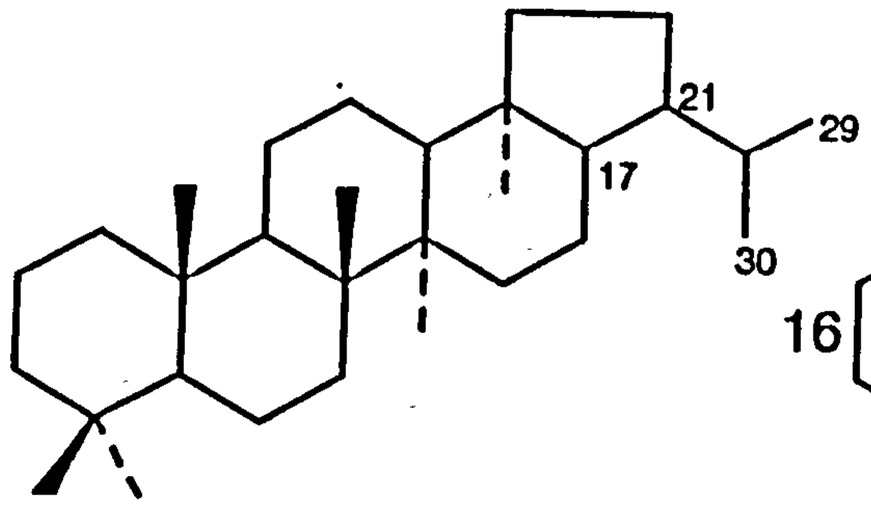

16

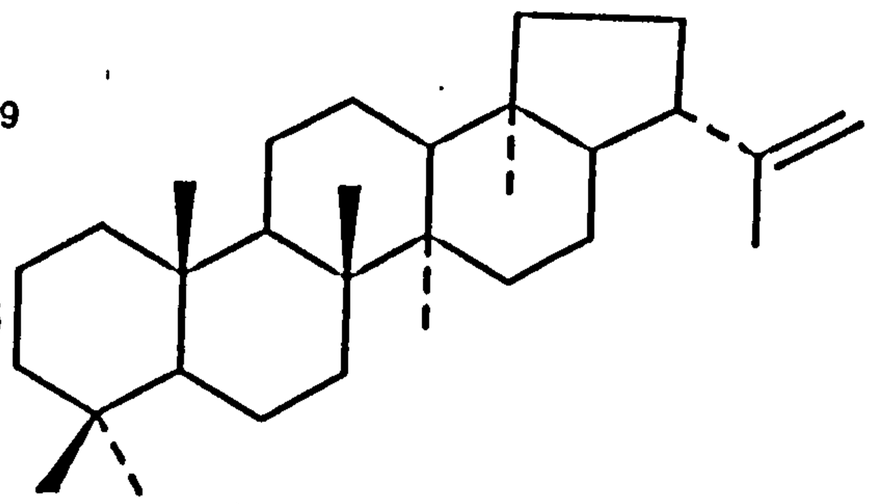

17

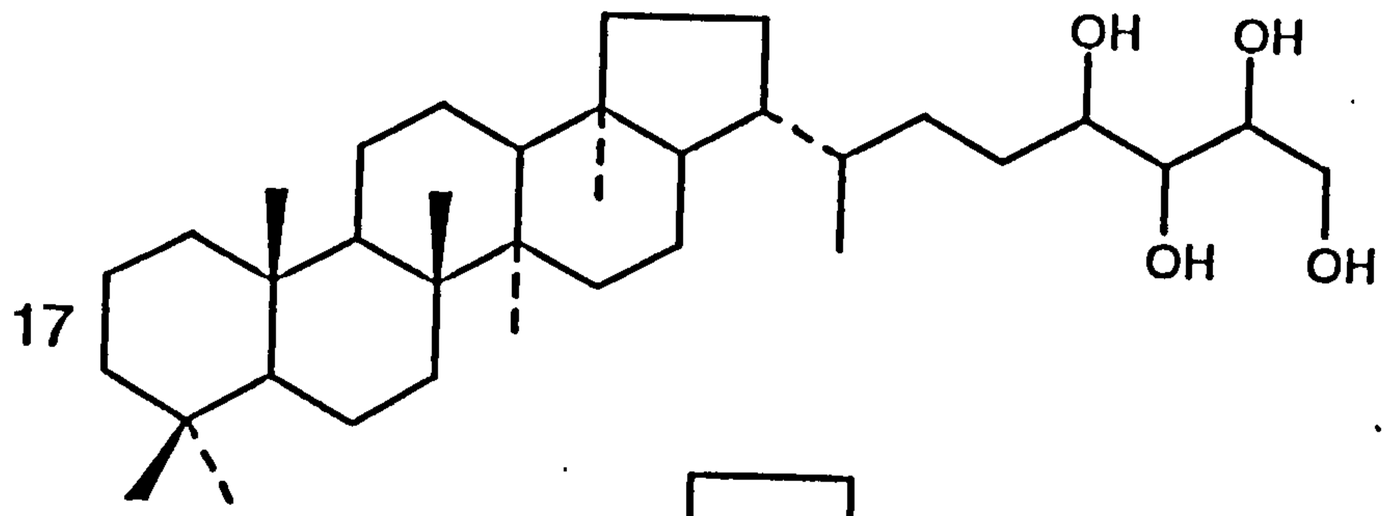

18

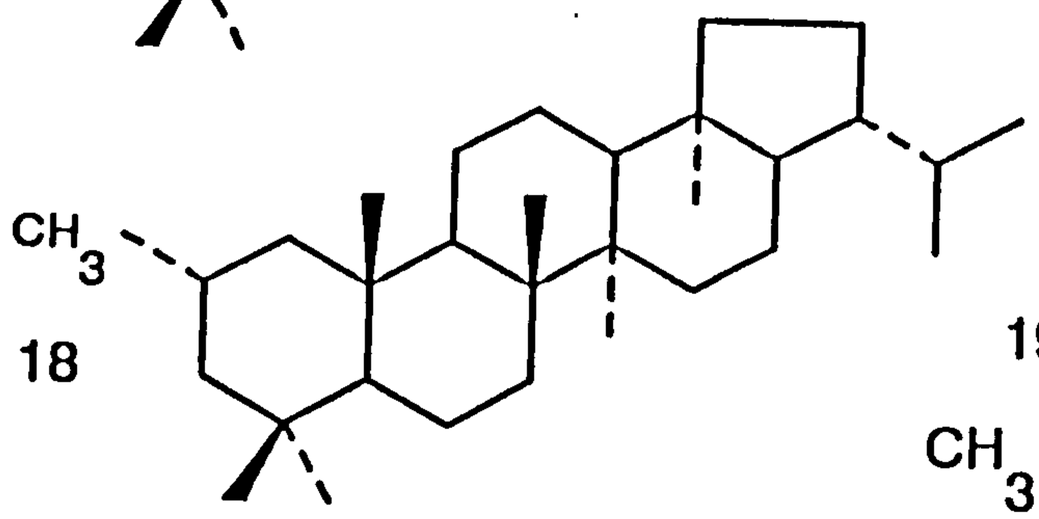

19

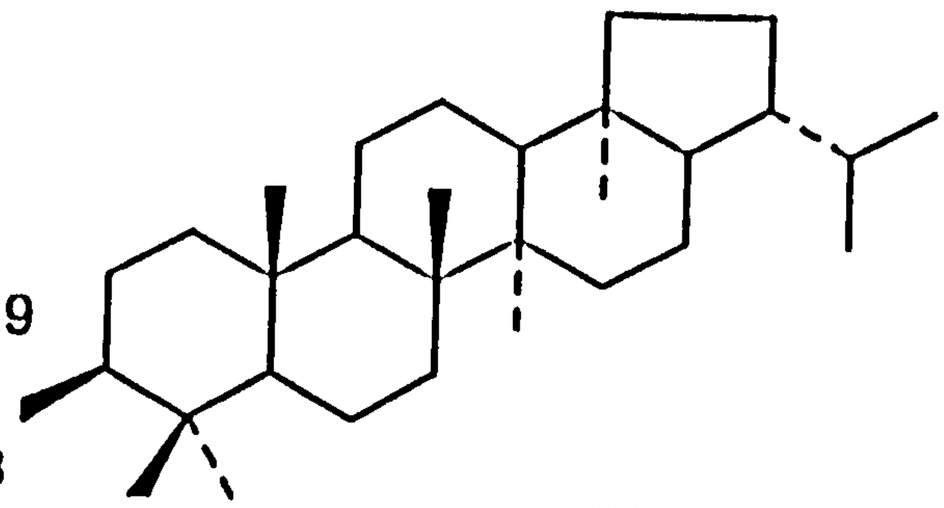

20

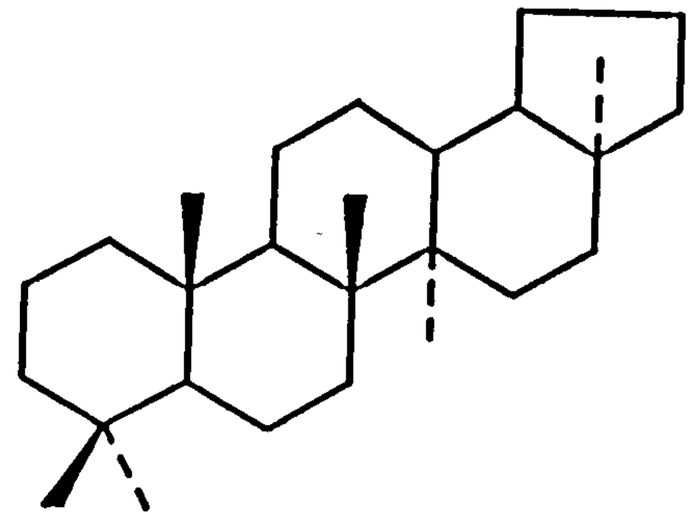

21

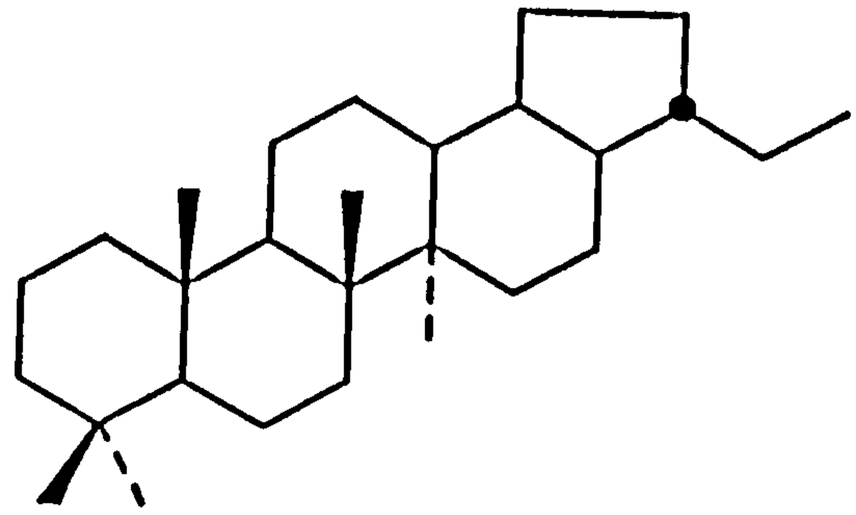

22

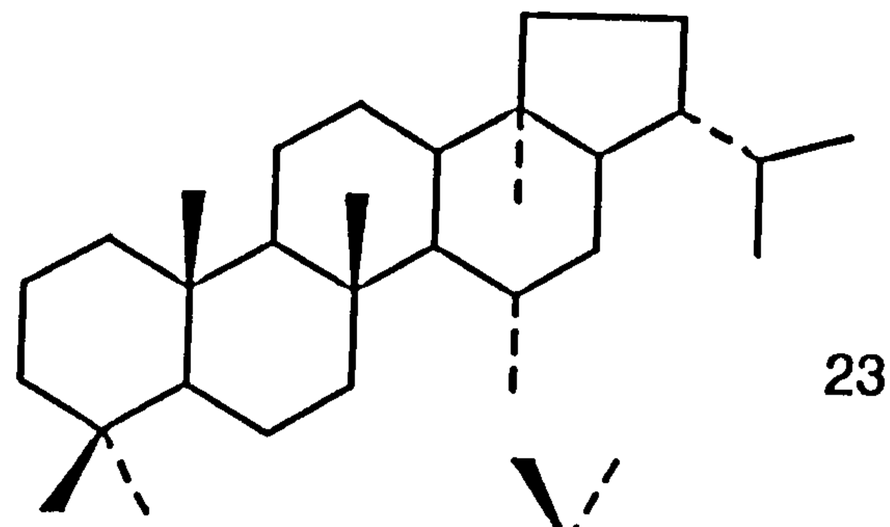

23

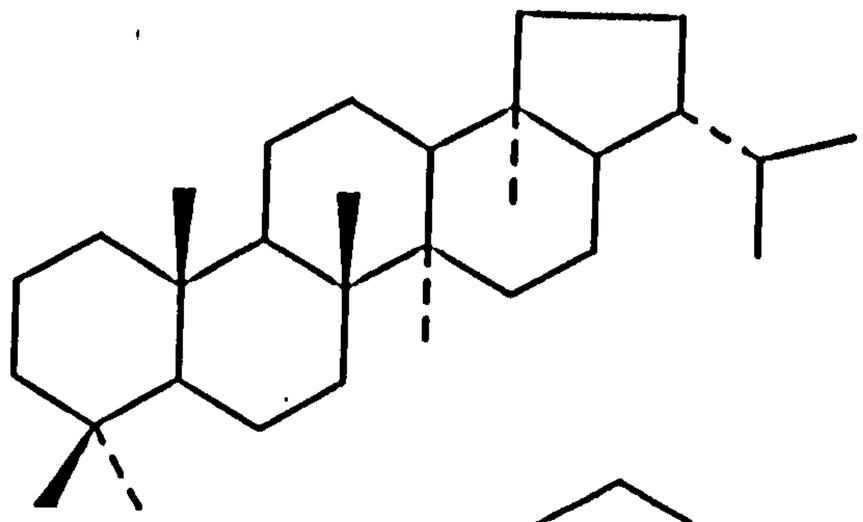

24

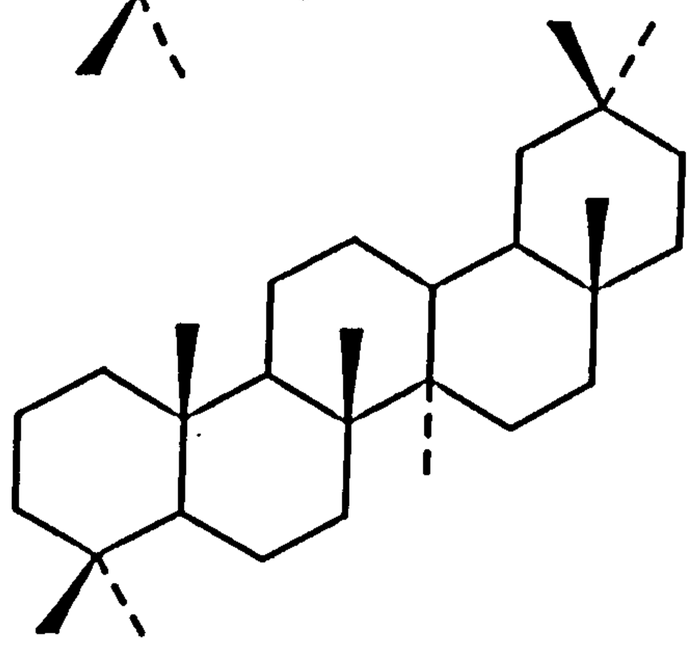

25

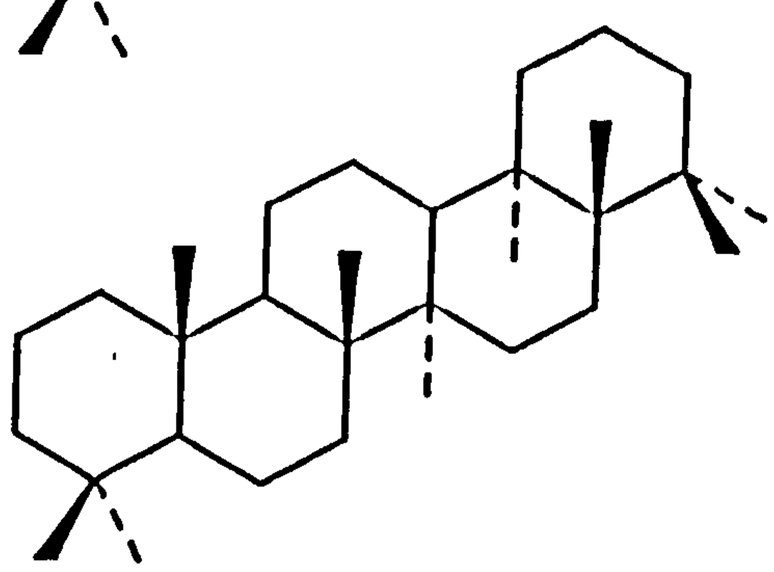

26

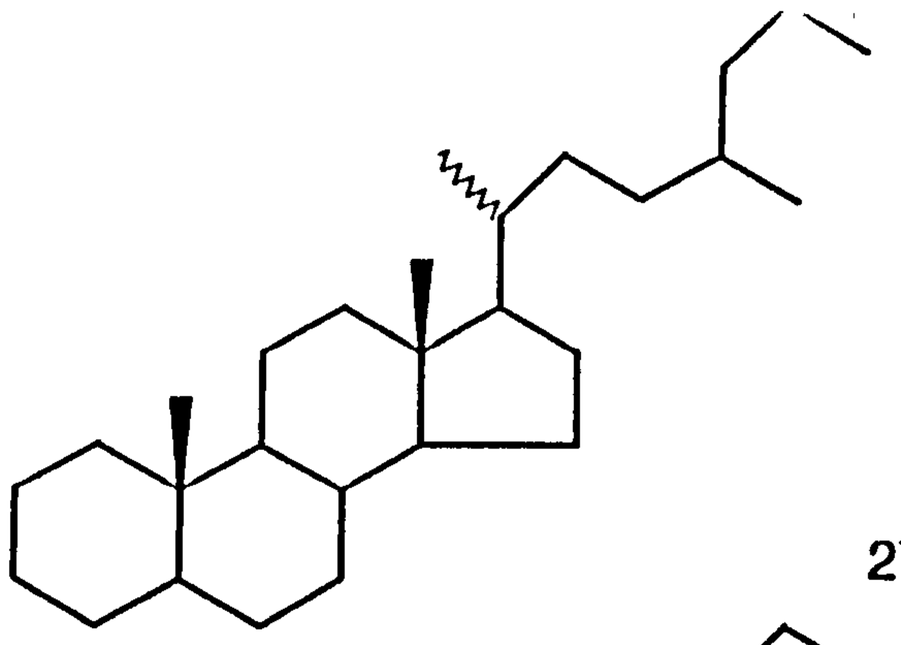

27

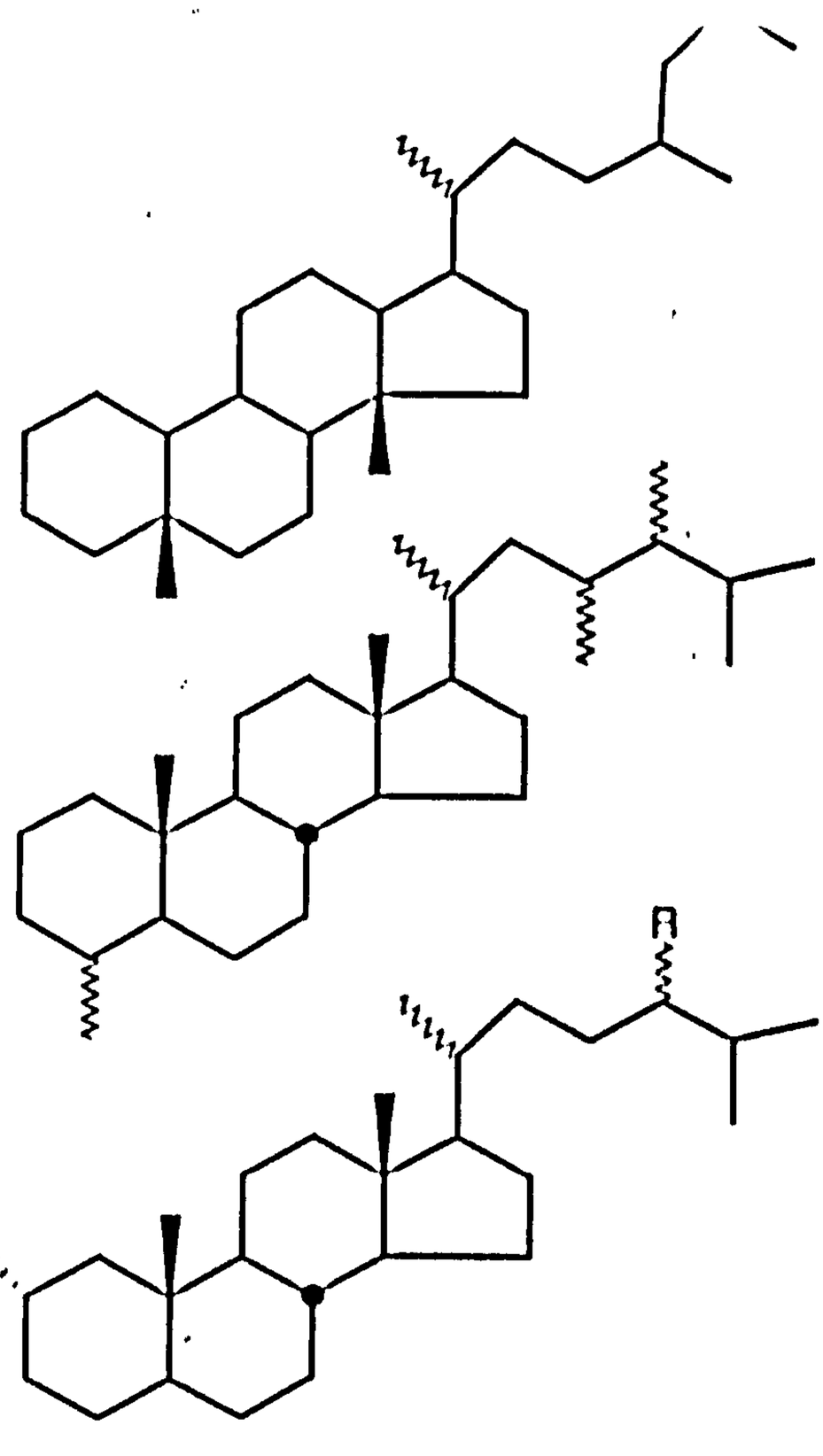

28

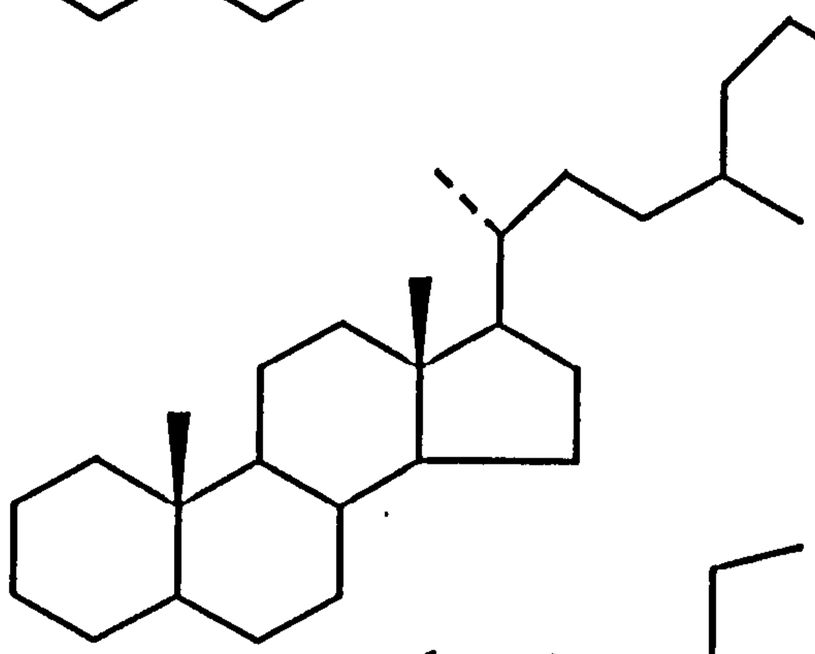

29

30

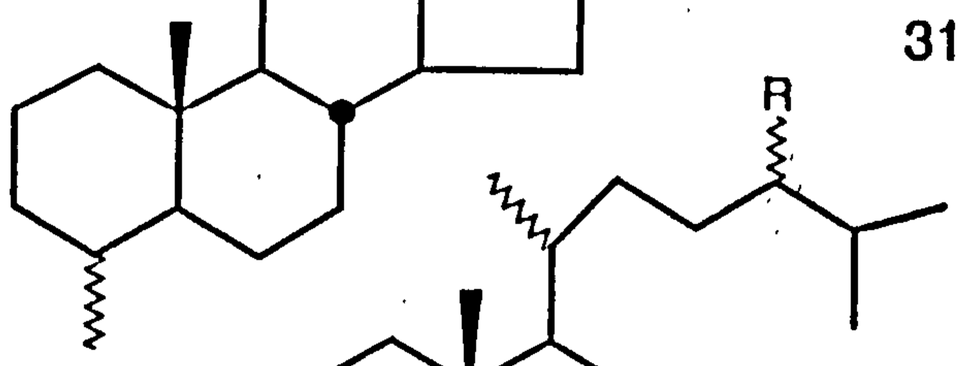

31

32

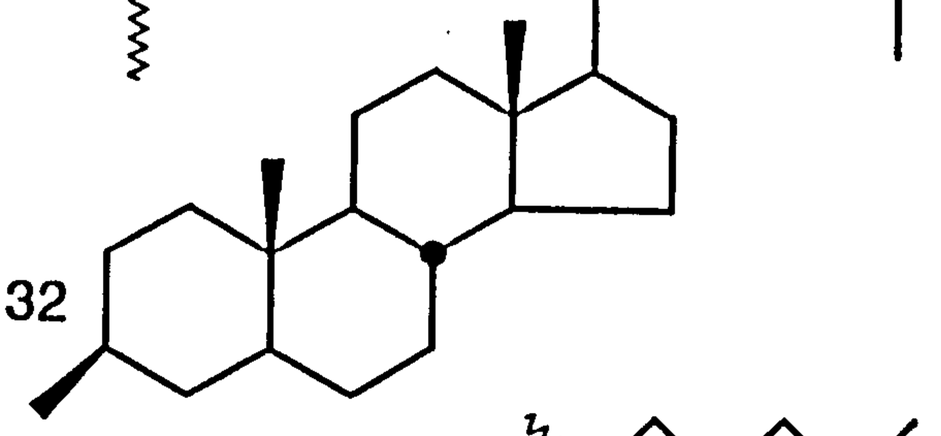

33

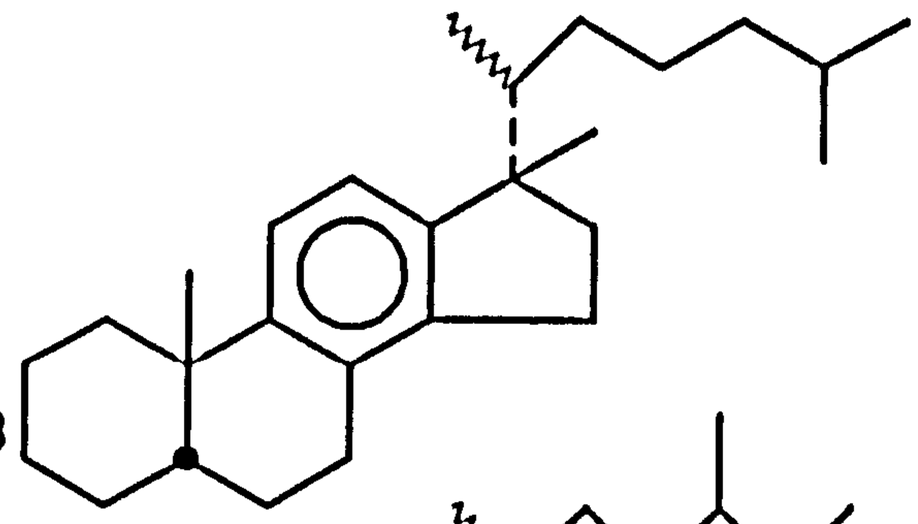

34

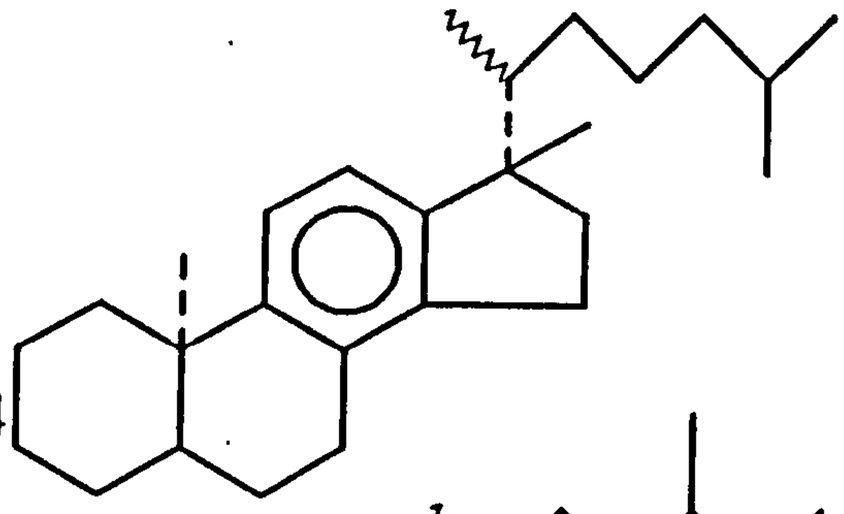

35

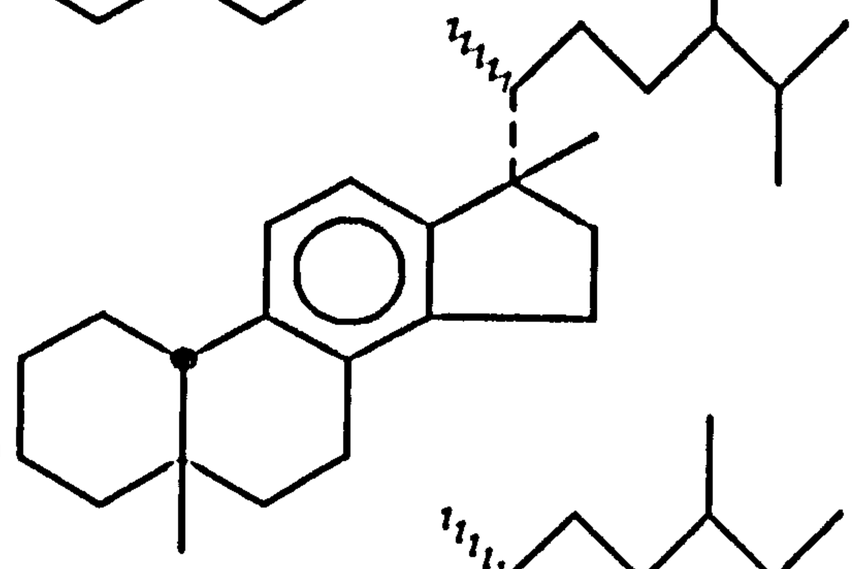

36

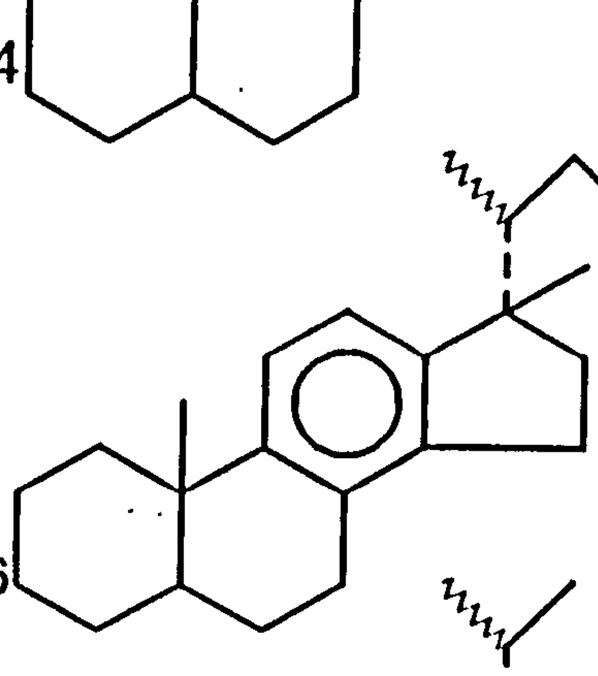

37

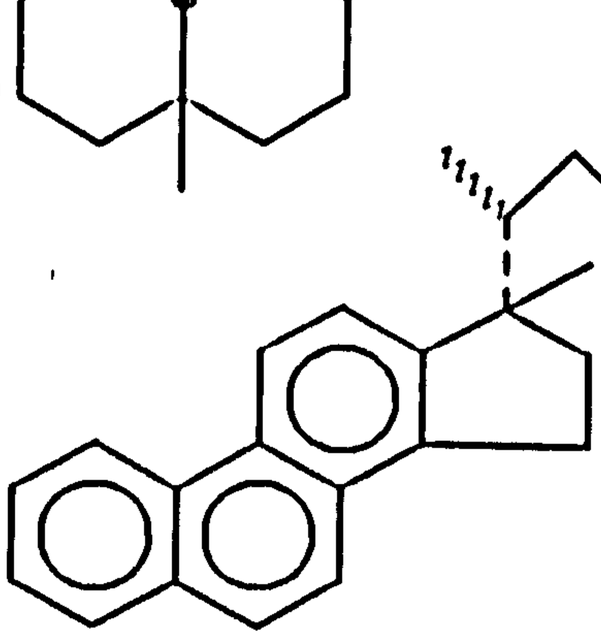

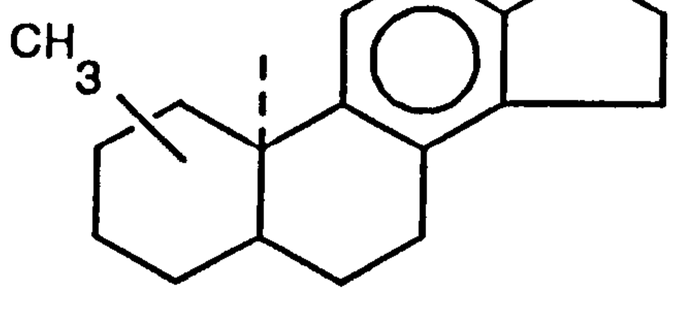

39

40

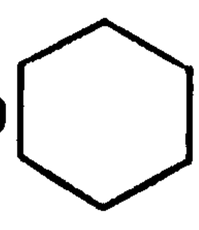

41

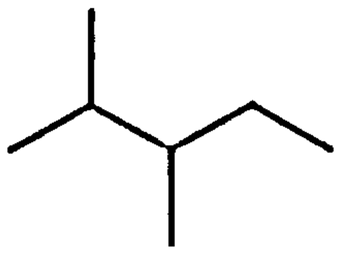

Appendix

Appendix 3.1 Geological and bulk geochemical data for source rocks.

well	depth (m)	age	lithology	spore fluorescence	VR/E
SOH-1	3192.50	Silurian	silty shale	MO-Red	0.75-1.00
SOH-1	3201.80	Silurian	silty shale	MO-Red	0.75-1.00
SOH-1	3398.40	Ordovician	shale-sandstone		1.19
MRK-1	3196.46	Ordovician	shale	MO-Red	0.75-1.00
MRK-1	3201.45	Ordovician	shale	MO-Red	0.75-1.00
MRK-1	3299.45	Ordovician	shale		>1.00
MRK-1	3306.45	Ordovician	shale		>1.00
MRK-1	3309.45	Ordovician	shale		>1.00
KA-1 bis	2605.65	Triassic	marl	Y-LO	0.4-0.5
KA-1 bis	3029.82	Silurian	shale	Y-LO	0.4-0.5
KA-1 bis	3060.90	Silurian	shale	Y-LO	0.4-0.5
KA-1 bis	3072.85	Silurian	shale	Y-LO	0.4-0.5
KA-1 bis	3168.55	Ordovician	shale		>1.00
KA-1 bis	3179.85	Ordovician	shale		>1.00
KA-1 bis	3182.85	Ordovician	shale		>1.00
RE-1	3040.00	Devonian	shale	Y-LO	0.4-0.5
RE-1	3050.25	Devonian	shale	Y-LO	0.4-0.5
RE-1	3103.90	Devonian	shale	Y-LO	0.4-0.5
RE-1	3114.70	Devonian	shale	Y-LO	0.4-0.5
RE-1	3202.20	Devonian	shale	LO-MO	0.65-0.75
RE-1	3346.20	Devonian	shale	LO-MO	0.65-0.75
RE-1	3354.40	Devonian	shale	LO-MO	0.65-0.75
RE-1	3438.26	Devonian	shale	LO-MO	0.65-0.75
ZAR-1	3450.98	Devonian	shale	Y-LO	0.4-0.5
ZAR-1	3514.20	Devonian	shale	Y-LO	0.4-0.5
ZAR-1	3994.65	Silurian	marly shale	LO-MO	0.65-0.75
REA-1	2764.56	Silurian	shale	Y-LO	0.4-0.5
REA-1	2768.21	Silurian	shale	Y-LO	0.4-0.5
ELB-3	2372.20	Triassic	marl	Y-LO	0.4-0.5
ELB-2	2379.00	Triassic	carb.shale	Y-LO	0.4-0.5

spore fluorescence:
MO-Red= middle orange-red
Y-LO= yellow-light orange
LO-MO= light orange-middle orange

Appendix 3.1 Geological and bulk geochemical data for source rocks.

well	depth (m)	age	lithology	spore fluorescence	VR/E
ZM-1	2388.40	Silurian	silty shale	Y-LO	0.4-0.5
ZM-1	2388.75	Silurian	silty shale	Y-LO	0.4-0.5
ZM-1	2483.58	Silurian	silty shale	LO-MO	0.65-0.75
ZM-1	2674.90	Ordovician	silty shale	LO-MO	0.65-0.75
ZM-1	2694.84	Ordovician	silty shale	LO-MO	0.65-0.75
ZM-1	2701.90	Ordovician	silty shale	LO-MO	0.65-0.75
RYB-1	3106.30	Devonian	shale	LO-MO	0.65-0.75
RYB-1	3110.20	Devonian	shale	LO-MO	0.65-0.75
RYB-1	3617.06	Devonian	shale	MO-Red	0.75-1.00
RYB-1	3627.50	Devonian	shale		1.34
RYB-1	3665.45	Devonian	shale		1.25
RYB-1	3704.50	Devonian	shale		1.23
RYB-1	3751.50	Devonian	shale		1.25
RYB-1	3762.40	Devonian	shale		1.31
RYB-1	3897.90	Devonian	shale		1.55
RYB-1	3901.80	Devonian	shale		1.57
RYB-1	4095.15	Devonian	shale		2.22
SED-1	2642.00	Devonian	silty shale	LO-MO	0.57
SED-1	2653.23	Devonian	silty shale	LO-MO	0.73
SED-1	2872.15	Devonian	shale-sandstone	LO-MO	0.96
SED-1	2877.10	Devonian	shale-sandstone	LO-MO	0.96
SED-1	3593.50	Devonian	shale-sandstone		>1.00
WT-1	3747.10	Devonian	shale	LO-MO	0.86
WT-1	3752.10	Devonian	shale	LO-MO	0.75
WT-1	3786.20	Devonian	shale	LO-MO	0.85
WT-1	3794.08	Devonian	shale	LO-MO	0.85
WT-1	4117.30	Devonian	shale		1.41
WT-1	4376.50	Devonian	shale		1.41
AKF-1	2250.06	Triassic	carb shale	LO-MO	0.62
AKF-1	2252.80	Triassic	carb shale	LO-MO	0.63

Appendix 3.2 Bulk data for source rocks.

well	depth (m)	age	lithology	%TOC	S1 kgHC/T rock	S2 kgHC/T rock	S1+S2 kgHC/T rock	S1/S1+S2	HI mg HC/ g org.C	Tmax °C
ZM-1	2388.40	Silurian	silty shale	1.01	0.09	0.59	0.68	0.13	58.42	431
ZM-1	2388.75	Silurian	silty shale	1.50	0.34	3.39	3.73	0.09	226.00	428
ZM-1	2483.58	Silurian	silty shale	0.34	0.07	0.36	0.43	0.16	105.88	435
ZM-1	2674.90	Ordovician	silty shale	0.65	0.22	0.56	0.78	0.28	86.15	436
ZM-1	2694.84	Ordovician	silty shale	1.52	0.90	0.91	1.81	0.50	59.87	424
ZM-1	2701.90	Ordovician	silty shale	1.74	0.85	7.11	7.96	0.11	408.62	443
KA-1 bis	2605.65	Triassic	marl	1.01	0.13	0.78	0.91	0.14	77.23	432
KA-1 bis	3029.82	Silurian	shale	1.46	0.39	1.68	2.07	0.19	115.07	441
KA-1 bis	3060.90	Silurian	shale	2.33	0.38	1.74	2.12	0.18	74.68	442
KA-1 bis	3072.85	Silurian	shale	3.22	0.86	5.53	6.39	0.13	171.74	423
KA-1 bis	3168.55	Ordovician	shale	0.56	0.19	0.87	1.06	0.18	155.36	441
KA-1 bis	3179.85	Ordovician	shale	0.58	0.25	1.43	1.68	0.15	246.55	441
KA-1	3182.85	Ordovician	shale	0.55	0.19	0.93	1.12	0.17	169.09	439
RE-1	3040.00	Devonian	shale	1.07	0.10	0.61	0.71	0.14	57.01	435
RE-1	3050.25	Devonian	shale	1.03	0.20	1.35	1.55	0.13	131.07	431
RE-1	3103.90	Devonian	shale	2.33	0.50	5.07	5.57	0.09	217.60	436
RE-1	3114.70	Devonian	shale	2.30	0.58	5.53	6.11	0.09	240.43	438
RE-1	3202.20	Devonian	shale	0.57	0.09	0.51	0.60	0.15	89.47	431
RE-1	3346.20	Devonian	shale	10.82	8.57	44.40	52.97	0.16	410.35	431
RE-1	3354.40	Devonian	shale	7.59	12.90	58.52	71.42	0.18	771.01	441
RE-1	3438.26	Devonian	shale	1.00	0.90	3.38	4.28	0.21	338.00	437
ZAR-1	3450.98	Devonian	shale	0.84	0.39	1.18	1.57	0.25	140.48	441
ZAR-1	3994.65	Silurian	marly shale	1.94	0.42	2.23	2.65	0.16	114.95	437
ELB-3	2372.20	Triassic	marl	1.11	0.07	0.54	0.61	0.11	48.65	433
RYB-1	3106.30	Devonian	shale	4.25	0.64	8.53	9.17	0.07	200.71	441
SED-1	2642.00	Devonian	silty shale	1.26	0.15	0.58	0.73	0.21	46.03	425
SED-1	2872.15	Devonian	silty shale	3.40	5.44	6.07	11.51	0.47	178.53	464
REA-1	2764.56	Silurian	shale	0.77	0.11	1.01	1.12	0.10	131.17	437
SOH-1	3192.50	Silurian	silty shale	0.4	0.43	0.19	0.62	0.69	47.50	423
MRK-1	3196.46	Ordovician	shale	0.41	0.10	0.16	0.26	0.38	39.02	438

Appendix 3.3 Bulk composition and geochemical data for source extracts.

well	depth(m)	age	%EOM/rock	EOM mg/org.C	%asph	%Sats	% Aro	%NSO	%Pol	Pr/Ph	Pr/n-C17	Ph/n-C18	CPI
ZM-1	2388.40	Silurian	0.14	138.60	11.14	35.52	36.08	17.26	28.39	1.42	0.54	0.37	1.00
ZM-1	2388.75	Silurian	0.26	173.30	6.98	52.32	32.29	8.41	15.39	1.65	0.75	0.59	1.09
ZM-1	2483.58	Silurian	0.05	147.00	8.89	51.86	20.26	18.99	27.88	1.65	0.10	0.06	1.09
ZM-1	2674.90	Ordovician	0.12	184.60	2.45	61.31	25.64	10.60	13.05	1.40	0.08	0.06	1.09
ZM-1	2694.84	Ordovician	0.29	190.80	2.44	57.86	31.77	7.93	10.37	1.44	0.15	0.13	1.09
ZM-1	2701.90	Ordovician	0.37	212.60	1.63	64.51	26.20	7.66	9.30	1.46	0.05	0.04	1.02
KA-1 bis	2605.65	Triassic	0.09	89.10	3.95	36.91	39.60	19.55	23.50	1.08	0.81	1.11	1.05
KA-1 bis	3029.82	Silurian	0.14	95.90	10.94	47.37	33.69	8.00	18.94	1.01	0.53	0.39	1.04
KA-1 bis	3060.90	Silurian	0.11	47.20	6.86	52.40	29.89	10.85	17.71	1.04	0.51	0.38	1.04
KA-1 bis	3072.85	Silurian	0.28	86.95	10.83	47.66	30.99	10.52	21.35	1.19	0.31	0.26	1.02
KA-1 bis	3168.82	Ordovician	0.09	160.70	5.50	65.61	20.30	8.59	14.09	1.25	0.02	0.02	1.05
KA-1 bis	3179.85	Ordovician	0.08	137.90	1.55	66.64	17.33	14.48	16.03	1.03	0.02	0.02	1.07
KA-1 bis	3182.85	Ordovician	0.06	109.10	1.29	65.18	18.23	15.31	16.59	1.03	0.02	0.02	1.06
RE-1	3040.00	Devonian	0.07	65.40	29.13	16.16	28.85	25.86	55.00	1.98	1.22	0.68	1.40
RE-1	3050.25	Devonian	0.07	66.60	23.79	37.62	28.83	9.77	33.55	1.30	1.02	0.87	1.12
RE-1	3114.70	Devonian	0.26	113.04	25.07	35.07	24.71	15.15	40.22	2.18	1.27	0.65	1.01
RE-1	3202.30	Devonian	0.03	52.60	2.07	72.12	20.54	5.27	7.34	1.44	0.51	0.32	1.02
RE-1	3346.20	Devonian	1.48	136.80	9.58	40.11	30.78	19.53	29.11	1.63	0.61	0.51	1.03
RE-1	3354.40	Devonian	2.43	320.00	22.93	38.19	25.68	13.20	36.12	1.41	0.85	0.68	1.01
RE-1	3438.26	Devonian	0.24	240.00	7.49	51.98	26.89	13.65	21.13	1.54	0.80	0.54	1.05
ZAR-1	3450.98	Devonian	0.14	166.60	9.84	49.21	26.28	14.67	24.51	1.54	0.50	0.36	1.01
ZAR-1	3994.65	Silurian	0.19	97.90	12.45	42.55	28.56	16.43	28.89	1.31	0.54	0.45	1.04
ELB-3	2372.20	Triassic	0.06	54.05	17.08	26.97	30.22	25.73	42.81	0.82	0.84	1.23	1.07
RYB-1	3106.30	Devonian	0.22	51.70	27.36	24.39	37.24	11.01	38.37	1.81	0.28	0.15	1.07
SED-1	2642.00	Devonian	0.11	87.00	12.57	28.54	35.61	23.29	35.85	2.71	0.62	0.22	1.09
REA-1	2764.57	Silurian	0.07	90.90	13.20	32.50	31.60	20.27	33.48	2.17	1.17	0.56	1.02
SOH-1	3192.50	Silurian	0.14	350.00	6.29	75.23	15.04	3.44	9.73	1.50	0.40	0.53	1.00
MRK-1	3196.46	Ordovician	0.03	73.00	3.54	60.04	22.12	14.30	17.84	1.40	0.02	0.02	1.04

Appendix 3.4 Molecular parameters predominantly related to source and depositional environment.

well	depth(m)	age	C27r/C27n	C29r/C29n	%C27	%C28	%C29	%C28t/C26t+C27t+C28t
ELB-3	2372.20	Triassic	n.d	n.d	9.80	21.56	67.70	74.40
KA-1 bis	2605.65	Triassic	6.57	4.52	8.70	21.74	69.57	63.50
KA-1 bis	3029.82	Silurian	10.50	4.40	30.77	23.08	46.15	59.40
KA-1 bis	3060.90	Silurian	10.77	4.72	40.63	18.75	40.63	51.35
KA-1 bis	3072.85	Silurian	11.50	5.48	24.32	24.32	51.35	53.40
RE-1	3040.00	Devonian	3.28	2.53	34.85	19.70	45.45	40.72
RE-1	3050.25	Devonian	3.44	1.94	40.01	21.43	38.57	46.09
RE-1	3114.70	Devonian	3.41	2.36	35.42	18.75	45.83	50.15
RE-1	3202.20	Devonian	9.40	4.63	26.80	24.40	48.80	48.01
RE-1	3346.20	Devonian	15.56	10.62	44.44	22.22	33.33	58.87
RE-1	3354.40	Devonian	14.10	9.40	45.45	18.18	36.36	59.50
RE-1	3438.26	Devonian	10.92	8.24	20.01	20.01	60.01	58.70
RYB-1	3106.30	Devonian	3.31	2.50	44.44	22.22	33.33	46.66
ZAR-1	3450.98	Devonian	7.67	4.01	25.01	25.01	50.01	50.01
ZAR-1	3994.65	Silurian	3.11	1.59	n.d	n.d	n.d	59.37
ZM-1	2388.75	Silurian	1.13	0.49	31.82	21.72	46.46	52.90
REA-1	2764.56	Silurian	3.38	1.07	32.98	17.02	50.01	46.30
ZM-1	2694.84	Ordovician	3.24	1.81	15.01	15.65	69.41	64.01
ZM-1	2701.90	Ordovician	11.33	3.97	15.01	10.01	75.01	70.50

C29r/C29n= C_{29} 13β(H),17α(H)(20S)/C_{29} 5α(H),14α(H),17a(H)(20S) (m/z 400.4100->m/z 217.2000, GC/MS/MRM)
C27r/C27n= C_{27} 13b(H),17a(H)(20S)/C_{27} 5α(H),14α(H),17α(H)(20S) (m/z 372.3800->m/z 217.2000, GC/MS/MRM))
C28t/C26t+C27t+C28t= total C_{28} triaromatic/total (C_{26}-C_{28}) triaromatic steroid (m/z 231.1170, GC/MS/EI, SIM)
%(C27-C29): relative proportions of 5α(H),14α(H),17α(H)-(C_{27}-C_{29}) (20R) steranes (m/z 217.1950, GC/MS/EI, SIM).
n.d-not determined.

Appendix 3.5 Molecular parameters predominantly related to source with some influence of maturity.

Well	depth(m)	age	C23T/C23T+C30hp	C30hp/C29st	%C27n	%C28n	%C29n	%C27r	%C28r	%C29r
ELB-3	2372.20	Triassic	0.53	13.90	35.47	10.34	54.19	49.69	9.22	41.09
KA-1 bis	2605.65	Triassic	0.01	3.12	15.97	16.81	67.22	23.71	17.74	58.55
KA-1 bis	3029.82	Silurian	0.47	3.50	23.36	34.58	42.06	33.82	32.37	33.82
KA-1 bis	3060.90	Silurian	0.44	3.61	37.15	9.82	53.03	48.63	7.07	44.30
KA-1 bis	3072.85	Silurian	0.50	3.58	36.43	8.37	55.20	49.77	6.89	43.34
RE-1	3040.00	Devonian	0.08	1.87	35.17	16.42	48.41	48.46	12.09	39.45
RE-1	3050.25	Devonian	0.11	1.14	37.95	10.01	52.04	48.39	11.57	40.04
RE-1	3114.70	Devonian	0.13	1.10	25.10	34.57	40.33	34.06	32.12	33.82
RE-1	3202.20	Devonian	0.17	2.48	27.37	7.44	65.19	41.48	9.82	48.70
RE-1	3346.20	Devonian	0.39	12.65	38.31	13.21	48.48	49.21	7.83	42.96
RE-1	3354.40	Devonian	0.40	10.52	48.65	7.82	43.53	48.34	8.40	43.25
RE-1	3438.26	Devonian	0.32	12.17	37.53	10.86	51.61	49.89	7.06	43.04
RYB-1	3106.30	Devonian	0.21	2.02	35.77	11.91	52.31	45.77	12.40	41.84
ZAR-1	3450.98	Devonian	0.54	3.13	35.54	11.99	52.47	50.72	6.43	42.85
ZAR-1	3994.65	Silurian	0.63	2.54	31.91	13.34	54.74	52.91	7.30	39.78
ZM-1	2388.75	Silurian	0.39	0.76	33.15	15.54	51.30	47.07	11.23	41.70
REA-1	2764.56	Silurian	0.58	16.51	42.94	18.40	38.65	56.75	6.13	37.12
ZM-1	2694.84	Ordovician	0.57	2.78	35.76	9.88	54.36	47.95	6.76	45.29
ZM-1	2701.90	Ordovician	0.60	20.33	31.77	6.73	61.49	34.22	7.55	58.23

$C_{23}T/C_{23}T+C_{30}$ hp= C_{23} tricyclic/C_{23}tricyclic+17α(H)-C_{30} hopane (m/z 318.3300->m/z 191.1800 & m/z 412.4100->m/z 191.1800 for C_{23} tricyclic and C_{30} hopane respectively).)
$C_{30}hp/C_{29}st$= 17α(H)-C_{30} hopane/5α(H),14α(H),17α(H)-C_{29} sterane(20R) (m/z 412.4100->m/z 191.1800 and m/z 400.4100->m/z 217.2000 for C_{30} hopane and C_{29} steranes).
r=rearranged sterane= 13β(H),17α(H) (20R); n=non-rearranged sterane= 5α(H),14α(H),17α(H) (20R) (%C_{27}, %C_{28} and %C_{29} steranes calculated from MRM traces).

Appendix 3.6 Molecular parameters predominantly related to maturity and source.

well	depth(m)	age	Ts/Tm	C_{29} βα/βα+αβ	C_{30} βα/βα+αβ	C29Ts/C29ab hp	C32 22S/22S+22R
ELB-3	2372.20	Triassic	0.16	0.97	0.92	0.07	0.55
KA-1 bis	2605.65	Triassic	0.30	0.89	0.85	0.19	0.58
KA-1 bis	3029.82	Silurian	17.60	0.84	0.84	n.d	0.57
KA-1 bis	3060.90	Silurian	19.87	0.97	0.94	n.d	0.66
KA-1 bis	3072.85	Silurian	19.57	0.90	0.98	n.d	0.66
RE-1	3040.00	Devonian	0.21	0.92	0.81	0.29	0.55
RE-1	3050.25	Devonian	0.36	0.93	0.96	0.29	0.62
RE-1	3114.70	Devonian	0.88	0.86	0.90	0.59	0.59
RE-1	3202.20	Devonian	1.10	0.91	0.95	0.61	0.62
RE-1	3346.20	Devonian	5.04	0.93	0.99	0.93	0.66
RE-1	3354.40	Devonian	6.09	0.93	0.97	0.85	0.68
RE-1	3438.26	Devonian	6.14	0.93	0.98	0.65	0.66
RYB-1	3106.30	Devonian	1.37	0.89	0.93	0.73	0.59
ZAR-1	3450.98	Devonian	11.25	0.85	0.97	1.95	0.64
ZAR-1	3994.65	Silurian	1.39	0.97	0.99	0.78	0.69
ZM-1	2388.75	Silurian	0.85	0.91	0.93	0.31	0.60
REA-1	2764.56	Silurian	0.12	0.88	0.92	0.07	0.65
ZM-1	2694.84	Ordovician	0.93	0.94	0.97	1.41	0.61
ZM-1	2701.90	Ordovician	3.09	0.95	0.98	0.86	0.68

T_s/T_m= 18α(H)-22,29,30-trisnorneohopane/17α(H)-22,29,30-trisnorhopane (m/z 370.3600-m/z 191.1800, GC/MS/MRM).

C_{29} βα/βα+αβ hp=17β(H),21α(H) - 30-norhopane/17β(H),21α(H)+17α(H),21β(H)-30-norhopane (m/z 398.3900->m/z 191.1800, GC/MS/MRM)

C_{30} βα/βα+αβ hp=17β(H),21α(H) hopane/17β(H),21α(H)+17α(H),21β(H)-hopane (412.4100->m/z 191.1800, GC/MS/MRM)

C_{29}Ts/C_{29}αβ hp=18α(H)-30-norneohopane/17α(H),21β(H)-30 norhopane/(m/z 398.3900->m/z 191.1800, GC/MS/MRM)

C_{32} 22S/22S+22R=17α(H),21β(H)-C_{32} (22S/22S+22R) (m/z 426.4200-m/z 191.1800, GC/MS/MRM)

TEXT BOUND INTO THE SPINE

Appendix 3.7 Molecular parameters related to maturity.

well	depth (m)	age	C29 20S/20S+20R	αββ/αββ+ααα	ARO ratio	cracking ratio	MTSI1	MTSI2
ELB-3	2372.20	Triassic	0.45	0.45	0.35	0.16	0.34	0.40
KA-1 bis	2605.65	Triassic	0.42	0.45	0.56	0.16	0.34	0.36
KA-1 bis	3029.82	Silurian	0.55	0.60	0.52	0.31	0.52	0.56
KA-1 bis	3060.90	Silurian	0.56	0.64	0.58	0.44	0.50	0.49
KA-1 bis	3072.85	Silurian	0.57	0.65	0.62	0.57	0.60	0.54
RE-1	3040.00	Devonian	0.34	0.30	0.23	0.30	0.24	0.20
RE-1	3050.25	Devonian	0.36	0.17	0.31	0.25	0.25	0.26
RE-1	3114.70	Devonian	0.38	0.29	0.62	0.13	0.42	0.39
RE-1	3202.20	Devonian	0.43	0.31	0.58	0.46	0.35	0.31
RE-1	3346.20	Devonian	0.55	0.64	0.70	0.61	0.53	0.63
RE-1	3354.40	Devonian	0.56	0.63	0.70	0.41	0.57	0.50
RE-1	3438.26	Devonian	0.57	0.68	0.56	0.38	0.51	0.45
RYB-1	3106.30	Devonian	0.35	0.35	0.58	0.51	0.85	0.92
ZAR-1	3450.98	Devonian	0.52	0.58	0.44	0.78	0.55	0.55
ZAR-1	3994.65	Silurian	0.56	0.55	n.m	0.41	0.50	0.51
ZM-1	2388.75	Silurian	0.45	0.32	0.49	0.12	0.53	0.50
REA-1	2764.56	Silurian	0.57	0.58	0.51	0.21	0.32	0.19
ZM-1	2694.84	Ordovician	0.51	0.60	n.m	0.72	0.61	0.53
ZM-1	2701.90	Ordovician	0.52	0.68	0.54	0.51	0.60	0.57

C29 20S/20S+20R= 5α(H),14α(H),17α(H)-C_{29} (20S/20S+20R) (m/z 217.1950, GC/MS/EI SIM)
αββ/αββ+ααα= 5α(H),14β(H),17β(H)-C_{29} (20R)/5α(H),14β(H),17β(H)-C_{29} (20R)+5α(H),14α(H),17α(H)-C_{29} (20R), (m/z 218.2040 and 217.1950, GC/MS/EI, SIM)
ARO ratio= steroid aromatisation= (total(C_{26}-C_{28}) triaromatic/total(triaromatic (C_{26}-C_{28}) & monoaromatic (C_{27}-C_{29}) steroids from m/z 231.1170 and m/z 253.1950 respectively, GC/MS/EI, SIM)
cracking ratio= (C_{20}+C_{21})/total(C_{20}+C_{21}+C_{26}+C_{27}+C_{28}) triaromatic steroid hydrocarbons (m/z 231.1170, GC/MS/EI SIM).
MTSI1 and MTSI2 (methyl triaromatic steroid indices 1 and 2 for C_{21} and C_{22} methylated triaromatic steroids, m/z 245.1130, GC/MS/EI, MRM)
MTSI1 and MTSI2= 2-methyl-+ 3-methyl/2-methyl-+3-methyl-+ 4-methyl-C_{21} and-C_{22} respectively.
n.m- not measurable (due to low intensity of aromatic steroid hydrocarbons.

Appendix 4.2 Molecular parameters predominantly related to source and depositional environment.

basin	well number	Age of reservoir)	Depth (reservoir)	C27r/C27n	C29r/C29n	%C27	%C28	%C29	%C28t/C26t+C27t+C28t
SE Constantine	DK-1	Conacian	1083m-1208m	2.35	1.29	24.70	27.90	46.80	46.02
SE Constantine	GKN-1	Cenomanian		9.29	4.62	n.d	n.d	n.d	n.d
Ghadames-El Borma	ELB-9	Triassic		10.46	10.23	33.30	12.50	54.10	64.05
Ghadames-El Borma	KA-2	Triassic		4.09	2.61	34.70	13.90	51.40	68.02
Ghadames-El Borma	ROM-1	Triassic		12.09	10.23	25.01	18.80	56.30	68.10
Sbaa	ODZ-1	Famenian	636m-662m	4.66	3.69	34.38	15.60	50.00	61.10
Sbaa	DECH-1	Strunian	613m-625m	5.12	4.19	35.30	15.70	49.02	69.08
Gassi Touil	GT-47	Lower Dev(TAGI)		8.64	4.06	41.80	20.90	37.30	69.07
Gassi Touil	GT-6	Upper Dev(TAGS)		10.00	4.78	34.50	20.70	44.80	54.20
Rhourd-Nouss	RN-48	Lower Dev(TAGI)		8.54	5.25	48.40	22.60	29.03	48.20
Rhourd-Nouss	RNSE-6	Upper Dev(TAGS)		4.09	2.18	23.08	11.50	65.40	80.20
Ain Amenas	ZR-115	Carboniferous		3.02	2.02	29.10	15.00	55.80	72.20
Ain Amenas	TG-22	Upper Dev(F2)		7.05	5.04	30.30	16.30	54.50	65.30

C29r/C29n= C_{29} 13β(H),17α(H)(20S)/C_{29} 5α(H),14α(H),17a(H)(20S) (m/z 400.4100->m/z 217.2000, GC/MS/MRM)
C27r/C27n= C_{27} 13b(H),17a(H)(20S)/C_{27} 5α(H),14α(H),17α(H)(20S) (m/z 372.3800->m/z 217.2000, GC/MS/MRM))
C28t/C26t+C27t+C28t= total C_{28} triaromatic/total (C_{26}-C_{28}) triaromatic steroid (m/z 231.1170, GC/MS/EI, SIM)
%(C27-C29): relative proportions of 5α(H),14α(H),17α(H)-(C_{27}-C_{29}) (20R) steranes (m/z 217.1950, GC/MS/EI, SIM).
n.d-not determined.

Appendix 4.3 Molecular parameters predominantly related to maturity and source.

basin	well number	age of reservoir	depth reservoir	Ts/Tm	C29N/C30hp	C29Ts/C29hp	C32 22S/22S+22R
SE Constantine	DK-1	Conacian	1083m-1208m	0.99	0.60	0.16	0.61
SE Constantine	GKN-1	Cenomanian		17.86	0.25	1.11	0.67
Ghadames-El Borma	ELB-9	Triassic		2.93	0.43	0.42	0.64
Ghadames-El Borma	KA-2	Triassic		3.14	0.43	0.61	0.65
Ghadames-El Borma	ROM-1	Triassic		4.69	0.45	0.86	0.63
Sbaa	ODZ-1	Famenian	636m-662m	3.16	0.43	0.49	0.63
Sbaa	DECH-1	Strunian	613m-625m	3.23	0.43	0.39	0.61
Gassi-Touil	GT-47	Low Dev(TAGI)		7.93	0.39	1.10	0.63
Gassi-Touil	GT-6	Upper Dev(TAGS)		5.81	0.63	0.59	0.64
Rhourd-Nouss	RN-48	Low Dev(TAGI)		6.94	1.22	0.49	0.63
Rhourd-Nouss	RNSE-6	Upper Dev(TAGS)		1.46	1.02	0.40	0.63
Ain Amenas	ZR-115	Carboniferous		1.02	0.64	0.23	0.62
Ain Amenas	TG-22	Upper Dev(F2)		4.03	0.44	0.59	0.61

T_s/T_m= 18α(H)-22,29,30-trisnorneohopane/17α(H)-22,29,30-trisnorhopane (m/z 370.3600-m/z 191.1800, GC/MS/MRM).

C_{29} βα/βα+αβ hp=17β(H),21α(H)-30-norhopane/17β(H),21α(H)+17α(H),21β(H)-30-norhopane (m/z 398.3900->m/z 191.1800, GC/MS/MRM)

C_{30} βα/βα+αβ hp=17β(H),21α(H) hopane/17β(H),21α(H)+17α(H),21β(H)-hopane (412.4100->m/z 191.1800, GC/MS/MRM)

C_{29}Ts/C_{29}αβ hp=18α(H)-30-norneohopane/17α(H),21β(H)-30 norhopane/(m/z 398.3900->m/z 191.1800, GC/MS/MRM)

C_{32} 22S/22S+22R=17α(H),21β(H)-C_{32} (22S/22S+22R) (m/z 426.4200-m/z 191.1800, GC/MS/MRM)

Appendix 4.4 Molecular parameters predominantly related to source with some influence of maturity.

basin	well number	age of reservoir	Depth(reservoir)	C23T/C23T+C30hp	C30 hp/C29st	%C27n	%C28n	%C29n	%C27r	%C28r	%C29r
SE Constantine	DK-1	Conacian	1083m-1208m	0.19	8.21	41.22	21.51	37.27	50.57	21.04	28.39
SE Constantine	GKN-1	Cenomanian		0.34	5.93	38.89	21.11	40.00	54.71	18.35	26.94
Ghadames-El Borma	ELB-9	Triassic		0.36	6.80	50.58	12.26	37.16	49.45	12.80	37.75
Ghadames-El Borma	KA-2	Triassic		0.35	3.50	41.12	9.78	49.10	46.40	9.11	44.48
Ghadames-El Borma	ROM-1	Triassic		0.59	3.47	43.64	11.72	44.64	43.53	9.16	47.31
Sbaa	ODZ-1	Famenian	636m-662m	0.34	8.68	39.45	12.72	47.82	45.22	10.22	44.55
Sbaa	DECH-1	Strunian	613m-625m	0.32	8.12	39.70	10.97	49.33	45.71	9.60	44.68
Gassi-Touil	GT-47	Low Dev(TAGI)		0.83	1.00	32.66	15.37	51.97	41.58	9.62	48.80
Gassi-Touil	GT-6	Upper Dev(TAGS)		0.69	1.35	32.32	12.22	55.46	43.51	10.44	46.05
Rhourd-Nouss	RN-48	Low Dev(TAGI)		0.63	0.87	36.39	16.34	47.28	37.89	9.01	53.09
Rhourd-Nouss	RNSE-6	Upper Dev(TAGS)		0.79	0.64	34.24	9.63	56.13	42.32	11.62	46.06
Ain Amenas	ZR-115	Carboniferous		0.00	2.89	35.50	12.40	52.10	45.24	9.86	44.90
Ain Amenas	TG-22	Upper Dev(F2)		0.36	6.45	41.23	11.61	47.16	49.31	10.26	40.43

$C_{23}T/C_{23}T+C_{30}$ hp= C_{23} tricyclic/C_{23}tricyclic+17α(H)-C_{30} hopane (m/z 318.3300->m/z 191.1800 & m/z 412.4100->m/z 191.1800 for C_{23} tricyclic and C_{30} hopane respectively).)
C_{30}hp/C_{29}st= 17α(H)-C_{30} hopane/5α(H),14α(H),17α(H)-C_{29} sterane(20R) (m/z 412.4100->m/z 191.1800 and m/z 400.4100->m/z 217.2000 for C_{30} hopane and C_{29} steranes).
r=rearranged sterane= 13β(H),17α(H) (20R); n=non-rearranged sterane: %C_{27}, C_{28} and %C_{29} 5α(H),14α(H),17α(H) (20R) (calculated from MRM traces, m/z 372.38, m/z 386.3900 and m/z 400.4100->m/z 217.2000).

Appendix 4.5 Molecular parameters related to maturity.

basin	well number	age of reservoir	depth (reservoir)	C29aaa 20S/20S+20R	αββ/αββ+ααα	ARO ratio	cracking ratio	IMTS1	IMTS2
SE Constantine	DK-1	Conacian	1083m-1208m	0.48	0.80	0.84	0.15	0.31	0.32
Ghadames-El Borma	ELB-9	Triassic		0.54	0.91	0.86	0.49	0.63	0.56
Ghadames-El Borma	KA-2	Triassic		0.53	0.49	0.88	0.22	0.59	0.48
Ghadames-El Borma	ROM-1	Triassic		0.50	0.87	n.m	0.72	0.61	0.57
Sbaa	ODZ-1	Famenian	636m-662m	0.50	0.77	n.m	0.31	0.62	0.45
Sbaa	DECH-1	Strunian	613m-625m	0.53	0.82	0.77	0.15	0.57	0.44
Sbaa	TOT-1	Tournaisian	593m	0.54	0.88	n.m	0.36	n.m	n.m
Illizi	STAH-40	Low Dev(F6)		n.m	n.m	n.m	n.m	n.m	n.m
Gassi-Touil	GT-47	Low Dev(TAGI)		0.54	0.78	n.m	0.57	n.m	n.m
Gassi-Touil	GT-6	Upper Dev(TAGS)		0.56	0.77	n.m	0.33	n.m	n.m
Rhourd-Nouss	RN-48	Low Dev(TAGI)		0.59	n.m	n.m	0.73	n.m	n.m
Rhourd-Nouss	RNSE-6	Upper Dev(TAGS)		0.47	0.38	n.m	0.64	0.68	0.55
Ain Amenas	ZR-115	Carboniferous		0.47	0.38	0.61	0.15	0.41	0.42
Ain Amenas	TG-22	Upper Dev(F2)		0.49	0.82	0.81	0.16	0.59	0.51

C29 20S/20S+20R= 5α(H),14α(H),17α(H)-C_{29} (20S/20S+20R) (m/z 217.1950, GC/MS/EI SIM)
αββ/αββ+ααα= 5α(H),14β(H),17β(H)-C_{29} (20R)/5α(H),14β(H),17β(H)-C_{29} (20R)+5α(H),14α(H),17α(H)-C_{29} (20R), (m/z 218.2040 and 217.1950, GC/MS/EI, SIM)
ARO ratio= steroid aromatisation= (total(C_{26}-C_{28}) triaromatic/total(triaromatic (C_{26}-C_{28}) & monoaromatic (C_{27}-C_{29}) steroids from m/z 231.1170 and m/z 253.1950 respectively, GC/MS/EI, SIM)
cracking ratio= (C_{20}+C_{21})/total(C_{20}+C_{21}+C_{26}+C_{27}+C_{28}) triaromatic steroid hydrocarbons (m/z 231.1170, GC/MS/EI SIM).
MTSI1 and MTSI2 (methyl triaromatic steroid indices 1 and 2 for C_{21} and C_{22} methylated triaromatic steroids, m/z 245.1130, GC/MS/EI, MRM)
MTSI1 and MTSI2= 2-methyl-+ 3-methyl/2-methyl-+3-methyl-+ 4-methyl-C_{21} and-C_{22} respectively.
n.m- not measurable (due to low intensity of aromatic steroid hydrocarbons.

Appendix 4.6 Paraffinicity and aromaticity parameters.

basin	well number	age of reservoir	depth (reservoir)	Bz/n-C6	Tol/n-C7	Isohep	Heptane	n-C7/2MC6	n-C7/MCH	n-C6/CHx
SE Constantine	DK-1	Conacian	1083m-1208m	0.26	0.46	0.72	25.81	3.04	1.39	1.58
SE Constantine	GKN-1	Cenomanian		0.23	0.49	1.08	27.41	2.73	1.38	2.54
Ghadames-El Borma	ROM-1	Triassic		0.10	0.30	1.90	31.72	3.08	1.31	2.66
Sbaa	ODZ-1	Famenian	636m-662m	0.01	0.19	1.62	30.33	3.94	0.95	1.27
Sbaa	DECH-1	Strunian	613m-625m	0.02	0.22	1.34	24.73	2.75	0.78	2.07
Sbaa	TOT-1	Tournaisian	593m	0.01	0.08	1.16	20.97	2.64	0.72	1.47
Illizi	MRK-12	Lower Dev(F6)		0.13	0.42	3.76	30.47	2.36	1.13	2.02
Illizi	STAH-40	Lower Dev(F6)		0.12	0.39	4.05	30.34	2.21	1.17	2.10
Illizi	MRK-16	Upper Dev		0.10	0.41	1.79	30.46	3.36	1.11	1.74
Illizi	STAH-8	Upper Dev		0.06	0.28	1.89	31.59	2.63	2.05	2.36
Illizi	WT-1	Lower Dev(TAGI)		0.20	0.09	2.93	34.45	3.45	1.30	2.66
Gassi Touil	GT-47	Lower Dev(TAGI)		0.37	0.48	7.50	31.12	1.83	1.46	2.78
Gassi Touil	GT-6	Upper Dev(TAGS)		0.40	0.48	7.71	31.07	1.81	1.46	2.87
Rhourd-Nouss	RN-48	Lower Dev(TAGI)		0.62	0.41	4.77	31.76	2.06	1.56	2.93
Rhourd-Nouss	RNSE-6	Upper Dev(TAGS)		0.55	0.54	3.77	35.01	2.08	1.69	2.67
Ain Amenas	ZR-115	Carboniferous		0.04	0.22	2.69	31.73	2.55	1.41	2.51
Ain Amenas	DL-127	Upper Dev(F2)		0.09	0.50	1.98	25.09	2.66	0.80	1.62
Ain Amenas	TG-22	Upper Dev(F2)		0.08	0.36	2.34	31.71	3.30	1.14	1.82

Bz=benzene
Tol/n-C7=Toluene/n-heptane
Isohep=Isoheptane index=(2-methyl- & 3-methylhexanes)/
(1cis-3-,1trans-3-,& 1trans-2-dimethylcyclopentanes)
Heptane= Heptane index= 100*n-heptane /total cyclohexane through methylcyclohexane+)
(Thompson, 1987)
n-C7/MCH=n-heptane/methylcyclohexane
n-C6/CHx=n-hexane/cyclohexane
n-C7/2MC6=n-heptane/2-methylhexane
+ excluding 1,cis-2-dimethylcyclopentane

influence of maturity.

well	depth(m)	age	Ts/Tm	C29Ts/C29hp	C23T/C23T+C30hp	C30hp/C29st	%C28t/C26t+C27t+C28t
ELB-3	2372.20	Triassic	0.16	0.07	0.53	13.90	74.40
KA-1 bis	2605.65	Triassic	0.30	0.19	0.01	3.12	63.50
KA-1 bis	3029.82	Silurian	17.60	n.d	0.47	3.50	59.40
KA-1 bis	3060.90	Silurian	19.87	n.d	0.44	3.61	51.35
KA-1 bis	3072.85	Silurian	19.57	n.d	0.50	3.58	53.40
RE-1	3040.00	Devonian	0.21	0.29	0.08	1.87	40.72
RE-1	3050.25	Devonian	0.36	0.29	0.11	1.14	46.09
RE-1	3114.70	Devonian	0.88	0.59	0.13	1.10	50.15
RE-1	3202.20	Devonian	1.10	0.61	0.17	2.48	48.01
RE-1	3346.20	Devonian	5.04	0.93	0.39	12.65	58.87
RE-1	3354.40	Devonian	6.09	0.85	0.40	10.52	59.50
RE-1	3438.26	Devonian	6.14	0.65	0.32	12.17	58.70
RYB-1	3106.30	Devonian	1.37	0.73	0.21	2.02	46.66
ZAR-1	3450.98	Devonian	11.25	1.95	0.54	3.13	50.01
ZAR-1	3994.65	Silurian	1.39	0.78	0.63	2.54	59.37
ZM-1	2388.75	Silurian	0.85	0.31	0.39	0.76	52.90
REA-1	2764.56	Silurian	0.12	0.07	0.58	16.51	46.30
ZM-1	2694.84	Ordovician	0.93	1.41	0.57	2.78	64.01
ZM-1	2701.90	Ordovician	3.09	0.86	0.60	20.33	70.50
ELB-9(oil)		Triassic	2.93	0.42	0.36	6.80	64.01
KA-2(oil)		Triassic	3.14	0.61	0.35	3.50	68.01
ROM-1(oil)		Triassic	4.69	0.86	0.59	3.47	68.01

T_s/T_m= 18α(H)-22,29,30-trisnorneohopane/17α(H)-22,29,30-trisnorhopane (m/z 370.3600-m/z 191.1800, GC/MS/MRM)

$C_{29}Ts/C_{29}\alpha\beta$ hp=18α(H)-30-norneohopane/17α(H),21β(H)-30 norhopane/(m/z 398.3900->m/z 191.1800, GC/MS/MRM)

$C_{23}T/C_{23}T+C_{30}$ hp= C_{23} tricyclic/C_{23}tricyclic+17α(H)-C_{30} hopane (m/z 318.3300->m/z 191.1800 & m/z 412.4100->m/z 191.1800 for C_{23} tricyclic and C_{30} hopane respectively).)

$C_{30}hp/C_{29}st$= 17α(H)-C_{30} hopane/5α(H),14α(H),17α(H)-C_{29} sterane(20R) (m/z 412.4100->m/z 191.1800 and m/z 400.4100->m/z 217.2000 for C_{30} hopane and C_{29} steranes).

C28t/C26t+C27t+C28t= total C_{28} triaromatic/total (C_{26}-C_{28}) triaromatic steroid (m/z 231.1170, GC/MS/EI, SIM)

Appendix 5.2 Molecular parameters related to maturity.

well	depth(m)	age	C29 20S/20S+20R	αββ/αββ+ααα	ARO ratio	cracking ratio	MTSI1	MTSI2
ELB-3	2372.20	Triassic	0.45	0.45	0.35	0.16	0.34	0.40
KA-1 bis	2605.65	Triassic	0.42	0.45	0.56	0.16	0.34	0.36
KA-1 bis	3029.82	Silurian	0.55	0.60	0.52	0.31	0.52	0.56
KA-1 bis	3060.90	Silurian	0.56	0.64	0.58	0.44	0.50	0.49
KA-1 bis	3072.85	Silurian	0.57	0.65	0.62	0.57	0.60	0.54
RE-1	3040.00	Devonian	0.34	0.30	0.23	0.30	0.24	0.20
RE-1	3050.25	Devonian	0.36	0.17	0.31	0.25	0.25	0.26
RE-1	3114.70	Devonian	0.38	0.29	0.62	0.13	0.42	0.39
RE-1	3202.20	Devonian	0.43	0.31	0.58	0.46	0.35	0.31
RE-1	3346.20	Devonian	0.55	0.64	0.70	0.61	0.53	0.63
RE-1	3354.40	Devonian	0.56	0.63	0.70	0.41	0.57	0.50
RE-1	3438.26	Devonian	0.57	0.68	0.56	0.38	0.51	0.45
RYB-1	3106.30	Devonian	0.35	0.35	0.58	0.51	0.85	0.92
ZAR-1	3450.98	Devonian	0.52	0.58	0.44	0.78	0.55	0.55
ZAR-1	3994.65	Silurian	0.56	0.55	n.m	0.41	0.50	0.51
ZM-1	2388.75	Silurian	0.45	0.32	0.49	0.12	0.53	0.50
REA-1	2764.56	Silurian	0.57	0.58	0.51	0.21	0.32	0.19
ZM-1	2694.84	Ordovician	0.51	0.60	n.m	0.72	0.61	0.53
ZM-1	2701.90	Ordovician	0.52	0.68	0.54	0.51	0.60	0.57
ELB-9(oil)		Triassic	0.54	0.91	0.86	0.49	0.63	0.56
KA-2(oil)		Triassic	0.53	0.63	0.88	0.22	0.59	0.48
ROM-1(oil)		Triassic	0.50	0.87	n.m	0.72	0.61	0.57

C29 20S/20S+20R= 5α(H),14α(H),17α(H)-C_{29} (20S/20S+20R) (m/z 217.1950, GC/MS/EI SIM)
αββ/αββ+ααα= 5α(H),14β(H),17β(H)-C_{29} (20R)/5α(H),14β(H),17β(H)-C_{29} (20R)+5α(H),14α(H),17α(H)-C_{29} (20R), (m/z 218.2040 and 217.1950, GC/MS/EI, SIM)
ARO ratio= steroid aromatisation= (total(C_{26}-C_{28}) triaromatic/total(triaromatic (C_{26}-C_{28}) & monoaromatic (C_{27}-C_{29}) steroids from m/z 231.1170 and m/z 253.1950 respectively, GC/MS/EI, SIM)
cracking ratio= (C_{20}+C_{21})/total(C_{20}+C_{21}+C_{26}+C_{27}+C_{28}) triaromatic steroid hydrocarbons (m/z 231.1170, GC/MS/EI SIM).
MTSI1 and MTSI2 (methyl triaromatic steroid indices 1 and 2 for C_{21} and C_{22} methylated triaromatic steroids, m/z 245.1130, GC/MS/EI, MRM)
MTSI1 and MTSI2= 2-methyl-+ 3-methyl/2-methyl-+3-methyl-+ 4-methyl-C_{21} and-C_{22} respectively.
n.m- not measurable (due to low intensity of aromatic steroid hydrocarbons.